ELECTROMAGNETIC/LASER ICE THICKNESS DATA FROM THE LABRADOR SHELF, 1994

J.S. Holladay and R. Moucha

Ocean Sciences Division
Maritimes Region
Fisheries and Oceans Canada

Bedford Institute of Oceanography
P.O. Box 1006
Dartmouth, Nova Scotia
Canada B2Y 4A2

1998

Canadian Contractor Report of Hydrography and Ocean Sciences 49

Fisheries and Oceans | Pêches et Océans

Canada

Canadian Contractor Report of Hydrography and Ocean Sciences 49

1998

Electromagnetic/Laser Ice Thickness Data from the Labrador Shelf, 1994

by

J. S. Holladay* and R. Moucha*

Ocean Sciences Division
Maritimes Region
Fisheries and Oceans Canada

Bedford Institute of Oceanography
P.O. Box 1006
Dartmouth, Nova Scotia
Canada, B2Y 4A2

---

* Vanguard Geophysics Inc.
66 Mann Avenue
Toronto, Ontario
Canada, M4S 2Y3
(formerly employed by Aerodat Inc.)

Cat. No. Fs 98-17/49E ISSN 071-6748

Correct Citation for this publication:

Holladay, J.S. and R. Moucha. 1998. Electromagnetic/Laser Ice Thickness Data from the Labrador Shelf, 1994. Can. Contract. Rep. Hydrogr. Ocean Sci. 49: viii + 340.

TABLE OF CONTENTS

ABSTRACT

Holladay, J.S. and R. Moucha. 1998. Electromagnetic/Laser Ice Thickness Data from the Labrador Shelf, 1994. Can. Contract. Rep. Hydrogr. Ocean Sci. 49: viii + 340.

Electromagnetic snow-plus-ice thickness data collected during the March, 1994 off the southern Labrador coast near Cartwright, has been post-processed and formatted for presentation. The ice thickness data includes data from long flight traverses over the mobile ice and short flight traverses over different ice types identified in ERS-1 satellite SAR imagery. The data are presented in both *profile map* and in *standard plot* formats. The *profile map* plots (Appendix C) consists of ice thickness data presented in profile form superimposed on a map of the area in a Lambert Conic Conformal projection. The *standard plot* contains ice thickness and high-pass filtered laser altimeter histograms along with profile plots of ice thickness, laser altimeter and high-pass filtered laser altimeter. All *standard plots* are shown in Appendix F and corresponds each to a 4 km segment of the flight traverse.

The EM observations showed that the EM ice sounding technique can clearly distinguish the ice properties of land-fast and mobile pack ice. The coastal land-fast ice was found to be relatively smooth and thin (1-1.5 m) and was covered by about a 20-40 cm layer of snow. Further offshore, the inshore mobile pack ice was thin, but was covered by a thinner layer of snow. The inshore pack ice was rafted at places to 4-6 m. Further offshore, the main pack ice was found to be 1.9 m thick on the average, with rafting of 2.5-4 m. The main pack ice was also covered by a thin (0-10 cm) layer of snow. In short, the EM sounding technique was proven to be a reliable observation tool which has the ability to collect large quantities of snow-plus-ice thickness data for validation of remotely sensed satellite data.

RÉSUMÉ

Holladay, J.S. and R. Moucha. 1998. Electromagnetic/Laser Ice Thickness Data from the Labrador Shelf, 1994. Can. Contract. Rep. Hydrogr. Ocean Sci. 49: viii + 340.

Les données de mesure électromagnétique de l'épaisseur de la combinaison neige-glace recueillies durant mars 1994 au large de la côte du sud du Labrador, près de Cartwright, ont été post-traitées et formattées en vue de leur présentation. Les données sur l'épaisseur de la glace incluent les données des cheminements en vol long au-dessus de la glace mobile et des cheminements en vol court au-dessus des divers types de glace identifiés par l'imagerie SAR du satellite ERS-1. Les données sont présentées en format *carte profil* et *tracé standard*. Les *cartes profils* (appendice C) consistent en des données sur l'épaisseur de la glace présentée en format profil surimposé sur une carte du secteur en projection conique conforme de Lambert. Le *tracé standard* contient des histogrammes des mesures de l'épaisseur de la glace et de l'altimètre laser à filtre passe-haut, ainsi que des profils des mesures de l'épaisseur de la glace, de l'altimètre laser et de l'altimètre laser à filtre passe-haut. Tous les *tracés standard* sont montrés à l'appendice F, et chacun d'entre eux correspond à un segment de 4 km du cheminement de vol.

Les observations électromagnétiques montrent que la technique du sondage électromagnétique de la glace permet de distinguer clairement les propriétés de la glace de la banquise côtière et celles du pack mobile. On a trouvé que la glace de la banquise était relativement lisse et mince (de 1 à 1,5 m) et couverte d'une couche de neige de 20 à 40 cm. Plus loin au large, le pack mobile côtier était mince, mais il était recouvert d'une couche de neige plus mince. La glace du pack côtier s'empilait par endroits jusqu'à une hauteur de 4 à 6 m. Encore plus loin au large, le pack principal avait une épaisseur moyenne de 1,9 m, avec des empilages de 2,5 à 4 m. Le pack principal était aussi couvert d'une mince couche de neige (de 0 à 10 cm). En résumé, la technique de sondage électromagnétique s'est avérée un outil d'observation fiable qui permet de recueillir de grandes quantités de données sur l'épaisseur de la combinaison neige-glace aux fins de la validation de données de télédétection obtenues par satellite.

LIST OF FIGURES

LIST OF TABLES

1. INTRODUCTION

The seasonal ice cover over the Newfoundland shelf poses a threat to safe operation of marine shipping, fishing activity and hydrocarbon exploration. Sea ice programs of the Department of Fisheries and Oceans (DFO), funded primarily by the Federal Panel of Energy and Resource Development, are investigating, through field programs and numerical modeling, the seasonal variability of pack ice properties such as southern ice extent, ice drift, ice concentration and ice thickness. One of these programs explores the use of the Electromagnetic (EM) Induction technique for measuring the thickness of pack ice. This report presents the data collected during the 1994 field survey.

The development of practical techniques to remotely measure ice characteristics such as ice and snow thicknesses and ridge depth profiles has been a goal of the Transportation Development Centre (TDC) and the Canadian Coast Guard (CCG) of Fisheries and Oceans, and of the Cold Regions Research and Engineering Laboratory of the US Army Corps of Engineers for many years. The airborne EM Induction technique has provided the most promising results to date. A number of prototype systems have been built, first at Geotech Ltd. of Markham, Ontario, and later at Aerodat Inc., of Mississauga, Ontario (a company which recently went into receivership). Two of the Aerodat prototypes were built between 1988 and 1991 for the U.S. and Canadian Governments, respectively. The Canadian version, called *Ice Probe*, was designed and manufactured as a pre-production prototype sensor under contract to TDC for deployment by CCG helicopters based on icebreakers as an aid to autonomous route selections. The pre-production prototype *Ice Probe* was transferred from TDC to CCG in 1993, and was field tested under an equipment loan to DFO during this program.

The ice thickness sensor, as configured for the DFO 1994 field project off Cartwright located on the southern Labrador coast, comprises an EM Induction sensor and a laser altimeter. The ground-penetrating Impulse Radar which was used during the 1992 St. Anthony, Newfoundland project (Prinsenberg *et al.*, 1996), was not used during this project. The basic EM method has been demonstrated in the Arctic (Kovacs and Holladay, 1989; Kovacs and Holladay, 1990); Prinsenberg *et al.*, 1992:, and off the Canadian East coast (Holladay et al., 1990; Rossiter et al., 1990, Prinsenberg *et al.*, 1993, Holladay., 1995). The system had been operationally tested during the previous spring and had been carried in one of the cargo holds aboard CCG's *Henry Larsen* during the whole of the previous summer.

The results will be presented after the field program, instrumentation and data collection technique are described. The Appendices list the dates when data was acquired (**Appendix A**), ice type summary (**Appendix B**), surface calibration data (**Appendix E**) as well as:

1. *Profile maps* of all survey data. These maps of the surveyed area contain superimposed ice thickness profiles. The maps are in a Lambert Conic Conformal projection (**Appendix C**).

2. *Summary tables* corresponding to the *standard plots*. The tables contain segment and entire survey line statistics such as; survey line length in km, average ice thickness and standard deviation, and sampling rates (**Appendix D**).
3. *Standard plots* of survey data broken up into 4 km segments. These plots contain the ice thickness and high-pass filtered (HPF) laser altimeter histograms along with corresponding profile plots that include the laser altimeter (**Appendix F**).

2. STUDY AREA AND FIELD WORK

2.1 STUDY AREA

The 1994 survey concentrated on land-fast and mobile pack ice east of the Labrador Coast. Here, prevailing westerly to northwesterly winds continually move the mobile pack ice southwards over the continental shelf. Beyond the shelf break, warm water of the Labrador Sea melts ice that is blown offshore. The predominant northwesterly to westerly winds cause an offshore ice-drift component which produces open water and thin ice conditions in coastal areas. In 1994 ice thickness and concentration increased with increasing distance from the shore until the main pack ice was encountered at about 50km offshore. The main pack ice consisted of a very rough consolidated floes made up of thick (1.5+ m) small floes and a few large smooth, thinner floes of uniform thickness (40-55 cm). These large floes were used to calibrate the sensor by flying over marked lines along which ice thickness measurements were made through augered ice holes.

2.2 DAILY FIELD LOG

Sunday, 20 February, 1994

S. Holladay (JSH) and I. Henderson of CCG packed the ice sensor gear at Charlottetown CG hangar for shipment to Goose Bay. The bird had two known problems at this point: the pitch monitor had failed late on Saturday, and the 100 kHz EM channels were subject to very serious drift errors. The latter problem had turned up a day earlier, but had not been corrected due to a lack of test equipment and time. The 2.5 kHz EM was being used instead of the 100 kHz for ice measurement, but failure of the pitch monitor prevented real-time measurements from being obtained.

Monday, 21 February, 1994

CCG truck delivered shipment to Canadian Air Cargo at Halifax. Shipment was pre-arranged, guaranteed for delivery on 22 February.

Thursday, 24 February, 1994

J. Lee (JL) and (JSH) departed Toronto for Goose Bay at 0650 EST (one day ahead of schedule, to allow extra time for bird repair). On arrival in Goose Bay, found all equipment already arrived at Canadian Air Cargo except the bird.

Friday, 25 February, 1994

JL and JSH arrived at Universal Hangar at 0815 local (Atlantic time). Gear was delivered by Canadian at about 1000, unpacked and ready for work on bird before 1200. Pitch problem was sorted out by approx. 1500: a broken wire (fatigued by vibration during the previous year's Arctic travels aboard the CCG's *Henry Larsen*). Checked out 100 kHz transmitter, receiver preamplifier, wiring, then tested for 100 kHz drift problem observed in Charlottetown: not measurable at this time. Decided to execute further tests on morning of 26 February.

Saturday, 26 February, 1994

Began by trying to identify the source of the 100 kHz drift. (Simultaneously, installation into the helicopter was substantially completed.) The 2.5 kHz transmitter was also checked out and one of the tuning capacitors replaced. Further testing indicated that this portion of the system was working nominally. Silicone compound was applied to all connectors to fix them in place. Finally, the bird was partially assembled and taken outside to test in a quieter environment. It was left running for about one hour. After this, the drift appeared to be normal, although a flight test was required to confirm fully normal operation. Finally, the new drag assembly was fitted to the bird. Rebalancing of the modified bird was scheduled for the morning.

Sunday, 27 February, 1994

Bird balancing was completed in the afternoon. The rest of the helicopter installation was also completed. In the afternoon, the first test flight was undertaken. The pitch, laser and EM sensors all worked properly, although the drift in the 100 kHz was not optimal (perhaps due to the short period of temperature equalization). The GPS did not operate properly due to an undocumented incompatibility between the Apollo 891 in QNS and the Trimble T2000 GPS receiver that had been used during the St. Anthony work. This was corrected in the late afternoon, for testing on Monday. Simon Prinsenberg (SP) and George Fowler (GF) arrived in the early afternoon from Cartwright. The plan for Monday, agreed to jointly, was to test fly the system after a proper temperature equalization, checking before the flight for proper GPS operation. A run over the salt water in Lake Melville was planned. Mobilization to Cartwright was scheduled to take place on Tuesday morning, with some EM (calibration) flying in the afternoon. All personal gear was to be shipped via LabAir to avoid overloading the helicopter.

Monday, 28 February, 1994

The weather started off poorly, and got rapidly worse. The principal factor was the wind, which started at about 10 knots and rose rapidly, with gusts to 50 knots. Blowing snow was therefore a serious problem. There was a fair bit of precipitation as well. High temperatures were roughly -10°C. There was no chance to test fly the system, as planned, nor was there a chance to mobilize to Cartwright. We therefore took the opportunity to:

1. Correct the GPS interface routine, which was still set up for the Trimble T2000.

2. Further investigate the drift in the 100 kHz channels. Outside drift testing indicated that significant drift was still present in the 100 kHz, although the 2.5 kHz was excellent.

3. Pack appropriate equipment for Cartwright. This was a problem, given the limited space in helicopters. Eventually, it was decided to send James Lee on the LabAir Twin Otter with all of the "extra" gear as excess baggage.

Tuesday, 1 March, 1994

Weather cold with snow. The forecast called for general clearing later in the day, so preparations continued to mobilize to Cartwright with both helicopters. JL left via Twin Otter at 0740, and the rest of the group moved to the Canadian (MM, SP, MS) and Universal (JSH, Carolyn Stewart (CS)) hangars. The gear was loaded FNYQ and QNS took off for Cartwright at about 1400. On the way into Cartwright (over Sandwich Tickle) a low-level run was made for calibration purposes. After unloading FNYQ, SP set out a calibration line north of Cartwright, 250m long with marker bags every 25m where ice thickness were obtained through augered ice holes.

Wednesday, 2 March, 1994

Weather clear and cold. JL went to airport to start transmitter warm-up. This failed. As it turned out, the bird computer had a failure in the board's battery-backed RAM disk which stored the boot information and bird program: The rest of the day was spent installing a replacement and getting the 2.5 kHz working properly again. Requested parts from Toronto to be sent with next shipment. By 2130, 2.5 kHz was working. Left computer running overnight to keep it warm.

Thursday, 3 March, 1994

Flew first test flight MAR03F1-3. No video was recorded during this flight. NAV failed during acquisition of the first two of these files, but was good for third. MAR03F1 included multiple passes over test line, attempting real-time ground truth calibration, which was not very successful. This may have been due to variations in ice thickness near the line or at the ends. MAR03F2 showed similar effects. It was concluded that the ice thickness in the vicinity of the test line was not uniform enough to be used for real-time recalibration (a better choice would be open water or very thin ice.) MAR03F3 used the previously-determined ground truth calibration factors (set up in PEI, in 1993) and yielded the most reasonable results: about 0.9 ± .1 m. After this pass over the check line, a second profile was run along the ice toward Cartwright, ending

just after the "tickle" (section of open water maintained by currents) between Huntingdon Island and the mainland.

A second flight, recorded in files MAR03F5-14, was performed in the afternoon. Most of these files failed at startup due to failure of the GPS data feed. This was a long flight, running out to the northeast, with significant air time near a floe site established by SP. Approximately eight passes were made in an E-W direction over the vicinity of the floe, including two directly over the floe site. After this, a long traverse was made back to the north of Huntingdon Island. In several instances, the GPS data feed to the acquisition system was interrupted, and it was necessary to restart the program to restore communications. Despite these difficulties, a good data set was gathered (see **Table 2.1**)

The first ERS-1 overflight occurred near midnight.

Friday, March 4, 1994

An early-morning departure was scheduled to coincide as nearly as possible with the ERS-1 overflight of the previous evening. As some selective navigation regarding ice types was required, CS flew as navigator, JSH operated. The objective of this flight was to profile the ice near South Wolf Island, and to fly over a ground-truth site (to be established concurrently) if possible. During the outbound leg, repeated dropouts in the GPS RS-232 interface were encountered: at the time, it was not clear whether this was a purely software-related error, or whether some type of hardware transmission error was leading to partial failure of the navigation interface software module.

In the afternoon, another flight was attempted, but snow reached the airport before the refueling operation at the fuel dump was completed. As this was expected to be a severe storm, the rest of the day was spent on data organization.

Saturday, March 5, 1994

The severe storm forecast on Friday was well underway on Saturday morning. The main effort therefore concentrated on plotting data for preliminary analysis. This was accomplished by early evening, and the process had been streamlined to the point where new flights would be very quick to process. The main factor slowing down the plotting was the shift to a new GPS receiver, and some strange behaviour observed with the GPS feed from this receiver: sorting this out required a significant amount of effort (which was not entirely successful by this point). By the end of the day, profile and colour bar charts of ice thickness had been prepared for the long traverse and the profiles near the floe site of March 3, as well as the profiles near South Wolf Island on March 4.

The snow had stopped by 1900, although the wind remained strong, and the forecast was for cold, clear weather on Sunday. Therefore, plans were made for further flying on Sunday morning. It was recognized, however, that difficulties would be encountered in getting out to the airport, since the road had not been plowed.

Sunday, March 6, 1994

As expected, the road was not plowed. Therefore, NYQ was used to ferry Gerry Nuttall (QNS pilot) and JL to airport. They returned to the hotel with the bird, and preparations began immediately for a survey flight. This first flight was executed flying to the south along the coast. The system returned to Cartwright without serious difficulties.

Once on the ground, transferred the data files to the post-processing computer. Map making began immediately, and the first map (from outer Table Bay to Point A) was printed in the early afternoon. The next was started immediately and printed by about 1440. The next flight was started immediately, using the morning's maps to aid in mission planning. This flight was mainly directed toward filling in the gap in the morning's coverage of the ERS-1 swath near South Wolf Island, and included some extra flying over ice thicknesses near this island. The return journey covered a variety of thick, heavily rafted ice, with occasional patches of thinner, less rafted ice left over from before the storm of Saturday. Almost all of the data obtained were contained in MAR06F13.

The second flight was processed immediately upon return to Cartwright. Colour bar and profile maps were provided to SP for planning purposes. The ERS-1 overflight was scheduled for later that night, so no comparison with SAR imagery was possible.

Monday, March 7, 1994

To test the hypothesis that the problems with navigation were caused by some kind of delay in real-time data processing or related activities, the CMOS setup of the main helicopter CPU was checked and set to the "high speed" mode. This did not eliminate the problem. The Transmitter coprocessor board was then swapped with the spare unit. The problem did not recur immediately, so a flight was initiated. While the problem did recur during this flight, it was not severe and the entire flight was stored in one data file. This flight, MAR07F1, ran well to the south, most of it within the ERS-1 swath. It reached the approximate location of SP's surface measurement site for the morning, then returned by a different route, including runs over Porcupine Bay, Ragged Rock Bay and Table Bay. It was discovered during this flight that the video recorder was no longer functional in a recording mode, although it was still capable of processing the incoming S-VHS signal and converting it to a composite signal for the monitor. It could also play back previously recorded tapes, so the playback circuits and mechanism were intact.

These data were processed immediately, and the morning's map was faxed to H. McRuer at about 1430. The afternoon's flying was delayed to take advantage of the ERS-1 images that were being downloaded by Mike Manore, but eventually had to take off without them.

This flight, stored originally as MAR07F1 and later renamed to MAR07F2, ran out over the southern side of Table Bay, through Indian Tickle and between Island of Ponds and Spotted Island, and out to Roundhill Island. It then turned due north, crossing through relatively loosely packed ice into very dense, heavily rubbled ice that appeared to continue for 10 km or more to the north and east. Well into this heavy pack, it turned roughly west and continued past Grady Island, crossing over the site of the sea-bottom profiler and a nearby iceberg (approximately 10 m freeboard, as measured with the bird's laser altimeter). The profile passed over several shears in the pack ice, at one of which considerable extension was exhibited by numerous leads parallel to the shear. It eventually passed onto more uniform ice south of Huntingdon Island. As has happened on some earlier flights, the analog record display of ice thickness was not printed.

This flight was processed in the early evening, and the resulting map provided to SP. Comparison to the newly downloaded ERS-1 images indicated excellent coverage of important contrasts and image areas during the two flights.

In the evening, the second flight was processed and provided to SP. JL also provided his new histogram extraction routine for assessment. This routine, run in a manner similar to GEOSTRIP, scans a data file and constructs a .CSV input file for Excel plotting. After some initial work, a number of minor required changes were found. A final task for the evening was to combine the two flights and plot a combined bar map.

Tuesday, 8 March, 1994

Weather started at -10°C, light wind from south, light cirrus clouds moving in. Forecast was for snow in afternoon, clear Wednesday. Started transmitters up as usual before 0800, took off for reconnaissance flight to north of Gannet Islands. Despite repeated attempts, could not operate in full data acquisition mode: on initiating the first drift correction, the GPS data feed would drop out. Tried a variety of different initial conditions, but never got system working while flying at this time. After landing at the airport, a number of attempts were made to resume operation, all unsuccessful. The weather closed in during the early afternoon, precluding further flying. During the afternoon, several more possible mechanisms for the interference were discussed, and JL went to the airport to try out some possible solutions.

Later in the evening, JL and JSH returned to the airport to try one more solution. It appeared that the helicopter computer's serial port attached to the Nav unit had been switched from 4800 baud to 9600 baud, while the port's buffers had not been changed. Increasing the buffer size would prevent saturation. To test this, the buffers were doubled in size. After this change was made, no failures in Nav data feed were observed during the rest of the survey work.

Wednesday, 9 March, 1994

A final flight was executed in the afternoon, after a snowy morning. This flight consisted of a run to Grady Island, then northeast to a point approximately 20 nm offshore, returning via the Gannet Islands and Cartwright. The flight went very smoothly, with no difficulties being experienced with any part of the equipment. Evidently, the correction to the serial buffer corrected the navigation problem. Some rough winds were experienced near the Gannets and other islands on the approach to Cartwright, but were not severe offshore.

After refueling, QNS returned to the airport, where JSH traded places with JL. JL and GN then attempted to reach Goose Bay, but could not make sufficient headway against the westerly winds which came up in the afternoon. JSH traveled to Goose Bay in the afternoon via LabAir, as did CS, taking all of the gear that would not fit into the helicopters for their return trip.

Thursday, 10 March, 1994

CS returned to Ottawa on the early morning flight. JSH and JL, assisted by MM and MS, packed the *Ice Probe* equipment for shipment back to Toronto via truck and returned to Toronto via the 1440 flight. Universal Helicopters was to handle the shipment of the equipment.

Friday, 11 March, 1994

JSH plotted up the final flight of 9 March, verifying that acquisition was fully successful.

2.3 FLIGHT SUMMARY

A flight summary for the entire research project can be found in **Table** 2.1. A detailed line by line flight summary can be found in **Appendix A**.

Date	File ID`s	Survey Route	Comments
3/3/94	MAR03F1-3	Marked line near Cartwright	Calibration check
	MAR03F4-14	Cartwright-Wolf-Table Bay-Cartwright-Iceberg	Some nav. problems, excellent results
4/3/94	MAR04F1-8	Cartwright-Wolf, vicinity-return to Cartwright	Some nav. problems, excellent results
	MAR04F9-12	Cartwright-Wolf, vicinity-return to Cartwright	Some nav. problems, excellent results
6/3/94	MAR06F1-9	Cartwright-Table Bay-Point A-SW to land-Black Tickle-Ragged Rock Bay-Stony Arm-return to Cartwright	Some nav. problems, excellent results
	MAR06F10-14	Cartwright-halfway to point A-Wolf-Grady-Cartwright	Some nav. problems, excellent results
7/3/94	MAR07F1	Cartwright-Table Bay-Ferret-Roundhill-South along 212° mag-North along 32° mag, Table Bay-Cartwright	Some nav. problems, excellent results
	MAR07F2	Ledge Is-S. of Indian Head Is and Spotted Is.-Roundhill Is.-north, then northwest to Grady Is-Cartwright.	Some nav. problems, excellent results (nav. problem corrected Mar 08)
9/3/94	MAR09F1	Cartwright-Grady-Offshore-Gannets-Cartwright	100% successful

Table 2.1: Flight Summary for 1994 Labrador Shelf Ice Measurement Work

3. INSTRUMENTATION

3.1 SENSORS IN THE BIRD

The EM induction sensor package is towed in a bird about 30 m beneath the helicopter between 15 to 30 m above the ice surface. Low frequency EM signals are transmitted by the antenna in the sensor bird and excite eddy currents in the sea water beneath the ice. These currents in turn generate secondary EM fields which are measured by the receiver, which is also mounted in the bird. The distance of the bird to the water/ice interface can be determined by measuring the amplitude and phase of the secondary field relative to the transmitted field.

The frequencies and antenna configurations available in the pre-production prototype *Ice Probe* system are 2.5 kHz in the coaxial mode and 100 kHz in the horizontal coplanar mode. During this project, the 2.5 kHz coaxial configuration was used. The transmitter and receiver antennas are separated by 3.0 m. The overall length of the bird is just under 4.0 m and its weight is about 125 kg. The bird is slung from the helicopter's cargo hook on a 30-meter tow cable which carries power and digital control signals down to the bird and digital data up to the helicopter.

An Optech G150 laser profilometer mounted in the sensor bird was used to measure the distance from the bird to the snow/air interface. Its footprint has a radius of less than .05 m when flying the sensor at an altitude of 15 to 20 m. In contrast, the radius of the EM sensor's footprint is much larger. It is comparable in size to the height of the sensor above the ice surface. A radar altimeter operating at about 2 GHz was mounted in the helicopter to assist the pilot in maintaining a steady survey attitude.

3.2 HELICOPTER INSTRUMENTATION

The *Ice Probe* system console was mounted on a rack in the back seat area of the helicopter in such a way that an operator could use the master computer/data logger and see the power distribution unit while viewing the annotated imagery from the video flight path monitoring camera on the CRT. A Panasonic AG-7400 S-VHS video recorder made an analog recording of this imagery for later use in assessing ice conditions below the helicopter. The camera was mounted in front of the forward passenger's seat, pointing downwards through the "chin bubble" of the helicopter, and observed the ice conditions and bird flight behavior.

The master computer controlled the entire system. It collated, reduced and logged EM and other incoming data onto magnetic media. It also controlled an auxiliary processor which inverted the data to ice thicknesses and other parameters, plotted the data on the graphic recorder, and generated a text overlay on the video flight path imagery including time, position and ice parameters. The helicopter was equipped with an Apollo GPS navigation unit. Data from this instrument were also logged on the EM computer and displayed on the CRT.

3.3 OTHER INSTRUMENTATION

Calibration and remotely sensed data were collected during the project to assess whether the *Ice Probe* sensor would be a good sampling technique to validate data collected either by fixed-wing aircraft (SLAR) or by satellite (SAR). To compare different data sets from different times, ice motion measurements in the region were collected by satellite tracked ice beacons to realign the data sets covered by the various observation techniques. Eleven ice beacons tracked by ARGOS satellite were deployed to monitor the pack ice motion. The locations of the beacons were monitored every 3 hours by the NOAA satellites as they passed overhead. The beacons were designed and built by MetOcean Ltd. of Dartmouth, N.S. and were deployed early in the project. Due to the uncertainty in the ARGOS location fix of 0.2 km, comparison of data sets were limited to large scale ice features.

SLAR and SAR data from the region were collected by the Canadian Ice Centre's surveillance aircraft and by the ERS-1 satellite. The SLAR data was collected by a Dash-7 equipped with a real aperture, side-looking airborne X-Band radar made by CAL Corporation. It collects data on both sides of the airplane covering a 100 km wide strip when data is acquired on a 1:1 million scale. More detail can be obtained by going to half or one-quarter of this scale but then the area covered reduces respectively to 50 and 25 km wide strips. The SLAR or SAR have the ability to map the surface in all weather conditions, and can identify ice morphologies (*i.e.* patchy ice *vs.* pack ice), ice edge locations and ice concentrations. Alongside the SLAR, the airborne imaging microwave radiometer (AIMR) measures the brightness temperature of the ice surface, which varies as a function of the ice morphology, snow cover and surface wetness. It complements the SLAR data by being able to discriminate most ice morphologies and deduce ice edge locations and ice concentrations.

The Earth Resources Satellite (ERS-1) uses a 5.3 GHz frequency C-band SAR to collect ice data from a polar orbit with a 3-day repeat cycle. In the image mode, the SAR obtains strips of high-resolution imagery, 100 m wide to the right of the satellite track. Imagery is built up from the time delay and strength of the returning radar beam which depends on roughness and dielectric properties of the reflecting surface. The resolution (pixel size) is 12.5 m. Comparison of the SAR (ERS-1) and SLAR data with the *Ice Probe* data are being published in a special J.G.R. issue covering ERS-1 data (Peterson *et al.* 1998).

4. AIRBORNE COLLECTION AND ANALYSIS

4.1 AIRBORNE DATA COLLECTION

Weather conditions during March 1994 were moderate. It was mostly clear with light winds and cold with an average temperature of -15 °C (**Table 4.1**). Long-range data collection missions over land-fast and pack ice were undertaken during which large quantities of airborne and surface (discussed in section **4.2**) ice thickness data were collected. A total of 801 km of EM data was collected, 399 km over land-fast ice and 402 km over pack ice (**Table 4.2**). In addition, a series of shorter validation flights were performed over land-fast and pack ice calibration sites (**Table 4.3**). A detailed summary of EM data collected for each date, flight and lined number can be found in **Appendix B**. A coastal map of the area surveyed with superimposed survey line flight paths can be seen in **Figure 4.1**. More detailed to scale coastal maps of the areas surveyed for each flight with superimposed survey line flight paths can be seen in **Figure 4.2 - Figure 4.12**.

Date	Temperature (°C)	Sky/Precipitation	Wind
2/3/94	-20	clear	light NW
3/3/94	-10	clear	light NW
4/3/94	-17	clear/overcast	light S
5/3/94	-12	blizzard	N/ NE
6/3/94	-25	clear	light NW
7/3/94	-18	clear	light NW
8/3/94	-9	overcast	light SE
9/3/94	-9	snowing	light NE

Table 4.1: Weather conditions summary.

Date	Land-fast ice (km)	Pack ice (km)
3/3/94	27.120	88.612
6/3/94	111.432	96.863
7/3/94	228.034	145.393
9/3/94	32.887	70.711
Total	399.473	401.579

Table 4.2: EM data sets for the land-fast and pack ice traverses.

Date	Flight	Line #	Ice Type	Date	Flight	Line #	Ice Type
3-Mar-94	3	10021	land-fast	3-Mar-94	14	10080	land-fast
		10022	land-fast			10090	land-fast
	11	10021	pack			10100	land-fast
		10022	pack			10111	land-fast
	12	10010	pack			10112	land-fast
		10020	pack			10113	land-fast
		10030	pack			10121	land-fast
		10040	pack			10122	land-fast
		10050	pack			10131	land-fast
		10061	pack			10132	land-fast
		10062	pack				
		10063	pack				
		10070	pack				
		10081	pack				
		10082	pack				

Table 4.3: Validation flight summary over land-fast and pack ice calibration sites.

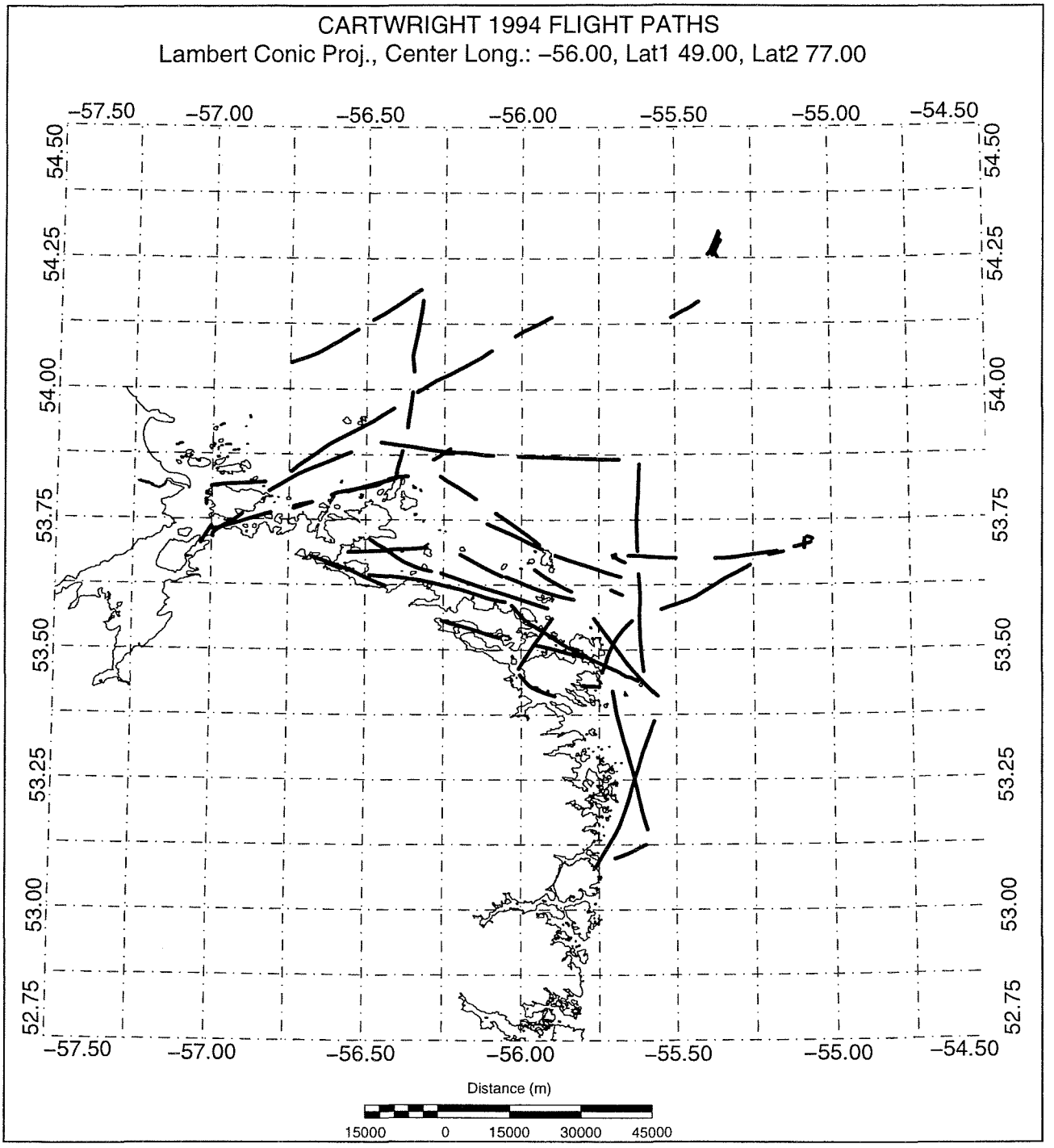

Figure 4.1: Cartwright coastal map with superimposed survey lines flight paths.

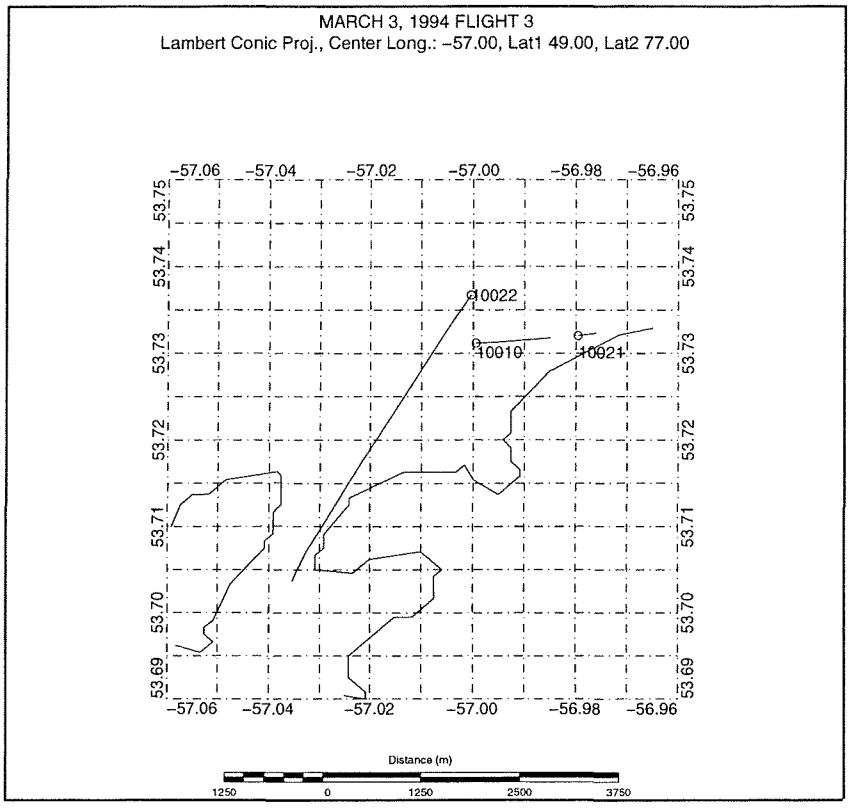

Figure 4.2: March 3, 1994 survey line flight paths, Flight # 3.

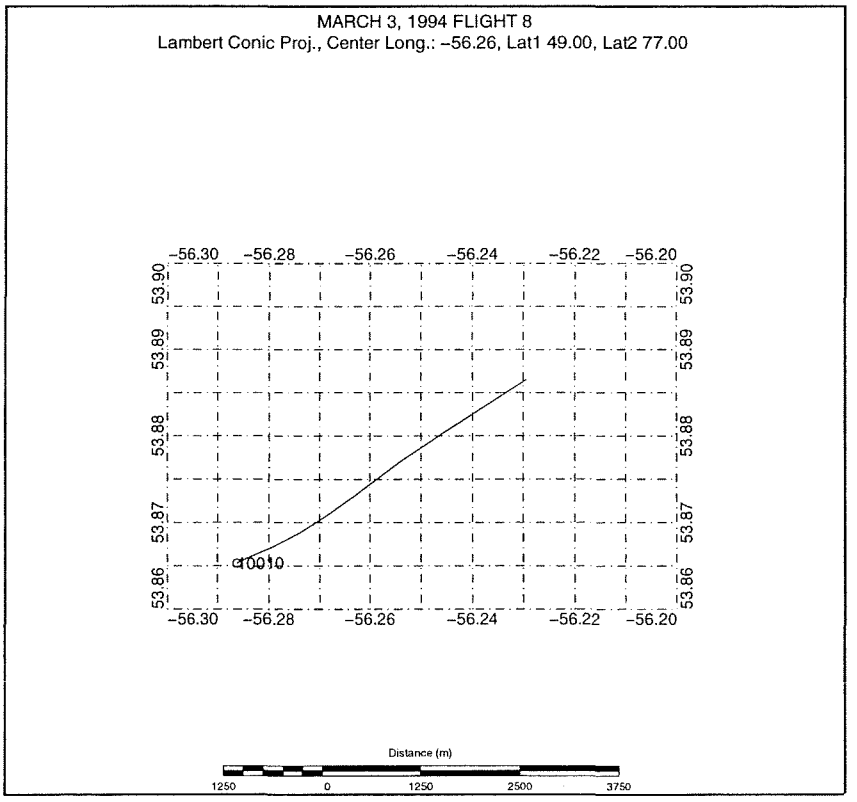

Figure 4.3: March 3, 1994 survey line flight paths, Flight # 8.

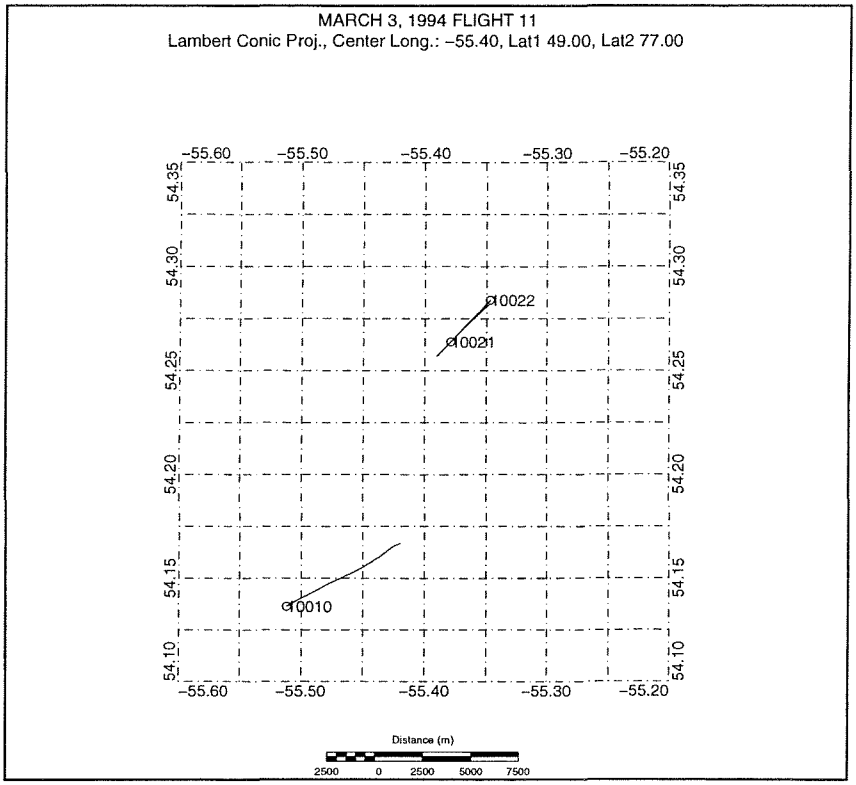

Figure 4.4: March 3, 1994 survey line flight path, Flight # 11 (pack ice calibration site).

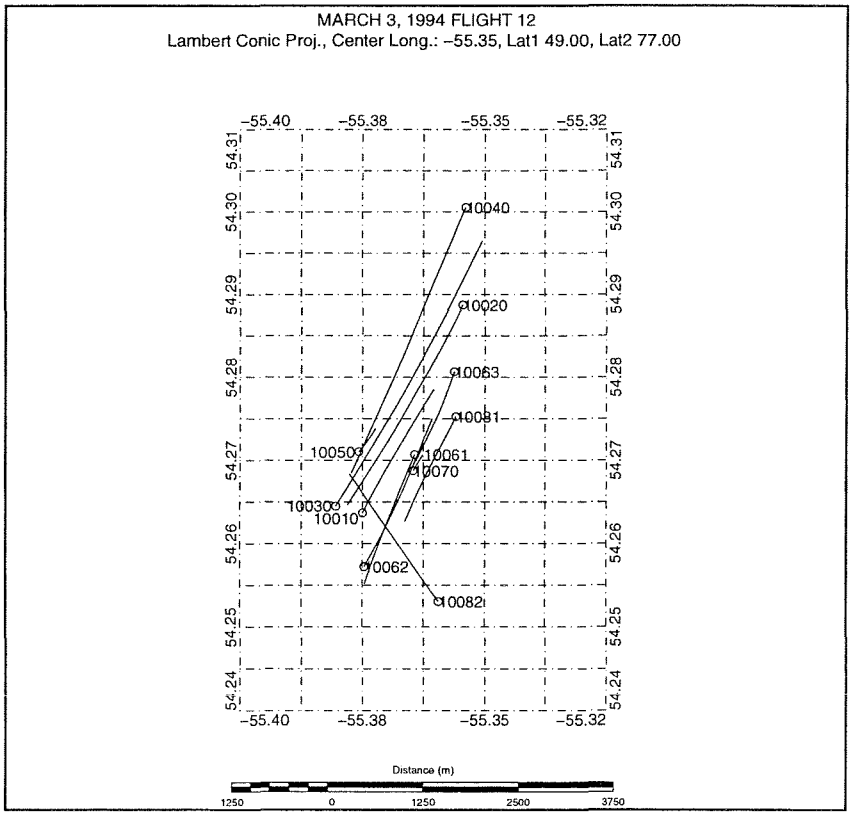

Figure 4.5: March 3, 1994 survey line flight path, Flight # 12 (pack ice calibration site).

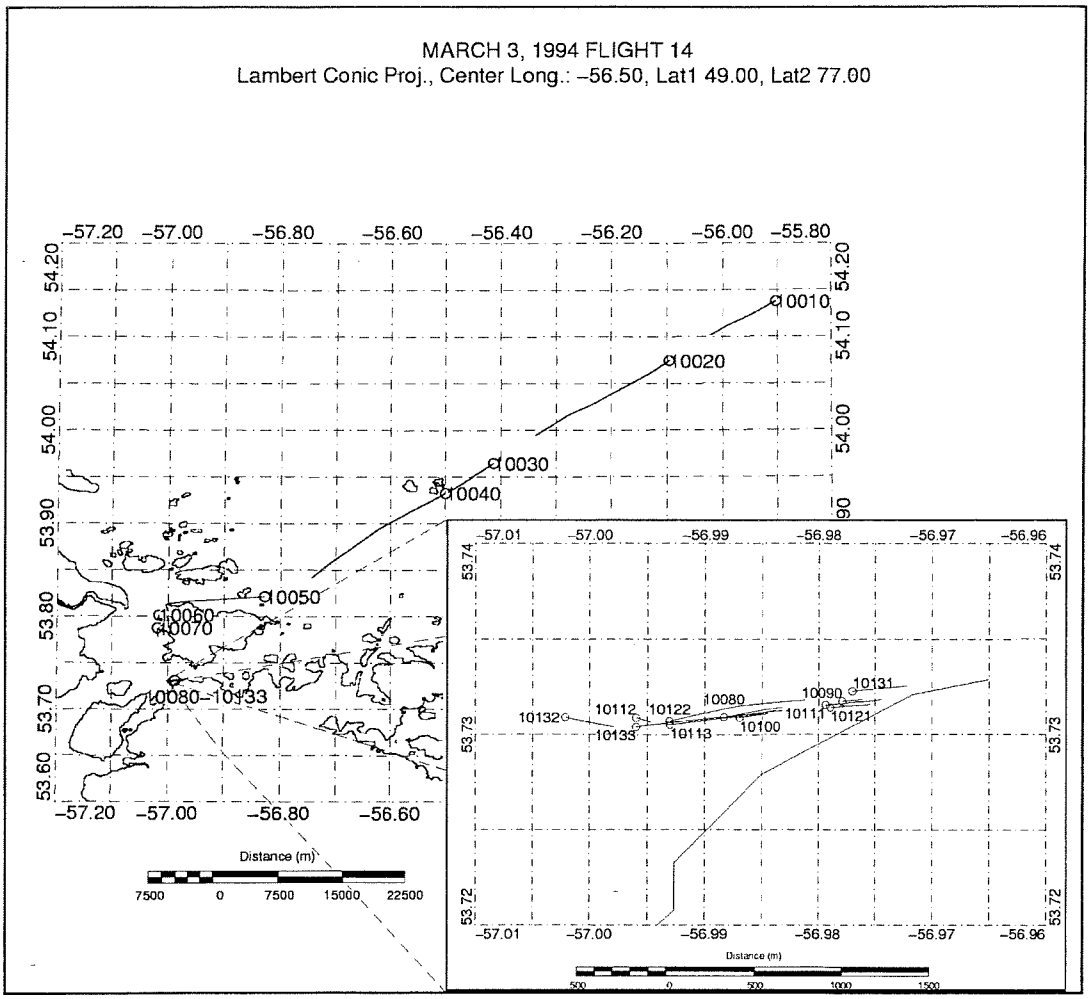

Figure 4.6: March 3, 1994 survey line flight path, Flight # 14 (land-fast calibration site).

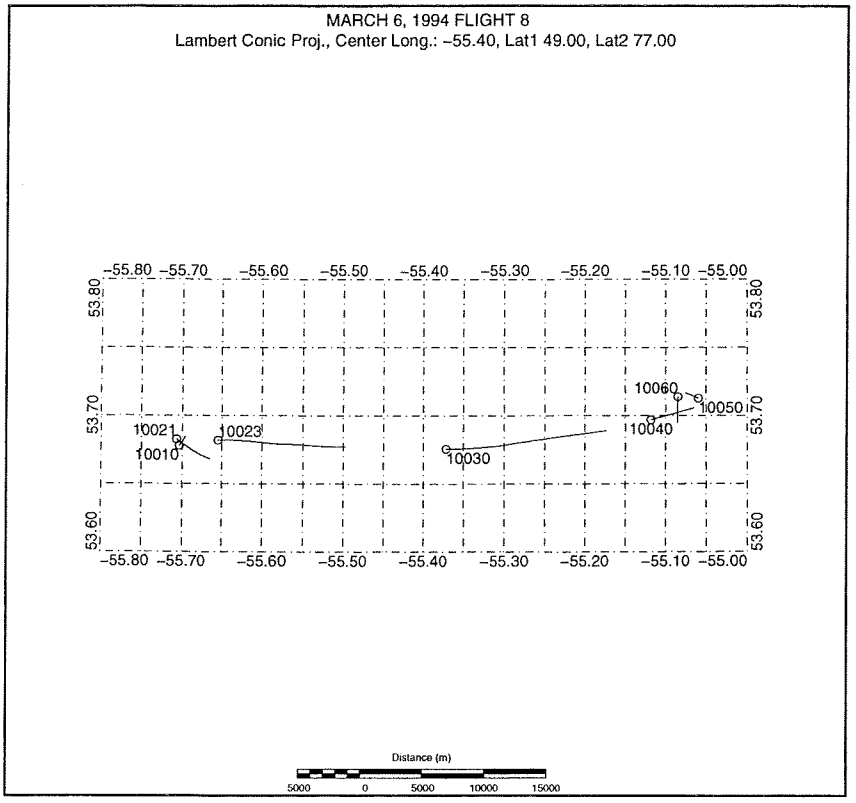

Figure 4.7: March 6, 1994 survey line flight path, Flight # 8.

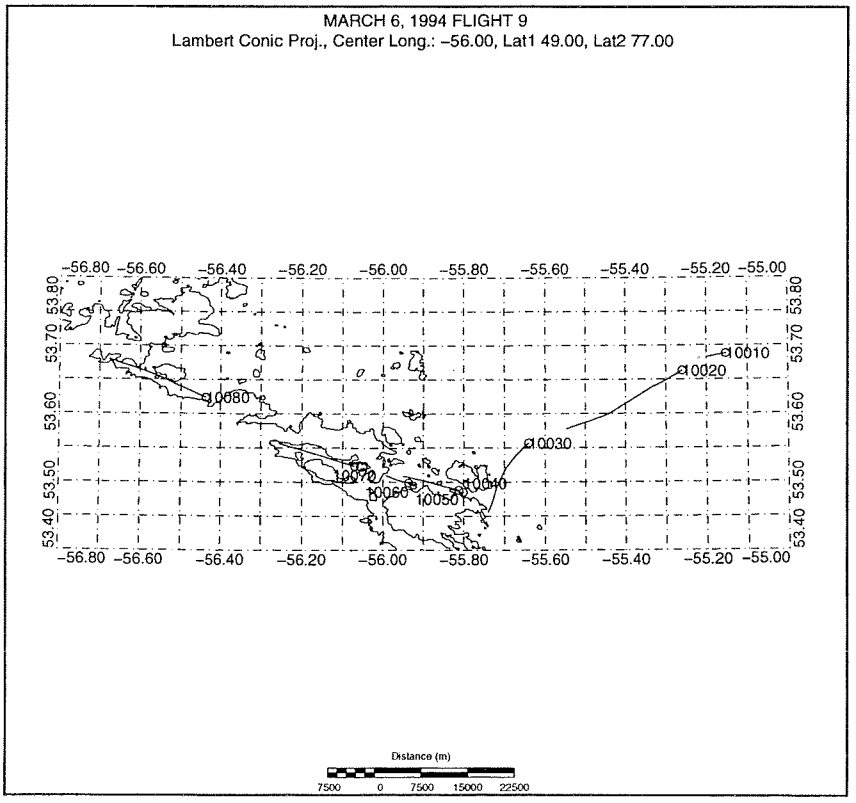

Figure 4.8: March 6, 1994 survey line flight path, Flight # 9.

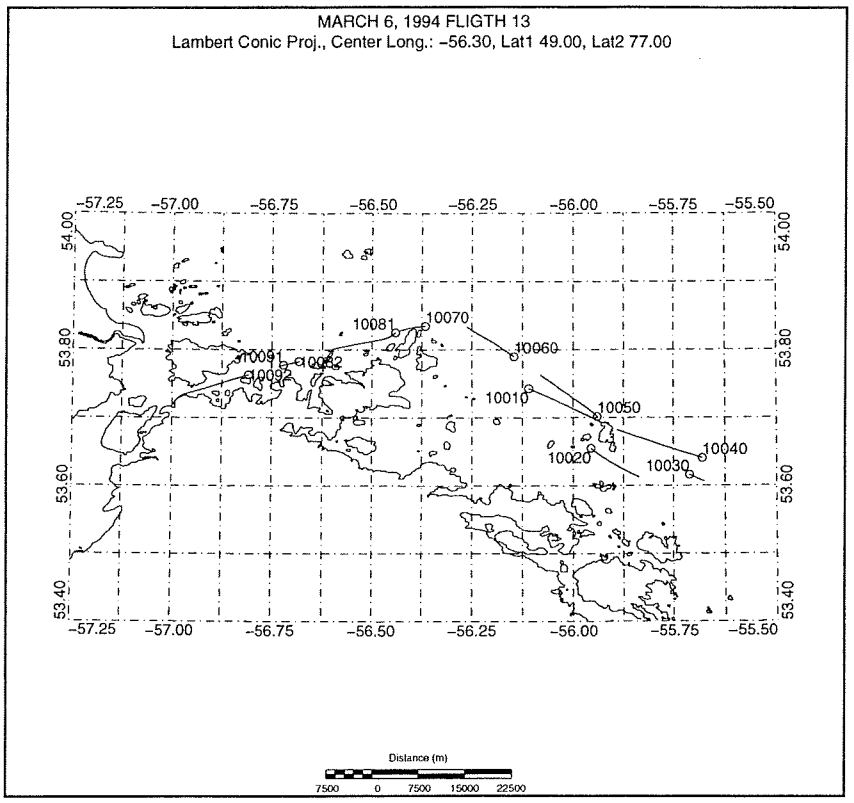

Figure 4.9: March 6, 1994 survey line flight path, Flight # 13.

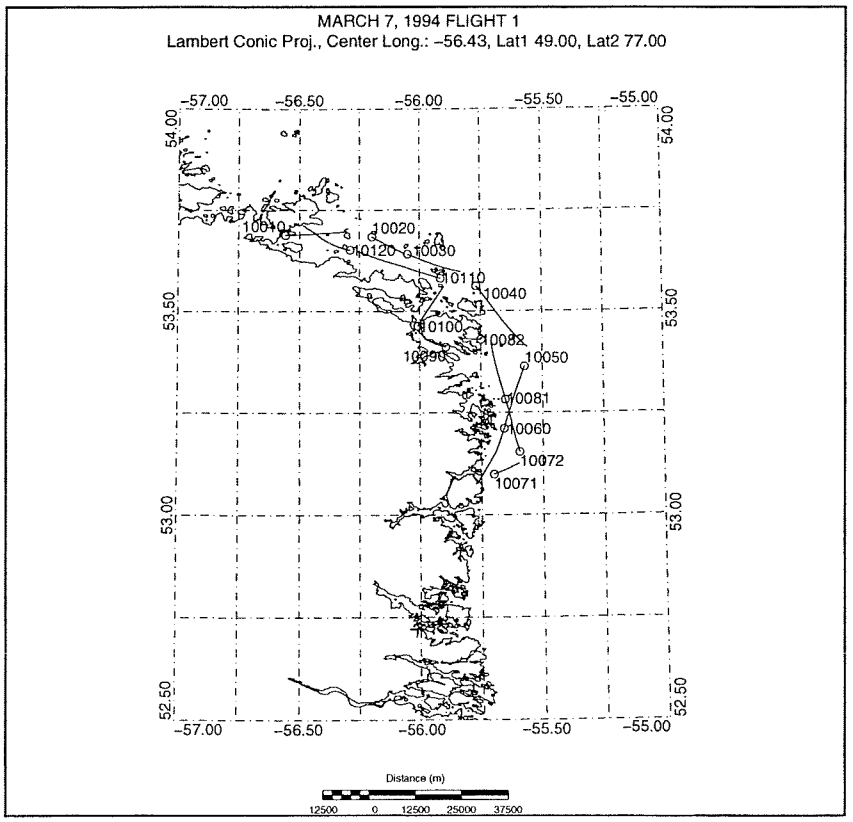

Figure 4.10: March 7, 1994 survey line flight path, Flight # 1.

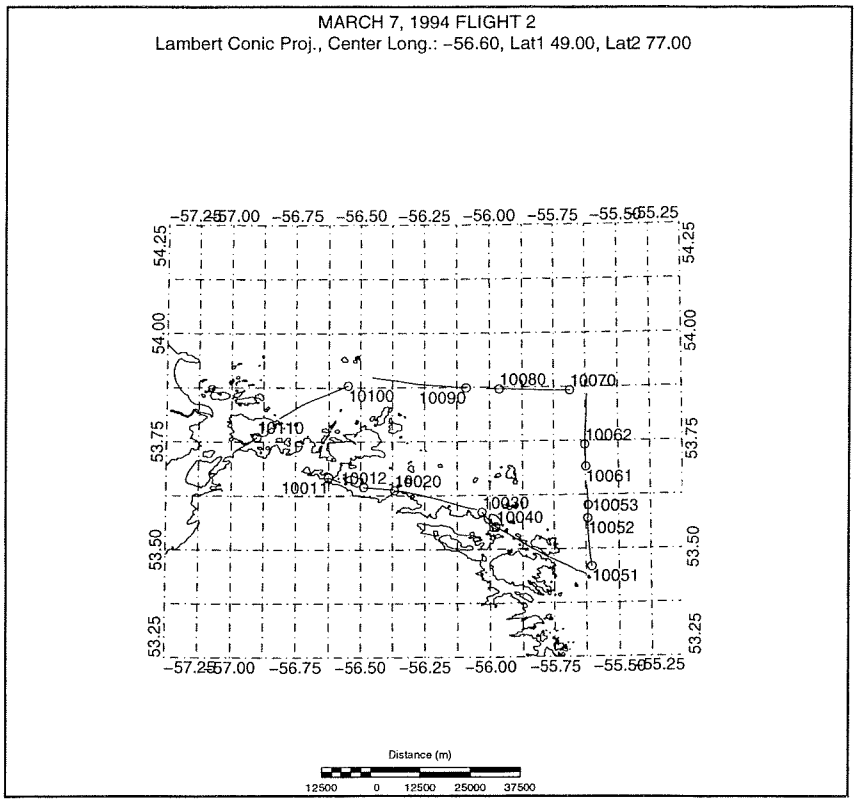

Figure 4.11: March 7, 1994 survey line flight path, Flight # 2.

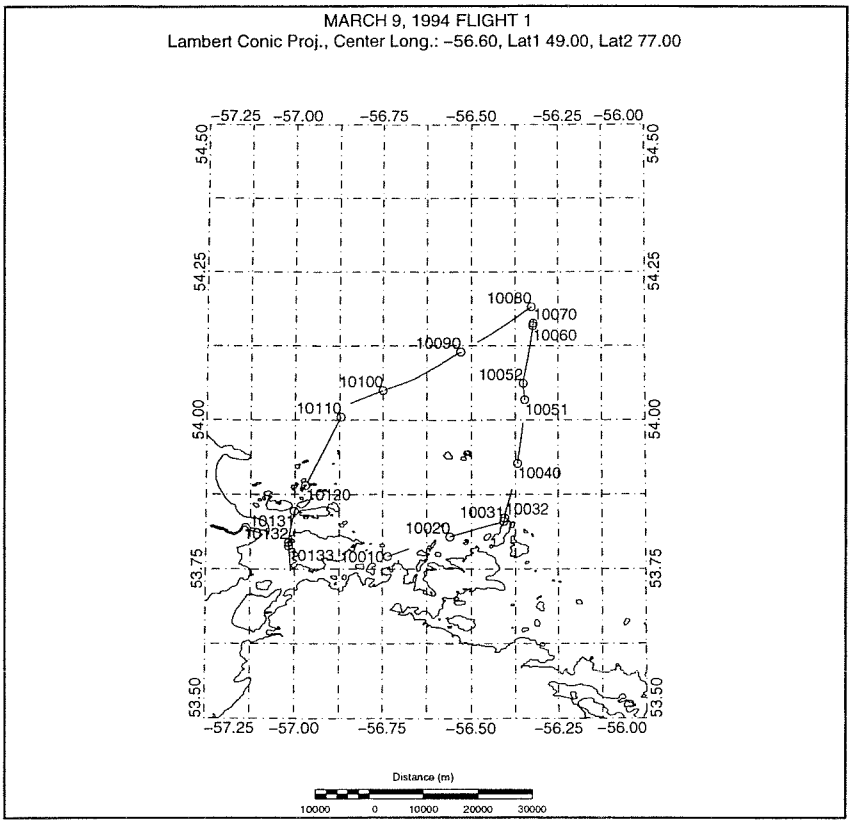

Figure 4.12: March 9, 1994 survey line flight path, Flight # 1.

4.2 SURFACE DATA

A second helicopter (FNYQ) was used to collect the surface calibration data, to mark the surveyed points with snow-filled garbage bags and to deploy satellite-tracked ice beacons. Ice thickness data was collected through hand-augured ice holes and snow depths with a metric snow staff. At selected locations ice chip samples from various depths of the ice sheet were collected to determine salinity content of the ice to verify the bulk ice salinity estimates obtained by the EM sensor and used in calculations of the speed of the electromagnetic signal in ice. Snow samples were also collected for salinity determinations after it was discovered that the thin snow layer on some pack ice floes had high salinity contents. It was thought possible that this might interfere with the radar and EM return signals although the real time processing for the EM did not encounter any problems. The ice and snow calibration and salinity data are listed in **Appendix E**.

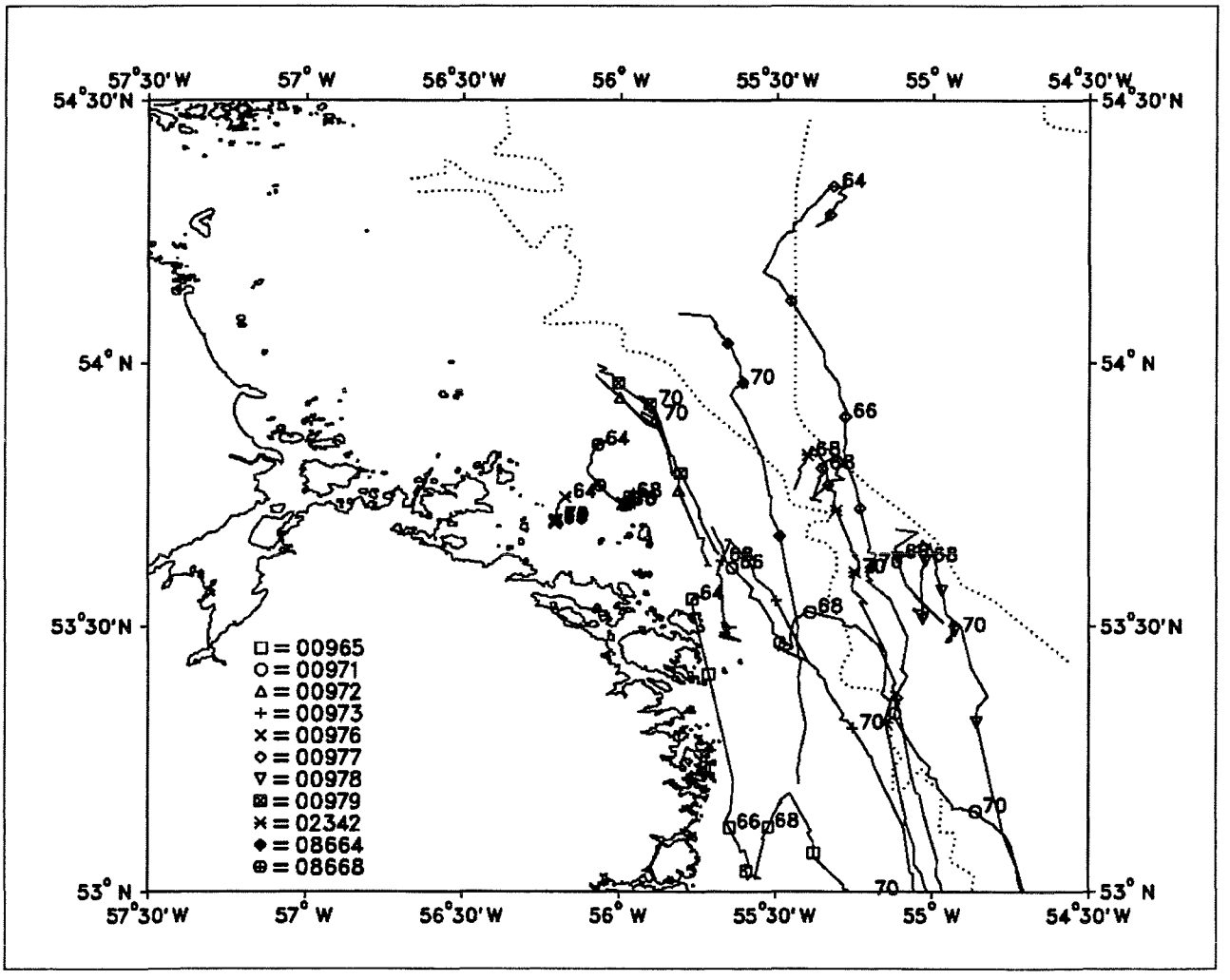

Figure 4.13: Trajectories of eleven beacons used to realign ice property data sets collected at different times. Numbers along the tracks refer to beacon locations in Julian days.

Eleven satellite tracked ice beacons were deployed by helicopters. This data can be found in Peterson *et al.*, 1995. The floes they were deployed on mainly consisted of undeformed flat ice that ranged in thickness of 0.5 m to 1.5 m. Most of the pack ice however consisted of deformed thicker ice with rafts of 2.5 to 4.0 m thick. The beacon trajectories (**Figure 4.13**) show that the offshore pack ice drifted onshore on March 5 (day 65) before drifting Southward parallel to the coastline. The two beacons on the near-shore ice #976 and #8668 remained stationary until past March 10 (day 70) as the ice they were on was constrained to the southeast by islands.

4.3 DATA ANALYSIS

4.3.1 Real time processing

The snow-plus-ice thickness is measured by first estimating the bird-to-water distance, then subtracting the bird-snow distance measured with the laser altimeter. Determining the distance of the bird to the water/ice interface is a complex inverse calculation and is performed on a secondary computer within the helicopter computer package. The amplitude and phase of the secondary signal depend not only on the bird's altitude above the ice surface, but also on the operating frequency, the ice conductivity and the sea water conductivity. The response can be numerically estimated in a precise and efficient manner for horizontally-layered ice and water layers of known thicknesses and conductivity (1D models), while approximations to the complex ice features (ridges) are more difficult and time-consuming to model. Using such models, the measured EM signals can be inverted to yield estimates of distances from the bird to the sea water surface on a point-by-point basis (1D model) or as a profile or grid data (2D and 3D models). The 1D inversion technique was used for the real-time data display during the 1992 St. Anthony survey and provided excellent accuracy over the relatively smooth ice conditions found at the calibration test sites. Full-scale inverse 2D or 3D modeling was not practical for the real-time data collection at this time. 2D ice structures were being interpreted using look-up tables similar to those constructed by Liu and Becker (1990) and successfully used on the 1991 Beaufort Sea data (Prinsenberg et al., 1992). Work was underway at this time to develop 2D and 3D ridge keel modeling.

4.3.2 Post-processing

Post-processing involves the extraction of data from binary files to XYZ format (geolocated, columnar ASCII files), smoothing and resampling of GPS data, high-pass filtering of the laser altimeter, and manual editing of data. Data extraction from binary to XYZ files introduces repetition of GPS values since the GPS data are sampled at .5 to 1 Hz whereas the EM data are sampled at 10 Hz. Though the GPS data are quite stable, GPS spikes do appear. Software was therefore developed to process the GPS data stream, specifically to despike, filter and resample it to match the sample rate for the ice thickness, conductivity and other data series derived from the EM data.

GPS filtering involves two procedures. The first procedure prepares the GPS data series (latitudes and longitudes) by removing anomalies (significant gaps and/or spikes in data) and adding synthesised or "contrived" data to minimise edge effects associated with filtering. The procedure also keeps track of where these anomalies occur to keep the user up to date. The second procedure utilises the information gathered by the first procedure to filter the GPS data series, using a weighted average filter. The filter is advanced in time through the prepared GPS data at the desired output sampling rate. The data points within the filter window are weighted, summed and output with a time stamp corresponding to the centre point of the filter window. The filtered GPS data stream is free of repeating values, spikes and large gaps. The associated data (ice thickness, laser altimeter, etc..) are then linearly interpolated to match the sampling rate of the filtered GPS data.

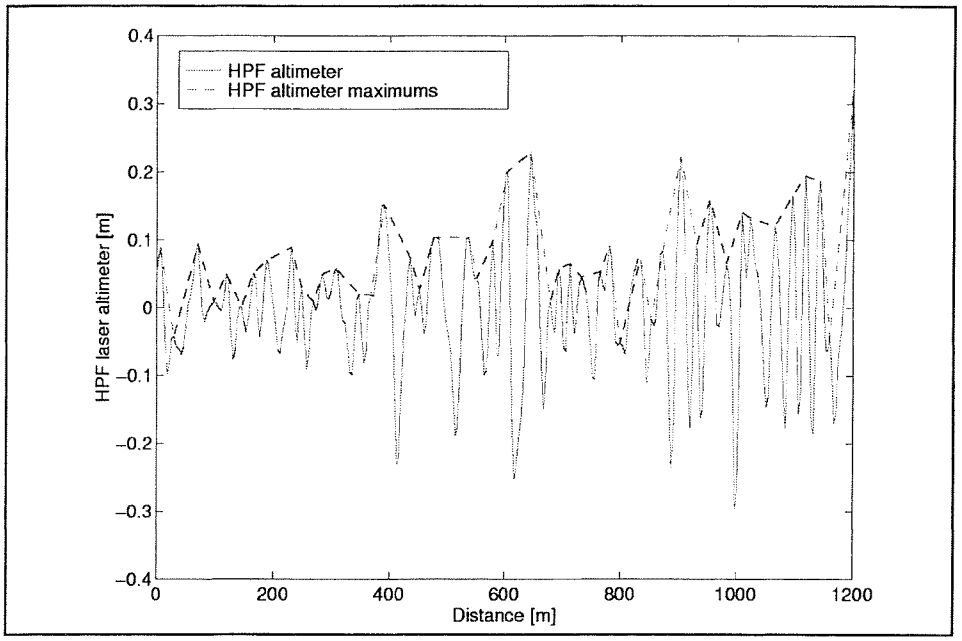

Figure 4.14: HPF laser data as obtained via Butterworth filtering (solid line) and HPF laser data minimums (discontinuous line).

Ice and snow surface roughness can be estimated by removing the helicopter motion (altitude variations of the helicopter) from the laser altimeter. An automated three step filtering technique (referred to here as the *minimum technique)* was used to separate the different signals (see Dierking 1995) following the GPS filtering (**Figure 4.14**). The laser altimeter data are filtered via a Butterworth low pass filter (LPF) with a spatial cut off frequency of 0.01 m^{-1} and a Nyquist frequency equal to the spatial sampling rate divided by 2. The high-pass filtered laser altimeter data series (HPFL) is then obtained by subtracting the LPF laser altimeter result from the laser data.

Minima in the HPFL are then located by numerical differentiation. The first derivative of the HPFL changes from negative to positive on each side of a minimum or trough. These changes in the slope are used to detected the troughs (**Figure 4.15**). The sequence of troughs are then

linearly interpolated to match the common sampling rate of the laser altimeter data series and then subtracted from it to obtain the estimated helicopter motion. The result is an approximate positive laser profile of the surface roughness. Small negative values in the surface roughness profile do occur, which are due to the combination of the linear interpolation and the points of inflection (**Figure 4.16**). The laser profile of the surface roughness is referred to as the HPF laser altimeter throughout this report.

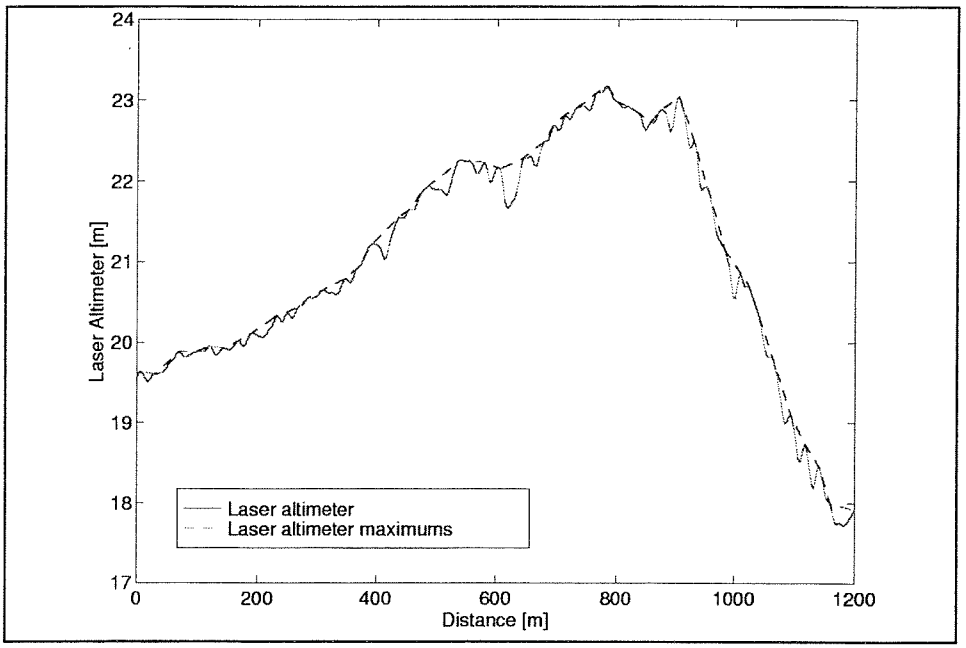

Figure 4.15: Estimating the helicopter motion using the computed HPF laser minimums.

One of the formats for presenting the data is the *standard plot* format (**Figure 4.17**). The *standard plot* contains ice thickness and HPF laser altimeter histograms along with profile plots of ice thickness, laser altimeter and HPF laser altimeter. The software that creates the *standard plot* excludes data corresponding to laser altimeter readings of 5 m or less and 25 m or greater from statistical calculations when the system is too low or high, respectively, to provide accurate measurements. In addition, data points that imply high apparent system velocities (over 83 m/s) are excluded. Survey lines are separated into segments for display. The start and end co-ordinates of each segment are displayed in the subtitle of the *standard plot*. Statistical tables are also created by the post-processing software (**Table 4.4**). These tables contain useful line and line segment information such as:

- Start and end coordinates of each survey line/segment.
- The number of samples/data in each survey line/segment.
- The length in kilometers of the survey line/segment.
- Mean and standard deviation of ice thickness in each survey line/segment.
- The average sampling rate in seconds and meters for each survey line. These are the final time interpolated sampling rates.

The post-processing software also has the ability to overlay profiles onto a geo-referenced map (**Figure 4.18**).

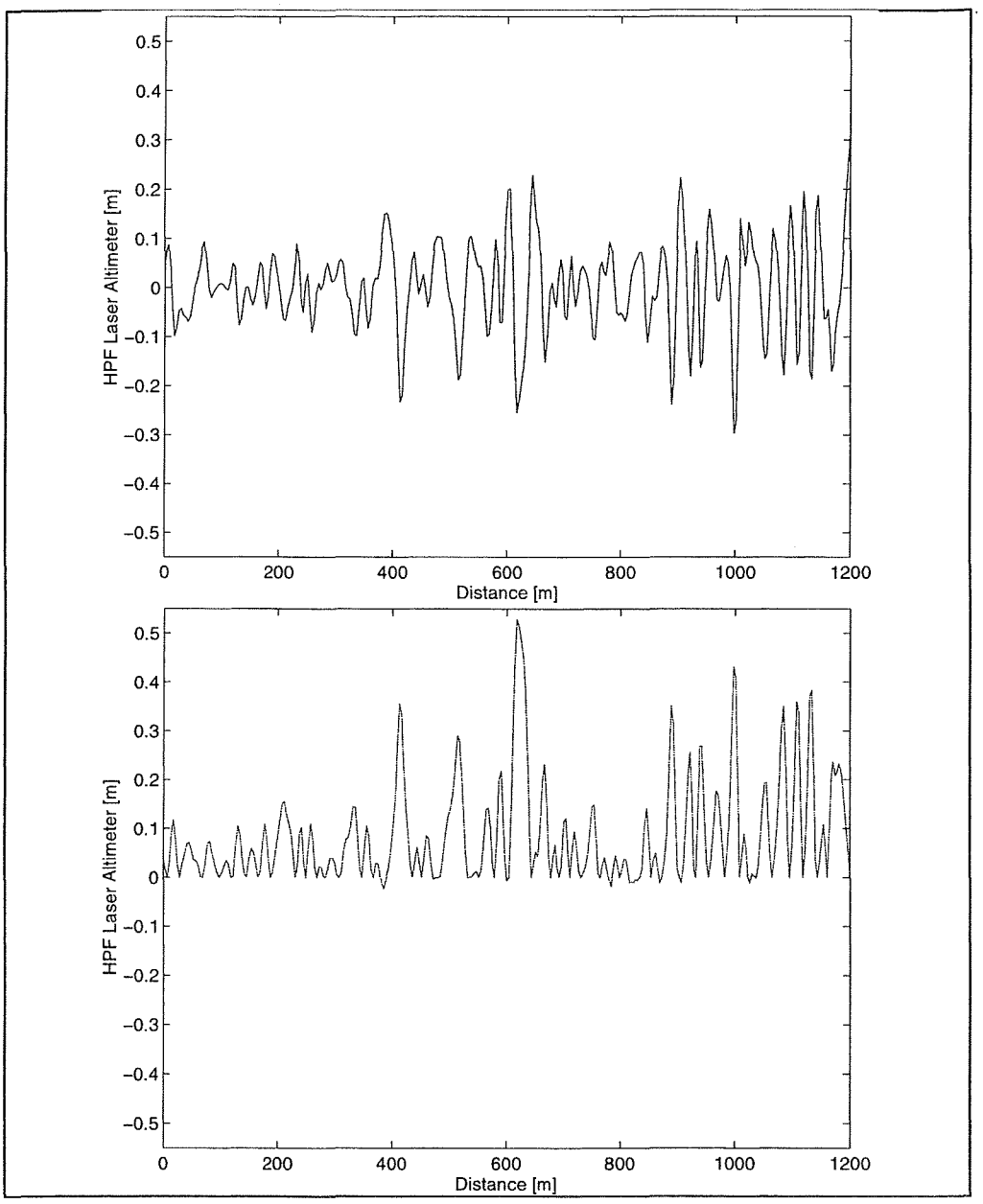

Figure 4.16: Comparing the HPF laser profile derived from Butterworth filtering (top) and the *maximum* technique (bottom).

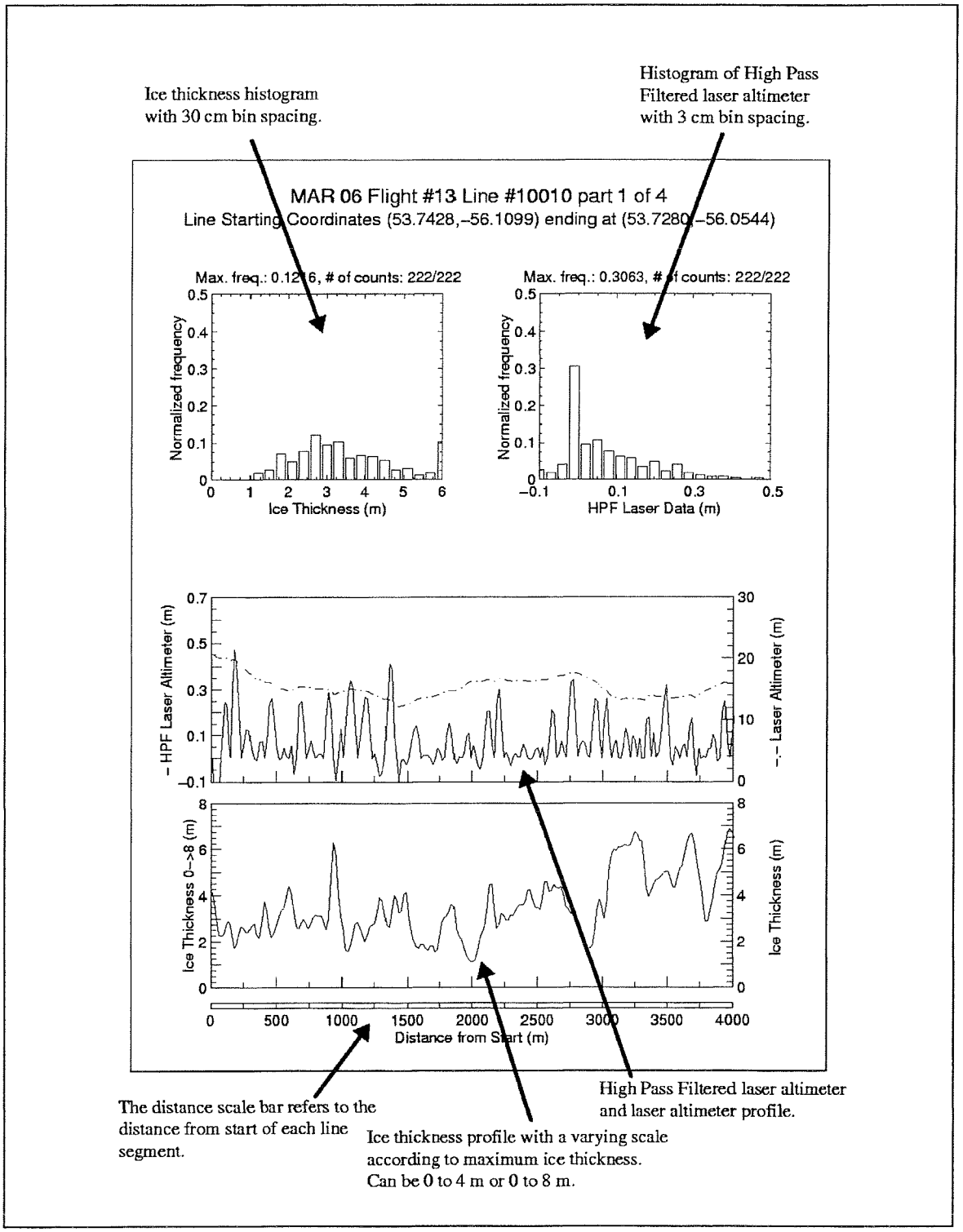

Figure 4.17: The *standard plot* format.

Line Number	Start		End		Number of Samples ICE	Length of Line/Seg. (km)	Ice Thickness (m)		Average Spacing (s) ICE	Average Spacing (m) ICE
	Lat. (deg. N)	Long. (deg. W)	Lat. (deg. N)	Long. (deg. W)			Mean	Std.		
10010	53.7428	-56.1099	53.7280	-56.0544	222	4.012	3.53	1.385		
	53.7280	-56.0544	53.7130	-55.9993	219	3.993	3.31	1.793		
	53.7130	-55.9993	53.6972	-55.9446	225	4.011	5.00	1.937		
	53.6972	-55.9446	53.6937	-55.9324	56	0.896	6.66	1.252		
Total	53.7428	-56.1099	53.6937	-55.9324	719	12.911	4.16	1.971	0.4	17.96
10020	53.6547	-55.9566	53.6344	-55.9065	223	4.008	0.31	0.662		
	53.6344	-55.9065	53.6172	-55.8534	216	4.000	2.12	1.436		
	53.6172	-55.8534	53.6124	-55.8369	72	1.207	2.92	1.076		
Total	53.6547	-55.9566	53.6124	-55.8369	509	9.215	1.44	1.513	0.4	18.10
10030	53.6158	-55.7112	53.6060	-55.6747	160	2.646	1.69	0.658		
Total	53.6158	-55.7112	53.6060	-55.6747	160	2.646	1.69	0.658	0.4	16.54

Table 4.4: Sample statistics table created by the post-processing software.

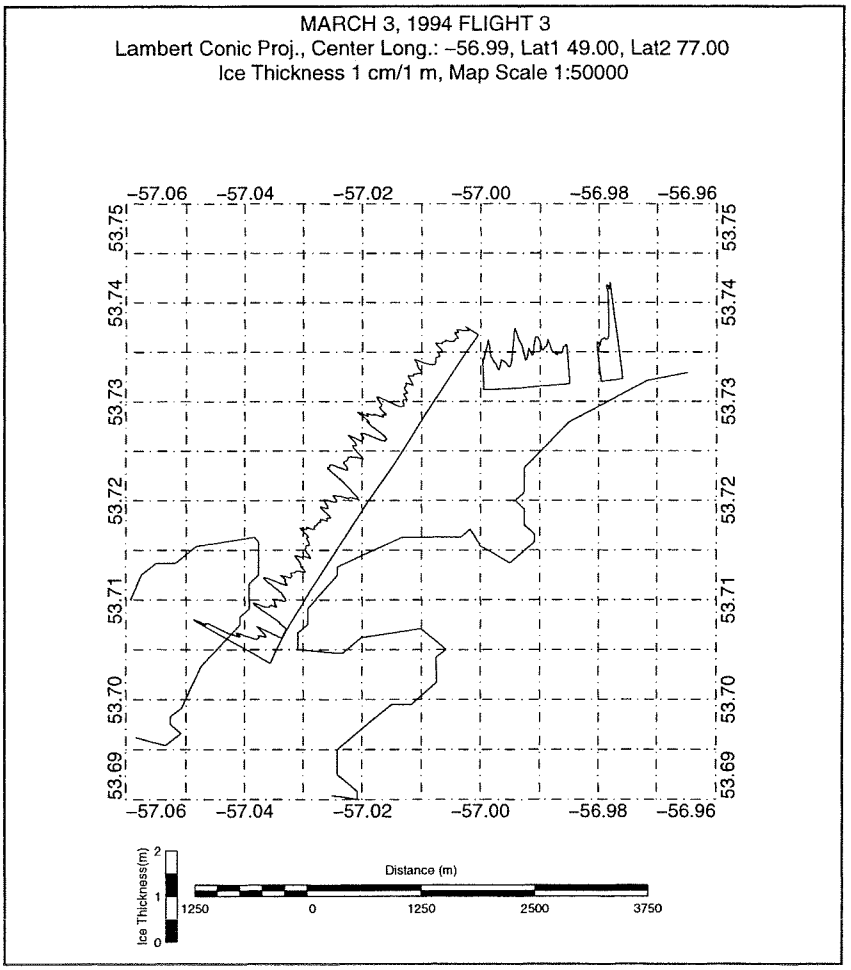

Figure 4.18: An ice thickness profile map (not to scale).

5. RESULTS

The system delivers extremely consistent estimates of ice thickness over relatively smooth, level ice, provided that wind conditions are not extreme so that the bird can be flown smoothly, with a minimum of pilot-induced swing. Cross winds caused particular problems when performing validation runs over short marked lines on the ice. Pilots with experience in flying EM systems can reduce the amount of bird swing considerably. Bird swing affects ice thickness estimates as follows: the laser altimeter's beam, which does not point straight down during a swing, will measure a larger distance to the surface, while the EM sensor continues to measure the shorter distance straight downward. Their difference will thus underestimate the snow-plus-ice thickness. The Production Prototype system being used now since 1996 by the Coast Guard reduces the effects of bird swing through the use of an accurate bird attitude sensor which corrects measurements for roll and tilt.

Sections of the post-processed data, presented as *standard plots*, were partitioned according to the homogeneity of ice conditions seen in the data and shown on ice charts provided by the Canadian Ice Services, Environment Canada. The *standard plots* for land-fast ice were then compared to the *standard* plots for pack ice. Due to the large amount of data collected, comparisons were made only between *standard plot* segments that contained 4 km of data. About 128 km of land-fast ice data was compared to 120 km of pack ice data. Significant differences were found between land-fast ice and pack ice data. These differences are illustrated in the following sections with the use of selected histograms and profiles.

5.1 LAND-FAST ICE

The *standard plots* for land-fast ice data pertained several unique characteristics. Overall, the ice thickness histograms were found to have a narrow distribution generally with a triangular or Gaussian shape. This histogram distribution ranged in majority from 0.7 m to 2.4 m with a maximum average count at 1.5 m. **Figure 5.1** shows the general characteristics of land-fast ice thickness histograms. The land-fast ice histograms that did not display these characteristics usually reflected the presence of old or new shear zones at the boundary between land-fast and mobile pack ice where ridging and rafting takes place (**Figure 5.2 (a)**). Some flights followed the land-fast-pack ice boundary according to the ice charts provided. These lines were classified as land-fast, but they do exhibit the characteristics of pack ice (**Figure 5.2 (b)**). In order to distinguish between coastal rubble/rafting and pack ice, one must take into account the location of the survey line and the associated ice thickness profile.

The ice thickness profiles for land-fast ice were found to be smooth (minimal variance in ice thickness) and generally contained fewer open leads (ice thickness of 0 m) than pack ice profiles. The land-fast ice thickness profiles were also found to contain fewer spikes than pack ice profiles. **Figure 5.3** shows the typical characteristics of ice thickness profiles for land-fast ice that correspond to the ice thickness histograms shown in **Figure 5.1**. The ice thickness profiles associated with histograms in **Figure 5.2** are shown in **Figure 5.4**.

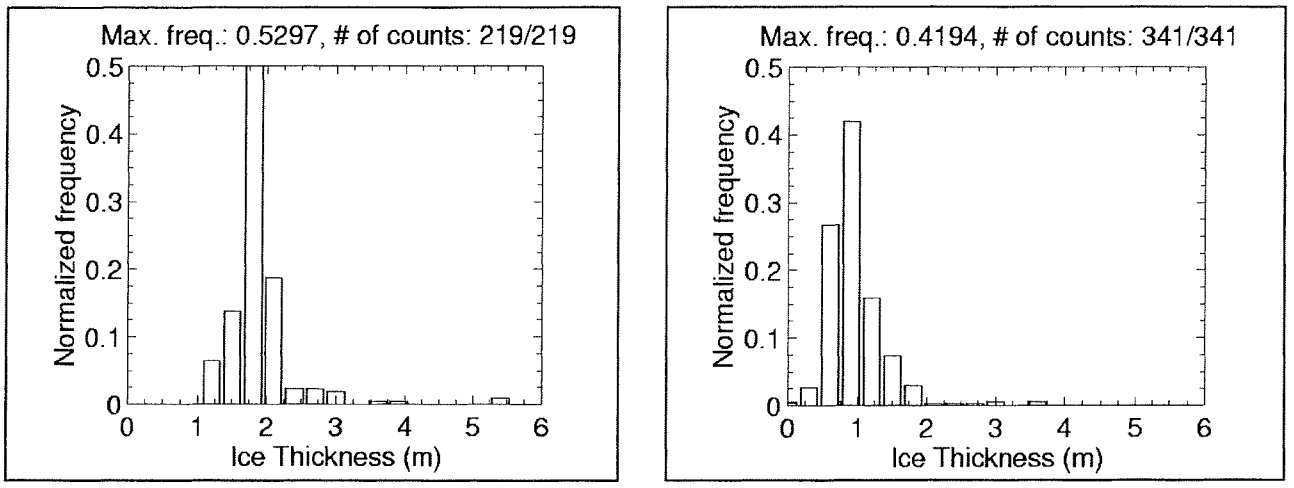

(a) (b)

Figure 5.1: Typical ice thickness histograms for land-fast ice:
(a) March 3, Flight 14 Line 10050; and (b) March 6, Flight 9 Line 10050.

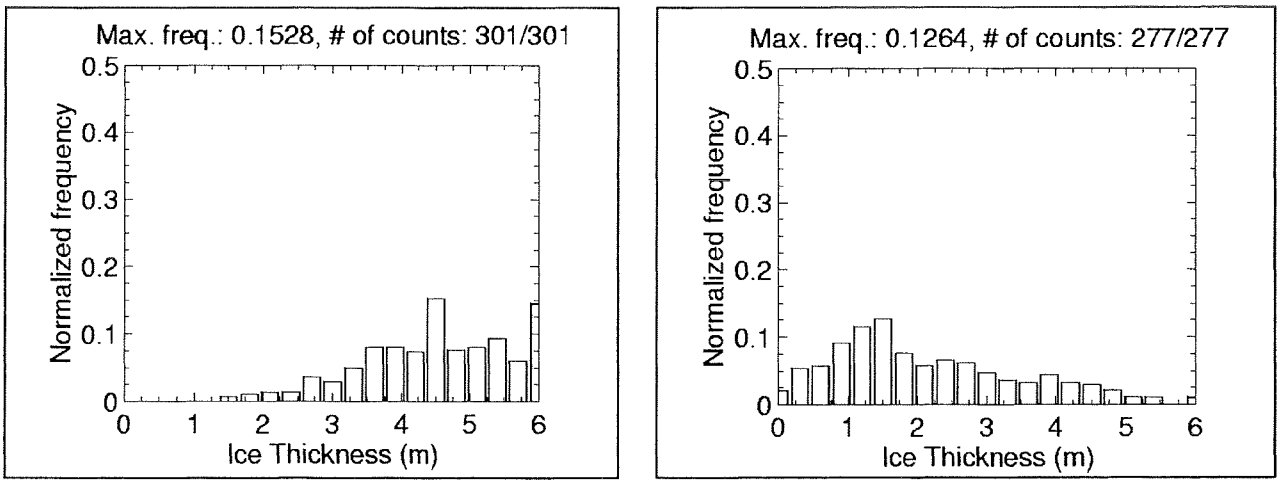

(a) (b)

Figure 5.2: Land-fast ice histograms due to a) coastal rubble and/or rafting, March 6, Flight 13 Line 10070 and b) misclassified land-fast ice March 6, Flight 9 Line 10030.

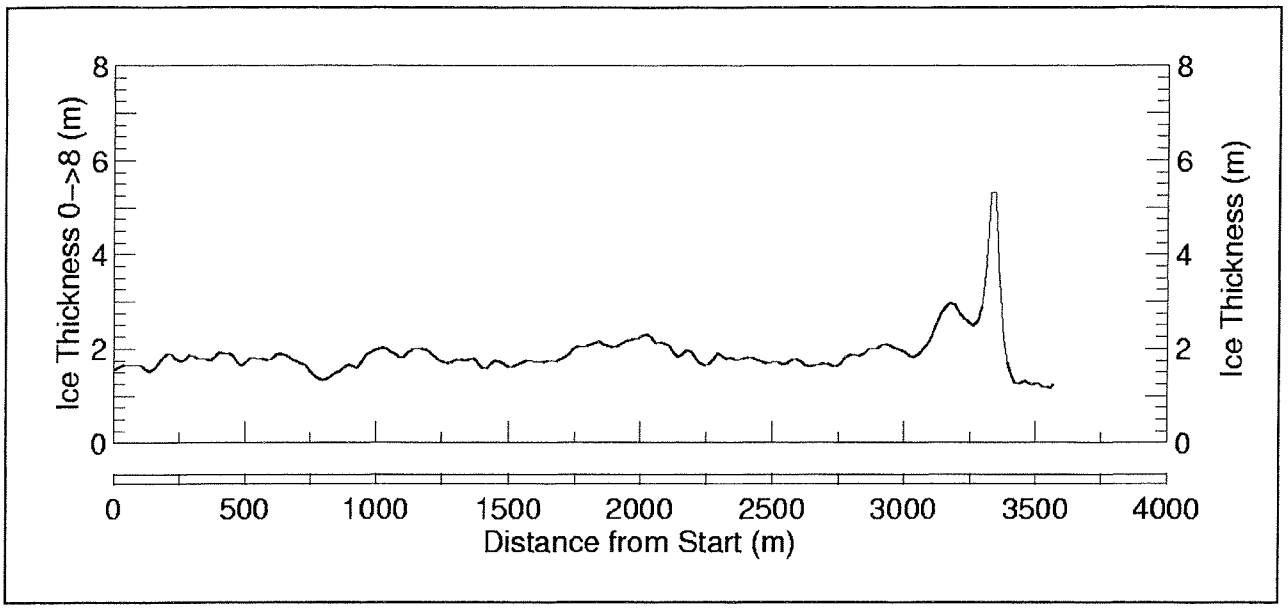

(a)

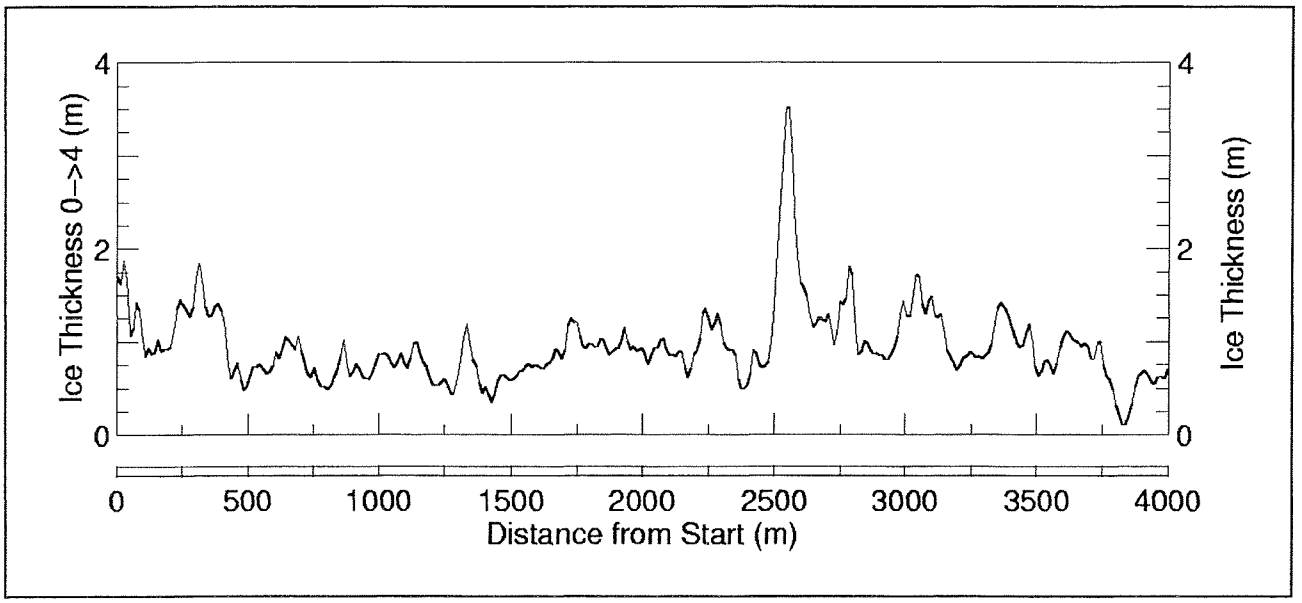

(b)

Figure 5.3: Typical ice thickness profiles for land-fast ice: (a) March 3, Flight 14 Line 10050; and (b) March 6, Flight 9 Line 10050.

Note the two figures have different ice thickness scales.

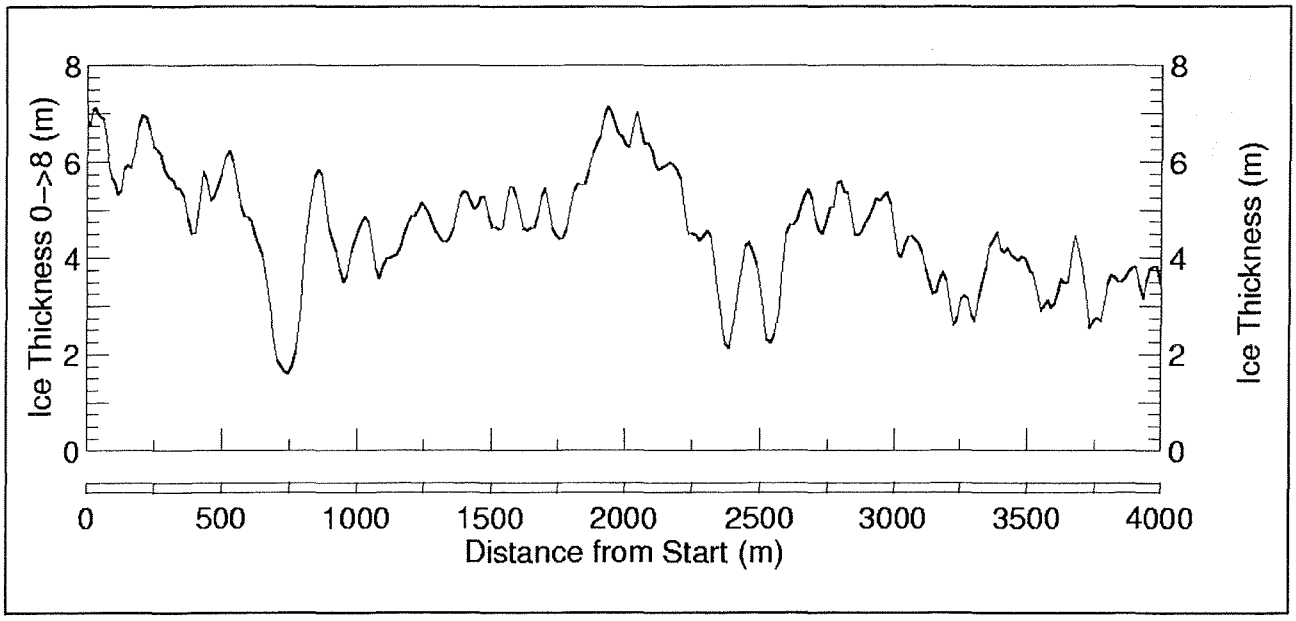

(a)

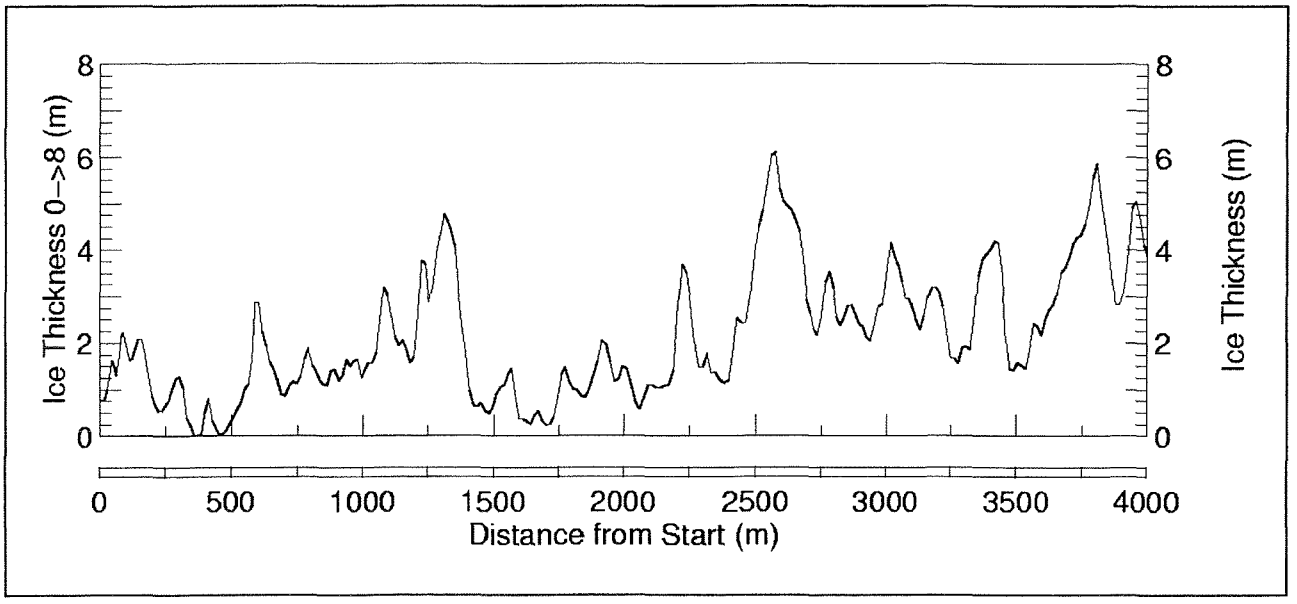

(b)

Figure 5.4: Land-fast ice profiles due to (a) coastal rubble and/or rafting, March 6, Flight 13 Line 10070; and (b) misclassified land-fast ice March 6, Flight 9 Line 10030.

The High Pass Filter (HPF) laser altimeter data, representing features of the snow and ice surface topography, also displayed some useful characteristics. The HPF histogram for land-fast ice was found to be distributed on the average from -0.09 m to 0.27 m with majority of the counts in the -0.07 m to 0.20 m range. The distribution was generally triangular or bell like. The maximum count of the HPF histogram was found to be, as expected, at 0 m, as the major portion of the topography consisted of flat snow-covered ice. **Figure 5.5** shows the general characteristics of the land-fast HPF laser altimeter histogram. As with the ice thickness histograms, there are some HPF laser altimeter histograms that do not contain the characteristics described. In addition to coastal effects, rafting, and misclassification there is the effect of the quality of flying. The HPF laser altimeter is greatly affected by highly variable altimeter data. A greater number of spikes shows up in the HPF laser altimeter profile for a flight in which the altitude of the bird varies significantly. These spikes tend to have a high amplitude and thus cause the histograms distribution to widen (**Figure 5.6** and **Figure 5.7**).

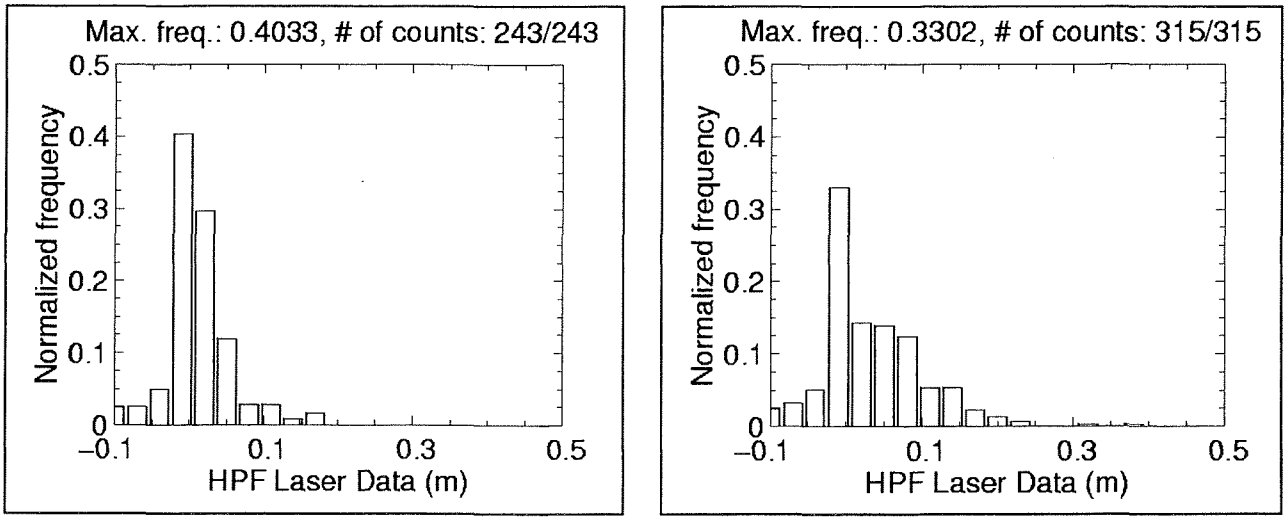

Figure 5.5: Typical HPF altimeter histograms for land-fast ice: (a) March 3, Flight 14 Line 10050; and (b) March 6, Flight 9 Line 10080.

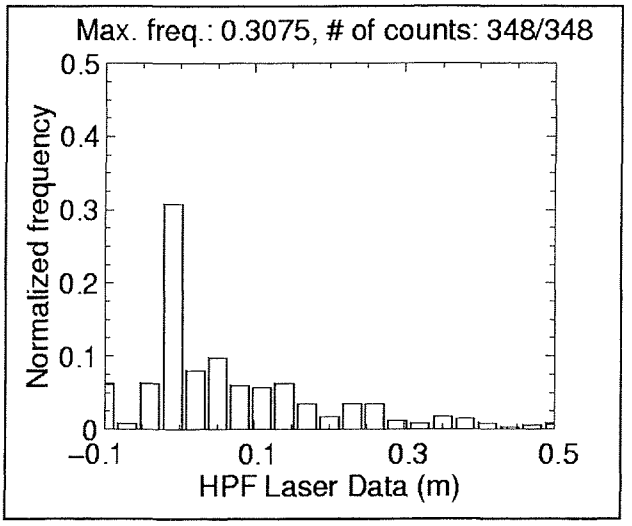

Figure 5.6: Land-fast ice HPF laser altimeter histogram due to a high varying altimeter: March 6, Flight 9 Line 10050.

The HPF laser altimeter profiles for land-fast ice were found to be generally smoother than the pack ice HPF laser altimeter profile. The land-fast profiles were also found to contain less number of spikes than the pack ice profiles. The amplitudes of the land-fast HPF laser altimeter spikes were also lower than that of the pack ice. **Figure 5.7 (b)** and **Figure 5.8** show the typical characteristics of an HPF laser altimeter profile for land-fast ice. It is again important to stress that the quality of flying greatly affects the HPF laser altimeter: classification of the surface snow and ice topography based solely on the HPF laser altimeter may not be accurate with the 1994 version of the Ice Probe. Since 1995, GPS-based roll and tilt sensors mounted in the Ice Probe have increased the quality of both the surface roughness data and the snow-plus-ice thickness data.

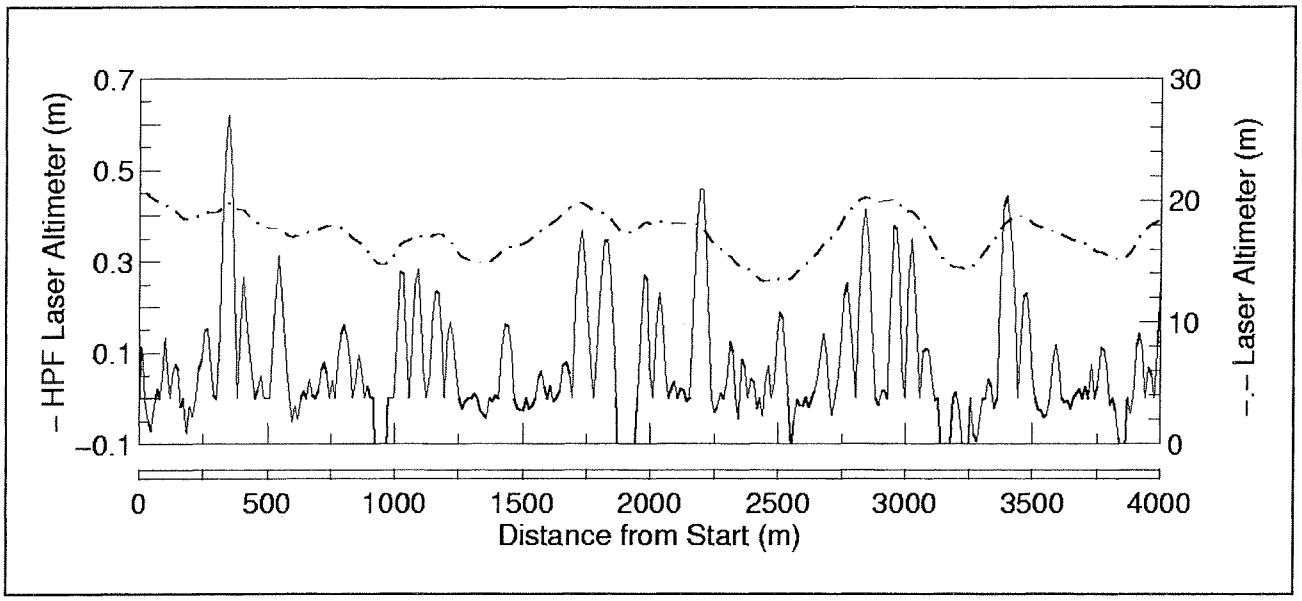

(a)

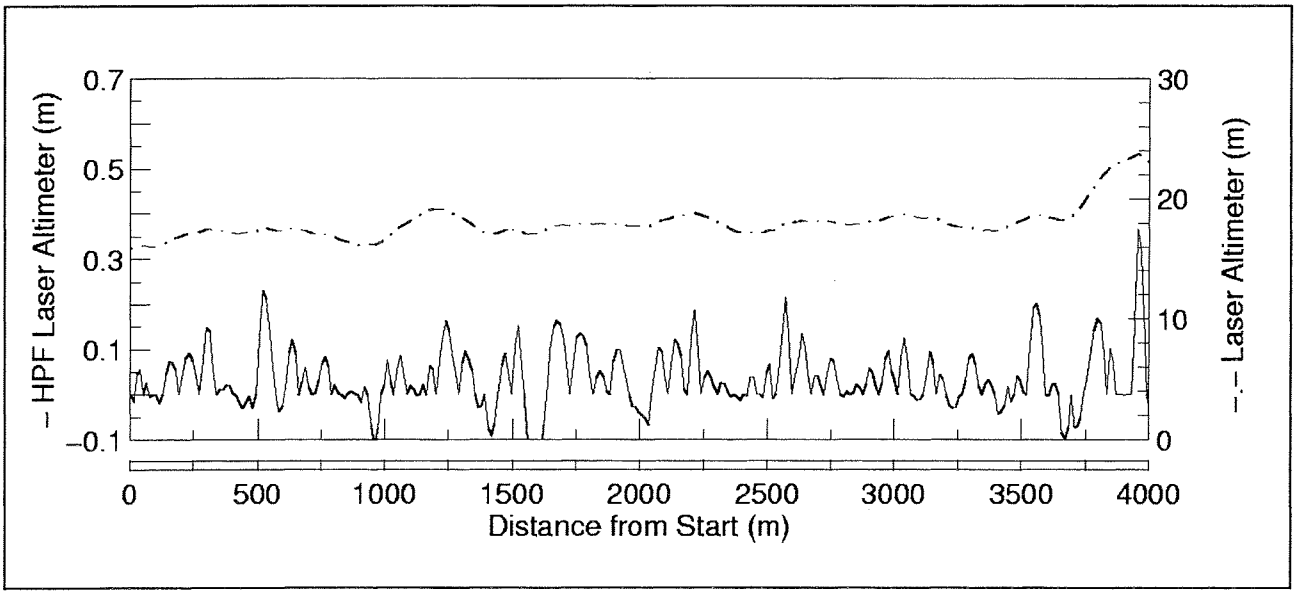

(b)

Figure 5.7: Comparison of HPF laser altimeter profiles of (a) a high variable altimeter profile from March 6, Flight 9 Line 10050; and (b) a smoother flight profile from March 6, Flight 9 Line 10080.

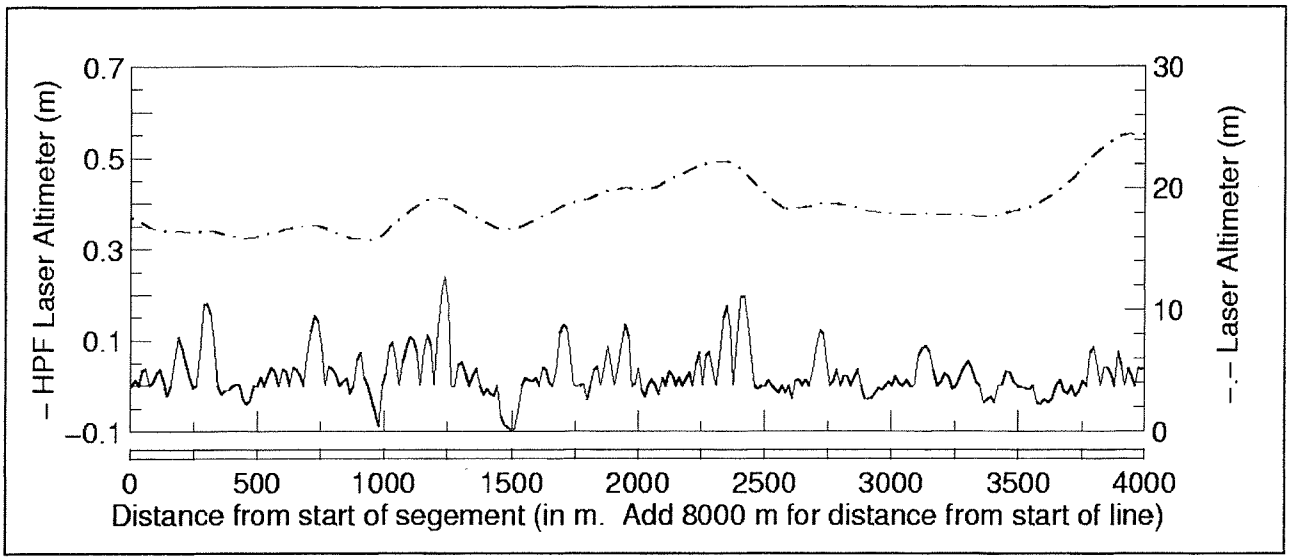

Figure 5.8: Typical land-fast ice HPF laser altimeter profile: March 6, Flight 13 Line 10092.

5.2 PACK ICE

The *standard plots* for pack ice displayed a number of characteristic features. Overall, the ice thickness histograms were found to have a wide quasi-Gaussian or a broad irregular distribution, suggesting that a wide variety of new and old ice areas are present in undeformed as well as deformed conditions. The majority of the counts for the ice thickness histogram for pack ice were found in the 1.0 m to 3.3 m range. The average maximum count was found to be 2.1 m. **Figure 5.9** show some of the characteristics pertaining to the ice thickness histograms of pack ice.

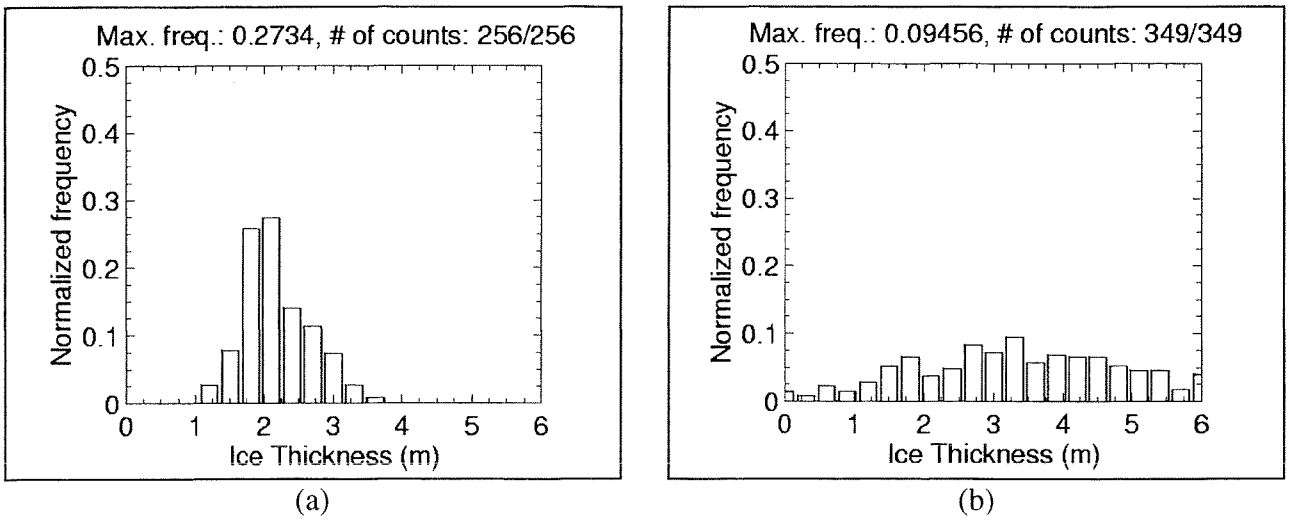

Figure 5.9: Typical ice thickness histograms for pack ice: (a) March 3, Flight 14 Line 10020; and (b) March 6, Flight 13 Line 10040.

The pack ice thickness profiles were found to be very rough (high variance in ice thickness) and overall contained large excursions (rafts and ridges) that were on the average 2 m above the average ice thickness for the segment. Typical ice thickness profiles for pack ice are shown in **Figure 5.10**.

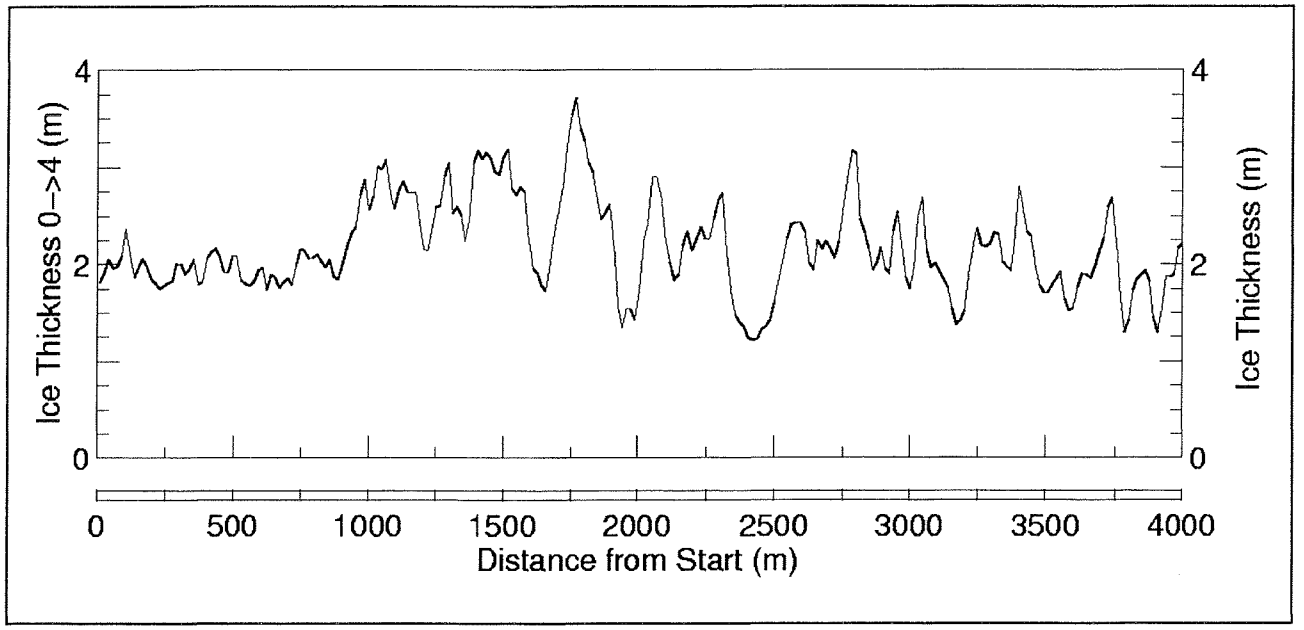

(a)

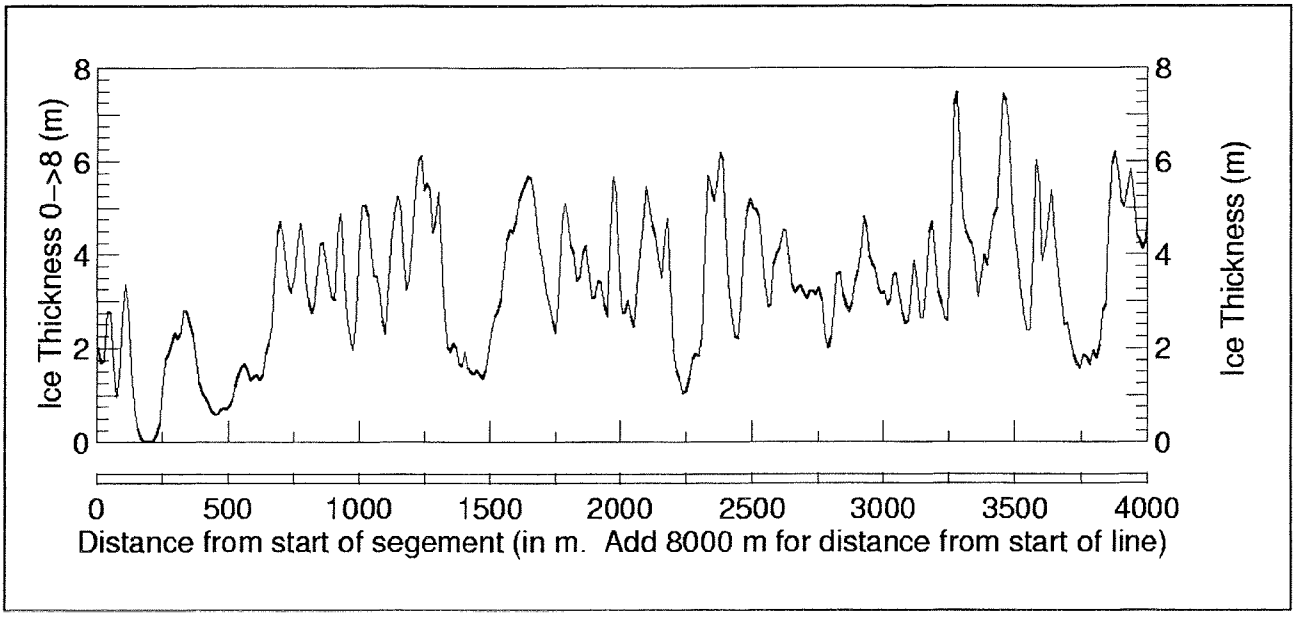

(b)

Figure 5.10: Typical ice thickness profiles for pack ice: (a) March 3, Flight 14 Line 10020; and (b) March 6, Flight 13 Line 10040.

Note: the two figures have different ice thickness scales.

The HPF laser altimeter histogram for pack ice was found to have an irregular distribution ranging on the average from -0.09 m to 0.39 m with the majority of counts between -0.04 m to 0.26 m. The pack ice surface and bottom topographies are thus rougher than those of land-fast ice. As for land-fast ice, the peak count for the HPF histogram was found to be at 0 m, indicating that, in spite of the rougher surface topography, most pack ice consists of relatively flat ice. **Figure 5.11** shows the general characteristics of a pack ice HPF histogram.

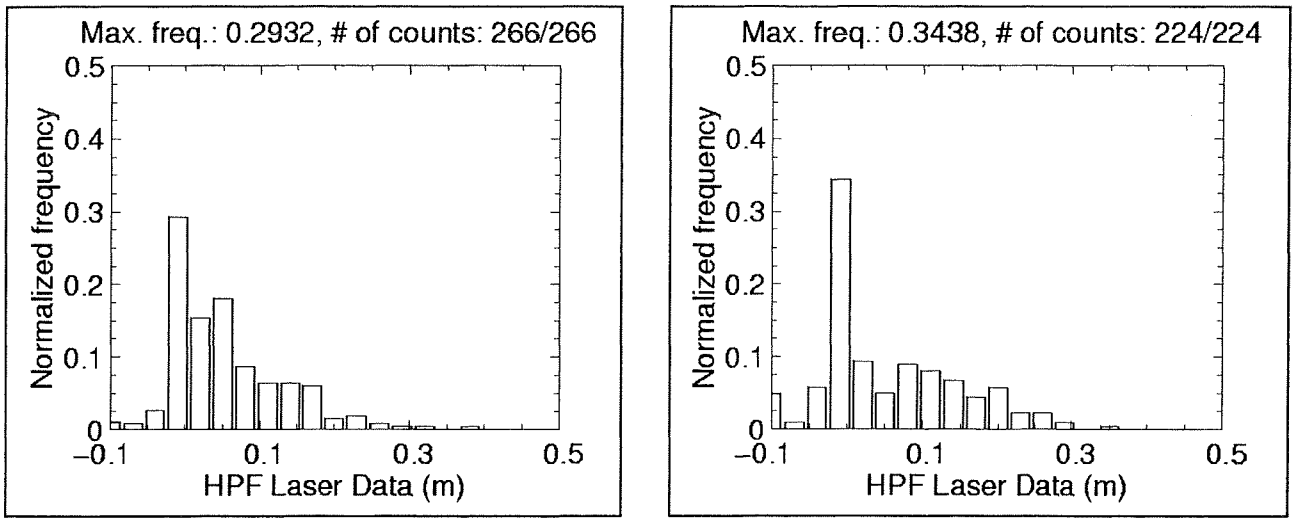

Figure 5.11: Typical HPF altimeter histogram for pack ice: (a) March 3 Flight 14 Line 10020; and (b) March 6 Flight 8 Line 10030.

The pack ice profiles for the HPF laser altimeter were found to have a high variance. The high number of spikes in the HPF profile was found to be typical of pack ice. **Figure 5.12** shows the typical characteristics of an HPF laser altimeter for pack ice. One should remember that the HPF laser altimeter is also affected by the quality of flying and this must be taken into account when analyzing HPF laser altimeter data.

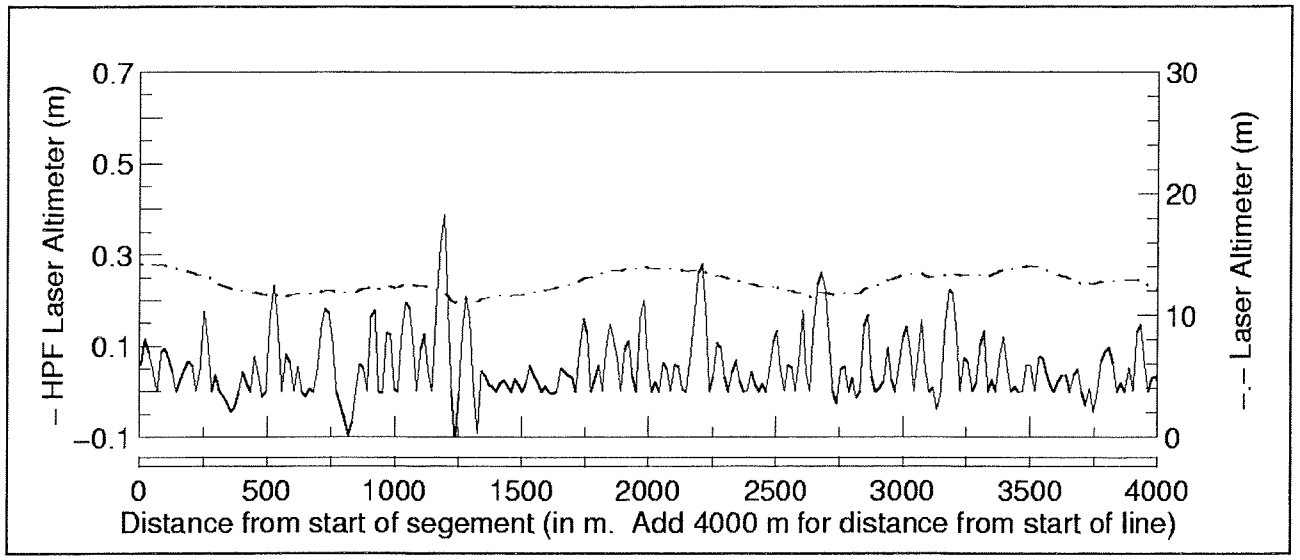

(a)

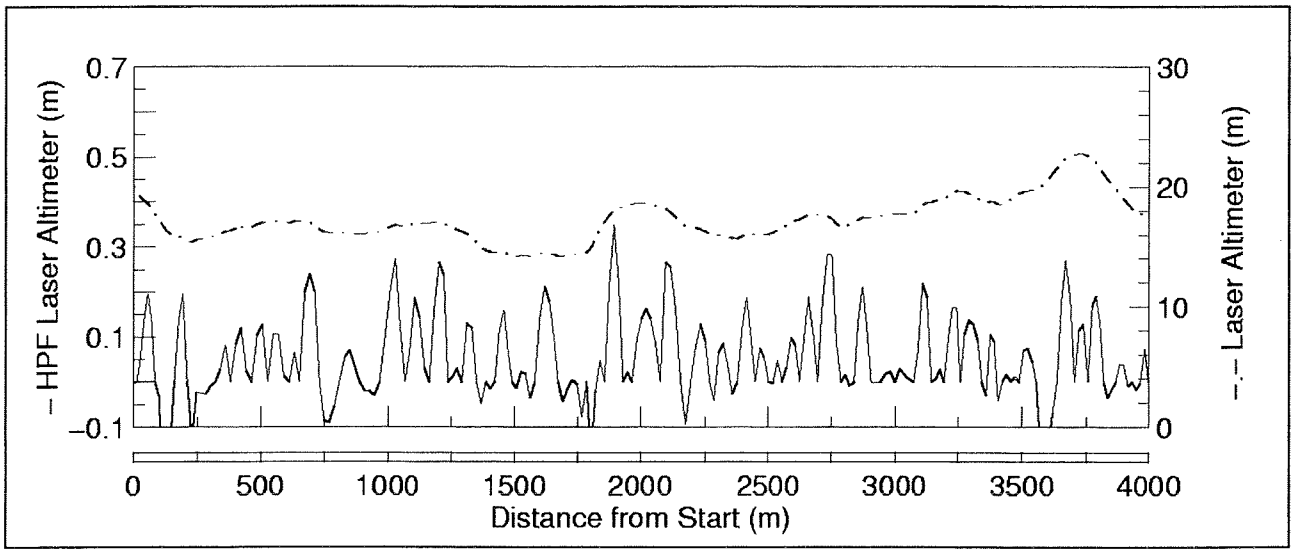

(b)

Figure 5.12: Typical pack ice HPF laser altimeter profiles: (a) March 3, Flight 14 Line 10020; and (b) March 6, Flight 8 Line 10030.

6. CONCLUSIONS

The *Ice Probe* data provides a clear distinction between ice types in land-fast and mobile pack ice. By comparing post-processed data for land-fast and pack ice it was possible to identify well-defined data characteristics pertaining to land-fast and pack ice types. This comparison started with the classification of ice type based on survey line position and ice charts. *Standard plots* were then used to identify characteristics for these ice types. These characteristics involved four data products: snow-plus-ice thickness histogram, snow-plus-ice thickness profile plot, High Pass Filter (HPF) laser altimeter histogram, and HPF laser altimeter profile plot. **Table 6.1** summarizes these four data products in relation to land-fast and pack ice.

Ice Type	Snow plus Ice Thickness		High Pass Filtered Laser	
	Histogram Distribution	Profile	Histogram Distribution	Profile
Land-fast	• narrow • triangular or Gaussian type • range 0.7 m to 2.4 m • average maximum at 1.5 m	• smooth • low variance	• narrow • triangular or Gaussian type • range -0.09 m to 0.27 m • majority of count -0.07 m to 0.20 m	• overall smooth • very few spikes • small spike amplitudes
Pack Ice	• wide • irregular • range 1.0 m to 3.3 m • average maximum at 1.5 m	• rough • high variance	• wide • irregular • range -0.09 m to 0.39 m • majority of count -0.04 m to 0.26 m	• overall rough • few spikes • large spike amplitudes

Table 6.1: Summary of the 4 data products in relation to land-fast and pack ice.

By using **Table 6.1** one can classify the ice as either land-fast or pack ice by first and foremost looking at the snow-plus-ice thickness histograms and profiles. The snow-plus-ice thickness histograms for land-fast ice were found to have a narrow distribution generally in a triangular or bell like formation indicating that a large fraction of the ice was undeformed and formed at the same time. The profiles of land-fast ice were generally smooth with low variance in ice thickness. In the case of pack ice, the histograms were found to have a wide irregular distribution and the corresponding profiles were generally rough with a high variance in ice thickness, i.e. ice was continually deformed and young ice was formed.

Once a classification has been made according to the snow-plus-ice thickness data one should take into account the surface topography, i.e. the HPF laser data. The HPF laser altimeter histograms for land-fast ice were overall found to have a triangular or bell like distribution. The HPF laser altimeter profile was also generally smoother and contained a few (if any) number of spikes. The HPF laser altimeter histogram distribution for pack ice was generally wide and irregular and the profile was rough with a greater amount of large amplitude spikes. However, it is important to note that the maximum histogram count for both ice types was at 0 m indicating that for both areas the majority of ice occurs as flat level ice.

By combining the classification results obtained from the snow-plus-ice thickness data and the surface topography one is able to classify the ice as either land-fast or pack ice. If a survey line was flown over both land-fast and pack ice, discrepancies between the classification results from the snow-plus-ice thickness and surface topography data may occur.

ACKNOWLEDGMENTS

The authors would like to thank the personnel of Universal Helicopters Ltd. and Canadian Helicopter Ltd. of Goose Bay for their help with the field work and for storage of the equipment. Pilots Gerry Nutall and Wayne Massie were a pleasure to fly with. S. Prinsenberg and I. Peterson are thanked for their support in the field and assistance in the analysis and interpretation of the data. The work was funded through the Ocean Sciences Division's Sea Ice Program of the Federal Panel of Energy, Research and Development.

REFERENCES

Dierking, W., 1995. Laser profiling of the ice surface topography during the Winter Weddell Gyre Study 1992. J. Geophys. Res., 100(C3), 4807-4820.

Holladay, J.S., J.R. Rossiter and A. Kovacs, 1990. Airborne measurements of sea-ice thickness using Electromagnetic induction sounding. In: Pro. 9th Conf. of Offshore Mechanics and Arctic Eng.: 309-315.

Holladay, J.S., 1995. Analysis of Electromagnetic/laser data over the Newfoundland Shelf in 1992. Can. Contract. Rep Hydrogr. Ocean Sci. 44: v + 318pp.

Kovacs, A. and J.S. Holladay, 1989. Airborne Sea Ice Thickness Sounding. In: Proc. Int. Conf. on Port and Ocean Eng. under Arctic Conditions. Lulea Univ. of Techn.: 1042-1052.

Kovacs, A. and J.S. Holladay, 1990. Sea-ice thickness measurements using a small airborne Electromagnetic sounding system. Geophysics No. 55(10): 1327-1337.

Liu, G. and A. Becker, 1990. Two-dimensional mapping of sea-ice keels with airborne electromagnetics: Geophysics No.55: 239-248.

Peterson, I.K., S.J. Prinsenberg and G.A. Fowler, 1995. Newfoundland Shelf sea ice program, 1993 and 1994. Can. Techn. Rep. of Hydrogr. and Ocean Sc., 167: vi + 129pp.

Peterson, I.K., S.J. Prinsenberg and J.S. Holladay and T. Carrieres, 1998. Ice thickness over Labrador shelf from EM-induction sounding: Comparison with ERS-1 SAR and airborne video data. J. Geophys. Res., Advances in Oceanography and Sea Ice Research using ERS-1 observations. In Press.

Prinsenberg, S.J., J.S. Holladay, J.R. Rossiter and L.A. Lalumiere, 1992. 1991 Beaufort Sea EM/Radar ice and snow sounding project. Can. Techn. Rep. of Hydrogr. and Ocean Sc., No 139: vi + 61pp.

Prinsenberg, S.J., J.S. Holladay and L.A. Lalumiere, 1993. 1992 Electromagnetic/Radar Ice and Snow Sounding Project over the Newfoundland Shelf in 1992. Can. Techn. Rep. of Hydrogr. and Ocean Sc., No 144: vii + 59pp.

Prinsenberg, S.J., I.K. Peterson and J.S. Holladay, 1996. Comparison of Airborne Electromagnetic Ice Thickness Data with NOAA/AVHRR and ERS-1/SAR Images. Atmosphere-Ocean 34(1): 185-205.

Rossiter, J.R., J.S. Holladay and L.A. Lalumiere, 1990. Validation of airborne sea ice thickness measurements using Electromagnetic Induction during LIMEX'89 (UP-C8-028). Rep. to Dept. Fish. and Oceans, Bedford Inst. of Oceanography., Contract FP953-8-08848/01-OSC.

APPENDICES

A. SURVEY LINE LISTING

Cartwright EM Ice Thickness Survey March 1994

The line numbers in this listing are taken directly from the logs. The line numbers in this table generally correspond to line numbers in the post-processed data by the following: L1 refers to line 10010, L2 to line 10020, ..., L11 to line 10110 etc.

Date	Flight ID	Line	Time Start	Time End	Remarks
3-Mar-94	MAR03F3	L1	9:16:41	9:17:20	First flight over marked line, no video, good run.
		L2	9:19:28	9:22:01	Flight to town
	MAR03F5	L1	13:27:38	13:28:08	Flight 2 over first marked line (10 bags), some bird swing to right of line.
	MAR03F6	L1	13:33:44	13:34:54	Enroute Grady Is., broken ice, in Bay?, lost NAV.
	MAR03F8	L1	13:47:40	13:49:06	
	MAR03F11	L1	14:10:27	14:14:04	Thick ice, ridge feature, and open water patches, low noise and drift
		L2	14:15:37	14:18:38	Open water (good 0 thickness meas.) Time lag checked 1.0 sec.
		L3	14:27:46	14:28:37	Eastbound flight near SP helicopter on ice floe.
		L4	14:29:37	14:31:16	Westbound flight near SP helicopter.
		L5	14:33:07	14:33:47	Start of eastbound line.
	MAR03F12	L1	14:40:11	14:41:11	Eastbound flight.
		L2	14:42:36	14:44:21	Westbound flight to south near SP ice floe site.
		L3	14:45:01	14:46:39	Flight near helicopter on ice floe.
		L4	14:48:44	14:50:50	Flight near marked SP marked ice floe.
		L5	14:54:01	14:55:31	Flight over short marked line, too low.
		L6	14:57:01	14:58:51	Flight near marked line.
		L7	14:58:51	14:59:41	Flight over short marked line by helicopter. Too low.
		L8	15:01:51	15:02:27	Eastbound flight over marked line.
		L9	15:03:31	15:04:21	Westbound approx. 100m to S of SP helicopter.
		L10	15:06:08	15:07:08	Small Iceberg overflight, maximum thickness 6.04 m.
	MAR03F14	L1	15:16:02	15:18:47	Flight (Nav. back on), Return to Cartwright then lost Nav.
		L2	15:25:50	15:29:51	Flight (Nav. back on) return to Cartwright.
		L3	15:32:23	15:40:18	Flight (Nav. back on) return to Cartwright.
		L4	15:42:21	15:52:54	Open water, thin grey white ice, pancake ice, and smooth sections.
		L5	15:55:20	16:01:40	Thin ice, open water sections, white and grey white ice and possible shoals
		L6	16:06:01	16:06:41	Flight over line near Huntington Is. to left of line. Low with bird swing.
		L7	16:08:34	16:09:02	Flight over marked line (to right of line), bird swing.
		L8	16:11:01	16:11:31	Flight over marked line, bird swing.
		L9	16:13:58	16:14:31	Flight over marked line, good, some bird swing.

Date	Flight ID	Line	Time Start	Time End	Remarks
4-Mar-94	MAR04F3	L1	8:29:56	8:31:03	Run to S. Wolf Is., N. Wolf and Ferret Is.
		L2	8:32:56	8:34:33	Some bad NAV.
	MAR04F5	L1	8:49:44	8:50:52	Short line
	MAR04F7	L1	9:09:44	9:11:09	Pictures 31-34 off East Wolf Is.
		L2	9:12:39	9:14:57	
		L3	9:17:06	9:17:53	Ended this line over Wolf. Is.
		L4	9:19:46	9:21:45	Wolf Is. numerous features
		L5	9:22:16	9:24:07	
		L6	9:27:05	9:28:54	S to N flight over Wolf Is.
		L7	9:30:20	9:31:55	
		L8	9:35:24	9:35:55	
		L9	9:36:04	9:37:44	Flight over marked line near SP helicopter, bird slightly left of line.
		L10	9:38:32	9:39:15	Run over marked line (5 bags), bird to right of line.
	MAR04F8	L1	9:50:10	9:54:12	Thin ice, broken gaps
		L2	9:57:24	10:00:32	Near marked line. Note, although not printed thicknesses saved to disk
6-Mar-94	MAR06F1	L1	10:18:04	10:21:04	Cartwright, Table Bay rerun part of line, Pt. A, Wolf Is return, no video
	MAR06F2	L1	10:25:36	10:26:23	Nav. ok, ridged small floes.
	MAR06F8	L1	10:47:31	10:50:30	Open water, thick floes, EM good, NAV OK, cross pattern over SP helicopter.
		L2	10:53:54	10:56:37	Followed other helicopter
		L3	10:59:28	11:03:17	Thin and thick ice mixed, NAV. OK.
		L4	11:06:27	11:11:27	NAV. OK.
		L5	11:32:46	11:14:37	Turn
		L6	11:15:15	11:16:10	Cross over helicopter, NAV. OK.
		L7	11:16:34	11:17:29	Landed on ice floe with SP, down at 11:22
	MAR06F9	L1	11:28:57	11:30:48	Site A onto Site B
		L2	11:33:12	11:44:00	NAV. OK, no video
		L3	11:47:25	11:53:18	Very rough, thick ice
		L4	11:57:12	12:02:08	Photo 8,9, over Black Tickle and Stoney Arm
		L5	12:05:08	12:07:24	Photo 9, 10, over smooth ice
		L6	12:10:28	12:17:16	Over shallow water, photo 11,12, Rocky Pt of land to L, Stoney Arm
		L7	12:24:52	12:33:42	Table Bay, flight over shoal
	MAR06F10	L1	15:48:09	15:49:53	Good EM data
	MAR06F11	L1	15:55:26	15:58:00	Nav OK, shear ridge, lost nav at end
	MAR06F13	L1	16:10:21	16:15:10	Heavy Ice
		L2	16:17:25	16:21:23	Thin ice to slightly thicker
		L3	16:26:00	16:27:05	
		L4	16:30:42	16:38:58	Nav OK. S. Wolf. Is. end of L4 -L5
		L5	16:41:32	16:47:59	Thin pancakes, transition to thicker ice
		L6	16:51:02	16:55:54	Shear ridge photo 14, smoother ice, approach tip of Grady Is.
		L7	16:59:36	17:01:50	Shearing of floes
		L8	17:02:10	17:08:00	Thin pans, slide 20,21,22
		L9	17:10:52	17:12:30	
		L10	17:15:20	17:21:40	Shoal to left, 0.8-0.9 m ice near test line, bags gone

Date	Flight ID	Line	Time Start	Time End	Remarks
7-Mar-94	MAR07F1	L1	10:33:51	10:40:25	Flight to Halfway Is., Table Bay, Ferret Is., Roundhill, S along 212 M
		L2	10:43:21	10:47:18	Ice >>100m near Is.?, thin ice, flat ice
		L3	10:49:14	10:55:06	N. Ferret Is., thin ice on app., open, thin, new ice, rafted, crs chg. Roundhill
		L4	10:57:18	11:05:33	Pack ice, open water areas, heading 212 deg. M.
		L5	11:08:00	11:22:48	Thick floes, open water, thin ice, grey ice and nilas.
		L6	11:25:26	11:28:14	Photo 8, 10, southbound leg?
		L7	11:30:05	11:43:58	Photo 21-24
		L8	11:45:46	11:47:25	Over a bay then south to Domino Pt.
		L9	11:47:33	11:47:42	Short line followed by run over Porcupine Bay.
		L10	11:50:32	11:54:46	Porcupine Bay, shallow in places
		L11	11:55:22	12:01:16	Edge of thin ice, flights over Is.
		L12	12:03:04	12:14:26	
		L13	12:16:57	12:17:28	Cross thick ice SW of Duck Is., Lookout Is., shoals, thick ice?
		L14	12:18:08	12:24:00	Thin rough surface, ridges, contrast, frozen lead.
	MAR07F2	L1	15:45:11	15:46:21	Flt. 2 Ledge Is., S of Spotted Is., to Roundhill Is, N to Pt. A, WNW to RDI then toward Grady Is., return to Cartwright.
		L2	15:49:38	15:52:51	Oblique crossing from 0.5 to 0.2m
		L3	15:55:21	16:04:41	Thicker ice, shear Ridge, smooth ice.
		L4	16:05:21	16:07:26	Small narrows between Indian Is., thinner smooth ice, flight over Is.
		L5	16:07:41	16:18:46	Thin 0.2m ice, chunks of thick 1.5m, thin and smooth ice.
		L6	16:20:41	16:29:04	Patches of open water and thick ice
		L7	16:31:08	16:38:40	Thick ice all around, bergy bit to right 1 km.
		L8	16:40:58	16:48:46	Heading WNW, thick ice 2-3 m, rough and broken ice.
		L9	16:48:52	16:50:18	Flight over iceberg.
		L10	16:52:43	17:02:31	Thinner smooth ice, open, ice 4-5m, many brash areas
		L11	17:05:36	17:13:31	Large pans with broken ice around, pans, ridges and thin ice <30 cm.
		L12	17:16:43	17:19:24	Approach to Huntington Is., ice 0.8-0.9, 1.1 m thick.
9-Mar-94	MAR09F1	L1	13:45:54	13:47:24	Offshore, Grady Is., Gannet Is., to Cartwright
		L2	13:50:22	13:53:59	Grady Is.
		L3	13:55:31	13:59:00	Shear ridge, ice thickness reading too thick?
		L4	14:01:52	14:05:58	Open water, ice edges, thin ice
		L5	14:08:40	14:16:02	Photos 3,4 over pack ice
		L6	14:16:04	14:16:17	Short line
		L7	14:16:20	14:16:49	
		L8	14:20:20	14:26:06	Iceberg photos, thick level ice floes
		L9	14:27:51	14:40:58	Long open lead, floes, grease ice, and open water
		L10	14:42:48	14:49:25	Smooth ice with pressure ridges, shear ridge, just S. of Is.
		L11	14:49:34	14:50:19	Island overflight
		L12	14:52:11	14:56:38	Shoals and ice

B. FLIGHT LINE ICE TYPE SUMMARY

It is important to note that the line numbers that do not end with 0 are the result of manual editing. These lines were split into numerous parts. For example, the line 10020 in March 3/94 Flight 3 was split into two parts therefore the line numbers 10021 and 10022 in tables.

Date	Flight #	Land-fast Ice				Pack Ice			
		Line #	Length (km)	Ave. Ice Thick. (m)	Subtotal Length (km)	Line #	Length (km)	Ave. Ice Thick. (m)	Subtotal Length (km)
3-Mar-94	3	10010	1.076	0.79					
		10021	0.367	1.31					
		10022	4.535	0.66					
					5.558				0
	8	10010	4.415	2.79					
					4.415				0
	11					10010	6.888	1.42	
						10021	2.841	1.41	
						10022	4.137	1.42	
					0				13.866
	12					10010	1.907	1.45	
						10020	3.092	1.24	
						10030	4.060	1.29	
						10040	3.880	1.37	
						10050	0.386	1.15	
						10061	1.850	1.88	
						10062	2.175	1.44	
						10063	1.350	1.57	
						10070	0.250	1.62	
						10081	1.549	1.23	
						10082	2.071	1.76	
					0				22.570

Date	Flight #	Land-fast Ice				Pack Ice			
		Line #	Length (km)	Ave. Ice Thick. (m)	Subtotal Length (km)	Line #	Length (km)	Ave. Ice Thick. (m)	Subtotal Length (km)
6-Mar-94	14					10010	8.774	1.70	
						10020	18.134	2.01	
						10030	6.338	1.76	
						10040	18.930	0.87	
		10050	11.568	1.23					
		10060	0.370	0.81					
		10070	1.088	0.87					
		10080	0.343	0.78					
		10090	0.116	1.93					
		10100	0.216	1.13					
		10111	0.325	2.42					
		10112	0.084	0.47					
		10113	0.563	1.16					
		10121	0.230	1.39					
		10122	0.795	0.69					
		10131	0.317	1.69					
		10132	0.287	0.47					
		10133	0.845	0.91					
					17.147				52.176
6-Mar-94	8					10010	0.863	1.48	
						10021	3.213	1.69	
						10022	10.393	1.41	
						10030	13.189	2.04	
						10040	3.636	1.74	
						10050	1.152	1.14	
						10060	2.127	1.47	
					0				34.573
	9					10010	3.111	1.83	
						10020	21.271	1.90	
		10030	13.278	1.81					
		10040	0.189	1.37					
		10050	9.330	0.91					
		10060	3.932	0.32					
		10070	12.837	0.81					
		10080	16.998	1.74					
					56.564				24.382

Date	Flight #	Land-fast Ice				Pack Ice			
		Line #	Length (km)	Ave. Ice Thick. (m)	Subtotal Length (km)	Line #	Length (km)	Ave. Ice Thick. (m)	Subtotal Length (km)
6-Mar-94	13	10010	12.911	4.16					
		10020	9.215	1.44					
						10030	2.646	1.69	
						10040	14.682	2.44	
						10050	11.531	4.36	
						10060	9.049	3.80	
		10070	4.268	4.49					
		10081	11.619	2.00					
		10082	2.378	1.44					
		10091	0.874	1.03					
		10092	13.603	1.37					
					54.868				37.908
7-Mar-94	1	10010	16.532	0.99					
		10020	10.076	2.43					
		10030	15.423	1.48					
						10040	21.714	2.04	
						10050	17.608	2.03	
		10060	15.889	0.45					
						10071	7.487	1.05	
						10072	14.634	1.39	
		10081	15.947	0.91					
		10082	3.737	0.26					
		10090	9.068	0.93					
		10100	13.017	0.85					
		10110	23.908	2.57					
		10120	14.692	0.77					
					138.289				61.443
	2	10011	3.347	0.72					
		10012	7.839	0.61					
		10020	21.375	1.67					
		10030	4.556	1.18					
		10040	26.534	1.39					

Date	Flight #	Land-fast Ice				Pack Ice			
		Line #	Length (km)	Ave. Ice Thick. (m)	Subtotal Length (km)	Line #	Length (km)	Ave. Ice Thick. (m)	Subtotal Length (km)
7-Mar-94	2					10051	12.309	1.90	
						10052	3.184	1.82	
						10053	5.114	1.94	
						10061	5.504	1.74	
						10062	13.047	1.97	
						10070	17.694	2.62	
						10080	3.212	2.90	
						10090	23.886	2.41	
		10100	19.395	2.18					
		10110	6.699	1.04					
					89.745				83.950
9-Mar-94	1	10010	4.221	1.75					
		10020	9.740	2.36					
		10031	0.536	5.05					
		10032	6.238	3.60					
						10040	7.645	2.40	
						10051	3.025	2.97	
						10052	10.765	2.79	
						10060	0.243	2.60	
						10070	0.770	2.99	
						10080	11.973	2.57	
						10090	15.924	2.08	
						10100	6.574	0.99	
						10110	13.792	1.63	
		10120	1.307	1.15					
		10131	5.787	2.14					
		10132	0.450	1.67					
		10133	4.608	3.01					
					32.887				70.711
Total		56		1.53	399.473	53		1.86	401.579

C. ICE THICKNESS PROFILE MAPS

MARCH 3, 1994 FLIGHT 8
Lambert Conic Proj., Center Long.: –56.26, Lat1 49.00, Lat2 77.00
Ice Thickness 1 cm/2 m, Map Scale 1:50000

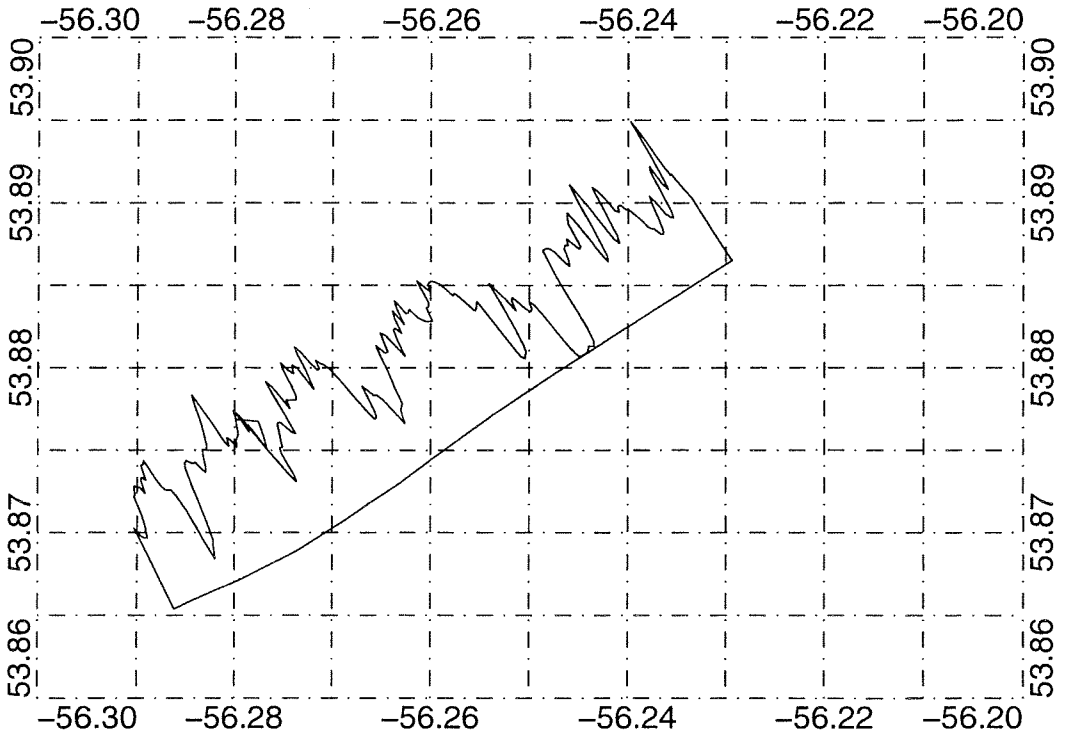

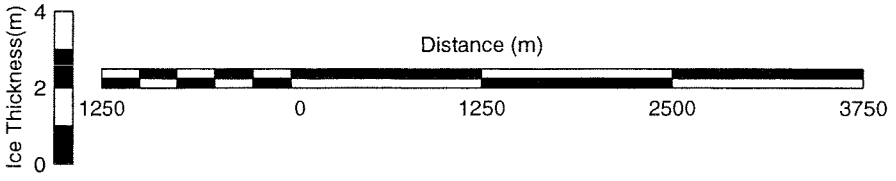

MARCH 3, 1994 FLIGHT 11
Lambert Conic Proj., Center Long.: −55.40, Lat1 49.00, Lat2 77.00
Ice Thickness 1 cm/2 m, Map Scale 1:200000

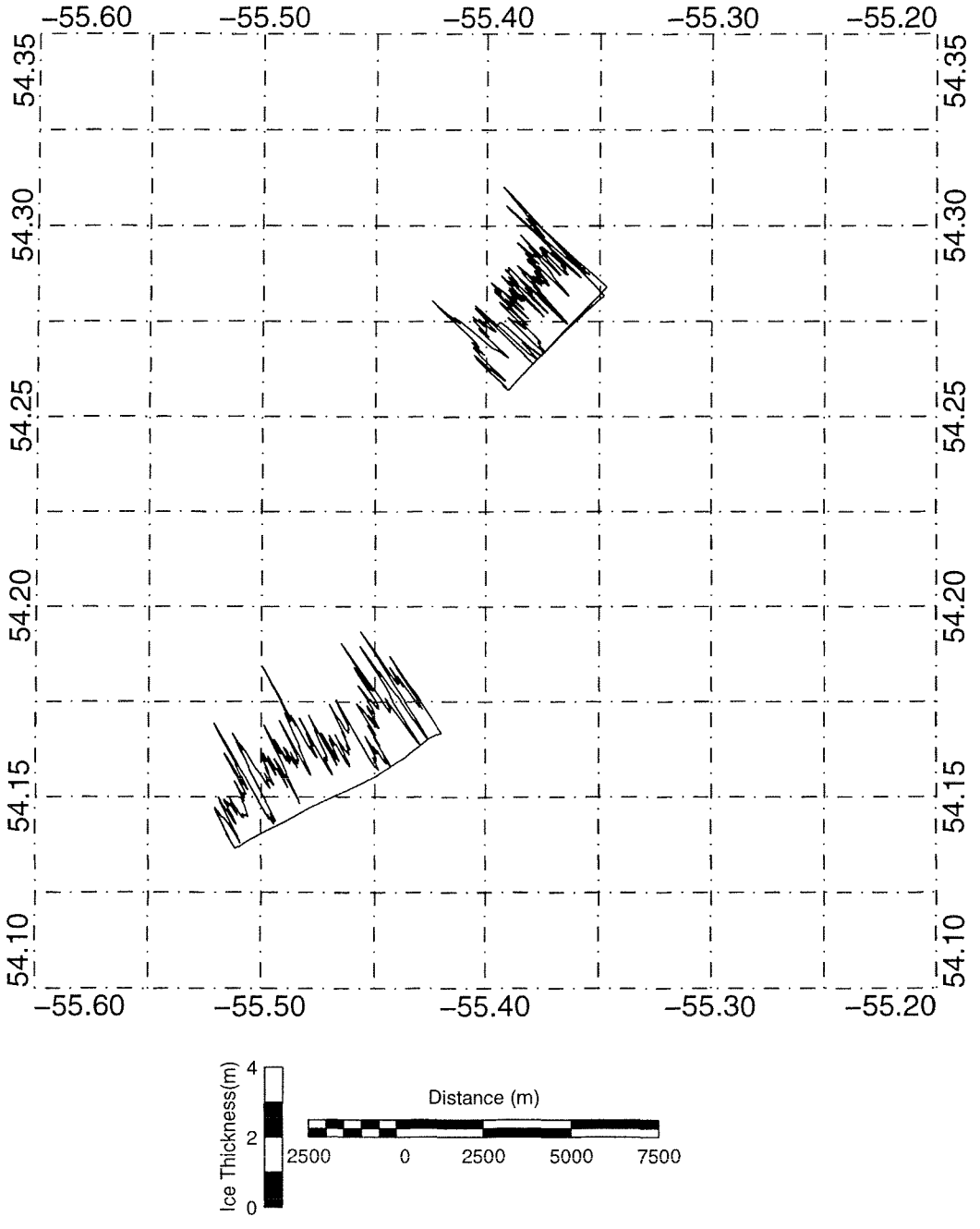

MARCH 3, 1994 FLIGHT 12
Lambert Conic Proj., Center Long.: −55.35, Lat1 49.00, Lat2 77.00
Ice Thickness 1 cm/2 m, Map Scale 1:50000

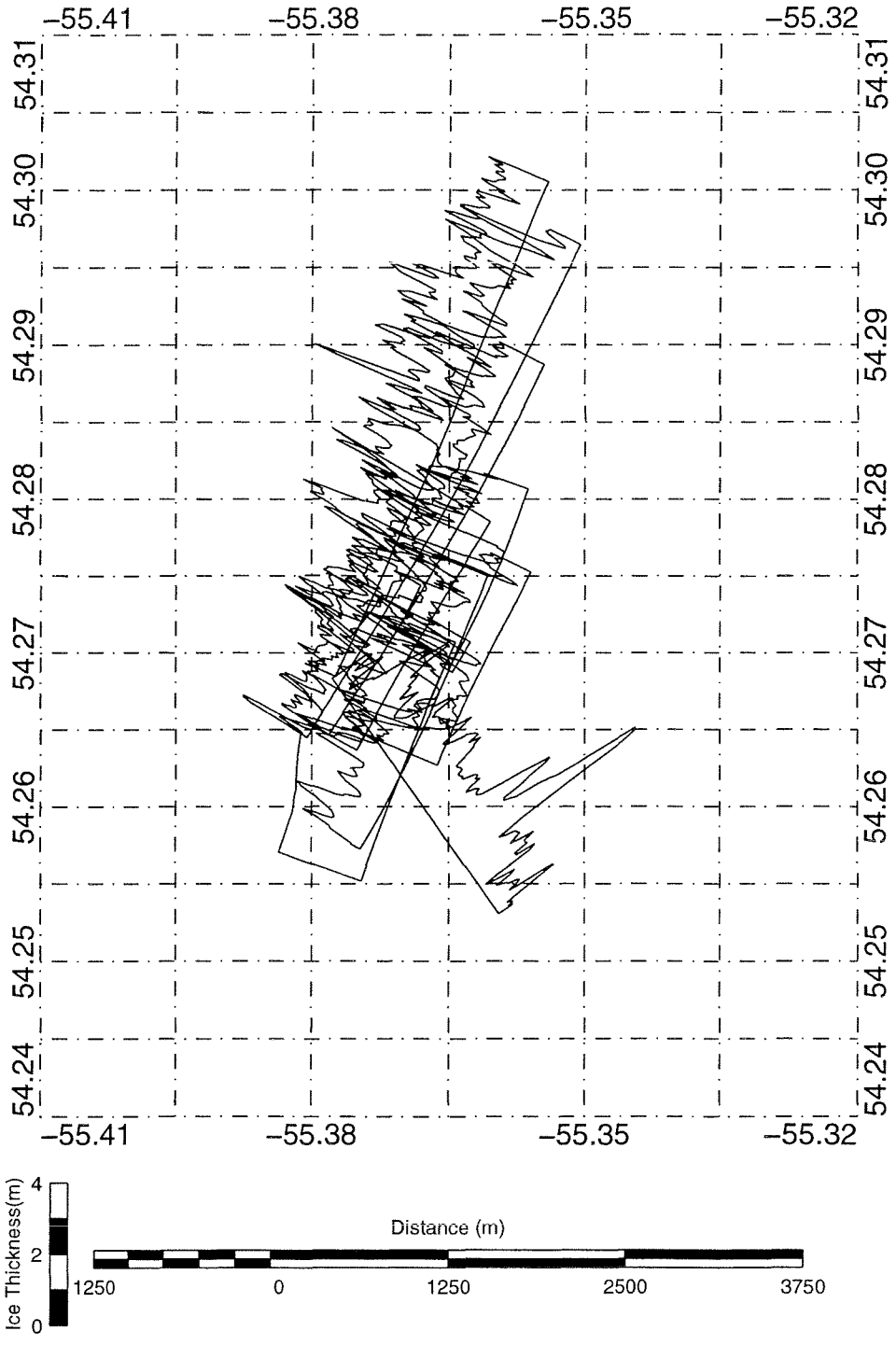

MARCH 3, 1994 FLIGHT 14
Lambert Conic Proj., Center Long.: -56.50, Lat1 49.00, Lat2 77.00
Ice Thickness 1 cm/2 m, Map Scale 1:575000

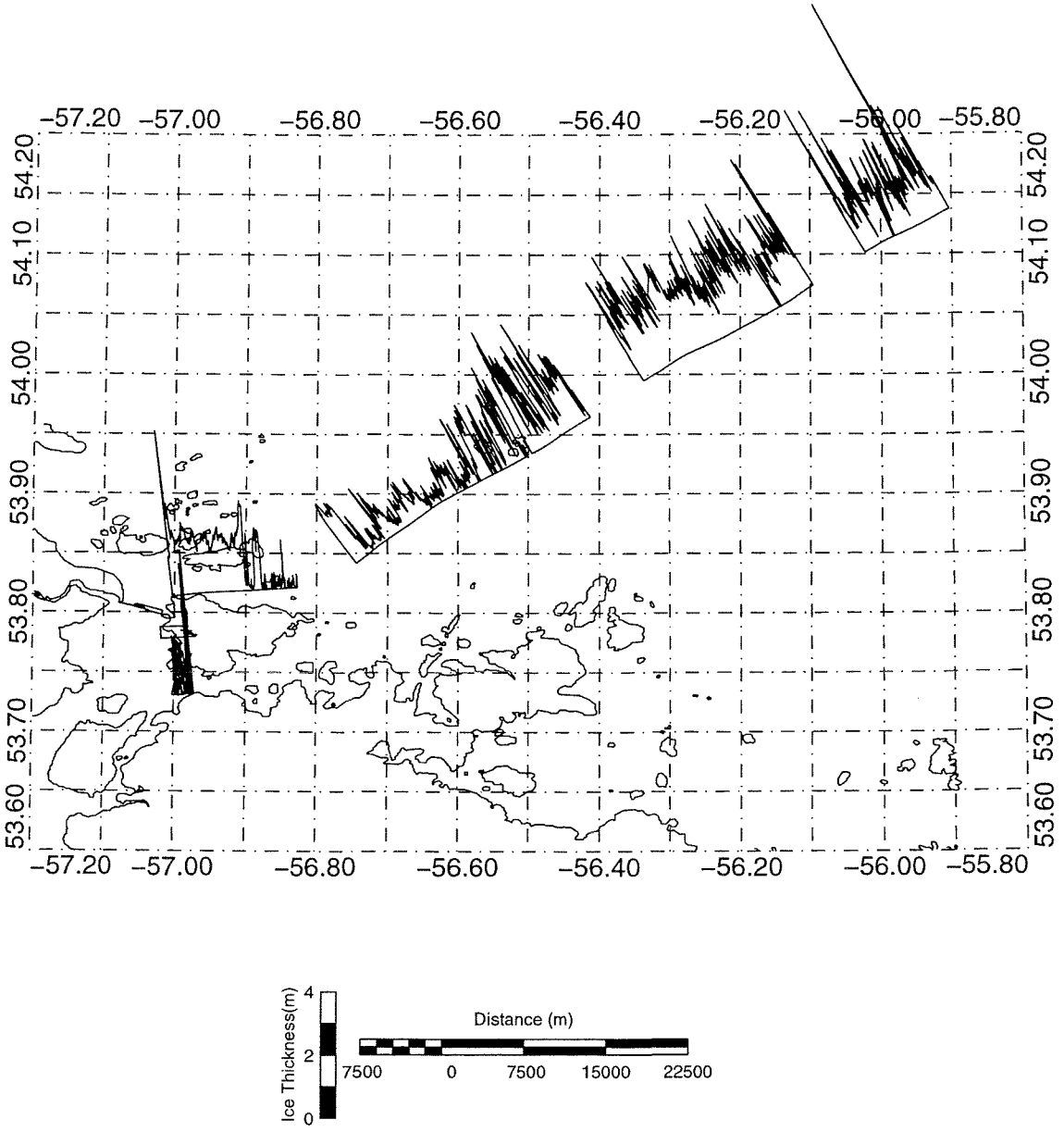

MARCH 6, 1994 FLIGHT 8
Lambert Conic Proj., Center Long.: −55.40, Lat1 49.00, Lat2 77.00
Ice Thickness 1 cm/2 m, Map Scale 1:350000

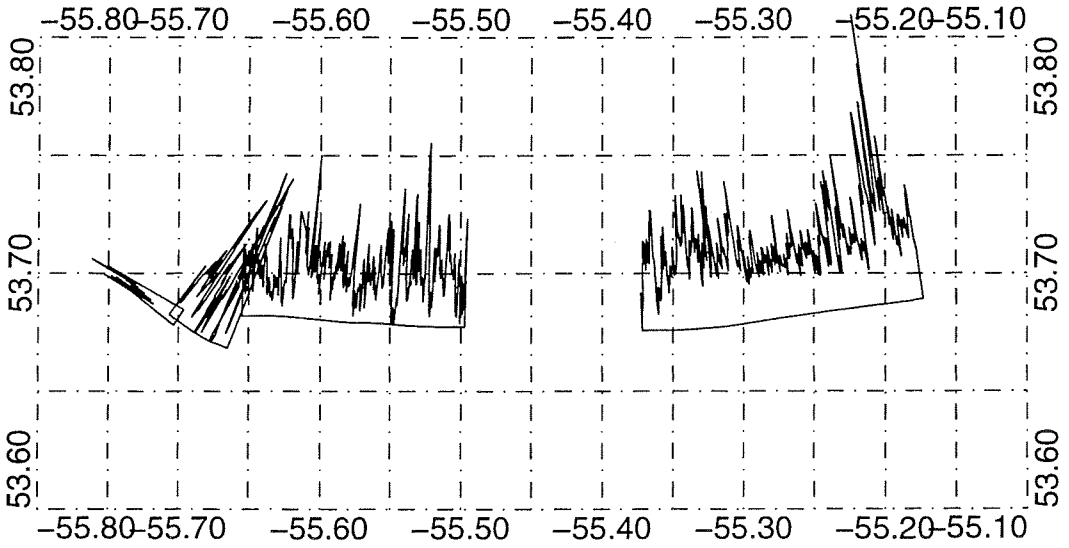

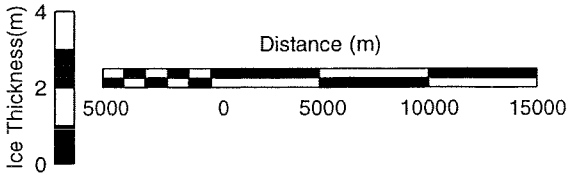

MARCH 6, 1994 FLIGHT 9
Lambert Conic Proj., Center Long.: −56.00, Lat1 49.00, Lat2 77.00
Ice Thickness 1 cm/2 m, Map Scale 1:625000

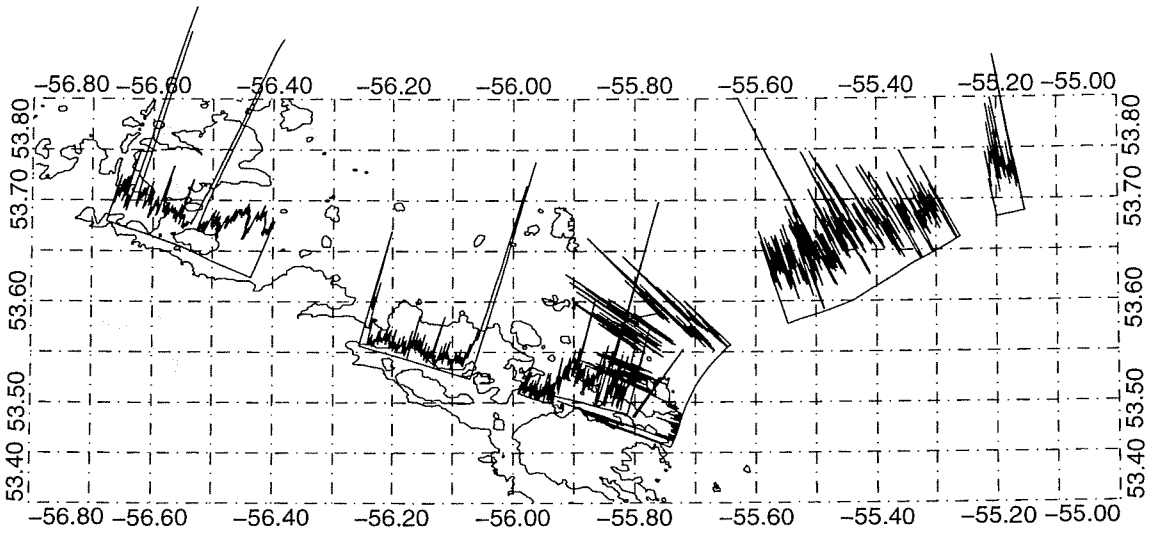

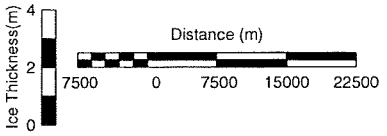

MARCH 6, 1994 FLIGHT 13
Lambert Conic Proj., Center Long.: −56.30, Lat1 49.00, Lat2 77.00
Ice Thickness 1 cm/2 m, Map Scale 1:625000

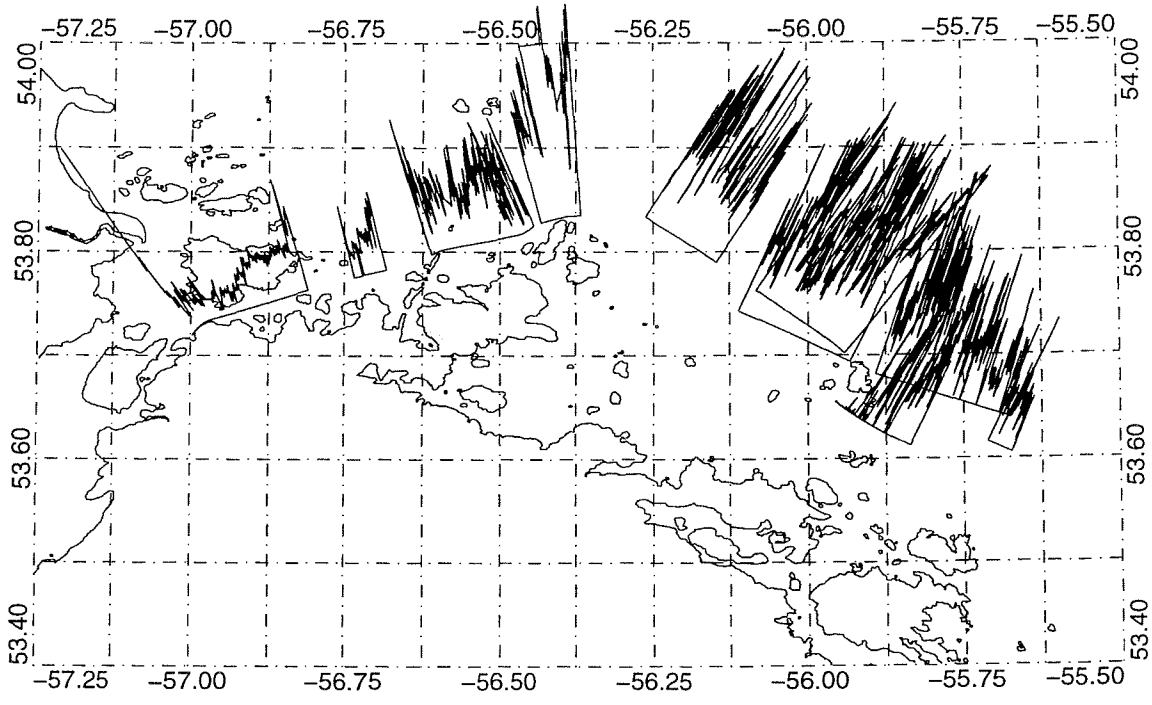

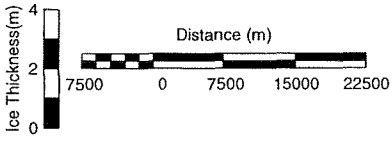

MARCH 7, 1994 FLIGHT 1
Lambert Conic Proj., Center Long.: −56.43, Lat1 49.00, Lat2 77.00
Ice Thickness 1 cm/2 m, Map Scale 1:1100000

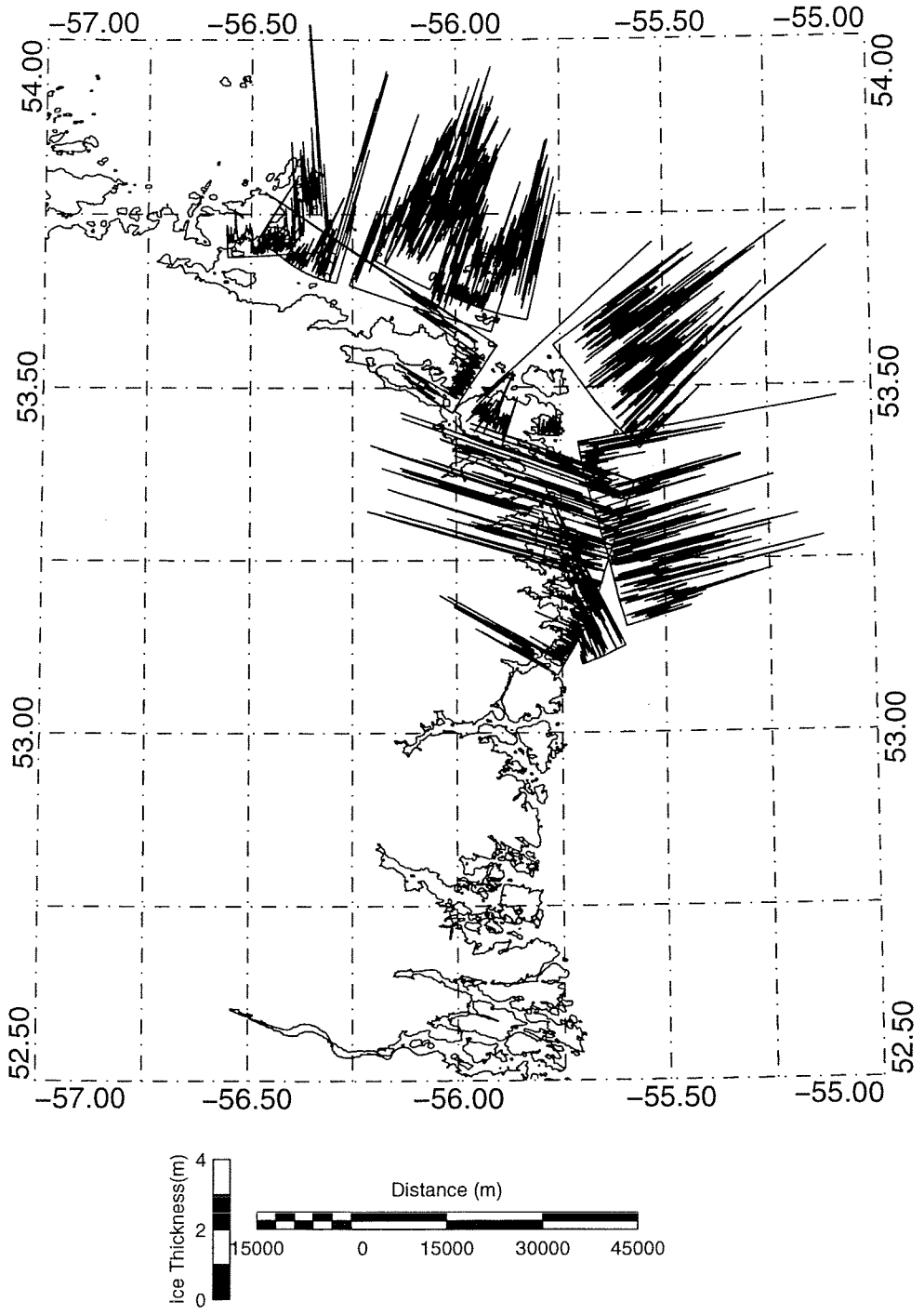

MARCH 7, 1994 FLIGHT 2
Lambert Conic Proj., Center Long.: –56.60, Lat1 49.00, Lat2 77.00
Ice Thickness 1 cm/2 m, Map Scale 1:1100000

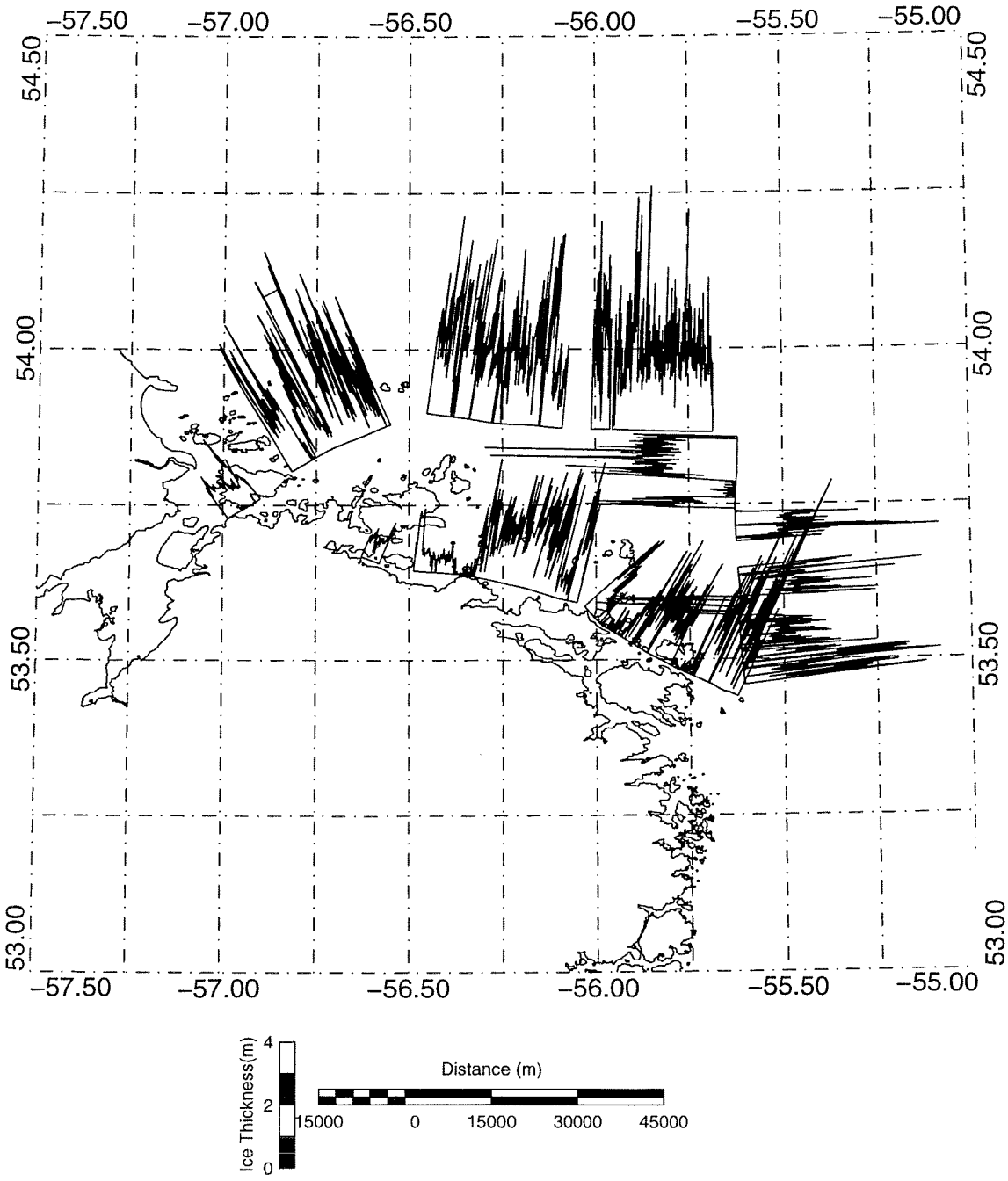

MARCH 9, 1994 FLIGHT 1
Lambert Conic Proj., Center Long.: −56.60, Lat1 49.00, Lat2 77.00
Ice Thickness 1 cm/2 m, Map Scale 1:700000

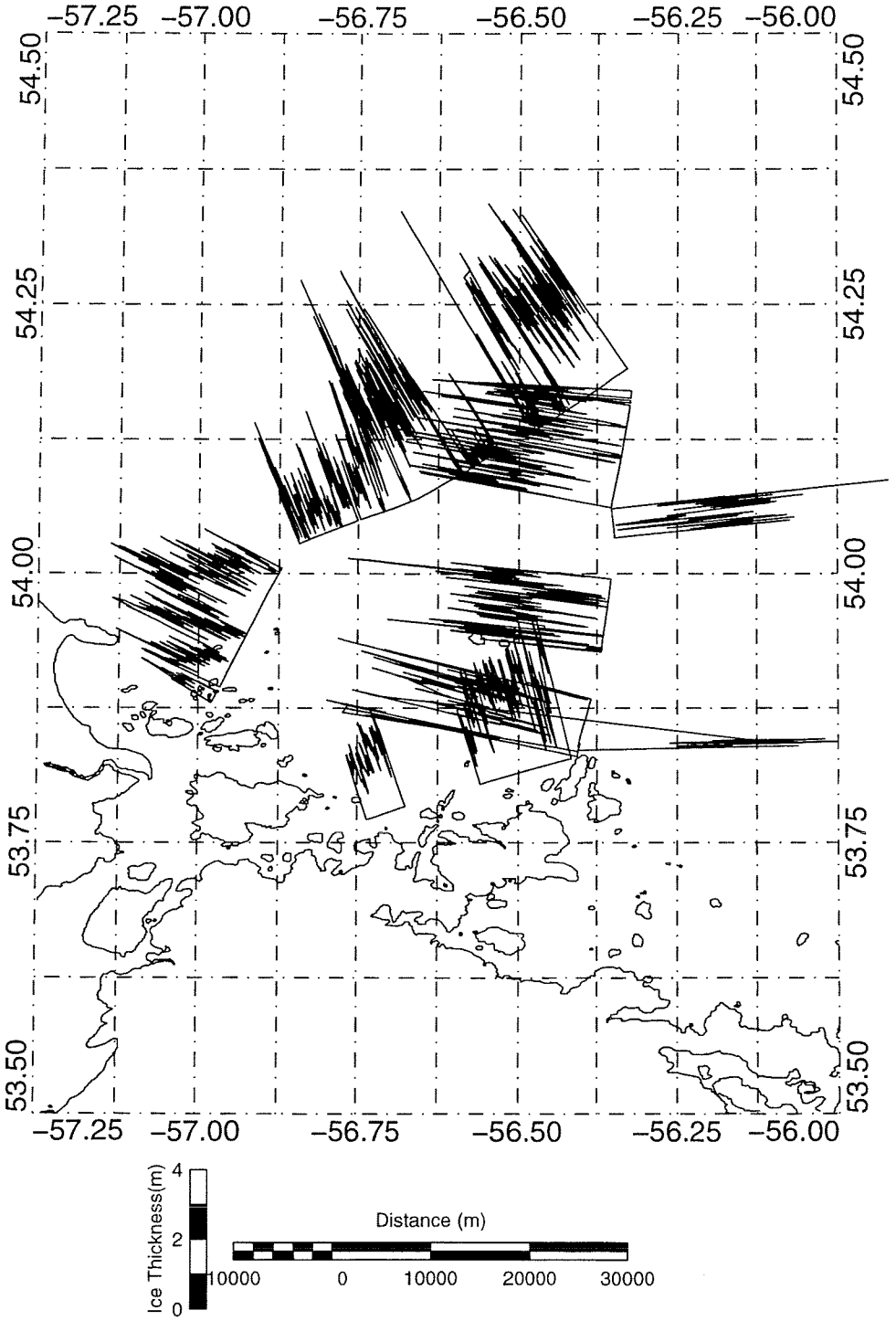

D. FLIGHT LINE STATISTICS

DATE: MAR03 Total Length: 4.415 km
FLIGHT # 08

Line	Start		End		Number of	Length of	Ice Thickness		Average	Average
Number	Lat. (deg. N)	Long. (deg. W)	Lat. (deg. N)	Long. (deg. W)	Samples	Line/Seg. (km)	Mean	Stdv.	Spacing (s)	Spacing (m)
10010	53.8654	-56.2862	53.8845	-56.2347	267	4.003	2.83	0.995		
	53.8845	-56.2347	53.8865	-56.2294	33	0.412	2.48	0.707		
Total	53.8654	-56.2862	53.8865	-56.2294	299	4.415	2.79	0.974	0.4	14.77

DATE: MAR03 Total Length: 13.866 km
FLIGHT #: 11

Line	Start		End		Number of	Length of	Ice Thickness		Average	Average
Number	Lat. (deg. N)	Long. (deg. W)	Lat. (deg. N)	Long. (deg. W)	Samples ICE	Line/Seg. (km)	Mean (m)	Stdv. (m)	Spacing (s)	Spacing (m)
10010	54.1364	-55.5115	54.1531	-55.4571	257	4.01	1.42	0.657		
	54.1531	-55.4571	54.1667	-55.4198	178	2.877	1.41	0.772		
Total	54.1364	-55.5115	54.1667	-55.4198	434	6.888	1.42	0.706	0.4	15.87
10021	54.2639	-55.3794	54.2816	-55.3481	200	2.841	1.54	0.844		
Total	54.2639	-55.3794	54.2816	-55.3481	200	2.841	1.54	0.844	0.4	14.2
10022	54.284	-55.3469	54.2577	-55.3891	305	4.003	1.56	0.666		
	54.2577	-55.3891	54.2568	-55.3904	14	0.134	0.7	0.512		
Total	54.284	-55.3469	54.2568	-55.3904	318	4.137	1.53	0.68	0.4	13.01

DATE: MAR03 Total Length: 22.570 km
FLIGHT #: 12

Line	Start		End		Number of	Length of	Ice Thickness		Average	Average
Number	Lat. (deg. N)	Long. (deg. W)	Lat. (deg. N)	Long. (deg. W)	Samples ICE	Line/Seg. (km)	Mean (m)	Stdv. (m)	Spacing (s)	Spacing (m)
10010	54.2637	-55.3750	54.2785	-55.3604	118	1.907	1.45	1.028		
Total	54.2637	-55.3750	54.2785	-55.3604	118	1.907	1.45	1.028	0.4	16.16
10020	54.2887	-55.3545	54.2647	-55.3781	254	3.092	1.24	0.656		
Total	54.2887	-55.3545	54.2647	-55.3781	254	3.092	1.24	0.656	0.4	12.17
10030	54.2645	-55.3805	54.2961	-55.3509	235	4.010	1.30	0.763		
	54.2961	-55.3509	54.2965	-55.3505	5	0.049	0.91	0.153		
Total	54.2645	-55.3805	54.2965	-55.3505	239	4.060	1.29	0.758	0.4	16.99
10040	54.3006	-55.3541	54.2685	-55.3774	304	3.880	1.37	0.686		
Total	54.3006	-55.3541	54.2685	-55.3774	304	3.880	1.37	0.686	0.4	12.76
10050	54.2710	-55.3757	54.2738	-55.3722	33	0.386	1.15	0.431		
Total	54.2710	-55.3757	54.2738	-55.3722	33	0.386	1.15	0.431	0.4	11.71
10061	54.2707	-55.3643	54.2552	-55.3745	159	1.850	1.88	1.051		
Total	54.2707	-55.3643	54.2552	-55.3745	159	1.850	1.88	1.051	0.4	11.63
10062	54.2572	-55.3746	54.2750	-55.3608	135	2.175	1.44	0.804		
Total	54.2572	-55.3746	54.2750	-55.3608	135	2.175	1.44	0.804	0.4	16.11

DATE: MAR03 Total Length: 22.570 km
FLIGHT #: 12

Line	Start		End		Number of	Length of	Ice Thickness		Average	Average
Number	Lat. (deg. N)	Long. (deg. W)	Lat. (deg. N)	Long. (deg. W)	Samples ICE	Line/Seg. (km)	Mean (m)	Stdv. (m)	Spacing (s)	Spacing (m)
10063	54.2807	-55.3563	54.2695	-55.3645	148	1.350	1.57	0.742		
Total	54.2807	-55.3563	54.2695	-55.3645	148	1.350	1.57	0.742	0.4	9.12
10070	54.2687	-55.3646	54.2707	-55.3627	29	0.250	1.62	0.832		
Total	54.2687	-55.3646	54.2707	-55.3627	29	0.250	1.62	0.832	0.4	8.61
10081	54.2753	-55.3560	54.2627	-55.3663	129	1.549	1.23	0.868		
Total	54.2753	-55.3560	54.2627	-55.3663	129	1.549	1.23	0.868	0.4	12.01
10082	54.2531	-55.3595	54.2683	-55.3777	158	2.071	1.76	1.022		
Total	54.2531	-55.3595	54.2683	-55.3777	158	2.071	1.76	1.022	0.4	13.11

DATE: MAR03 Total Length: 69.323 km
FLIGHT #: 14

Line	Start		End		Number of	Length of	Ice Thickness		Average	Average
Number	Lat. (deg. N)	Long. (deg. W)	Lat. (deg. N)	Long. (deg. W)	Samples ICE	Line/Seg. (km)	Mean	Stdv.	Spacing (s)	Spacing (m)
10010	54.1378	-55.9029	54.1210	-55.9573	271	4.014	1.68	0.886		
	54.1210	-55.9573	54.1049	-56.0121	270	3.997	1.69	0.712		
	54.1049	-56.0121	54.1015	-56.0222	56	0.763	1.83	0.981		
Total	54.1378	-55.9029	54.1015	-56.0222	595	8.774	1.70	0.823	0.4	14.75
10020	54.0744	-56.0960	54.0551	-56.1477	262	4.005	1.65	0.723		
	54.0551	-56.1477	54.0379	-56.2015	266	4.008	2.19	0.519		
	54.0379	-56.2015	54.0220	-56.2562	258	3.996	1.85	0.460		
	54.0220	-56.2562	54.0045	-56.3094	256	3.992	2.18	0.479		
	54.0045	-56.3094	53.9946	-56.3372	141	2.134	2.32	0.702		
Total	54.0744	-56.0960	53.9946	-56.3372	1179	18.134	2.01	0.624	0.4	15.38
10030	53.9647	-56.4131	53.9449	-56.4642	246	4.008	1.67	0.793		
	53.9449	-56.4642	53.9342	-56.4948	144	2.330	1.91	1.002		
Total	53.9647	-56.4131	53.9342	-56.4948	389	6.338	1.76	0.884	0.4	16.29
10040	53.9326	-56.5002	53.9156	-56.5542	241	4.017	1.28	0.897		
	53.9156	-56.5542	53.8987	-56.6079	234	3.989	0.79	0.661		
	53.8987	-56.6079	53.8787	-56.6586	239	4.010	0.55	0.343		
	53.8787	-56.6586	53.8583	-56.7085	234	3.989	0.69	0.383		
	53.8583	-56.7085	53.8417	-56.7431	175	2.925	1.11	0.806		
Total	53.9326	-56.5002	53.8417	-56.7431	1119	18.930	0.87	0.702	0.4	16.92

DATE: MAR03 Total Length: 69.323 km
FLIGHT #: 14

Line	Start		End		Number of	Length of	Ice Thickness		Average	Average
Number	Lat. (deg. N)	Long. (deg. W)	Lat. (deg. N)	Long. (deg. W)	Samples ICE	Line/Seg. (km)	Mean	Stdv.	Spacing (s)	Spacing (m)
10050	53.8214	-56.8271	53.8189	-56.8880	244	4.011	0.40	0.603		
	53.8189	-56.8880	53.8170	-56.9487	243	3.993	1.48	0.694		
	53.8170	-56.9487	53.8132	-57.0025	219	3.563	1.87	0.483		
Total	53.8214	-56.8271	53.8132	-57.0025	704	11.568	1.23	0.867	0.4	16.43
10060	53.8014	-57.0163	53.7982	-57.0177	29	0.370	0.81	0.243		
Total	53.8014	-57.0163	53.7982	-57.0177	29	0.370	0.81	0.243	0.4	12.75
10070	53.7876	-57.0191	53.7779	-57.0181	69	1.088	0.87	0.134		
Total	53.7876	-57.0191	53.7779	-57.0181	69	1.088	0.87	0.134	0.4	15.77
10080	53.7309	-56.9884	53.7314	-56.9832	34	0.343	0.78	0.189		
Total	53.7309	-56.9884	53.7314	-56.9832	34	0.343	0.78	0.189	0.4	10.08
10090	53.7318	-56.9779	53.7318	-56.9761	17	0.116	1.93	1.000		
Total	53.7318	-56.9779	53.7318	-56.9761	17	0.116	1.93	1.000	0.4	6.84
10100	53.7309	-56.9870	53.7313	-56.9838	29	0.216	1.13	0.389		
Total	53.7309	-56.9870	53.7313	-56.9838	29	0.216	1.13	0.389	0.4	7.46
10111	53.7316	-56.9794	53.7318	-56.9744	33	0.325	2.42	1.088		
Total	53.7316	-56.9794	53.7318	-56.9744	33	0.325	2.42	1.088	0.4	9.84

DATE: MAR03 Total Length: 69.323 km
FLIGHT #: 14

Line	Start		End		Number of	Length of	Ice Thickness		Average	Average
Number	Lat. (deg. N)	Long. (deg. W)	Lat. (deg. N)	Long. (deg. W)	Samples ICE	Line/Seg. (km)	Mean	Stdv.	Spacing (s)	Spacing (m)
10112	53.7309	-56.9959	53.7307	-56.9947	15	0.084	0.47	0.363		
Total	53.7309	-56.9959	53.7307	-56.9947	15	0.084	0.47	0.363	0.4	5.59
10113	53.7305	-56.9930	53.7311	-56.9845	49	0.563	1.16	0.312		
Total	53.7305	-56.9930	53.7311	-56.9845	49	0.563	1.16	0.312	0.4	11.50
10121	53.7314	-56.9789	53.7316	-56.9754	24	0.230	1.39	0.635		
Total	53.7314	-56.9789	53.7316	-56.9754	24	0.230	1.39	0.635	0.4	9.59
10122	53.7307	-56.9931	53.7318	-56.9812	58	0.795	0.69	0.452		
Total	53.7307	-56.9931	53.7318	-56.9812	58	0.795	0.69	0.452	0.4	13.71
10131	53.7323	-56.9770	53.7326	-56.9722	30	0.317	1.69	1.011		
Total	53.7323	-56.9770	53.7326	-56.9722	30	0.317	1.69	1.011	0.4	10.57
10132	53.7309	-57.0021	53.7304	-56.9978	30	0.287	0.47	0.356		
Total	53.7309	-57.0021	53.7304	-56.9978	30	0.287	0.47	0.356	0.4	9.56
10133	53.7304	-56.9959	53.7313	-56.9832	68	0.845	0.91	0.177		
Total	53.7304	-56.9959	53.7313	-56.9832	68	0.845	0.91	0.177	0.4	12.42

DATE: MAR06 Total Length: 34.573 km
FLIGHT #: 08

Line	Start		End		Number of	Length of	Ice Thickness		Average	Average
Number	Lat. (deg. N)	Long. (deg. W)	Lat. (deg. N)	Long. (deg. W)	Samples ICE	Line/Seg. (km)	Mean (m)	Stdv. (m)	Spacing (s)	Spacing (m)
10010	53.6781	-55.7036	53.6846	-55.6964	74	0.863	1.48	0.443		
Total	53.6781	-55.7036	53.6846	-55.6964	74	0.863	1.48	0.443	0.4	11.66
10021	53.6827	-55.7067	53.6683	-55.6647	183	3.213	1.69	1.101		
Total	53.6827	-55.7067	53.6683	-55.6647	183	3.213	1.69	1.101	0.4	17.56
10023	53.6820	-55.6547	53.6800	-55.5939	228	4.016	1.39	0.613		
	53.6800	-55.5939	53.6779	-55.5335	223	3.995	1.36	0.690		
	53.6779	-55.5335	53.6773	-55.4974	133	2.382	1.57	0.873		
Total	53.6820	-55.6547	53.6773	-55.4974	582	10.393	1.41	0.708	0.4	17.86
10030	53.6757	-55.3716	53.6775	-55.3110	224	4.001	2.02	0.701		
	53.6775	-55.3110	53.6829	-55.2508	223	4.016	1.77	0.476		
	53.6829	-55.2508	53.6876	-55.1908	229	3.993	2.32	1.215		
	53.6876	-55.1908	53.6892	-55.1731	71	1.180	2.11	0.507		
Total	53.6757	-55.3716	53.6892	-55.1731	744	13.189	2.04	0.857	0.4	17.73
10040	53.6970	-55.1179	53.7057	-55.0648	219	3.636	1.74	0.426		
Total	53.6970	-55.1179	53.7057	-55.0648	219	3.636	1.74	0.426	0.4	16.60
10050	53.7126	-55.0595	53.7167	-55.0756	129	1.152	1.14	0.540		
Total	53.7126	-55.0595	53.7167	-55.0756	129	1.152	1.14	0.540	0.4	8.93

DATE: MAR06 Total Length: 34.573 km
FLIGHT #: 08

Line	Start		End		Number of	Length of	Ice Thickness		Average	Average
Number	Lat. (deg. N)	Long. (deg. W)	Lat. (deg. N)	Long. (deg. W)	Samples ICE	Line/Seg. (km)	Mean (m)	Stdv. (m)	Spacing (s)	Spacing (m)
10060	53.7137	-55.0847	53.6946	-55.0857	134	2.127	1.47	0.364		
Total	53.7137	-55.0847	53.6946	-55.0857	134	2.127	1.47	0.364	0.4	15.87

DATE: MAR06 Total Length: 81.000 km
FLIGHT #: 09

Line	Start		End		Number of	Length of	Ice Thickness		Average	Average
Number	Lat. (deg. N)	Long. (deg. W)	Lat. (deg. N)	Long. (deg. W)	Samples ICE	Line/Seg. (km)	Mean (m)	Stdv. (m)	Spacing (s)	Spacing (m)
10010	53.6879	-55.1532	53.6823	-55.1994	274	3.111	1.83	0.721		
Total	53.6879	-55.1532	53.6823	-55.1994	274	3.111	1.83	0.721	0.4	11.35
10020	53.6628	-55.2598	53.6450	-55.3123	304	4.002	1.35	0.663		
	53.6450	-55.3123	53.6271	-55.3650	308	4.009	1.69	0.835		
	53.6271	-55.3650	53.6084	-55.4166	297	3.994	2.26	0.807		
	53.6084	-55.4166	53.5929	-55.4709	296	3.997	2.26	0.928		
	53.5929	-55.4709	53.5815	-55.5283	317	4.003	1.87	0.669		
	53.5815	-55.5283	53.5776	-55.5463	101	1.266	2.14	0.474		
Total	53.6628	-55.2598	53.5776	-55.5463	1618	21.271	1.90	0.841	0.4	13.15

DATE: MAR06 Total Length: 81.000 km
FLIGHT #: 09

Line	Start		End		Number of	Length of	Ice Thickness		Average	Average
Number	Lat. (deg. N)	Long. (deg. W)	Lat. (deg. N)	Long. (deg. W)	Samples ICE	Line/Seg. (km)	Mean (m)	Stdv. (m)	Spacing (s)	Spacing (m)
10030	53.5569	-55.6415	53.5308	-55.6829	277	4.003	2.14	1.365		
	53.5308	-55.6829	53.4999	-55.7132	270	3.998	2.74	0.918		
	53.4999	-55.7132	53.4660	-55.7333	249	4.003	0.58	0.963		
	53.4660	-55.7333	53.4556	-55.7412	86	1.274	1.38	1.298		
Total	53.5569	-55.6415	53.4556	-55.7412	879	13.278	1.81	1.415	0.4	15.11
10040	53.4849	-55.8011	53.4859	-55.8034	24	0.189	1.37	0.554		
Total	53.4849	-55.8011	53.4859	-55.8034	24	0.189	1.37	0.554	0.4	7.87
10050	53.4881	-55.8121	53.4972	-55.8705	348	4.003	1.07	0.890		
	53.4972	-55.8705	53.5063	-55.9291	341	4.008	0.96	0.419		
	53.5063	-55.9291	53.5087	-55.9486	117	1.319	0.32	0.237		
Total	53.4881	-55.8121	53.5087	-55.9486	804	9.330	0.91	0.698	0.4	11.60
10070	53.5234	-56.0703	53.5340	-56.1282	330	4.011	1.34	2.069		
	53.5340	-56.1282	53.5446	-56.1860	318	3.999	0.48	0.275		
	53.5446	-56.1860	53.5543	-56.2441	307	3.993	0.41	0.160		
	53.5543	-56.2441	53.5566	-56.2561	67	0.834	1.58	0.937		
Total	53.5234	-56.0703	53.5566	-56.2561	1019	12.837	0.81	1.297	0.4	12.60

DATE: MAR06 Total Length: 81.000 km
FLIGHT #: 09

Line	Start		End		Number of	Length of	Ice Thickness		Average	Average
Number	Lat. (deg. N)	Long. (deg. W)	Lat. (deg. N)	Long. (deg. W)	Samples ICE	Line/Seg. (km)	Mean (m)	Stdv. (m)	Spacing (s)	Spacing (m)
10080	53.6239	-56.4367	53.6379	-56.4926	311	4.003	1.89	0.268		
	53.6379	-56.4926	53.6532	-56.5475	315	4.003	1.73	1.707		
	53.6532	-56.5475	53.6655	-56.6045	304	4.005	1.37	1.321		
	53.6655	-56.6045	53.6771	-56.6618	315	3.996	2.12	2.544		
	53.6771	-56.6618	53.6796	-56.6762	83	0.991	1.18	0.258		
Total	53.6239	-56.4367	53.6796	-56.6762	1324	16.998	1.74	1.646	0.4	12.84
10060e	53.4986	-55.9347	53.5096	-55.9918	358	3.986	0.31	0.213		
Total	53.4986	-55.9347	53.5096	-55.9918	358	3.986	0.31	0.213	0.4	11.08

DATE: MAR06 Total Length: 92.776 km
FLIGHT #: 13

Line	Start		End		Number of	Length of	Ice Thickness		Average	Average
Number	Lat. (deg. N)	Long. (deg. W)	Lat. (deg. N)	Long. (deg. W)	Samples ICE	Line/Seg. (km)	Mean (m)	Stdv. (m)	Spacing (s)	Spacing (m)
10010	53.7428	-56.1099	53.7280	-56.0544	222	4.012	3.530	1.385		
	53.7280	-56.0544	53.7130	-55.9993	219	3.993	3.310	1.793		
	53.7130	-55.9993	53.6972	-55.9446	225	4.010	5.000	1.937		
	53.6972	-55.9446	53.6937	-55.9324	56	0.896	6.660	1.252		
Total	53.7428	-56.1099	53.6937	-55.9324	719	12.911	4.160	1.971	0.4	17.960
10020	53.6547	-55.9566	53.6344	-55.9065	223	4.008	0.310	0.662		
	53.6344	-55.9065	53.6172	-55.8534	216	4.000	2.120	1.436		
	53.6172	-55.8534	53.6124	-55.8369	72	1.207	2.920	1.076		
Total	53.6547	-55.9566	53.6124	-55.8369	509	9.215	1.440	1.513	0.4	18.100
10030	53.6158	-55.7112	53.6060	-55.6747	160	2.646	1.690	0.658		
Total	53.6158	-55.7112	53.6060	-55.6747	160	2.646	1.690	0.658	0.4	16.540
10040	53.6406	-55.6802	53.6515	-55.7379	331	4.002	1.520	0.962		
	53.6515	-55.7379	53.6629	-55.7954	334	4.001	2.180	0.993		
	53.6629	-55.7954	53.6741	-55.8531	349	4.004	3.340	1.484		
	53.6741	-55.8531	53.6822	-55.8913	222	2.676	2.810	1.212		
Total	53.6406	-55.6802	53.6822	-55.8913	1233	14.682	2.440	1.376	0.4	11.910

DATE: MAR06 Total Length: 92.776 km
FLIGHT #: 13

Line	Start		End		Number of	Length of	Ice Thickness		Average	Average
Number	Lat. (deg. N)	Long. (deg. W)	Lat. (deg. N)	Long. (deg. W)	Samples ICE	Line/Seg. (km)	Mean (m)	Stdv. (m)	Spacing (s)	Spacing (m)
10050	53.7018	-55.9410	53.7241	-55.9887	343	4.005	4.850	1.636		
	53.7241	-55.9887	53.7446	-56.0385	318	4.001	4.010	1.440		
	53.7446	-56.0385	53.7629	-56.0823	300	3.525	4.180	1.813		
Total	53.7018	-55.9410	53.7629	-56.0823	959	11.531	4.360	1.671	0.4	12.020
10060	53.7898	-56.1465	53.8098	-56.1972	315	4.013	3.370	1.257		
	53.8098	-56.1972	53.8283	-56.2493	328	3.999	4.330	1.362		
	53.8283	-56.2493	53.8335	-56.2625	88	1.037	3.340	1.210		
Total	53.7898	-56.1465	53.8335	-56.2625	729	9.049	3.800	1.384	0.4	12.410
10070	53.8348	-56.3666	53.8286	-56.4266	301	4.011	4.600	1.193		
	53.8286	-56.4266	53.8280	-56.4303	24	0.257	3.070	0.424		
Total	53.8348	-56.3666	53.8280	-56.4303	324	4.268	4.490	1.221	0.4	13.170
10081	53.8251	-56.4422	53.8127	-56.4983	318	4.004	1.760	0.917		
	53.8127	-56.4983	53.8062	-56.5581	305	3.997	2.160	0.656		
	53.8062	-56.5581	53.7971	-56.6105	267	3.618	2.100	0.672		
Total	53.8251	-56.4422	53.7971	-56.6105	888	11.619	2.000	0.783	0.4	13.080
10082	53.7826	-56.6835	53.7775	-56.7186	180	2.378	1.440	0.477		
Total	53.7826	-56.6835	53.7775	-56.7186	180	2.378	1.440	0.477	0.4	13.210

DATE: MAR06 Total Length: 92.776 km
FLIGHT #: 13

Line	Start		End		Number of	Length of	Ice Thickness		Average	Average
Number	Lat. (deg. N)	Long. (deg. W)	Lat. (deg. N)	Long. (deg. W)	Samples ICE	Line/Seg. (km)	Mean (m)	Stdv. (m)	Spacing (s)	Spacing (m)
10091	53.7772	-56.7205	53.7753	-56.7334	73	0.874	1.030	0.399		
Total	53.7772	-56.7205	53.7753	-56.7334	73	0.874	1.030	0.399	0.4	11.980
10092	53.7629	-56.8087	53.7524	-56.8670	289	4.012	1.740	0.464		
	53.7524	-56.8670	53.7417	-56.9248	279	3.992	1.280	0.362		
	53.7417	-56.9248	53.7299	-56.9819	287	4.000	0.820	0.262		
	53.7299	-56.9819	53.7191	-56.9976	115	1.599	1.990	1.833		
Total	53.7629	-56.8087	53.7191	-56.9976	967	13.603	1.370	0.834	0.4	14.070

DATE: MAR07 Total Length: 199.787 km
FLIGHT #: 01

Line	Start		End		Number of	Length of	Ice Thickness		Average	Average
Number	Lat. (deg. N)	Long. (deg. W)	Lat. (deg. N)	Long. (deg. W)	Samples ICE	Line/Seg. (km)	Mean (m)	Stdv. (m)	Spacing (s)	Spacing (m)
10010	53.6882	-56.5551	53.6896	-56.4943	232	4.015	0.66	0.178		
	53.6896	-56.4943	53.6916	-56.4339	222	3.987	0.33	0.192		
	53.6916	-56.4339	53.6938	-56.3733	225	4.006	0.80	0.569		
	53.6938	-56.3733	53.6966	-56.3128	229	4.002	2.11	1.610		
	53.6966	-56.3128	53.6968	-56.3048	35	0.523	1.16	0.700		
Total	53.6882	-56.5551	53.6968	-56.3048	939	16.532	0.99	1.087	0.4	17.61
10020	53.6837	-56.1973	53.6665	-56.1441	235	4.003	2.37	1.148		
	53.6665	-56.1441	53.6498	-56.0902	231	4.009	2.14	1.005		
	53.6498	-56.0902	53.6416	-56.0622	120	2.064	3.10	0.788		
Total	53.6837	-56.1973	53.6416	-56.0622	584	10.076	2.43	1.085	0.4	17.25
10030	53.6409	-56.0507	53.6277	-55.9942	236	4.006	1.49	1.219		
	53.6277	-55.9942	53.6145	-55.9378	232	4.006	0.17	0.176		
	53.6145	-55.9378	53.6039	-55.8800	221	4.001	1.98	1.333		
	53.6039	-55.8800	53.5972	-55.8296	193	3.410	2.44	1.137		
Total	53.6409	-56.0507	53.5972	-55.8296	879	15.423	1.48	1.359	0.4	17.55

DATE: MAR07 Total Length: 199.787 km
FLIGHT #: 01

Line	Start		End		Number of	Length of	Ice Thickness		Average	Average
Number	Lat. (deg. N)	Long. (deg. W)	Lat. (deg. N)	Long. (deg. W)	Samples ICE	Line/Seg. (km)	Mean (m)	Stdv. (m)	Spacing (s)	Spacing (m)
10040	53.5611	-55.7668	53.5322	-55.7309	235	4.000	2.30	0.995		
	53.5322	-55.7309	53.5033	-55.6950	233	4.004	2.83	1.492		
	53.5033	-55.6950	53.4744	-55.6590	229	4.007	2.00	0.980		
	53.4744	-55.6590	53.4470	-55.6199	221	3.997	2.02	1.084		
	53.4470	-55.6199	53.4212	-55.5781	222	3.992	1.56	1.546		
	53.4212	-55.5781	53.4107	-55.5592	99	1.713	0.80	0.624		
Total	53.5611	-55.7668	53.4107	-55.5592	1234	21.714	2.04	1.311	0.4	17.60
10050	53.3629	-55.5715	53.3292	-55.5924	255	4.008	2.12	1.645		
	53.3292	-55.5924	53.2954	-55.6127	254	4.006	2.40	1.838		
	53.2954	-55.6127	53.2612	-55.6307	251	3.988	2.08	2.081		
	53.2612	-55.6307	53.2269	-55.6489	254	4.007	1.73	1.598		
	53.2269	-55.6489	53.2131	-55.6553	109	1.599	1.64	2.004		
Total	53.3629	-55.5715	53.2131	-55.6553	1119	17.608	2.03	1.832	0.4	15.74
10071	53.0989	-55.6999	53.1119	-55.6441	241	4.007	0.58	0.575		
	53.1119	-55.6441	53.1257	-55.5974	214	3.479	1.59	1.092		
Total	53.0989	-55.6999	53.1257	-55.5974	454	7.487	1.05	0.995	0.4	16.49

DATE: MAR07 Total Length: 199.787 km
FLIGHT #: 01

Line	Start		End		Number of	Length of	Ice Thickness		Average	Average
Number	Lat. (deg. N)	Long. (deg. W)	Lat. (deg. N)	Long. (deg. W)	Samples ICE	Line/Seg. (km)	Mean (m)	Stdv. (m)	Spacing (s)	Spacing (m)
10081	53.2819	-55.6506	53.3165	-55.6671	289	4.010	0.94	0.932		
	53.3165	-55.6671	53.3510	-55.6835	282	3.996	1.43	1.111		
	53.3510	-55.6835	53.3859	-55.6975	282	3.996	0.35	0.206		
	53.3859	-55.6975	53.4209	-55.7076	273	3.945	0.91	1.050		
Total	53.2819	-55.6506	53.4209	-55.7076	1123	15.947	0.91	0.977	0.4	14.20
10090	53.4110	-55.8923	53.4231	-55.9492	277	4.015	0.80	0.305		
	53.4231	-55.9492	53.4451	-55.9957	277	3.989	0.78	0.185		
	53.4451	-55.9957	53.4521	-56.0065	82	1.065	1.84	1.956		
Total	53.4110	-55.8923	53.4521	-56.0065	634	9.068	0.93	0.818	0.4	14.30
10100	53.4633	-56.0083	53.4938	-55.9760	270	4.009	0.74	0.547		
	53.4938	-55.9760	53.5234	-55.9421	277	3.993	0.27	0.165		
	53.5234	-55.9421	53.5534	-55.9087	273	4.005	1.00	0.896		
	53.5534	-55.9087	53.5609	-55.9000	72	1.009	2.98	1.663		
Total	53.4633	-56.0083	53.5609	-55.9000	889	13.017	0.85	1.022	0.4	14.64

DATE: MAR07 Total Length: 199.787 km
FLIGHT #: 01

Line	Start		End		Number of	Length of	Ice Thickness		Average	Average
Number	Lat. (deg. N)	Long. (deg. W)	Lat. (deg. N)	Long. (deg. W)	Samples ICE	Line/Seg. (km)	Mean (m)	Stdv. (m)	Spacing (s)	Spacing (m)
10110	53.5803	-55.9143	53.5915	-55.9719	286	4.005	2.26	0.747		
	53.5915	-55.9719	53.6026	-56.0295	275	3.999	1.95	0.799		
	53.6026	-56.0295	53.6136	-56.0873	295	4.009	1.97	1.707		
	53.6136	-56.0873	53.6243	-56.1451	282	3.996	4.47	1.162		
	53.6243	-56.1451	53.6361	-56.2023	282	4.002	2.87	0.707		
	53.6361	-56.2023	53.6478	-56.2580	289	3.897	1.94	0.897		
Total	53.5803	-55.9143	53.6478	-56.2580	1704	23.908	2.57	1.400	0.4	14.03
10120	53.6513	-56.2899	53.6616	-56.3478	293	4.002	1.76	2.389		
	53.6616	-56.3478	53.6781	-56.4018	292	4.010	0.59	0.499		
	53.6781	-56.4018	53.6994	-56.4505	282	3.996	0.29	0.232		
	53.6994	-56.4505	53.7125	-56.4846	193	2.684	0.23	0.331		
Total	53.6513	-56.2899	53.7125	-56.4846	1057	14.692	0.77	1.441	0.4	13.90
10060e	53.2107	-55.6565	53.1768	-55.6762	263	4.003	0.34	0.274		
	53.1768	-55.6762	53.1440	-55.7007	224	4.001	0.28	0.202		
	53.1440	-55.7007	53.1130	-55.7312	277	4.010	0.16	0.153		
	53.1130	-55.7312	53.0825	-55.7608	283	3.929	1.01	0.951		
Total	53.2107	-55.6565	53.0825	-55.7608	1044	15.956	0.46	0.628	0.4	14.69

DATE: MAR07 Total Length: 199.787 km
FLIGHT #: 01

Line	Start		End		Number of	Length of	Ice Thickness		Average	Average
Number	Lat. (deg. N)	Long. (deg. W)	Lat. (deg. N)	Long. (deg. W)	Samples ICE	Line/Seg. (km)	Mean (m)	Stdv. (m)	Spacing (s)	Spacing (m)
10072e	53.1536	-55.5934	53.1881	-55.6106	255	4.008	1.43	0.781		
	53.1881	-55.6106	53.2230	-55.6246	239	3.993	1.28	1.176		
	53.2230	-55.6246	53.2580	-55.6388	268	4.013	1.59	1.308		
	53.2580	-55.6388	53.2807	-55.6500	187	2.638	1.24	1.048		
Total	53.1536	-55.5934	53.2807	-55.6500	946	15.028	1.40	1.109	0.4	15.33
10082e	53.4294	-55.7535	53.4310	-55.8051	240	3.431	0.18	0.148		
Total	53.4294	-55.7535	53.4310	-55.8051	240	3.331	0.18	0.148	0.4	13.98

DATE: MAR07 Total Length: 173.695 km
FLIGHT #: 02

Line	Start		End		Number of	Length of	Ice Thickness		Average	Average
Number	Lat. (deg. N)	Long. (deg. W)	Lat. (deg. N)	Long. (deg. W)	Samples ICE	Line/Seg. (km)	Mean (m)	Stdv. (m)	Spacing (s)	Spacing (m)
10011	53.6672	-56.6265	53.6565	-56.5791	215	3.347	0.72	0.204		
Total	53.6672	-56.6265	53.6565	-56.5791	215	3.347	0.72	0.204	0.4	15.57
10012	53.6444	-56.4877	53.6415	-56.4271	255	4.015	0.79	0.532		
	53.6415	-56.4271	53.6384	-56.3694	250	3.825	0.43	0.223		
Total	53.6444	-56.4877	53.6384	-56.3694	504	7.839	0.61	0.447	0.4	15.55

DATE: MAR07 Total Length: 173.695 km
FLIGHT #: 02

Line	Start		End		Number of	Length of	Ice Thickness		Average	Average
Number	Lat. (deg. N)	Long. (deg. W)	Lat. (deg. N)	Long. (deg. W)	Samples ICE	Line/Seg. (km)	Mean (m)	Stdv. (m)	Spacing (s)	Spacing (m)
10020	53.6370	-56.3664	53.6318	-56.3065	261	4.002	0.46	0.690		
	53.6318	-56.3065	53.6236	-56.2475	258	4.003	1.82	0.598		
	53.6236	-56.2475	53.6152	-56.1885	264	4.010	2.18	0.536		
	53.6152	-56.1885	53.6044	-56.1308	264	3.992	2.24	0.732		
	53.6044	-56.1308	53.5948	-56.0725	261	4.001	1.38	1.019		
	53.5948	-56.0725	53.5924	-56.0522	93	1.367	2.43	0.777		
Total	53.6370	-56.3664	53.5924	-56.0522	1396	21.375	1.67	0.992	0.4	15.31
10030	53.5860	-56.0313	53.5594	-55.9906	267	4.004	1.34	0.827		
	53.5594	-55.9906	53.5560	-55.9846	40	0.551	0.12	0.139		
Total	53.5860	-56.0313	53.5560	-55.9846	306	4.556	1.18	0.874	0.4	14.89
10040	53.5522	-55.9762	53.5336	-55.9242	259	4.013	0.24	0.248		
	53.5336	-55.9242	53.5138	-55.8737	251	4.003	1.44	0.785		
	53.5138	-55.8737	53.4964	-55.8211	251	3.988	1.54	0.508		
	53.4964	-55.8211	53.4800	-55.7673	256	4.012	0.70	0.893		
	53.4800	-55.7673	53.4650	-55.7126	252	3.988	1.35	1.185		
	53.4650	-55.7126	53.4483	-55.6593	229	4.009	2.45	1.066		
	53.4483	-55.6593	53.4404	-55.6241	177	2.523	2.47	1.530		
Total	53.5522	-55.9762	53.4404	-55.6241	1669	26.534	1.39	1.197	0.4	15.90

DATE: MAR07 Total Length: 173.695 km
FLIGHT #: 02

Line	Start		End		Number of	Length of	Ice Thickness		Average	Average
Number	Lat. (deg. N)	Long. (deg. W)	Lat. (deg. N)	Long. (deg. W)	Samples ICE	Line/Seg. (km)	Mean (m)	Stdv. (m)	Spacing (s)	Spacing (m)
10051	53.4593	-55.6041	53.4951	-55.6108	248	4.015	2.61	1.600		
	53.4951	-55.6108	53.5309	-55.6158	238	3.997	1.78	1.356		
	53.5309	-55.6158	53.5668	-55.6175	233	3.998	1.35	0.643		
	53.5668	-55.6175	53.5695	-55.6175	22	0.298	1.19	0.142		
Total	53.4593	-55.6041	53.5695	-55.6175	738	12.309	1.90	1.359	0.4	16.68
10052	53.5708	-55.6175	53.5994	-55.6154	198	3.184	1.82	0.795		
Total	53.5708	-55.6175	53.5994	-55.6154	198	3.184	1.82	0.795	0.4	16.08
10053	53.6009	-55.6154	53.6369	-55.6192	246	4.013	1.92	0.959		
	53.6369	-55.6192	53.6467	-55.6207	68	1.102	2.05	0.710		
Total	53.6009	-55.6154	53.6467	-55.6207	313	5.114	1.94	0.912	0.4	16.34
10061	53.6898	-55.6241	53.7259	-55.6263	239	4.017	1.84	0.995		
	53.7259	-55.6263	53.7392	-55.6268	96	1.487	1.49	0.967		
Total	53.6898	-55.6241	53.7392	-55.6268	334	5.504	1.74	0.999	0.4	16.48
10062	53.7406	-55.6268	53.7767	-55.6245	247	4.016	1.04	1.201		
	53.7767	-55.6245	53.8125	-55.6210	240	3.996	1.93	1.220		
	53.8125	-55.6210	53.8483	-55.6190	251	3.991	2.68	0.945		
	53.8483	-55.6190	53.8577	-55.6184	68	1.044	2.13	0.855		
Total	53.7406	-55.6268	53.8577	-55.6184	803	13.047	1.97	1.322	0.4	16.25

DATE: MAR07 Total Length: 173.695 km
FLIGHT #: 02

Line	Start		End		Number of	Length of	Ice Thickness		Average	Average
Number	Lat. (deg. N)	Long. (deg. W)	Lat. (deg. N)	Long. (deg. W)	Samples ICE	Line/Seg. (km)	Mean (m)	Stdv. (m)	Spacing (s)	Spacing (m)
10070	53.8662	-55.6856	53.8666	-55.7467	264	4.013	2.45	0.601		
	53.8666	-55.7467	53.8677	-55.8075	265	3.995	2.71	0.760		
	53.8677	-55.8075	53.8689	-55.8684	262	3.999	2.45	0.595		
	53.8689	-55.8684	53.8705	-55.9293	263	4.001	3.09	1.369		
	53.8705	-55.9293	53.8710	-55.9550	113	1.687	2.06	0.790		
Total	53.8662	-55.6856	53.8710	-55.9550	1163	17.694	2.62	0.932	0.4	15.21
10080	53.8710	-55.9620	53.8717	-56.0109	208	3.212	2.90	1.214		
Total	53.8710	-55.9620	53.8717	-56.0109	208	3.212	2.90	1.214	0.4	15.44
10090	53.8737	-56.0913	53.8771	-56.1522	248	4.014	2.28	1.435		
	53.8771	-56.1522	53.8796	-56.2129	243	3.994	2.37	0.994		
	53.8796	-56.2129	53.8825	-56.2737	244	4.006	2.30	0.951		
	53.8825	-56.2737	53.8883	-56.3339	243	4.002	2.10	0.900		
	53.8883	-56.3339	53.8930	-56.3942	247	3.995	2.45	1.333		
	53.8930	-56.3942	53.8979	-56.4527	244	3.874	2.92	0.910		
Total	53.8737	-56.0913	53.8979	-56.4527	1464	23.886	2.41	1.136	0.4	16.32

DATE: MAR07 Total Length: 173.695 km
FLIGHT #: 02

Line	Start		End		Number of	Length of	Ice Thickness		Average	Average
Number	Lat. (deg. N)	Long. (deg. W)	Lat. (deg. N)	Long. (deg. W)	Samples ICE	Line/Seg. (km)	Mean (m)	Stdv. (m)	Spacing (s)	Spacing (m)
10100	53.8796	-56.5496	53.8656	-56.6058	250	4.008	1.83	0.960		
	53.8656	-56.6058	53.8520	-56.6621	245	3.992	2.57	1.087		
	53.8520	-56.6621	53.8377	-56.7179	247	4.003	2.28	1.620		
	53.8377	-56.7179	53.8196	-56.7706	244	4.003	1.71	1.192		
	53.8196	-56.7706	53.8041	-56.8149	212	3.388	2.55	1.006		
Total	53.8796	-56.5496	53.8041	-56.8149	1194	19.395	2.18	1.254	0.4	16.24
10110	53.7607	-56.9004	53.7409	-56.9510	231	4.006	1.01	0.391		
	53.7409	-56.9510	53.7277	-56.9852	164	2.693	1.09	0.141		
Total	53.7607	-56.9004	53.7277	-56.9852	394	6.699	1.04	0.315	0.4	17.00

E. SURFACE CALIBRATION DATA

(Station data also listed in Peterson et al., 1995)

Station 1.1 Calibration Line off Black Head, Cartwright
(spacing 25m, Tuesday 1 March, 1994)

Stn #	Ice cm	Snow cm	Free board cm	Snow +Ice cm	
11	78	17	1	95	3 bags
--	30	--	--		
12	68	25	0	93	
--	20	--	--		
13	62	24	0	86	
--	24	--	--		
14	62	32	-6	94	
--	22	--	--		
15	74	9	0	83	
--	18	--	--		
16	86	27	2	113	
--	20	--	--		
17	66	32	-1	98	
--	22	--	--		
18	84	20	2	104	
--	17	--	--		
19	72	30	-1	102	
--	20	--	--		
20	72	25	0	97	2 bags

Station 2.1 Landfast ice (Stooney Arm)
Large flat ice cover inside a bay.
Snow floaded ice: salty froozen slush layer of 6cm.

Date:	March 2, 1994	Latitude:	53 29.56N
Time:	09:05 EST	Longitude:	056 02.56W
Wind:	Light NW	Temp:	-20°C/clear
Depth:	14.3m		

Stn #	Ice cm	Snow cm	Free board cm	Snow +Ice cm
1	70	25	-7	95
2	72	22-28	-6	97
3	72	20-30	-4	97

refroozen slush layer of 6cm (14ppt)
Surface crust layer of 1cm (0ppt)

Station 3.3 Calibration Floe Pack Ice
Small floe in rough ridged ice
North of iceberg/ARGOS beacon #977

Date:	March 3, 1994	Latitude:	54 16.24N
Time:	15:00 EST	Longitude:	055 21.78W
Wind:	Calm	Temp:	-8°C/overcast

Stn #	Ice cm	Snow cm	Free board cm	Snow +Ice cm
1	104	6	16	110
2	104	2	12	106
3	+++	2	12	+++
4	102	2	10	104
5	63*	2	6	65*

* rafted with 8cm of slush between rafts
floe 15x35m, ridge blocks 45-50cm/one large block 95cm
Slush layer between floes 64ppt

Station 4.1 Calibration Floe Pack Ice
Flat large floe made of pancake ice
North of Wolf Island/Argos Beacon 976

Date:	March 4, 1994	Latitude:	53 44.75N
Time:	09:15 EST	Longitude:	056 09.91W
Wind:	5kmph/180	Temp:	-12°C/overcast

Stn #	Ice cm	Snow cm	Free board cm	Snow +Ice cm		
1	35	4	1	39	black bag	
	35	5	1	40	small ridge	
2	49	4	3	53		
	49	3	3	52		
3	47	5	2	53		
	42	4	2	46		
4	94	4	4	98	orange bag	(rafted)

Stn. seperated by 25m plus in between samples.
(line SE-NW, sampled by Ice Probe at 09:45)

Snow and ice salinities

Between ***Stn 2*** and ***3*** (ARGOS beacon #976)

bottle #	depth (cm)	Salinity ppt
64659	Snow	13.0
64652	5	8.0
64660	25	6.0
64665	45	10.0

Station 4.2 Calibration Floe Pack Ice
Flat large floe made of pancake ice
South of Wolf Island/Argos Beacon 965

Date:	March 4, 1994	Latitude:	53 33.29N
Time:	10:30 EST	Longitude:	055 45.58W
Wind:	Calm	Temp:	-12°C/clouds to SW

Stn #	Ice cm	Snow cm	Free board cm	Snow +Ice cm
1	56	5	3	60
2	57	7	4	64
3	56	5	3	61

Stns. near helicopter

Snow and ice salinities (near ARGOS beacon #965)

bottle #	depth (cm)	Salinity ppt
64658	1	16.0
64667	15	8.0
64656	35	8.0

Station 4.3 Black Tickle thin ice station
Flat rafted floe, SE of one-day old ice
SW of black Tickle

Date:	March 4, 1994	Latitude:	53 25.73N
Time:	11:30 EST	Longitude:	055 44.60W
Wind:	Calm	Temp:	-12°C/clouds SE

Stn #	Ice cm	Snow cm	Free board cm	Snow +Ice cm
1	57	4	8	61
2	56	4	8	60
3	52*	4	8	56*

* rafted, 8cm slush between rafted layers
Stns. near helicopter (floe 30x30m)
Thin ice 9cm/black and 16cm/grey
Large area to NE and inbay to East bordering landfast ice

Salinities ***Stn. 4.3*** Thin black ice: surface (auger) and 20x20cm lose sheat

bottle #	depth (cm)	Salinity ppt
64657	auger	16.0
64655	sheat	17.0

Station 6.1 15km east of Wolf Island.
Large composite floe.

Date:	March 6, 1994	Latitude:	53 41.26N
Time:	10:30 EST	Longitude:	055 42.37W
Wind:	5mph NW	Temp:	-25°C/clear

Stn #	Ice cm	Snow cm	Free board cm	Snow +Ice cm
1	103	6	7	110
2	103	5	6	109
3	107	6	7	114

Salinities ***Stn. 6.1***

bottle #	depth (cm)	Salinity ppt
64659	snow	3.0
64658	2	13.0
64652	25	9.0
64655	45	8.0
64656	65	10.0

Station 6.3 Black Tickle: south of thin ice area.

Date:	March 6, 1994	Latitude:	53 25.79N
Time:	12:50 EST	Longitude:	055 45.18W
Wind:	5mph NW	Temp:	-25°C/clear

bottle #	depth (cm)	Salinity ppt
64657	snow	3.0
64666	slush	35.0
64663	ice	14.0

Station 6.5 Rocky Bay: Reflector on large thin ice area.
(second visit March 7, afternoon)

Date:	March 6, 1994	Latitude:	53 29.88N
Time:	17:20 EST	Longitude:	055 58.70W
Wind:	5mph NW	Temp:	-25°C/clear

bottle #	depth (cm)	Salinity ppt
64667	0-2 snow	37.0
64665	2-4 slush	35.0
64660	5	9.0
64644*	1	12.0
64645*	10	6.0

Ice 21cm thick and 1cm of freeboard.
* done March 7

Station 7.1 5km SE off Spotted Island
Large composite floe

Date:	March 7, 1994	Latitude:	53 29.90N
Time:	09:30 EST	Longitude:	055 40.47W
Wind:	calm	Temp:	-18°C/clear

Stn #	Ice cm	Snow cm	Free board cm	Snow +Ice cm
1	75	2	7	77
2	76	2	8	78
3	77	2	8	79

Temperature staff beacon #973.

Salinities ***Stn. 7.1***

bottle #	depth (cm)	Salinity ppt
64650	snow	6.0
64658	1	16.0
64659	10	15.0
64649	20	10.0
64666	30	23.0 (rafted slush layer)
64667	45	14.0

Station 7.2 Start of large thin area, 40km south of Roundhill Island.

Date:	March 7, 1994	Latitude:	53 02.66N
Time:	10:30 EST	Longitude:	055 38.37W
Wind:	calm	Temp:	-18°C/clear

bottle #	depth (cm)	Salinity ppt
64652	frost*	82.0
64657	sheat	20.0
64663	5	20.0

10-12cm of ice.

Station 8.1 Brighter part of Rocky Bay on ERS-1 image.

Date:	March 8, 1994	Latitude:	53 29.98N
Time:	09:50 EST	Longitude:	055 56.26W
Wind:	Calm	Temp:	-9°C/clear

bottle #	depth (cm)	Salinity ppt
64647	soft snow	36.0
64654	hard snow	35.0
64655	2	9.0
64658	10	10.0
64651	20	5.0

30cm of ice but 20cm of slush wind pushed it downwind.
Hard snow in 1m waves 9cm amplitude filled with 5cm of soft snow.

Station 8.2 Porcupine Bay, a bay facing southeast.

Date:	March 8, 1994	Latitude:	
Time:	10:10 EST	Longitude:	
Wind:	SW 10-15mph	Temp:	-9°C/clear

Stn #	Ice cm	Snow cm	Free board cm	Snow +Ice cm
1	15	5	0	20
2	16	6	0	22
3	15	5	0	20

bottle #	depth (cm)	Salinity ppt
64649	snow	33.0
64666	5	7.0

Station 9.1 Northeast of Grady Island

Date:	March 9, 1994	Latitude:	53 58.62
Time:	14:30 EST	Longitude:	056 04.63
Wind:	NW 10-15mph	Temp:	-9°C/overcast

Stn #	Ice cm	Snow cm	Free board cm	Snow +Ice cm
1	107	2	10	127
2	107	2	10	127
3	107	2	10	127

bottle #	depth (cm)	Salinity ppt
64644	snow	3.0
64657	5	12.0
64646	25	21.0
64661	35	26.0
64648	55	27.0
64665	80	12.0

F. STANDARD PLOTS

MAR 03 Flight #08 Line #10010 part 1 of 2
Line Starting Coordinates (53.8654,–56.2862) ending at (53.8845,–56.2347)

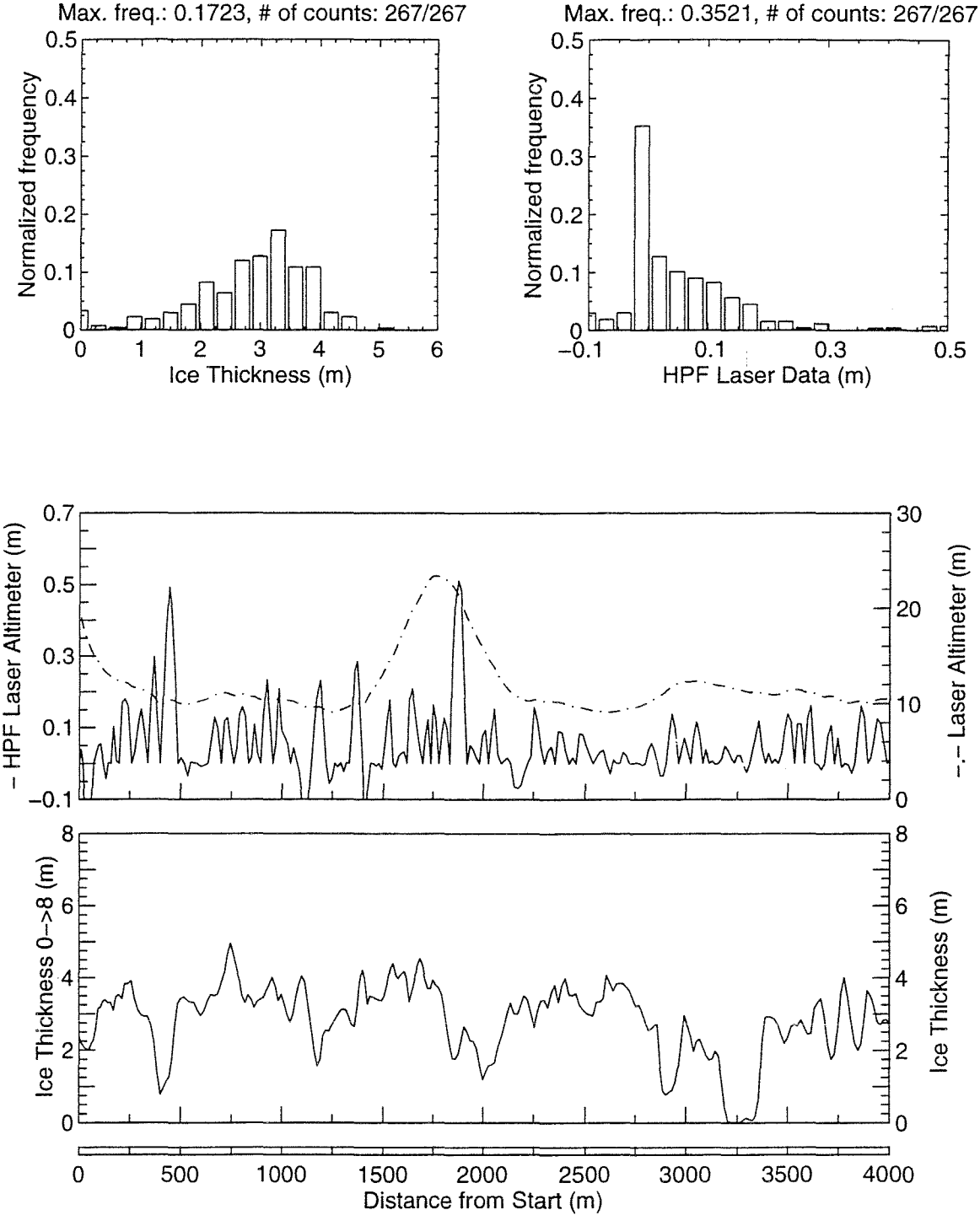

MAR 03 Flight #08 Line #10010 part 2 of 2

Line Starting Coordinates (53.8845,–56.2347) ending at (53.8865,–56.2294)

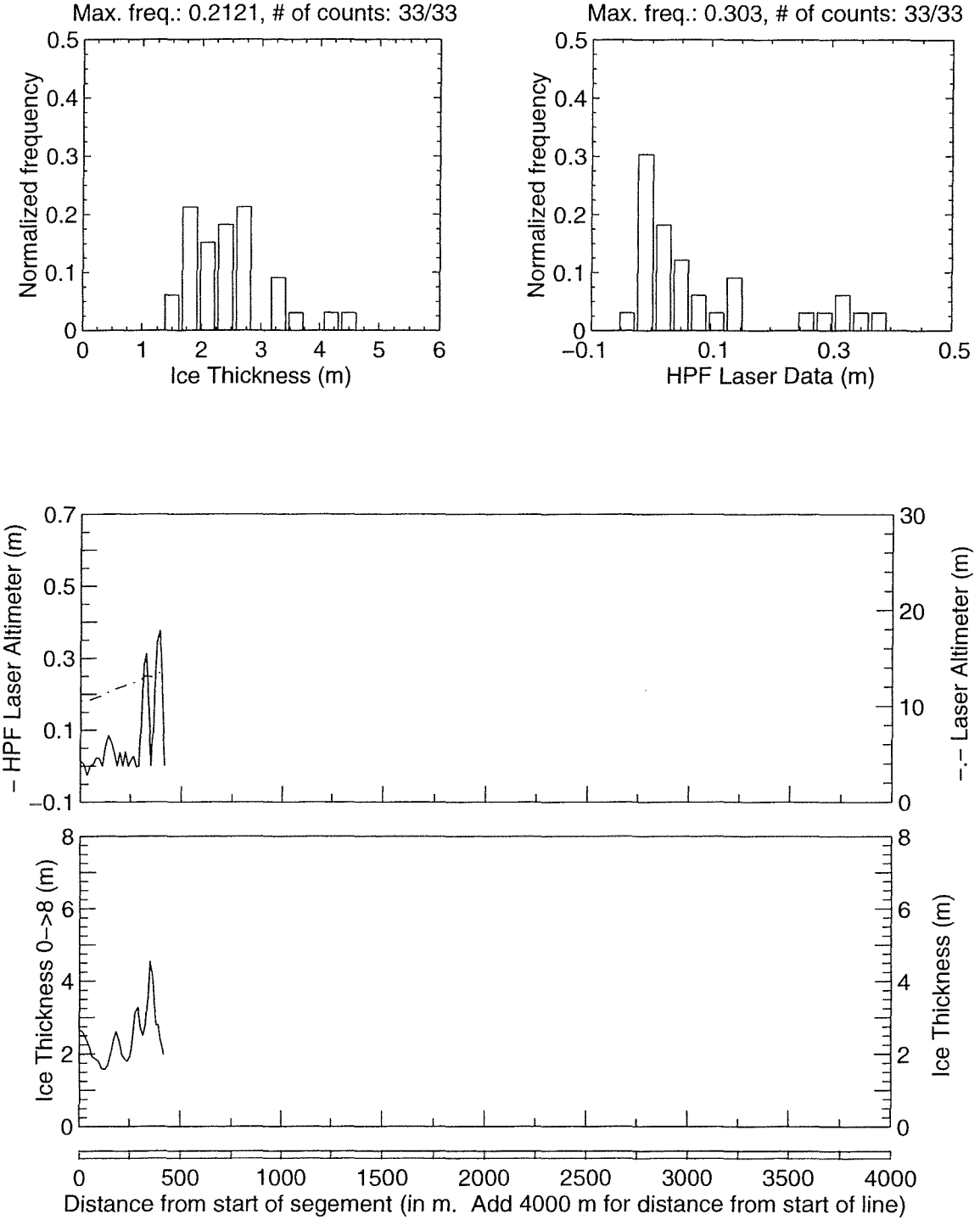

MAR 03 Flight #11 Line #10010 part 1 of 2

Line Starting Coordinates (54.1364,–55.5115) ending at (54.1531,–55.4571)

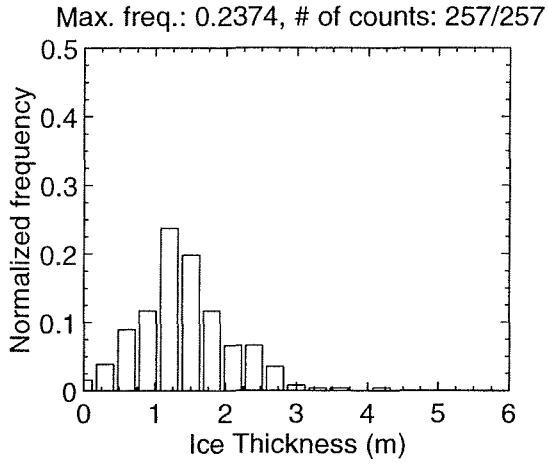

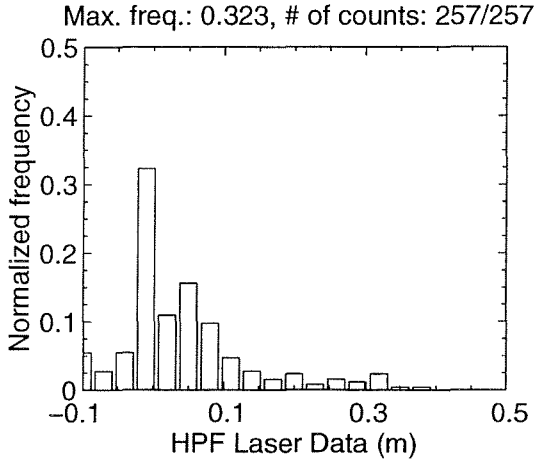

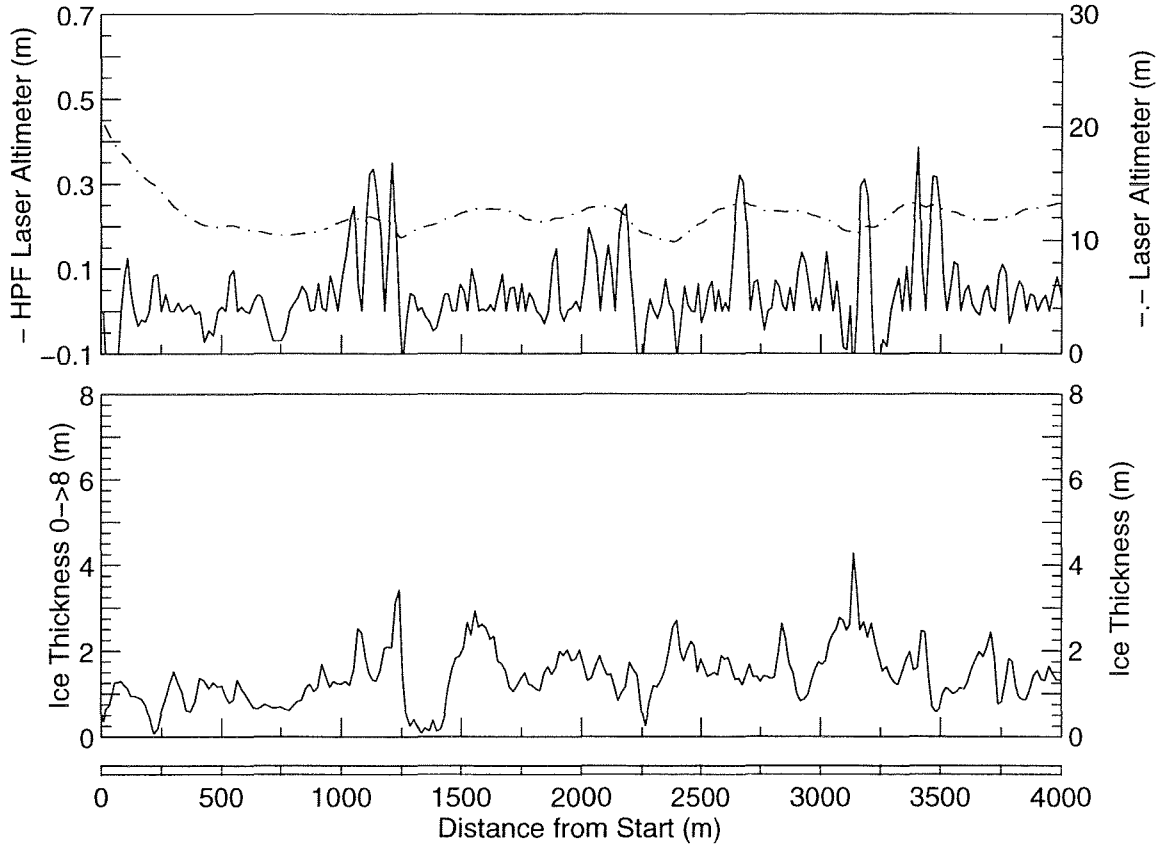

MAR 03 Flight #11 Line #10010 part 2 of 2

Line Starting Coordinates (54.1531,–55.4571) ending at (54.1667,–55.4198)

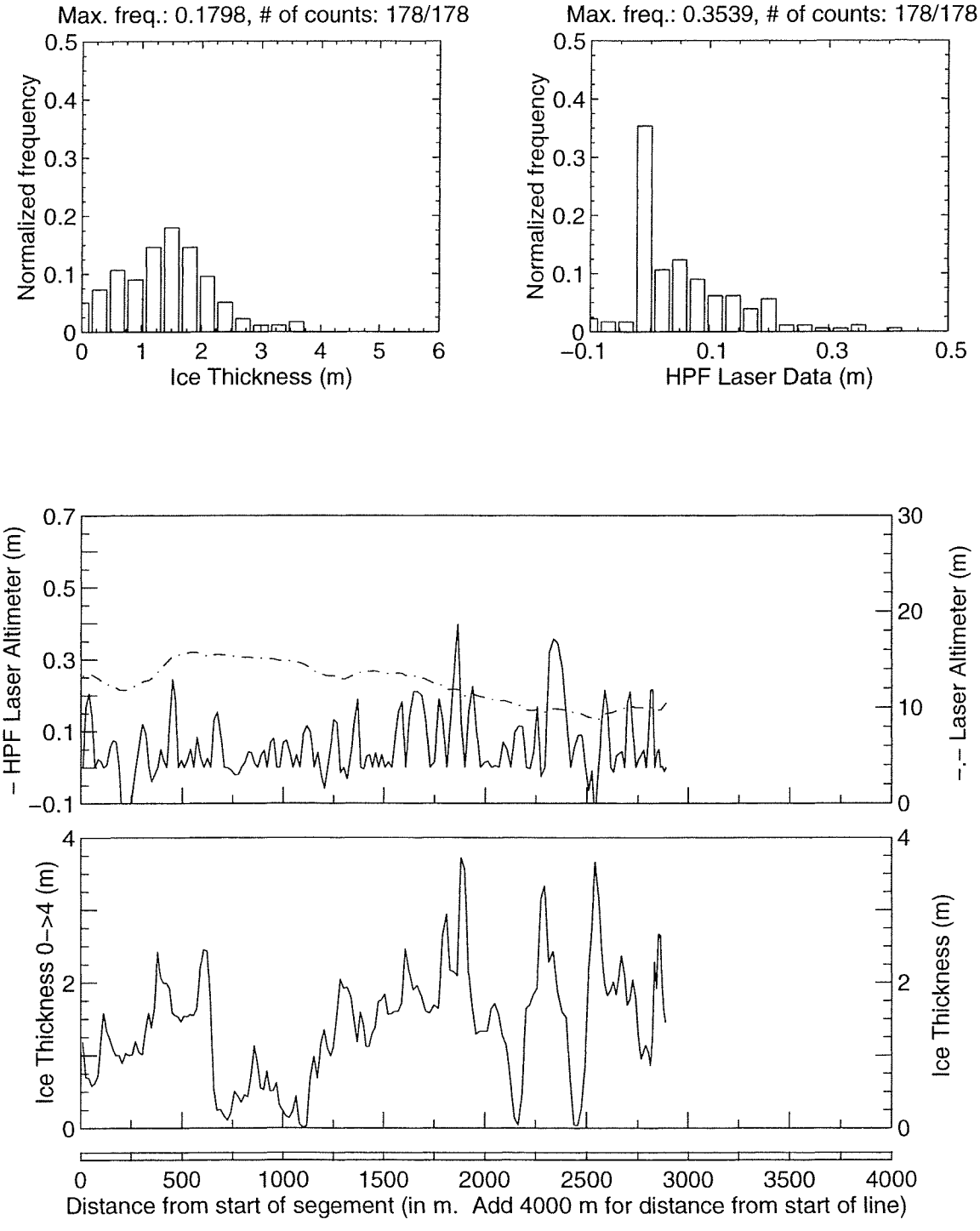

MAR 03 Flight #11 Line #10021 part 1 of 1

Line Starting Coordinates (54.2639,–55.3794) ending at (54.2816,–55.3481)

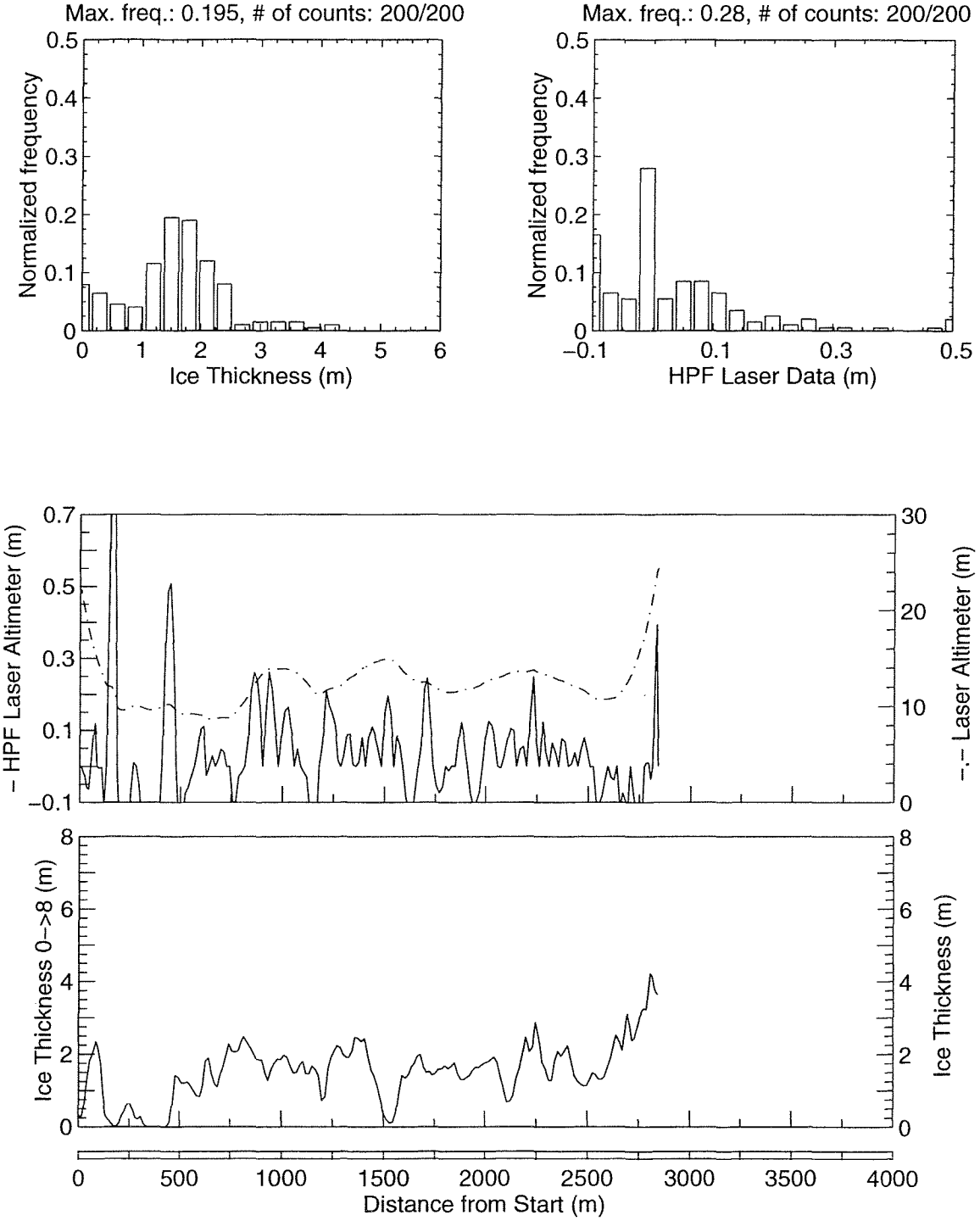

MAR 03 Flight #11 Line #10022 part 1 of 2

Line Starting Coordinates (54.2840,–55.3469) ending at (54.2577,–55.3891)

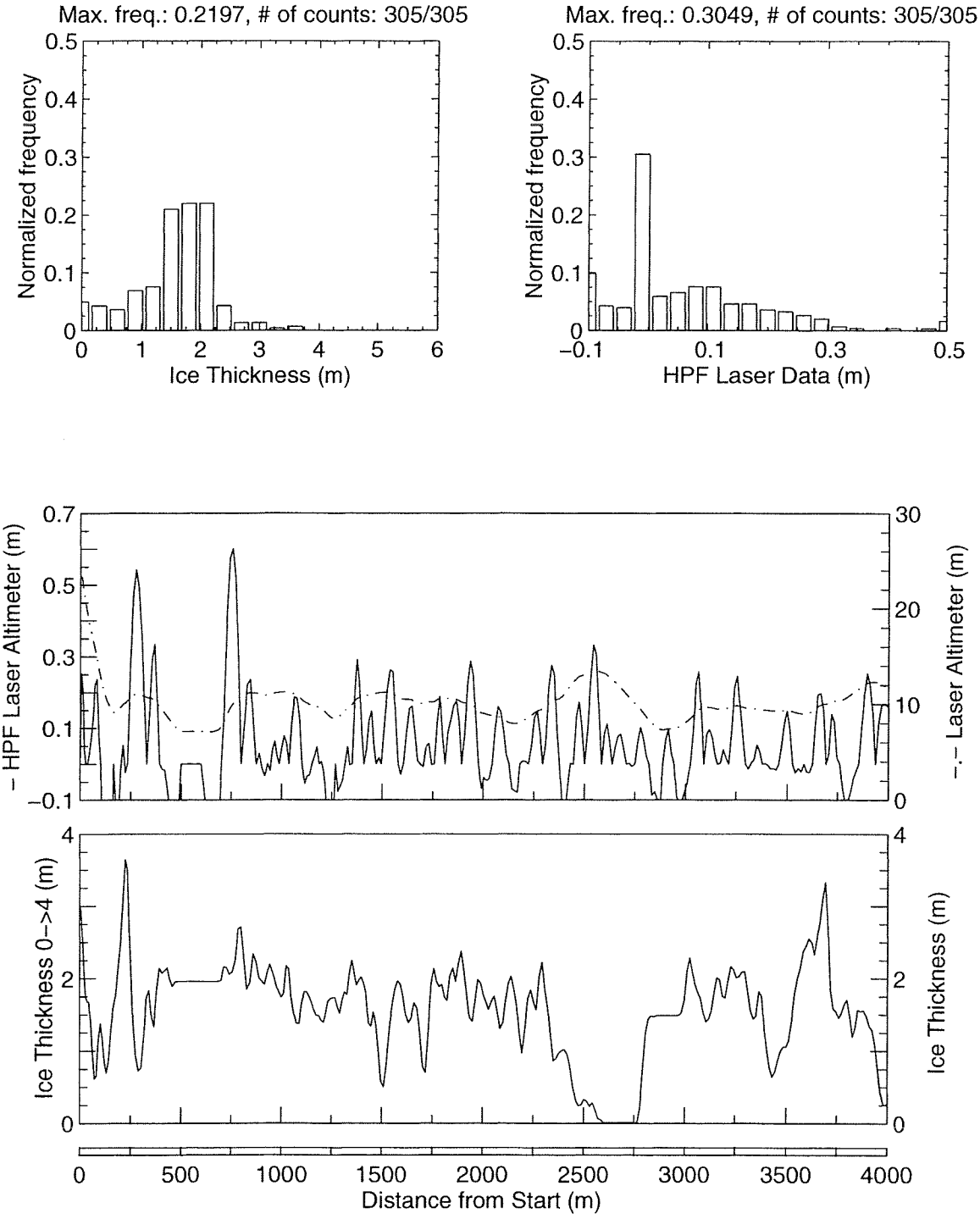

MAR 03 Flight #11 Line #10022 part 2 of 2

Line Starting Coordinates (54.2577,–55.3891) ending at (54.2568,–55.3904)

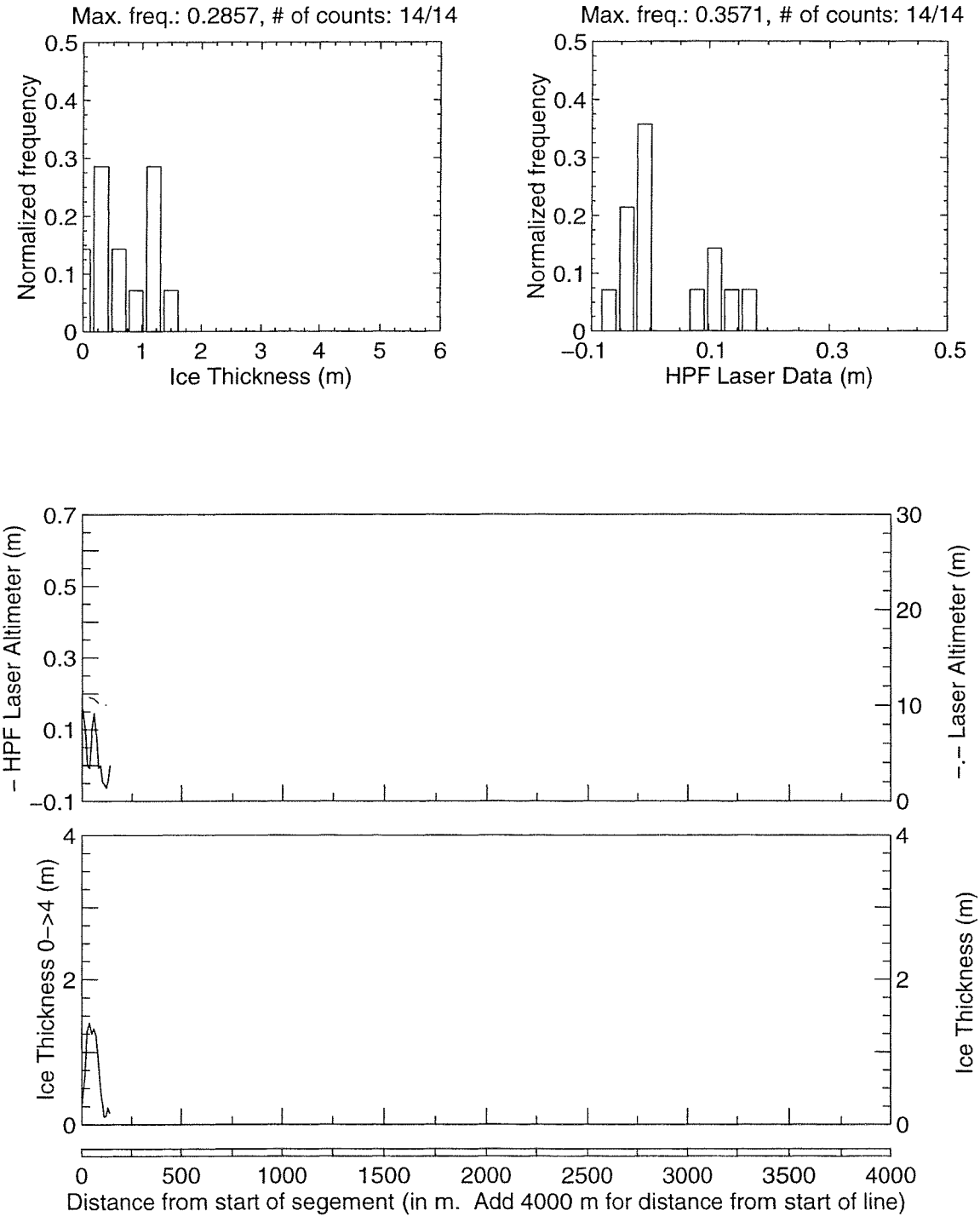

MAR 03 Flight #12 Line #10010 part 1 of 1

Line Starting Coordinates (54.2637,–55.3750) ending at (54.2785,–55.3604)

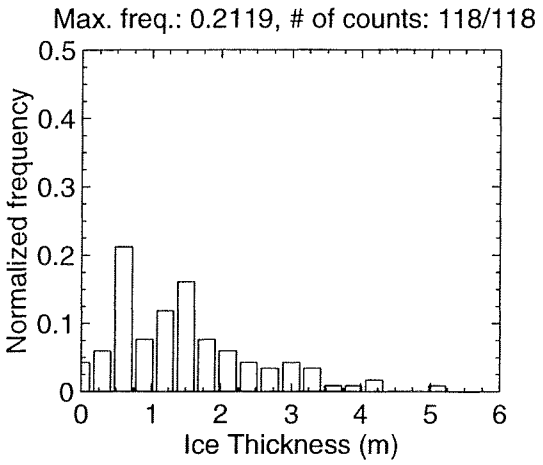

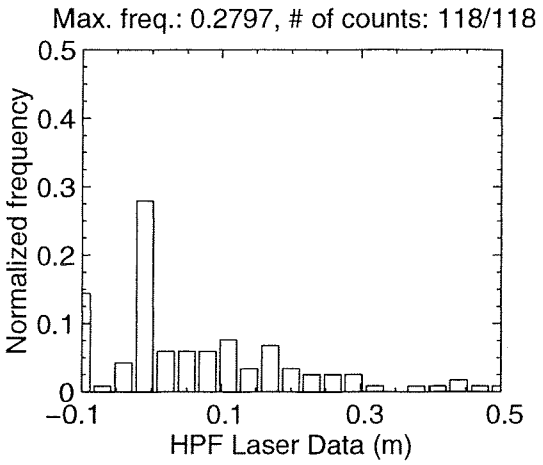

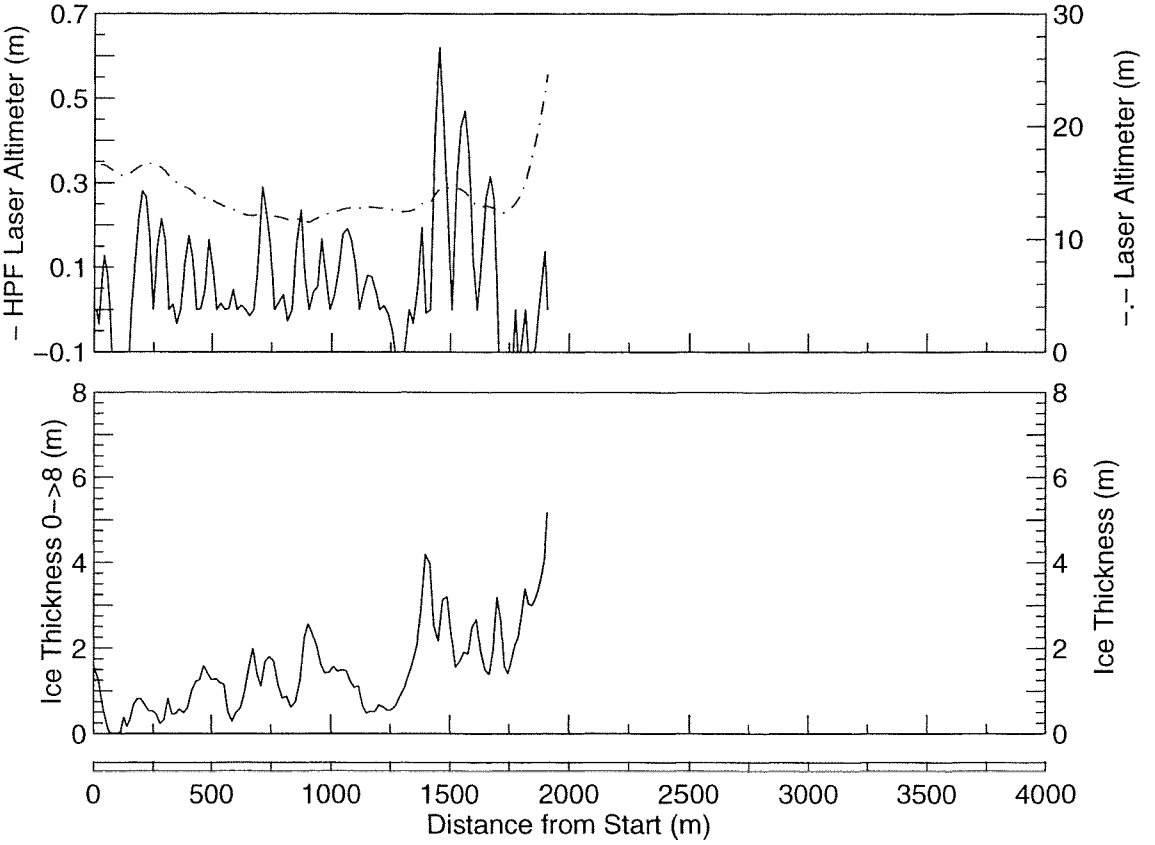

MAR 03 Flight #12 Line #10020 part 1 of 1

Line Starting Coordinates (54.2887,–55.3545) ending at (54.2647,–55.3781)

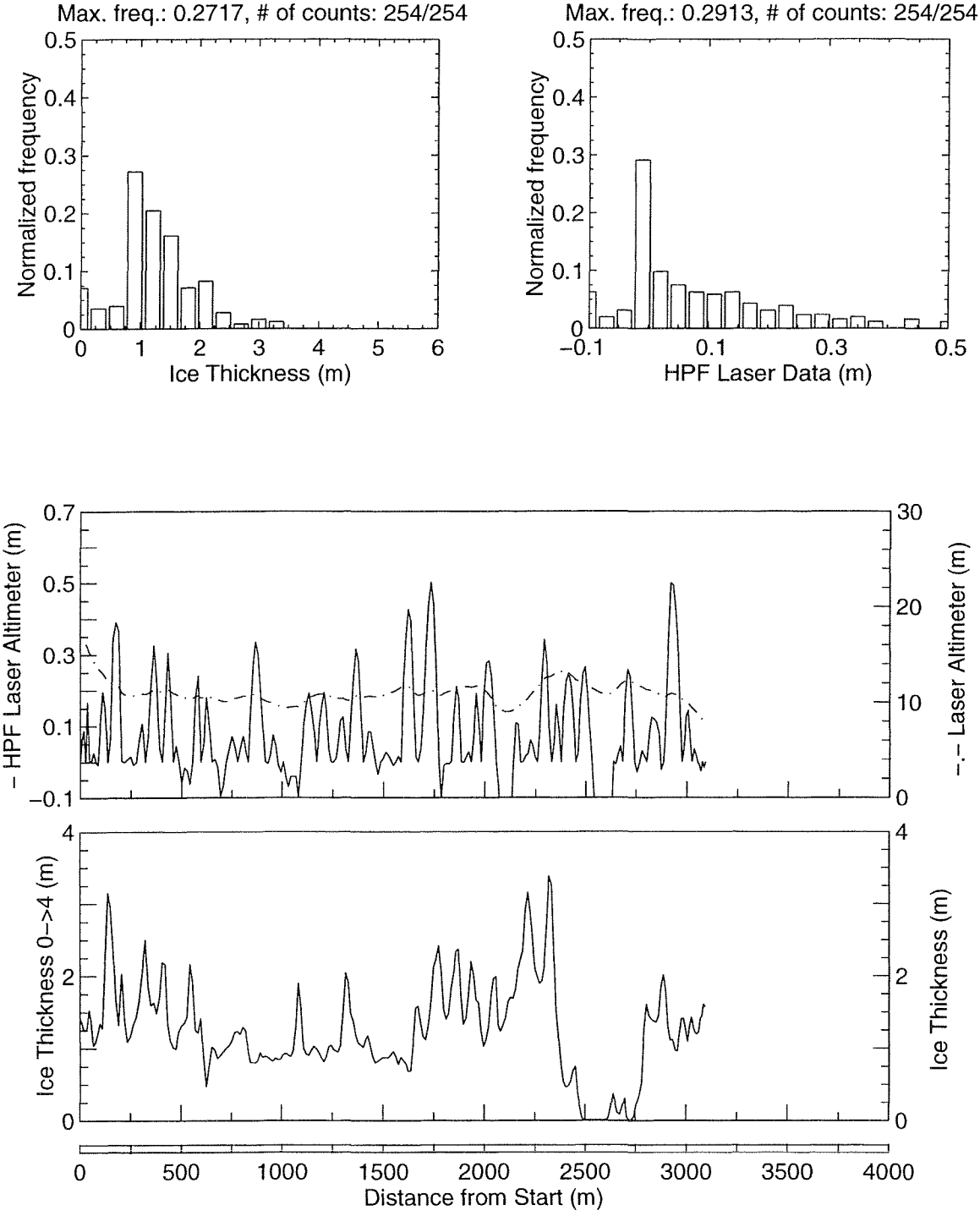

MAR 03 Flight #12 Line #10030 part 1 of 2

Line Starting Coordinates (54.2645,–55.3805) ending at (54.2961,–55.3509)

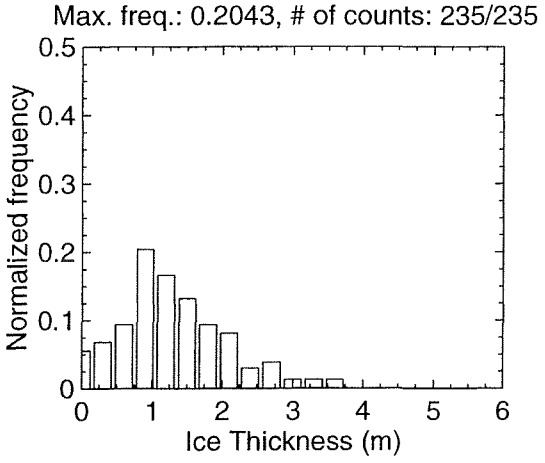

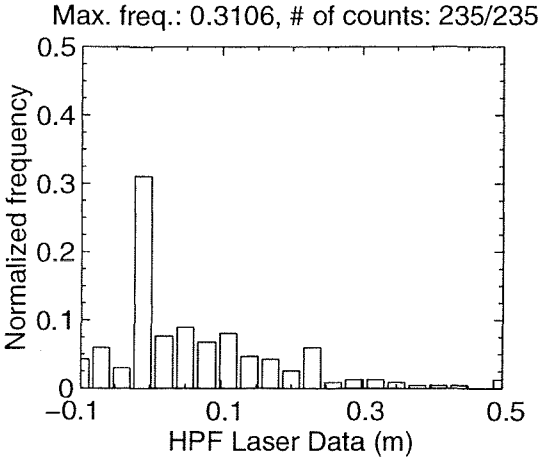

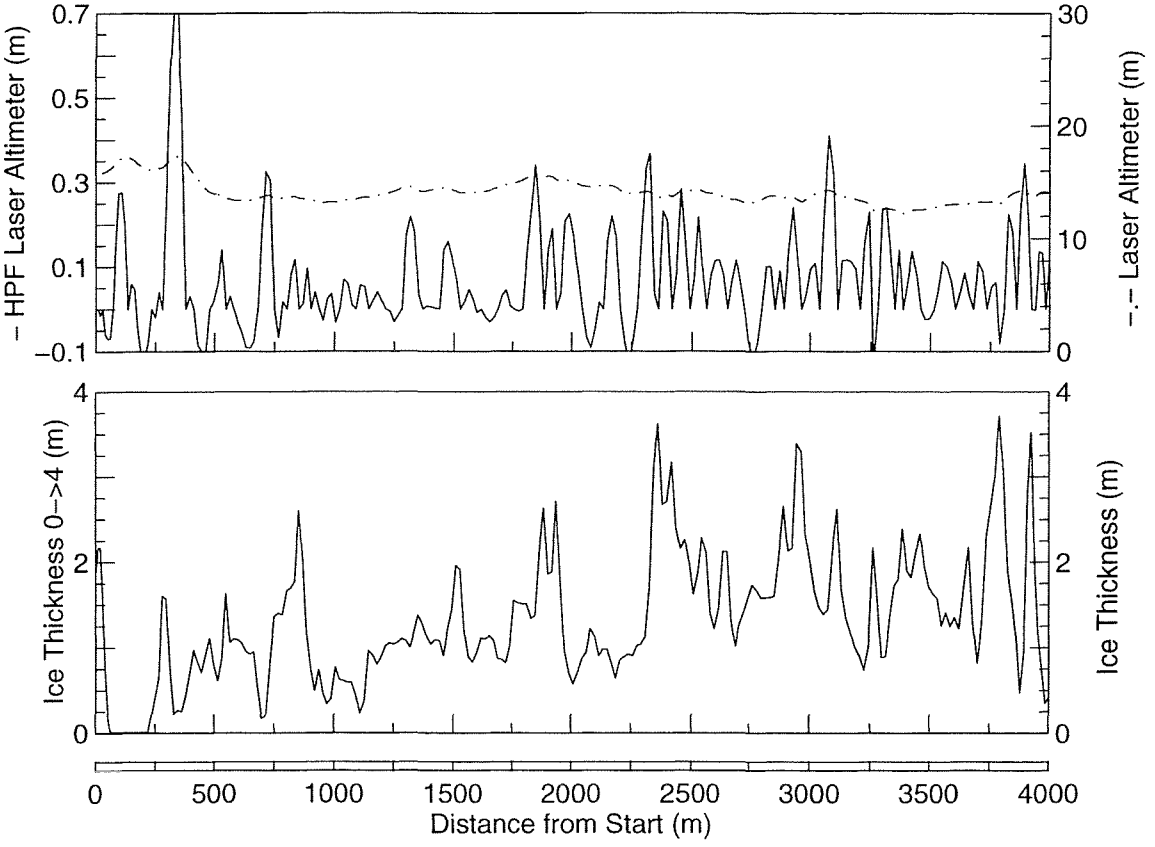

MAR 03 Flight #12 Line #10030 part 2 of 2

Line Starting Coordinates (54.2961,–55.3509) ending at (54.2965,–55.3505)

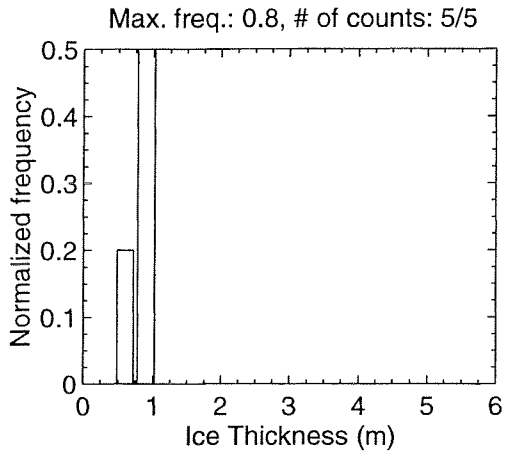

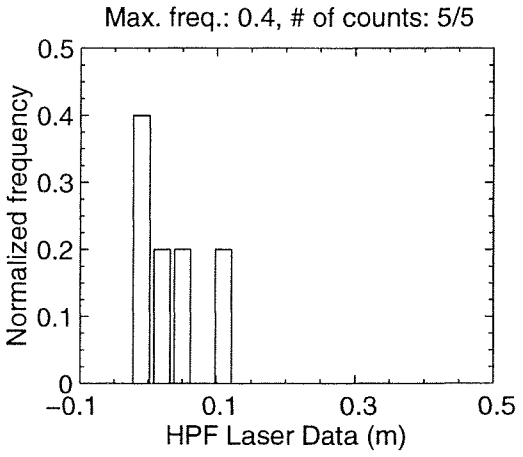

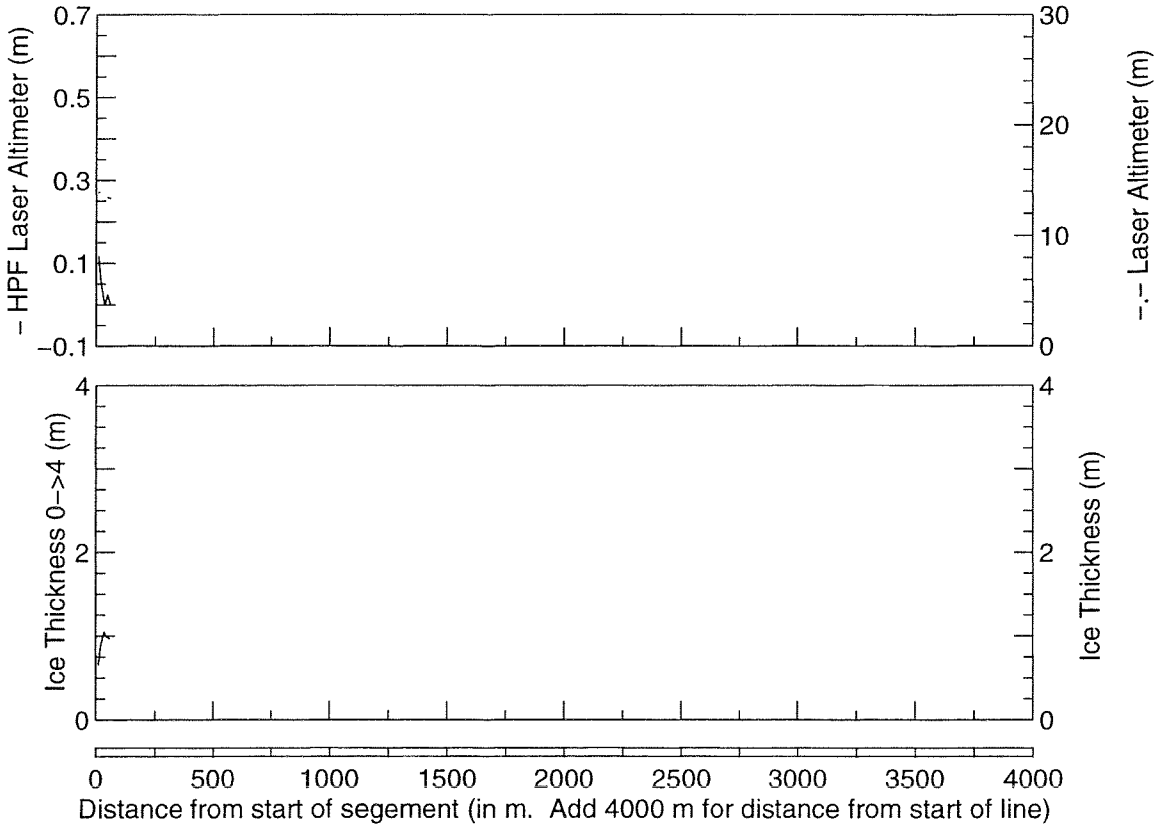

MAR 03 Flight #12 Line #10040 part 1 of 1

Line Starting Coordinates (54.3006,−55.3541) ending at (54.2685,−55.3774)

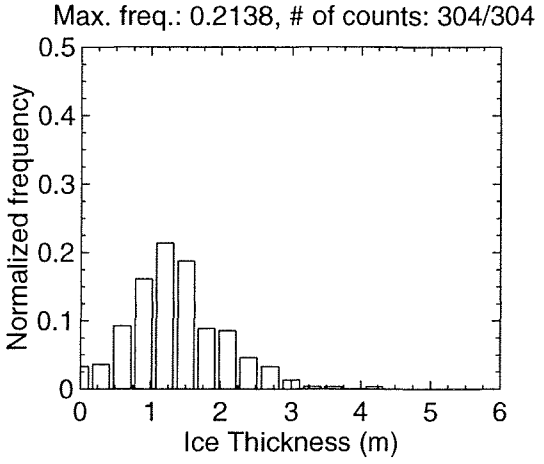

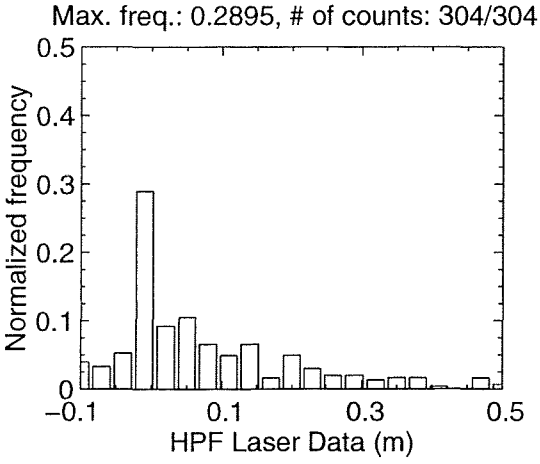

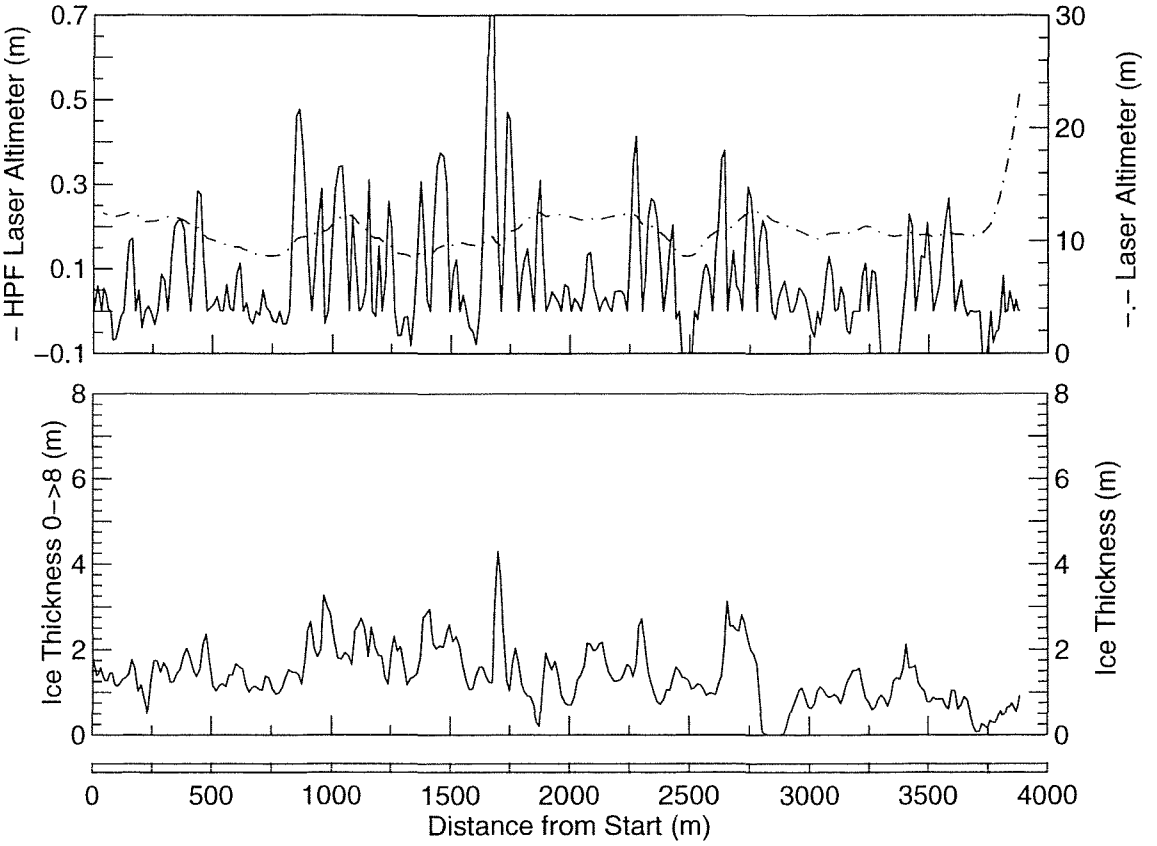

MAR 03 Flight #12 Line #10050 part 1 of 1

Line Starting Coordinates (54.2710,–55.3757) ending at (54.2738,–55.3722)

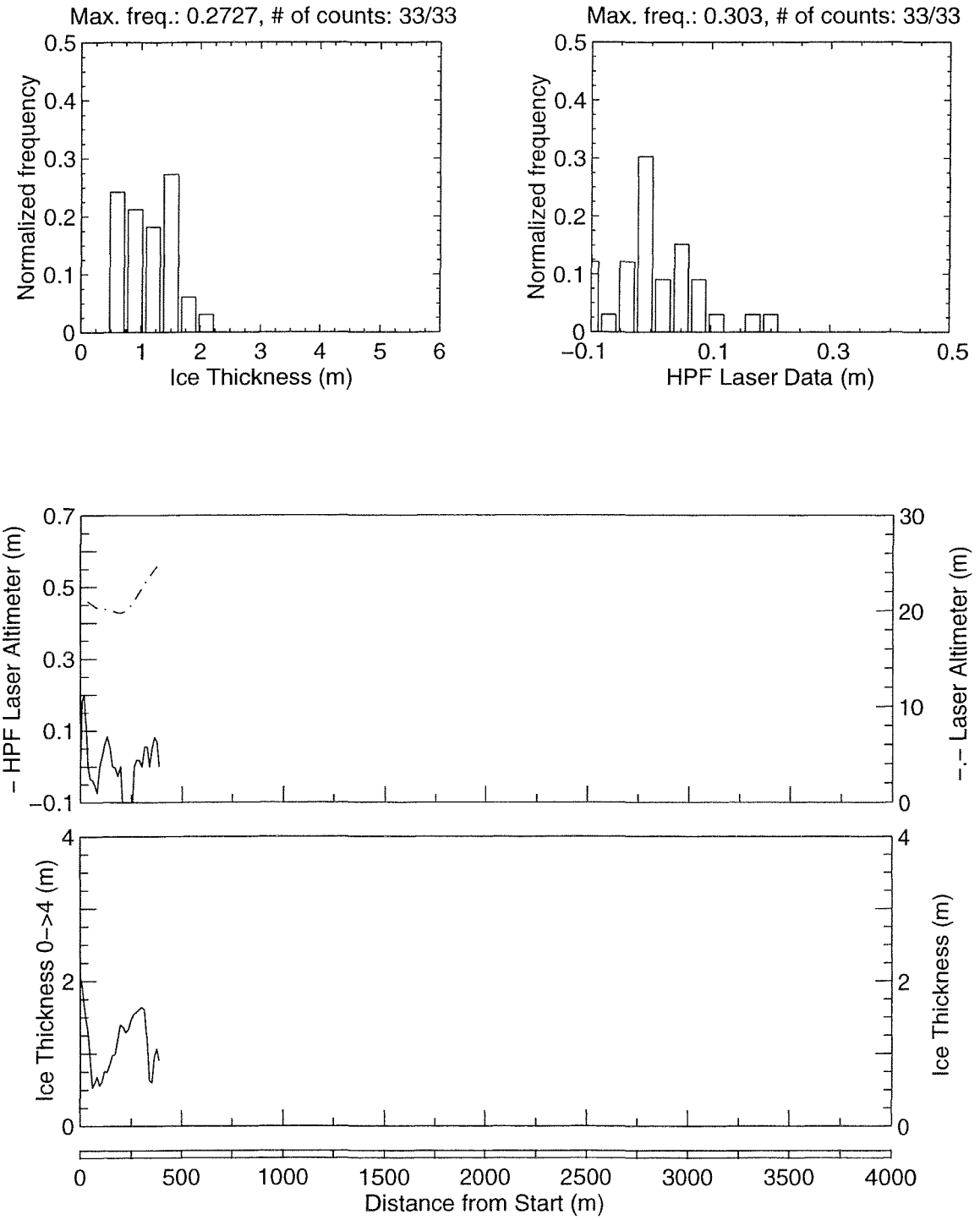

MAR 03 Flight #12 Line #10061 part 1 of 1

Line Starting Coordinates (54.2707,–55.3643) ending at (54.2552,–55.3745)

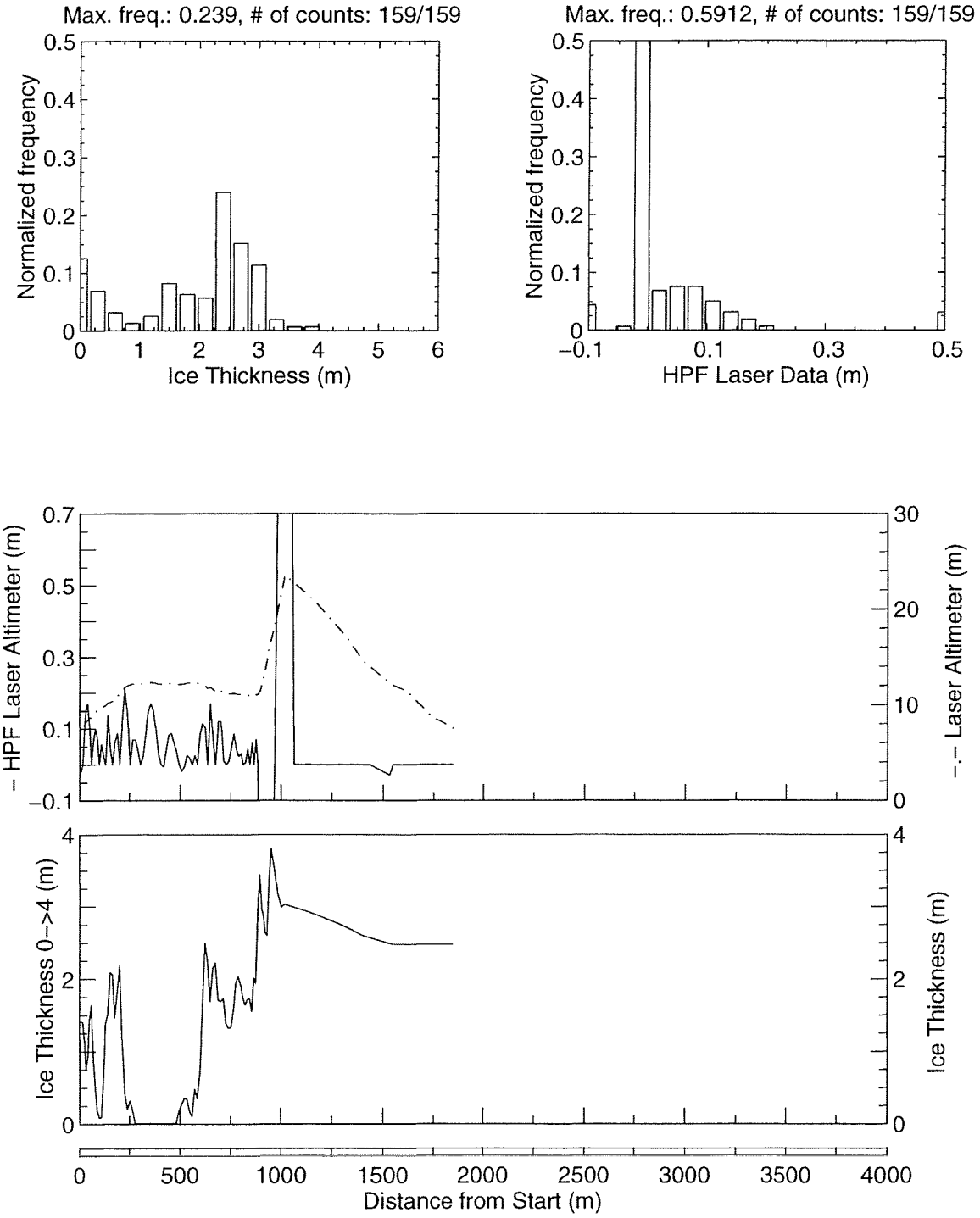

MAR 03 Flight #12 Line #10062 part 1 of 1

Line Starting Coordinates (54.2572,–55.3746) ending at (54.2750,–55.3608)

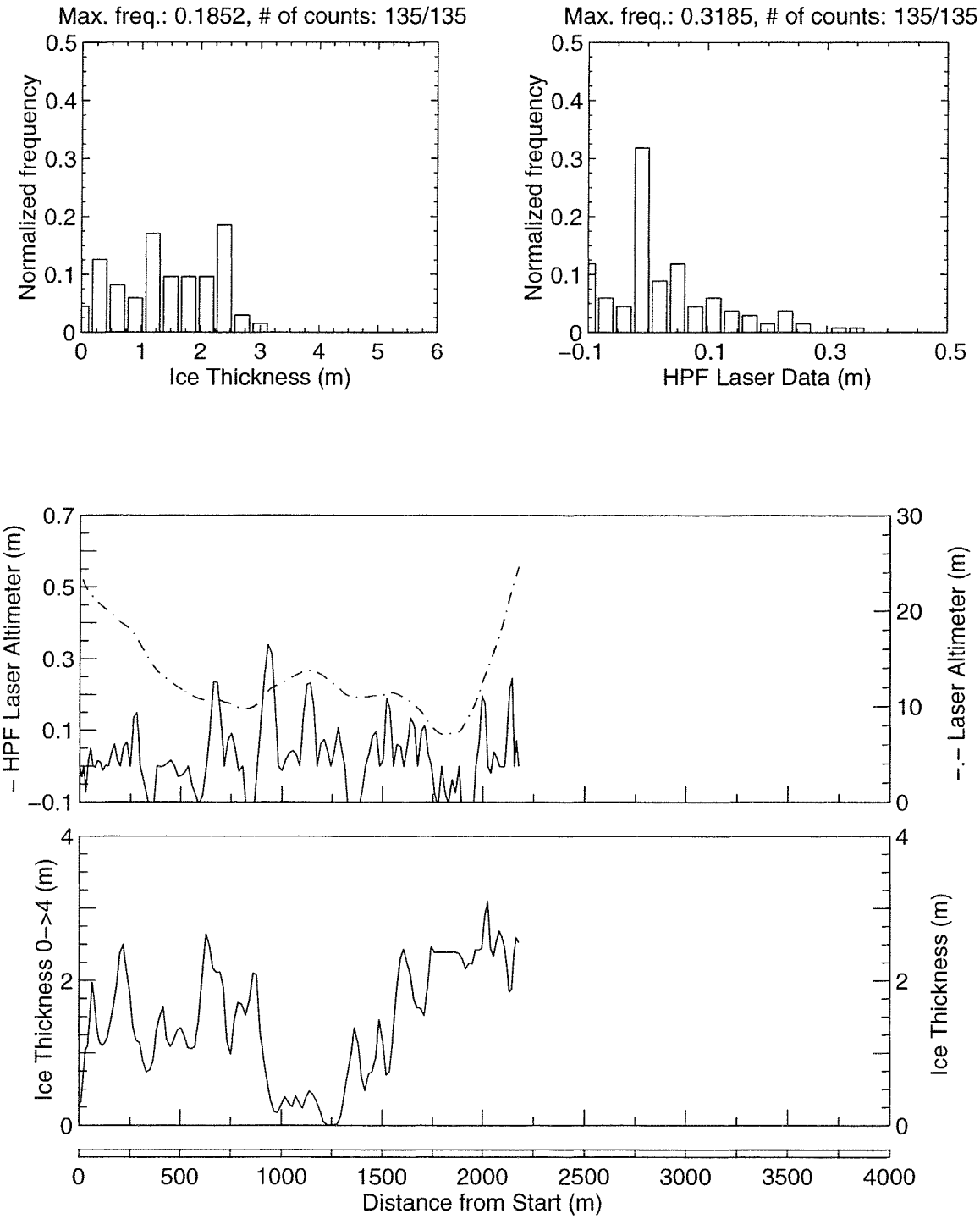

MAR 03 Flight #12 Line #10063 part 1 of 1

Line Starting Coordinates (54.2807,−55.3563) ending at (54.2695,−55.3645)

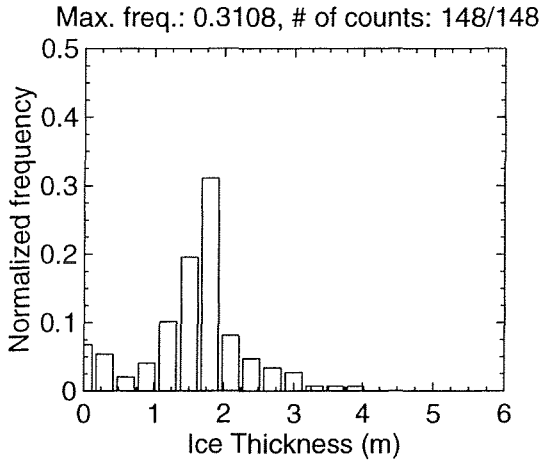

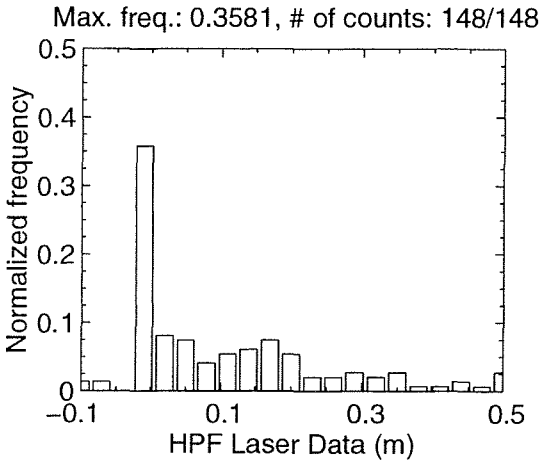

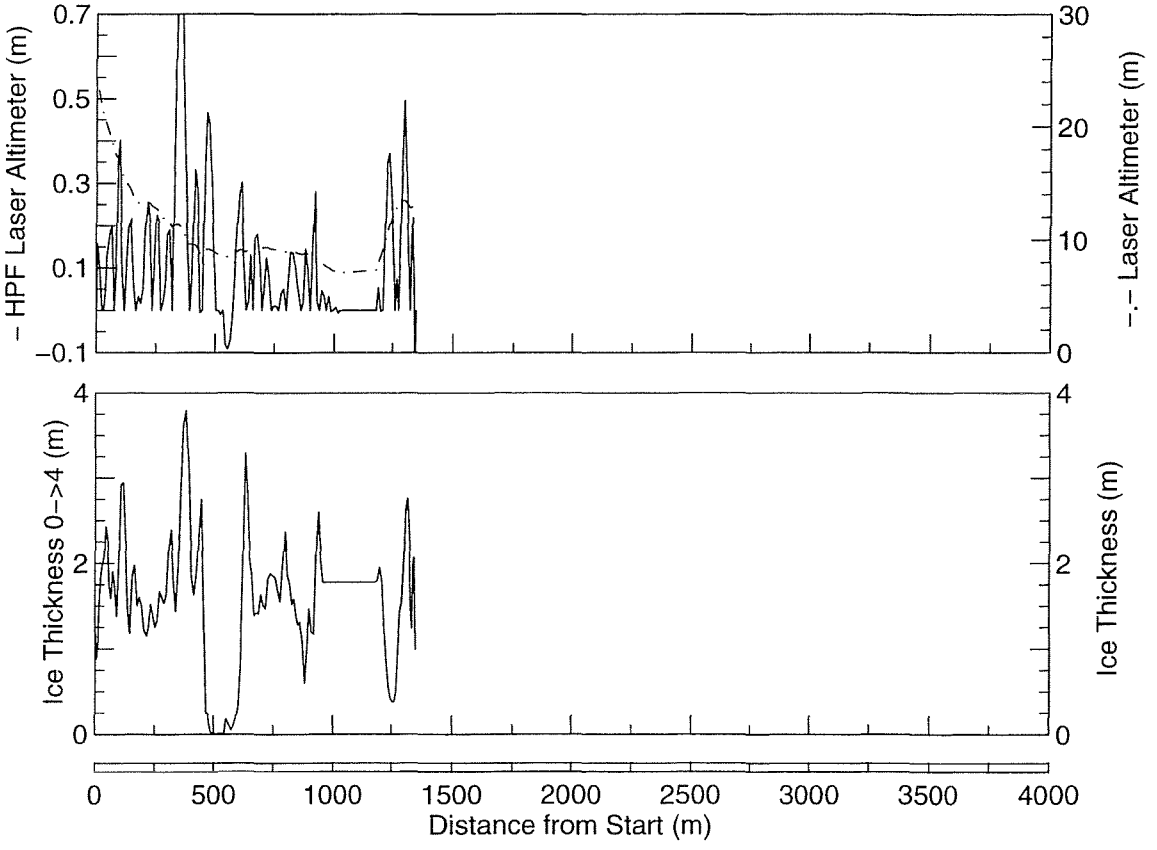

MAR 03 Flight #12 Line #10070 part 1 of 1

Line Starting Coordinates (54.2687,–55.3646) ending at (54.2707,–55.3627)

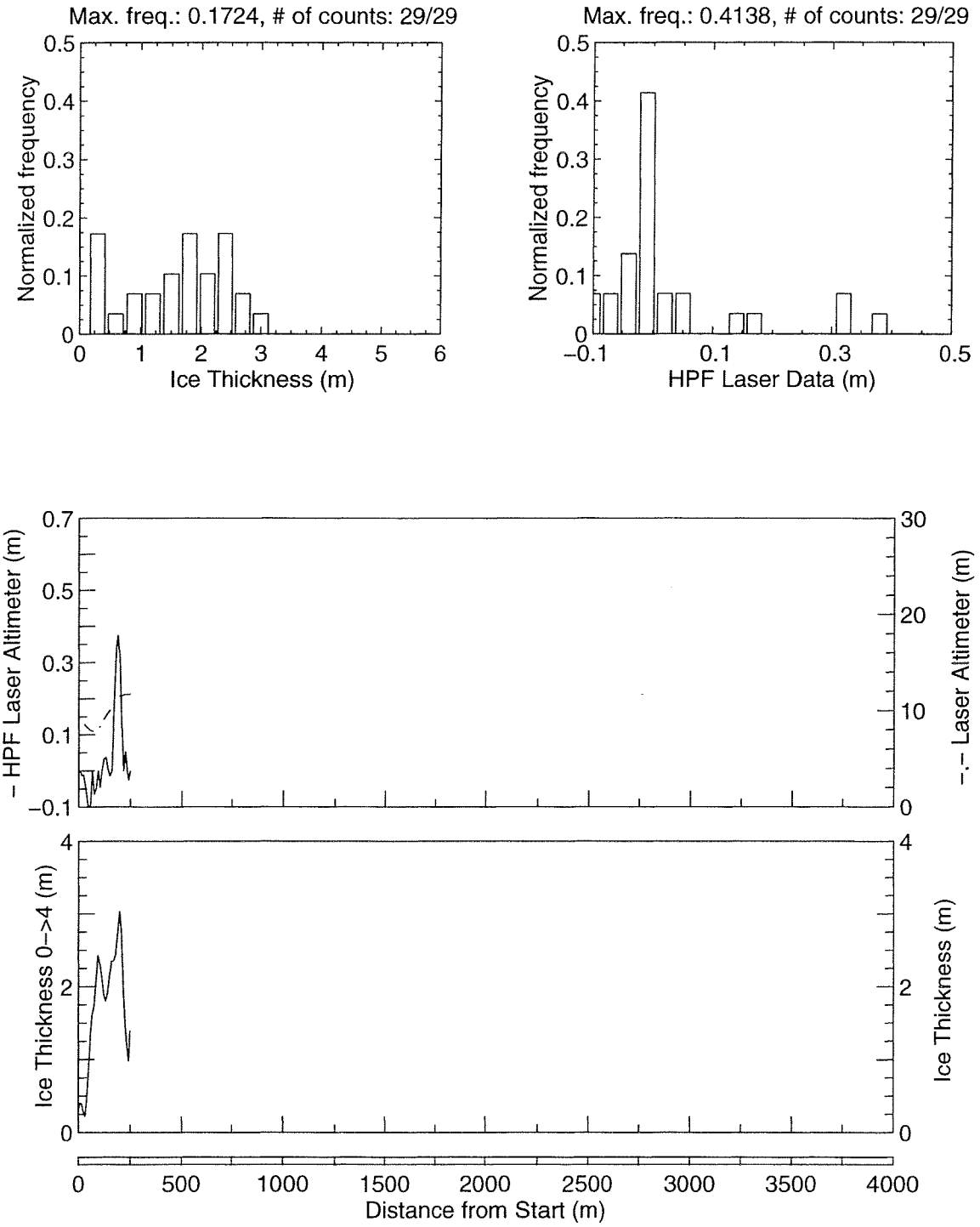

MAR 03 Flight #12 Line #10081 part 1 of 1

Line Starting Coordinates (54.2753,–55.3560) ending at (54.2627,–55.3663)

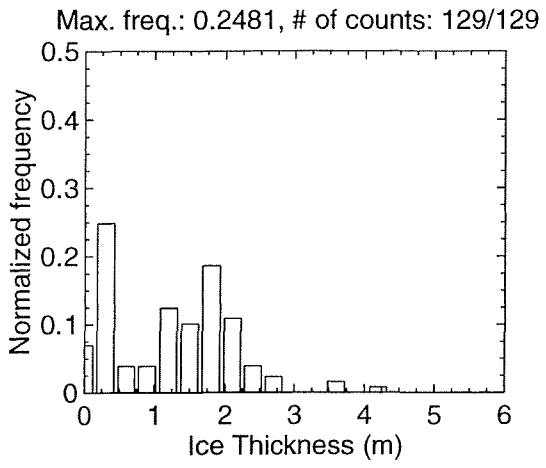

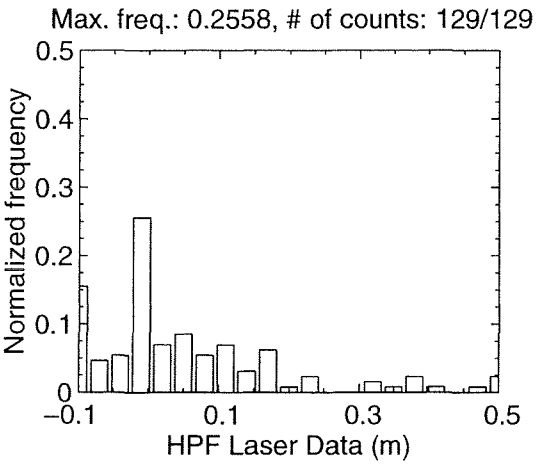

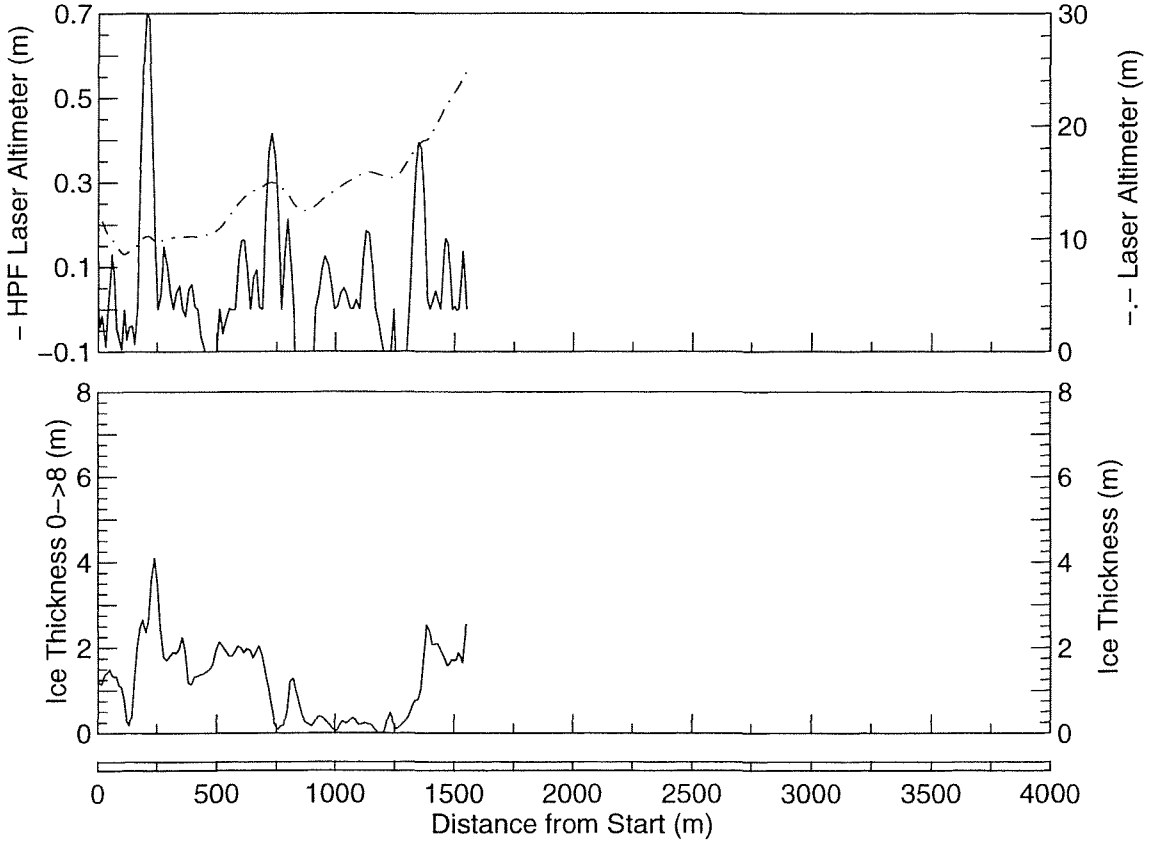

MAR 03 Flight #12 Line #10082 part 1 of 1

Line Starting Coordinates (54.2531,–55.3595) ending at (54.2683,–55.3777)

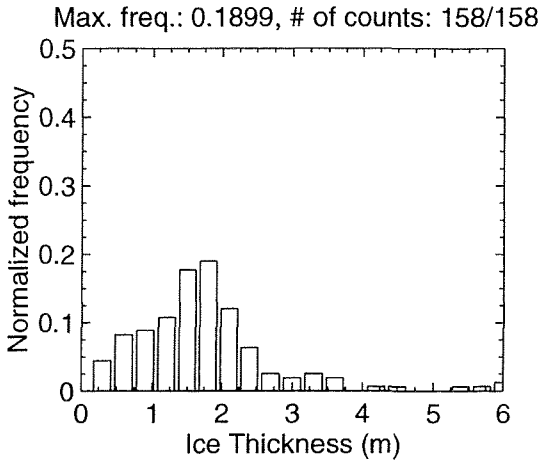

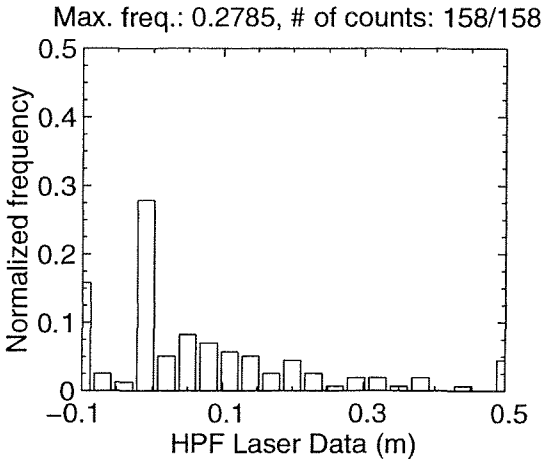

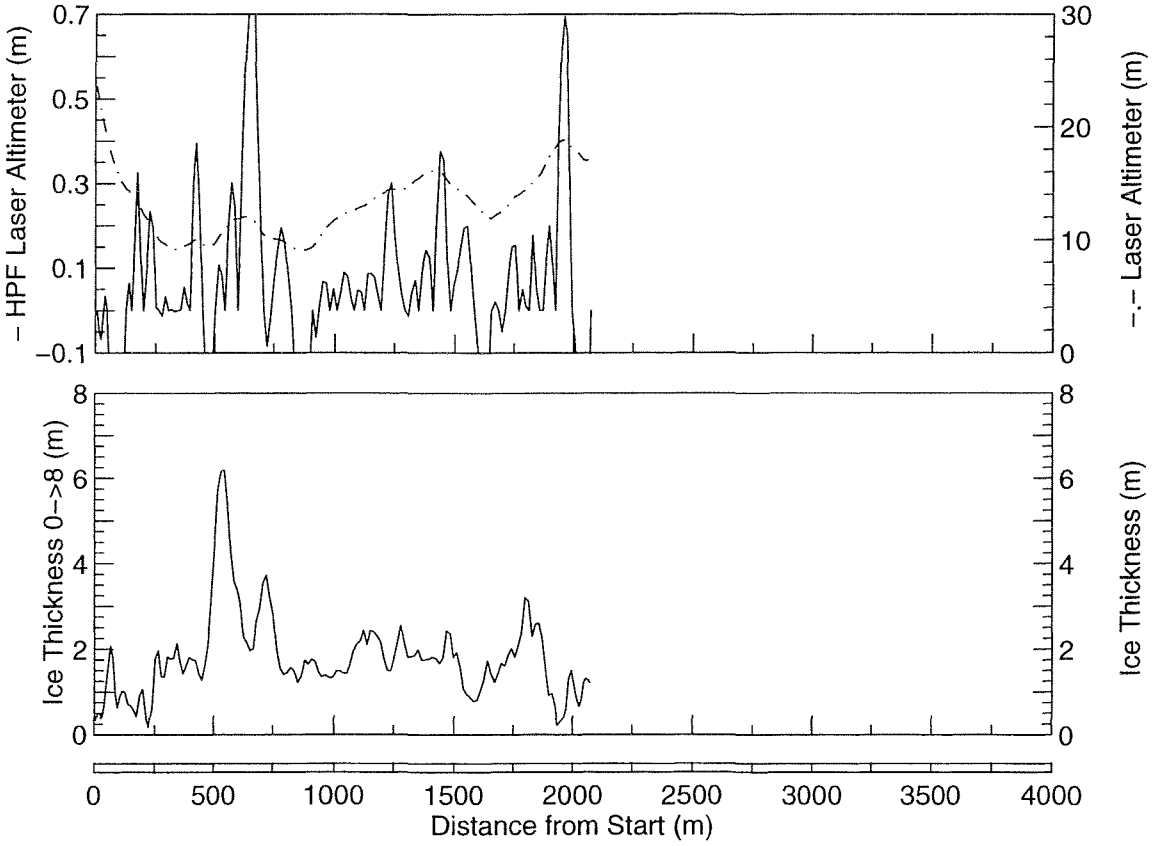

MAR 03 Flight #14 Line #10010 part 1 of 3

Line Starting Coordinates (54.1378,−55.9029) ending at (54.1210,−55.9573)

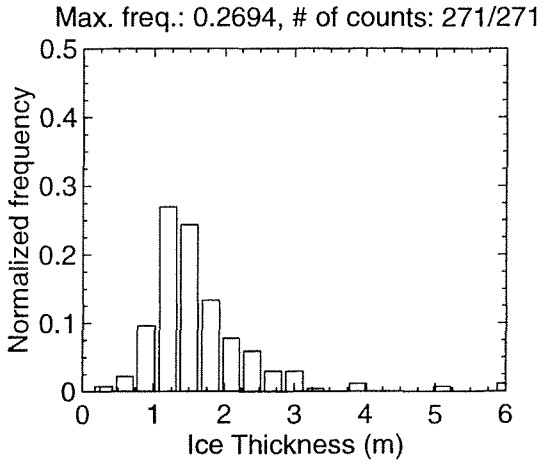

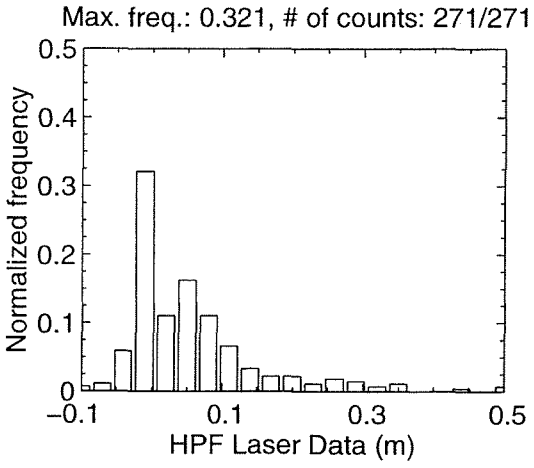

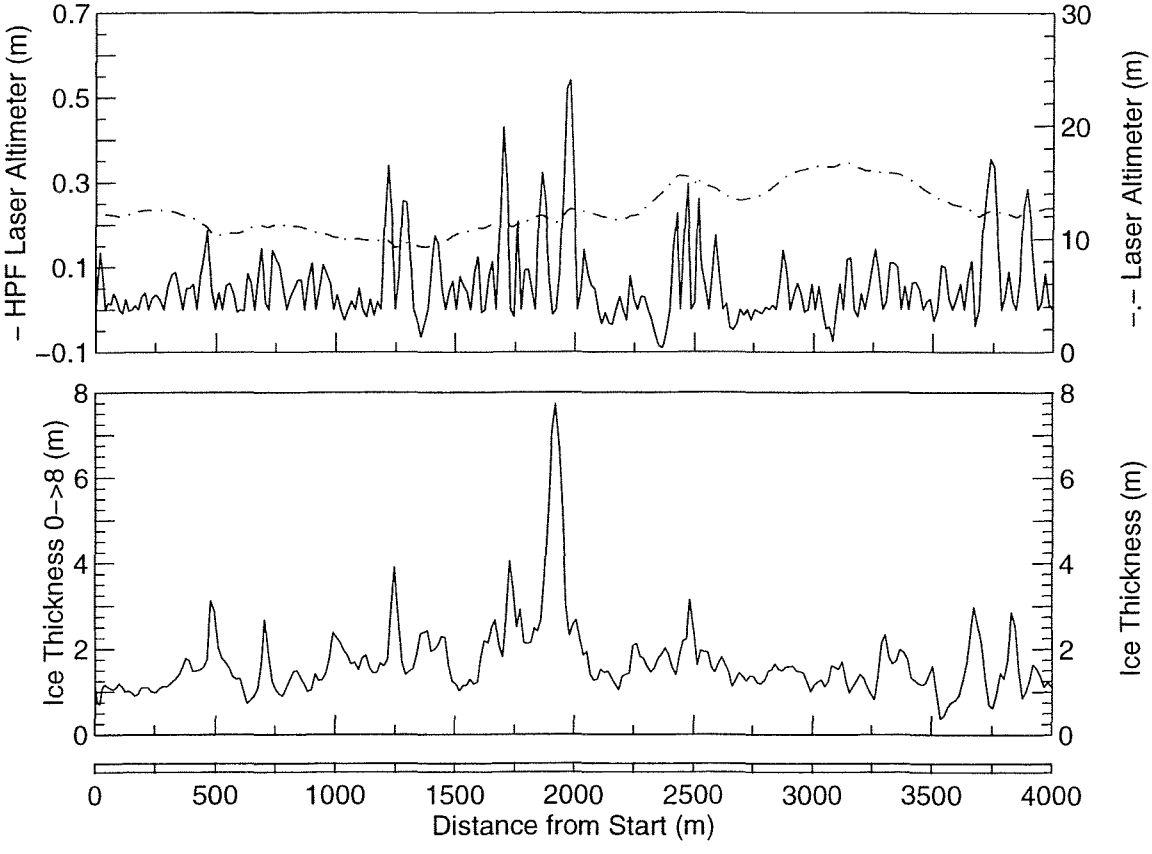

MAR 03 Flight #14 Line #10010 part 2 of 3

Line Starting Coordinates (54.1210,–55.9573) ending at (54.1049,–56.0121)

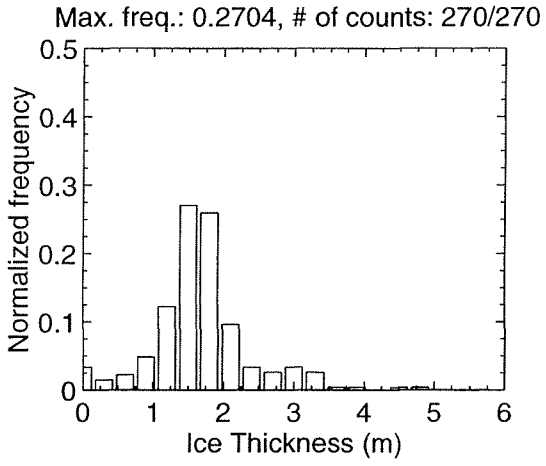

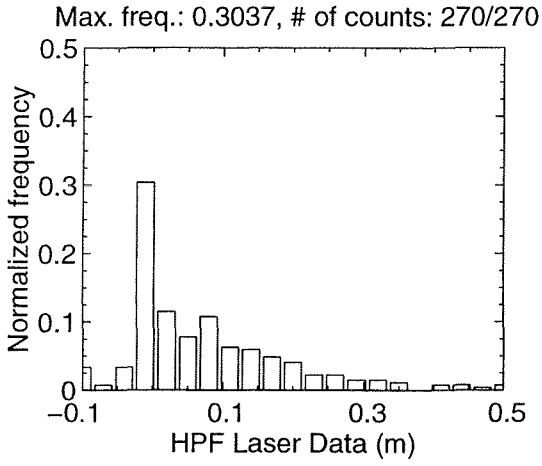

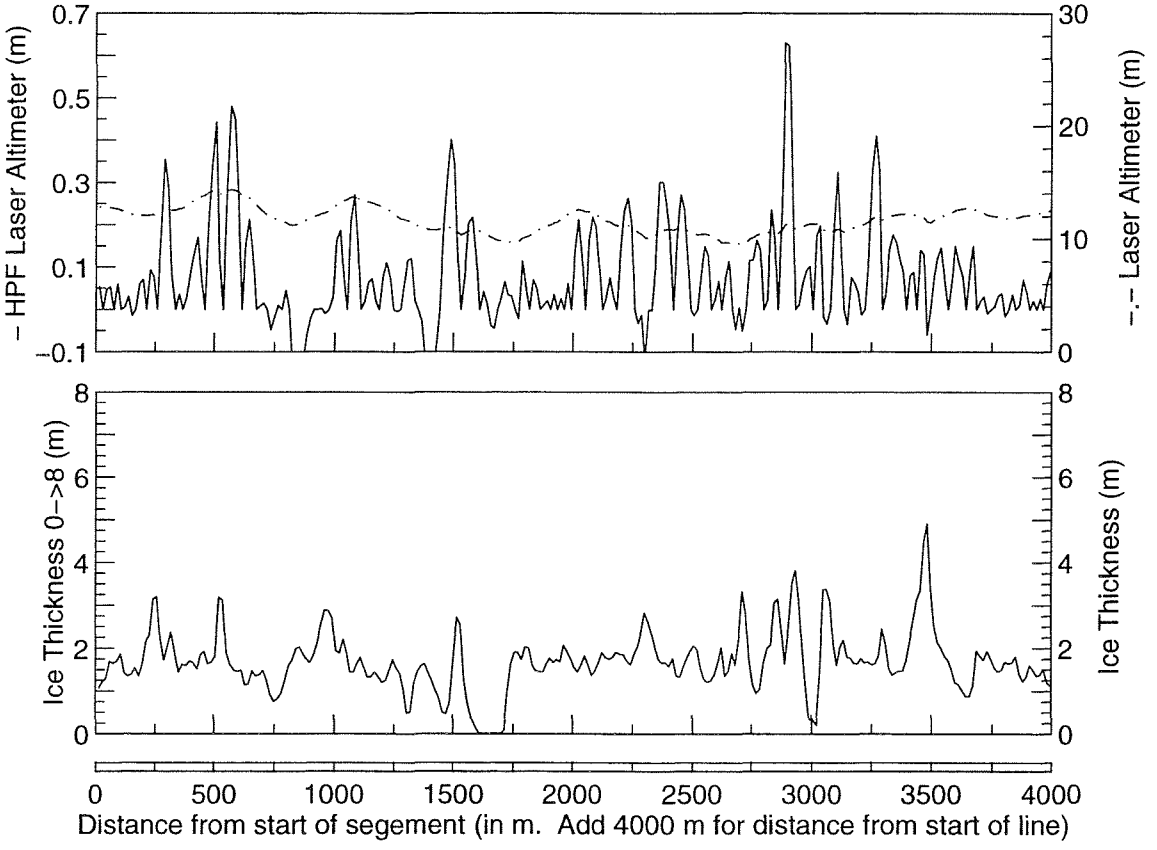

MAR 03 Flight #14 Line #10010 part 3 of 3

Line Starting Coordinates (54.1049,–56.0121) ending at (54.1015,–56.0222)

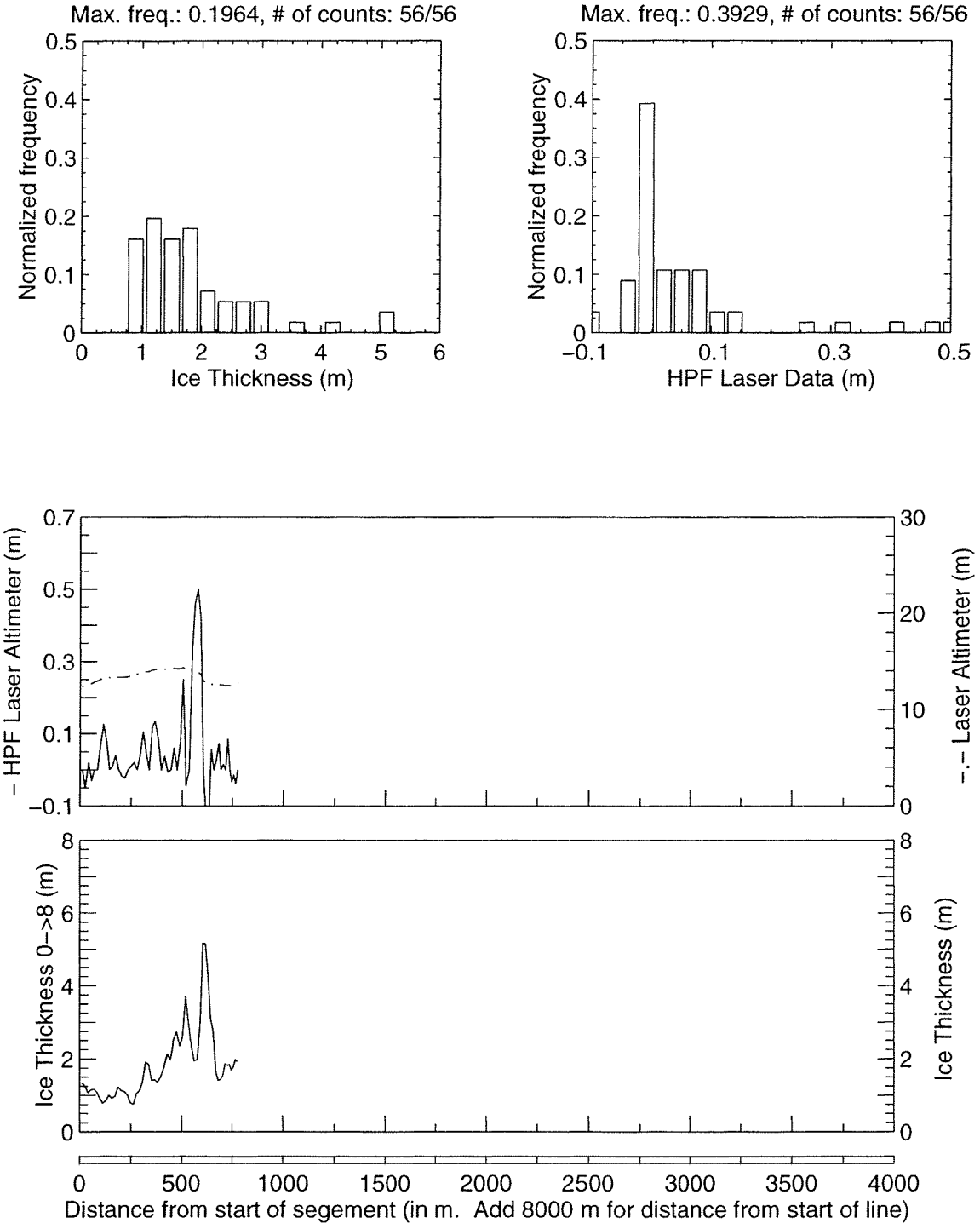

MAR 03 Flight #14 Line #10020 part 1 of 5

Line Starting Coordinates (54.0744,–56.0960) ending at (54.0551,–56.1477)

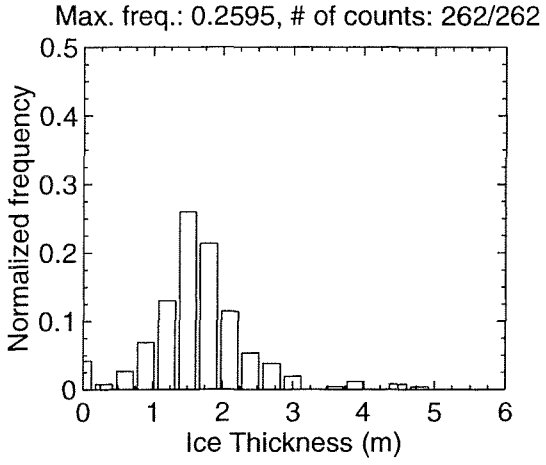

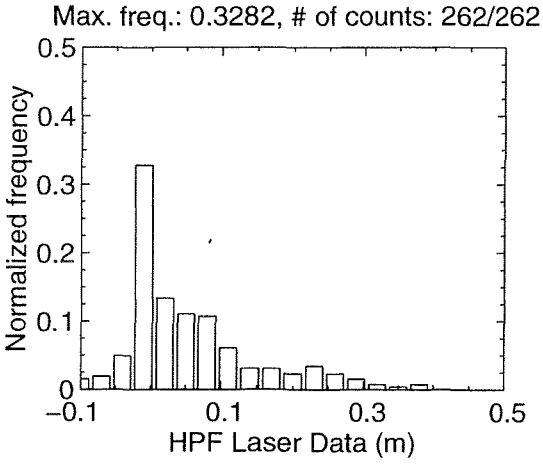

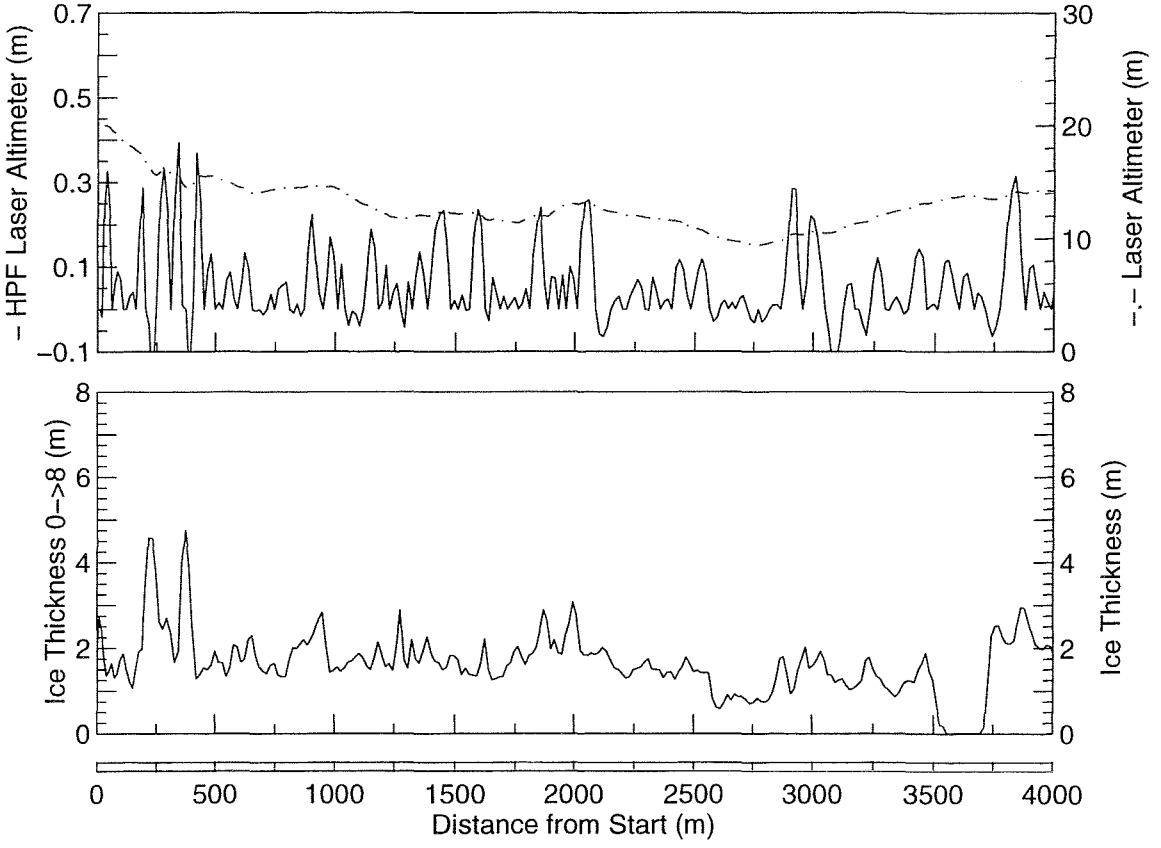

MAR 03 Flight #14 Line #10020 part 2 of 5

Line Starting Coordinates (54.0551,–56.1477) ending at (54.0379,–56.2015)

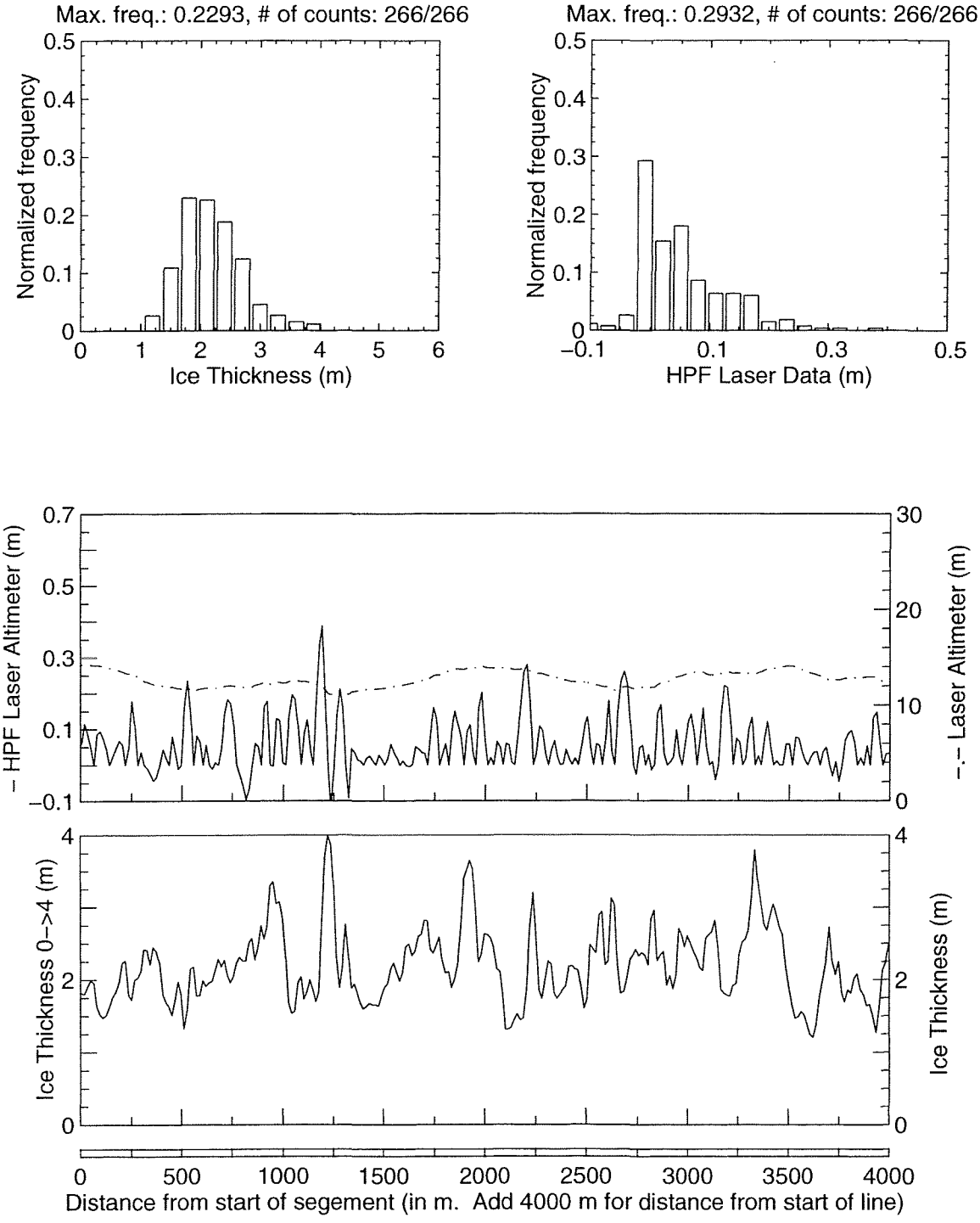

MAR 03 Flight #14 Line #10020 part 3 of 5

Line Starting Coordinates (54.0379,–56.2015) ending at (54.0220,–56.2562)

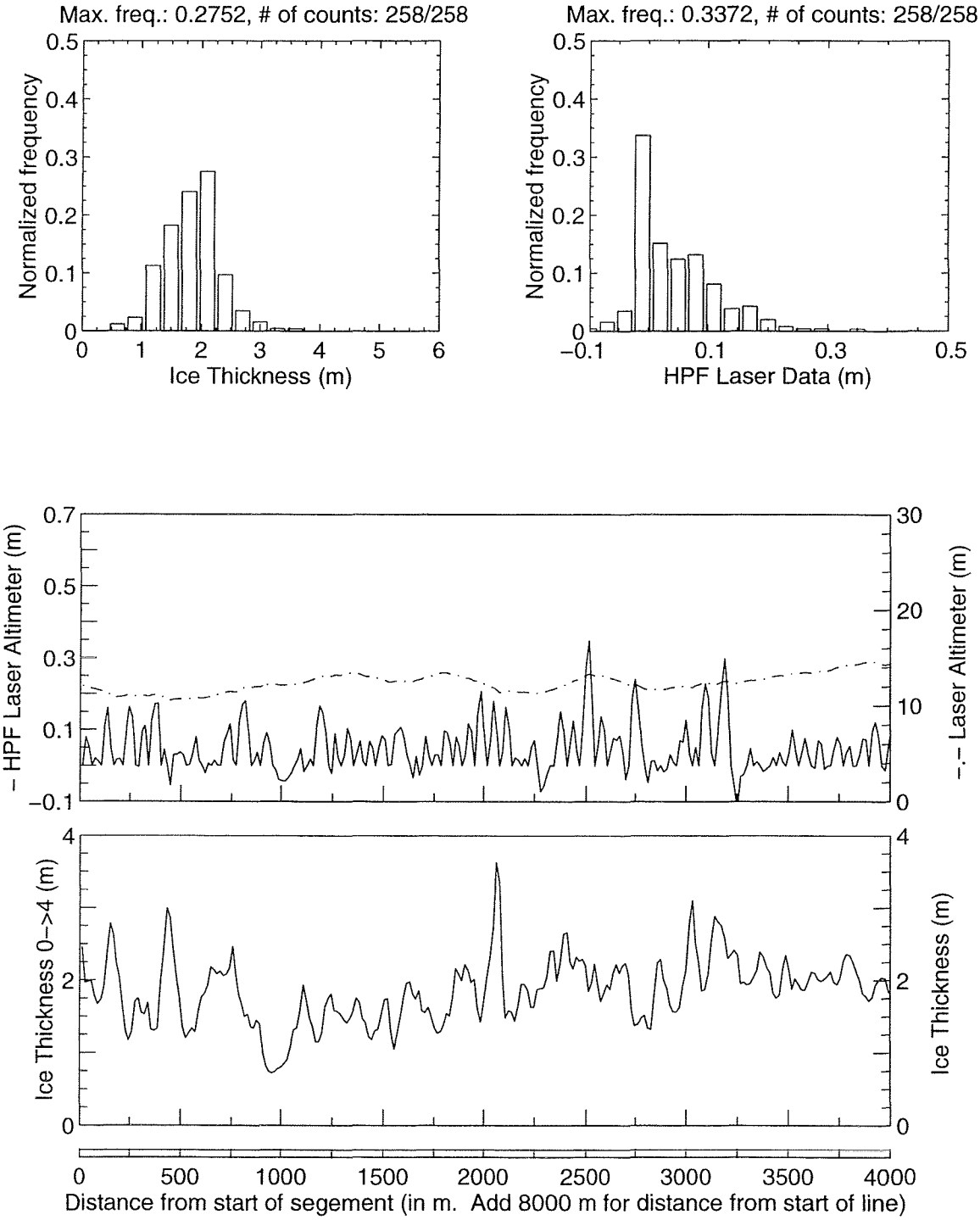

MAR 03 Flight #14 Line #10020 part 4 of 5

Line Starting Coordinates (54.0220,–56.2562) ending at (54.0045,–56.3094)

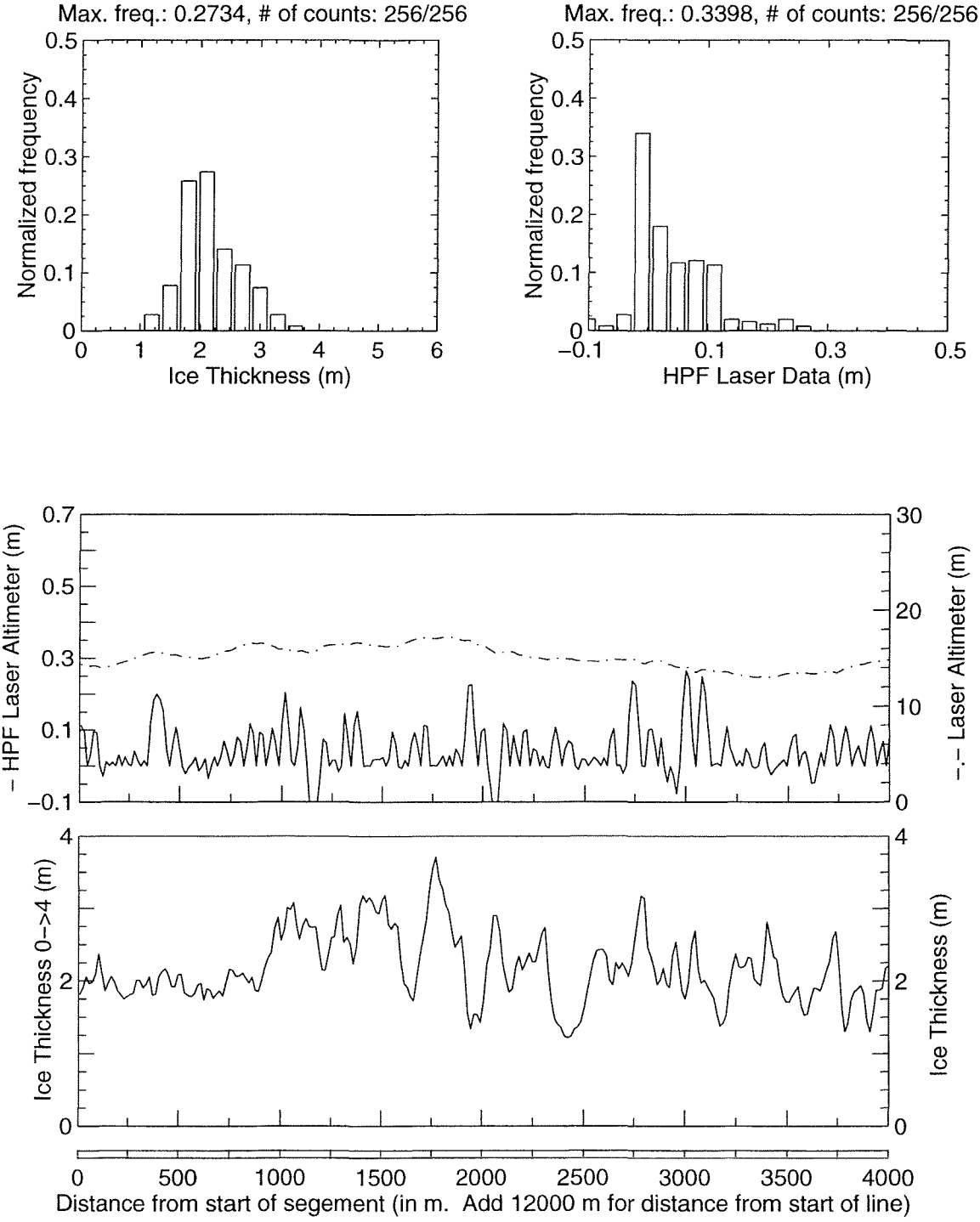

MAR 03 Flight #14 Line #10020 part 5 of 5

Line Starting Coordinates (54.0045,–56.3094) ending at (53.9946,–56.3372)

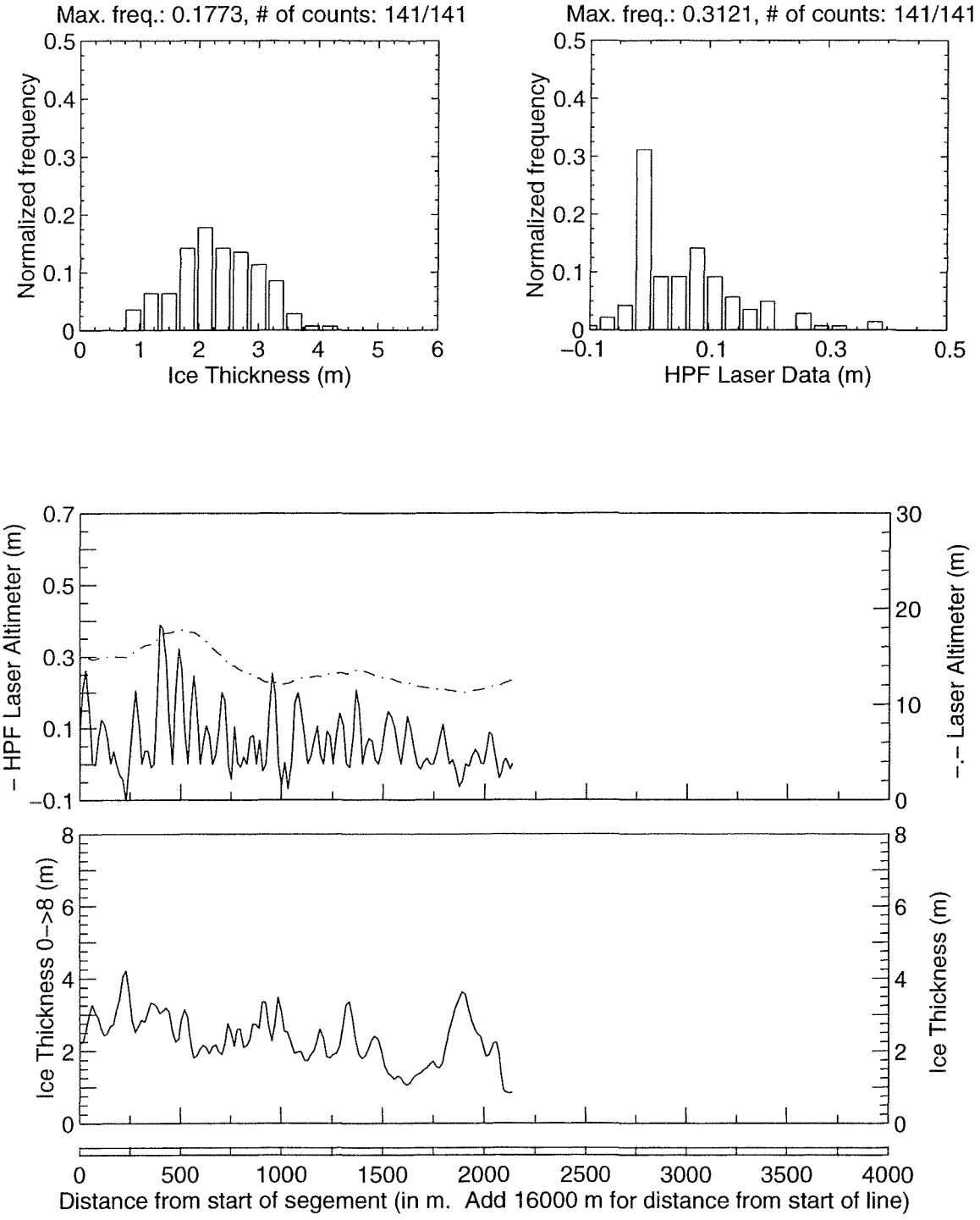

MAR 03 Flight #14 Line #10030 part 1 of 2

Line Starting Coordinates (53.9647,–56.4131) ending at (53.9449,–56.4642)

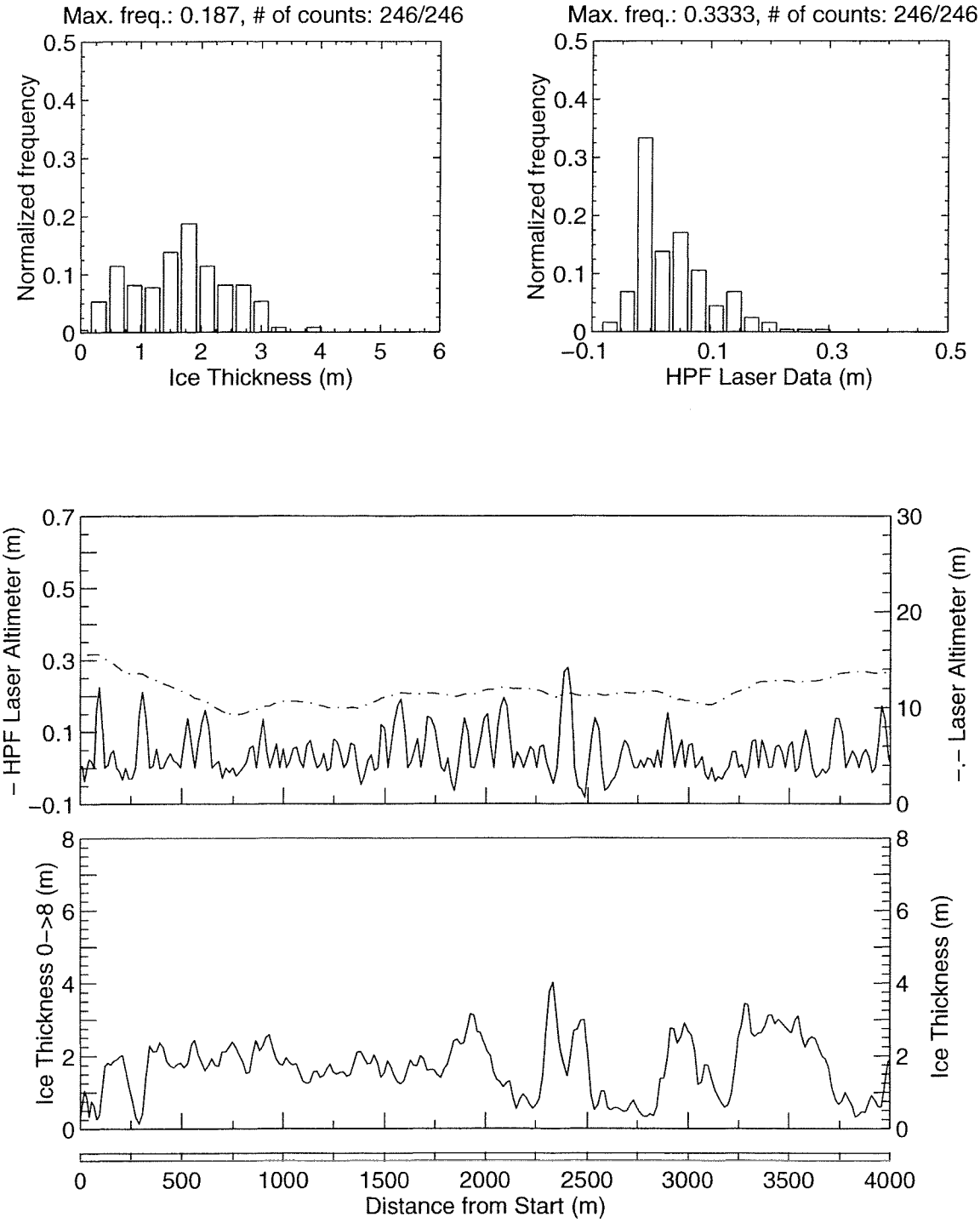

MAR 03 Flight #14 Line #10030 part 2 of 2

Line Starting Coordinates (53.9449,−56.4642) ending at (53.9342,−56.4948)

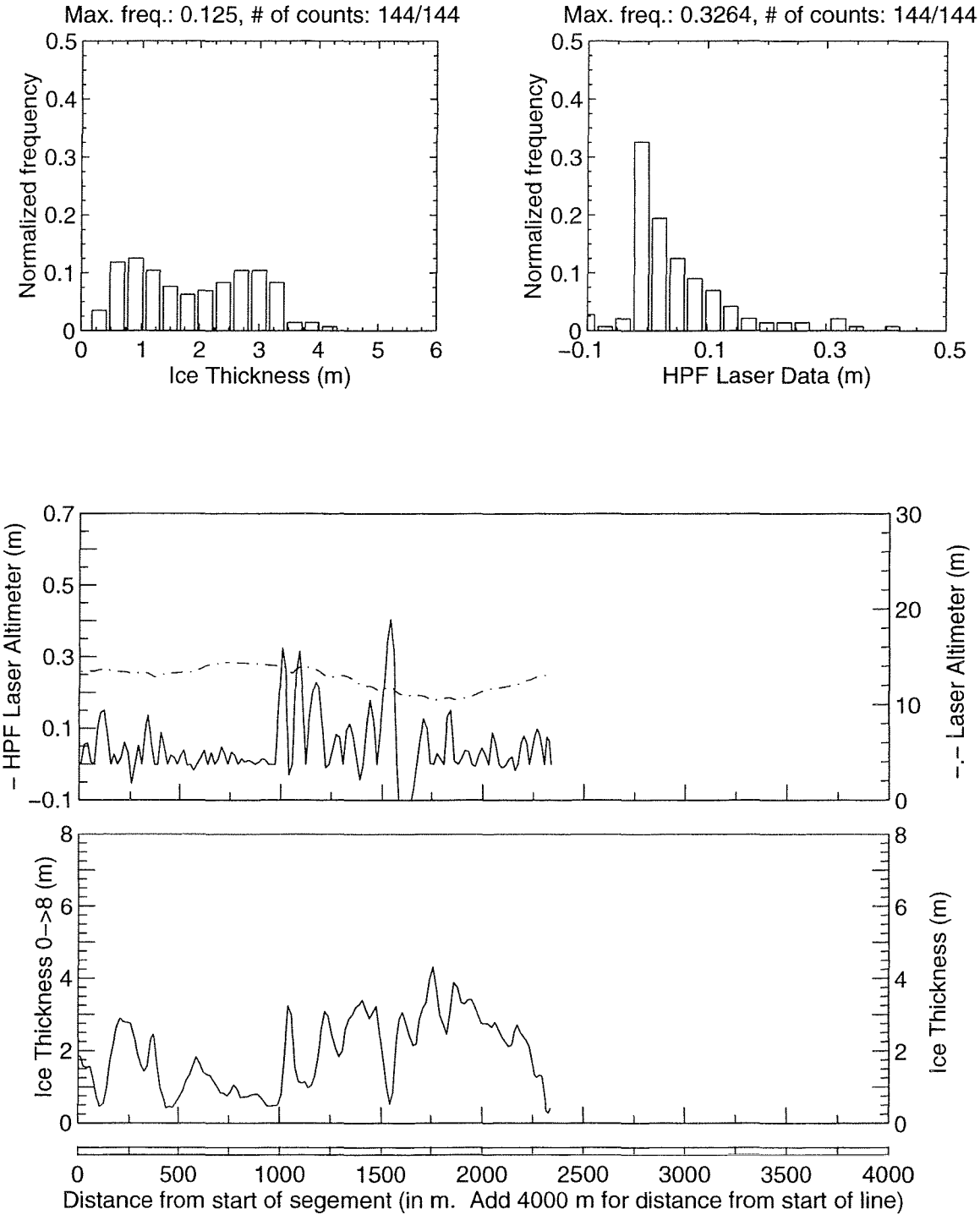

MAR 03 Flight #14 Line #10040 part 1 of 5

Line Starting Coordinates (53.9326,–56.5002) ending at (53.9156,–56.5542)

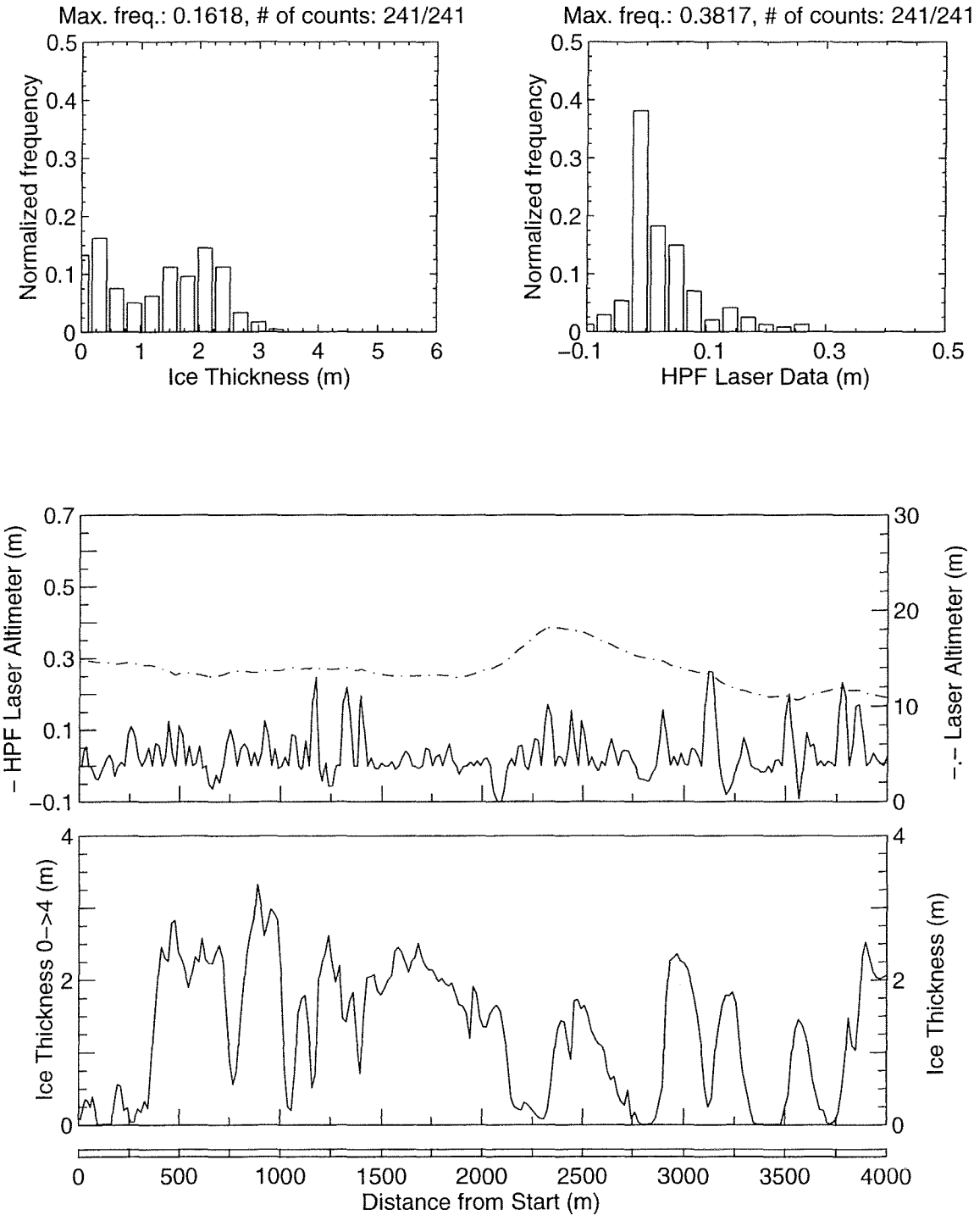

MAR 03 Flight #14 Line #10040 part 2 of 5

Line Starting Coordinates (53.9156,–56.5542) ending at (53.8987,–56.6079)

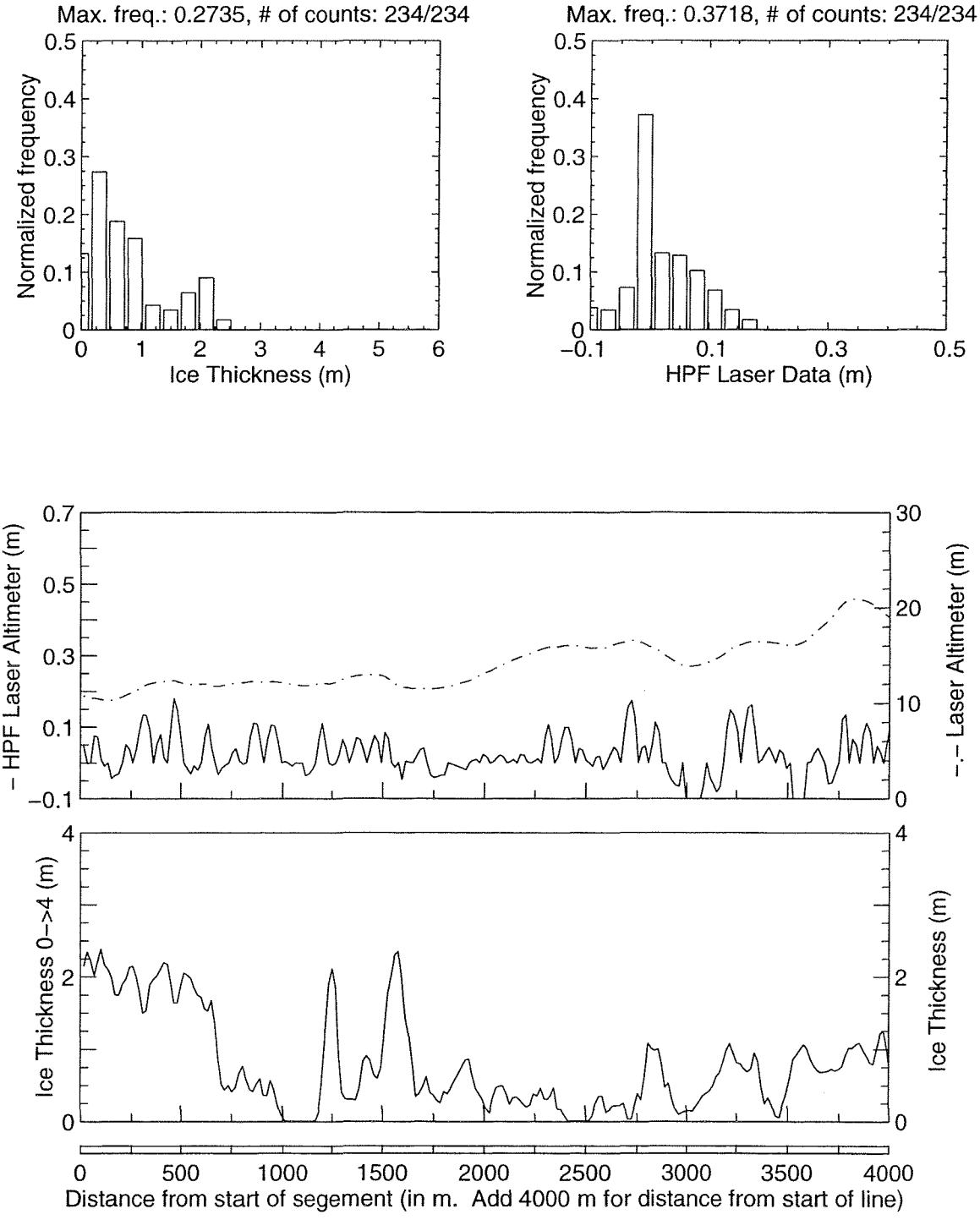

MAR 03 Flight #14 Line #10040 part 3 of 5

Line Starting Coordinates (53.8987,−56.6079) ending at (53.8787,−56.6586)

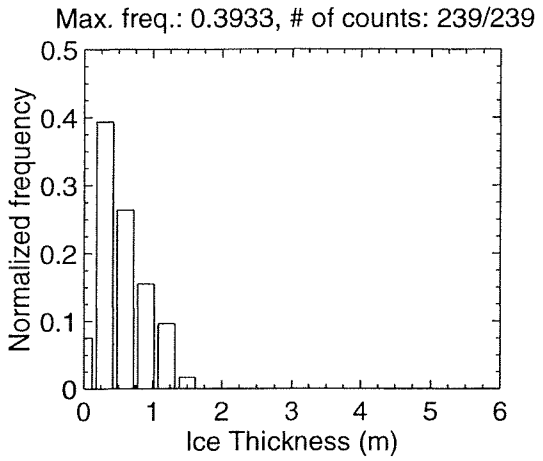

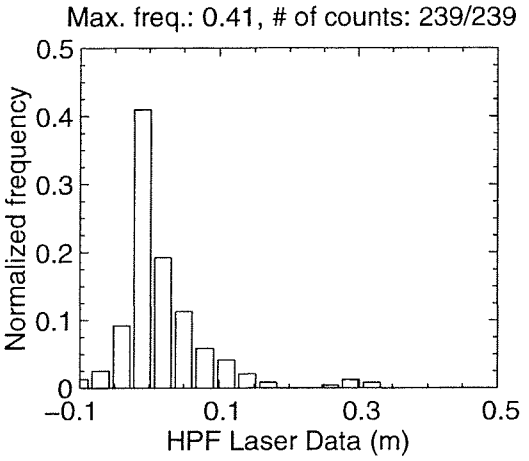

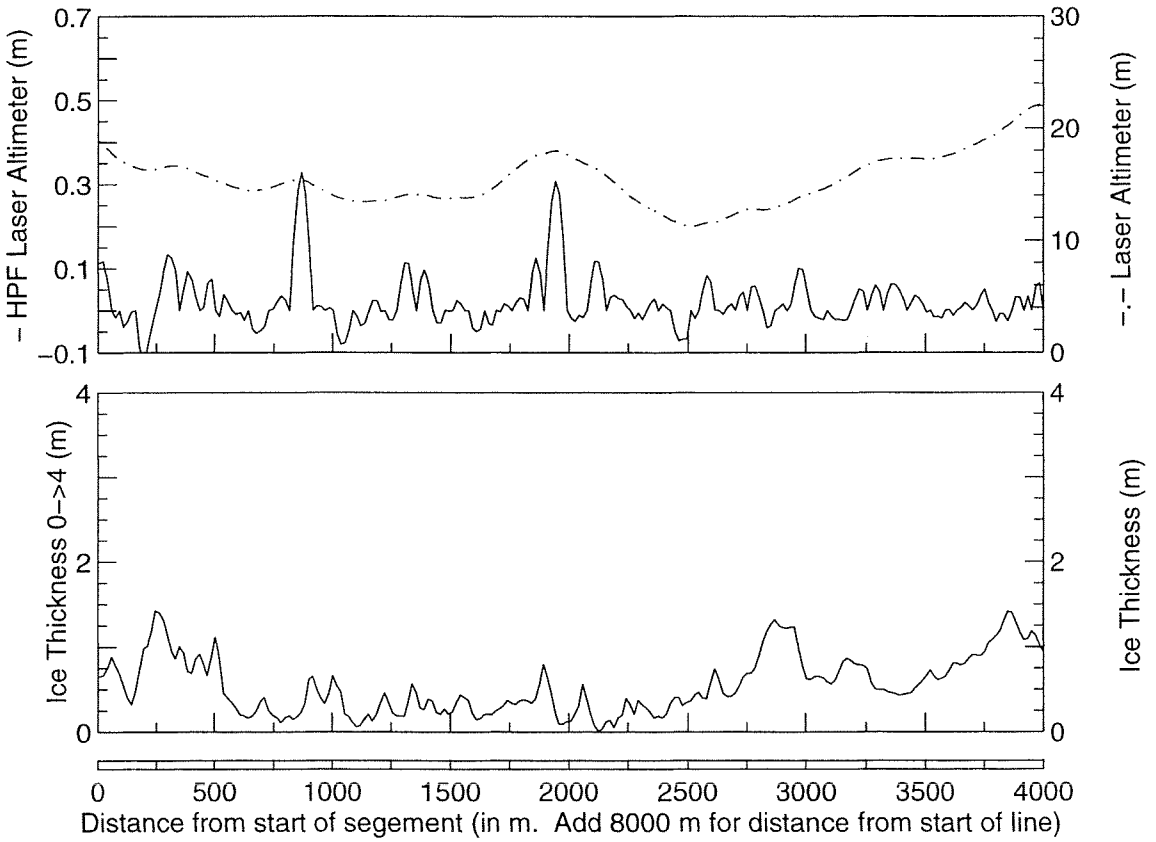

MAR 03 Flight #14 Line #10040 part 4 of 5

Line Starting Coordinates (53.8787,–56.6586) ending at (53.8583,–56.7085)

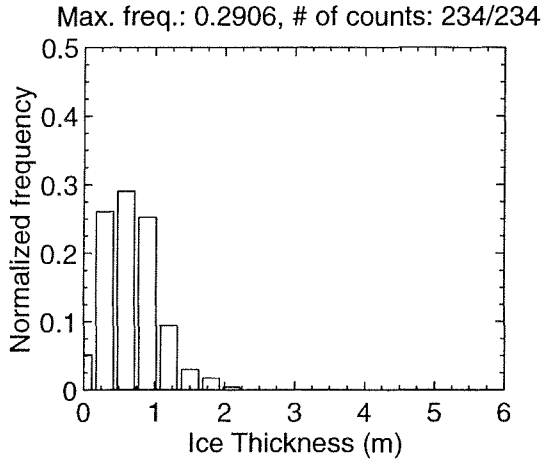

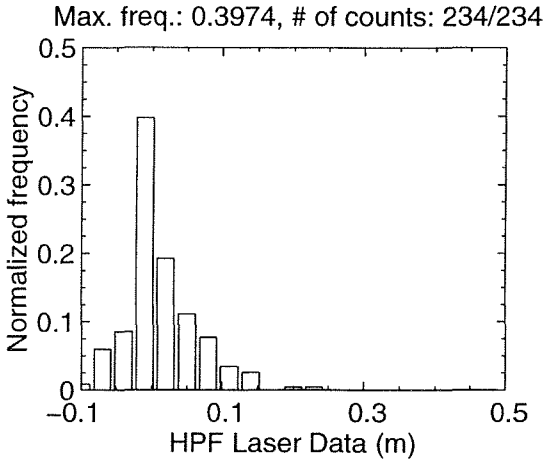

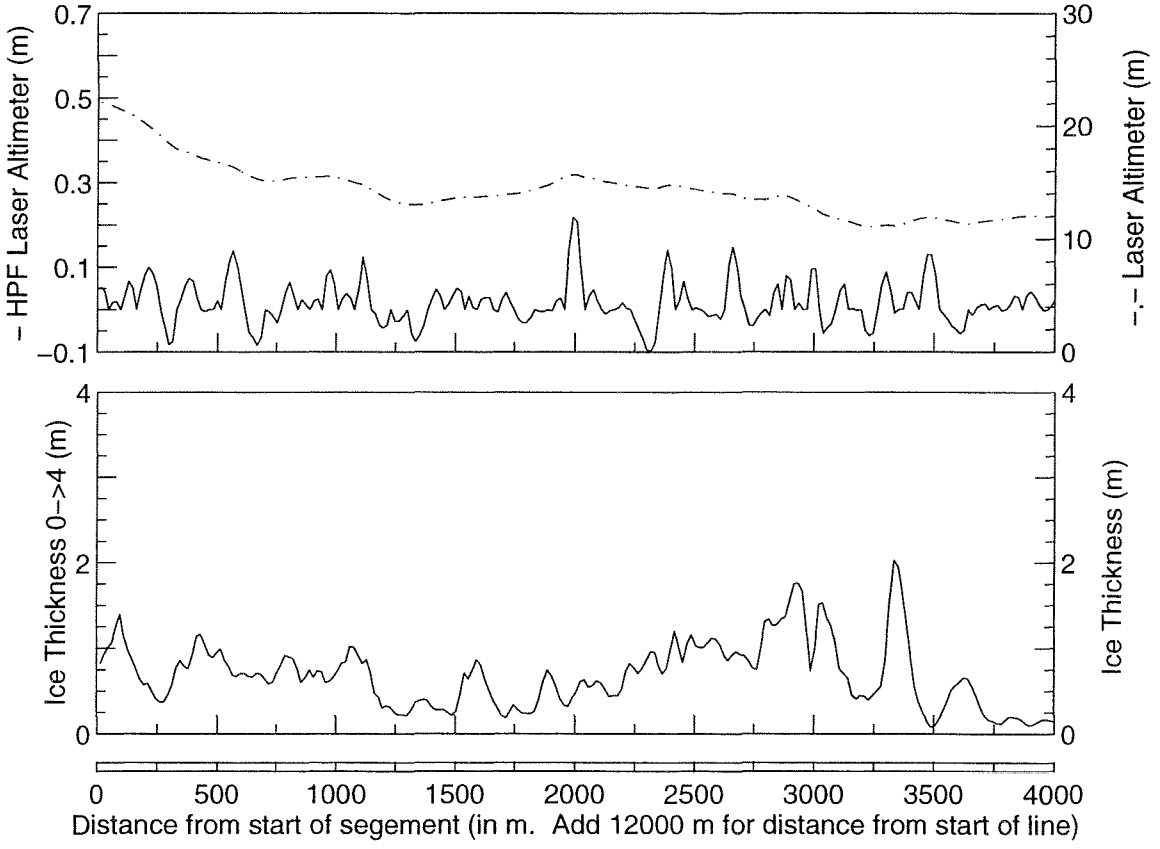

MAR 03 Flight #14 Line #10040 part 5 of 5

Line Starting Coordinates (53.8583,–56.7085) ending at (53.8417,–56.7431)

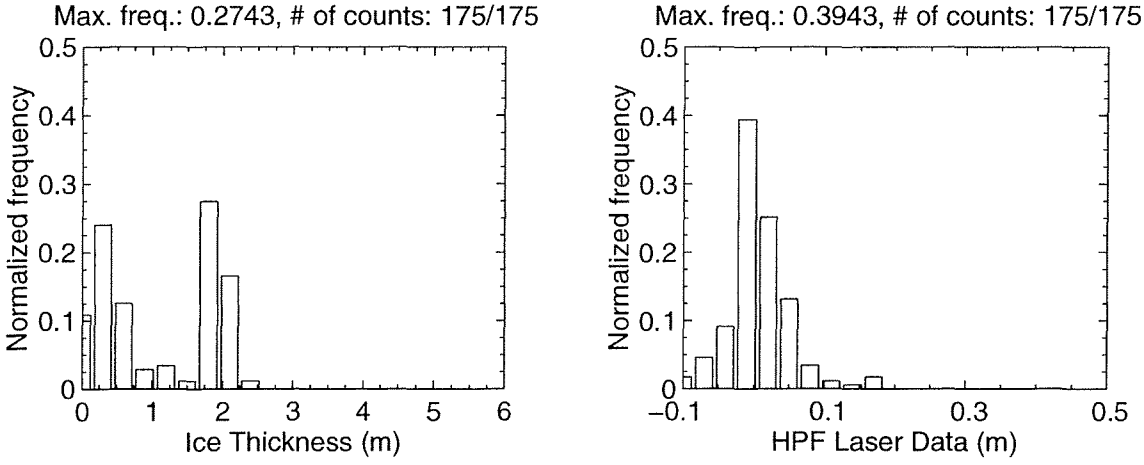

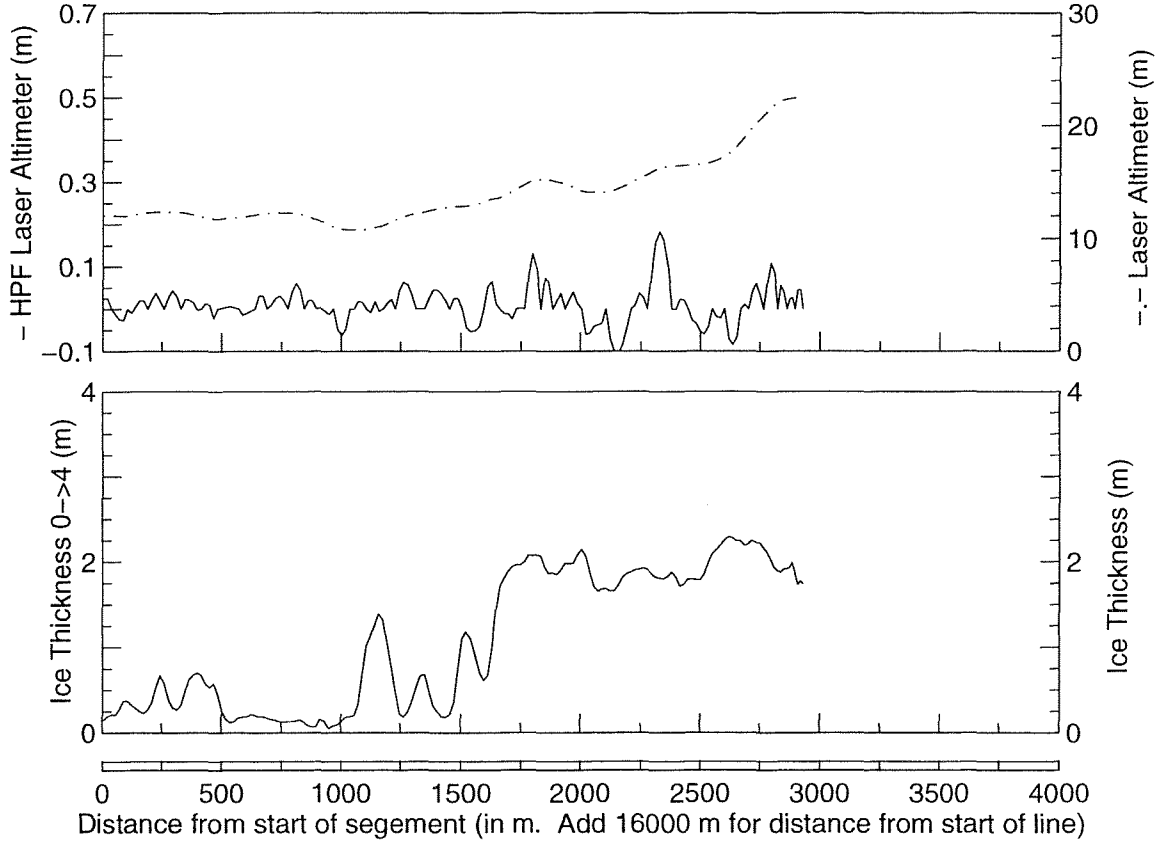

MAR 03 Flight #14 Line #10050 part 1 of 3

Line Starting Coordinates (53.8214,–56.8271) ending at (53.8189,–56.8880)

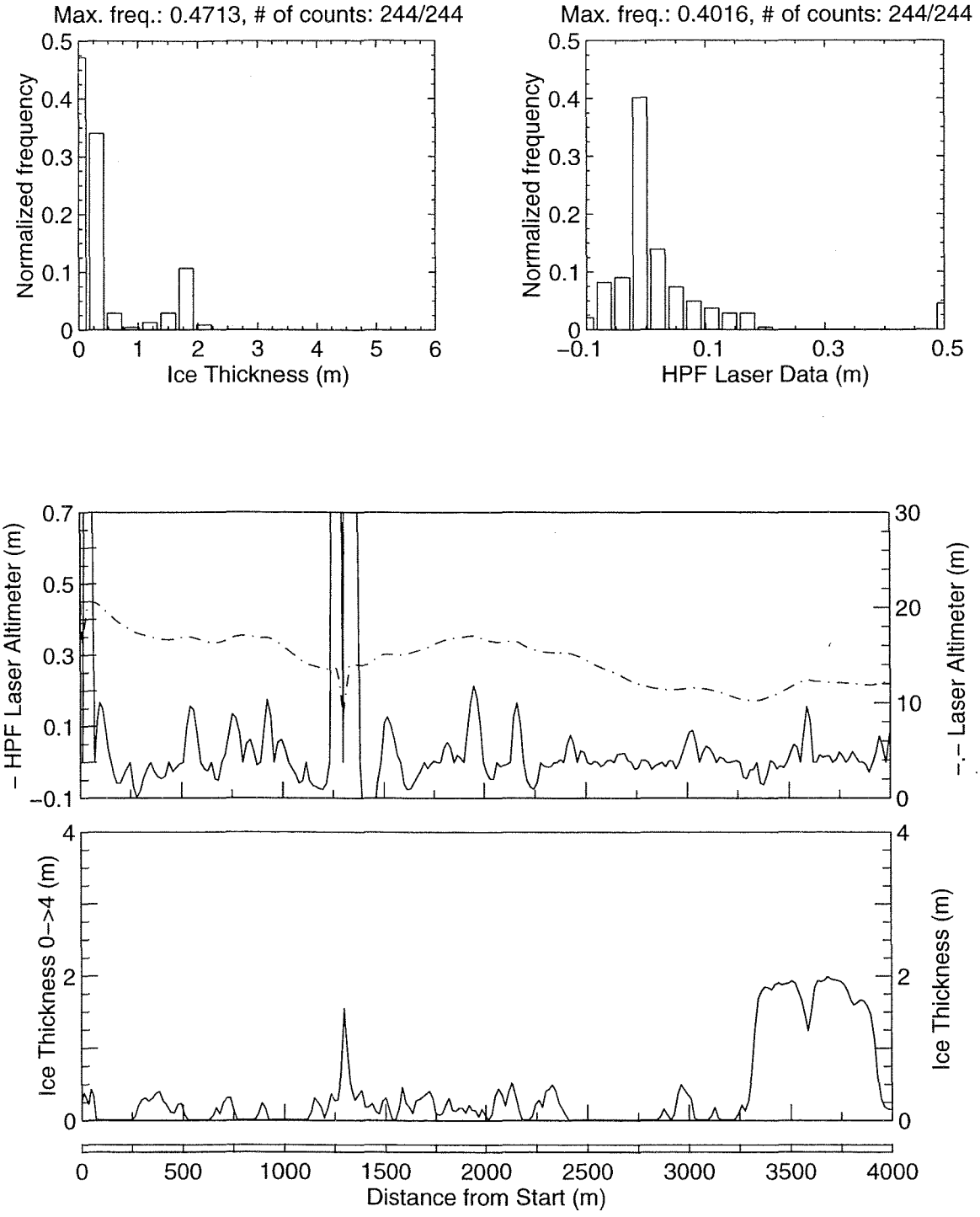

MAR 03 Flight #14 Line #10050 part 2 of 3

Line Starting Coordinates (53.8189,–56.8880) ending at (53.8170,–56.9487)

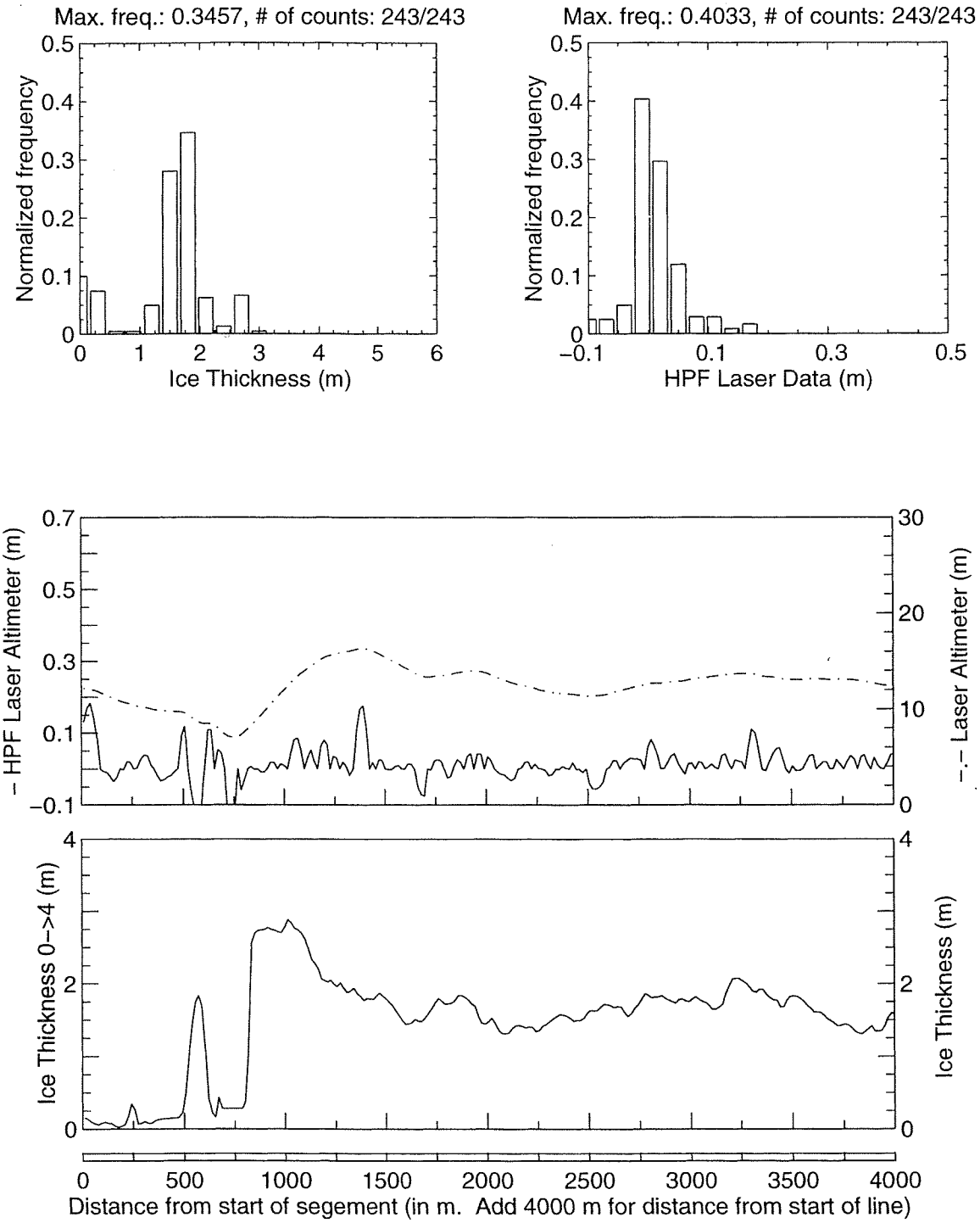

MAR 03 Flight #14 Line #10050 part 3 of 3

Line Starting Coordinates (53.8170,–56.9487) ending at (53.8132,–57.0025)

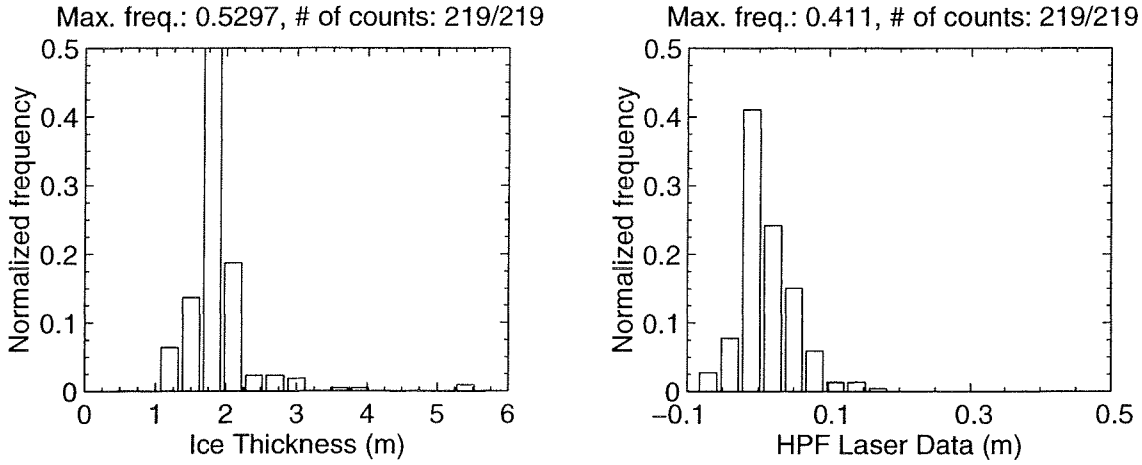

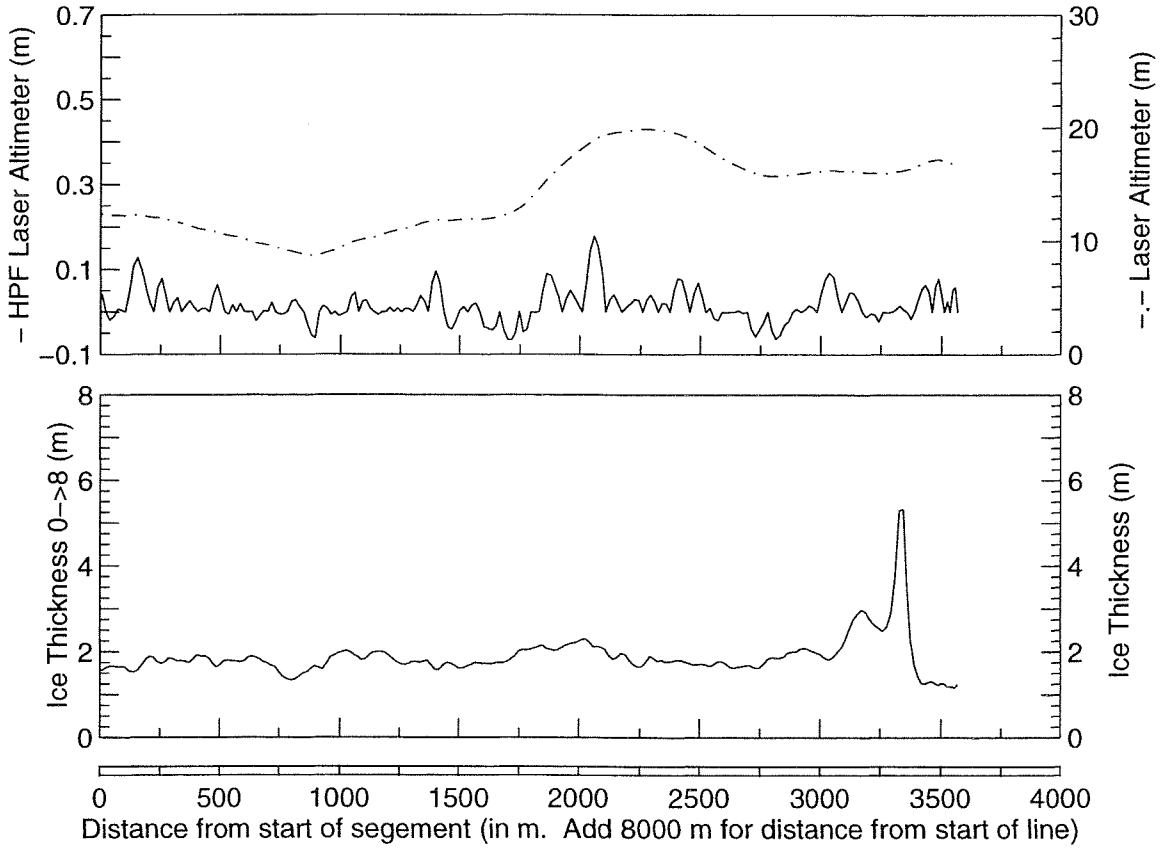

MAR 03 Flight #14 Line #10060 part 1 of 1

Line Starting Coordinates (53.8014,–57.0163) ending at (53.7982,–57.0177)

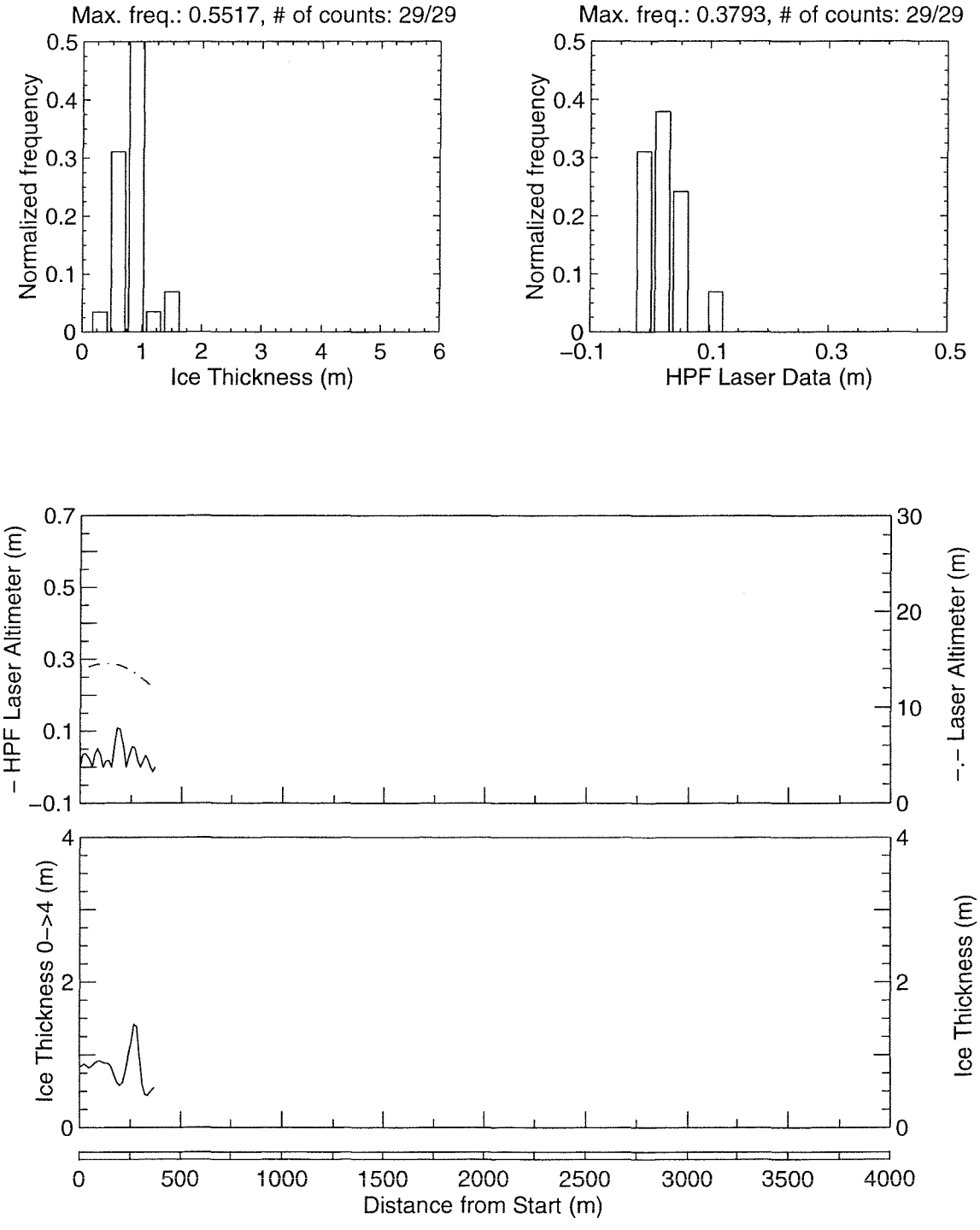

MAR 03 Flight #14 Line #10070 part 1 of 1

Line Starting Coordinates (53.7876,–57.0191) ending at (53.7779,–57.0181)

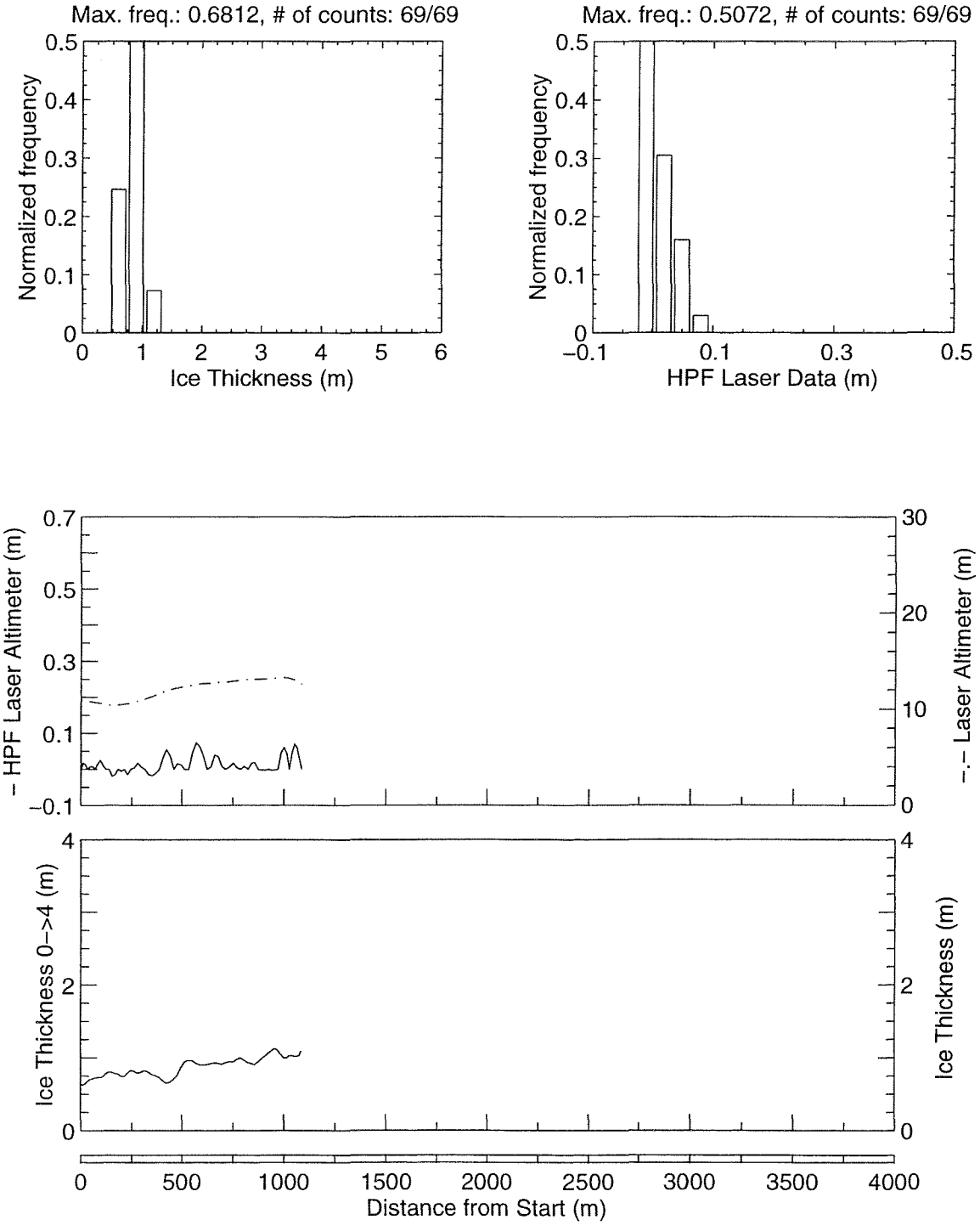

MAR 03 Flight #14 Line #10080 part 1 of 1

Line Starting Coordinates (53.7309,–56.9884) ending at (53.7314,–56.9832)

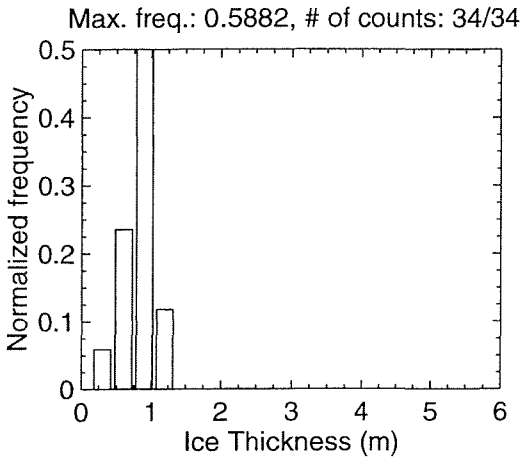

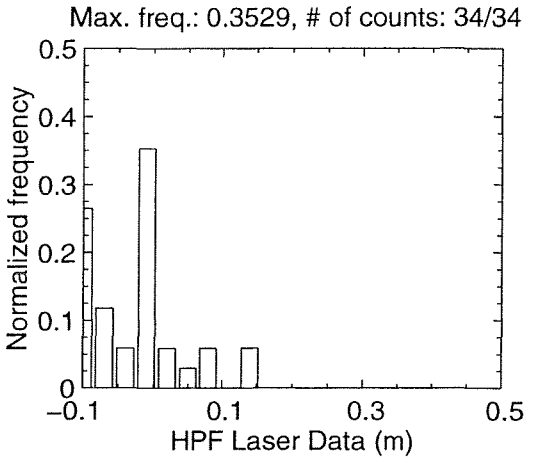

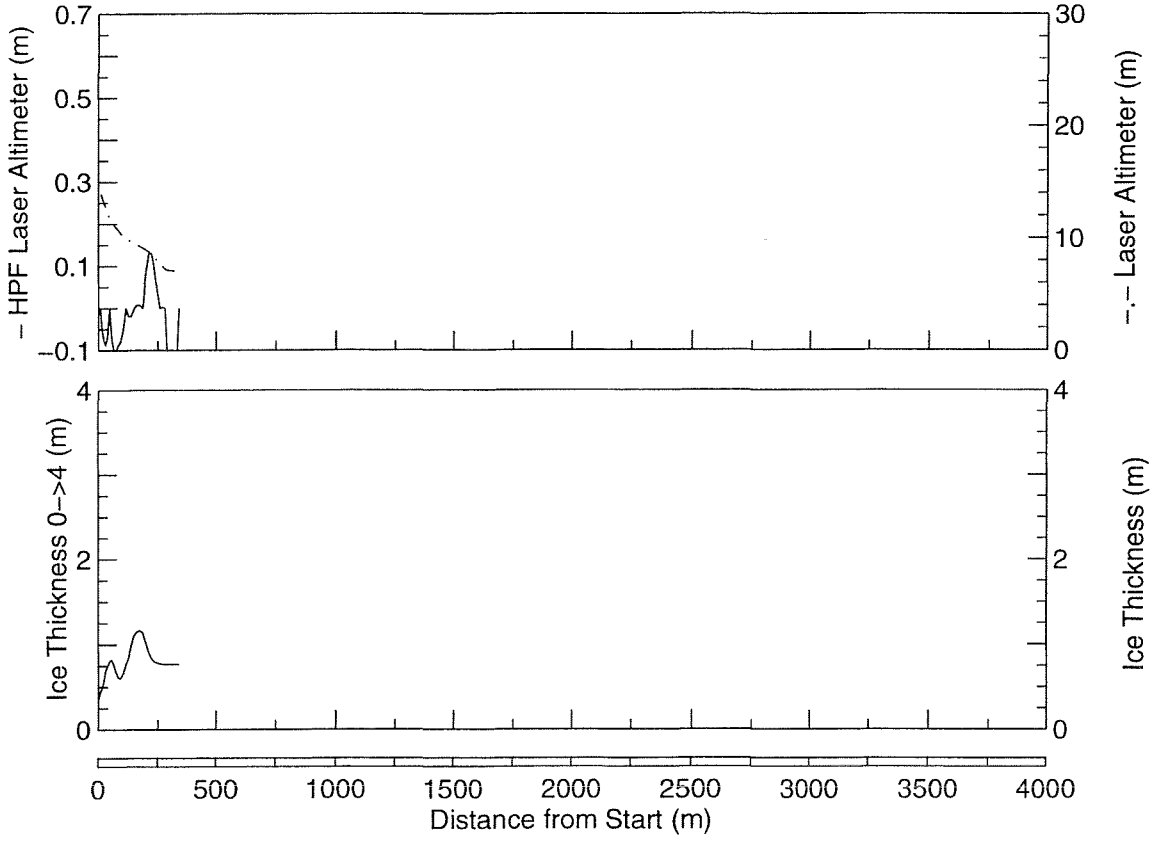

MAR 03 Flight #14 Line #10090 part 1 of 1

Line Starting Coordinates (53.7318,–56.9779) ending at (53.7318,–56.9761)

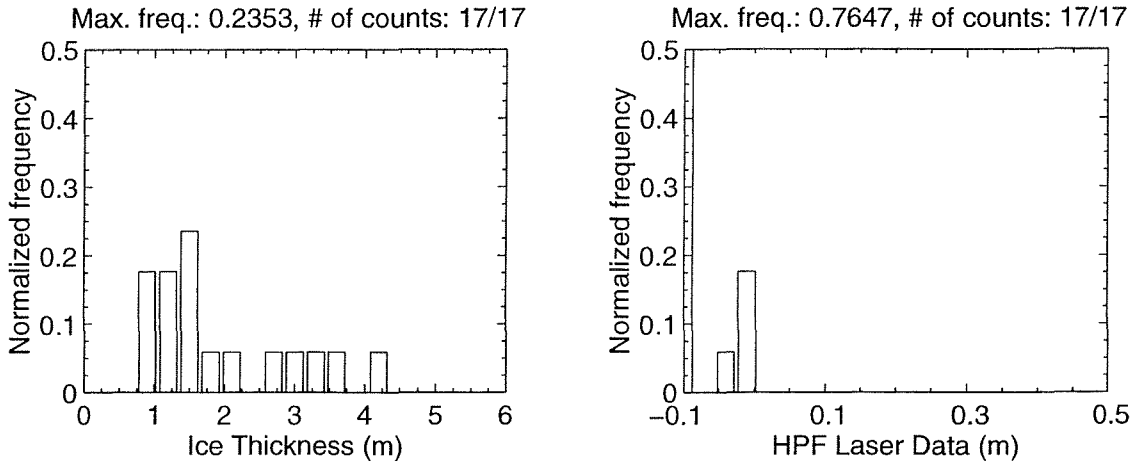

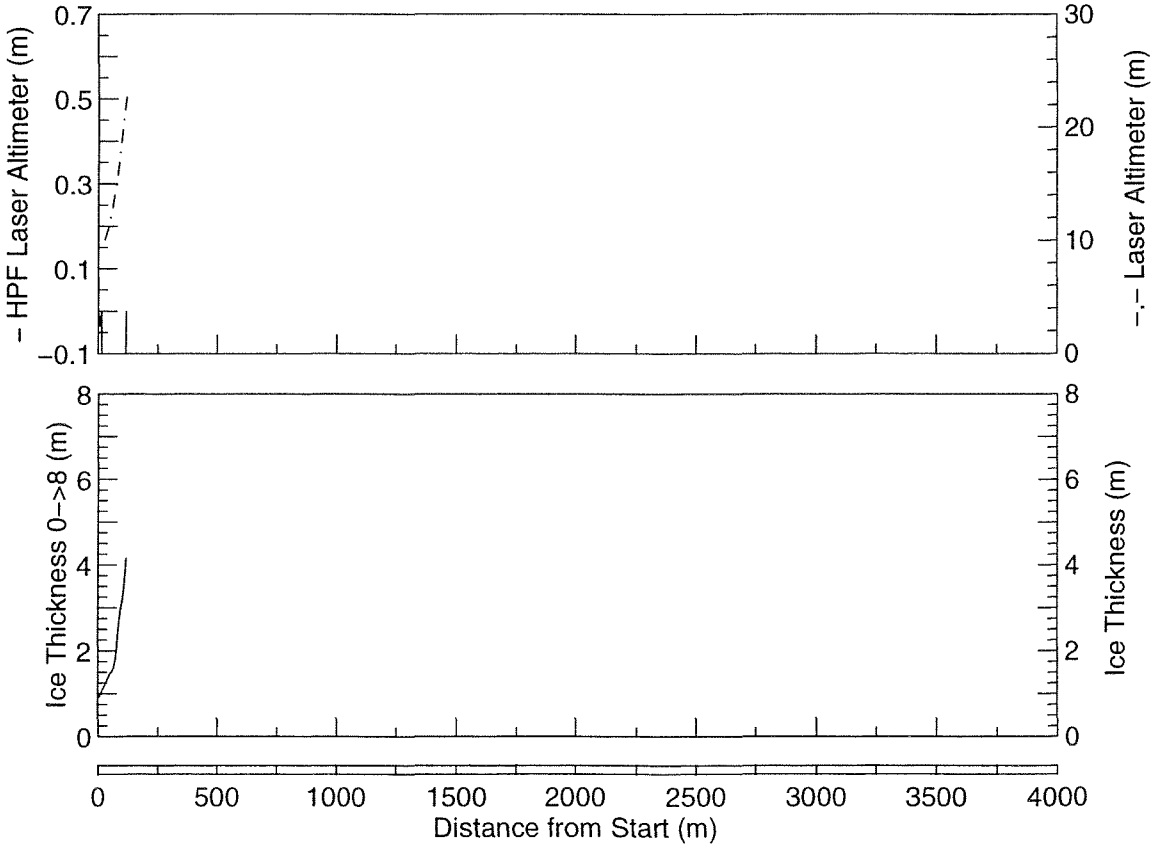

MAR 03 Flight #14 Line #10100 part 1 of 1

Line Starting Coordinates (53.7309,–56.9870) ending at (53.7313,–56.9838)

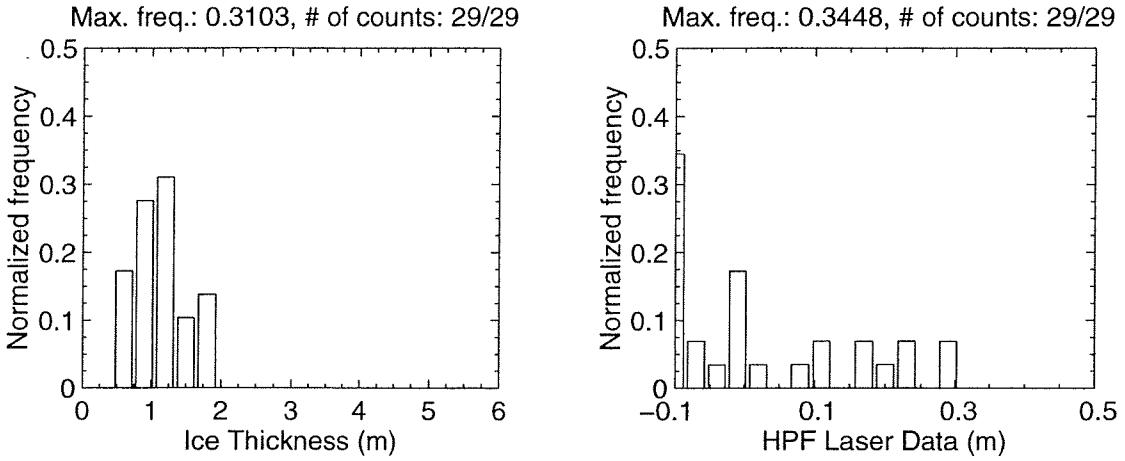

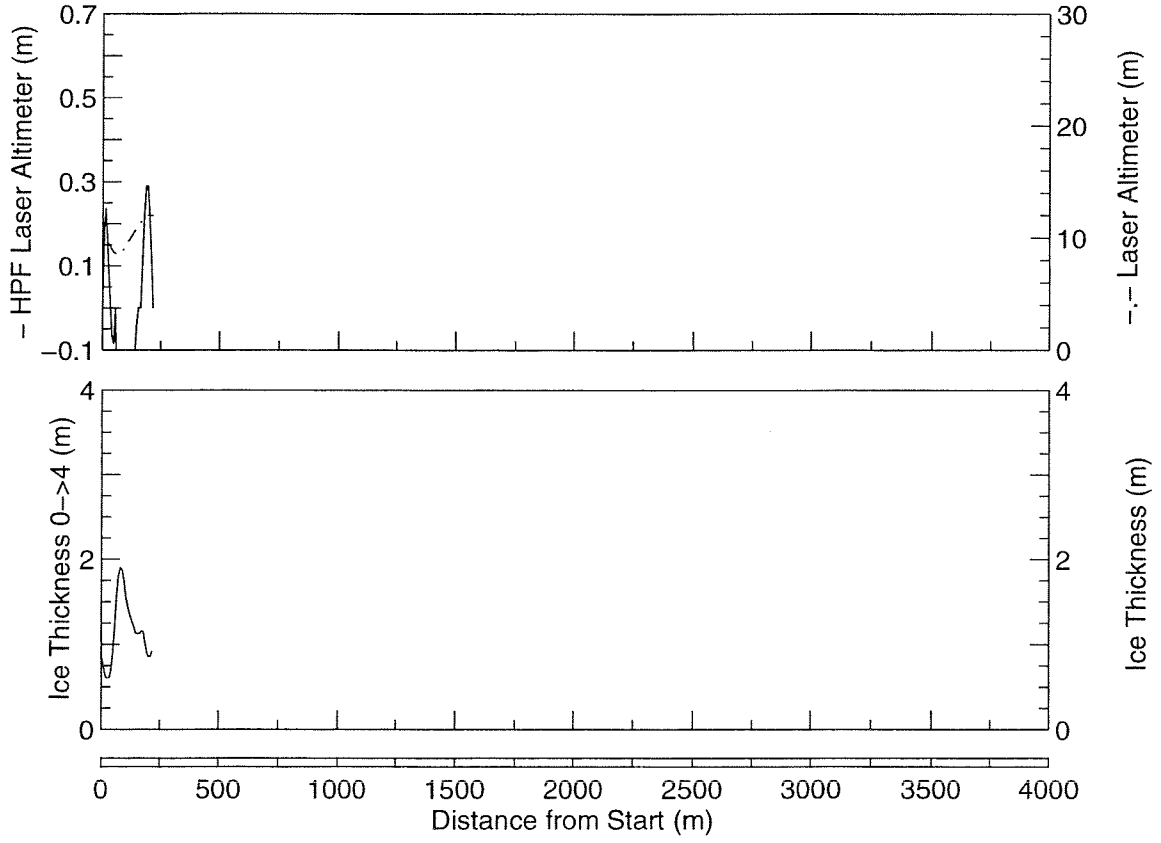

MAR 03 Flight #14 Line #10111 part 1 of 1

Line Starting Coordinates (53.7316,–56.9794) ending at (53.7318,–56.9744)

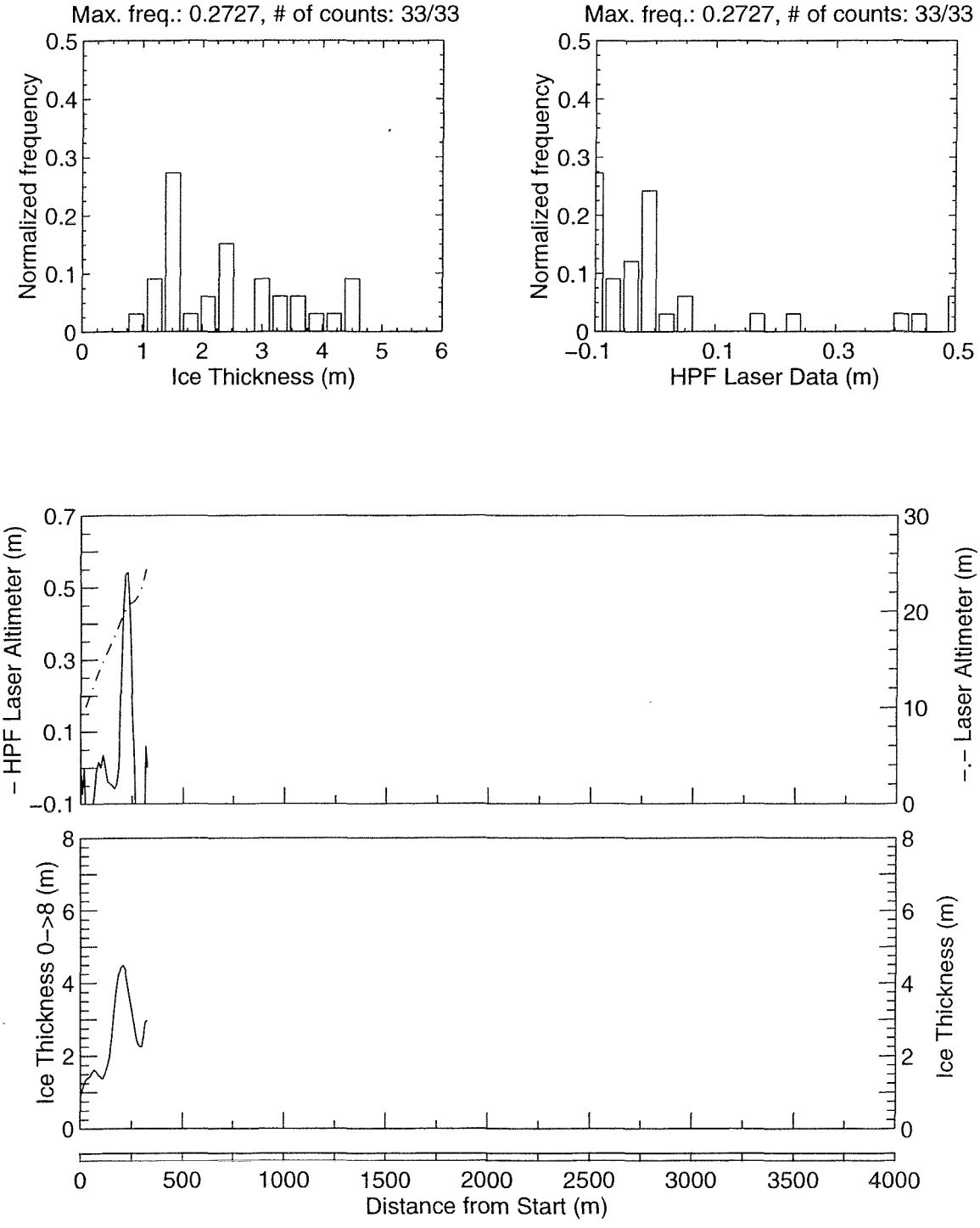

MAR 03 Flight #14 Line #10112 part 1 of 1

Line Starting Coordinates (53.7309,–56.9959) ending at (53.7307,–56.9947)

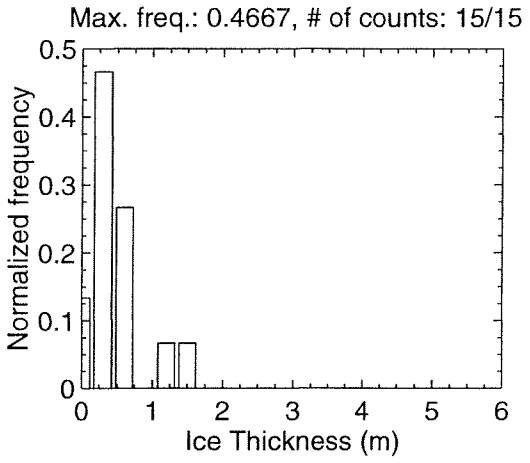

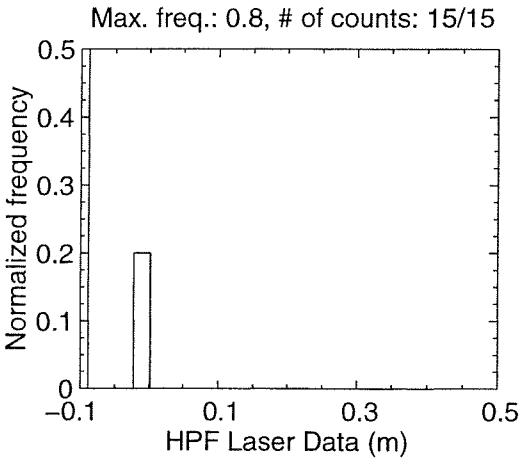

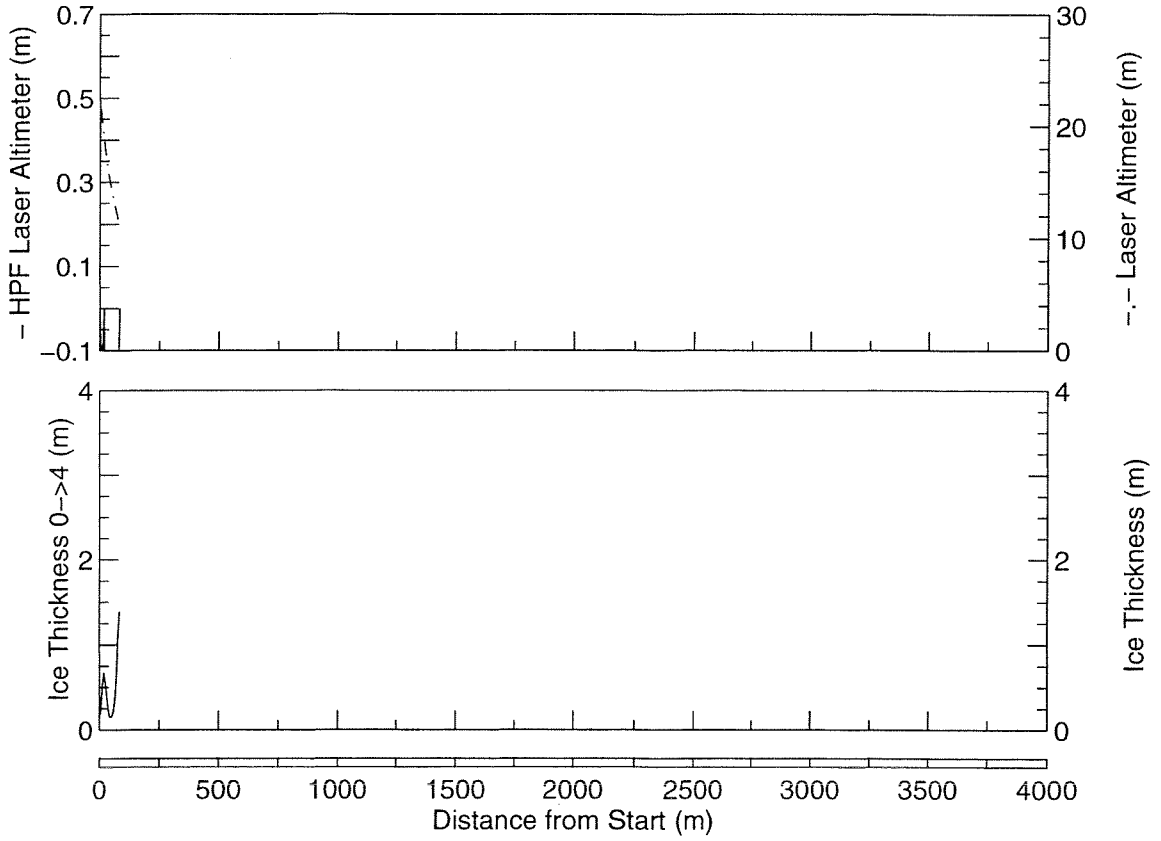

MAR 03 Flight #14 Line #10113 part 1 of 1

Line Starting Coordinates (53.7305,–56.9930) ending at (53.7311,–56.9845)

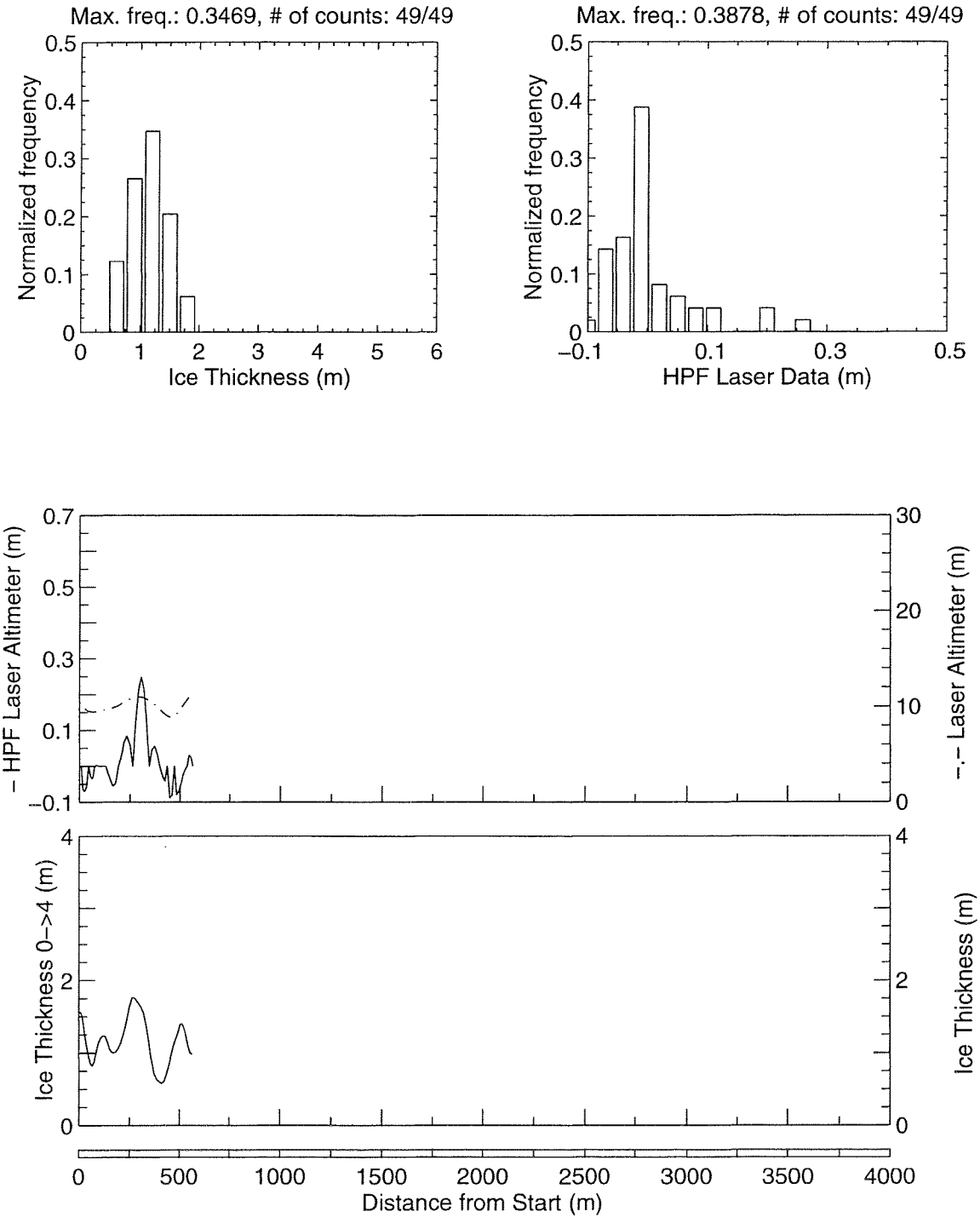

MAR 03 Flight #14 Line #10121 part 1 of 1

Line Starting Coordinates (53.7314,–56.9789) ending at (53.7316,–56.9754)

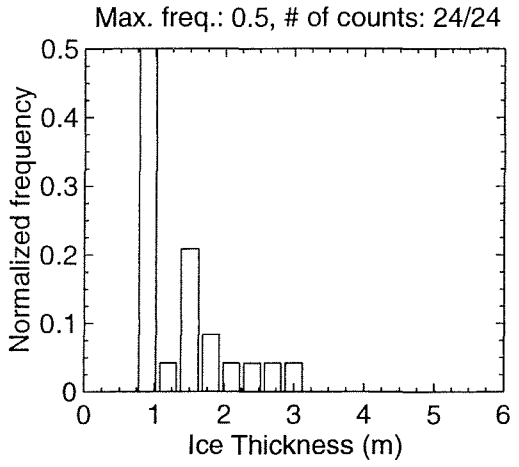

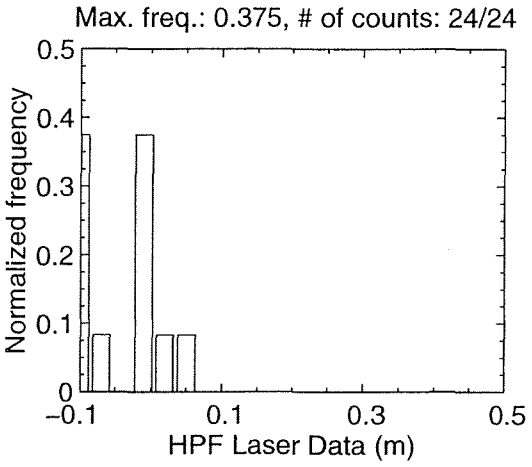

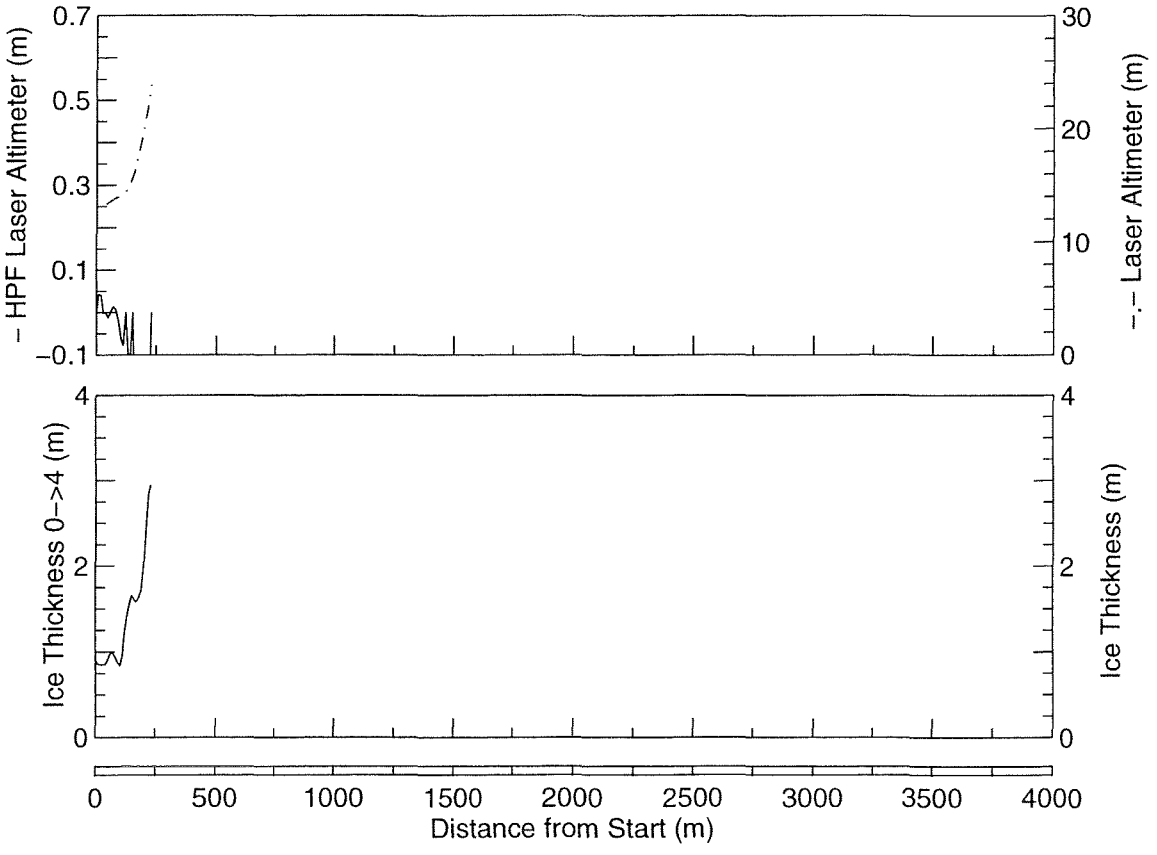

MAR 03 Flight #14 Line #10122 part 1 of 1

Line Starting Coordinates (53.7307,−56.9931) ending at (53.7318,−56.9812)

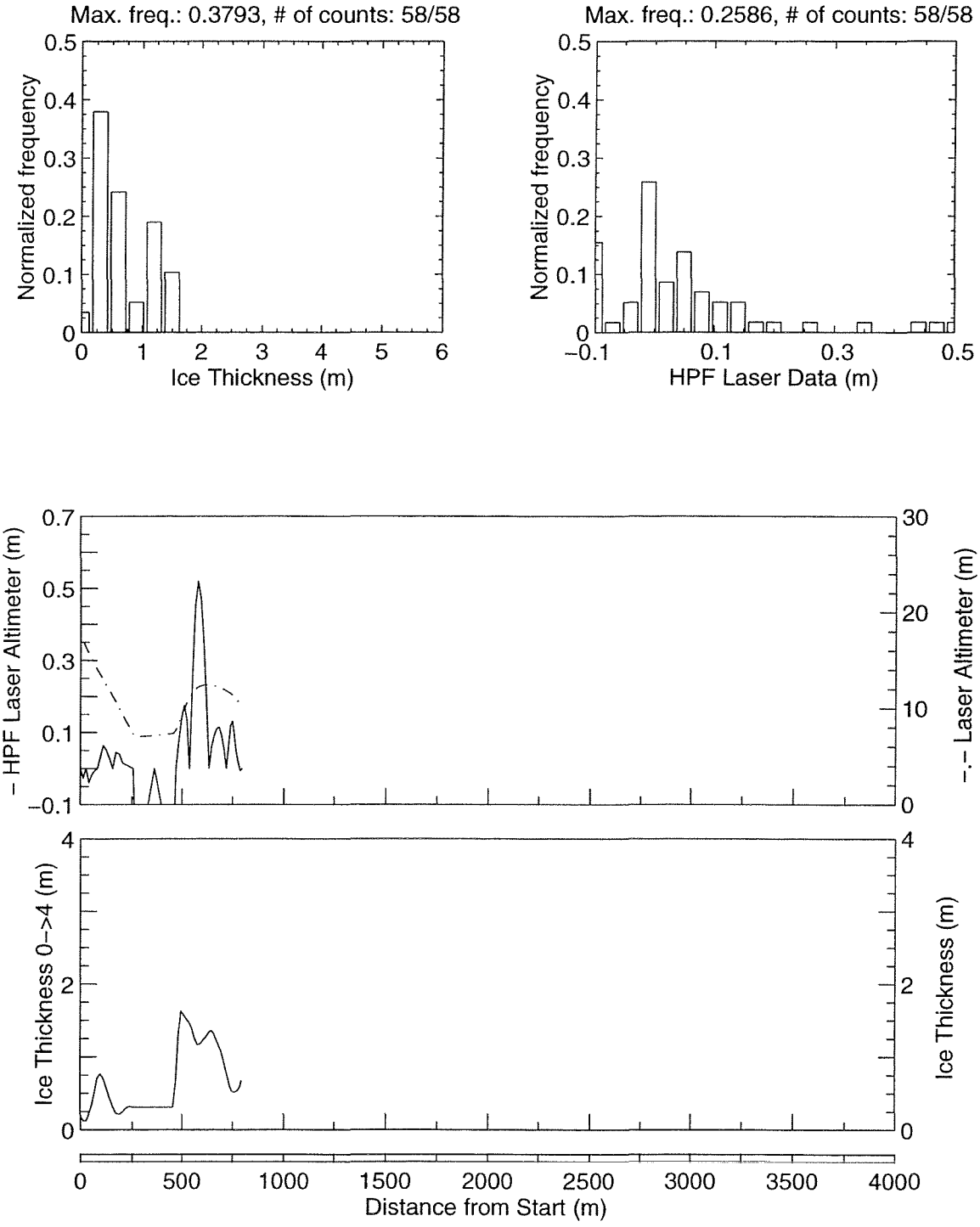

MAR 03 Flight #14 Line #10131 part 1 of 1

Line Starting Coordinates (53.7323,–56.9770) ending at (53.7326,–56.9722)

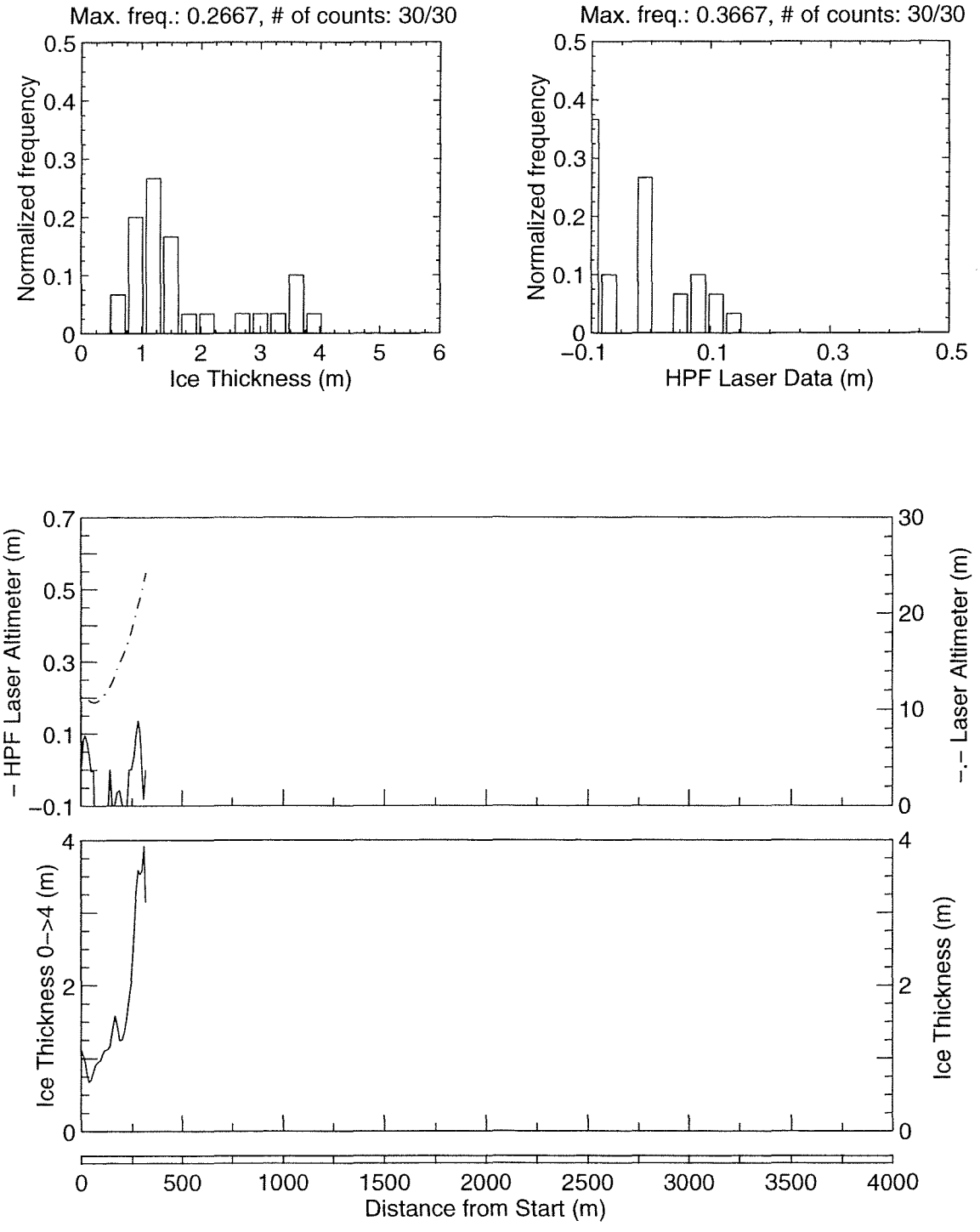

MAR 03 Flight #14 Line #10132 part 1 of 1

Line Starting Coordinates (53.7309,–57.0021) ending at (53.7304,–56.9978)

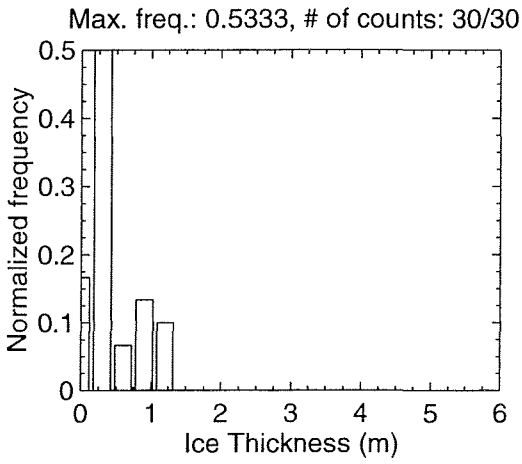

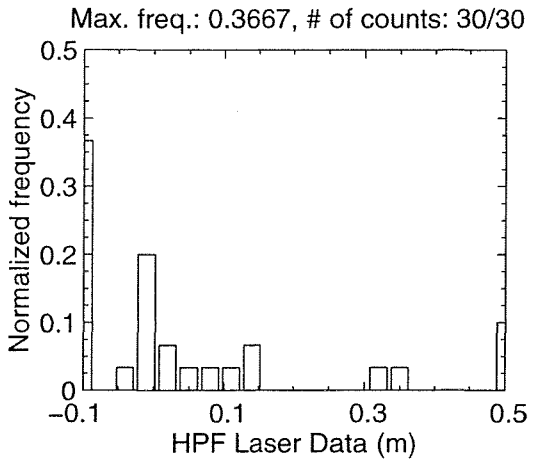

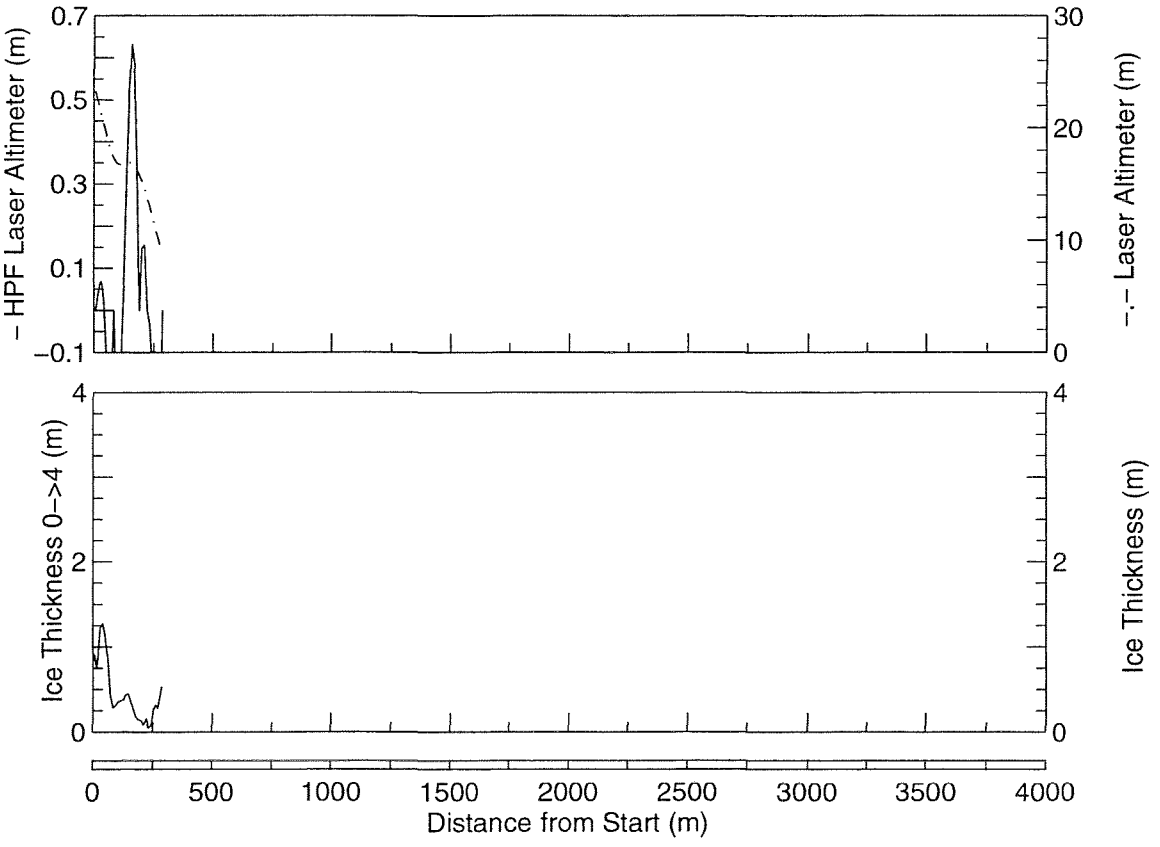

MAR 03 Flight #14 Line #10133 part 1 of 1

Line Starting Coordinates (53.7304,–56.9959) ending at (53.7313,–56.9832)

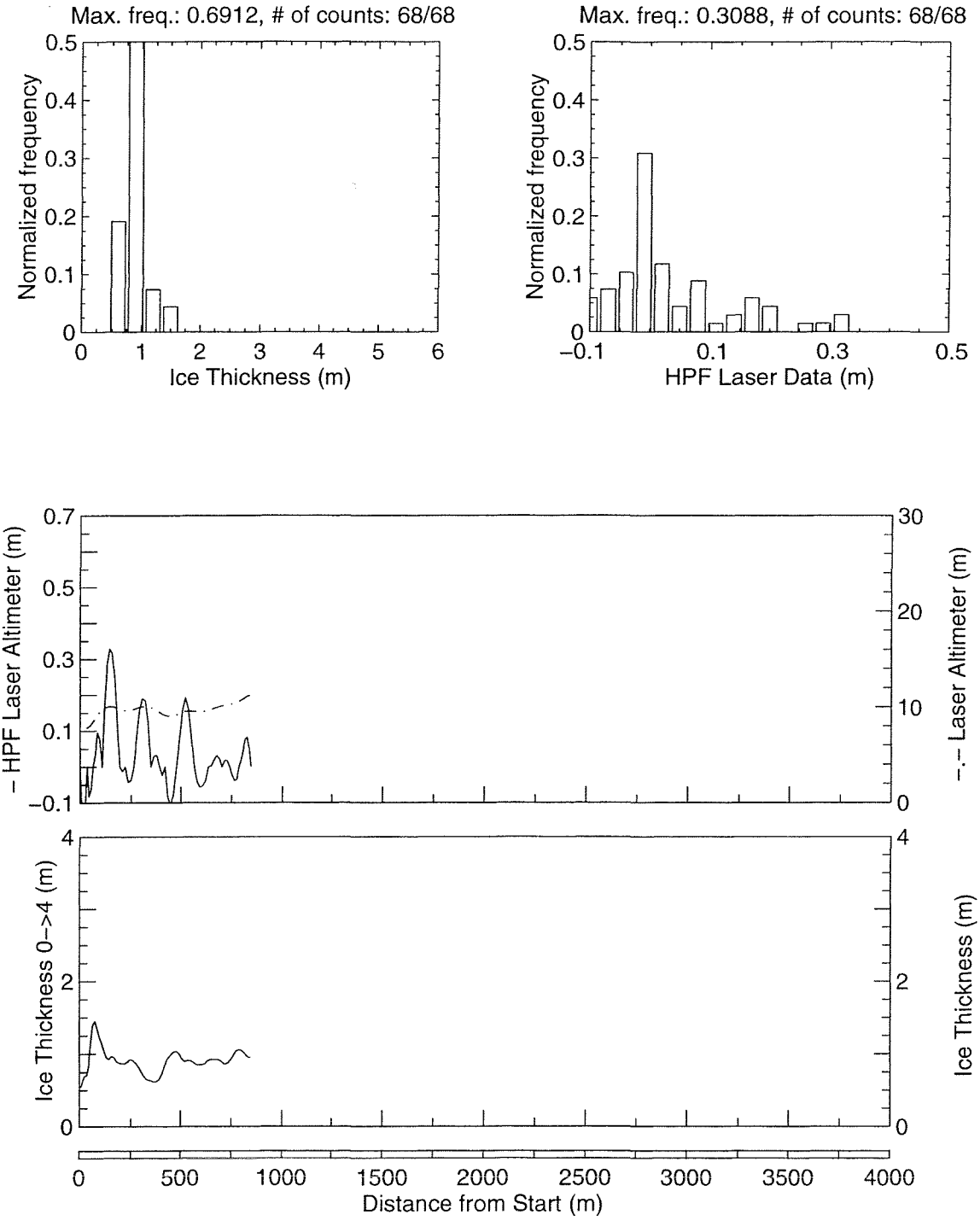

MAR 06 Flight #08 Line #10010 part 1 of 1

Line Starting Coordinates (53.6781,–55.7036) ending at (53.6846,–55.6964)

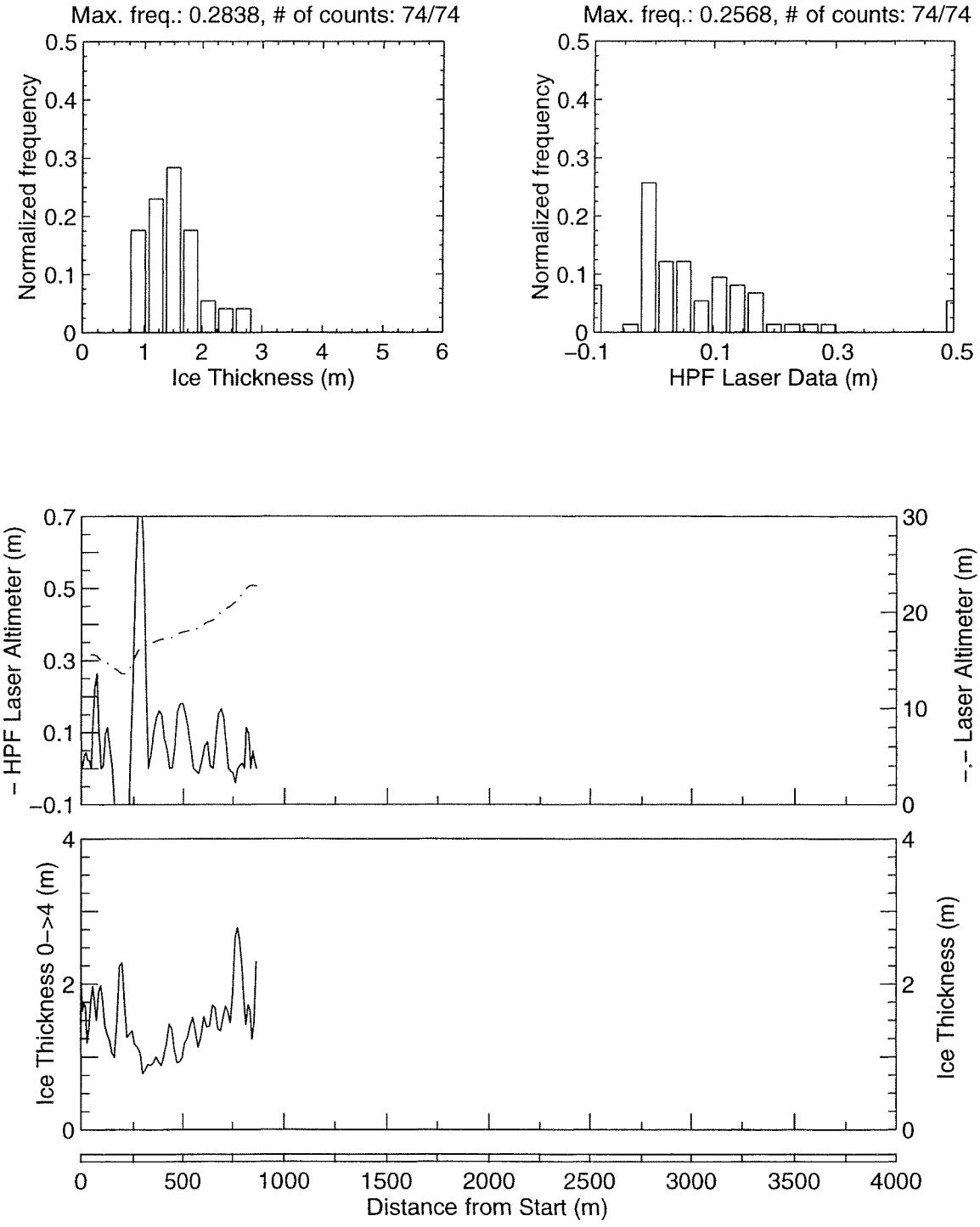

MAR 06 Flight #08 Line #10021 part 1 of 1

Line Starting Coordinates (53.6827,–55.7067) ending at (53.6683,–55.6647)

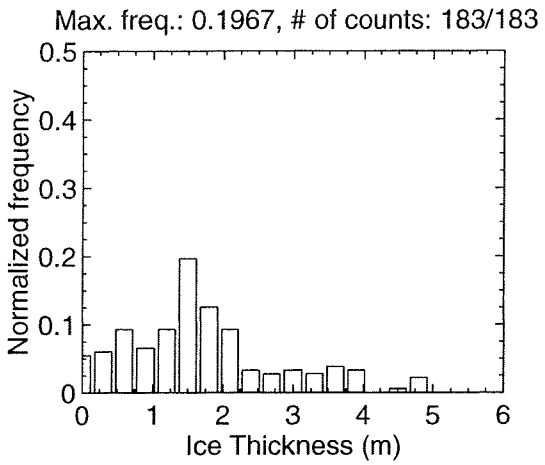

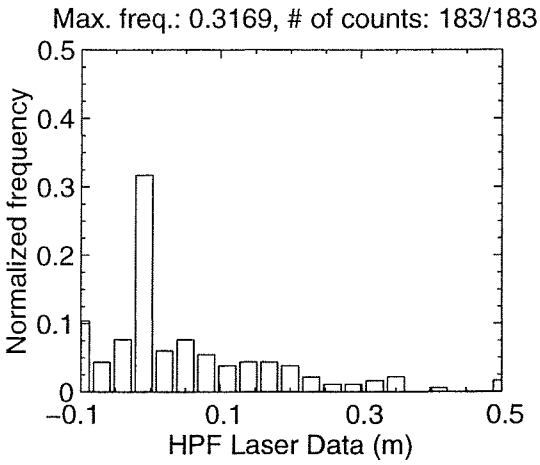

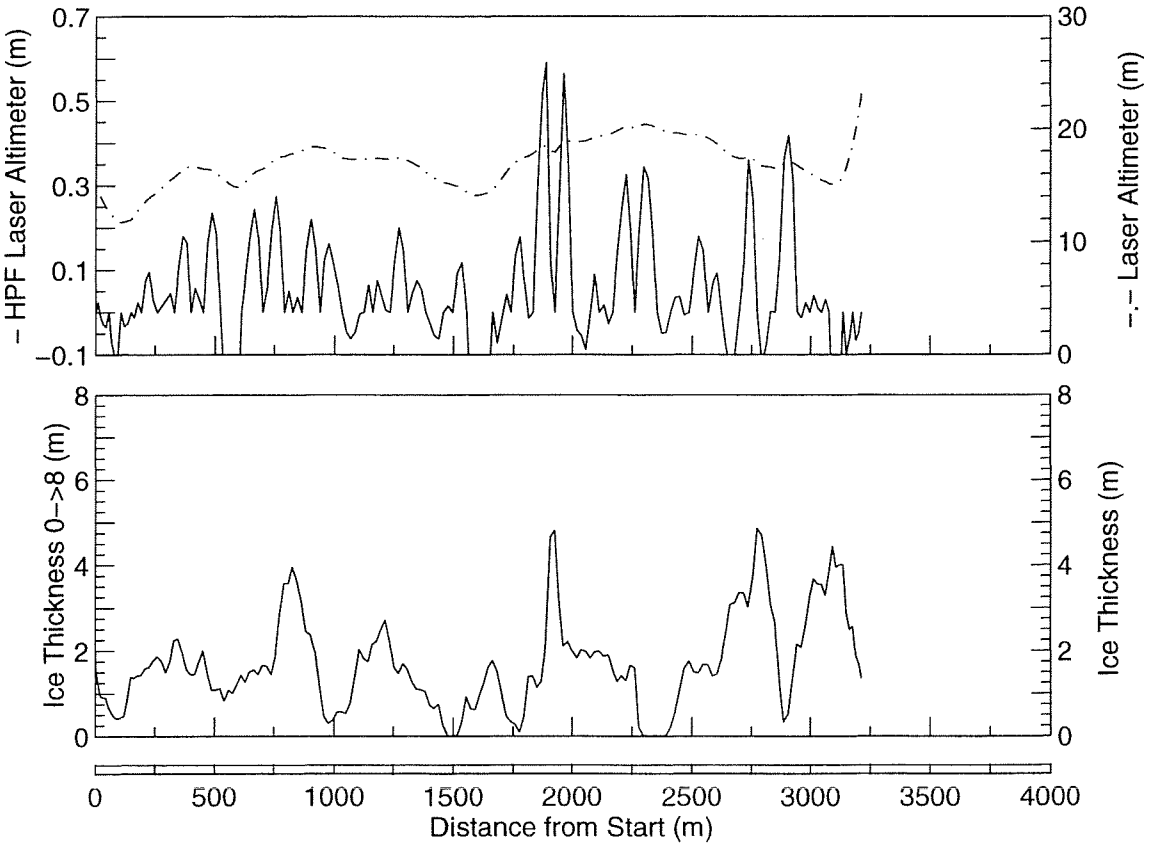

MAR 06 Flight #08 Line #10023 part 1 of 3

Line Starting Coordinates (53.6820,–55.6547) ending at (53.6800,–55.5939)

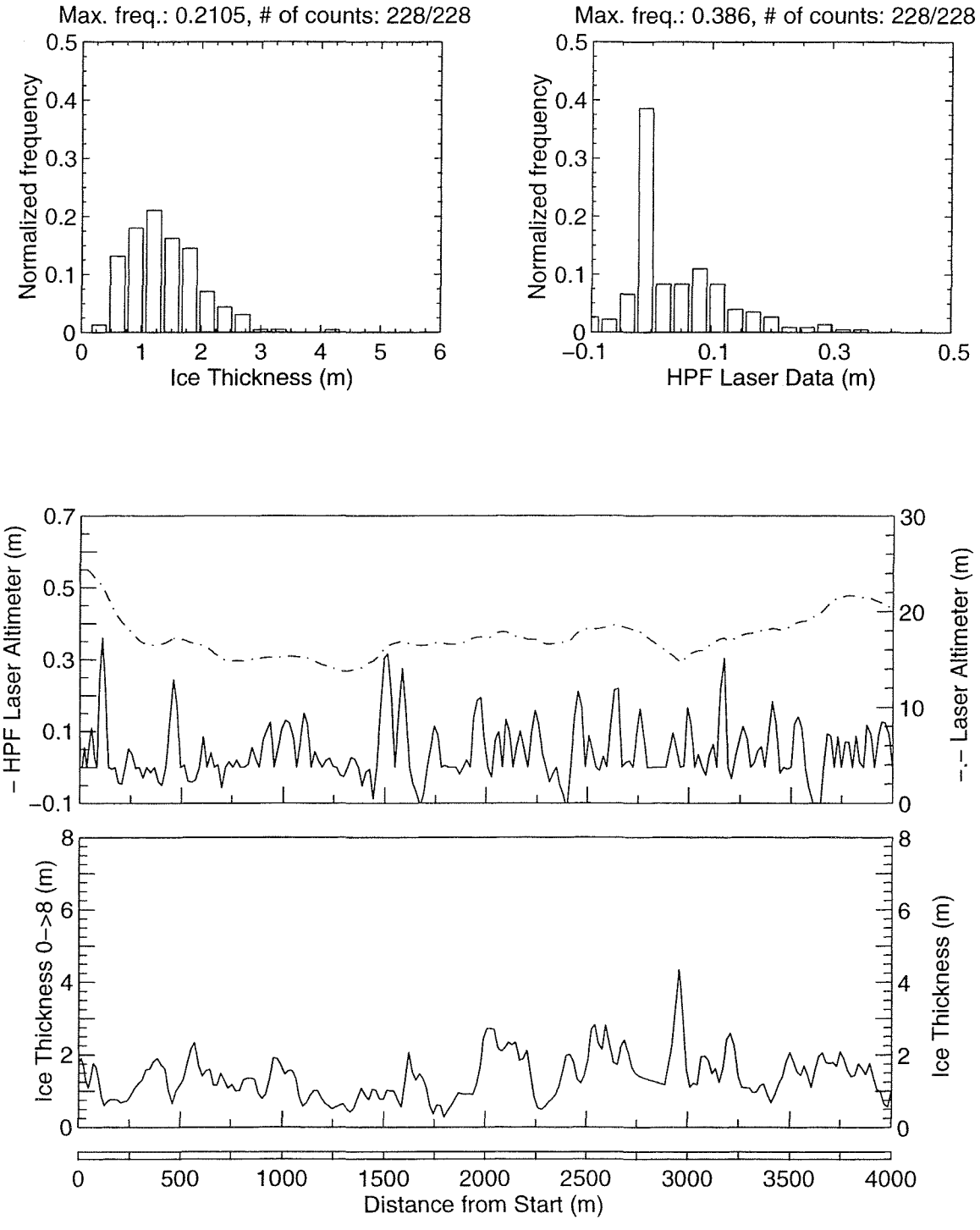

MAR 06 Flight #08 Line #10023 part 2 of 3

Line Starting Coordinates (53.6800,–55.5939) ending at (53.6779,–55.5335)

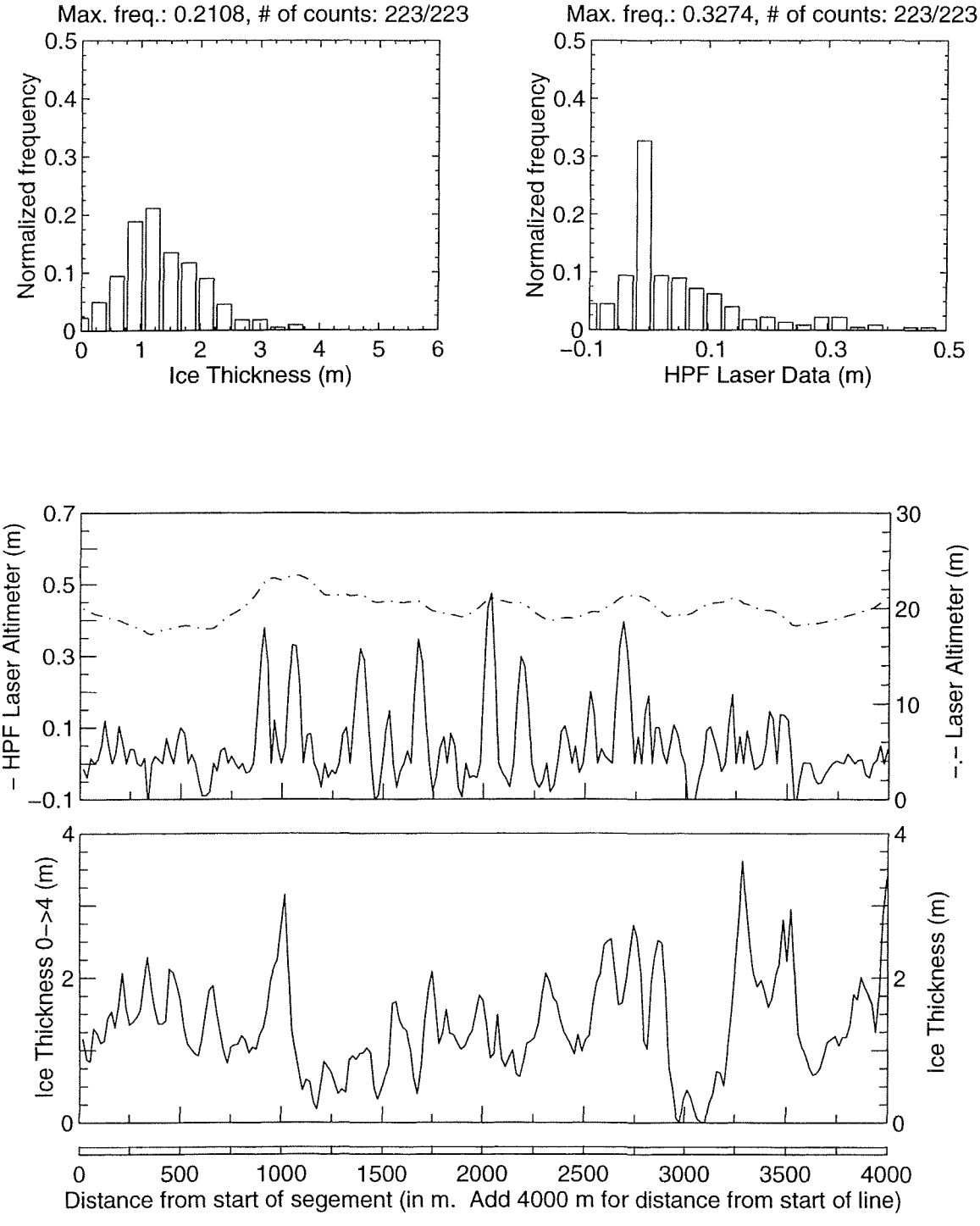

MAR 06 Flight #08 Line #10023 part 3 of 3

Line Starting Coordinates (53.6779,–55.5335) ending at (53.6773,–55.4974)

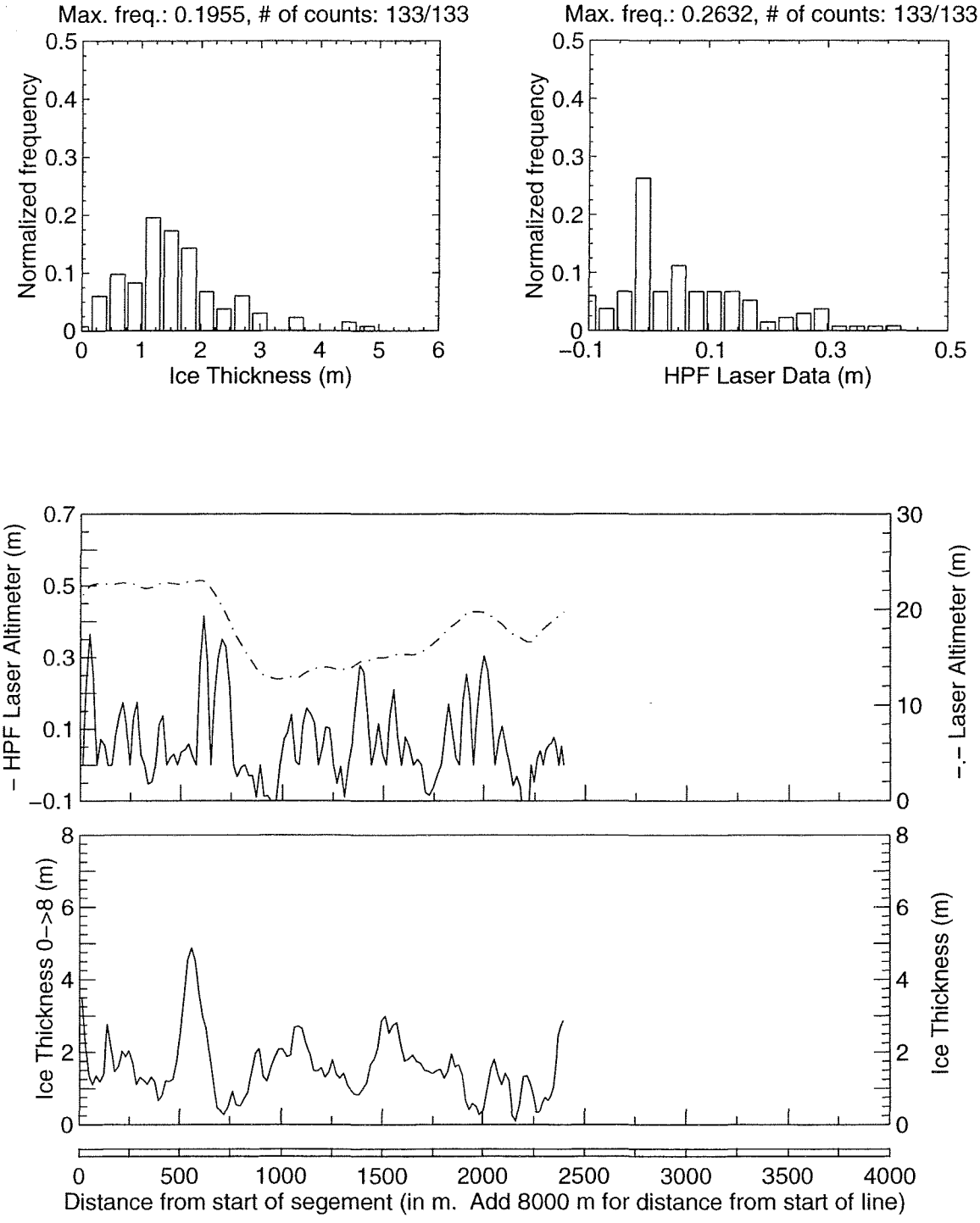

MAR 06 Flight #08 Line #10030 part 1 of 4

Line Starting Coordinates (53.6757,–55.3716) ending at (53.6775,–55.3110)

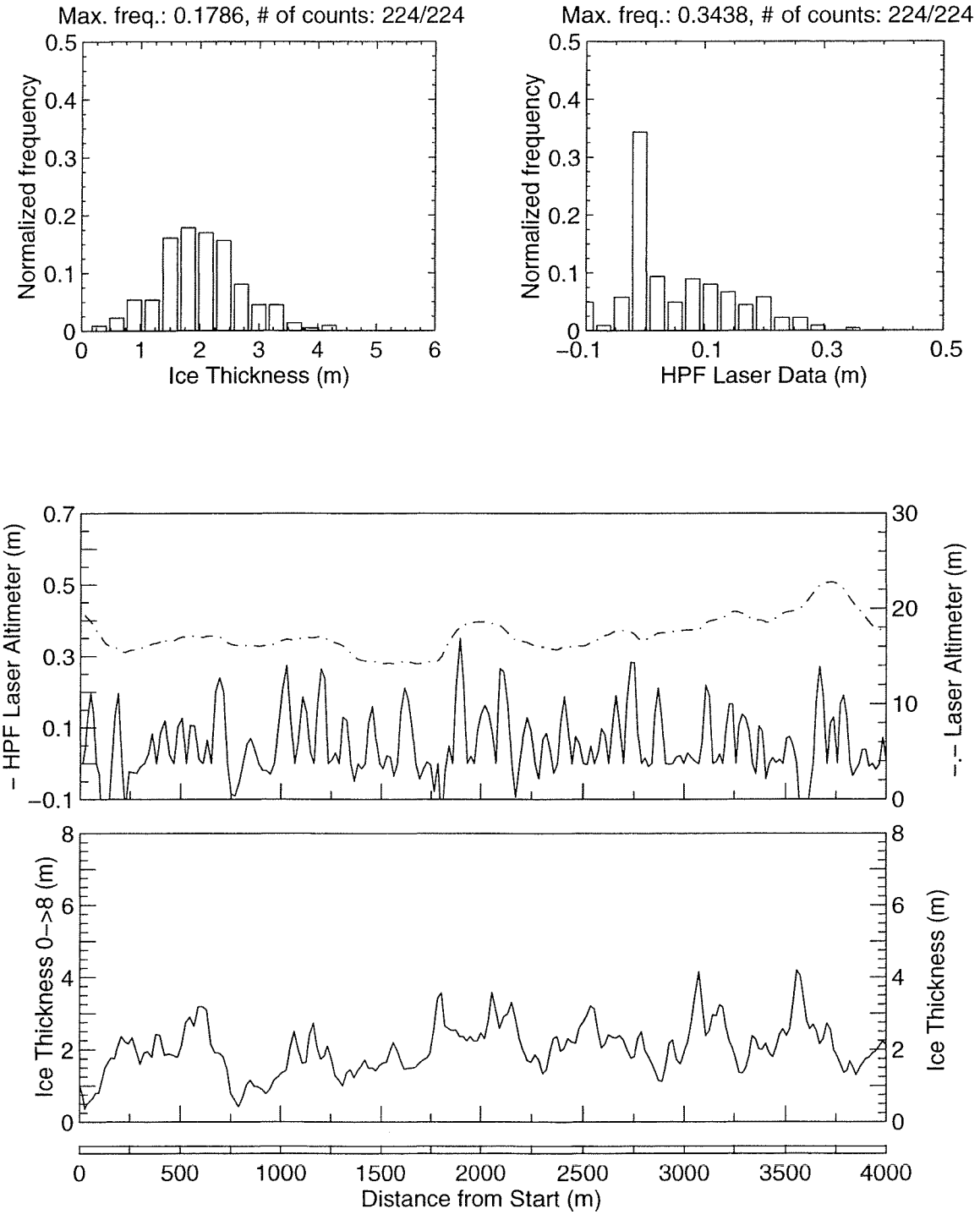

MAR 06 Flight #08 Line #10030 part 2 of 4

Line Starting Coordinates (53.6775,–55.3110) ending at (53.6829,–55.2508)

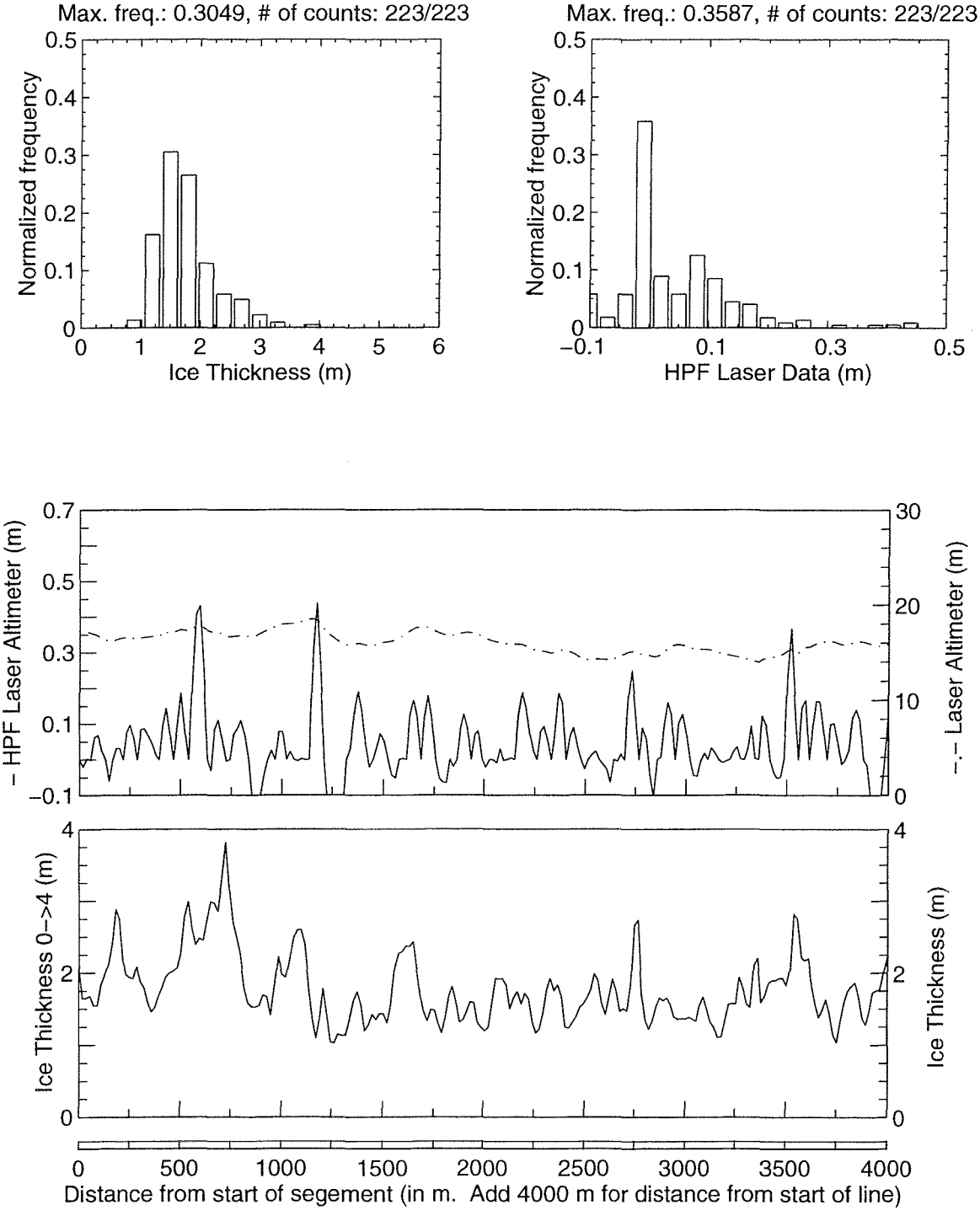

MAR 06 Flight #08 Line #10030 part 3 of 4

Line Starting Coordinates (53.6829,–55.2508) ending at (53.6876,–55.1908)

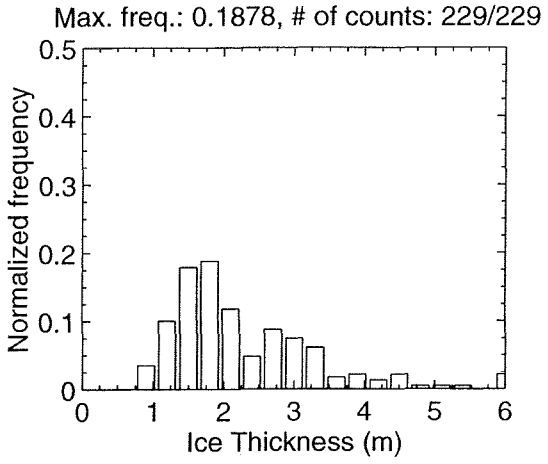

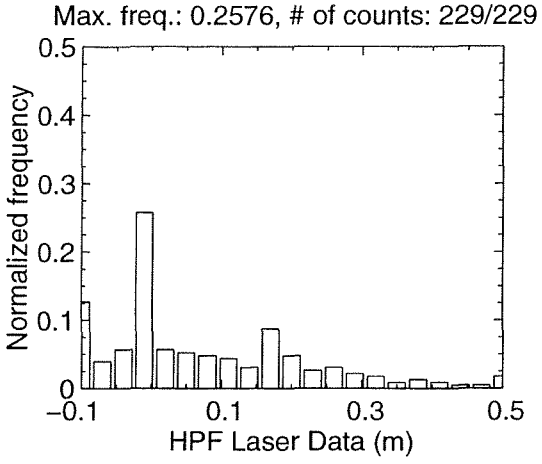

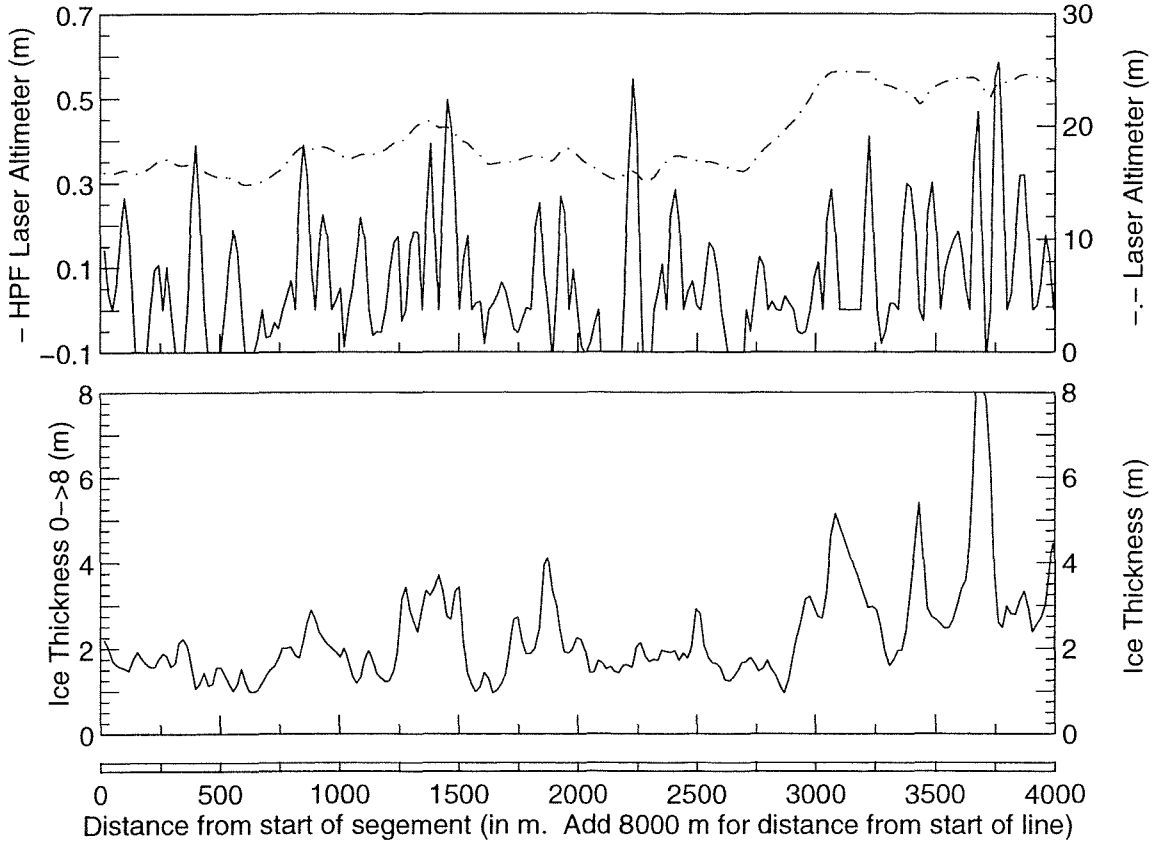

MAR 06 Flight #08 Line #10030 part 4 of 4

Line Starting Coordinates (53.6876,–55.1908) ending at (53.6892,–55.1731)

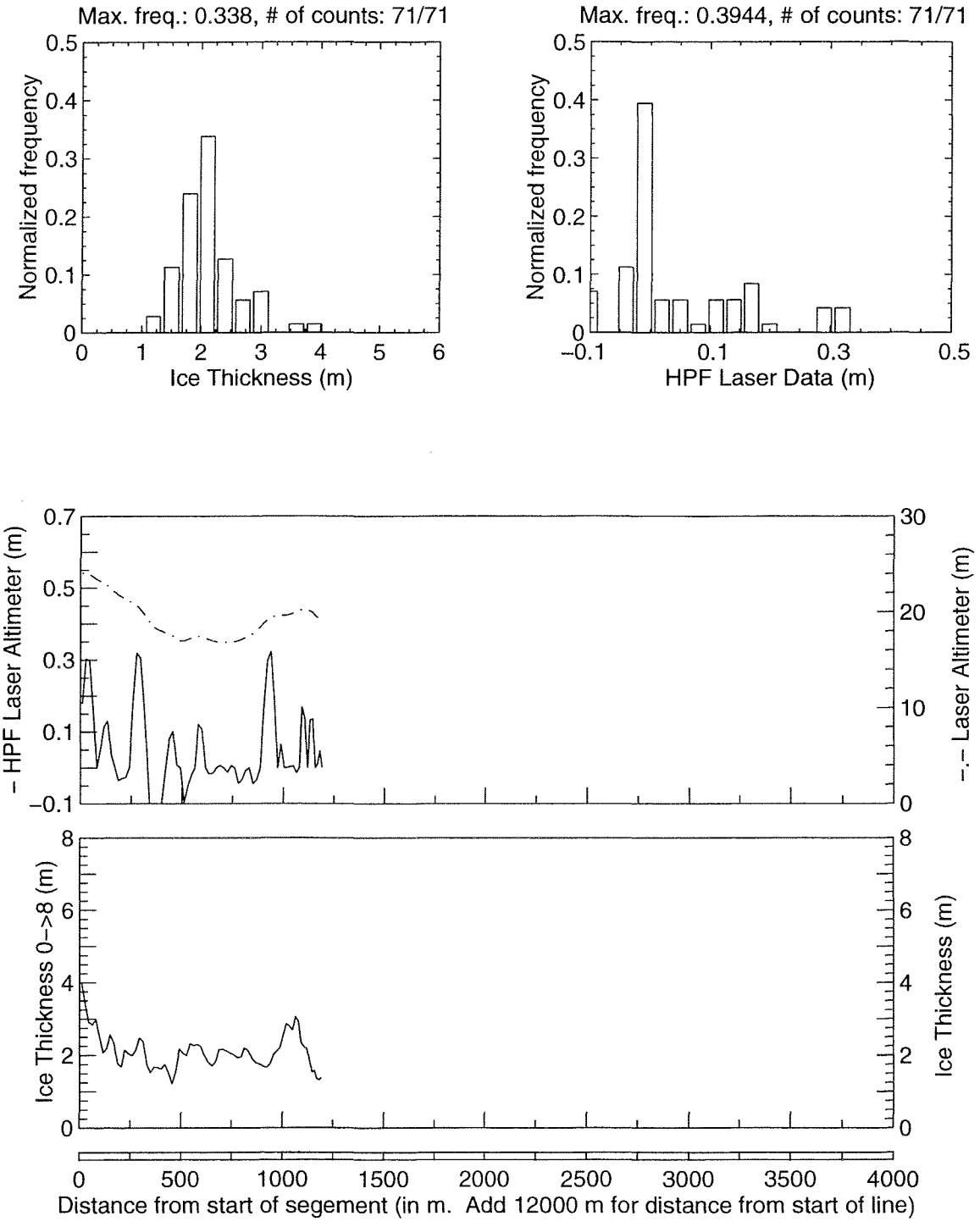

MAR 06 Flight #08 Line #10040 part 1 of 1

Line Starting Coordinates (53.6970,–55.1179) ending at (53.7057,–55.0648)

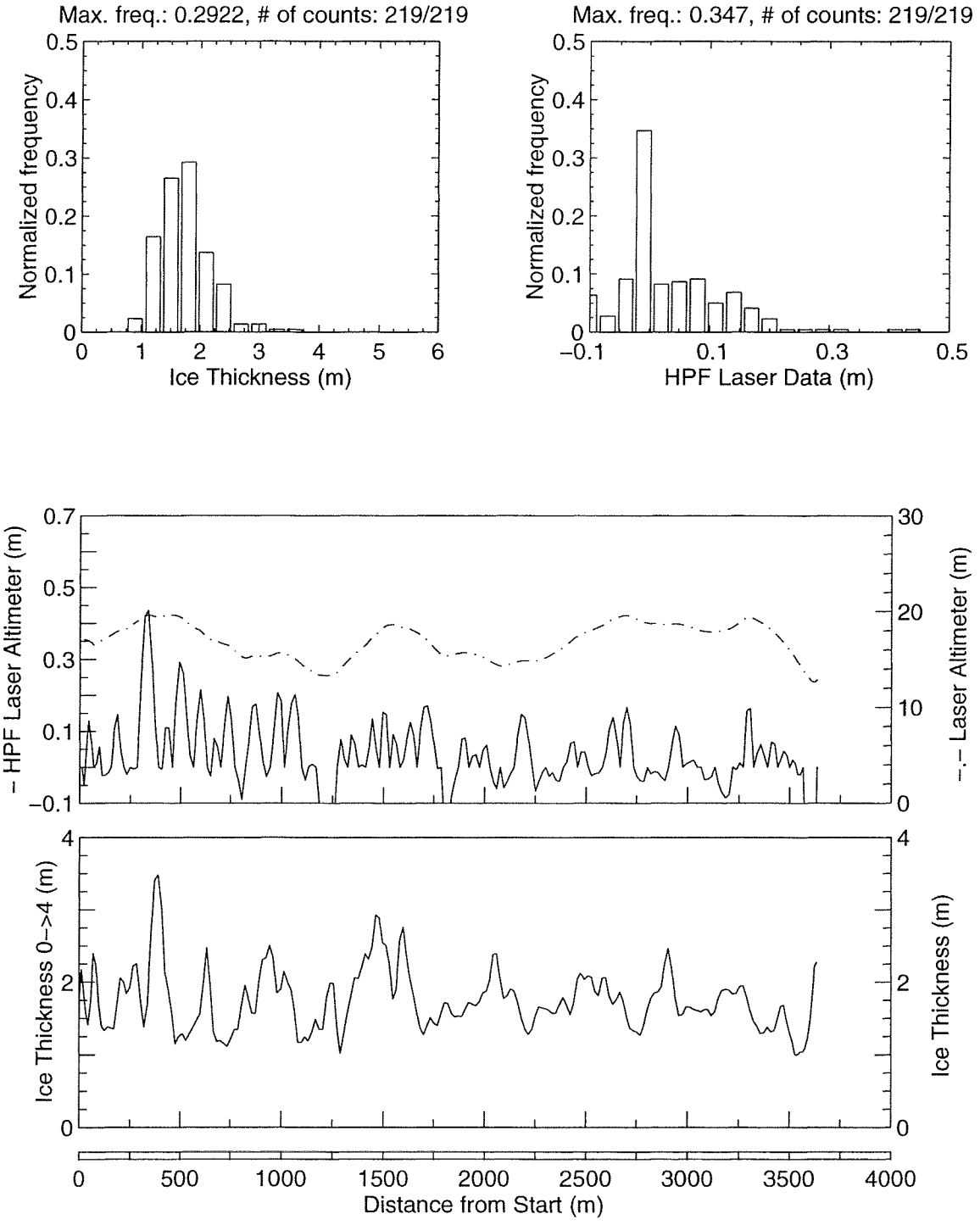

MAR 06 Flight #08 Line #10050 part 1 of 1

Line Starting Coordinates (53.7126,–55.0595) ending at (53.7167,–55.0756)

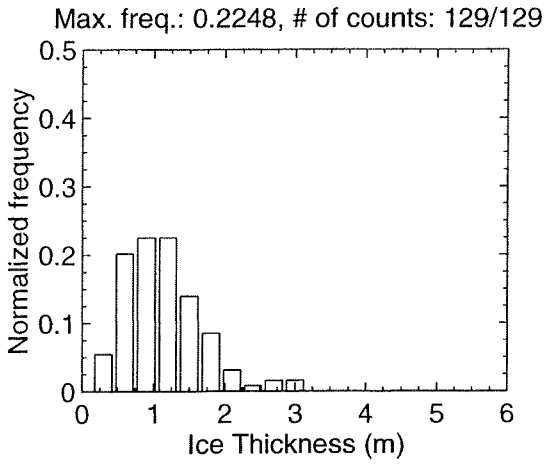

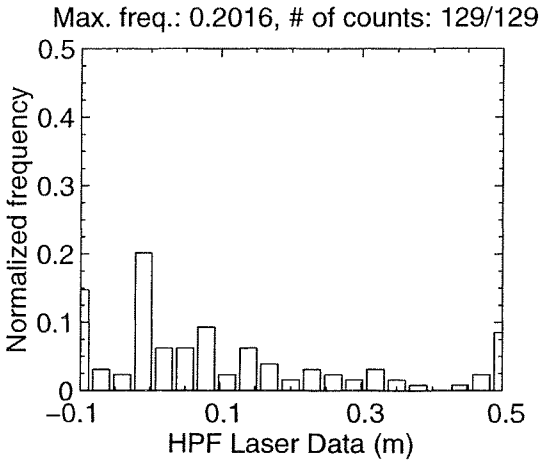

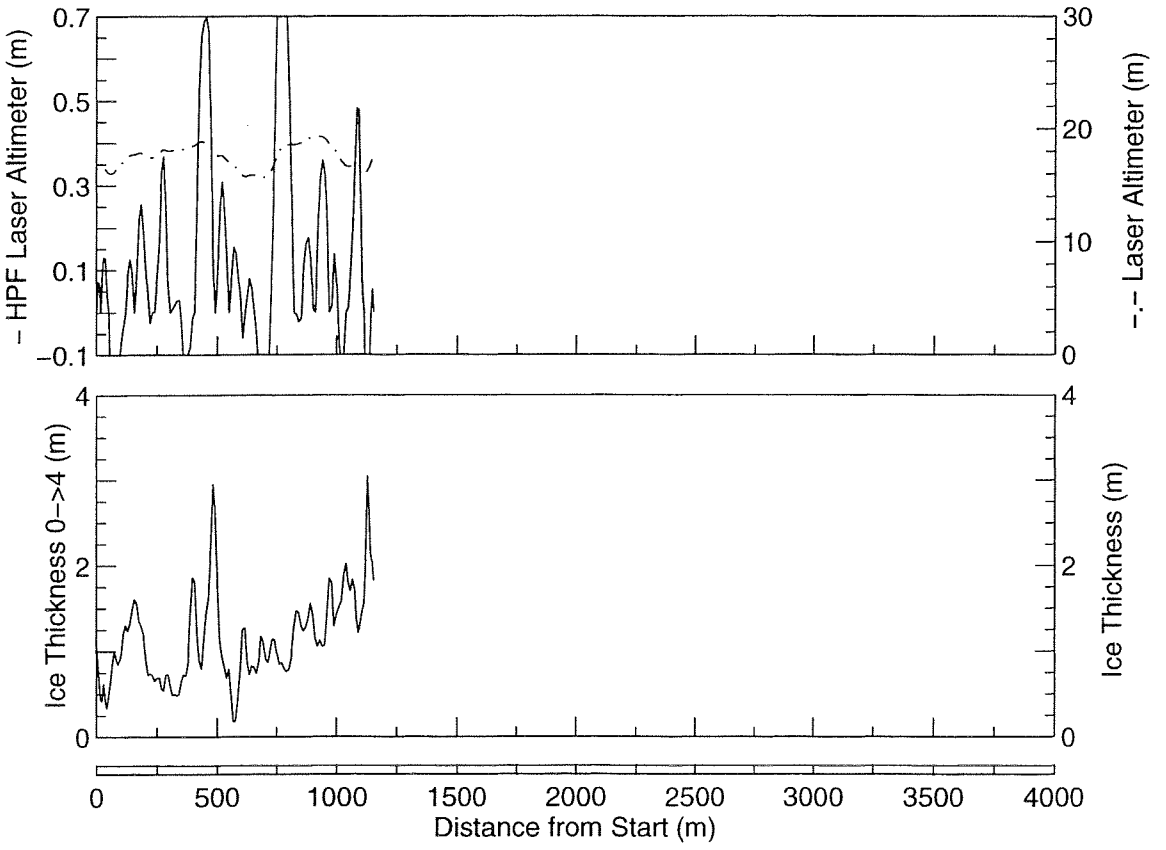

MAR 06 Flight #08 Line #10060 part 1 of 1

Line Starting Coordinates (53.7137,–55.0847) ending at (53.6946,–55.0857)

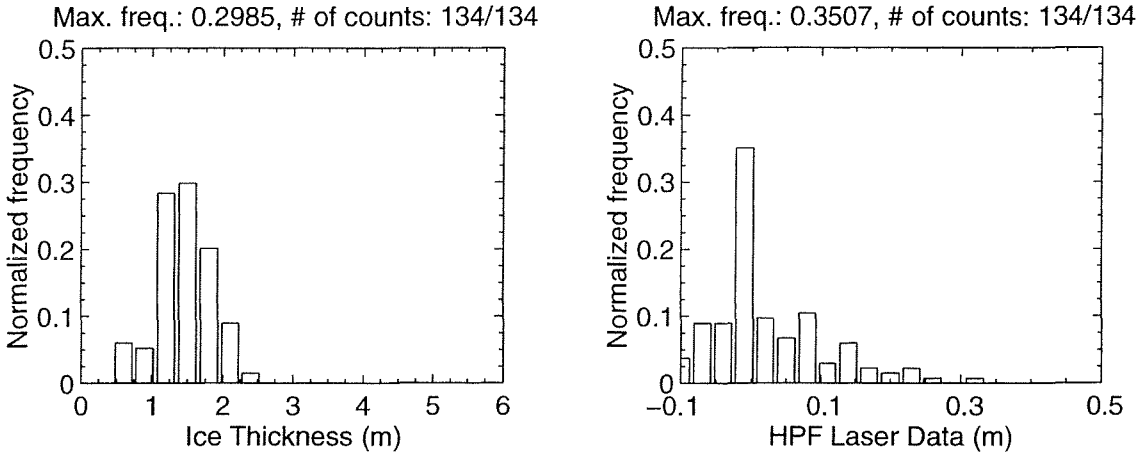

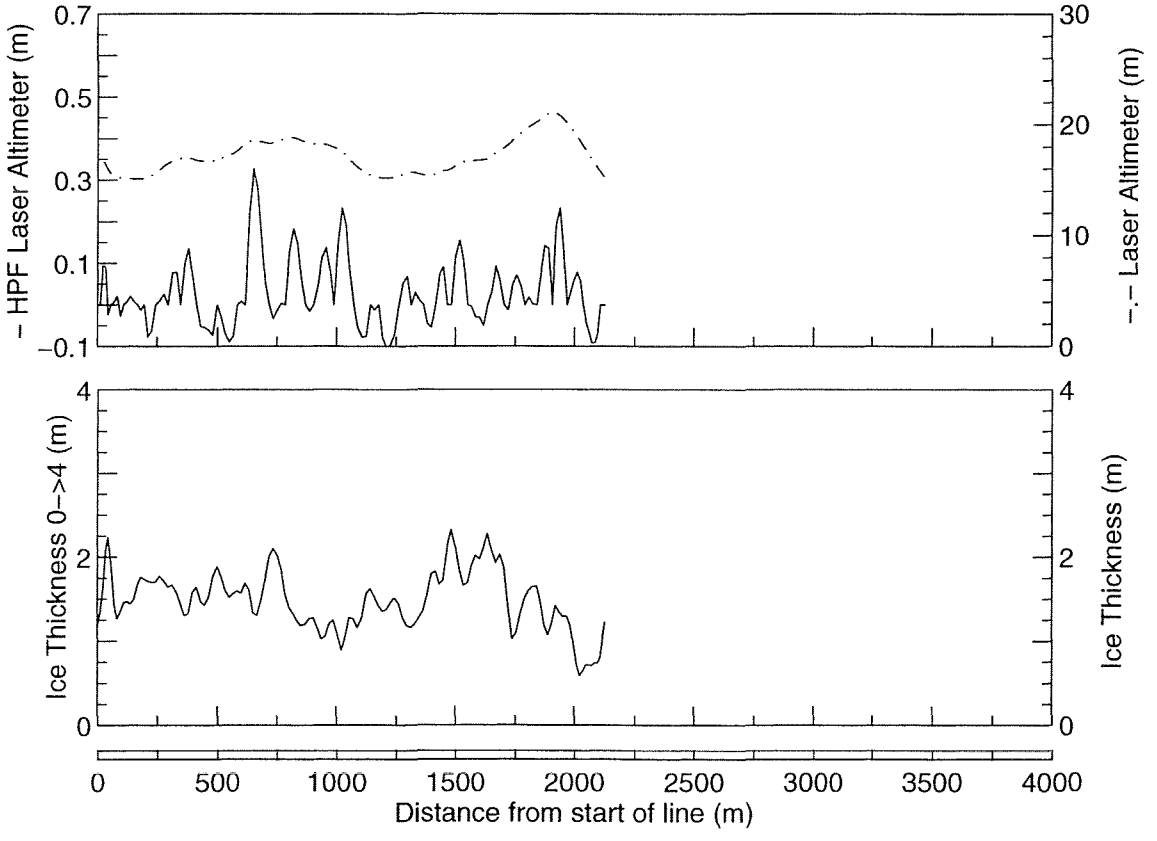

MAR 06 Flight #09 Line #10010 part 1 of 1

Line Starting Coordinates (53.6879,–55.1532) ending at (53.6823,–55.1994)

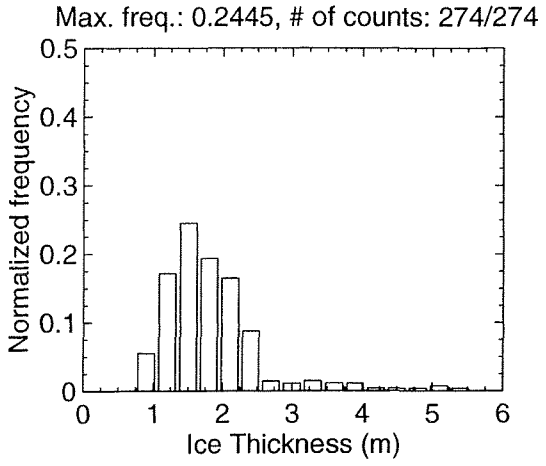

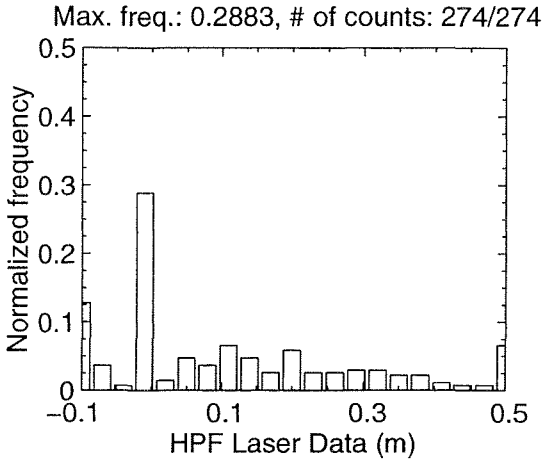

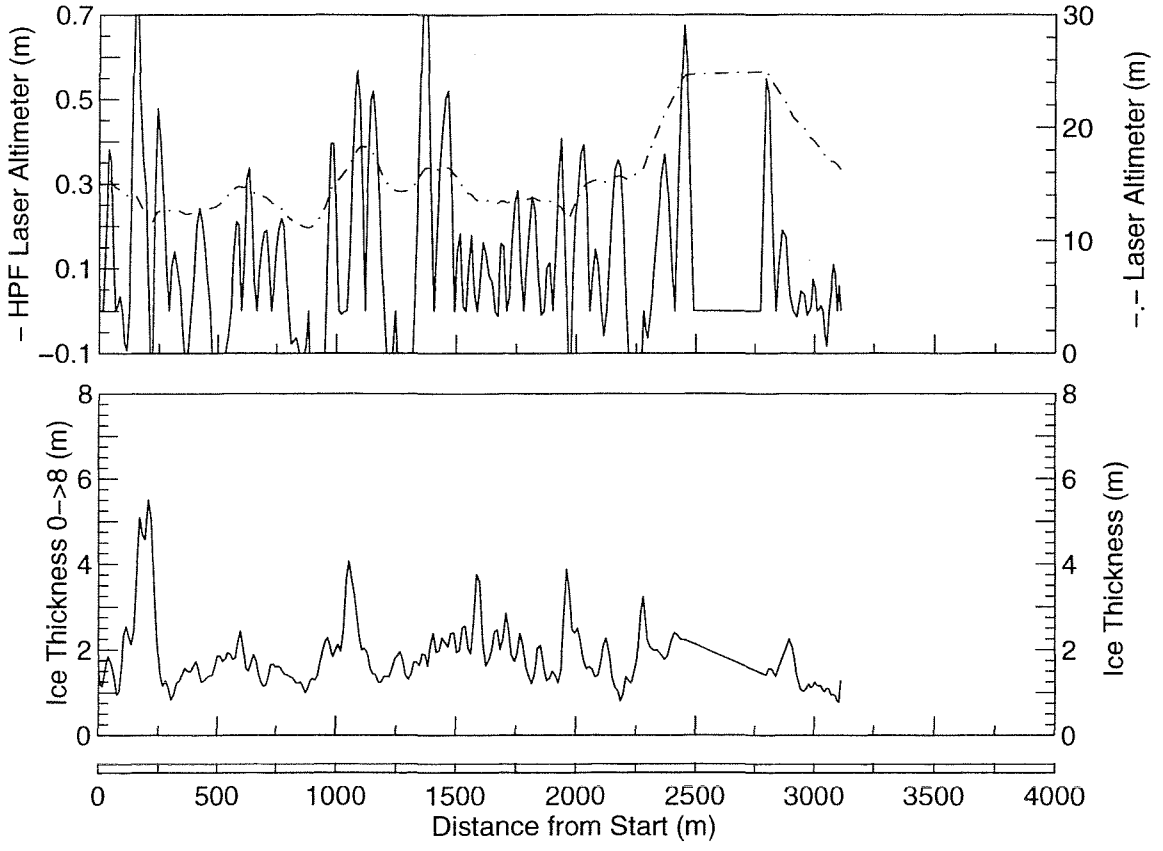

MAR 06 Flight #09 Line #10020 part 1 of 6

Line Starting Coordinates (53.6628,–55.2598) ending at (53.6450,–55.3123)

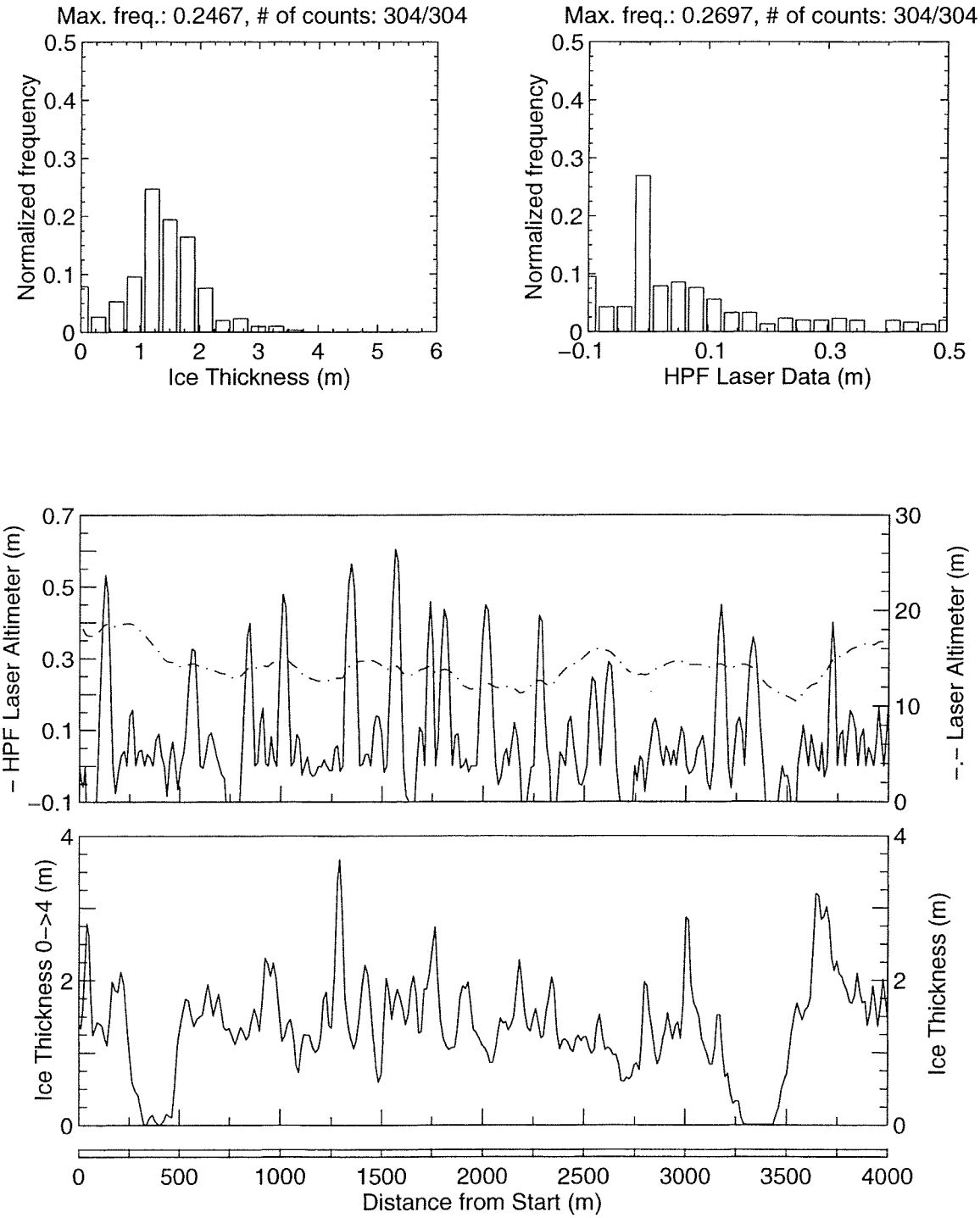

MAR 06 Flight #09 Line #10020 part 2 of 6

Line Starting Coordinates (53.6450,–55.3123) ending at (53.6271,–55.3650)

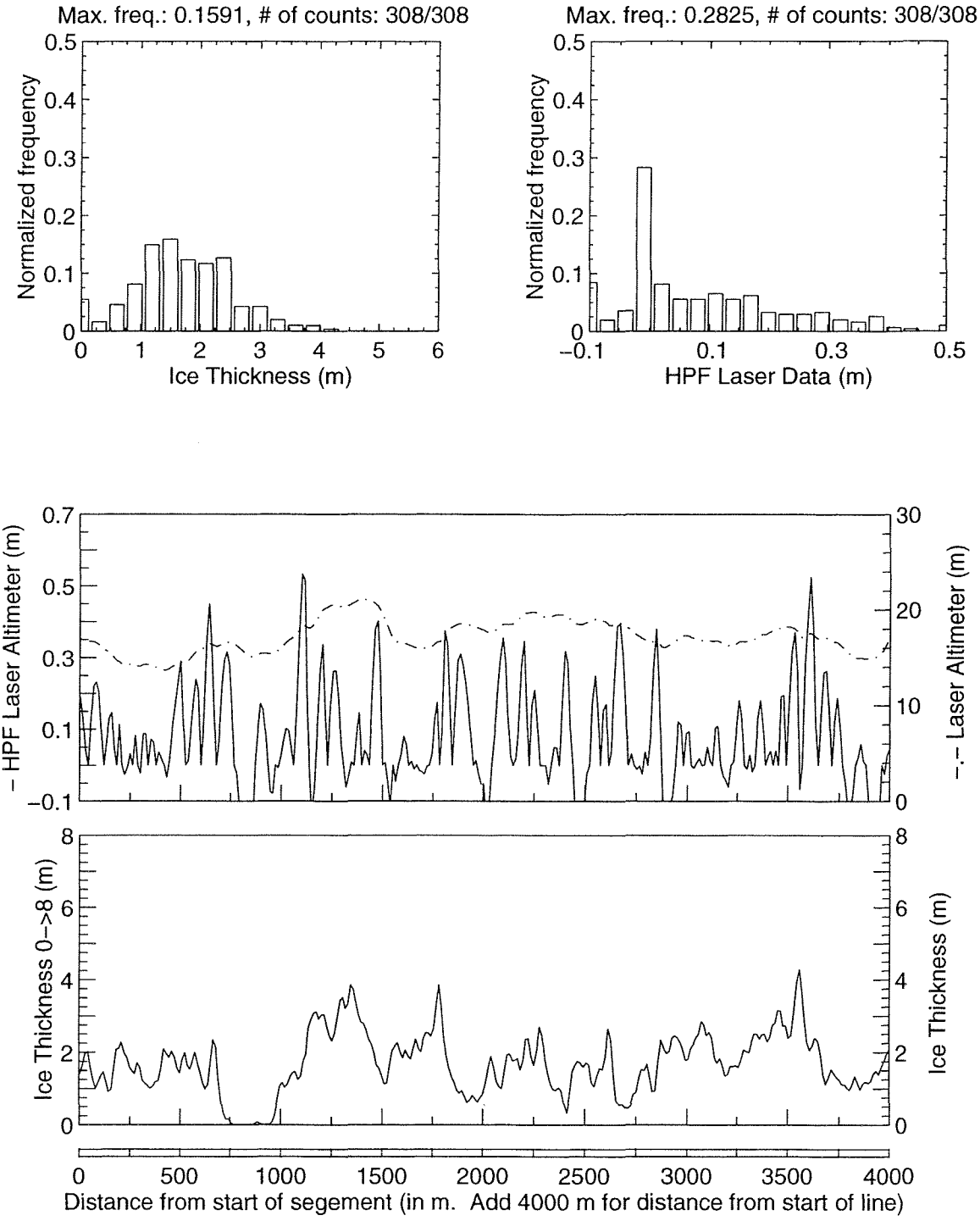

MAR 06 Flight #09 Line #10020 part 3 of 6

Line Starting Coordinates (53.6271,–55.3650) ending at (53.6084,–55.4166)

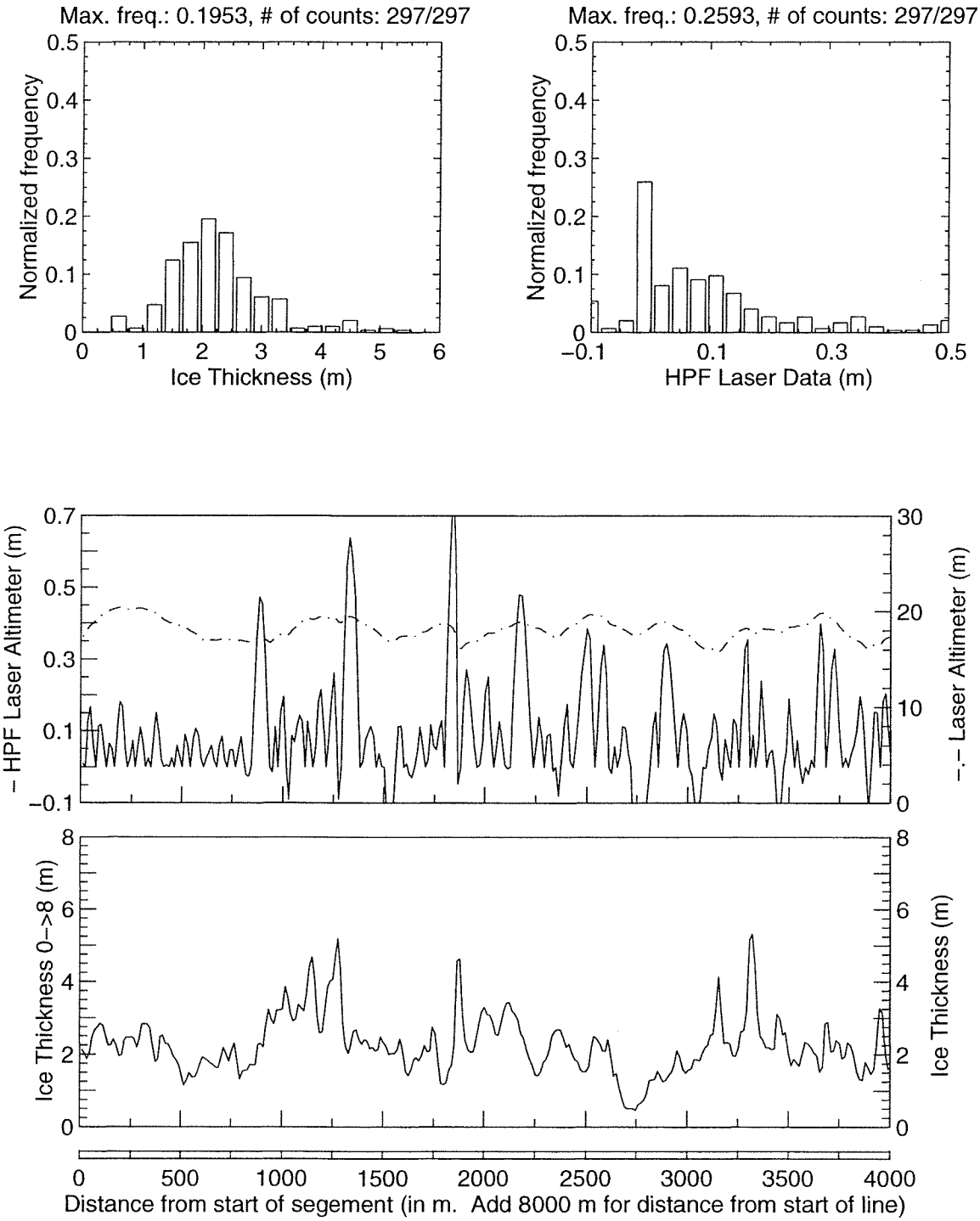

MAR 06 Flight #09 Line #10020 part 4 of 6

Line Starting Coordinates (53.6084,–55.4166) ending at (53.5929,–55.4709)

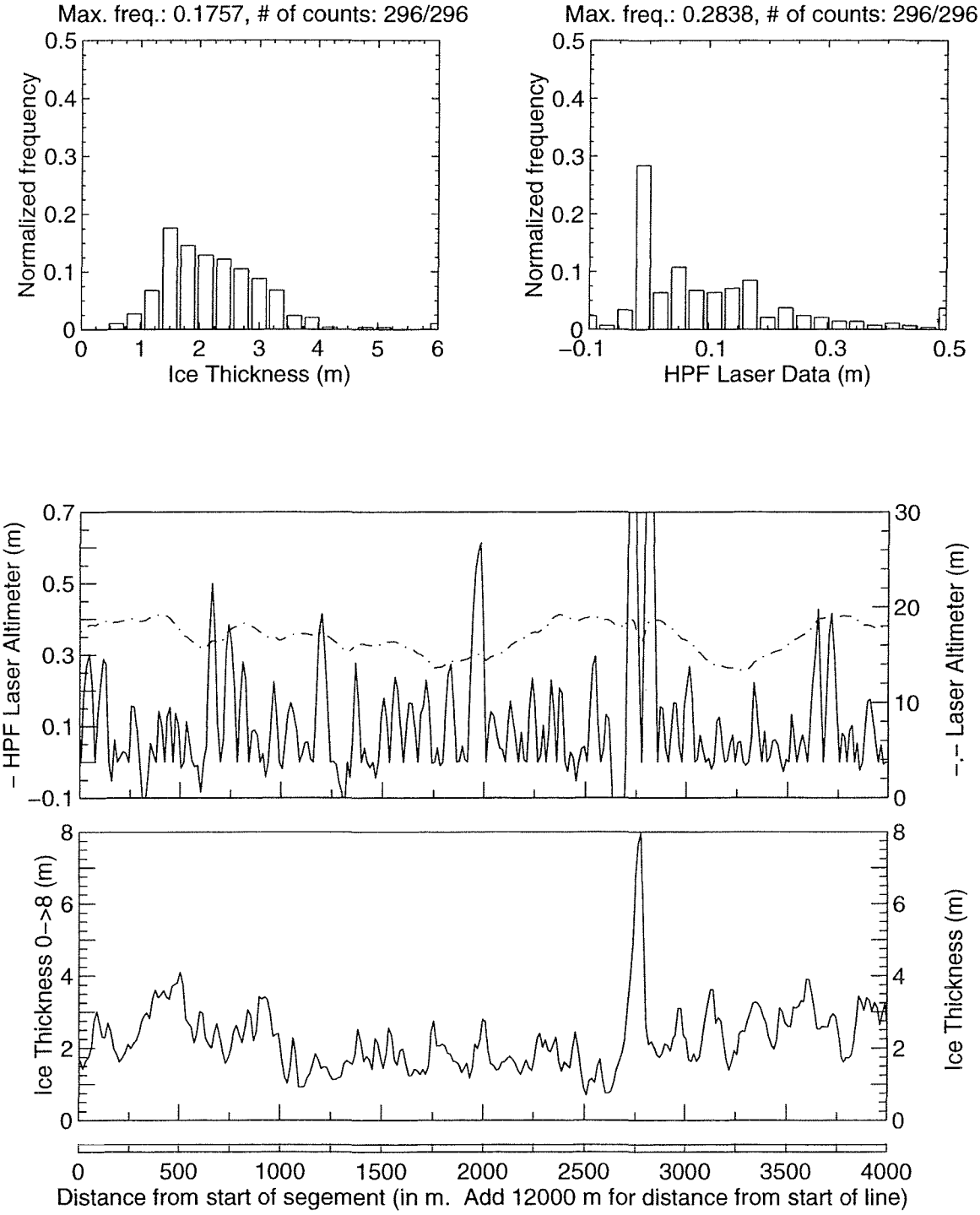

MAR 06 Flight #09 Line #10020 part 5 of 6

Line Starting Coordinates (53.5929,–55.4709) ending at (53.5815,–55.5283)

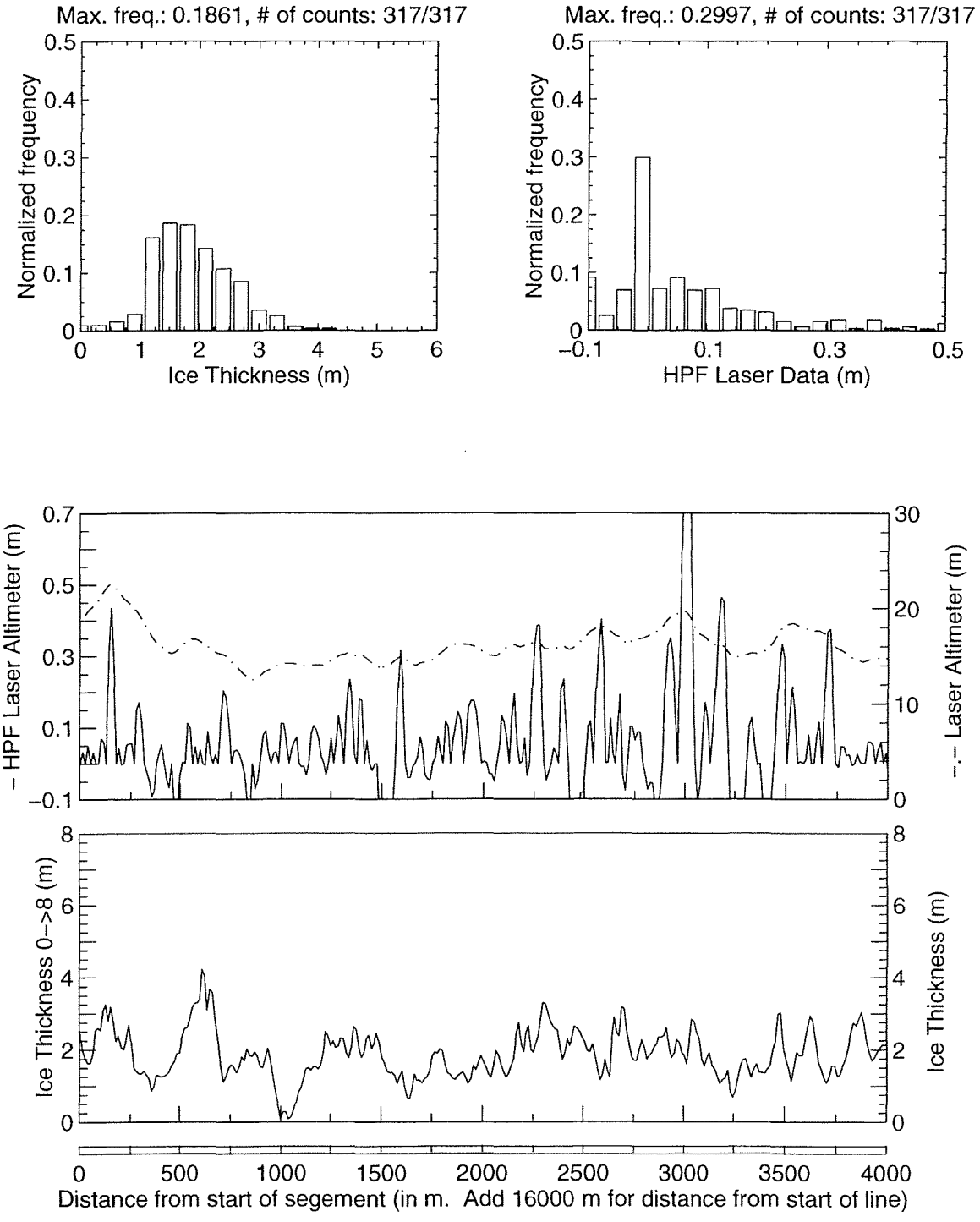

MAR 06 Flight #09 Line #10020 part 6 of 6

Line Starting Coordinates (53.5815,–55.5283) ending at (53.5776,–55.5463)

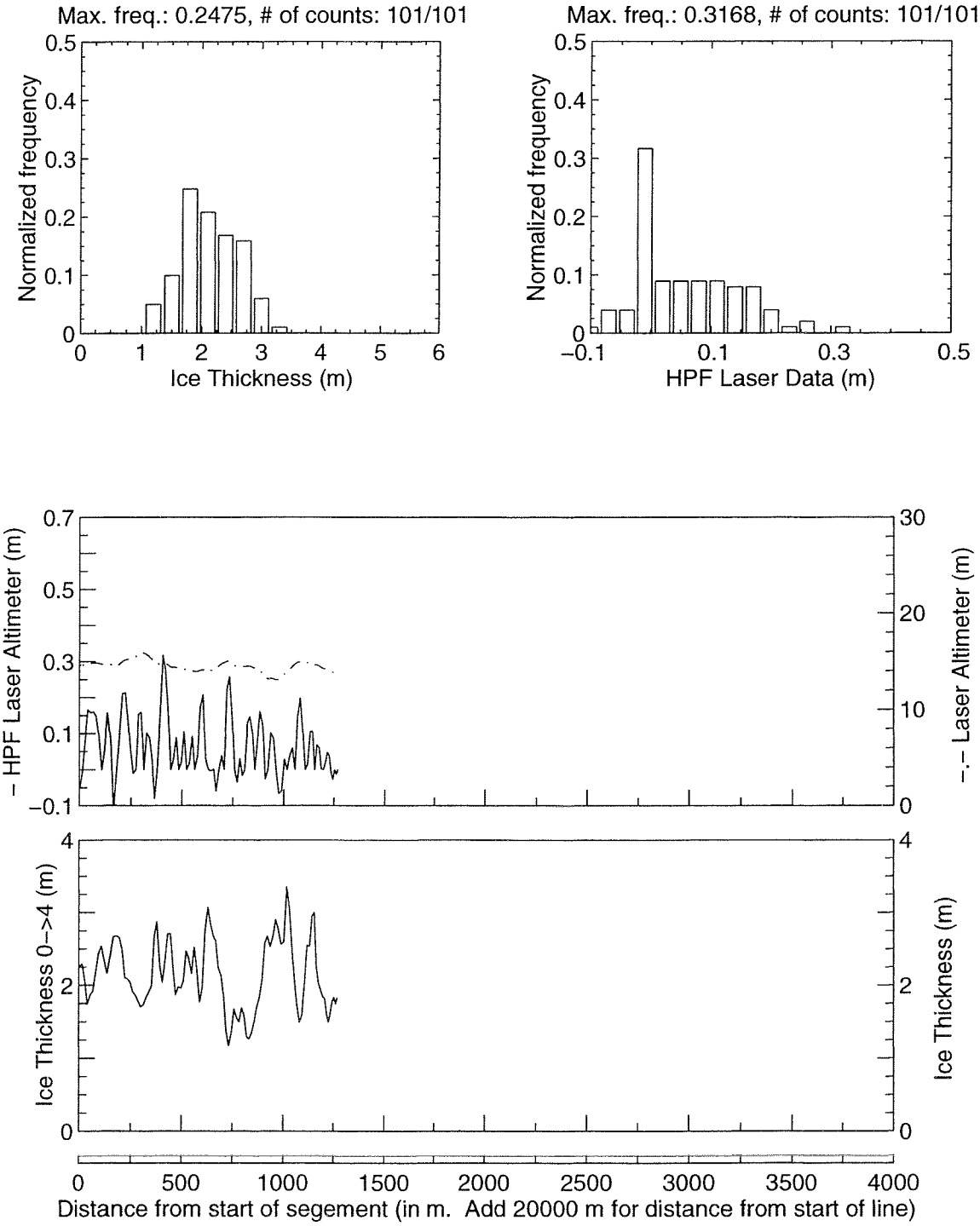

MAR 06 Flight #09 Line #10030 part 1 of 4

Line Starting Coordinates (53.5569,–55.6415) ending at (53.5308,–55.6829)

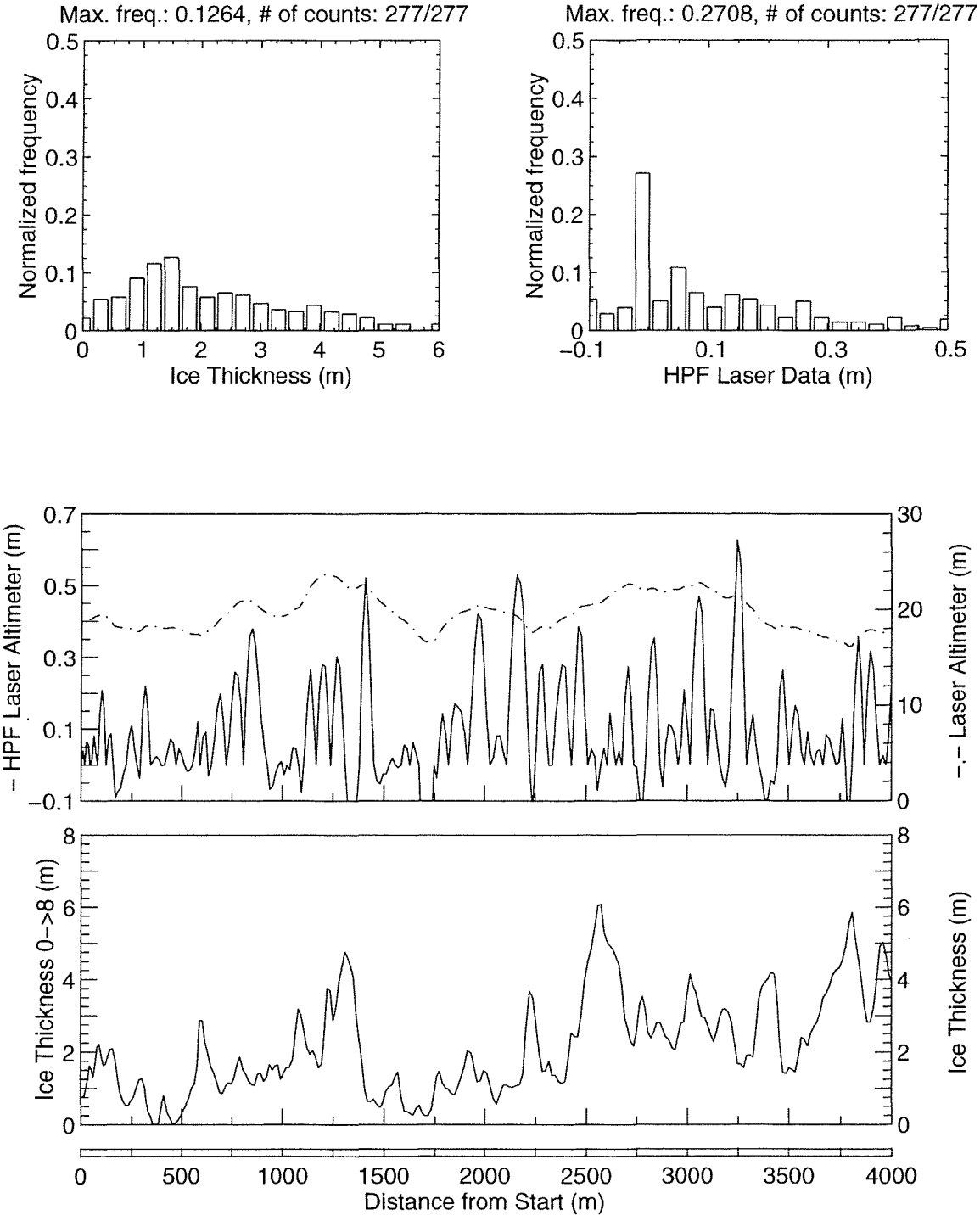

MAR 06 Flight #09 Line #10030 part 2 of 4

Line Starting Coordinates (53.5308,–55.6829) ending at (53.4999,–55.7132)

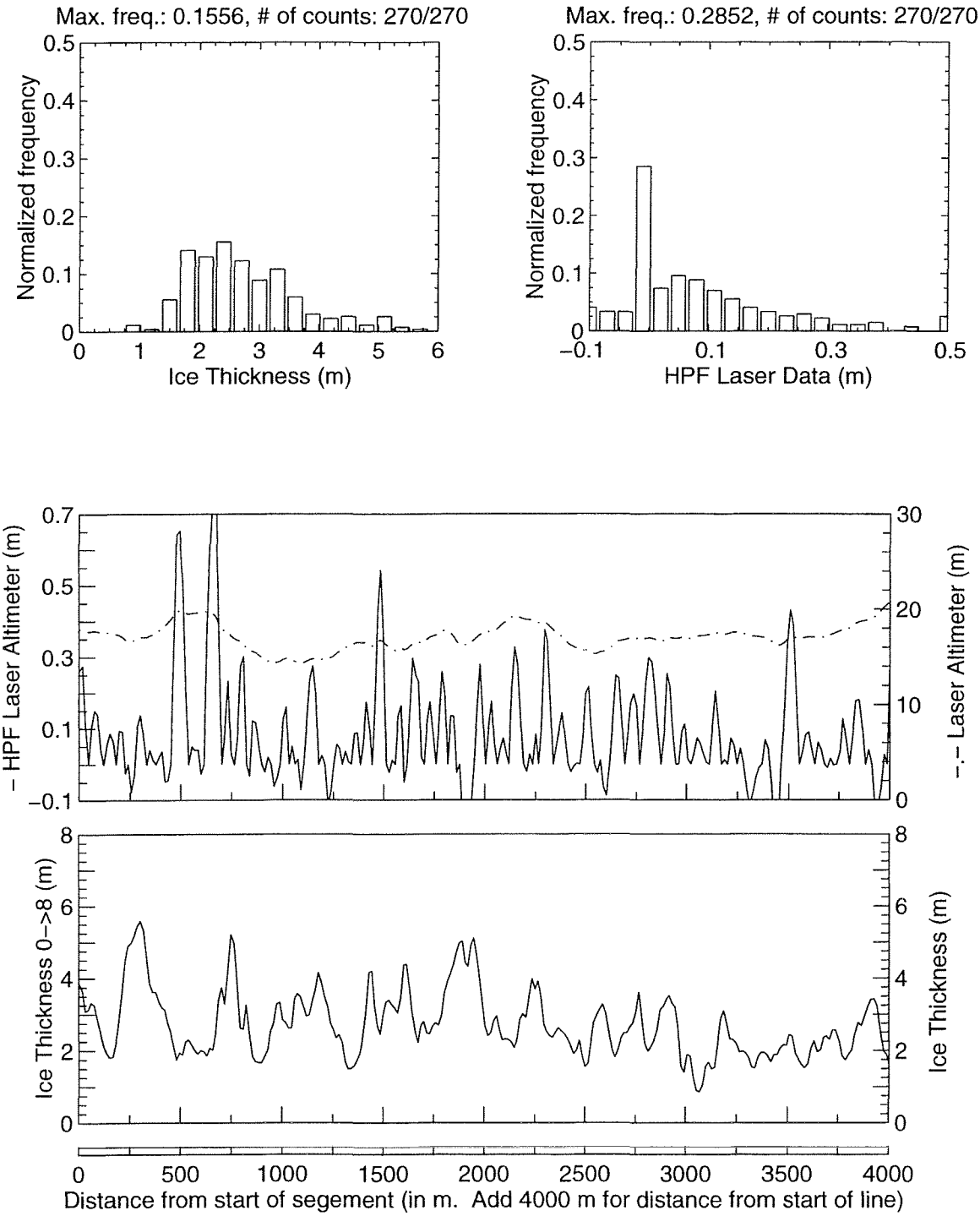

MAR 06 Flight #09 Line #10030 part 3 of 4

Line Starting Coordinates (53.4999,–55.7132) ending at (53.4660,–55.7333)

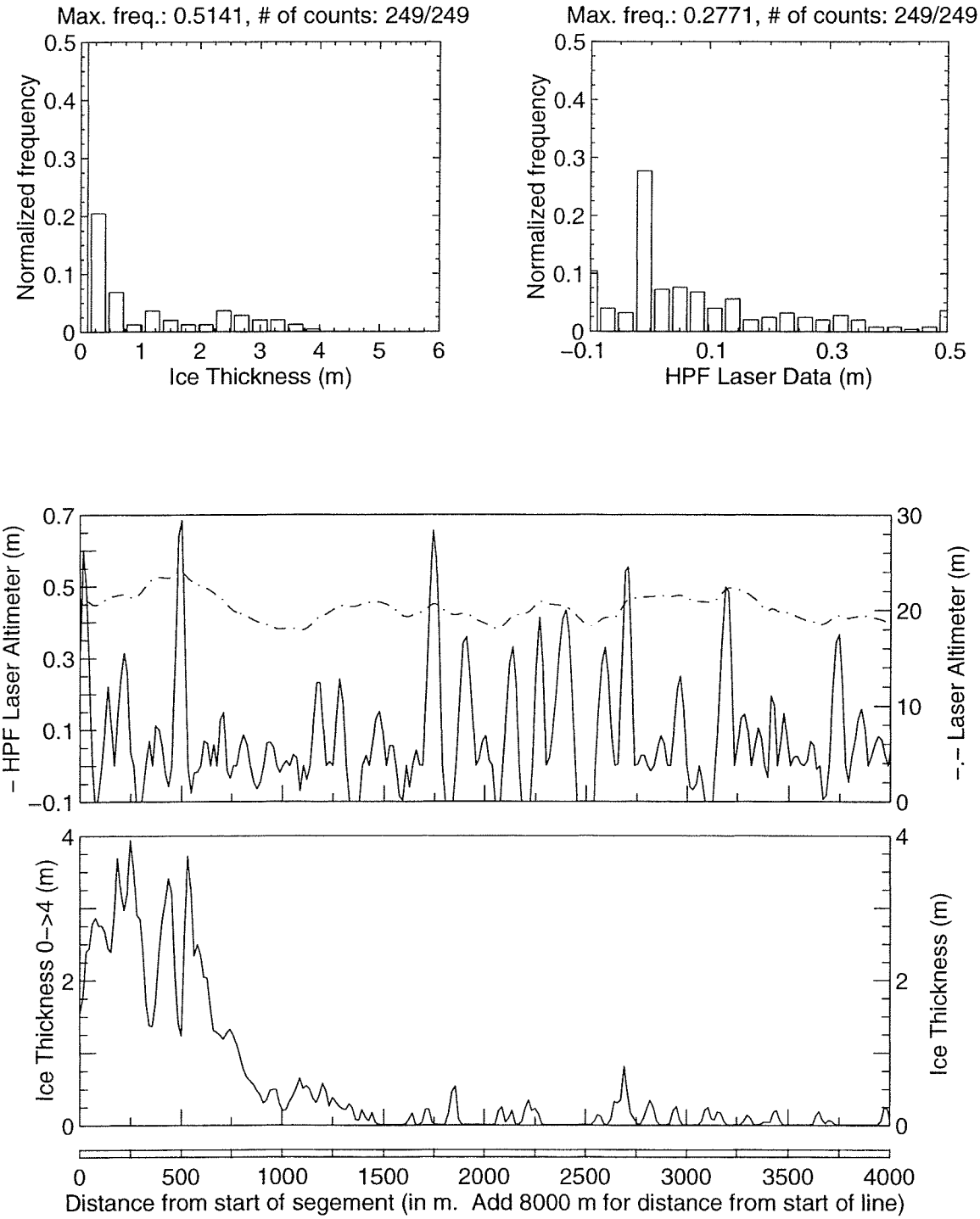

MAR 06 Flight #09 Line #10030 part 4 of 4

Line Starting Coordinates (53.4660,–55.7333) ending at (53.4556,–55.7412)

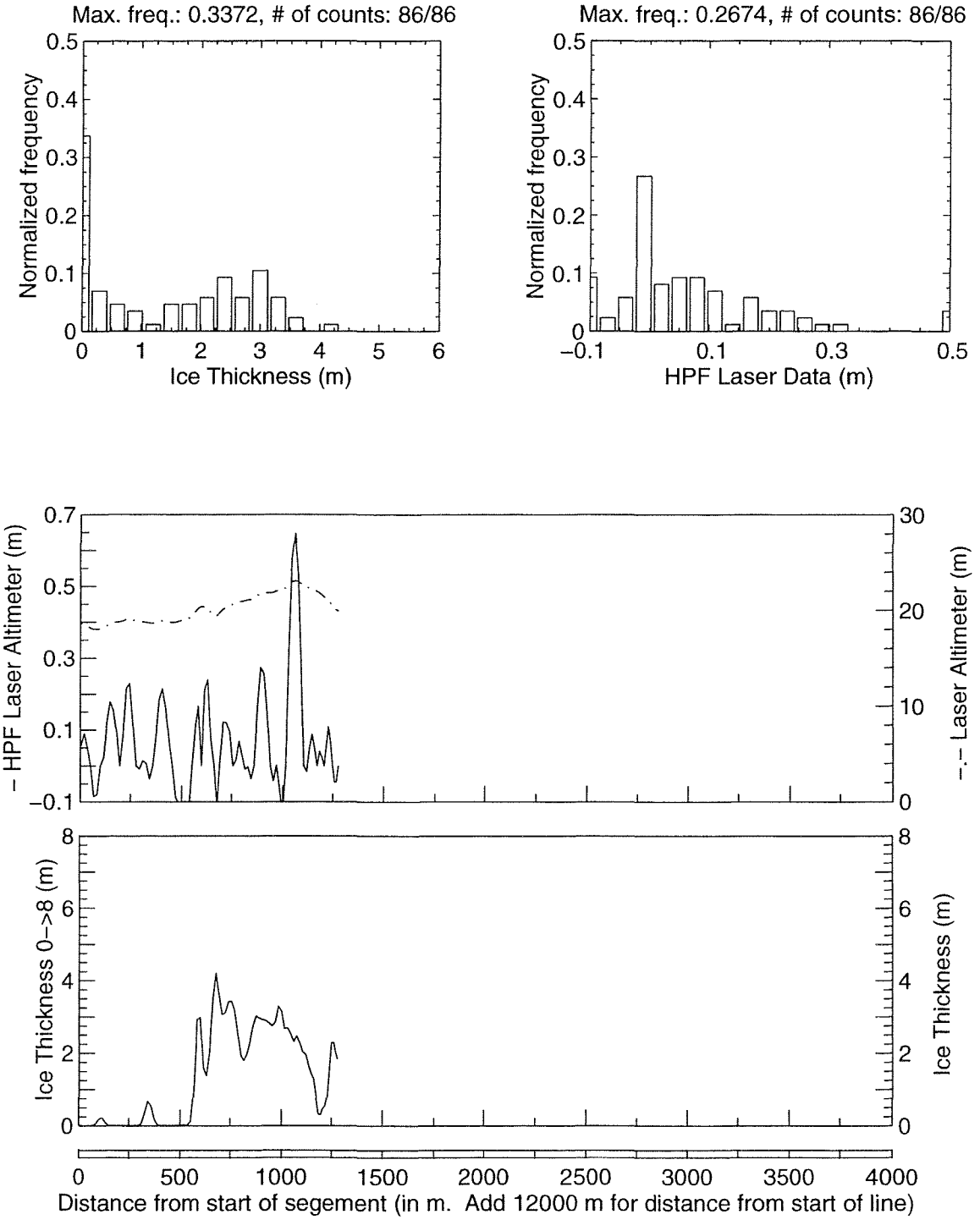

MAR 06 Flight #08 Line #10040 part 1 of 1

Line Starting Coordinates (53.6970,–55.1179) ending at (53.7057,–55.0648)

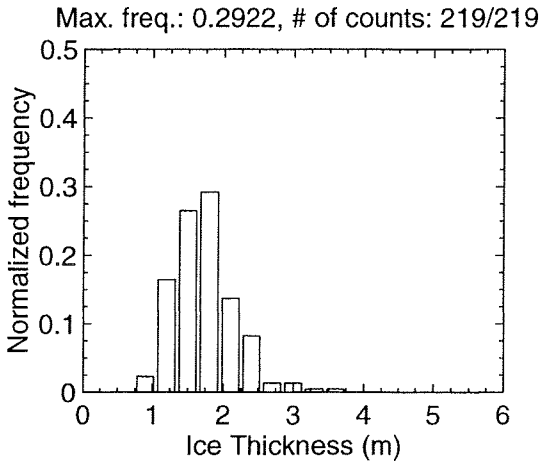

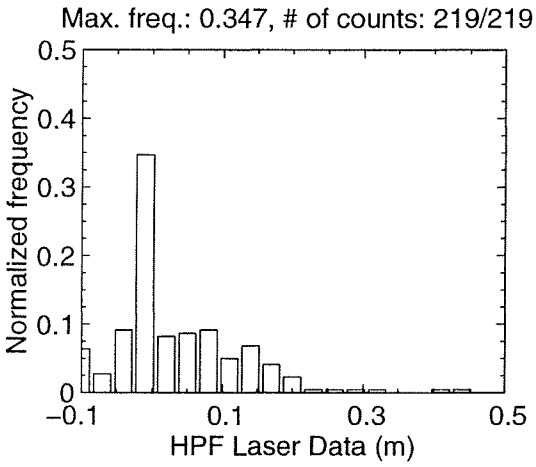

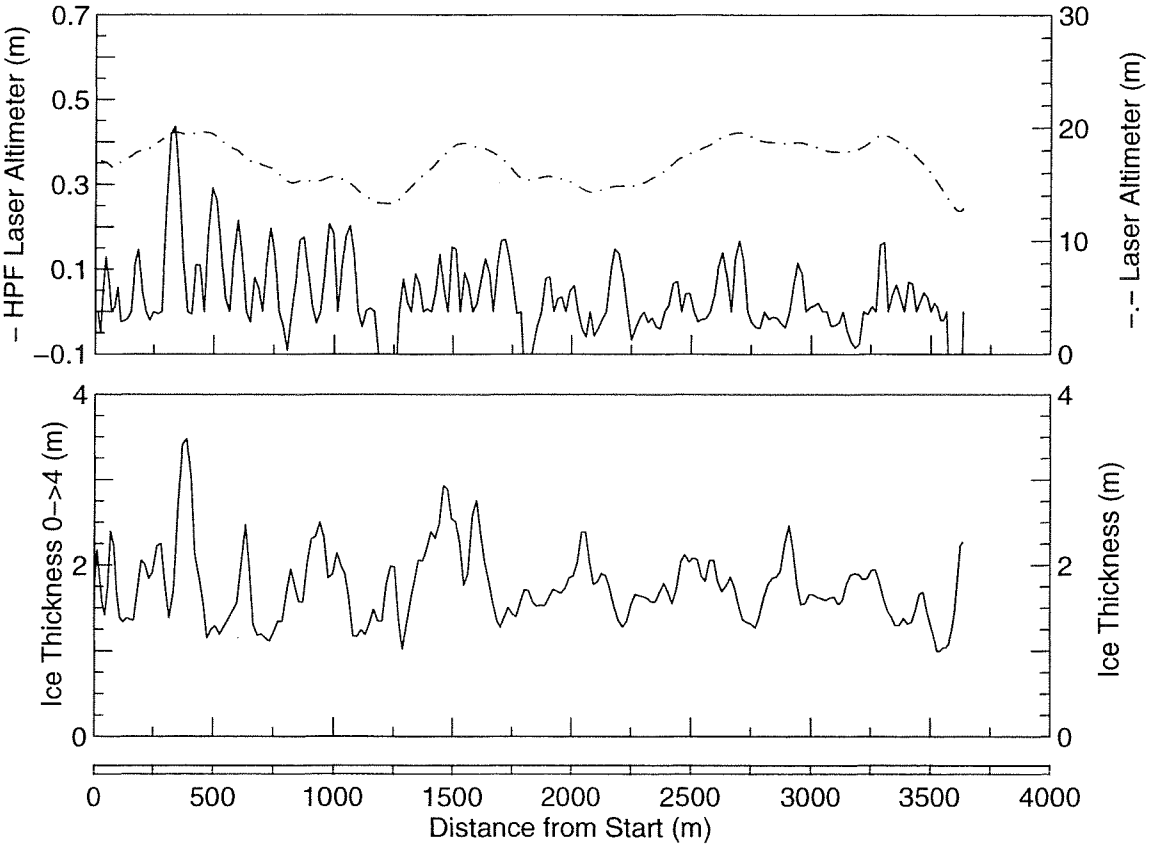

MAR 06 Flight #09 Line #10050 part 1 of 3

Line Starting Coordinates (53.4881,−55.8121) ending at (53.4972,−55.8705)

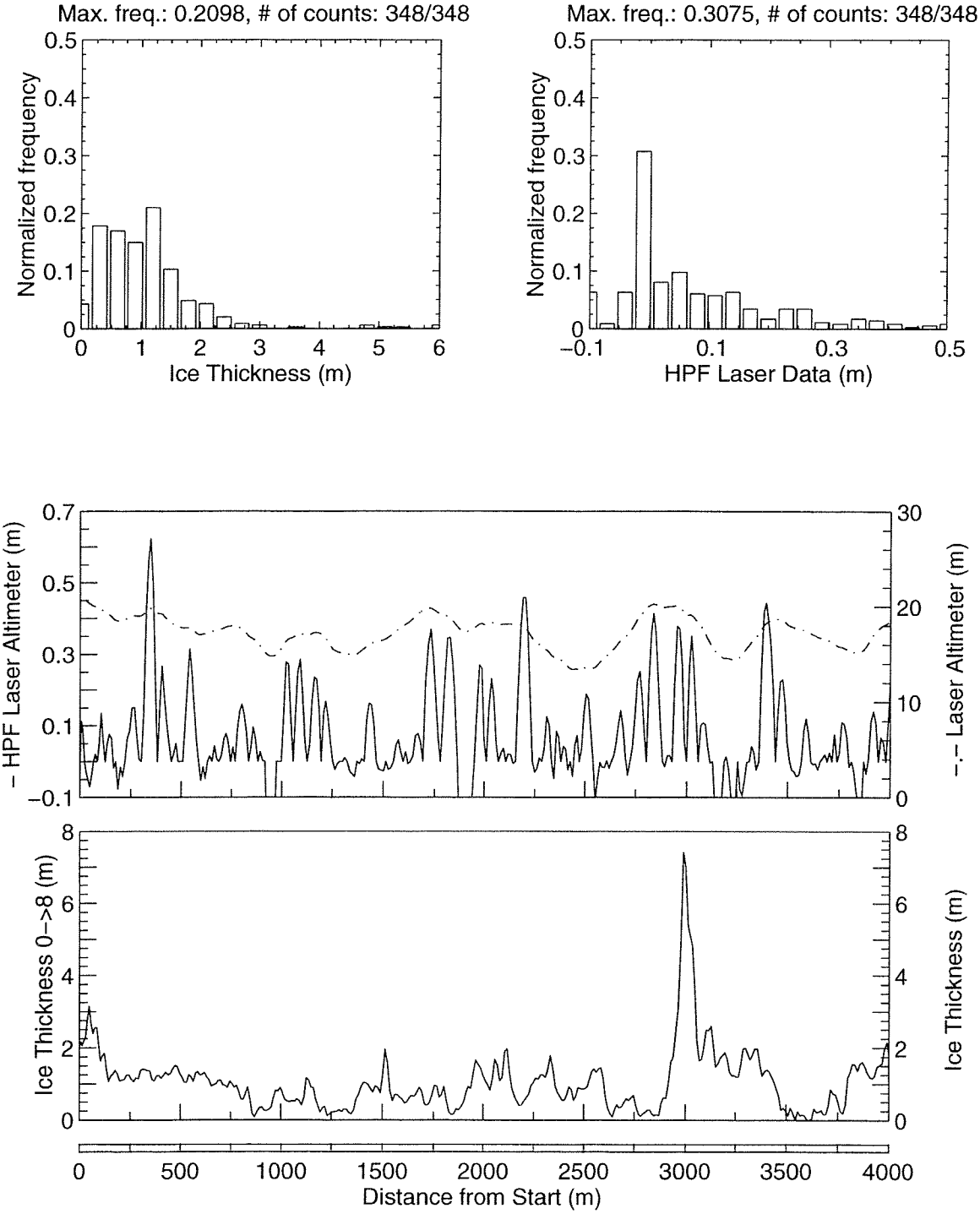

MAR 06 Flight #09 Line #10050 part 2 of 3

Line Starting Coordinates (53.4972,–55.8705) ending at (53.5063,–55.9291)

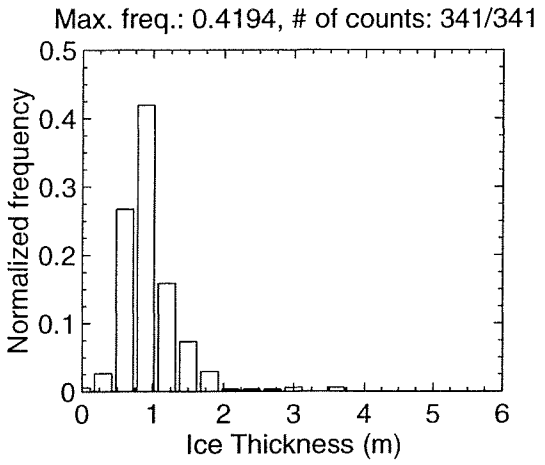

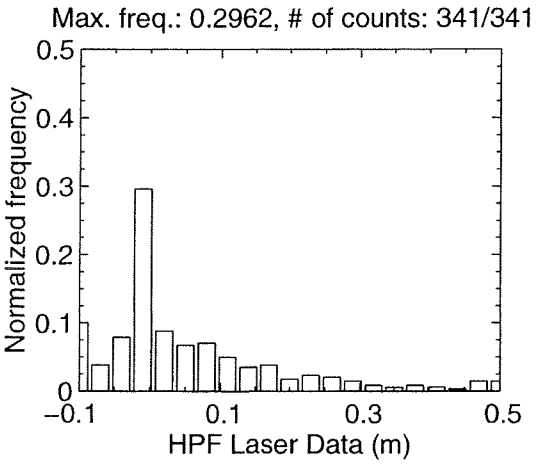

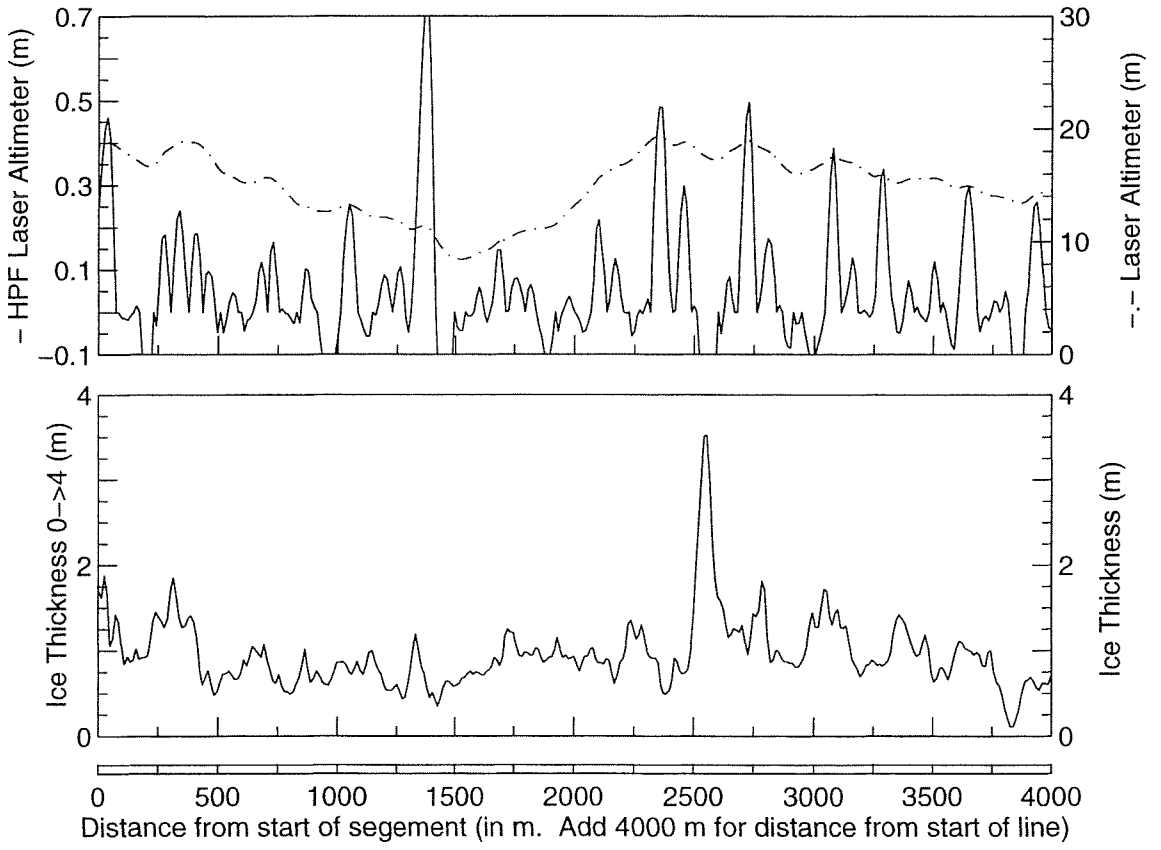

MAR 06 Flight #09 Line #10050 part 3 of 3

Line Starting Coordinates (53.5063,–55.9291) ending at (53.5087,–55.9486)

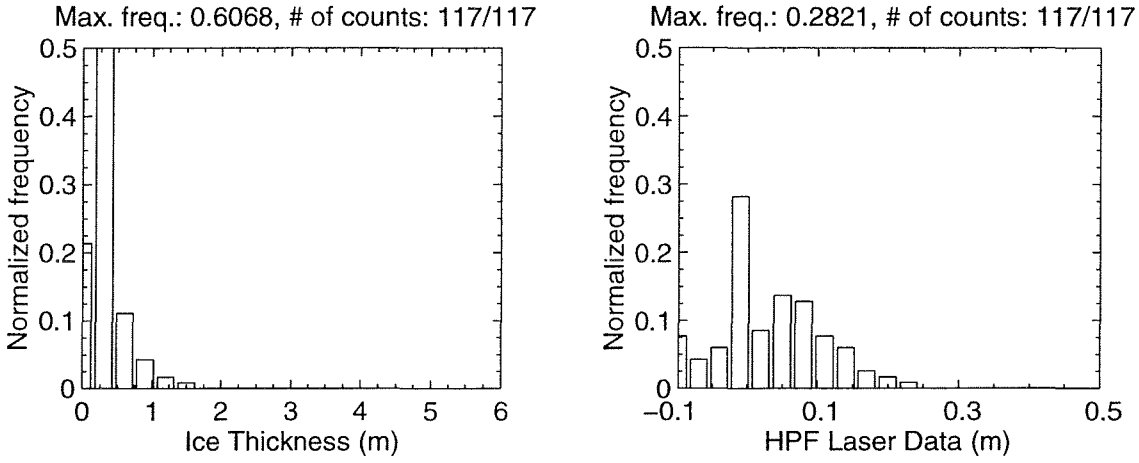

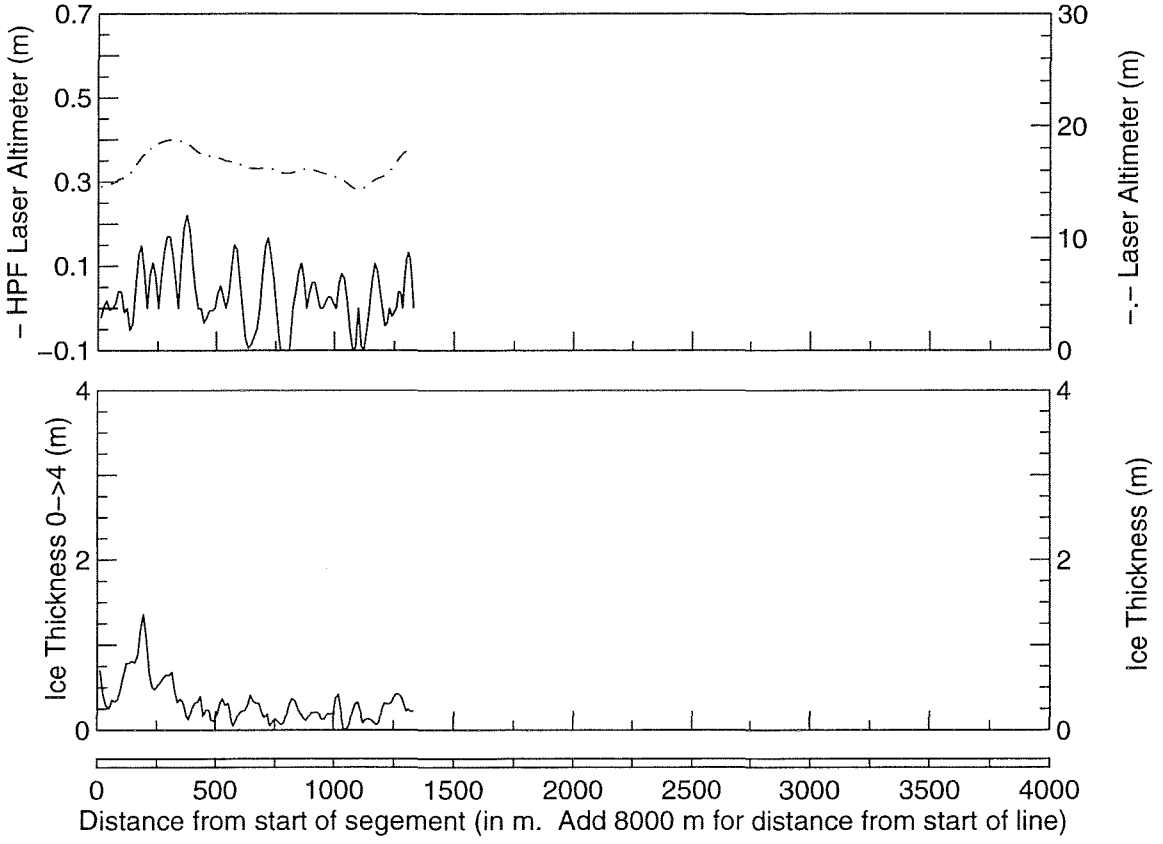

MAR 06 Flight #09 Line #10070 part 1 of 4

Line Starting Coordinates (53.5234,–56.0703) ending at (53.5340,–56.1282)

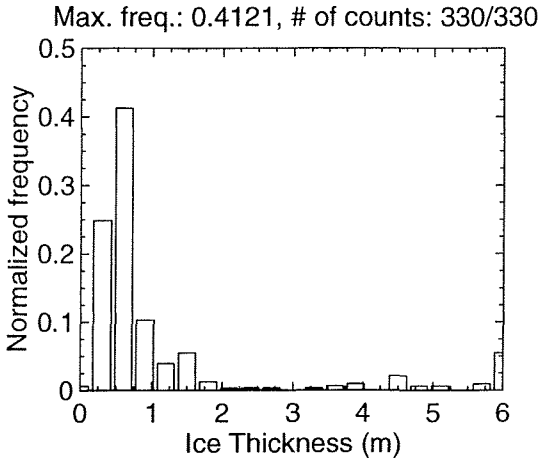

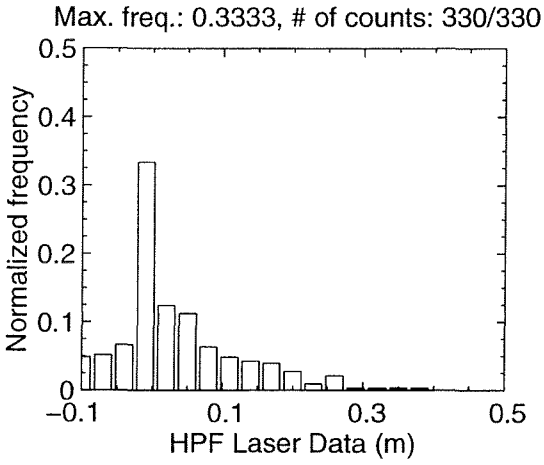

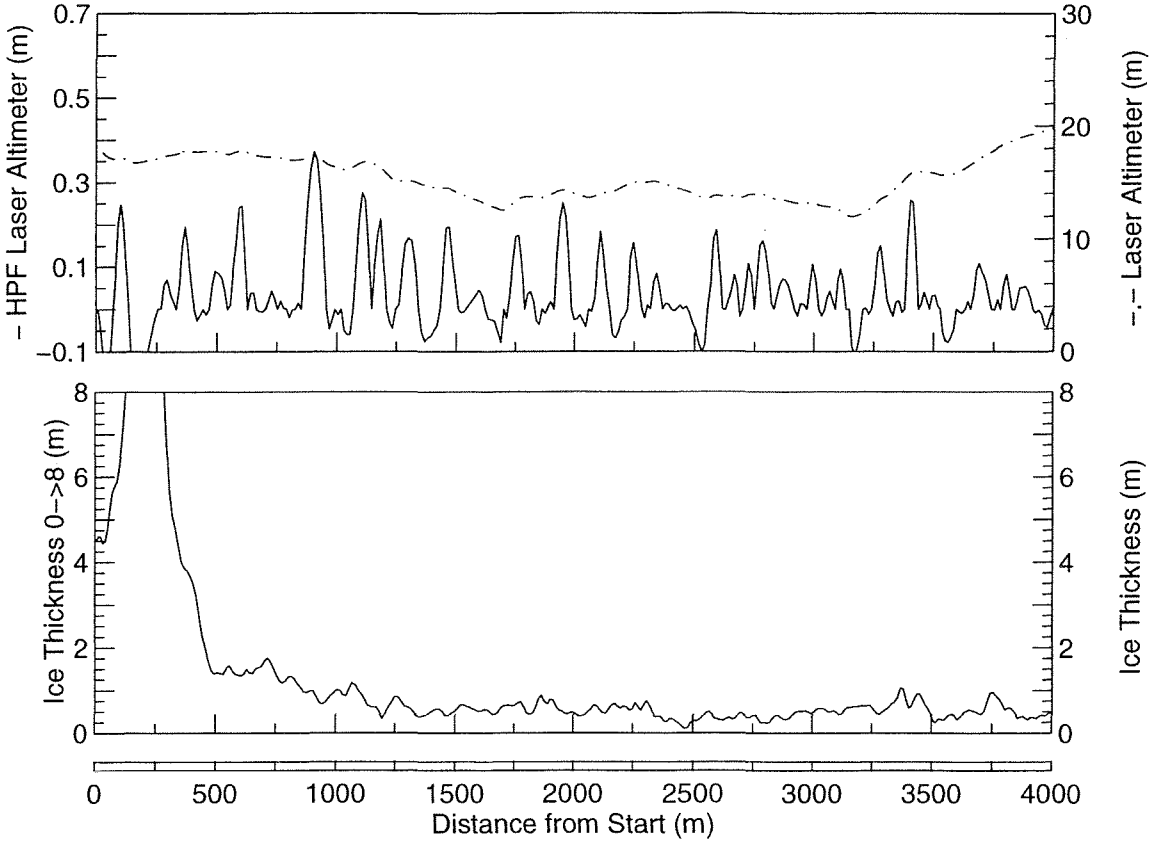

MAR 06 Flight #09 Line #10070 part 2 of 4

Line Starting Coordinates (53.5340,−56.1282) ending at (53.5446,−56.1860)

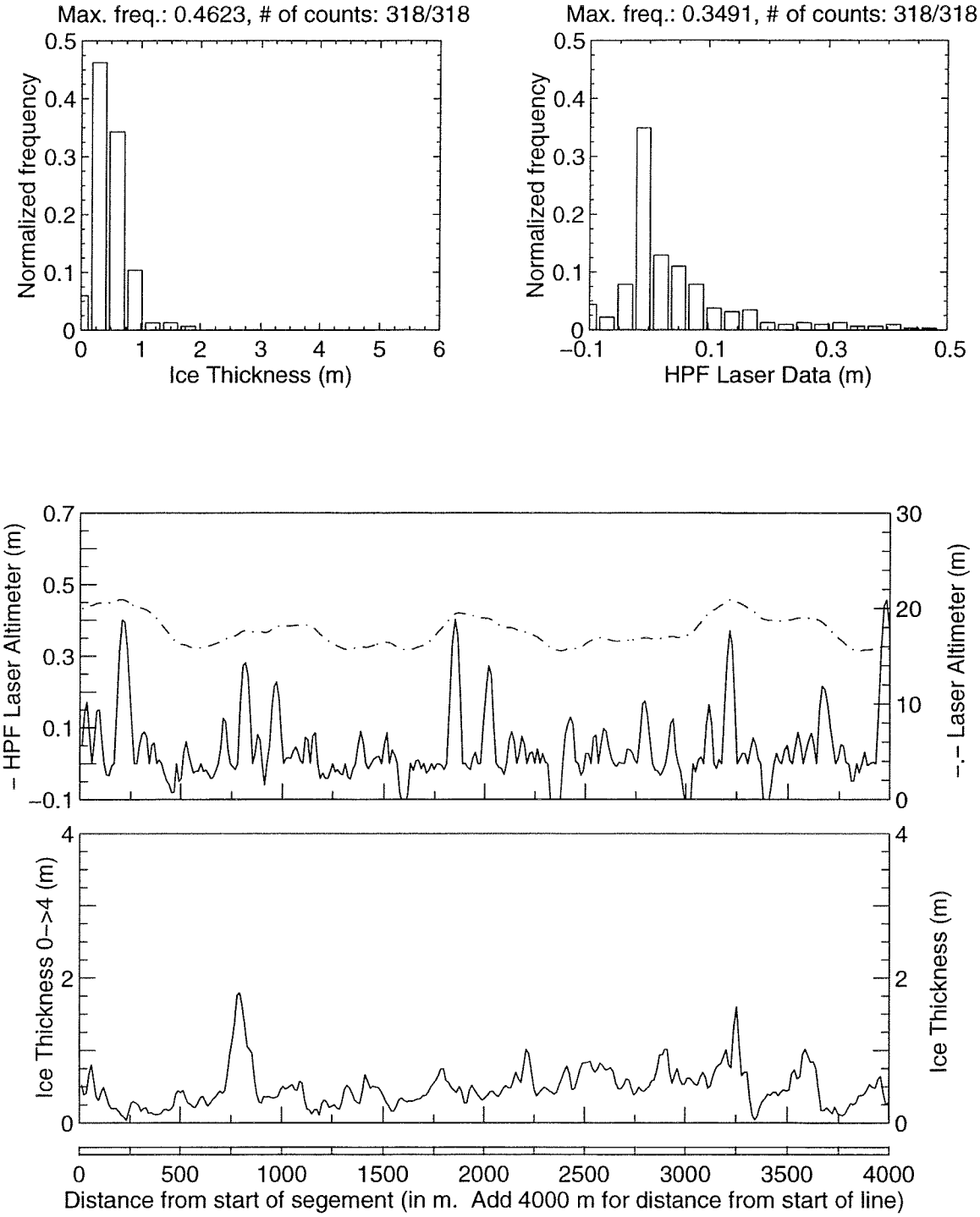

MAR 06 Flight #09 Line #10070 part 3 of 4

Line Starting Coordinates (53.5446,−56.1860) ending at (53.5543,−56.2441)

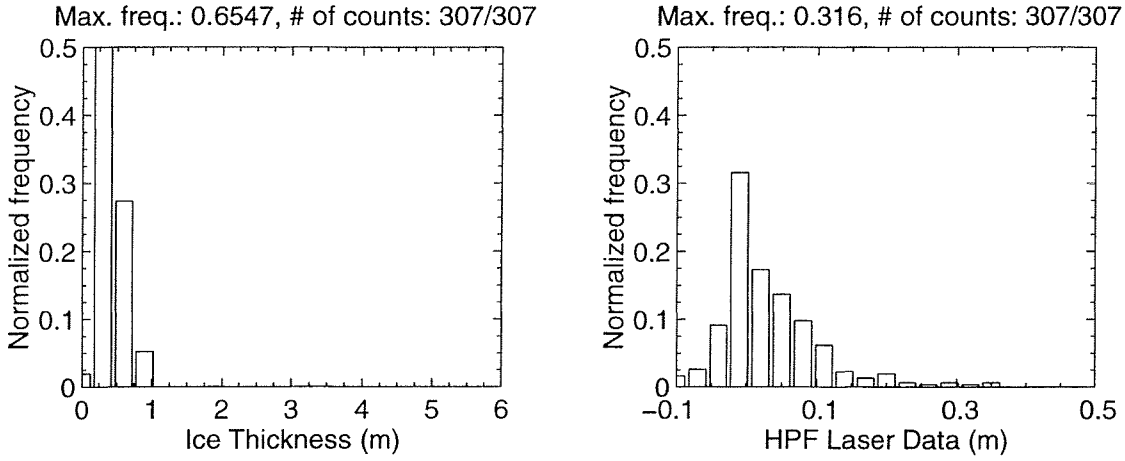

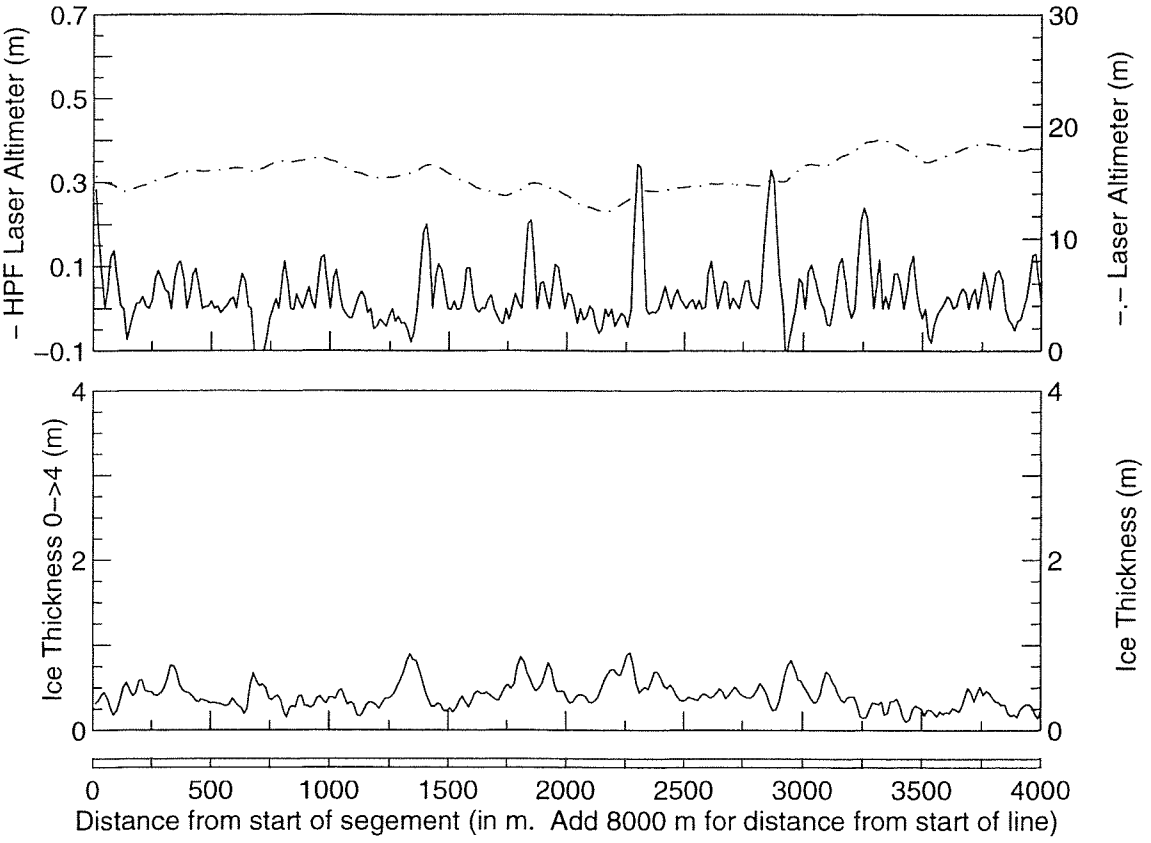

MAR 06 Flight #09 Line #10070 part 4 of 4

Line Starting Coordinates (53.5543,–56.2441) ending at (53.5566,–56.2561)

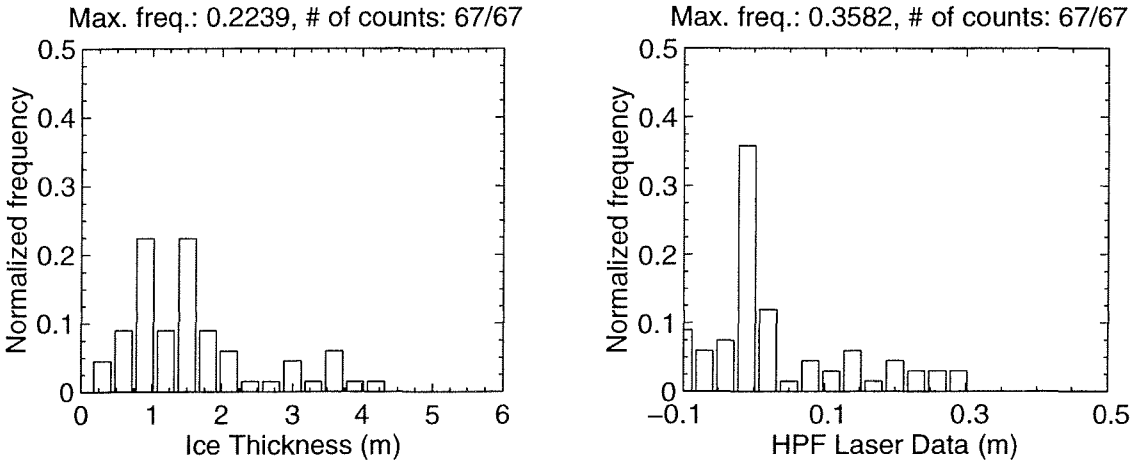

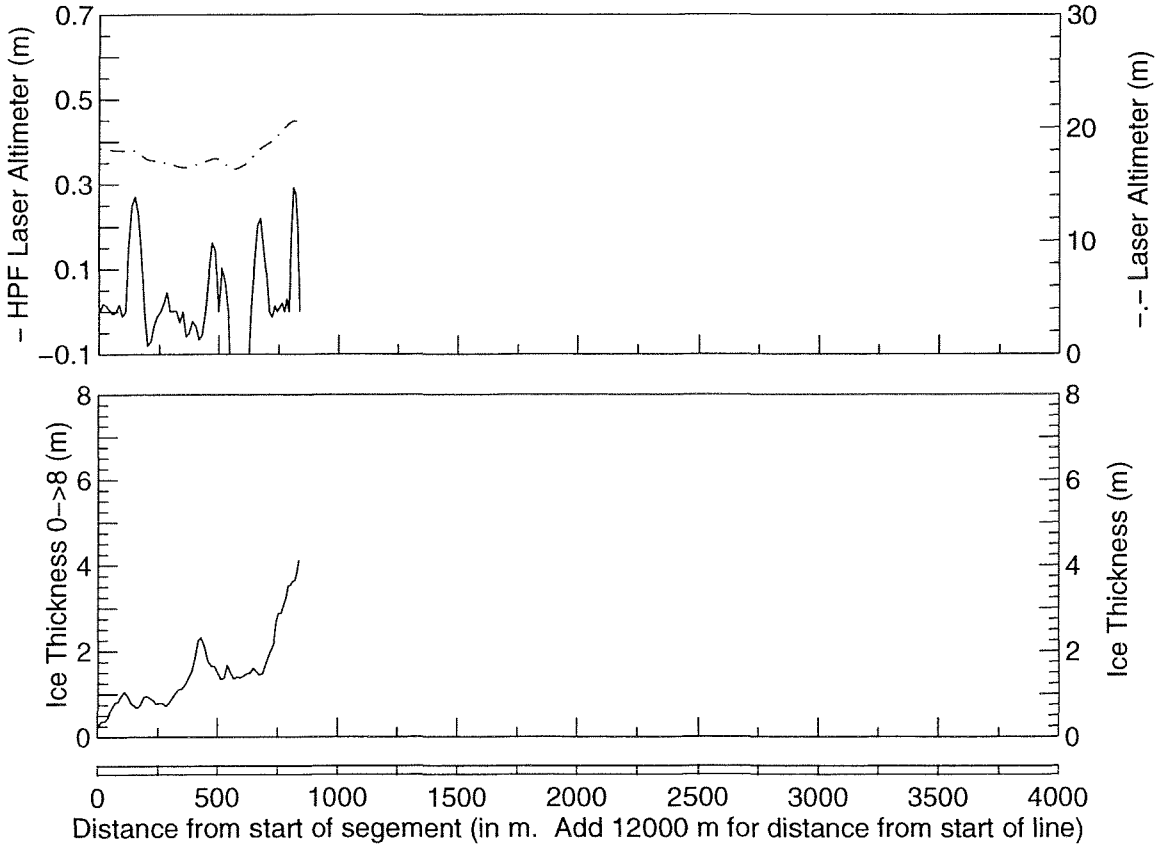

MAR 06 Flight #09 Line #10080 part 1 of 5

Line Starting Coordinates (53.6239,−56.4367) ending at (53.6379,−56.4926)

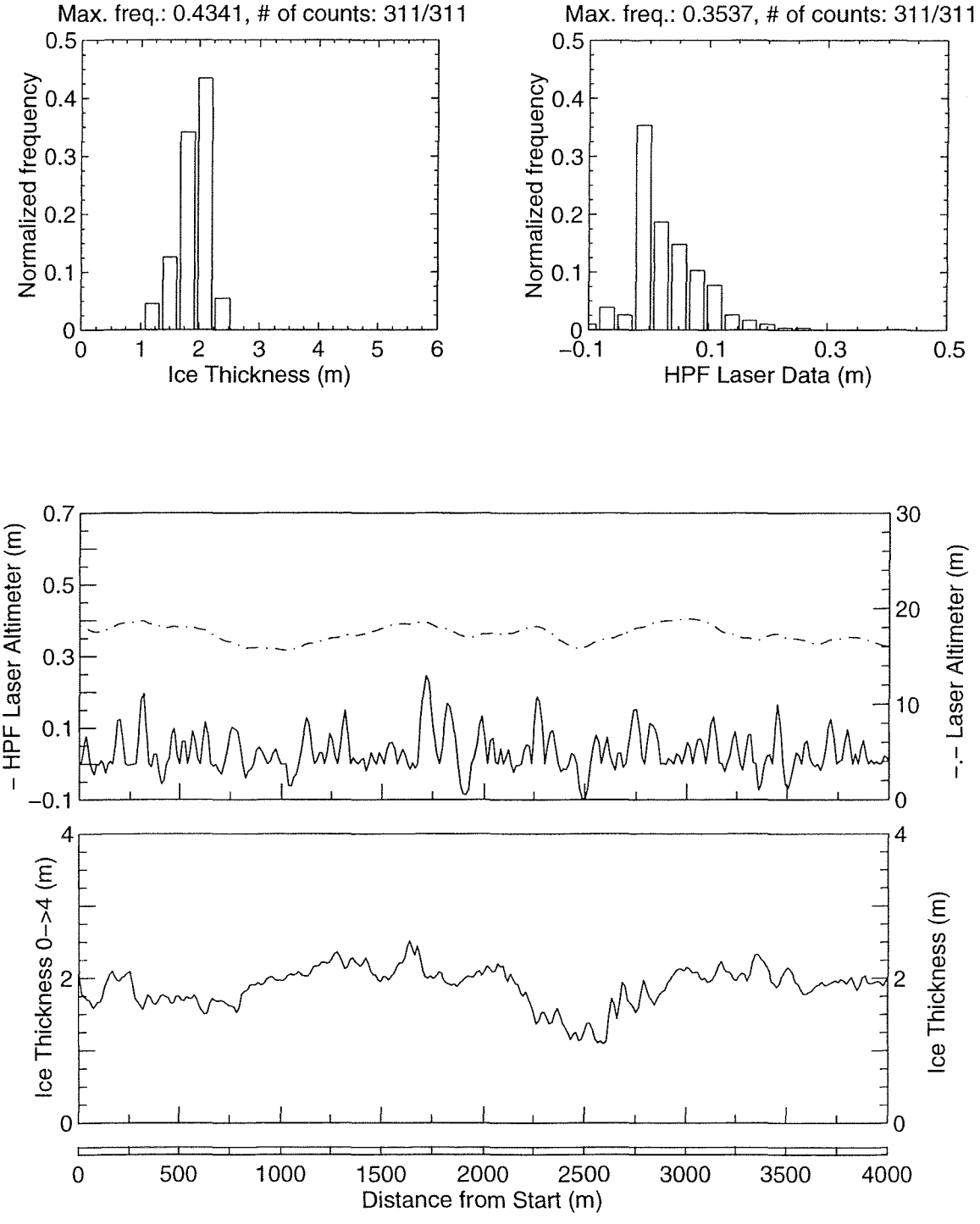

MAR 06 Flight #09 Line #10080 part 2 of 5

Line Starting Coordinates (53.6379,–56.4926) ending at (53.6532,–56.5475)

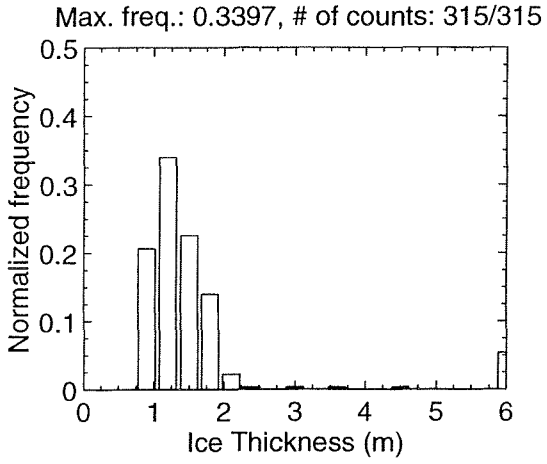

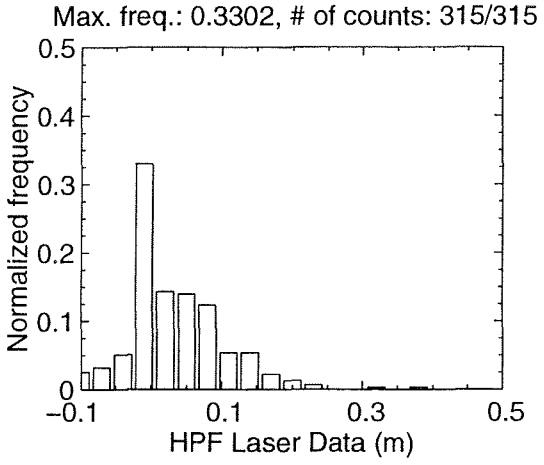

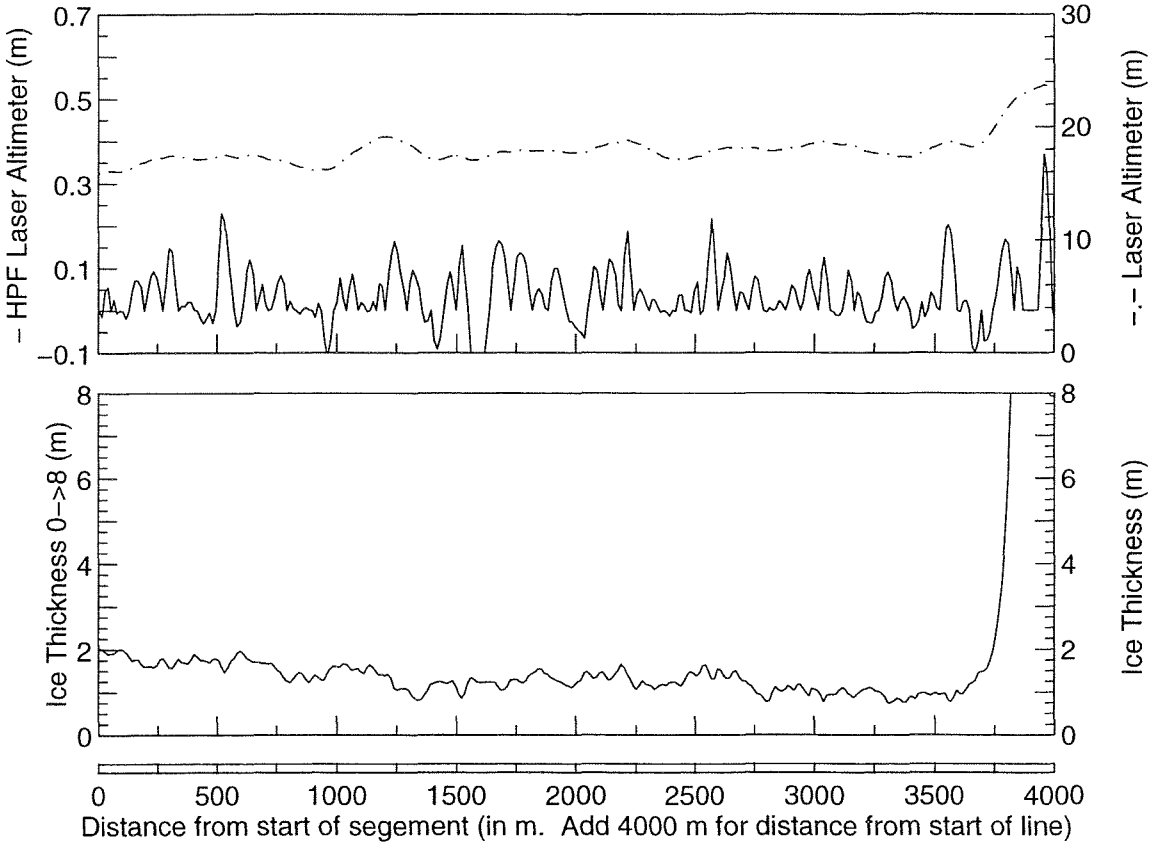

MAR 06 Flight #09 Line #10080 part 3 of 5

Line Starting Coordinates (53.6532,–56.5475) ending at (53.6655,–56.6045)

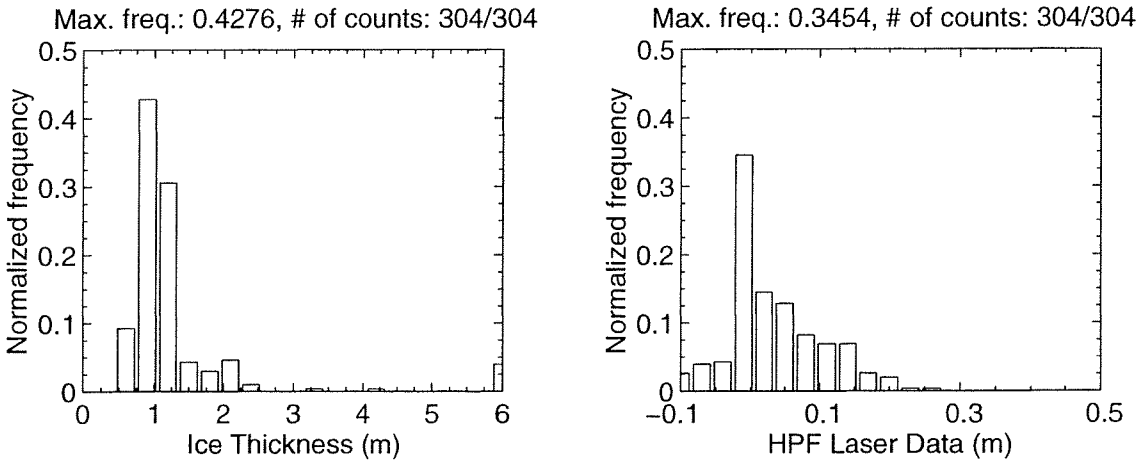

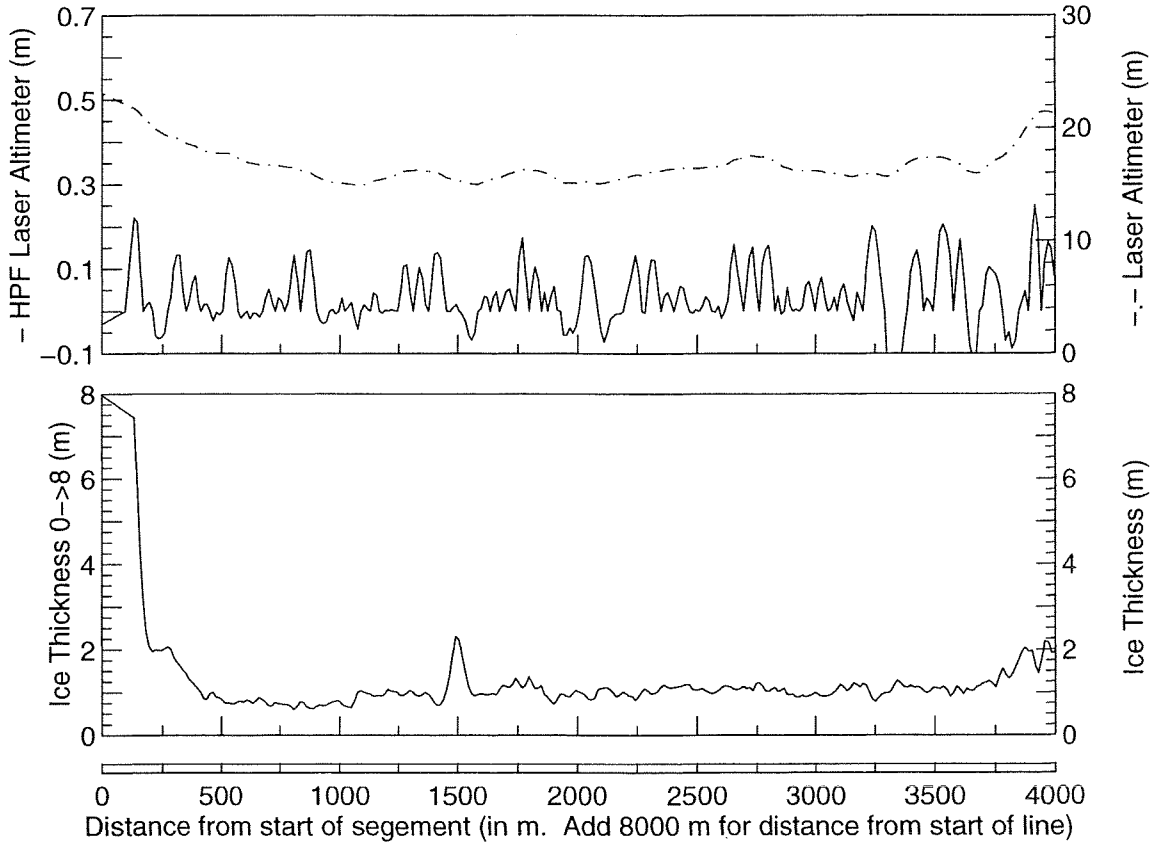

MAR 06 Flight #09 Line #10080 part 4 of 5

Line Starting Coordinates (53.6655,–56.6045) ending at (53.6771,–56.6618)

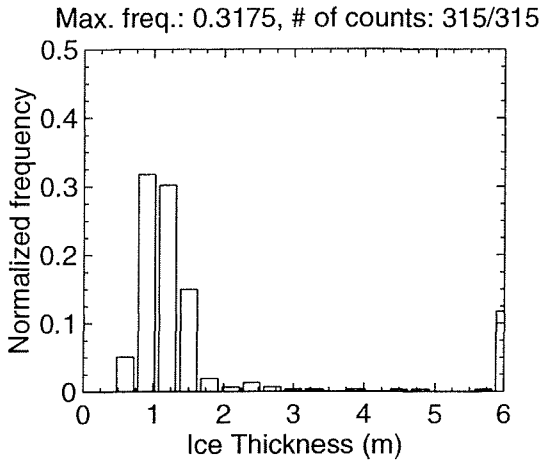

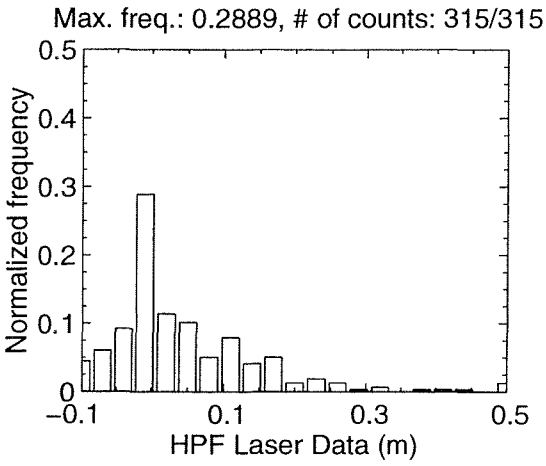

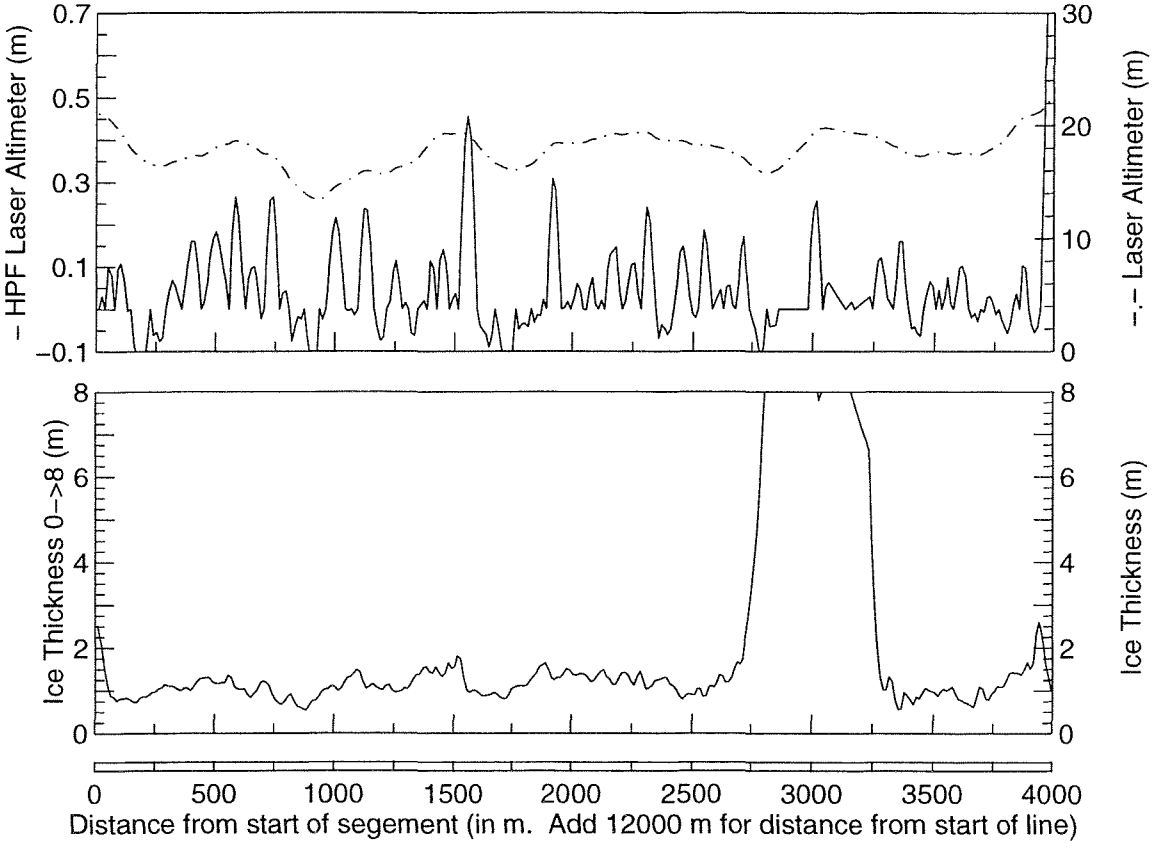

MAR 06 Flight #09 Line #10080 part 5 of 5

Line Starting Coordinates (53.6771,–56.6618) ending at (53.6796,–56.6762)

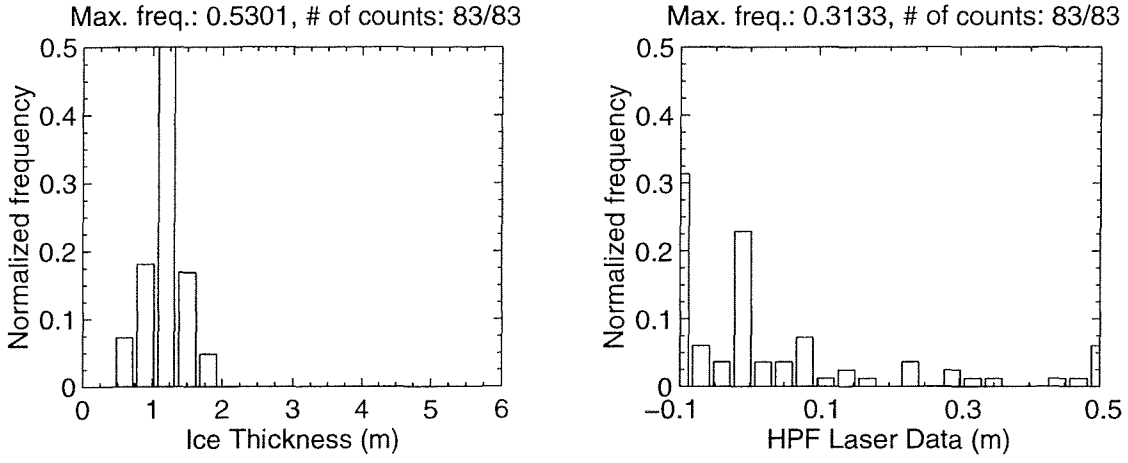

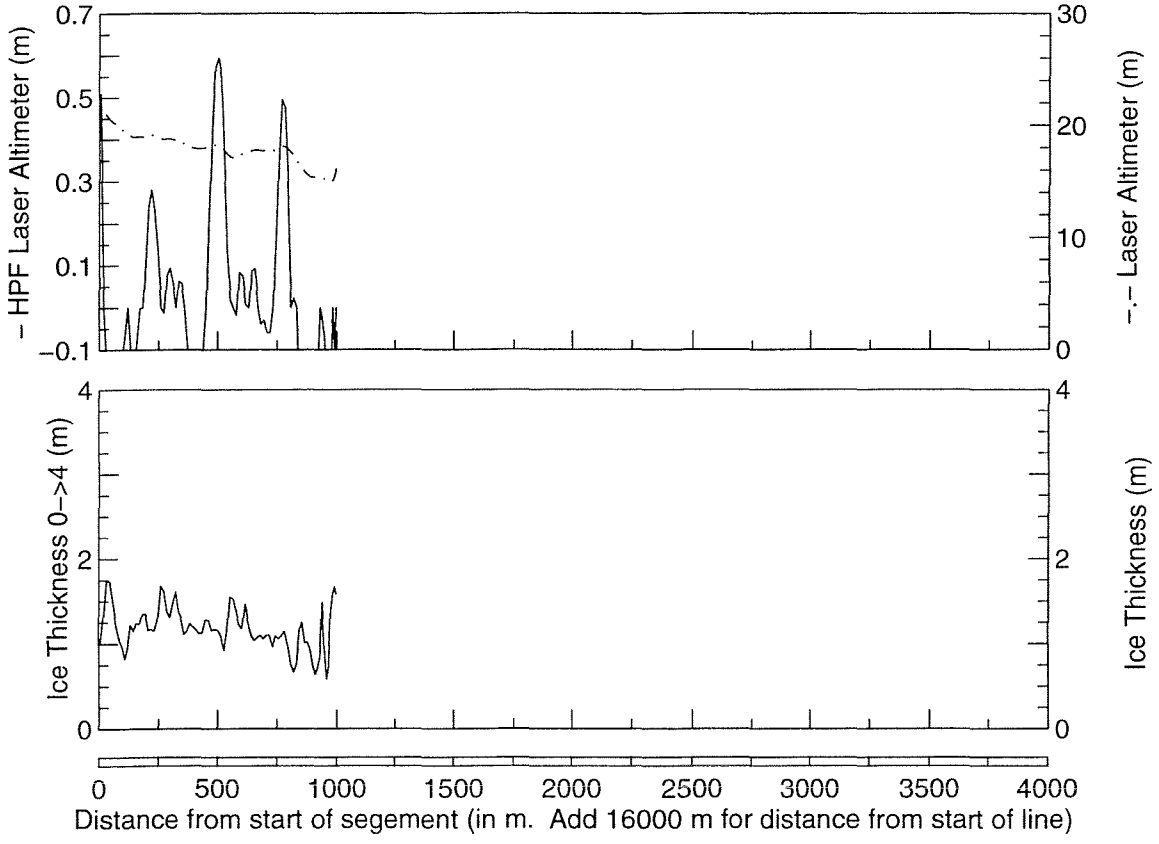

MAR 06 Flight #09 Line #10060 part 1 of 2

Line Starting Coordinates (53.4986,–55.9347) ending at (53.5097,–55.9922)

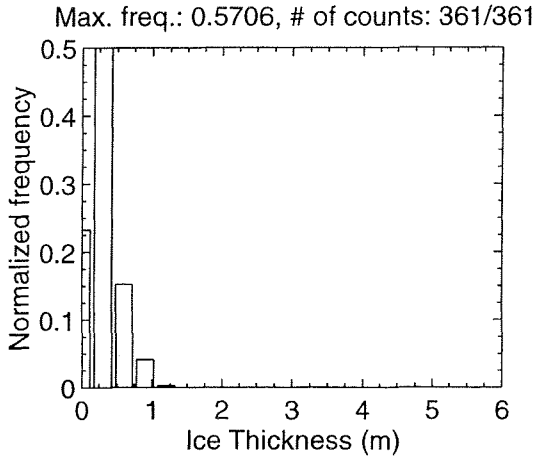

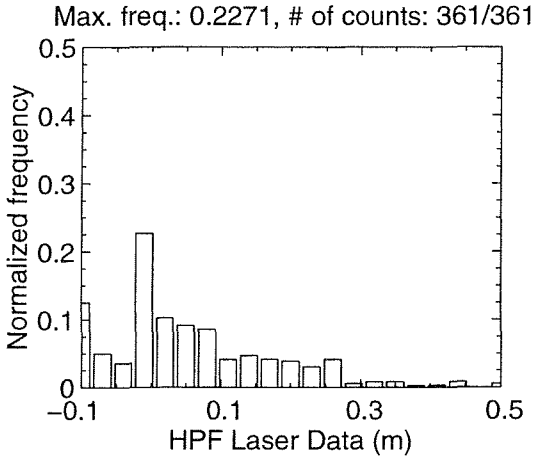

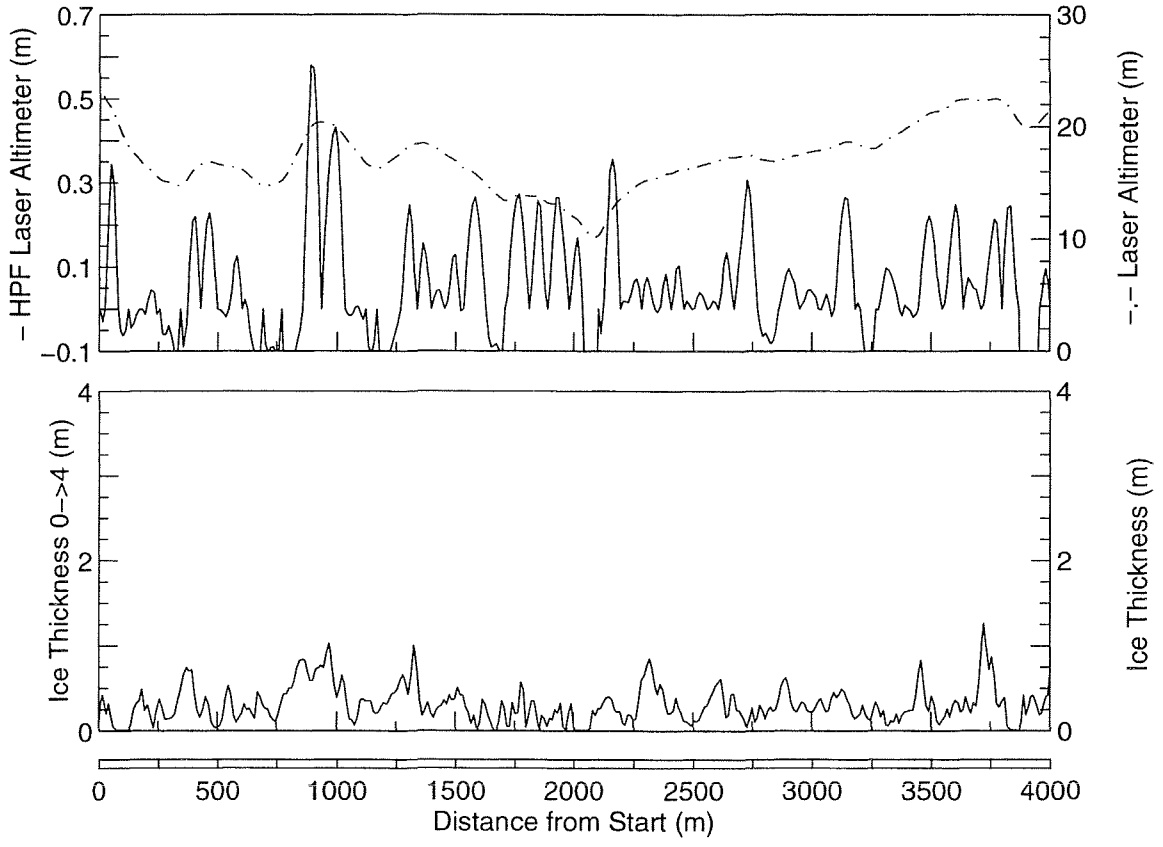

MAR 06 Flight #13 Line #10010 part 1 of 4

Line Starting Coordinates (53.7428,–56.1099) ending at (53.7280,–56.0544)

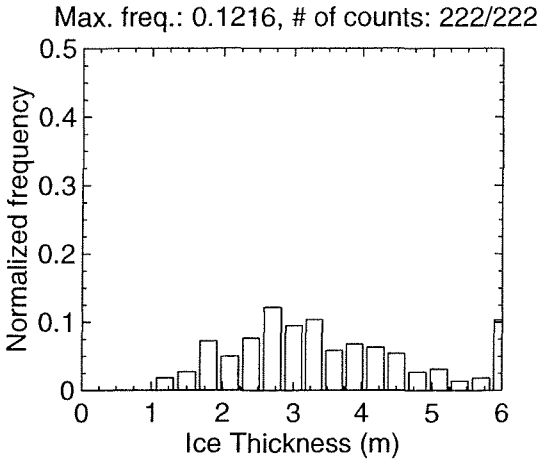

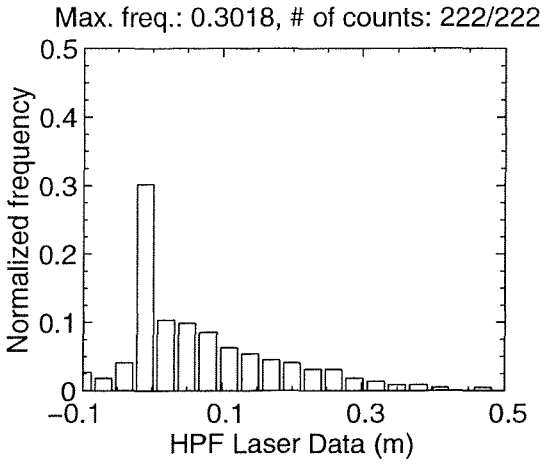

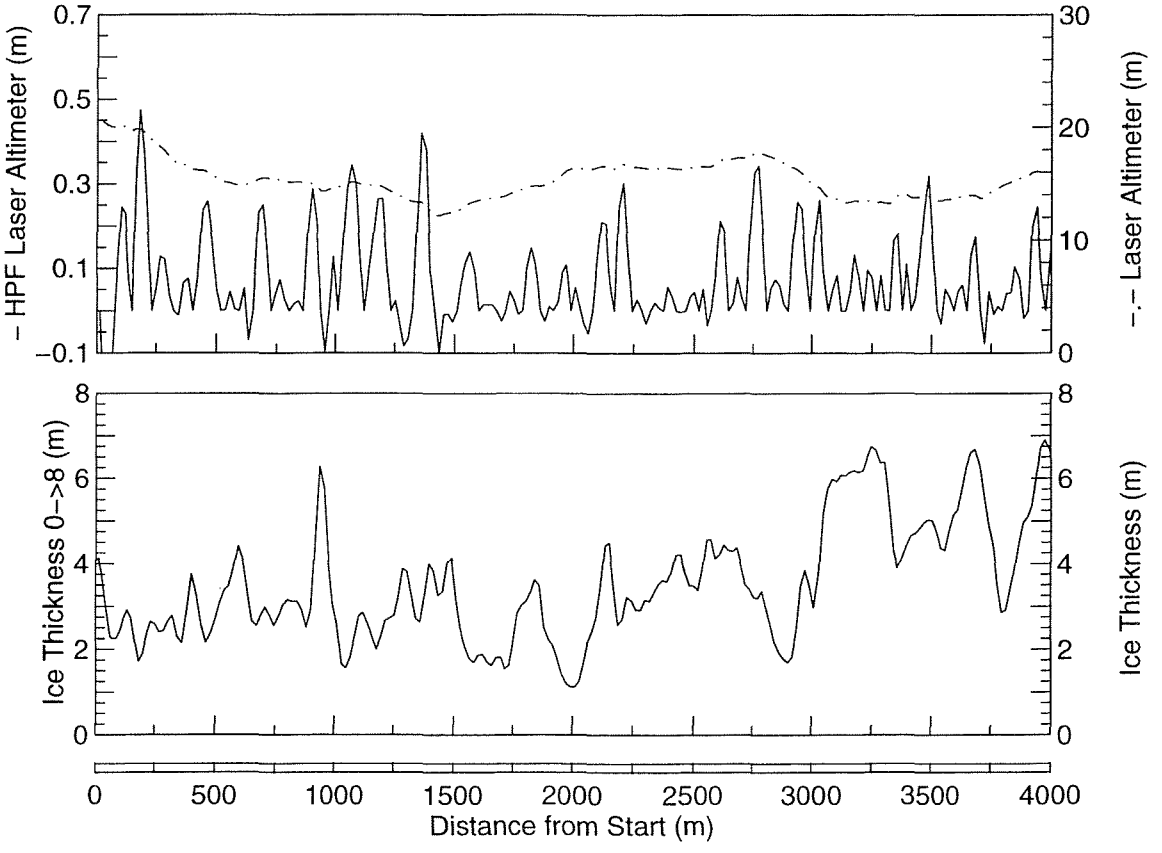

MAR 06 Flight #13 Line #10010 part 2 of 4

Line Starting Coordinates (53.7280,–56.0544) ending at (53.7130,–55.9993)

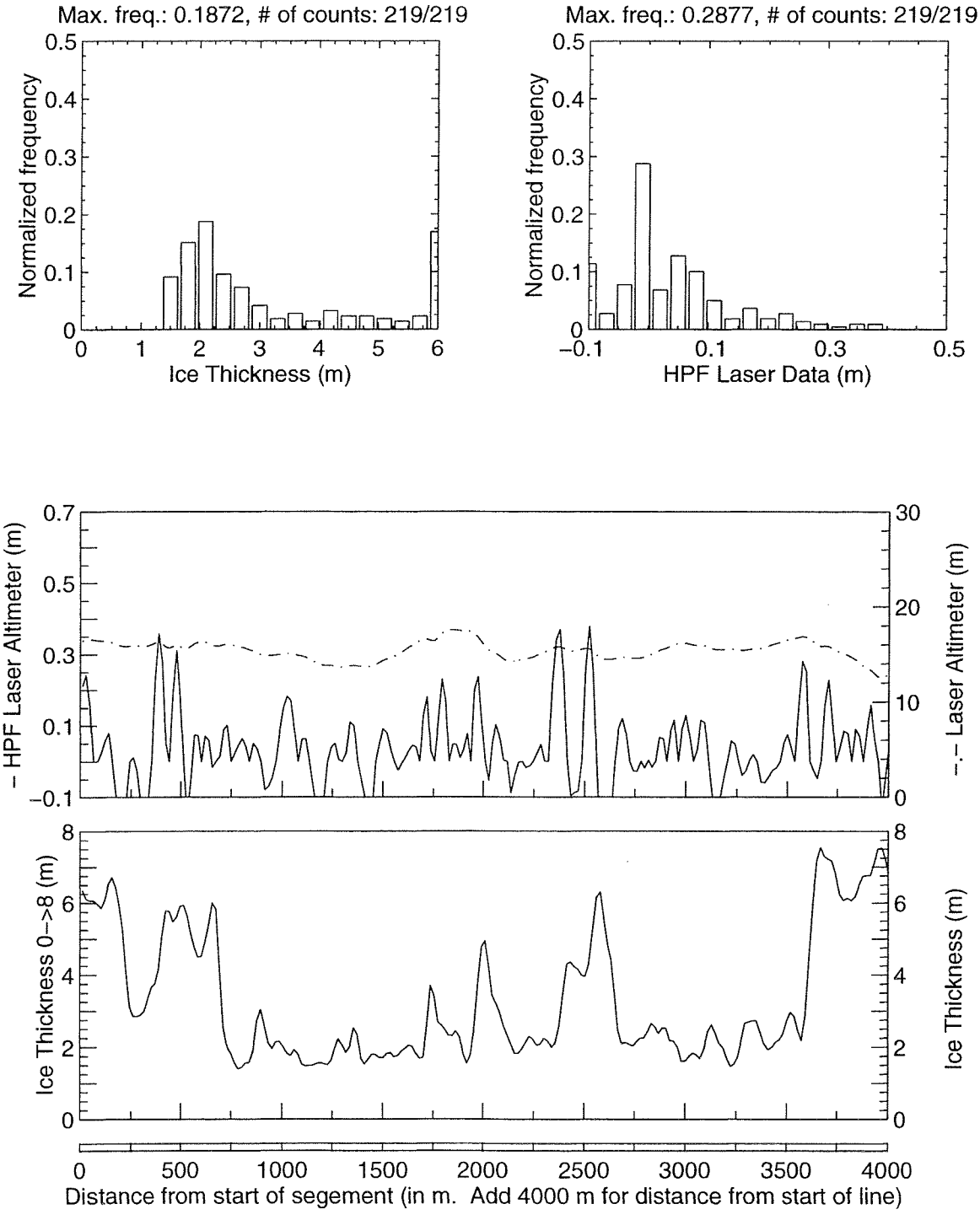

MAR 06 Flight #13 Line #10010 part 3 of 4

Line Starting Coordinates (53.7130,–55.9993) ending at (53.6972,–55.9446)

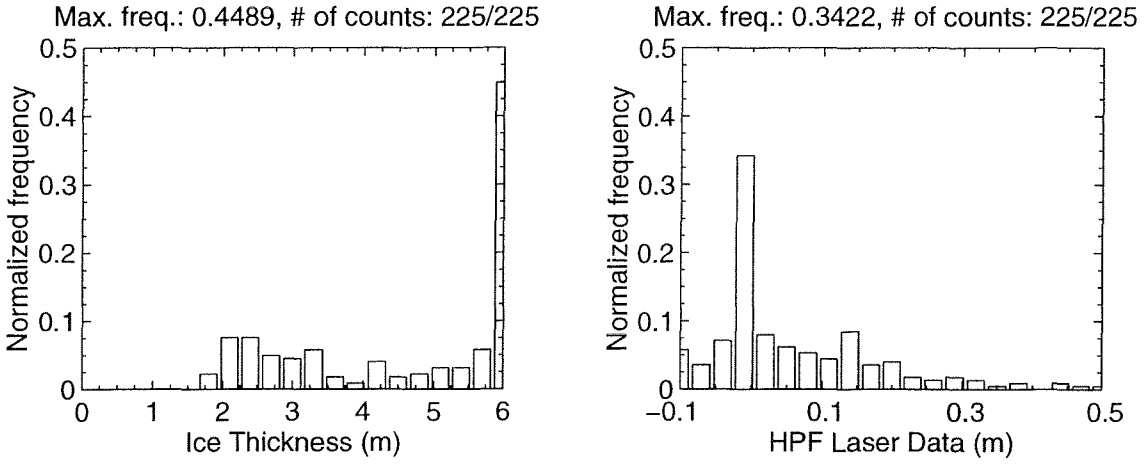

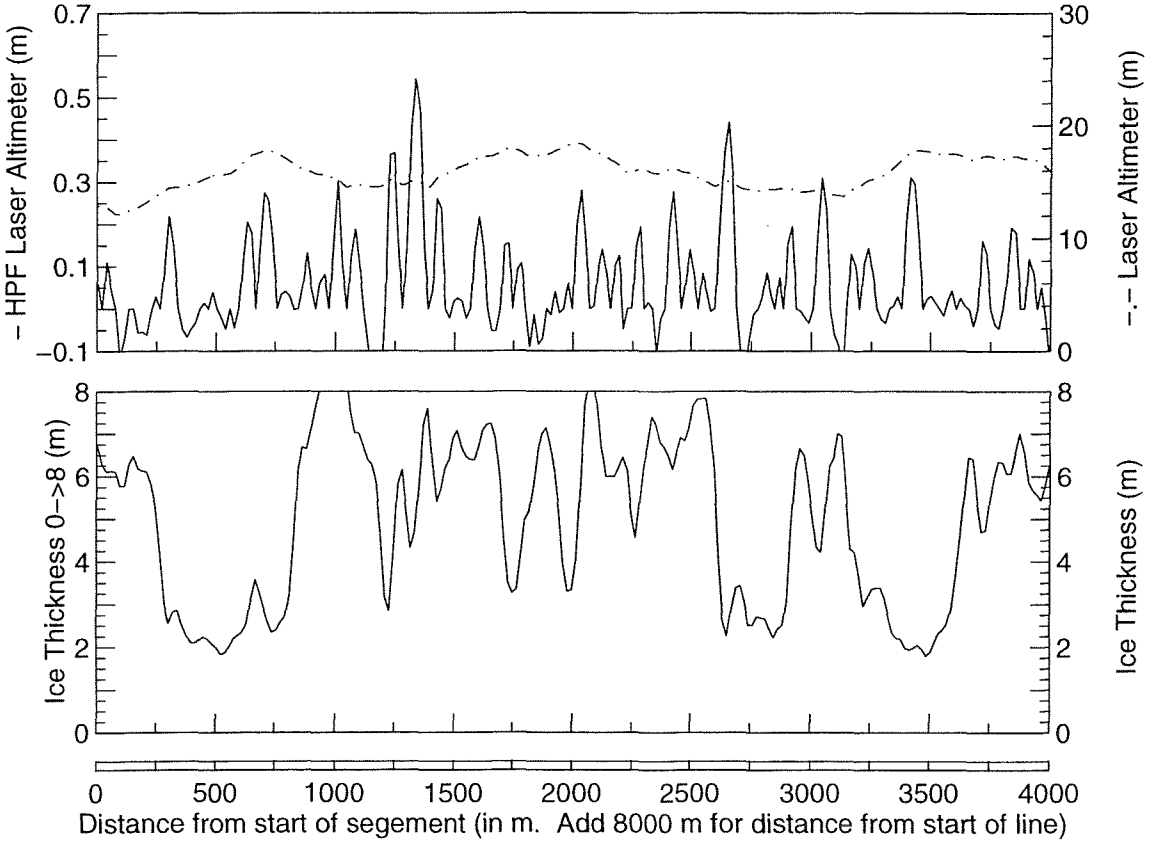

MAR 06 Flight #13 Line #10010 part 4 of 4

Line Starting Coordinates (53.6972,–55.9446) ending at (53.6937,–55.9324)

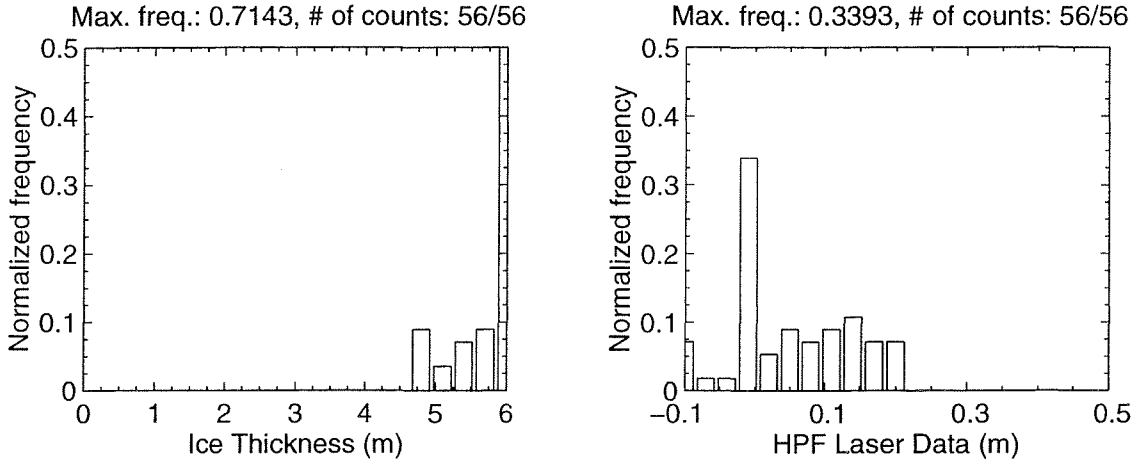

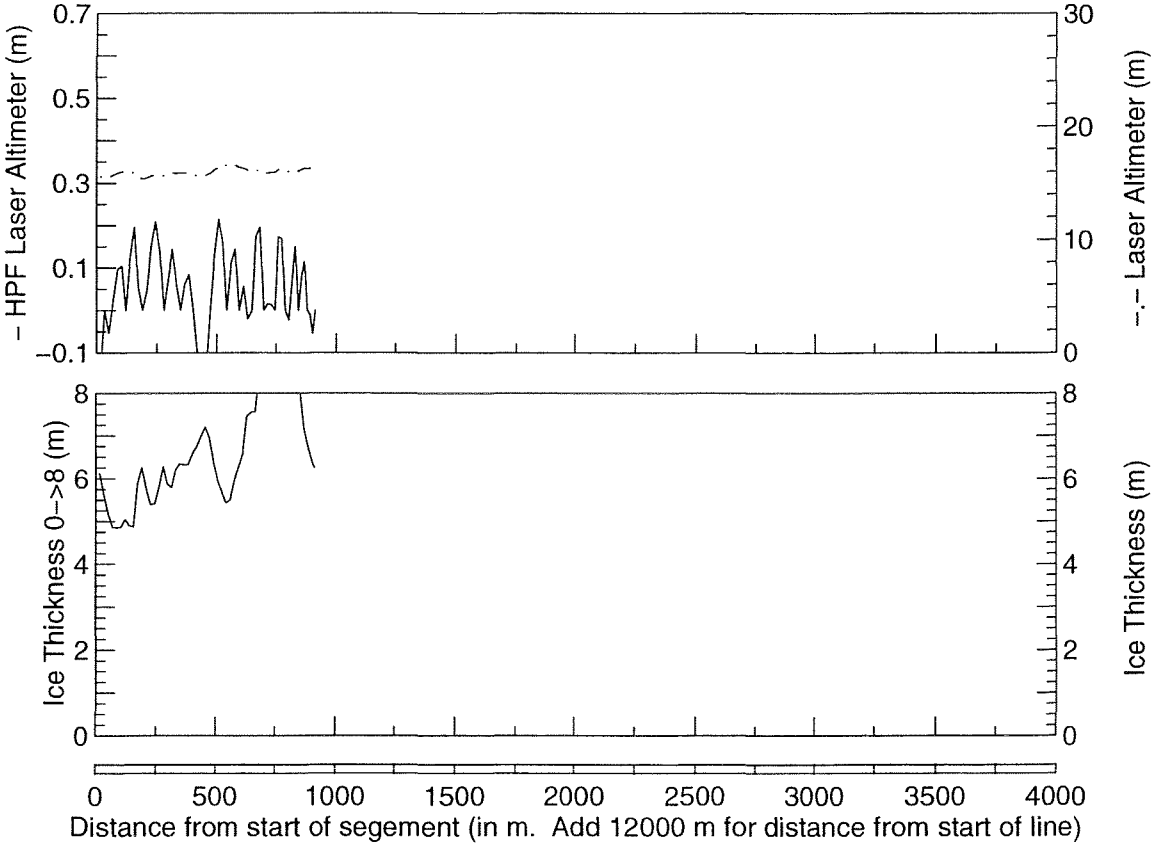

MAR 06 Flight #13 Line #10020 part 1 of 3

Line Starting Coordinates (53.6547,–55.9566) ending at (53.6344,–55.9065)

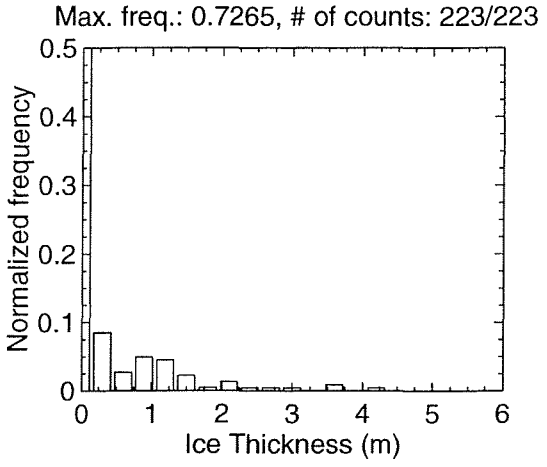

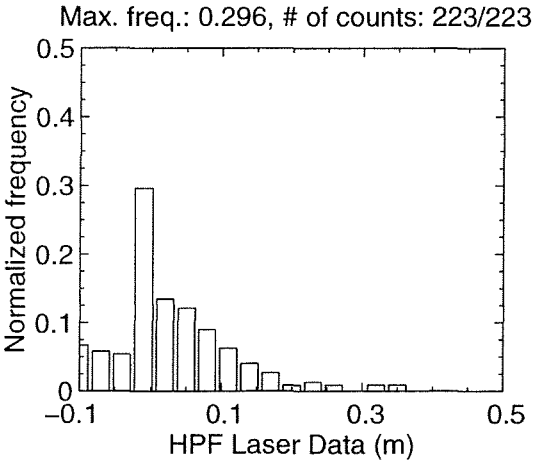

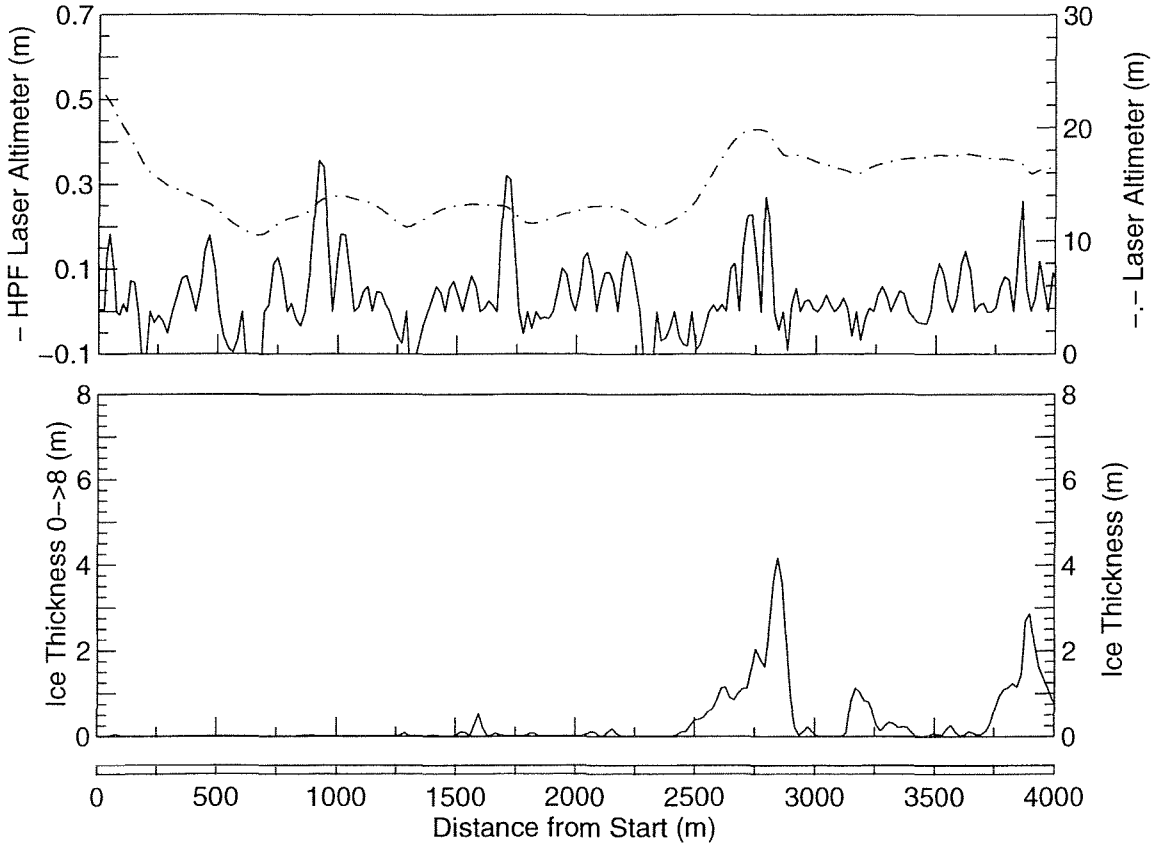

MAR 06 Flight #13 Line #10020 part 2 of 3

Line Starting Coordinates (53.6344,–55.9065) ending at (53.6172,–55.8534)

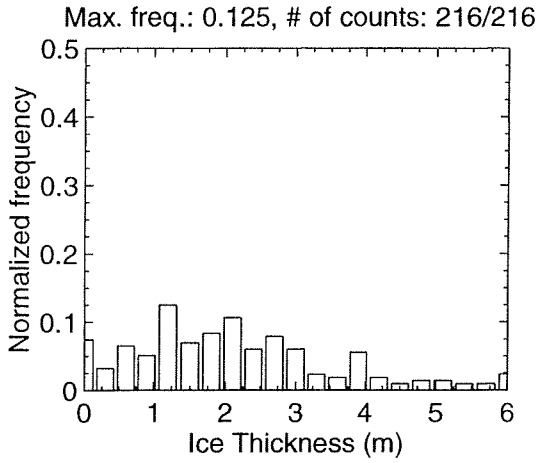

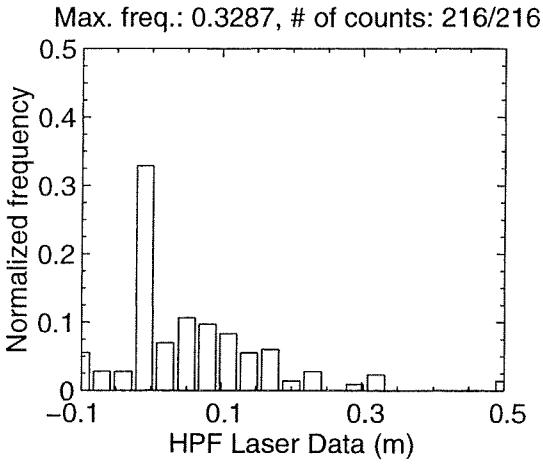

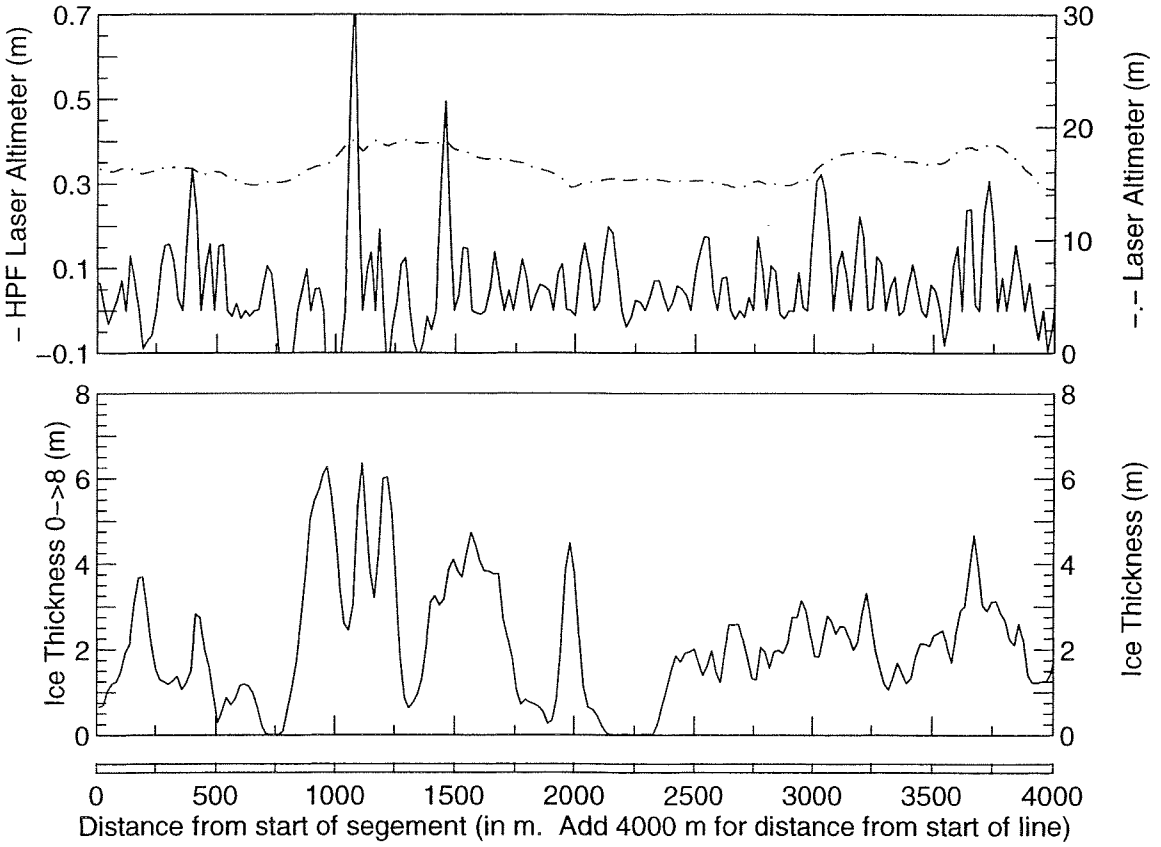

MAR 06 Flight #13 Line #10020 part 3 of 3

Line Starting Coordinates (53.6172,–55.8534) ending at (53.6124,–55.8369)

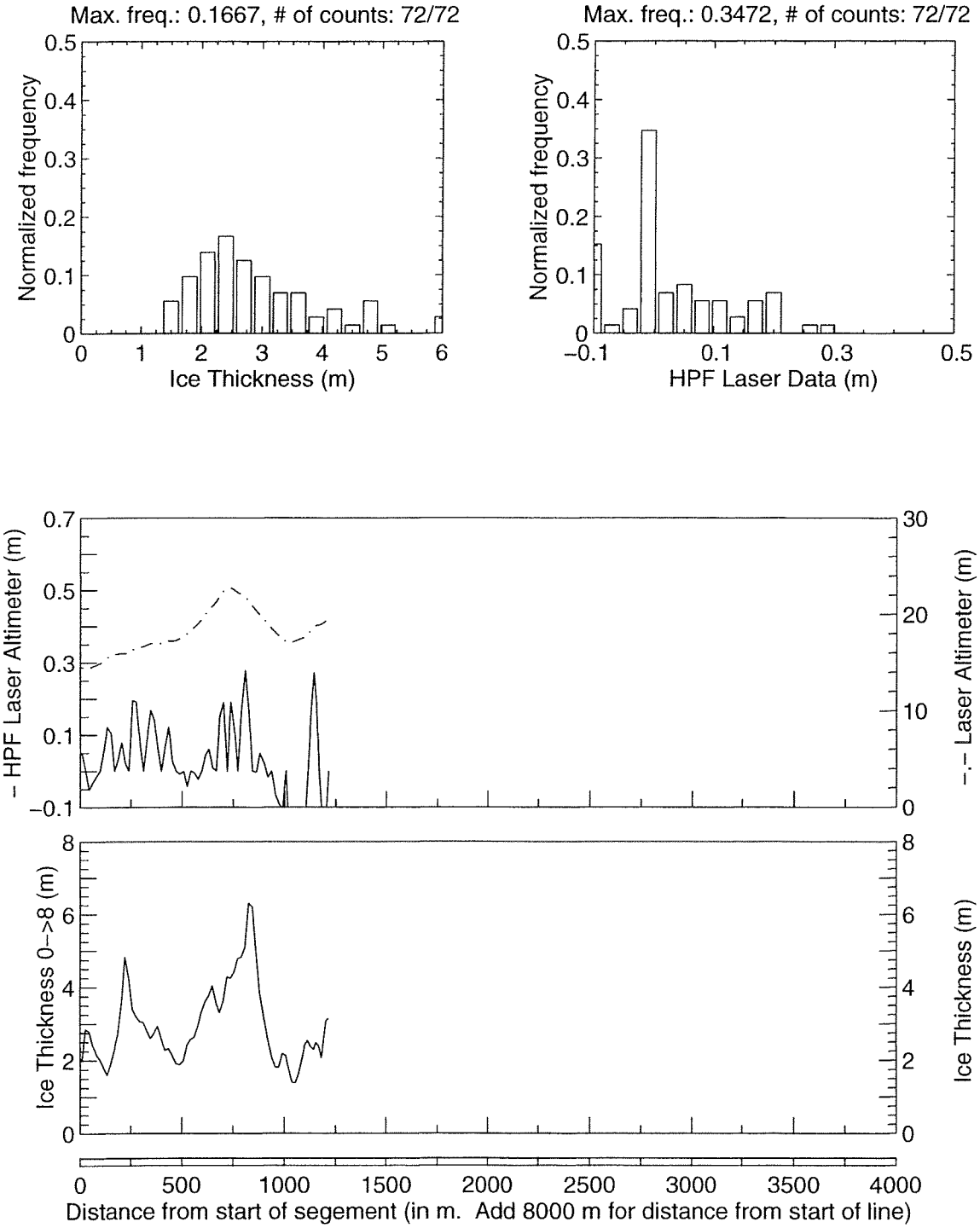

MAR 06 Flight #13 Line #10030 part 1 of 1

Line Starting Coordinates (53.6158,–55.7112) ending at (53.6060,–55.6747)

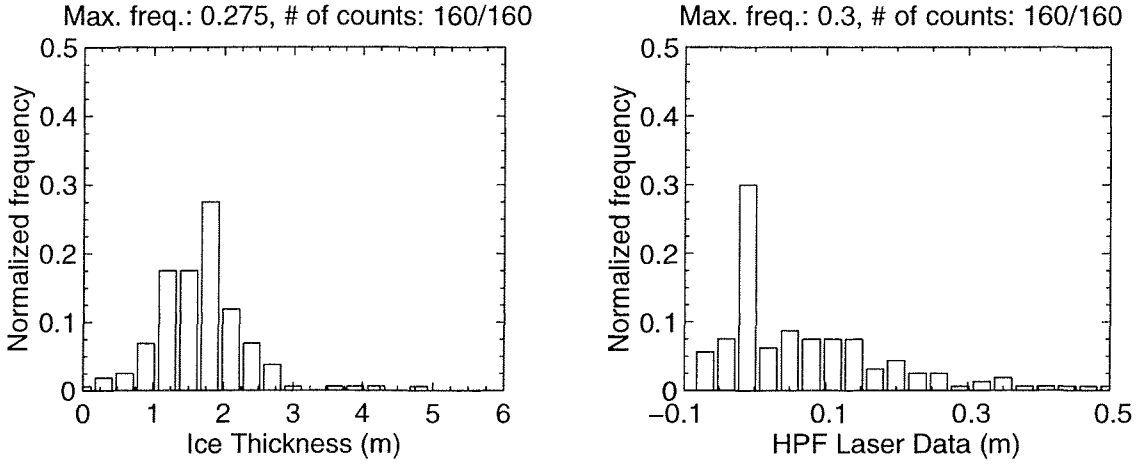

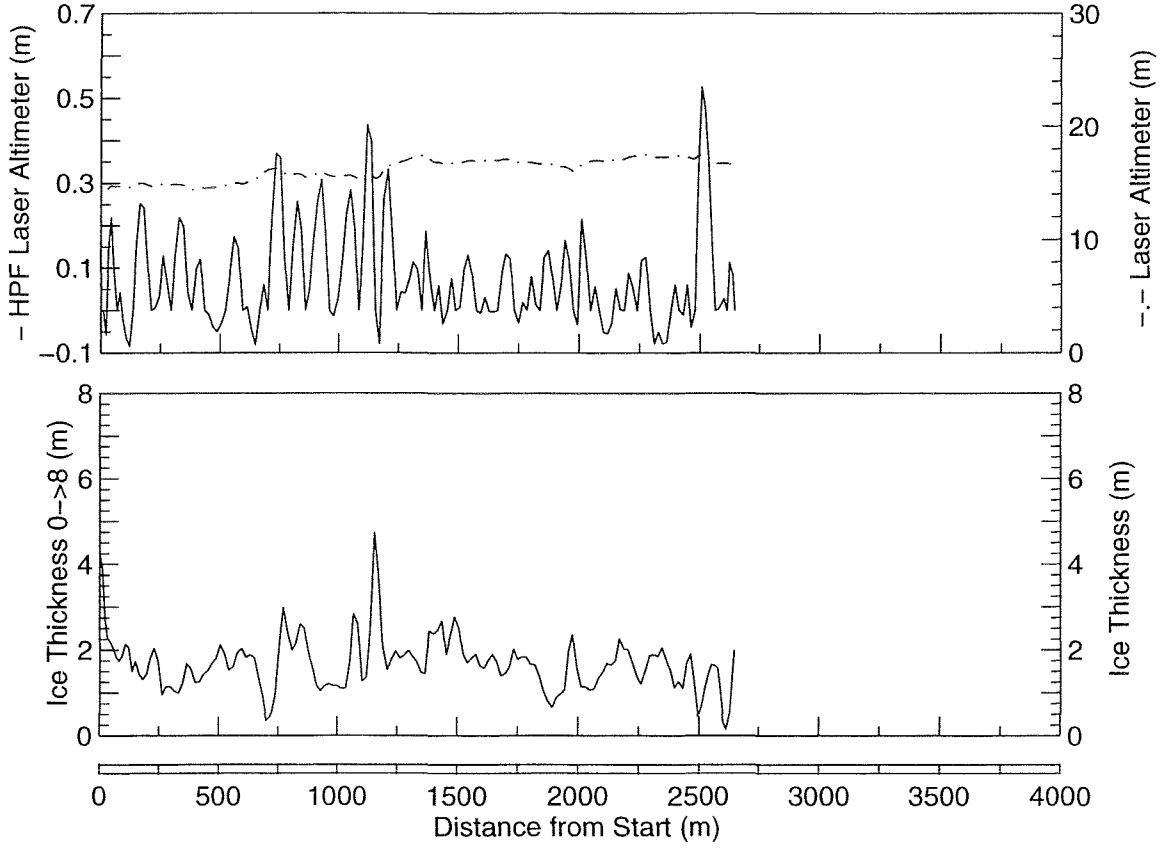

MAR 06 Flight #13 Line #10040 part 1 of 4

Line Starting Coordinates (53.6406,–55.6802) ending at (53.6515,–55.7379)

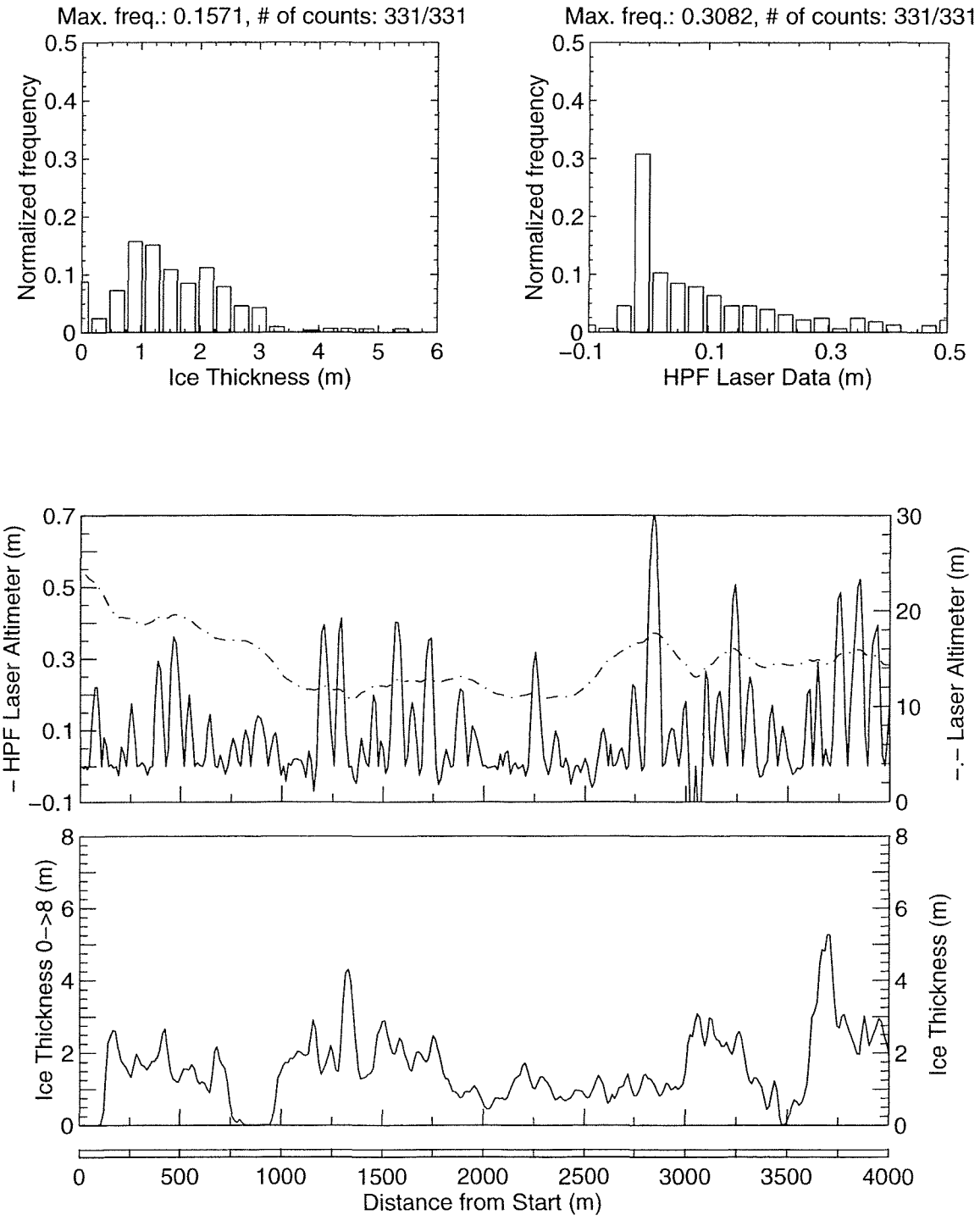

MAR 06 Flight #13 Line #10040 part 2 of 4

Line Starting Coordinates (53.6515,–55.7379) ending at (53.6629,–55.7954)

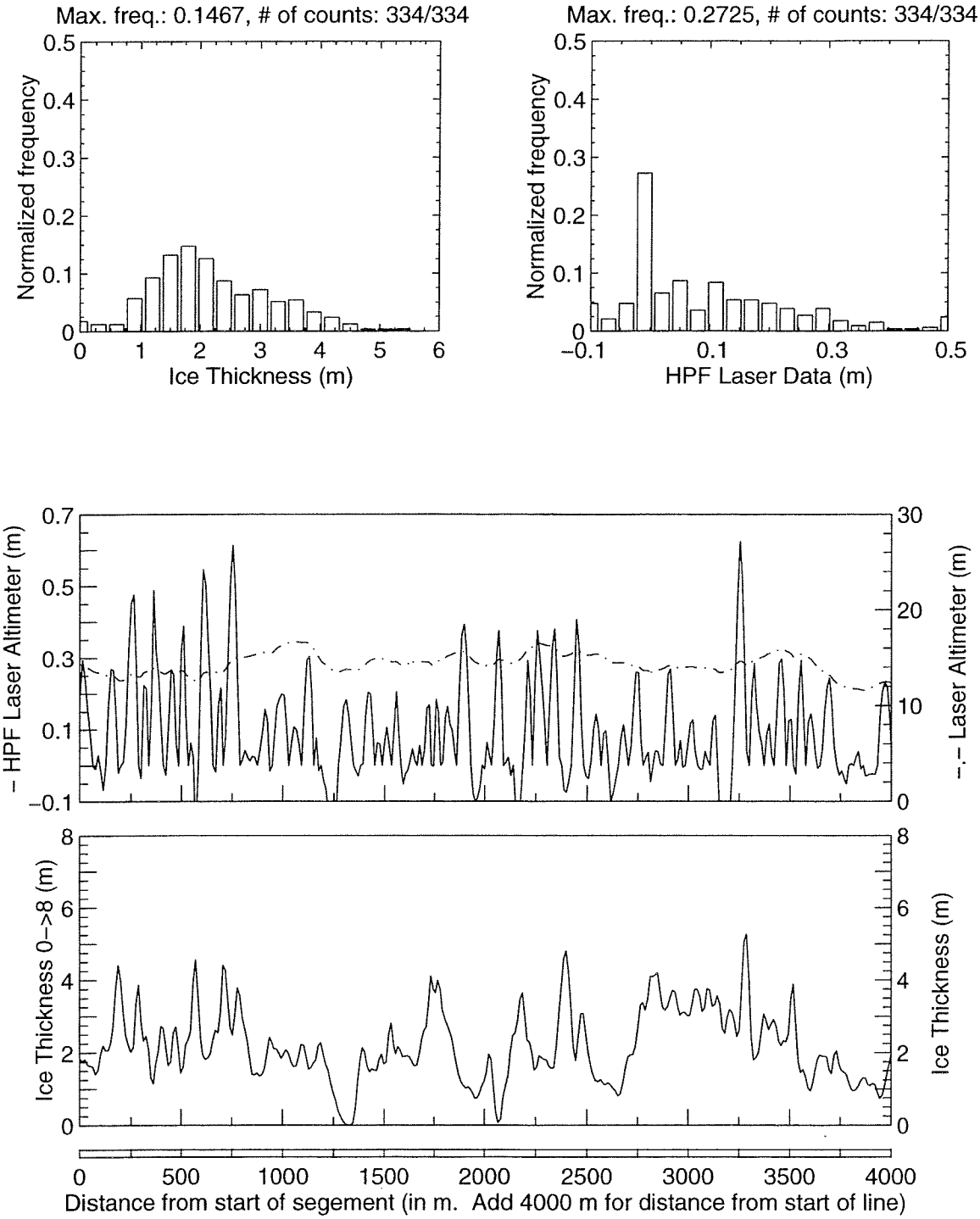

MAR 06 Flight #13 Line #10040 part 3 of 4

Line Starting Coordinates (53.6629,–55.7954) ending at (53.6741,–55.8531)

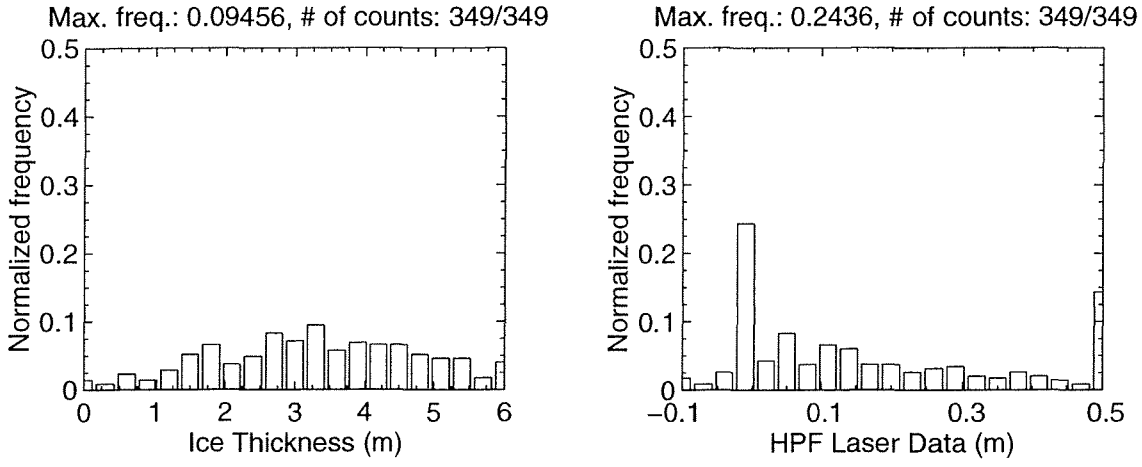

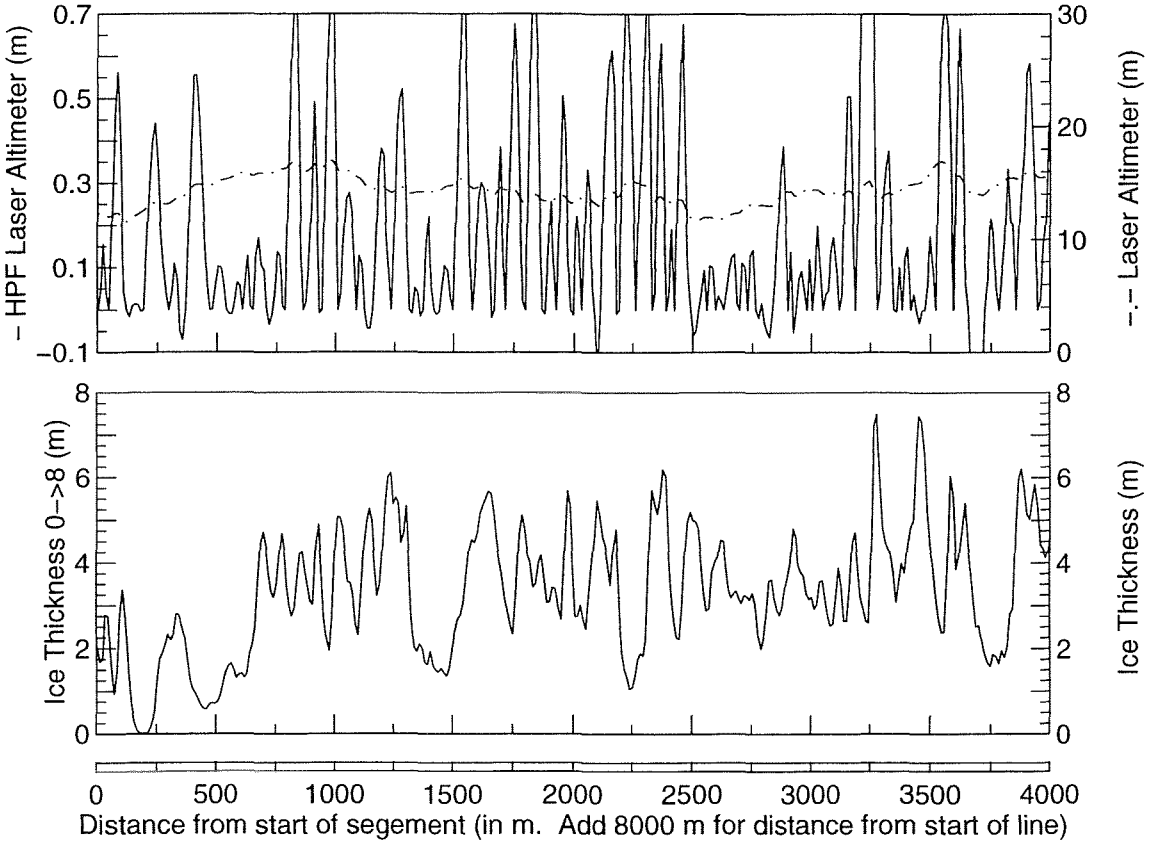

MAR 06 Flight #13 Line #10040 part 4 of 4

Line Starting Coordinates (53.6741,–55.8531) ending at (53.6822,–55.8913)

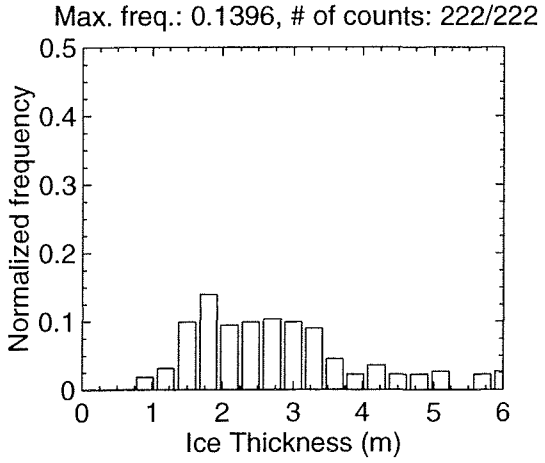

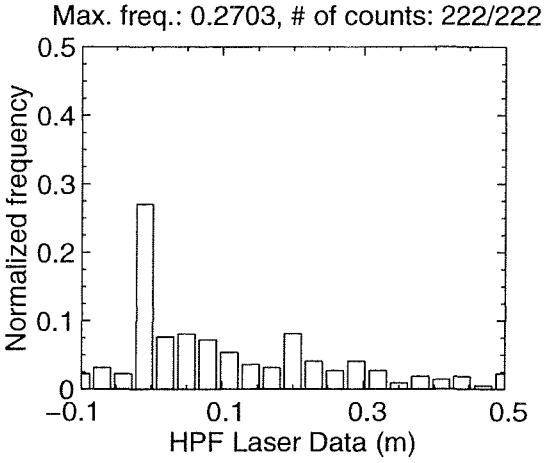

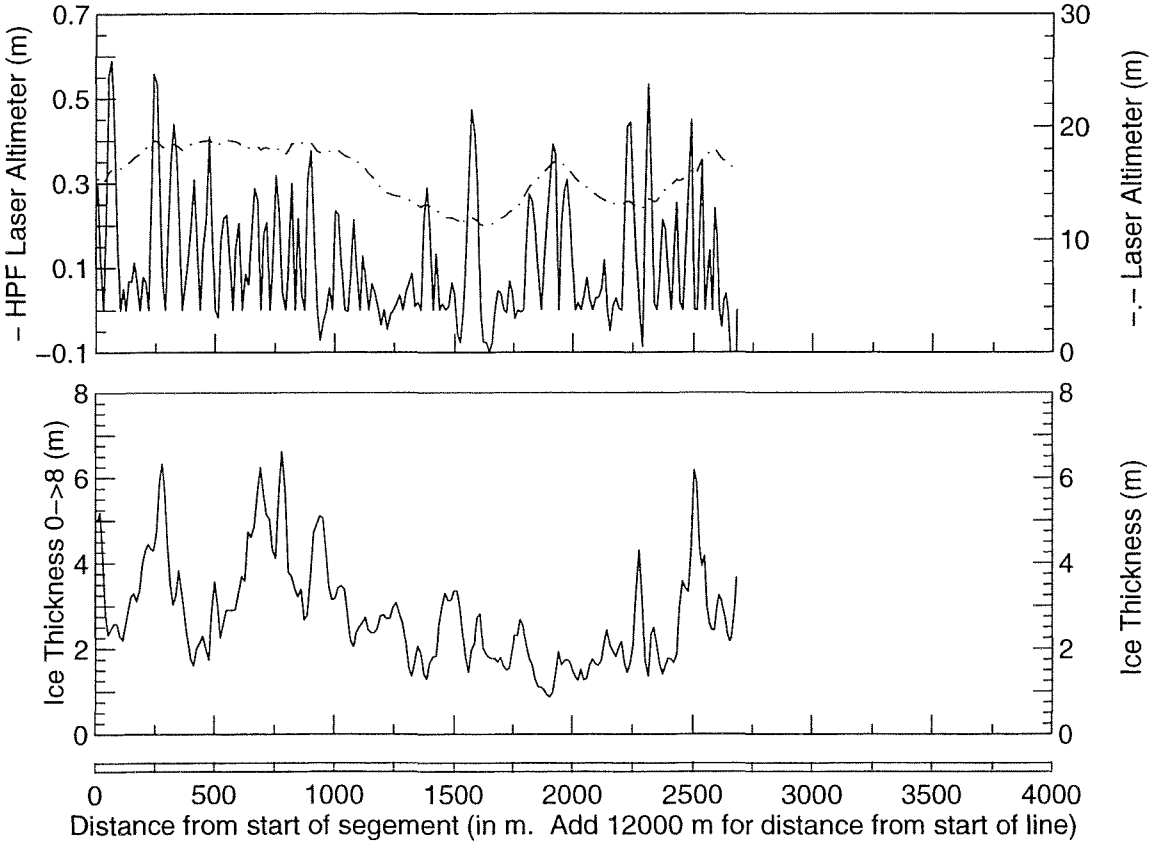

MAR 06 Flight #13 Line #10050 part 1 of 3

Line Starting Coordinates (53.7018,–55.9410) ending at (53.7241,–55.9887)

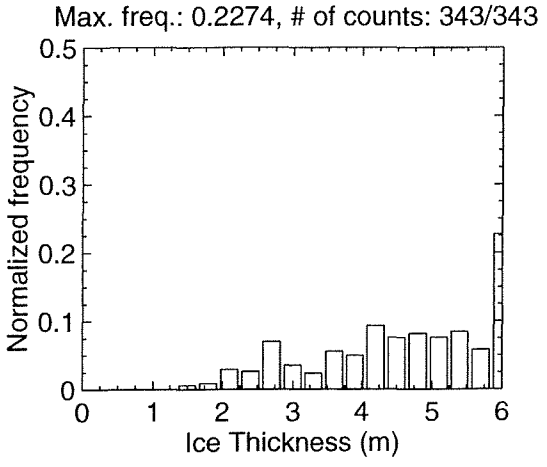

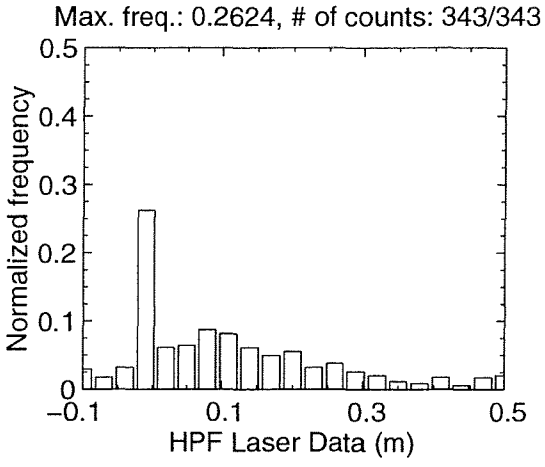

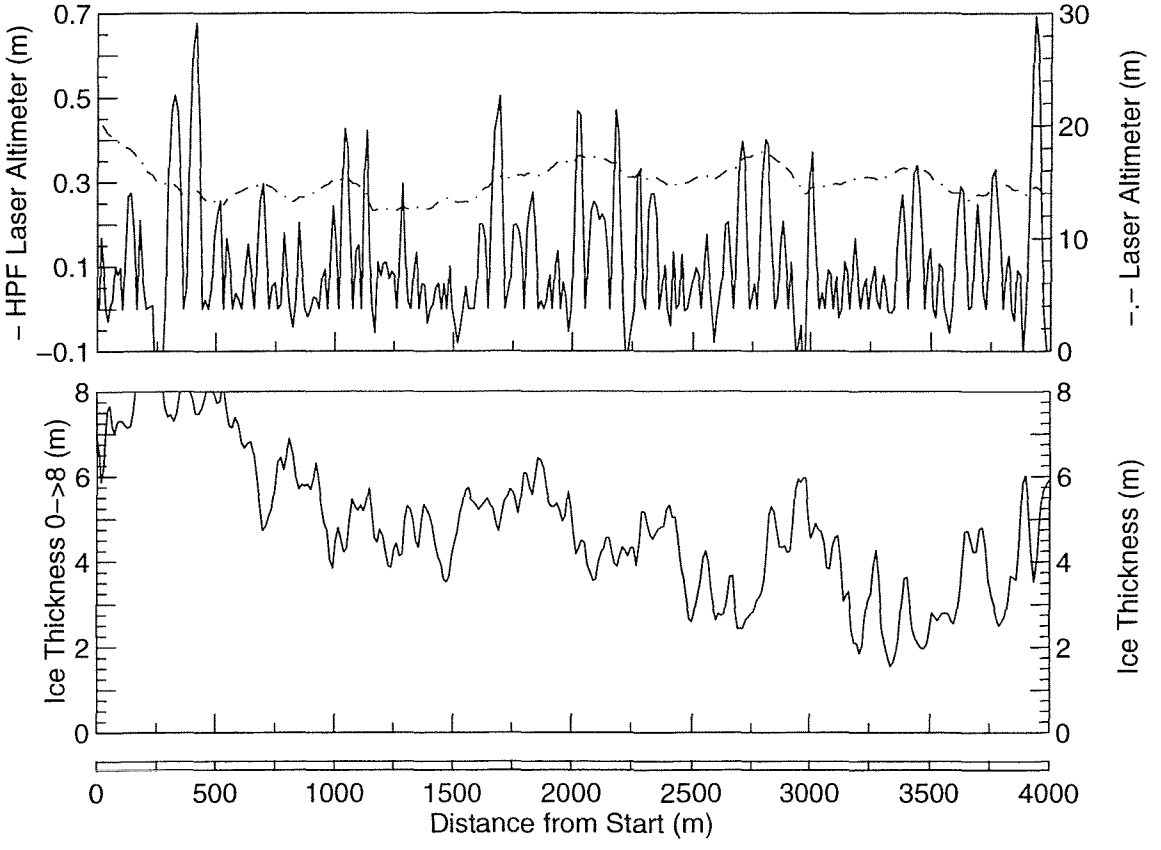

MAR 06 Flight #13 Line #10050 part 2 of 3

Line Starting Coordinates (53.7241,–55.9887) ending at (53.7446,–56.0385)

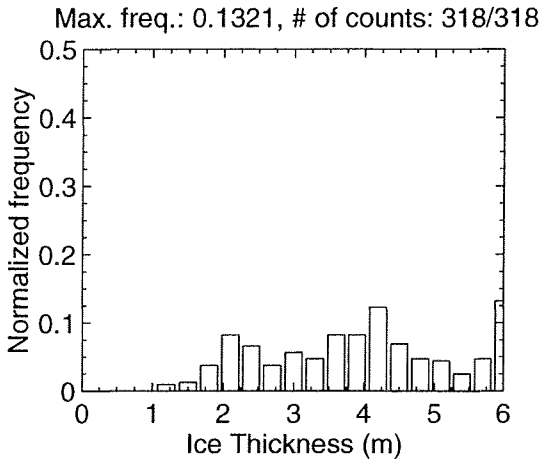

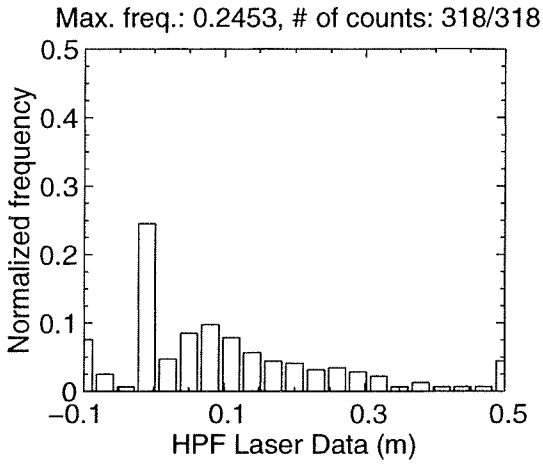

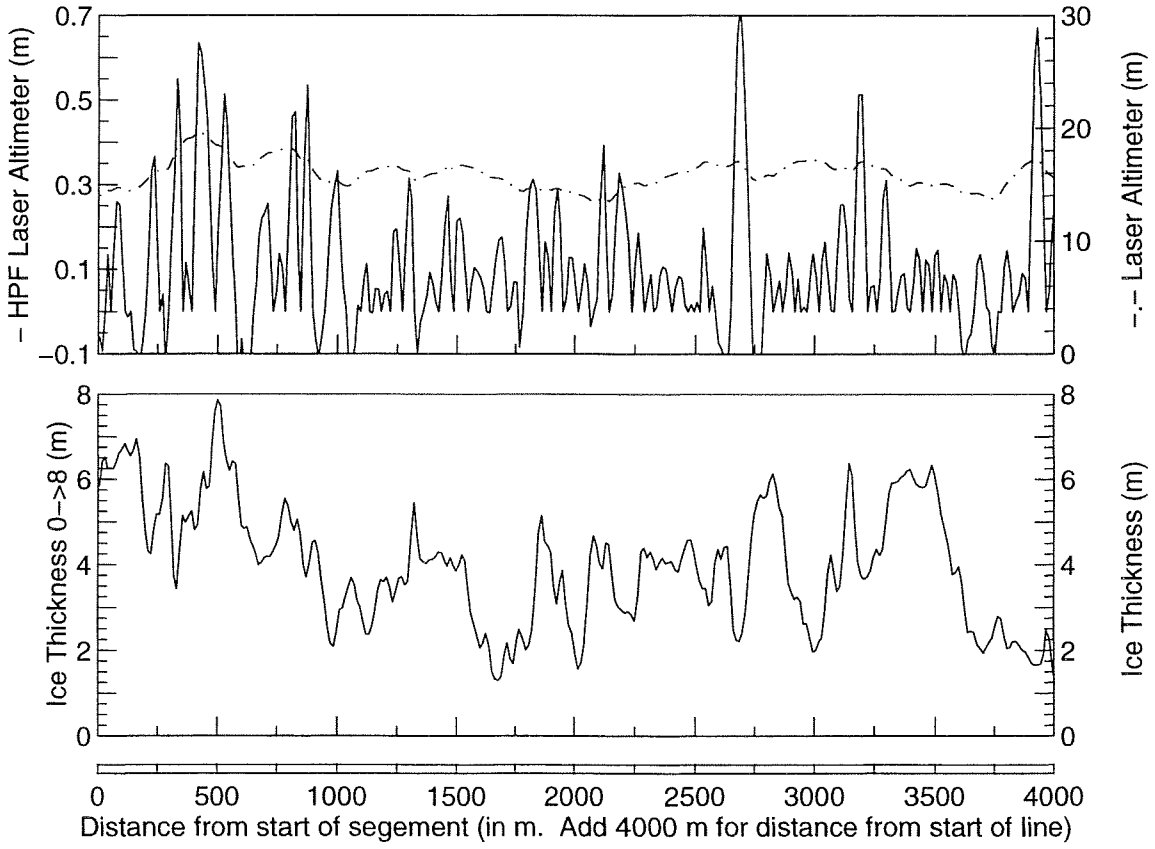

MAR 06 Flight #13 Line #10050 part 3 of 3

Line Starting Coordinates (53.7446,–56.0385) ending at (53.7629,–56.0823)

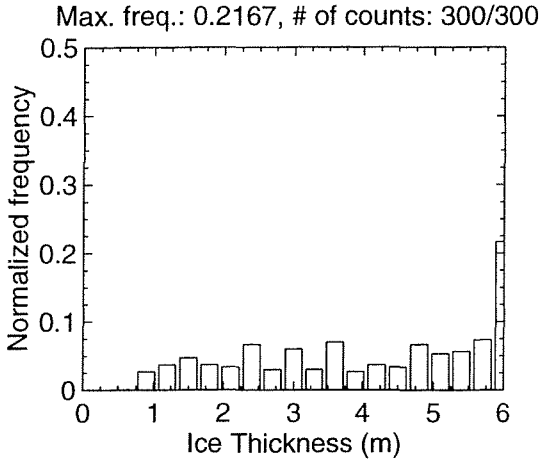

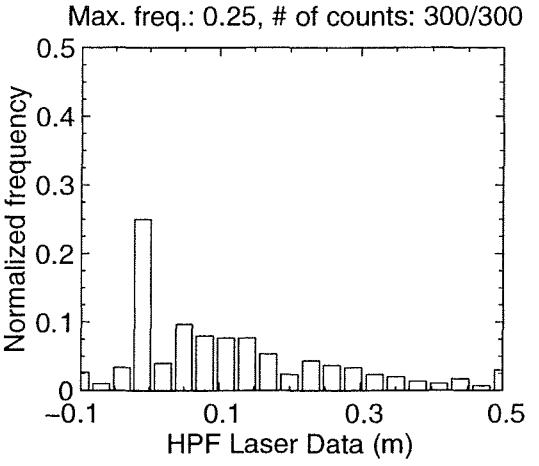

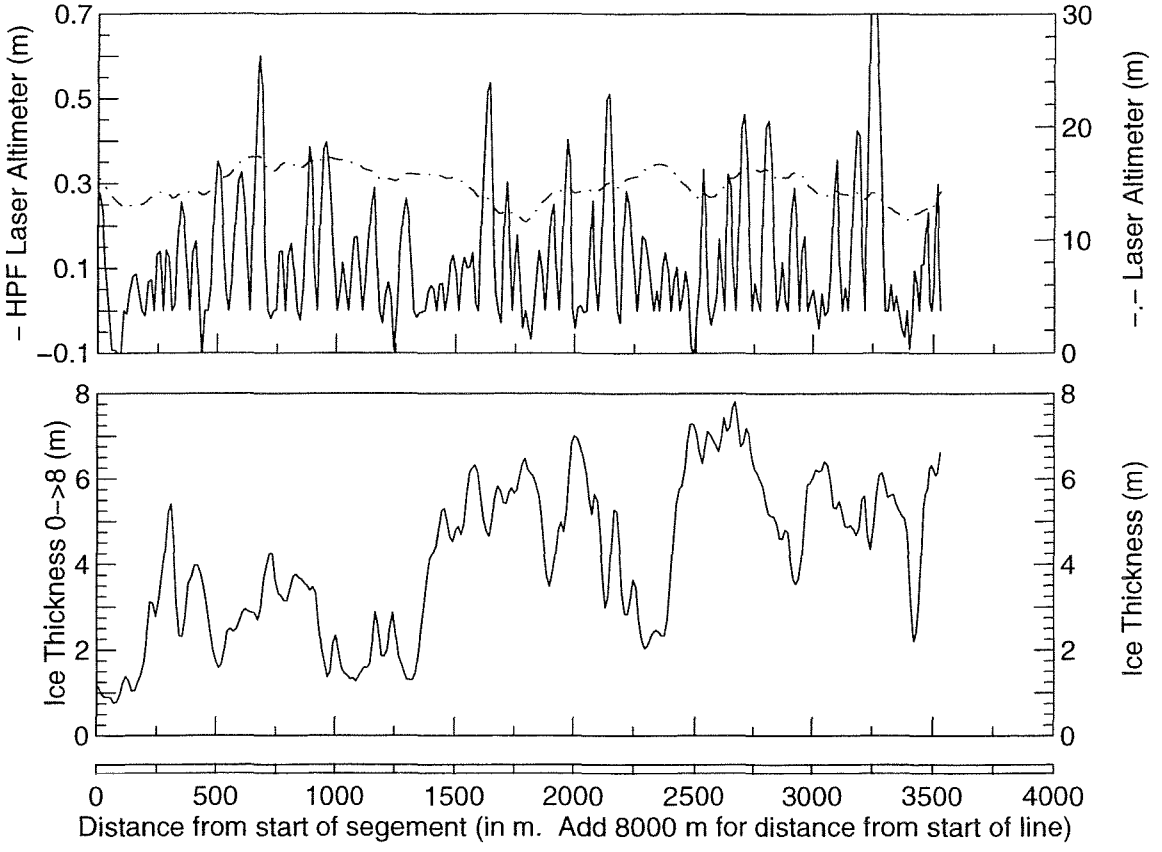

MAR 06 Flight #13 Line #10060 part 1 of 3

Line Starting Coordinates (53.7898,–56.1465) ending at (53.8098,–56.1972)

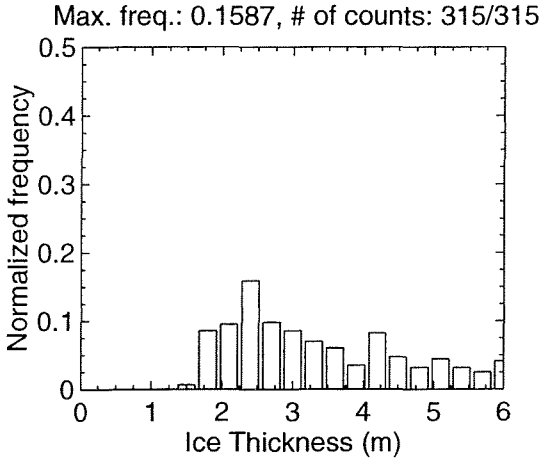

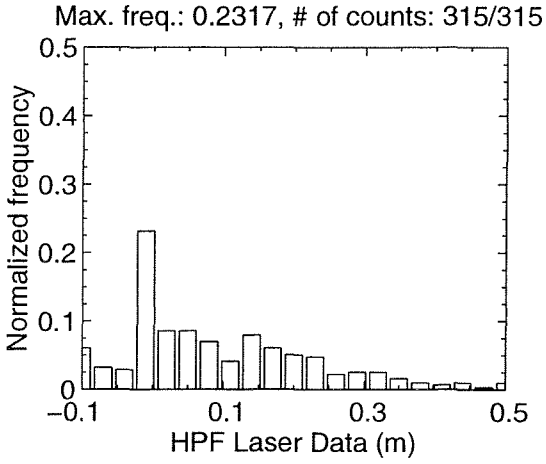

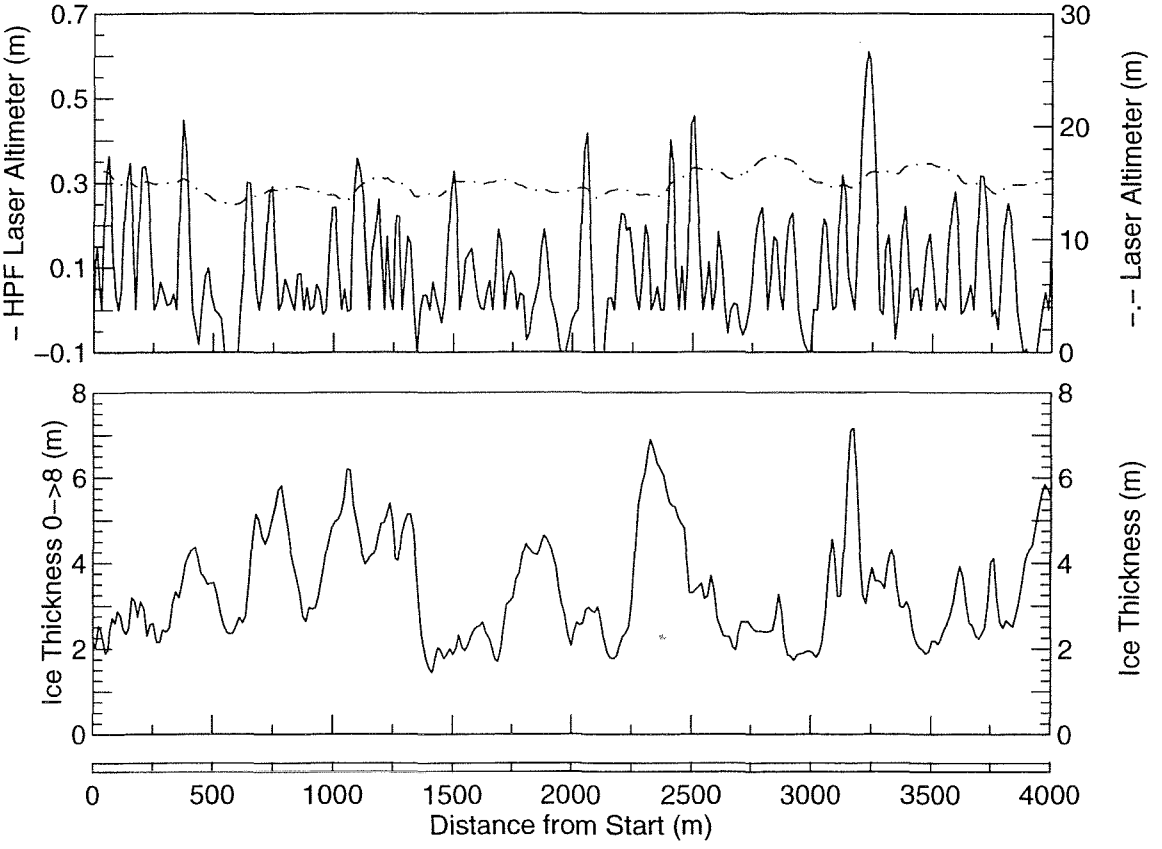

MAR 06 Flight #13 Line #10060 part 2 of 3

Line Starting Coordinates (53.8098,–56.1972) ending at (53.8283,–56.2493)

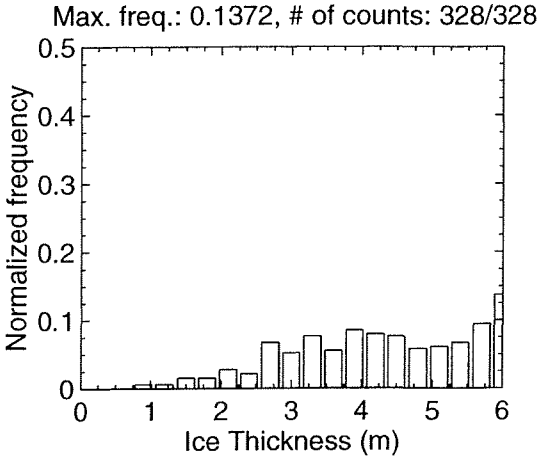

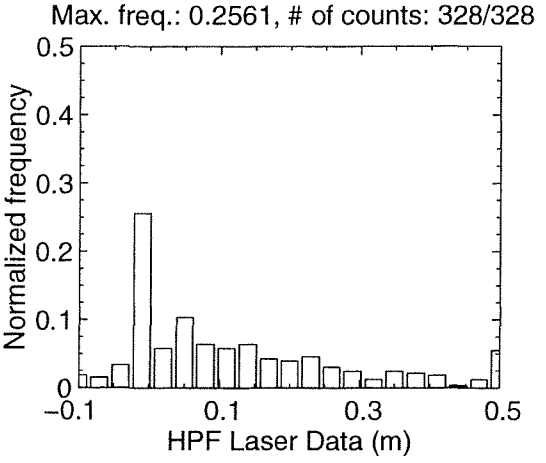

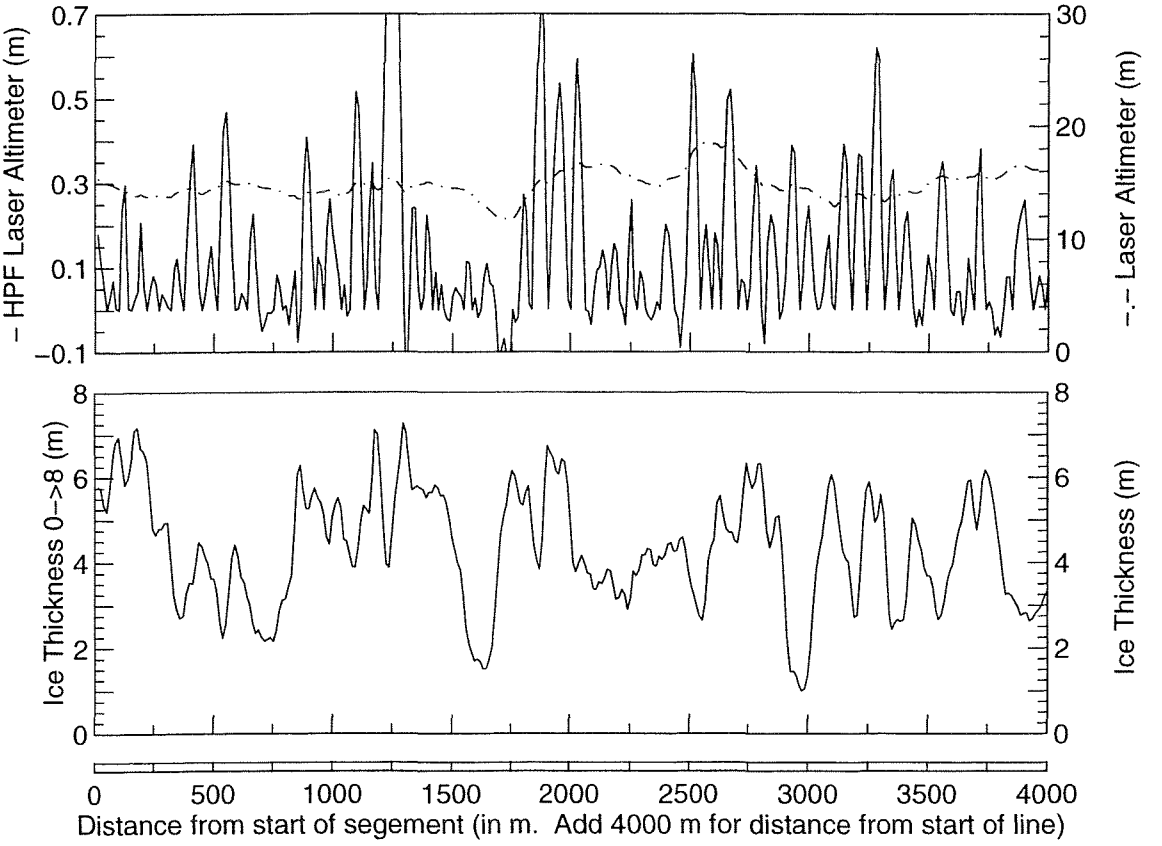

MAR 06 Flight #13 Line #10060 part 3 of 3

Line Starting Coordinates (53.8283,–56.2493) ending at (53.8335,–56.2625)

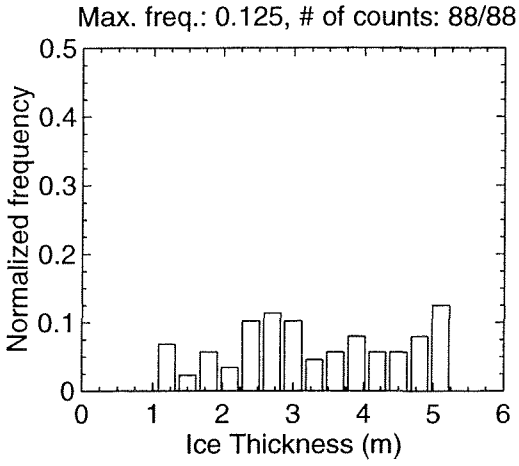

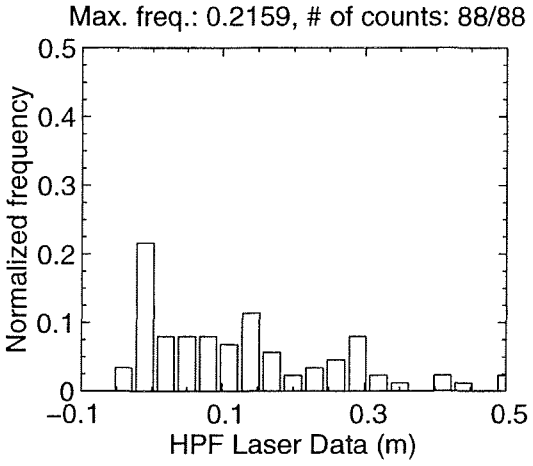

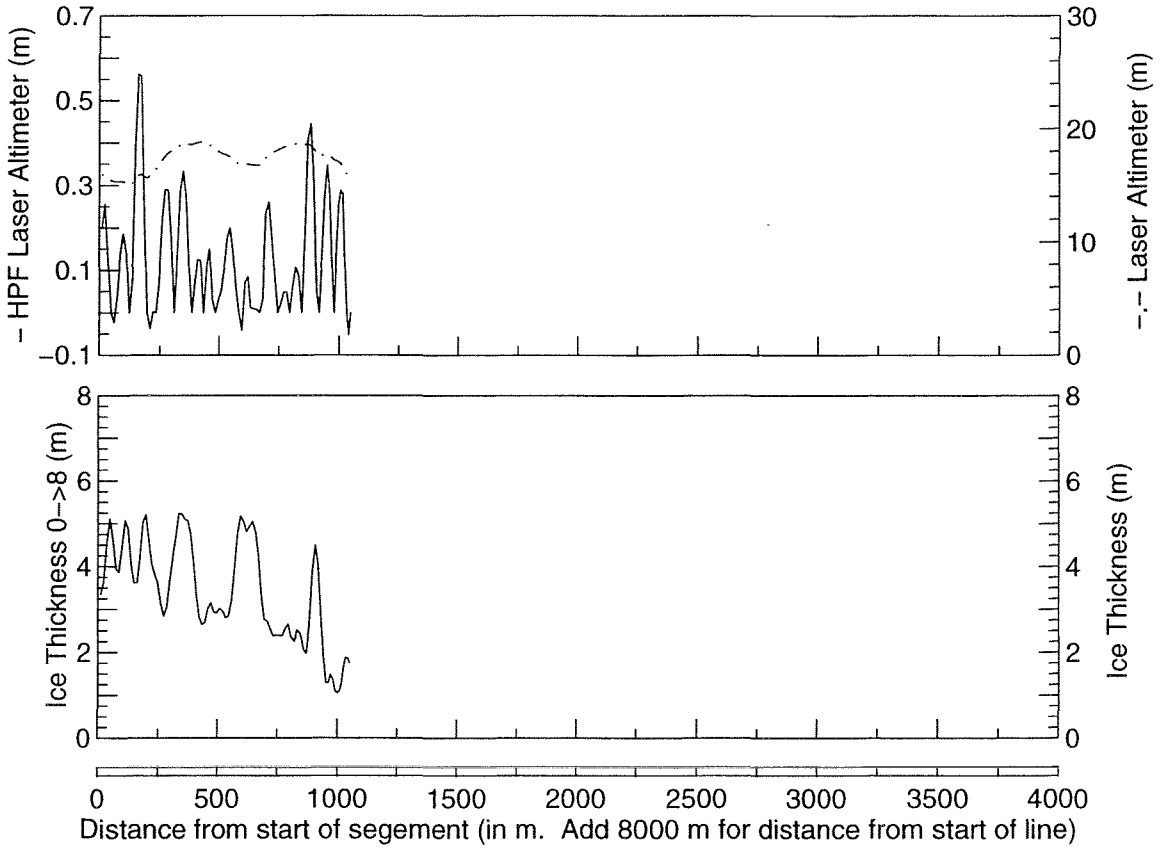

MAR 06 Flight #13 Line #10070 part 1 of 2

Line Starting Coordinates (53.8348,–56.3666) ending at (53.8286,–56.4266)

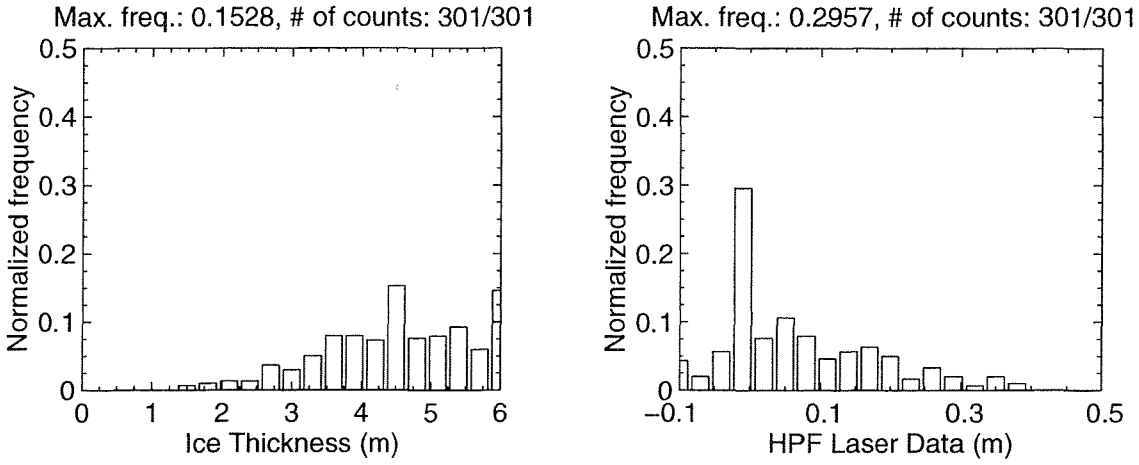

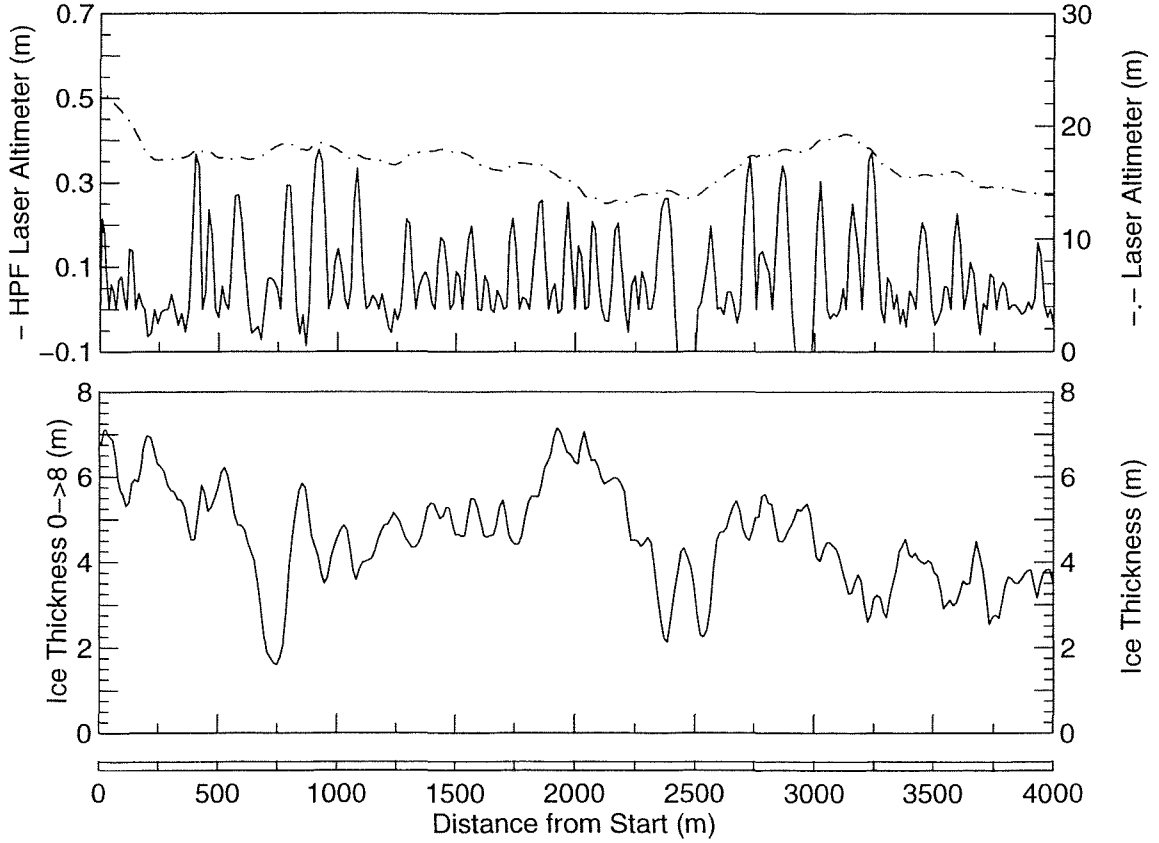

MAR 06 Flight #13 Line #10070 part 2 of 2

Line Starting Coordinates (53.8286,–56.4266) ending at (53.8280,–56.4303)

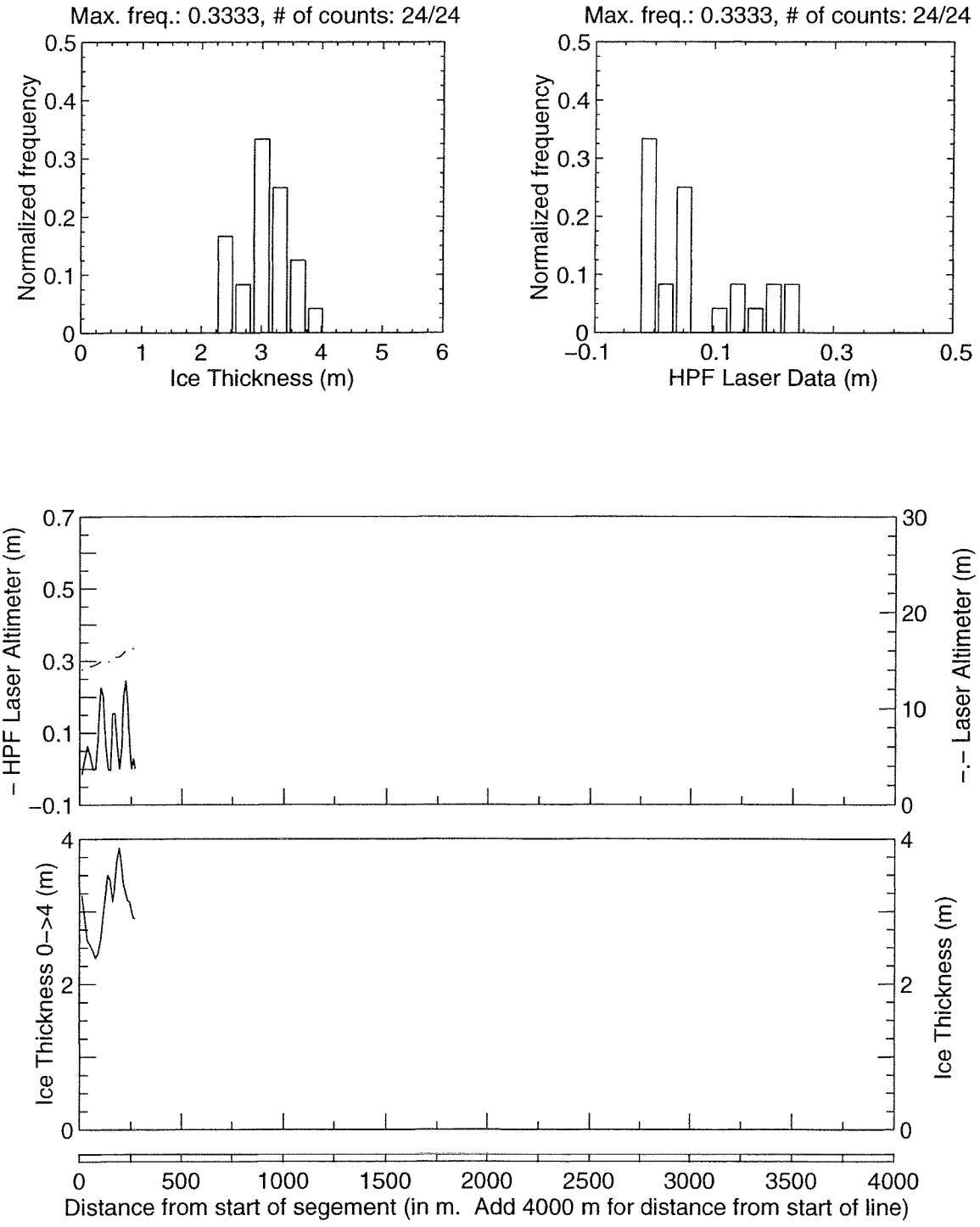

MAR 06 Flight #13 Line #10081 part 1 of 3

Line Starting Coordinates (53.8251,–56.4422) ending at (53.8127,–56.4983)

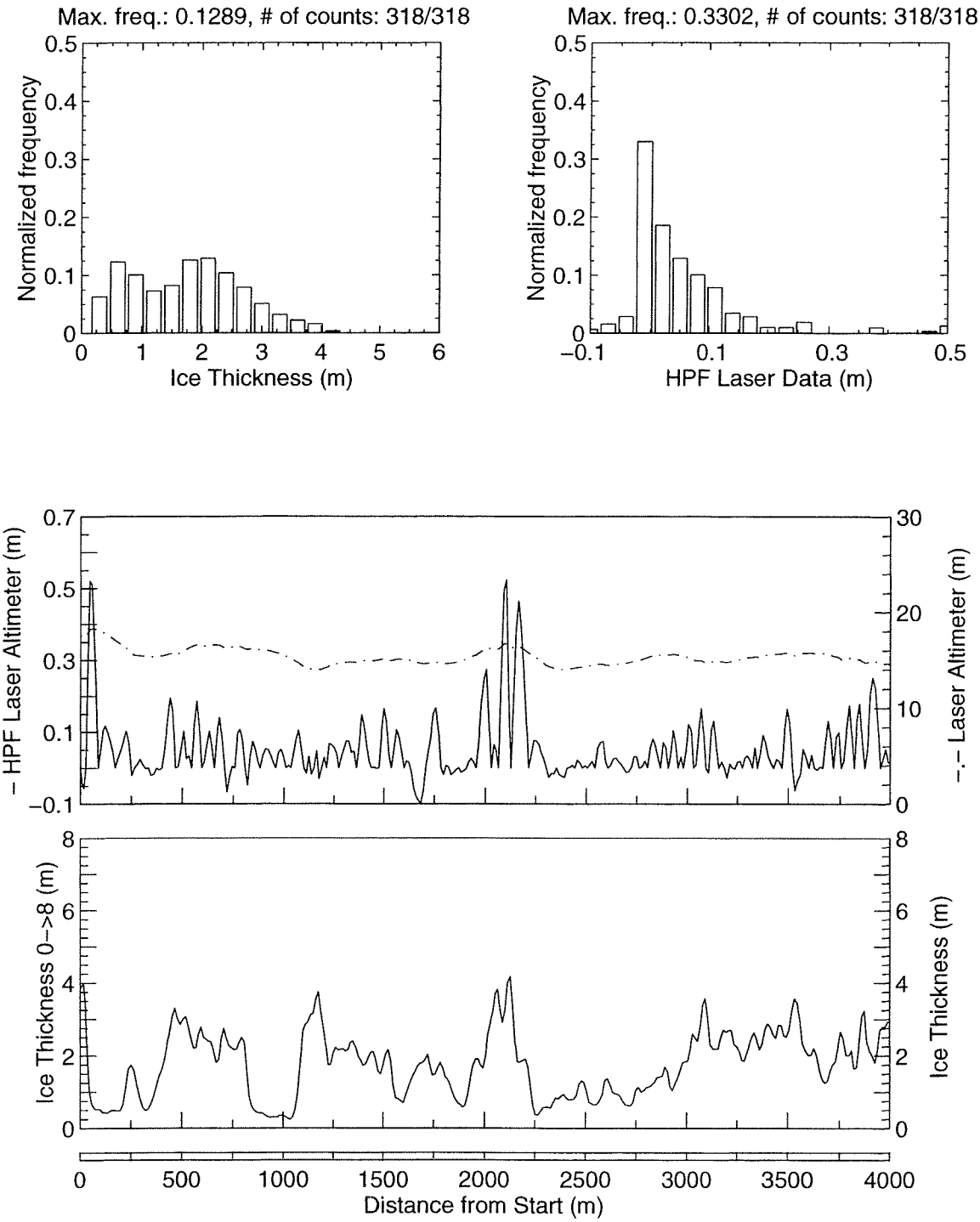

MAR 06 Flight #13 Line #10081 part 2 of 3

Line Starting Coordinates (53.8127,–56.4983) ending at (53.8062,–56.5581)

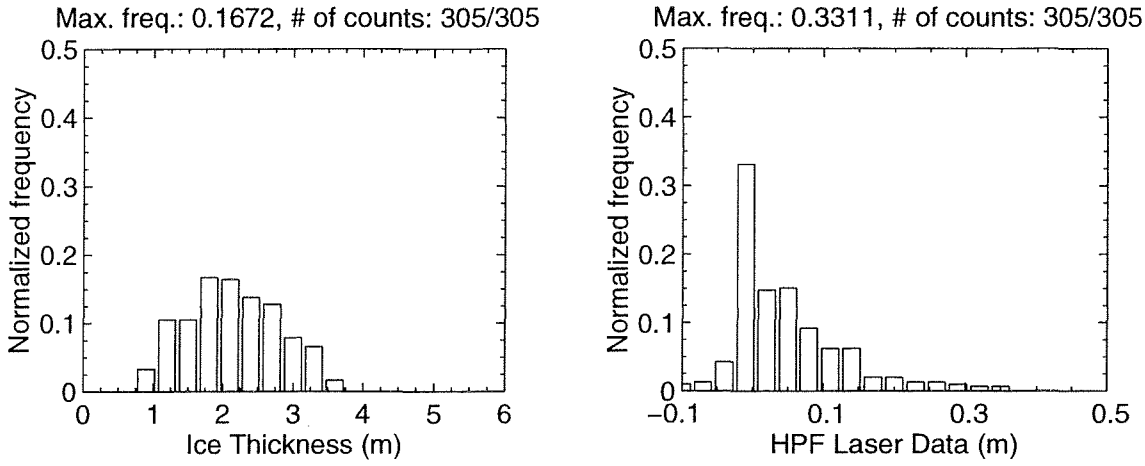

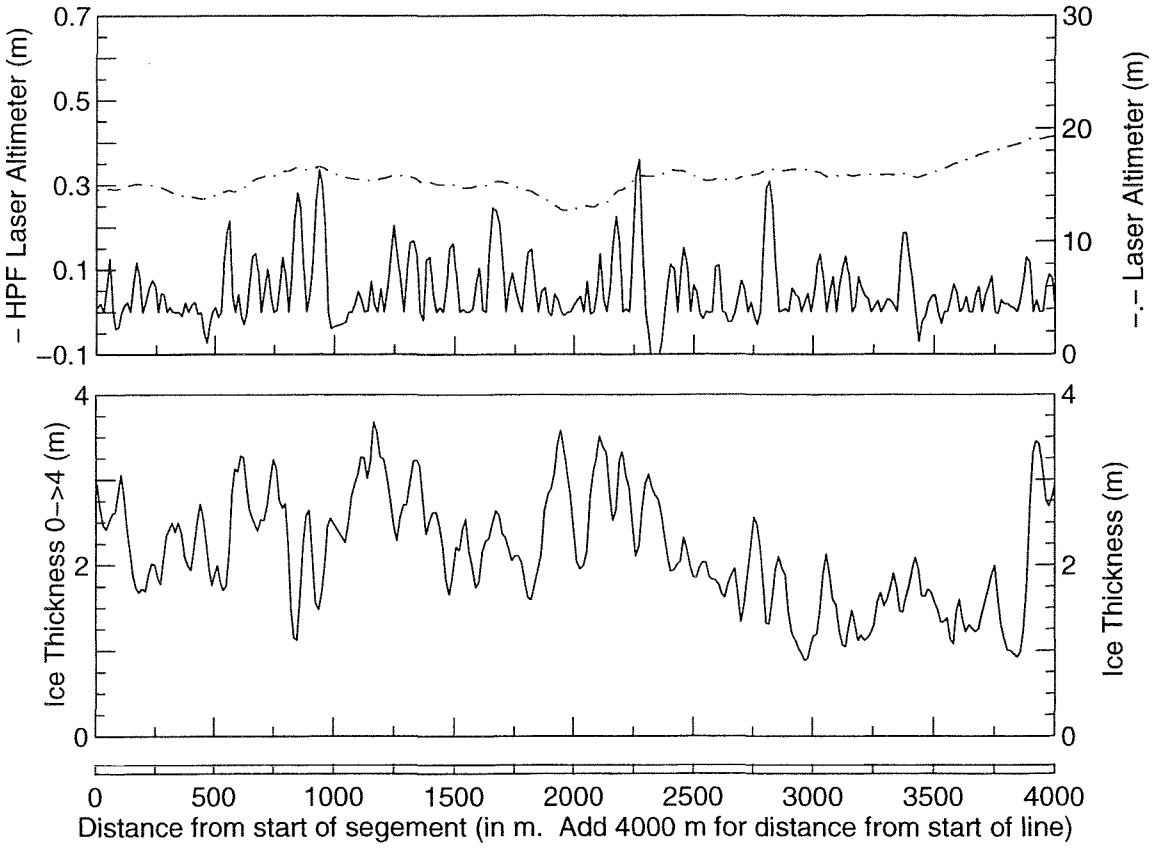

MAR 06 Flight #13 Line #10081 part 3 of 3

Line Starting Coordinates (53.8062,–56.5581) ending at (53.7971,–56.6105)

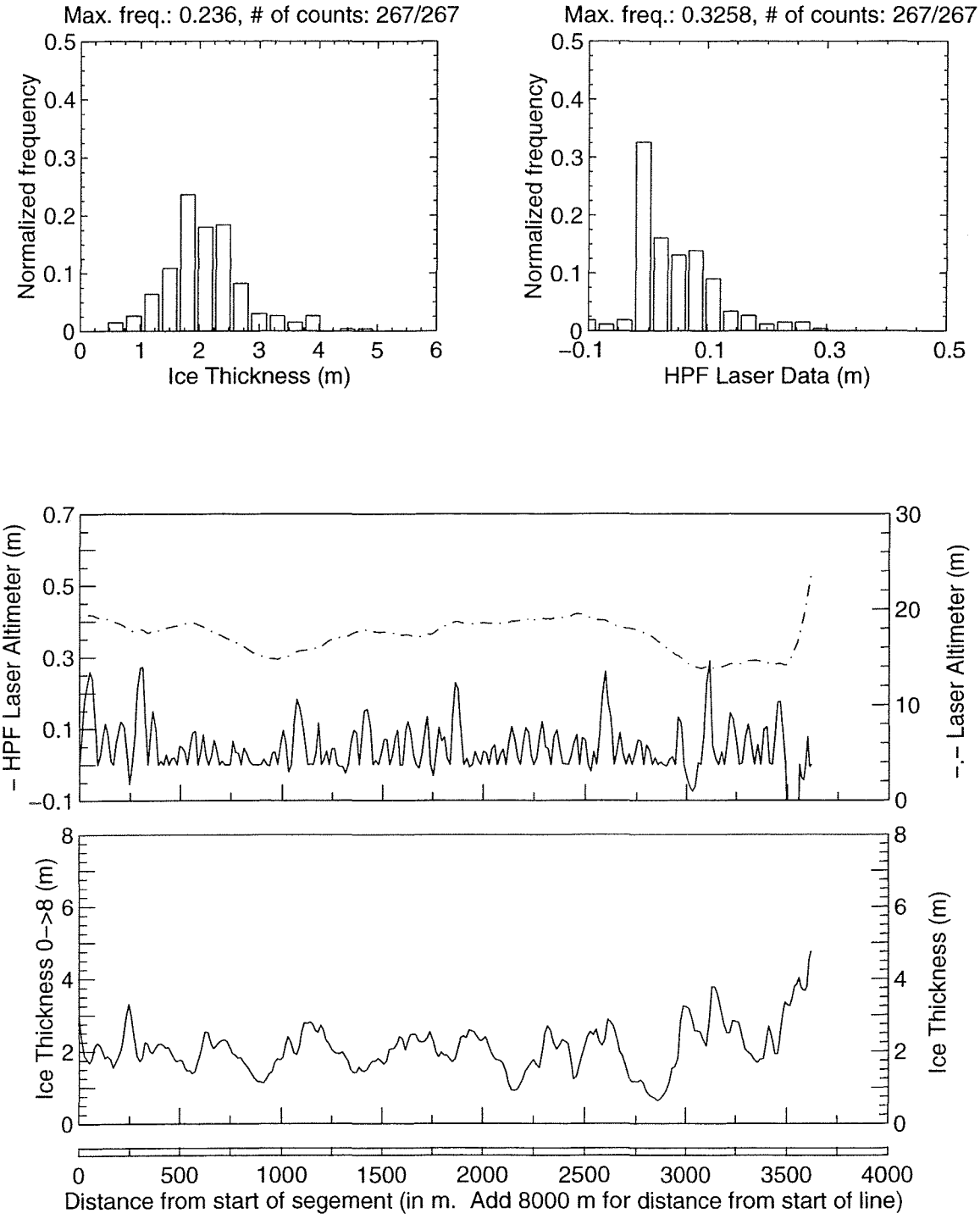

MAR 06 Flight #13 Line #10082 part 1 of 1

Line Starting Coordinates (53.7826,–56.6835) ending at (53.7775,–56.7186)

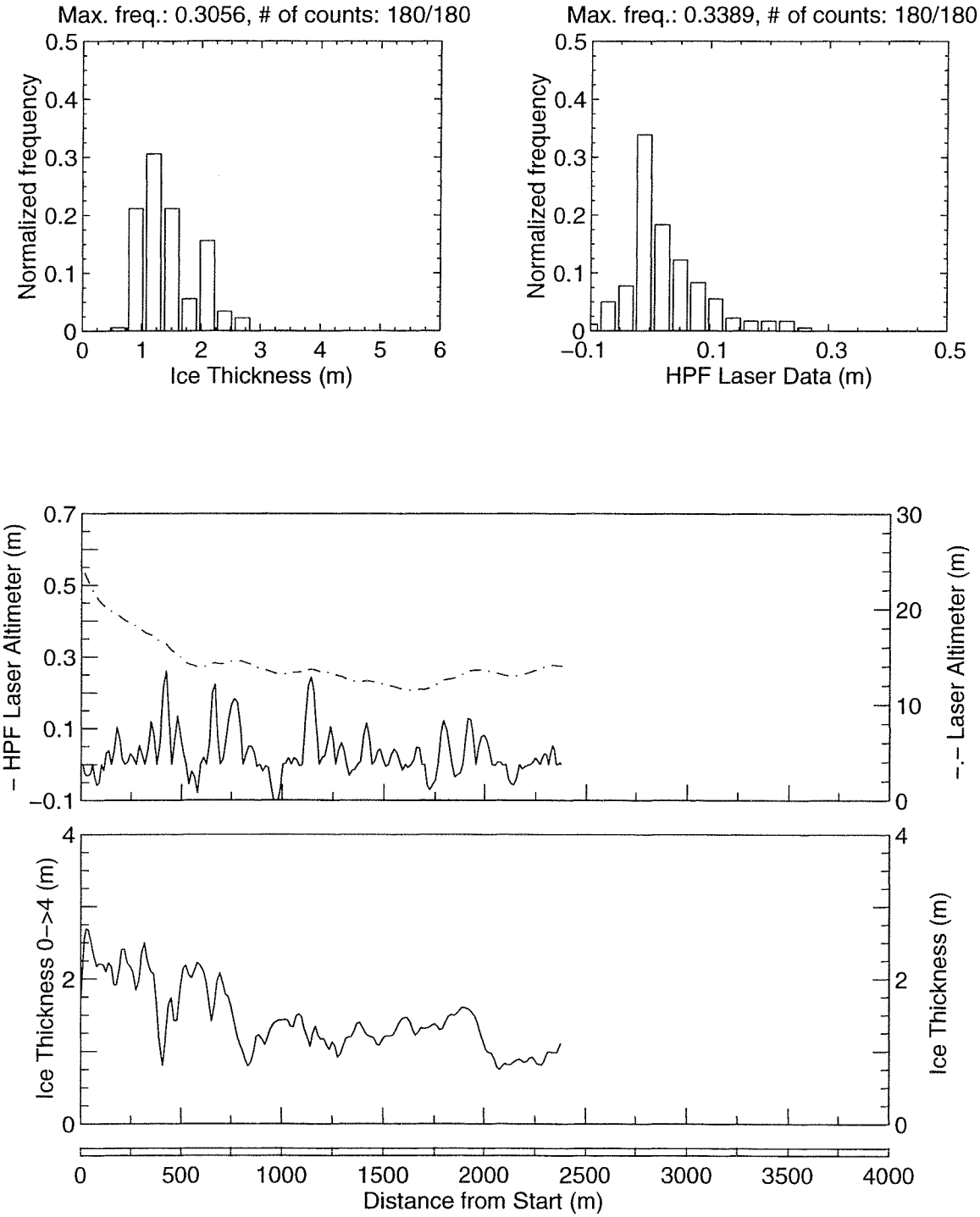

MAR 06 Flight #13 Line #10091 part 1 of 1

Line Starting Coordinates (53.7772,–56.7205) ending at (53.7753,–56.7334)

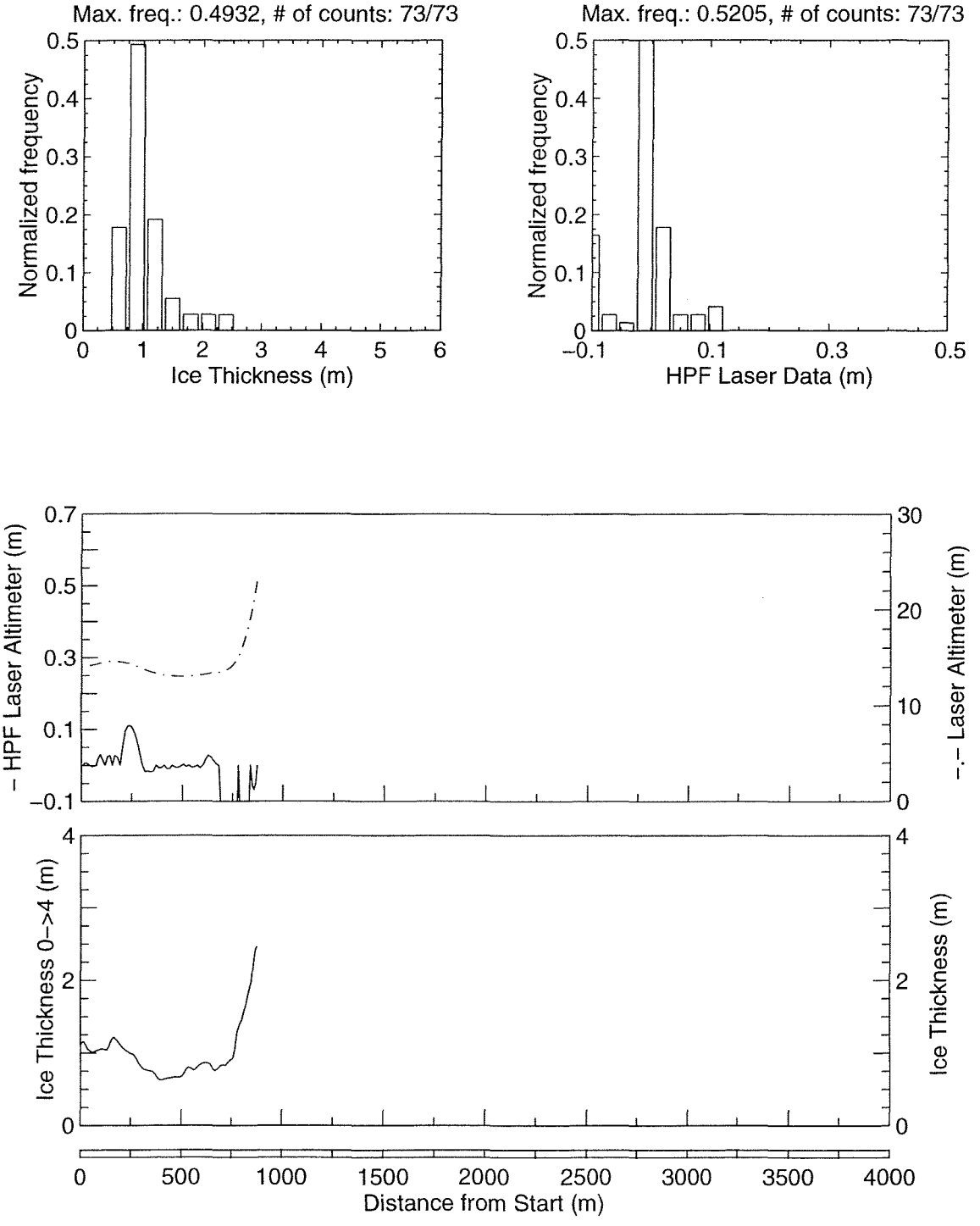

MAR 06 Flight #13 Line #10092 part 1 of 4

Line Starting Coordinates (53.7629,–56.8087) ending at (53.7524,–56.8670)

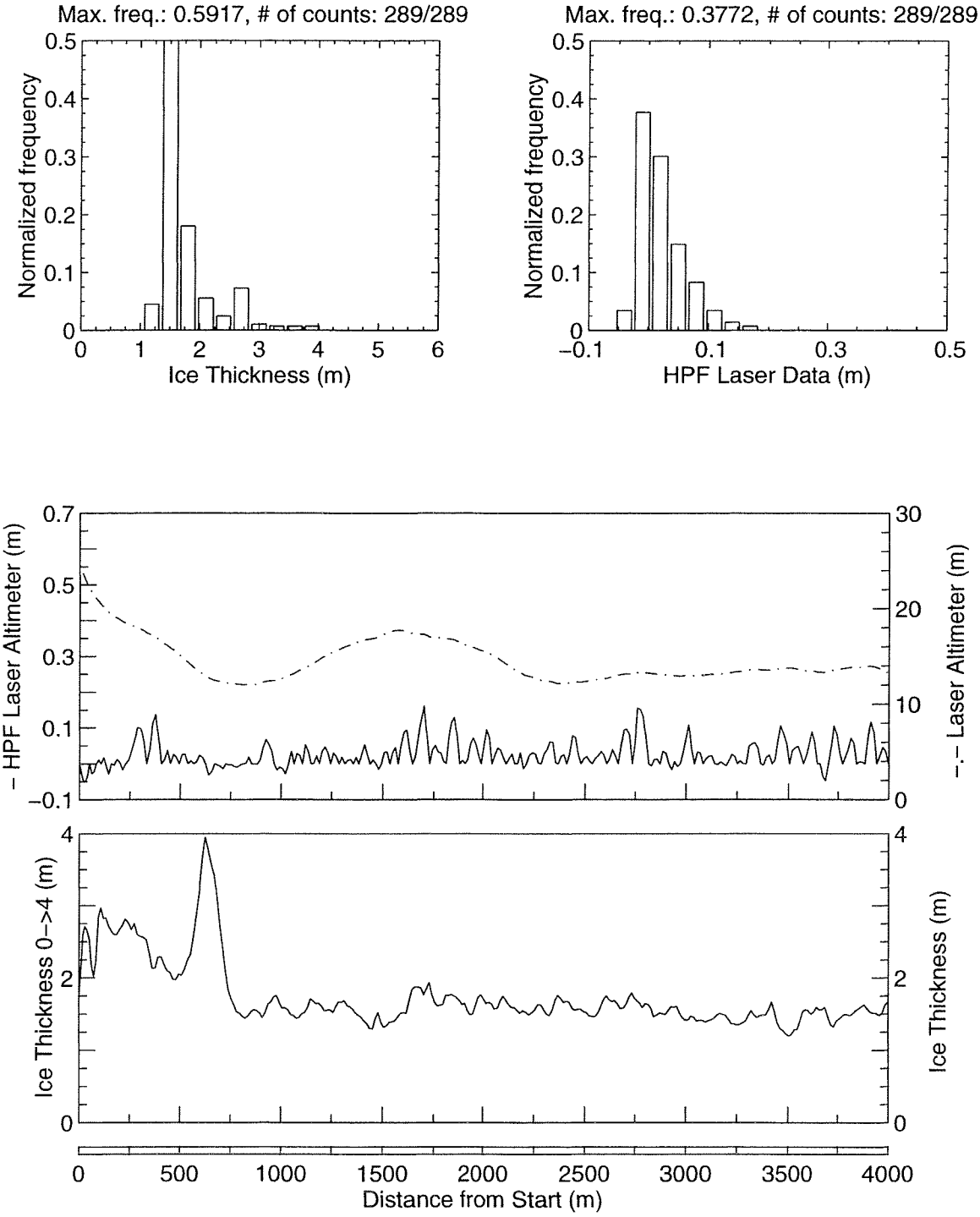

MAR 06 Flight #13 Line #10092 part 2 of 4

Line Starting Coordinates (53.7524,–56.8670) ending at (53.7417,–56.9248)

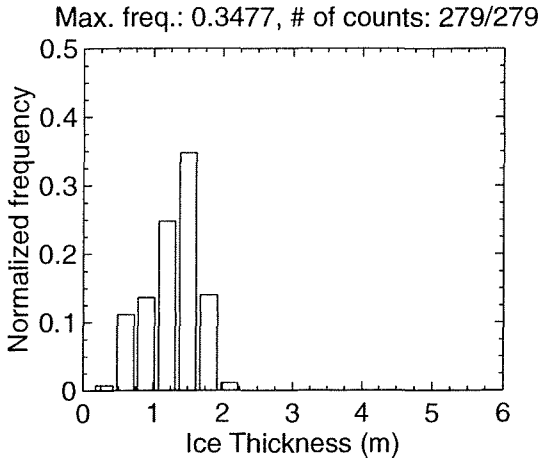

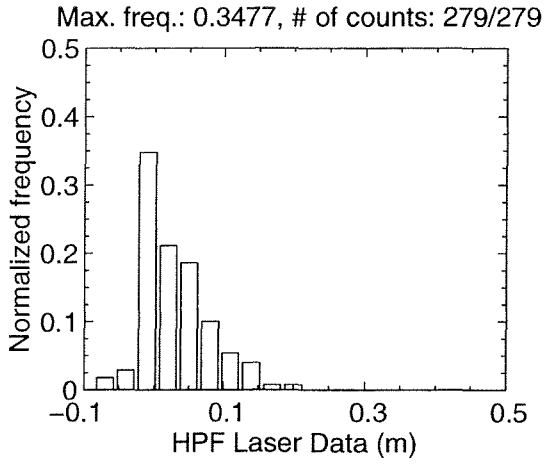

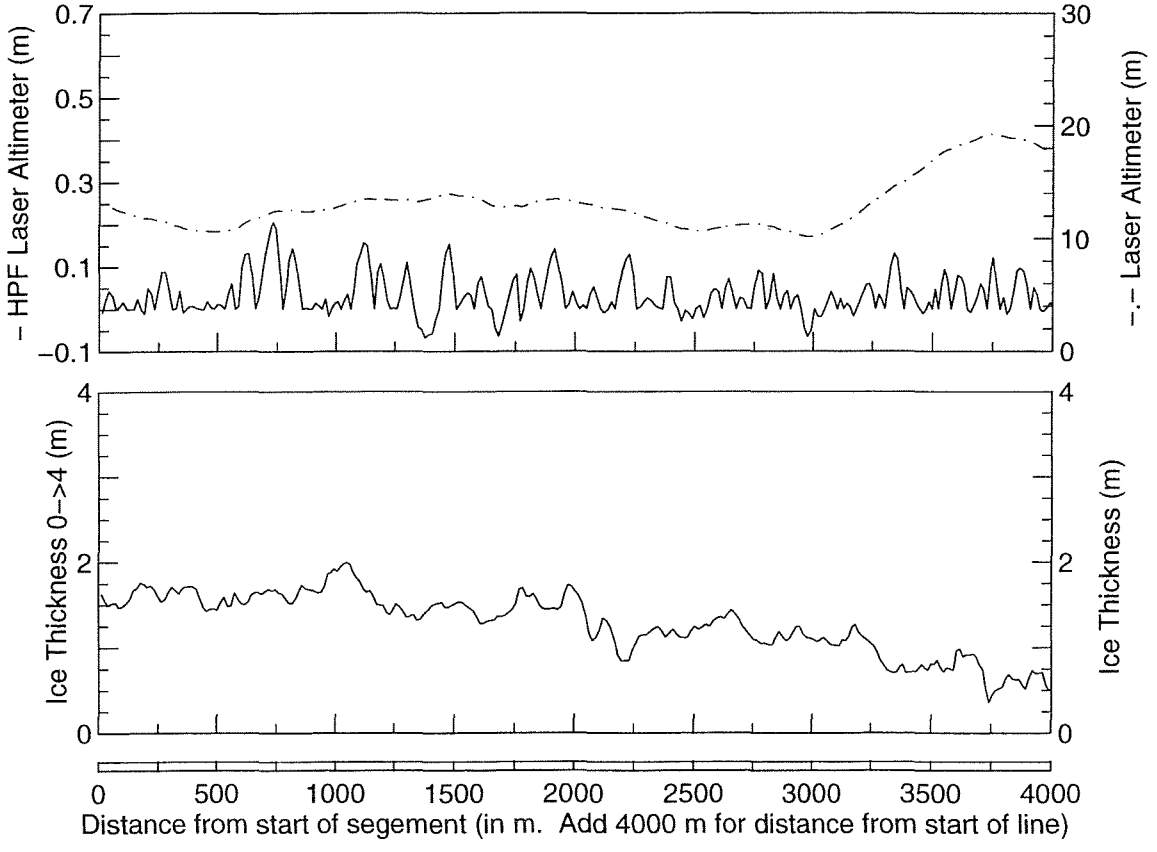

MAR 06 Flight #13 Line #10092 part 3 of 4

Line Starting Coordinates (53.7417,–56.9248) ending at (53.7299,–56.9819)

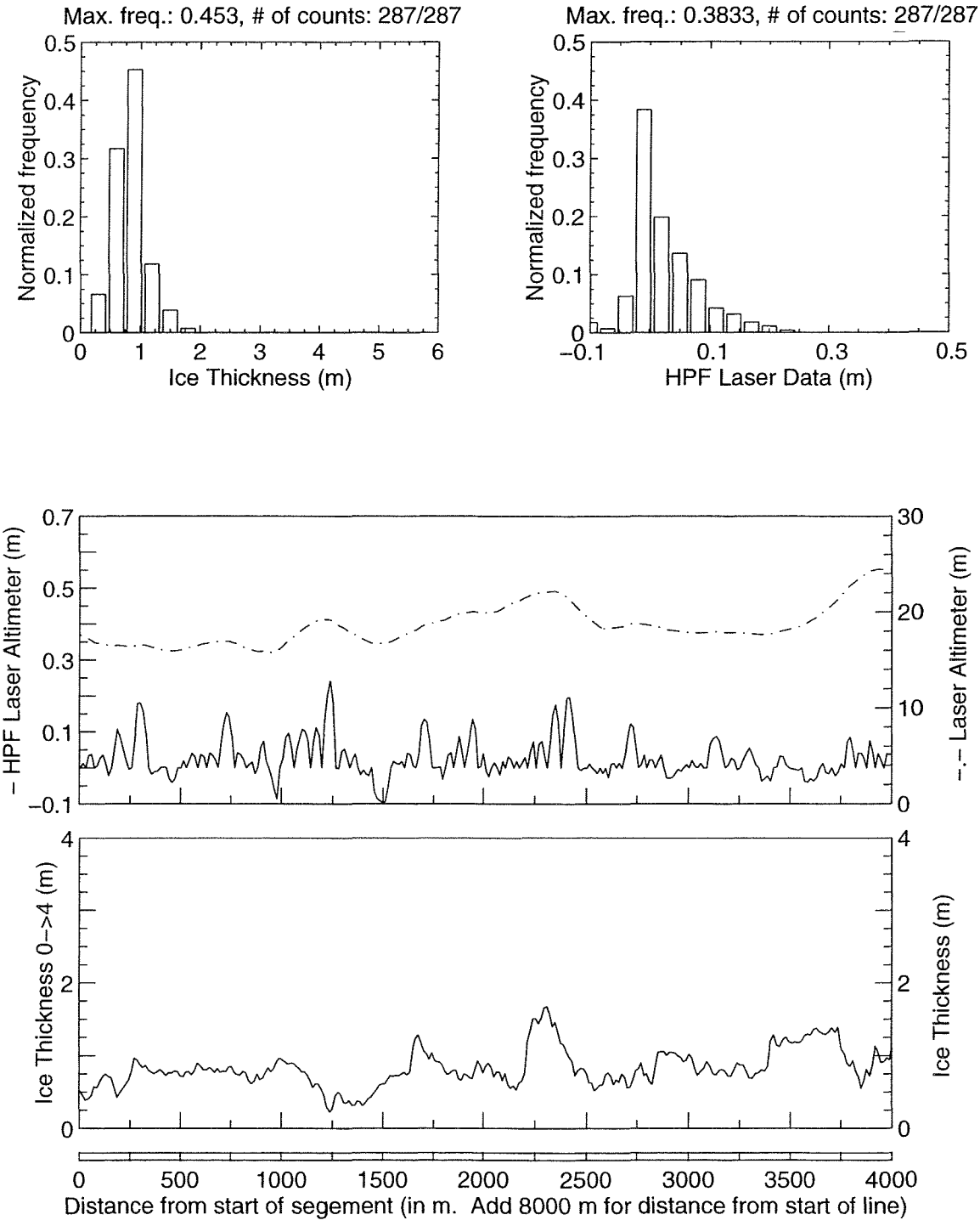

MAR 06 Flight #13 Line #10092 part 4 of 4

Line Starting Coordinates (53.7299,–56.9819) ending at (53.7191,–56.9976)

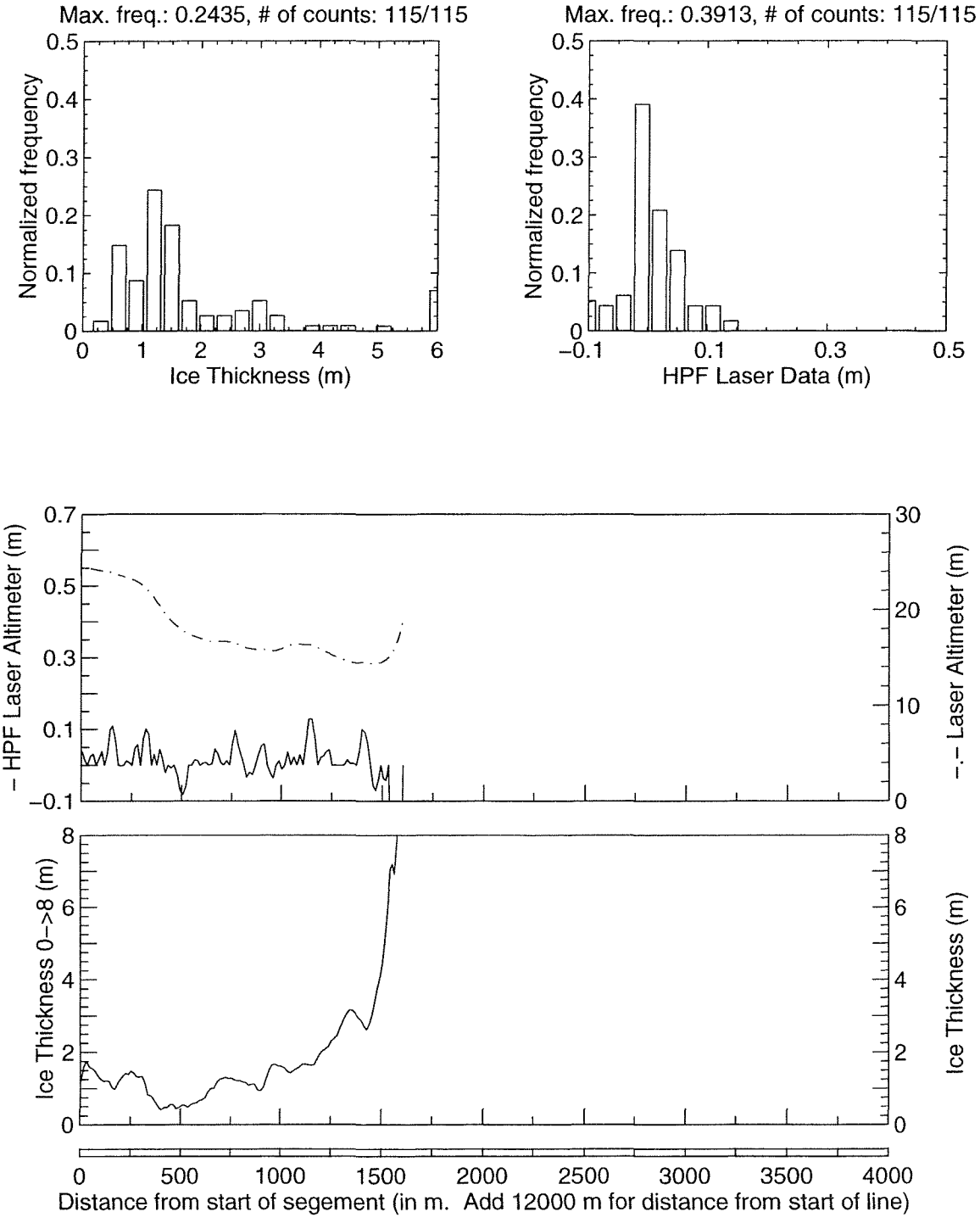

MAR 07 Flight #01 Line #10010 part 1 of 5

Line Starting Coordinates (53.6882,–56.5551) ending at (53.6896,–56.4943)

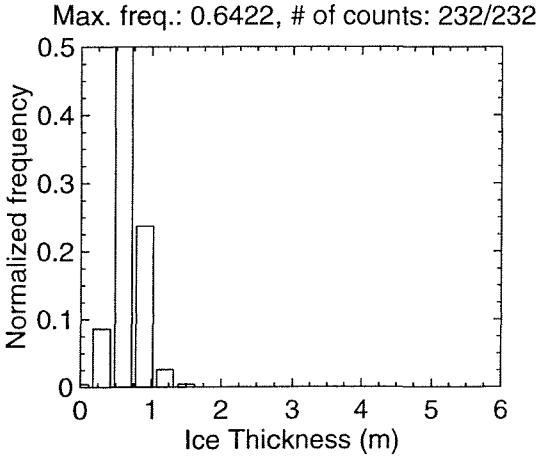

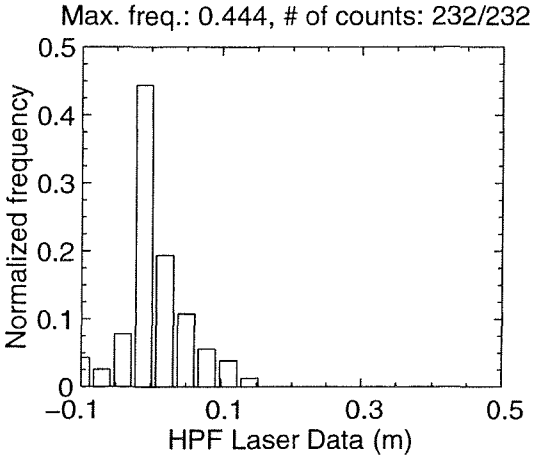

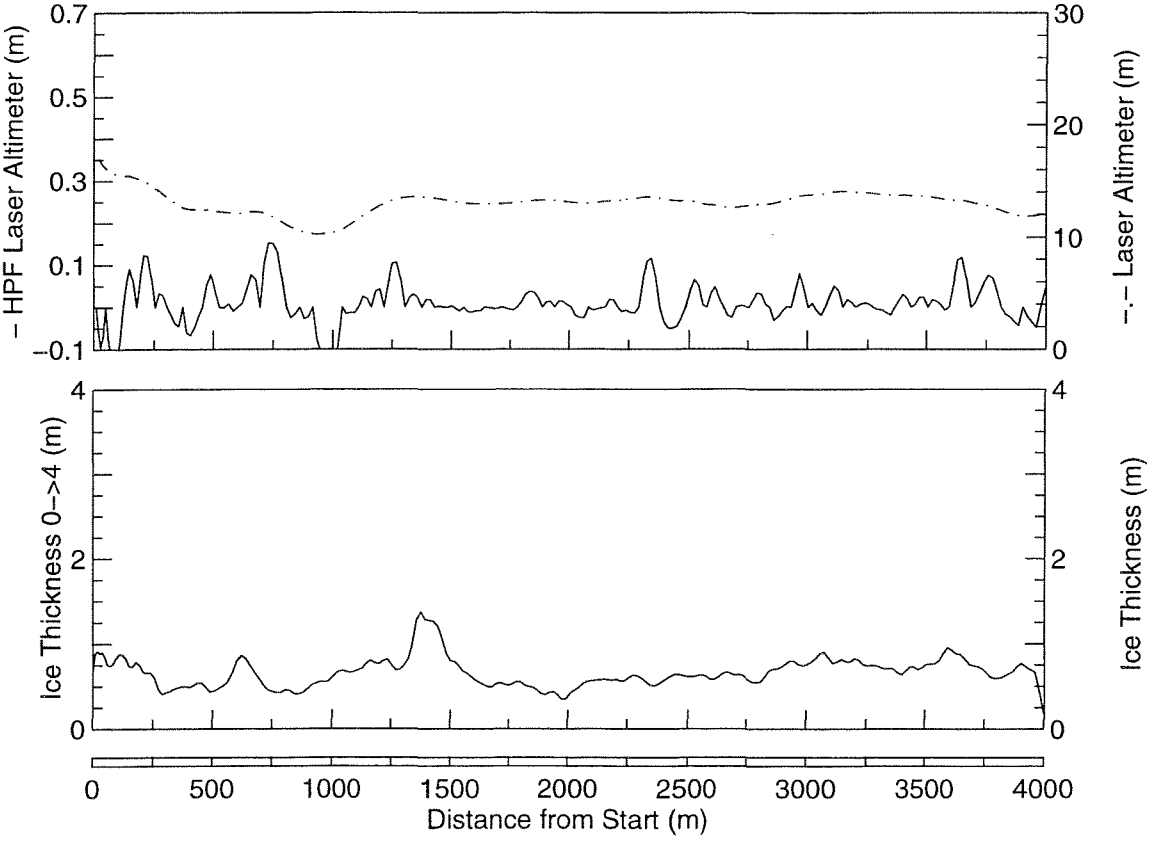

MAR 07 Flight #01 Line #10010 part 2 of 5

Line Starting Coordinates (53.6896,–56.4943) ending at (53.6916,–56.4339)

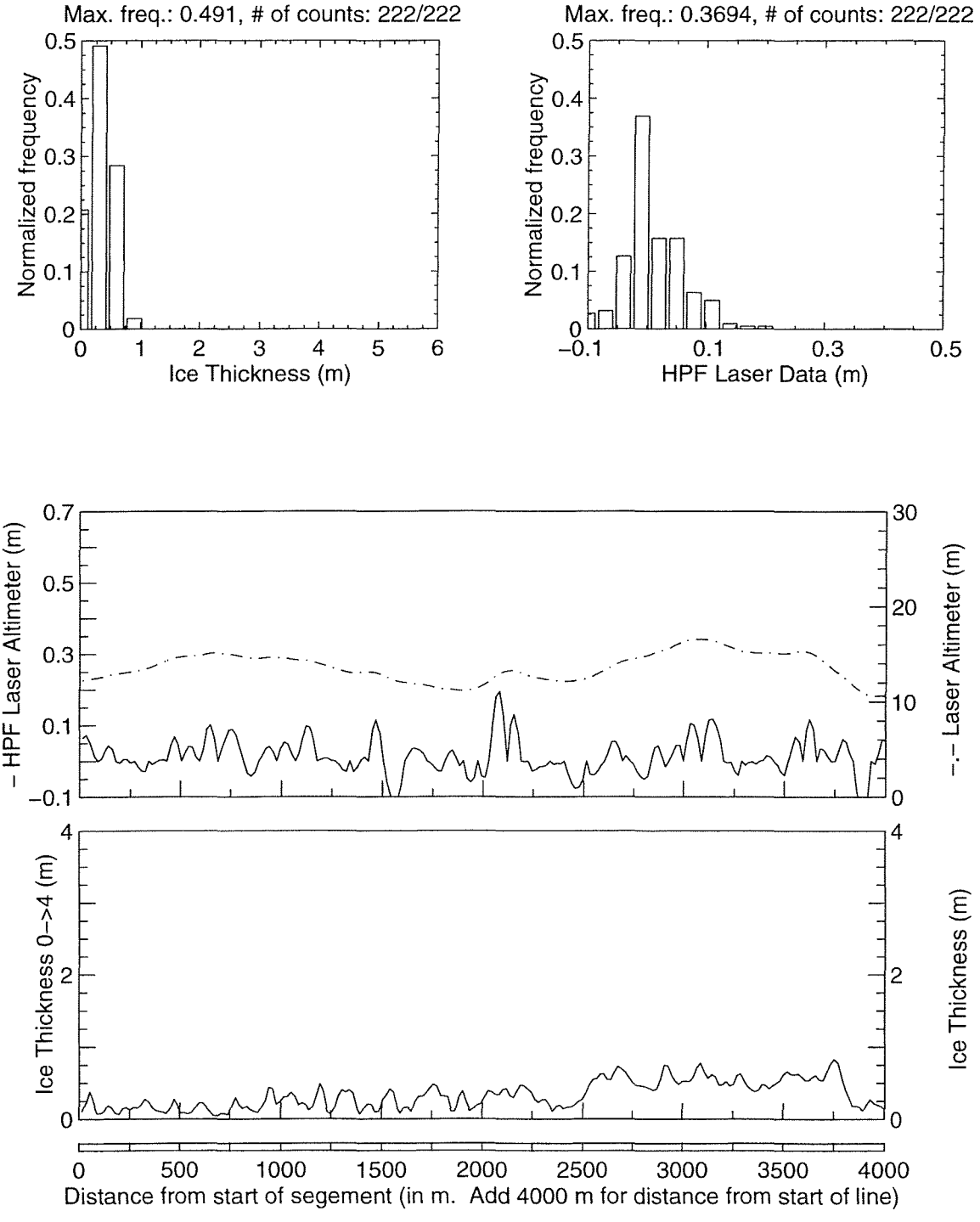

MAR 07 Flight #01 Line #10010 part 3 of 5

Line Starting Coordinates (53.6916,–56.4339) ending at (53.6938,–56.3733)

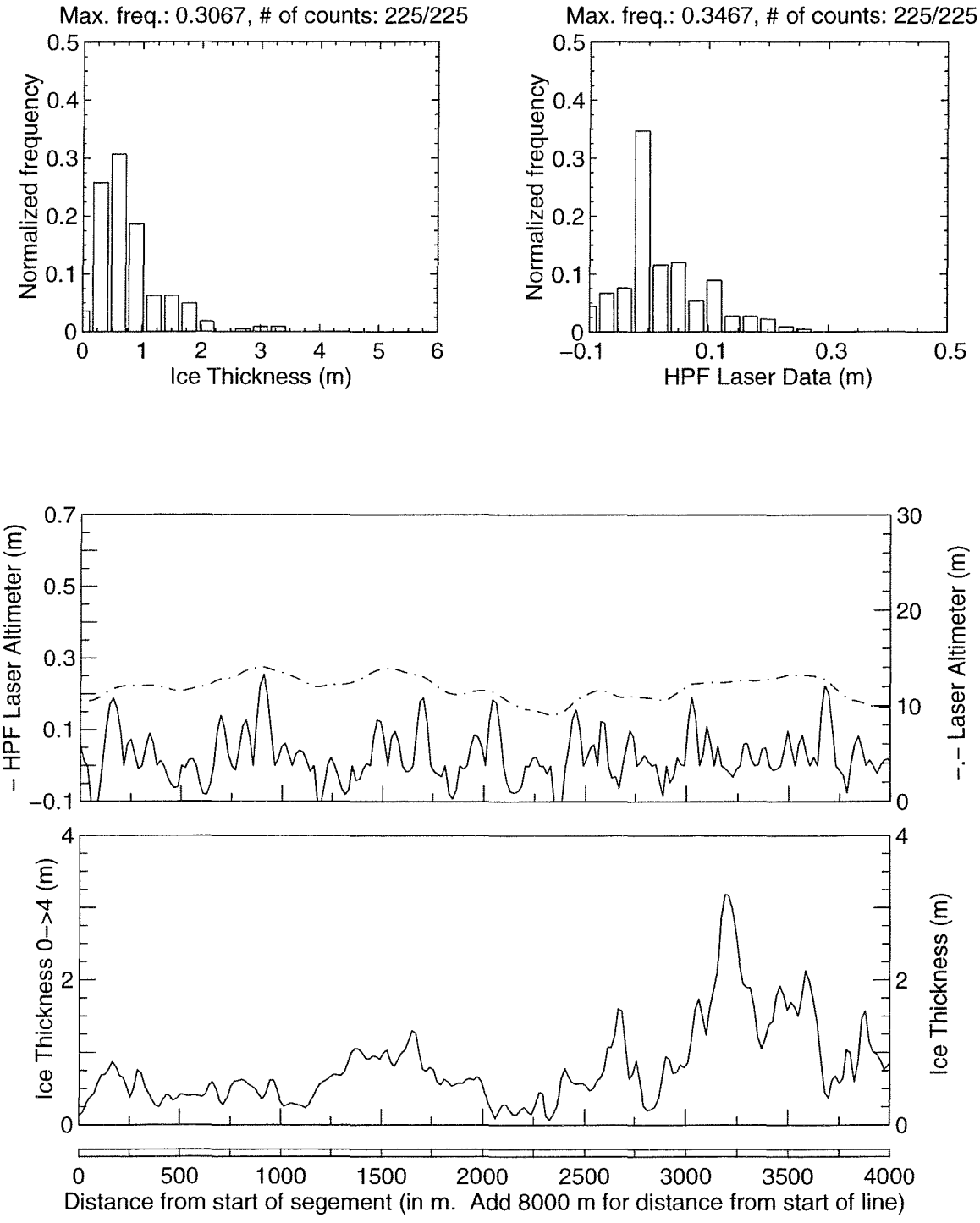

MAR 07 Flight #01 Line #10010 part 4 of 5

Line Starting Coordinates (53.6938,–56.3733) ending at (53.6966,–56.3128)

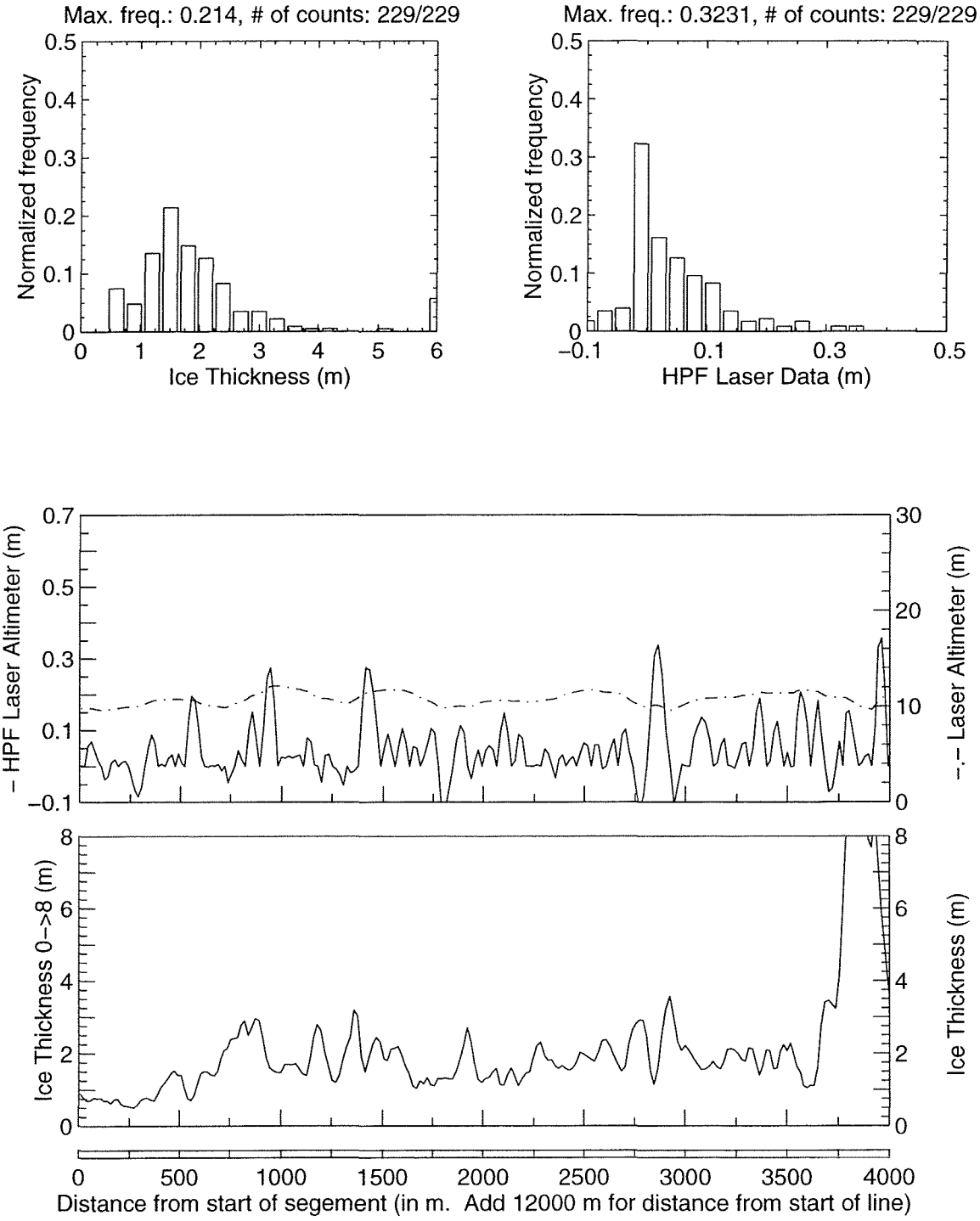

MAR 07 Flight #01 Line #10010 part 5 of 5

Line Starting Coordinates (53.6966,–56.3128) ending at (53.6968,–56.3048)

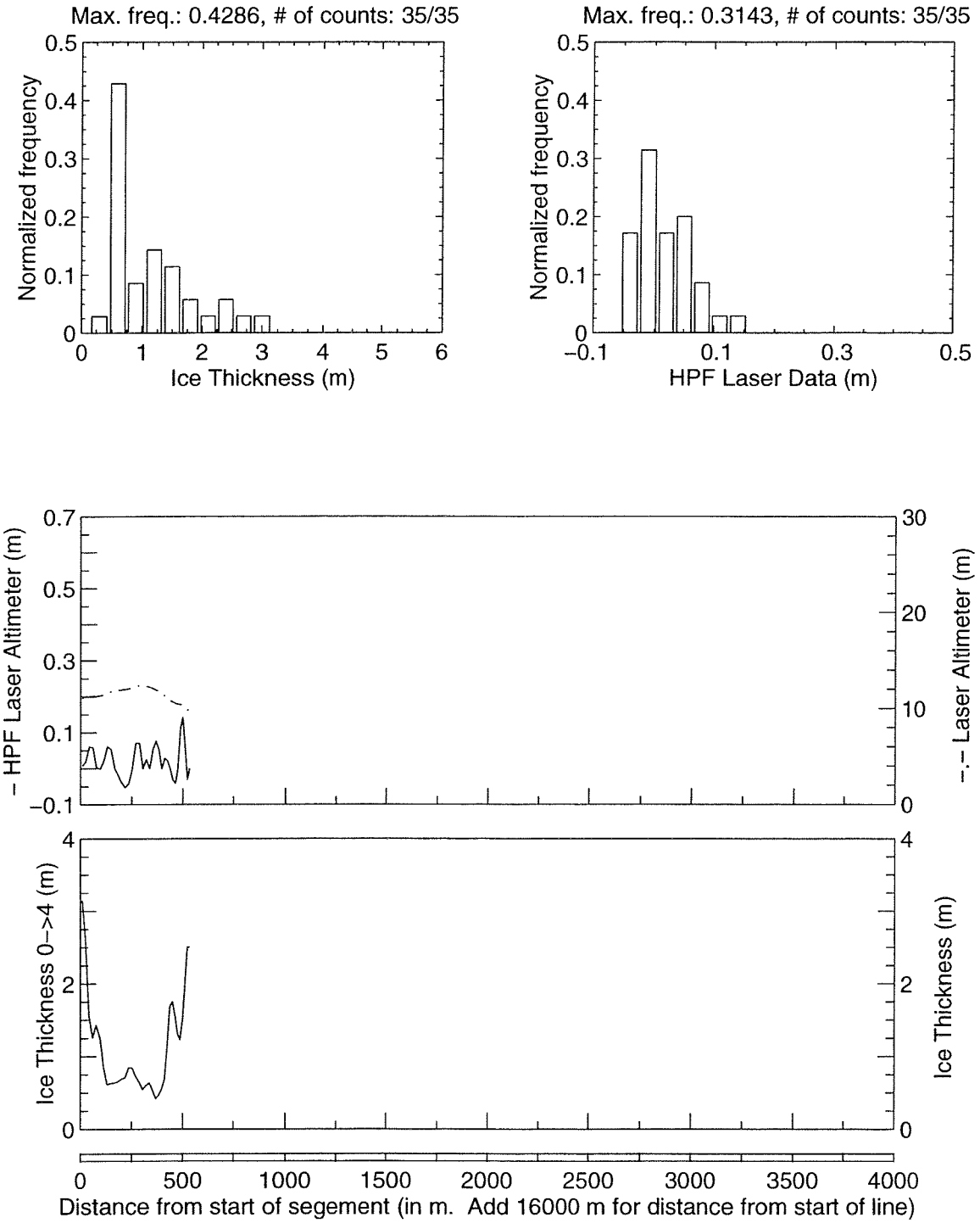

MAR 07 Flight #01 Line #10020 part 1 of 3

Line Starting Coordinates (53.6837,–56.1973) ending at (53.6665,–56.1441)

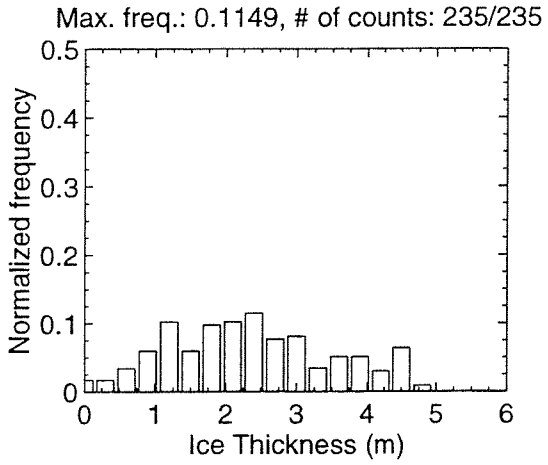

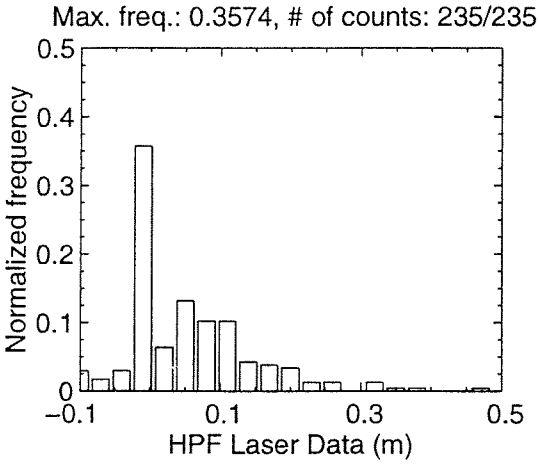

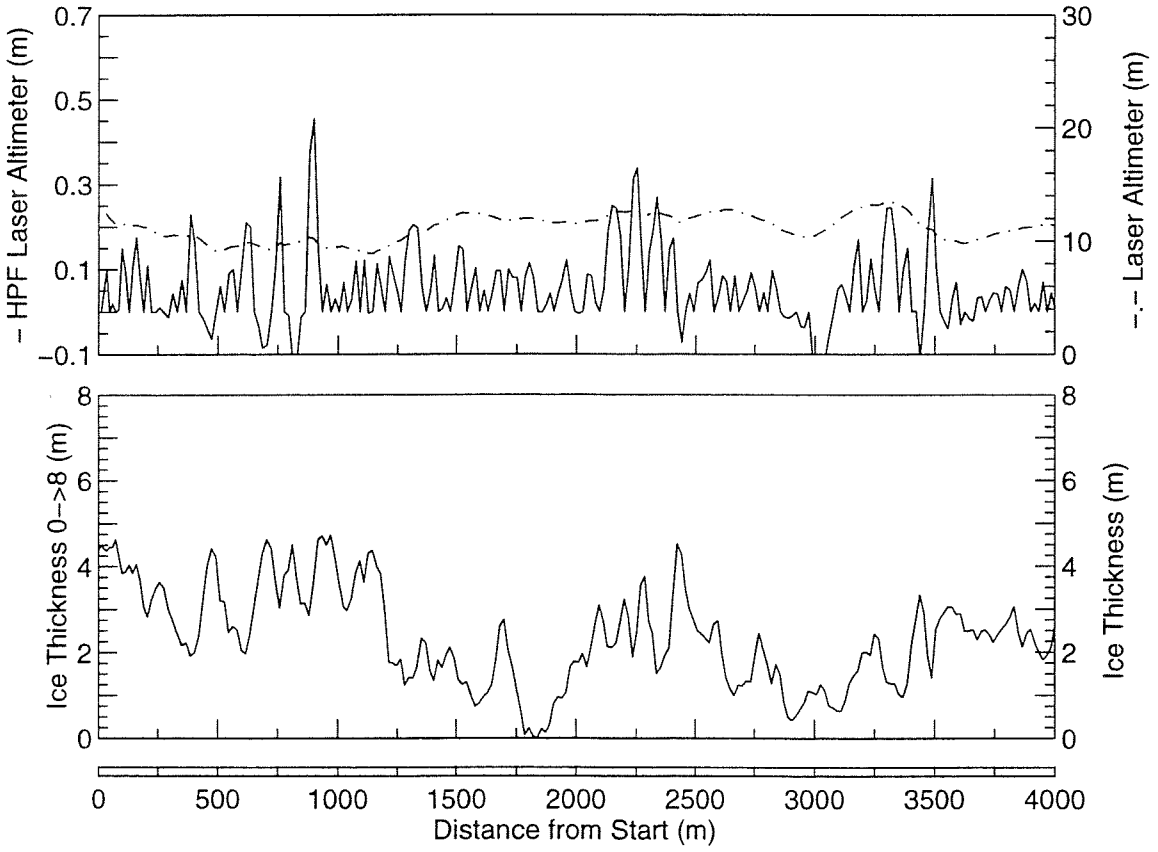

MAR 07 Flight #01 Line #10020 part 2 of 3

Line Starting Coordinates (53.6665,–56.1441) ending at (53.6498,–56.0902)

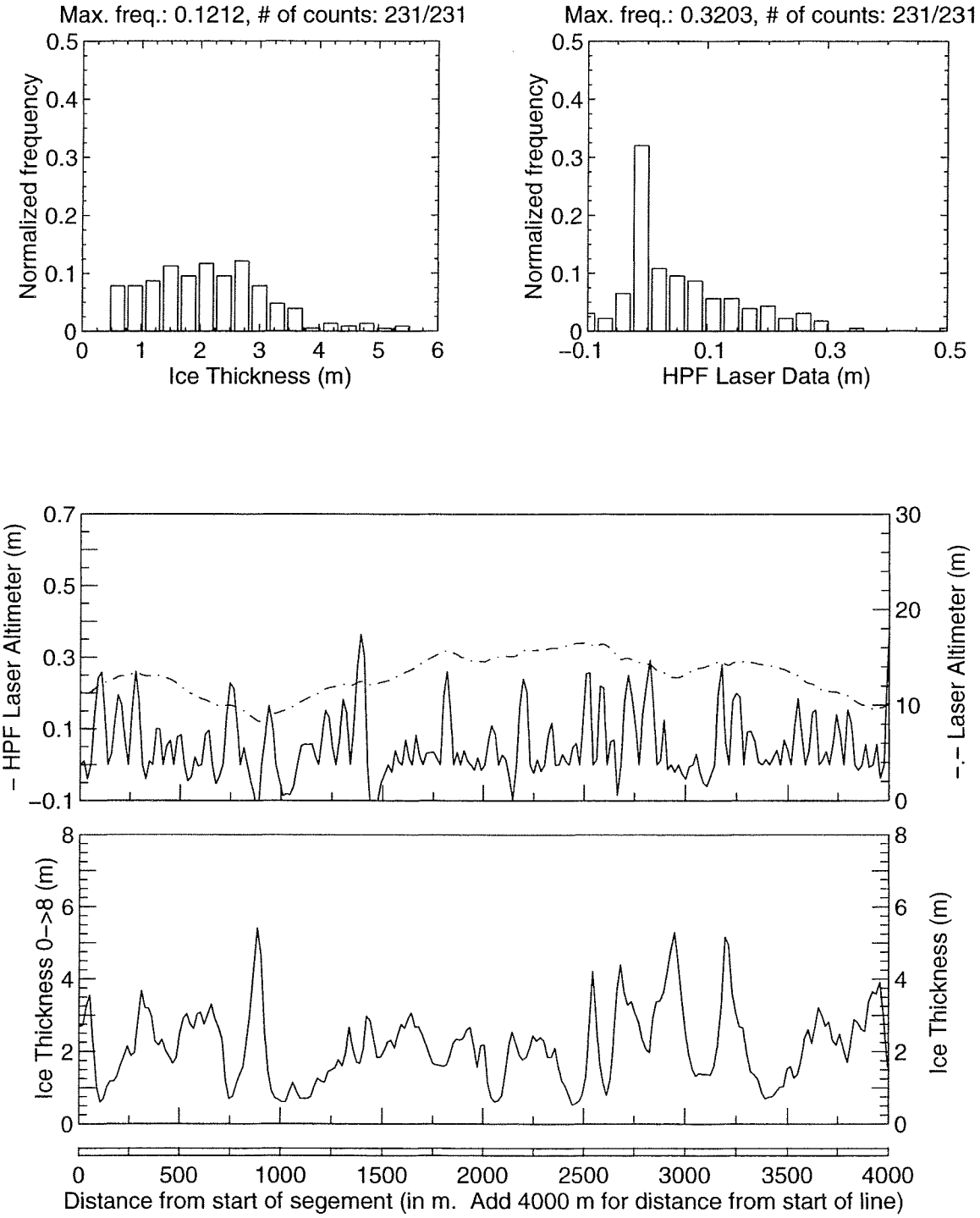

MAR 07 Flight #01 Line #10020 part 3 of 3

Line Starting Coordinates (53.6498,–56.0902) ending at (53.6416,–56.0622)

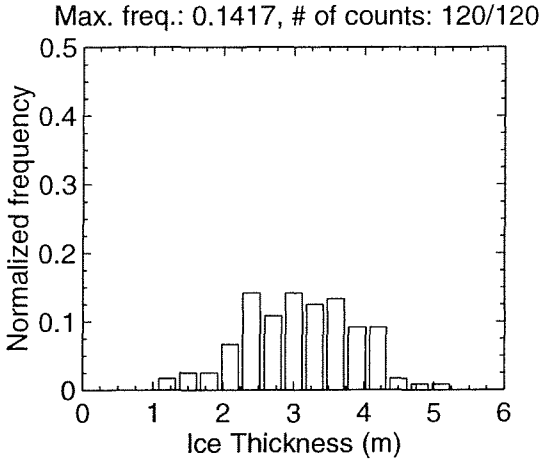

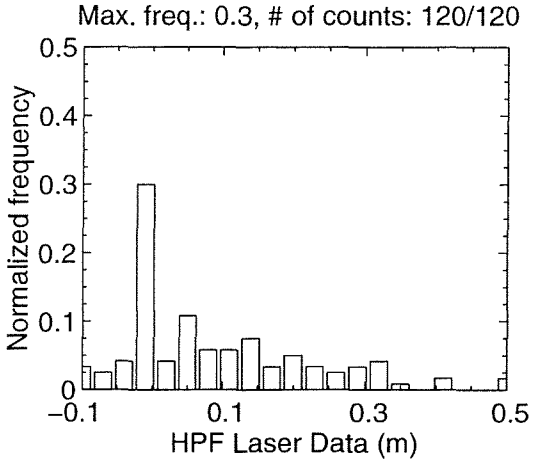

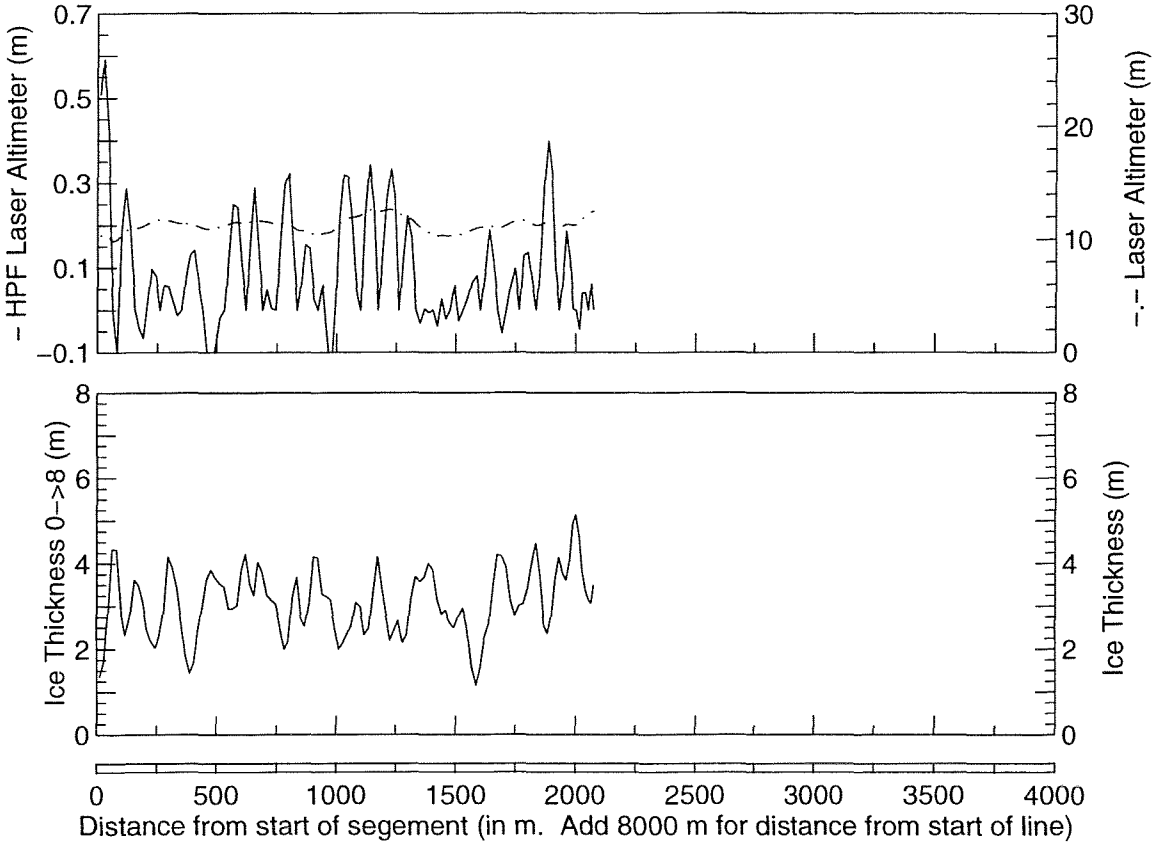

MAR 07 Flight #01 Line #10030 part 1 of 4

Line Starting Coordinates (53.6409,–56.0507) ending at (53.6277,–55.9942)

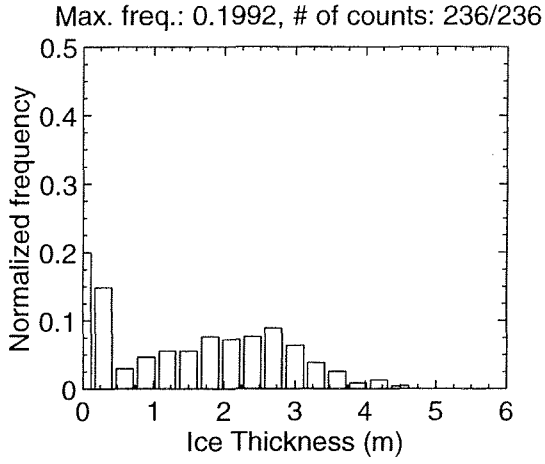

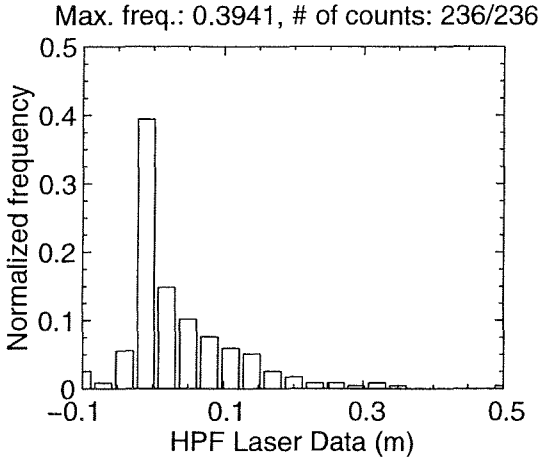

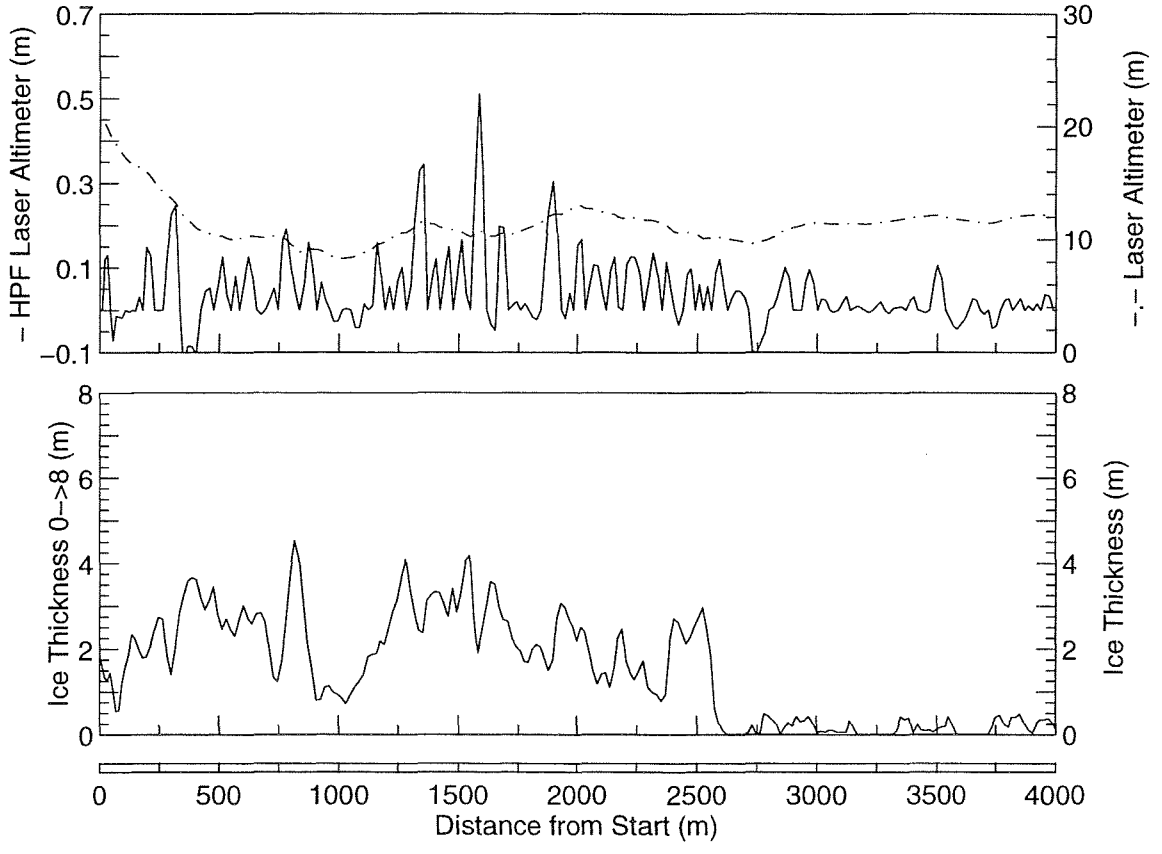

MAR 07 Flight #01 Line #10030 part 2 of 4

Line Starting Coordinates (53.6277,–55.9942) ending at (53.6145,–55.9378)

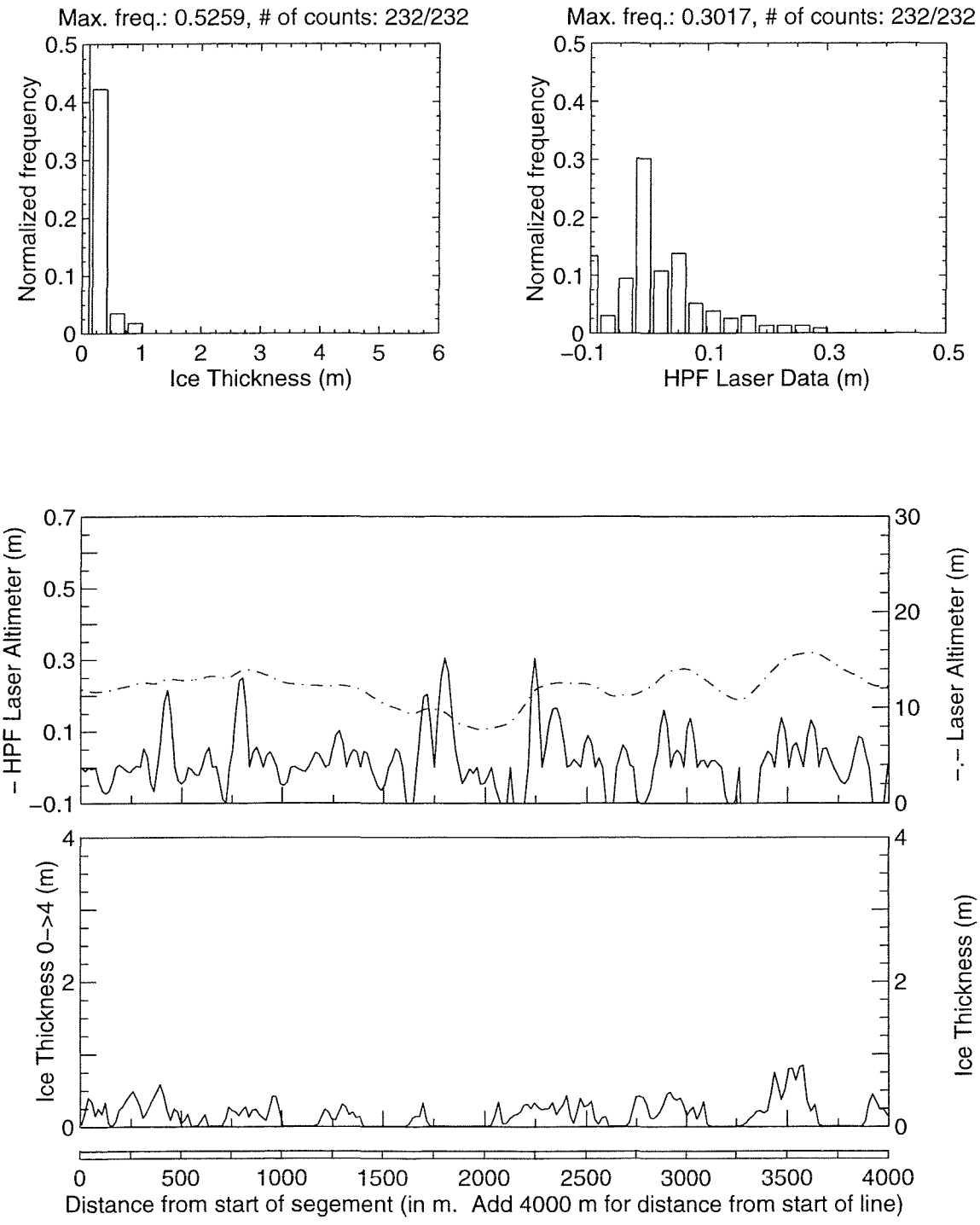

MAR 07 Flight #01 Line #10030 part 3 of 4

Line Starting Coordinates (53.6145,–55.9378) ending at (53.6039,–55.8800)

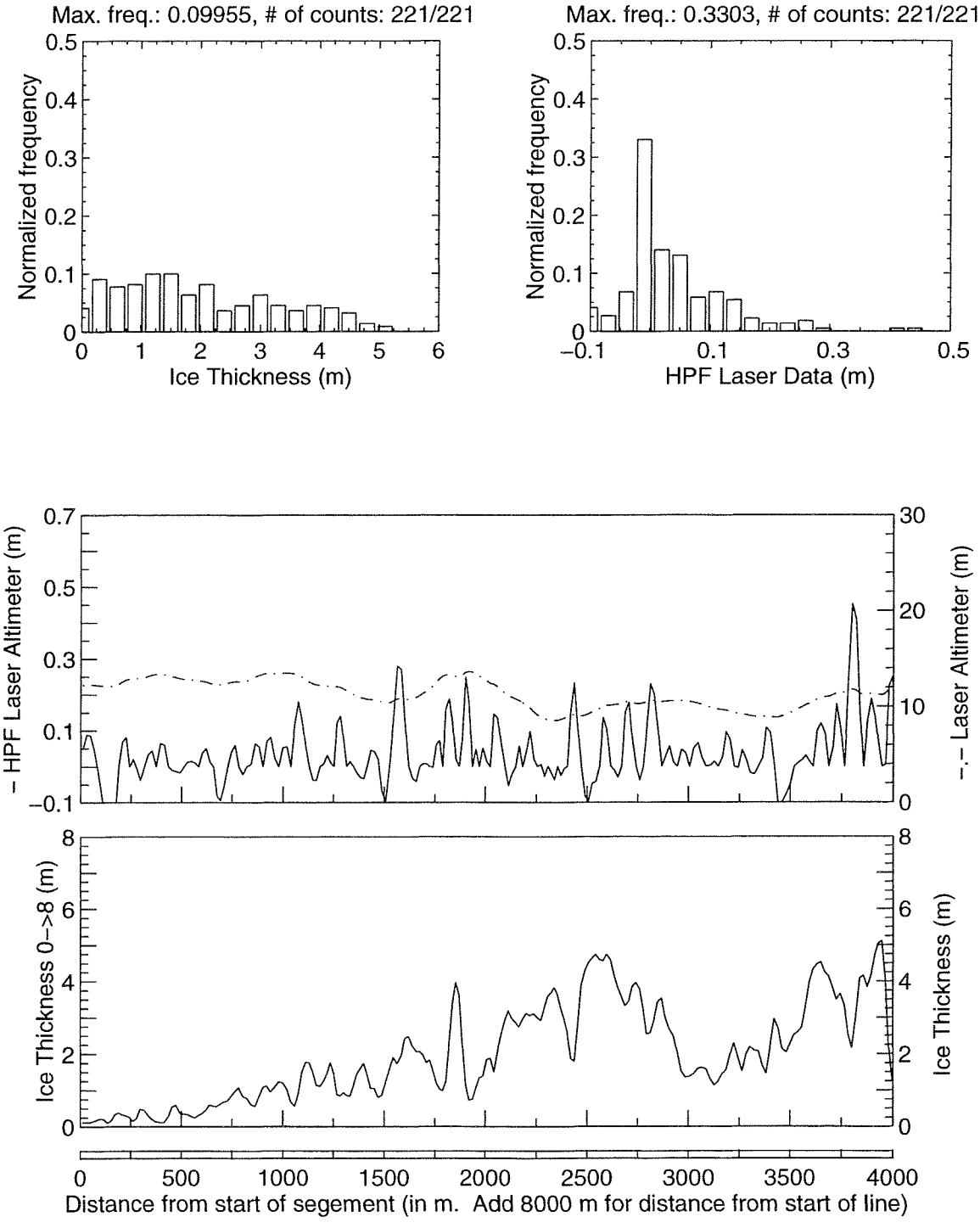

MAR 07 Flight #01 Line #10030 part 4 of 4

Line Starting Coordinates (53.6039,–55.8800) ending at (53.5972,–55.8296)

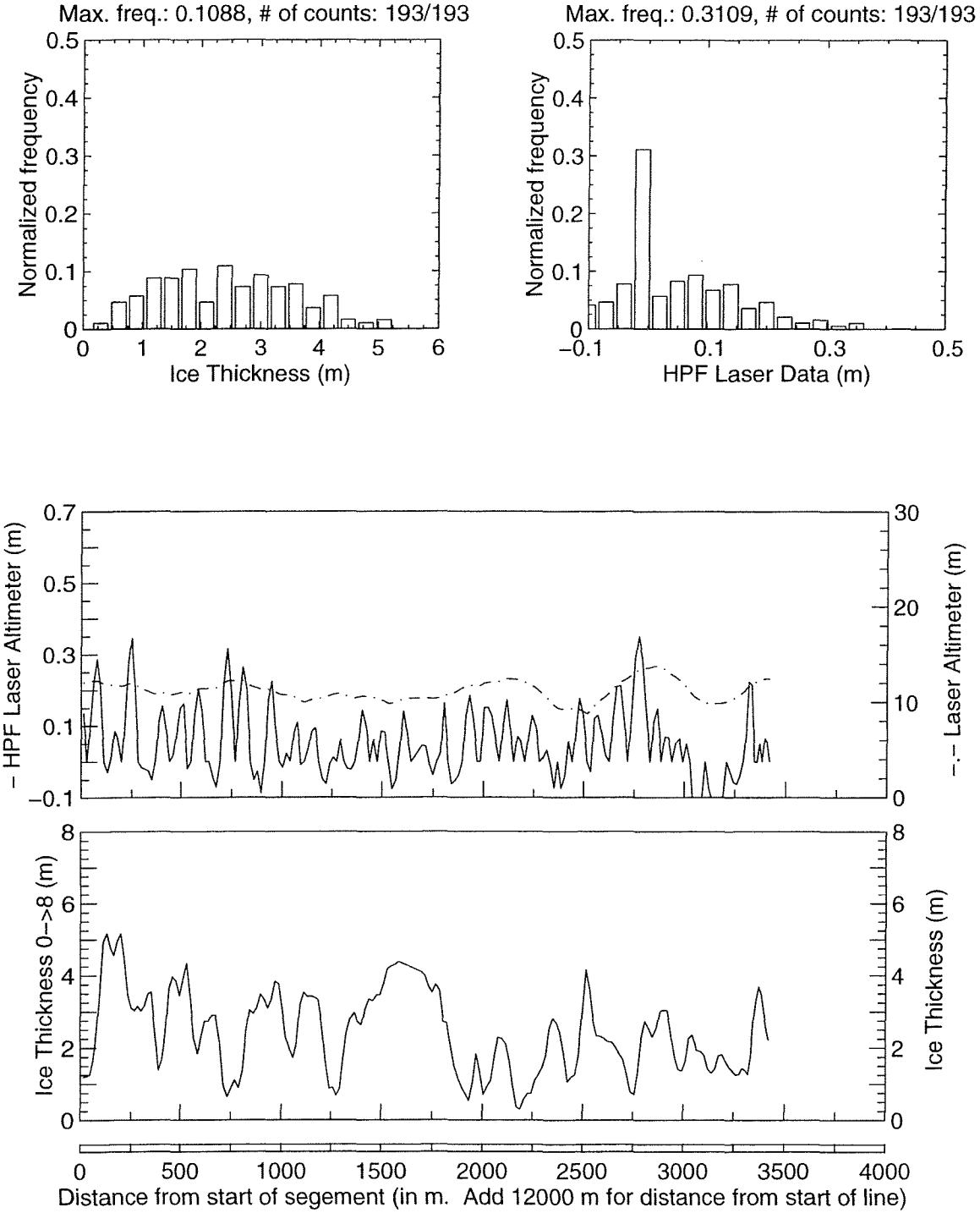

MAR 07 Flight #01 Line #10040 part 1 of 6

Line Starting Coordinates (53.5611,–55.7668) ending at (53.5322,–55.7309)

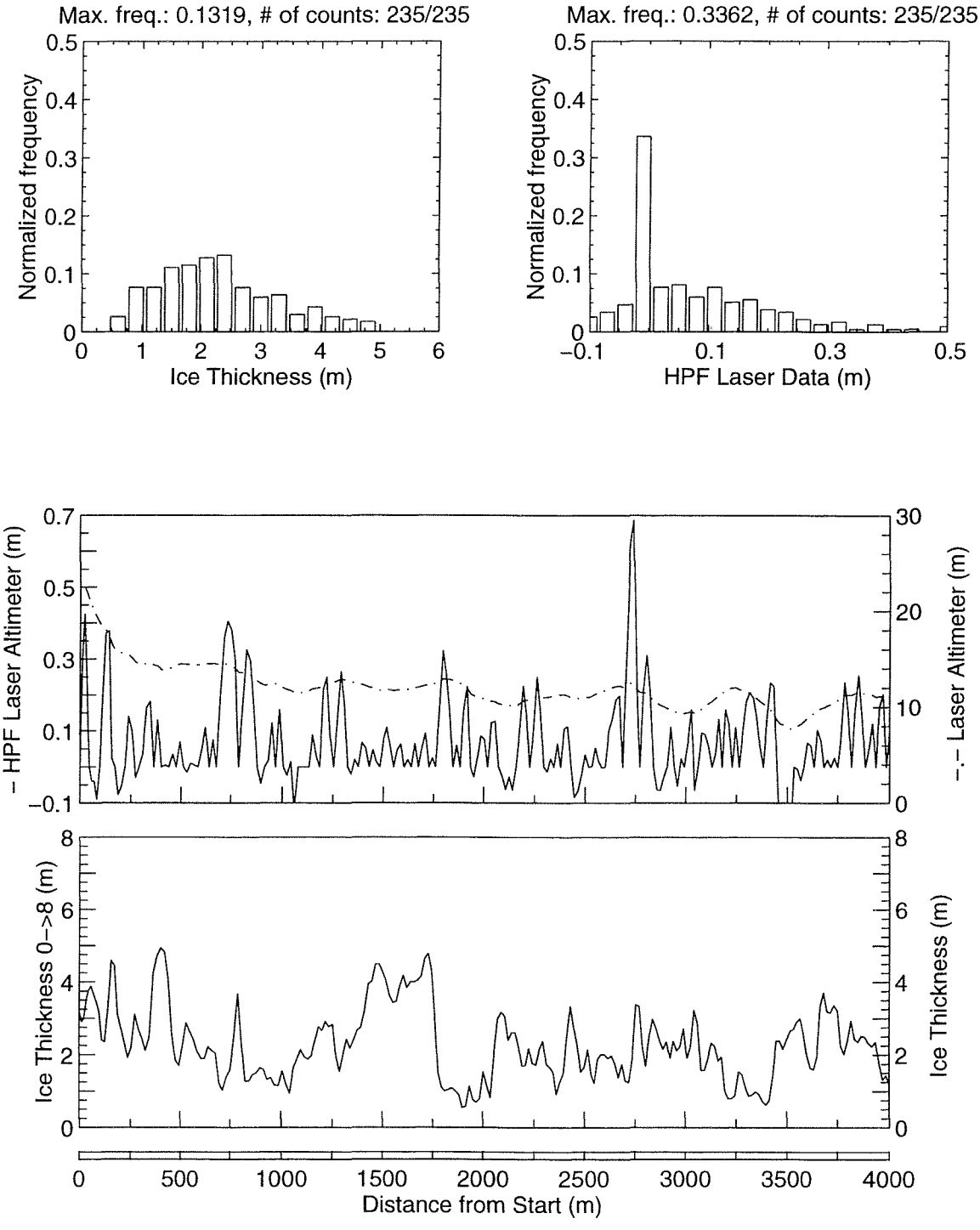

MAR 07 Flight #01 Line #10040 part 2 of 6

Line Starting Coordinates (53.5322,–55.7309) ending at (53.5033,–55.6950)

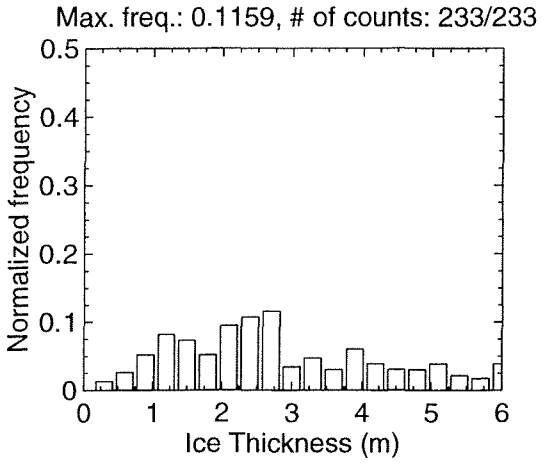

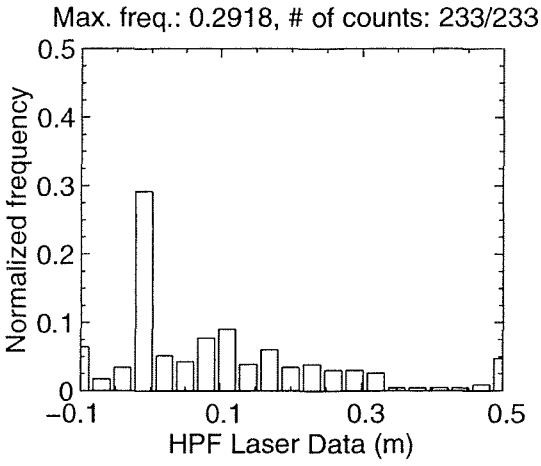

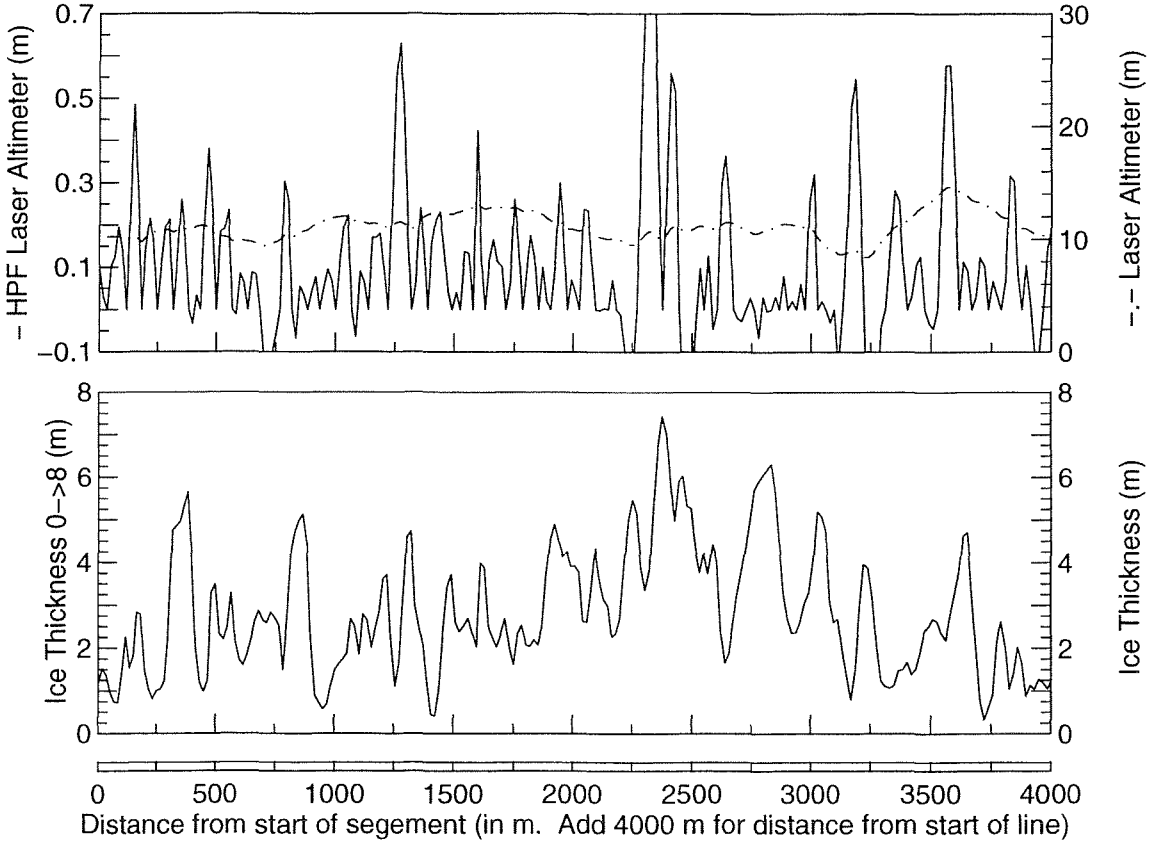

MAR 07 Flight #01 Line #10040 part 3 of 6

Line Starting Coordinates (53.5033,–55.6950) ending at (53.4744,–55.6590)

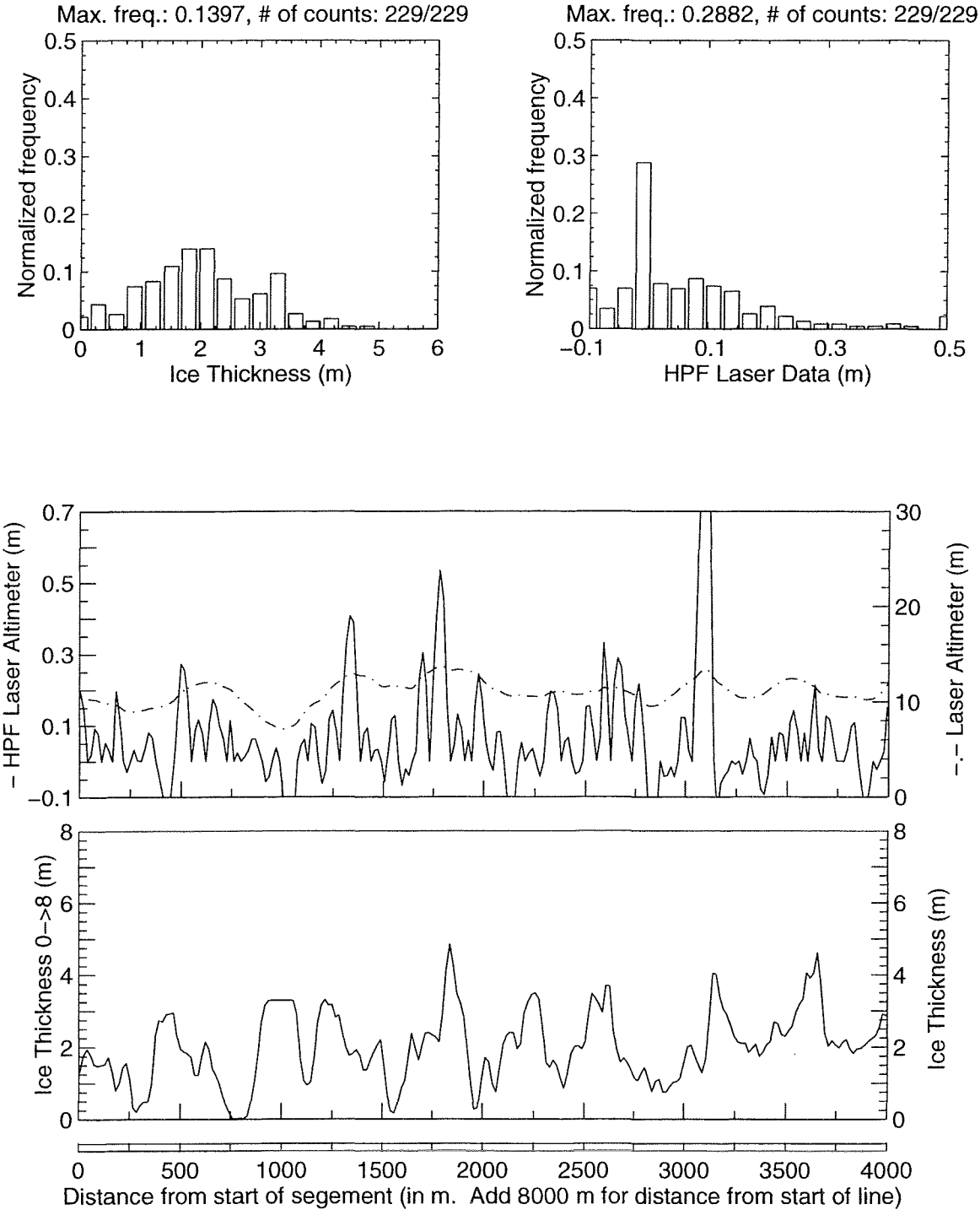

MAR 07 Flight #01 Line #10040 part 4 of 6

Line Starting Coordinates (53.4744,–55.6590) ending at (53.4470,–55.6199)

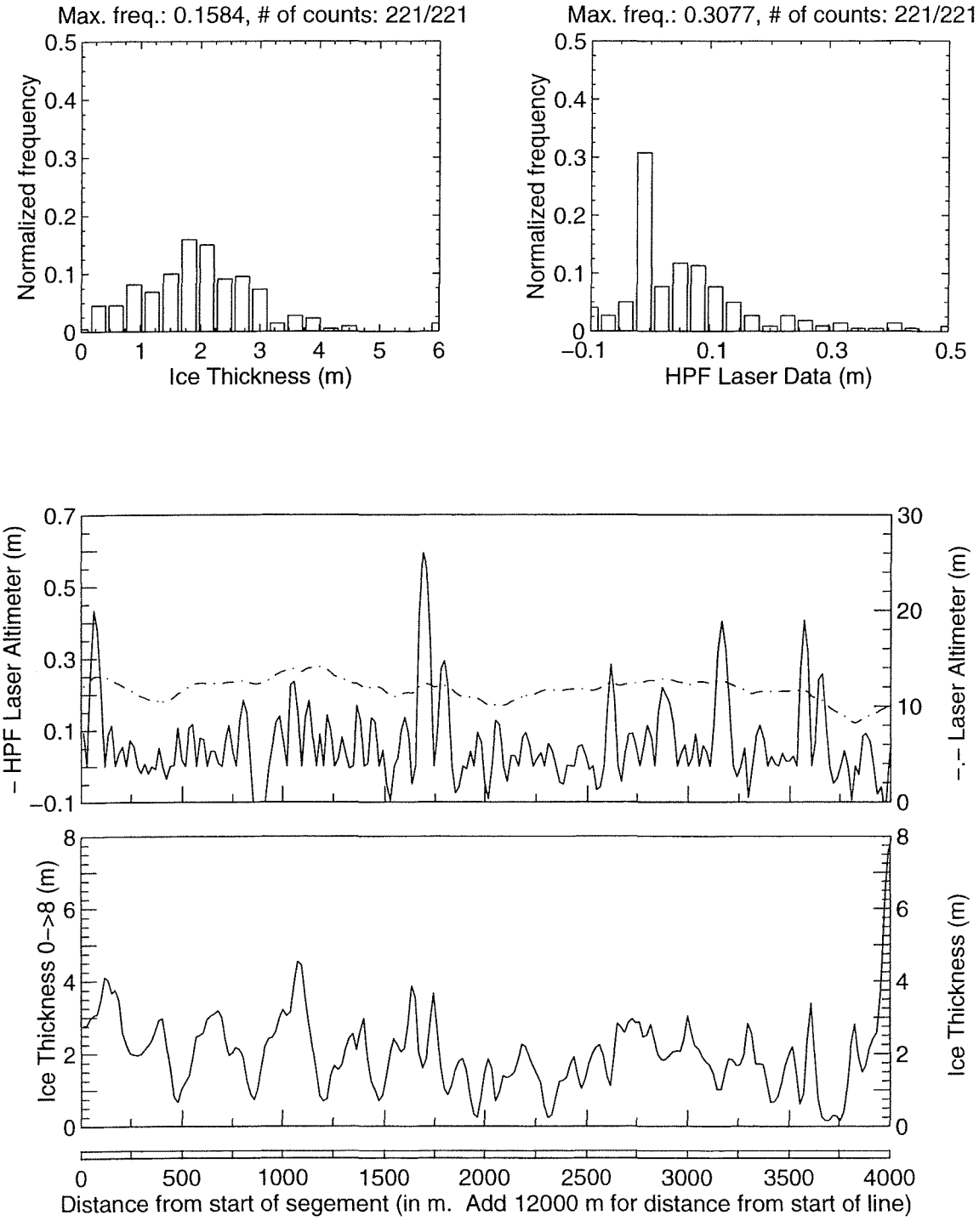

MAR 07 Flight #01 Line #10040 part 5 of 6

Line Starting Coordinates (53.4470,–55.6199) ending at (53.4212,–55.5781)

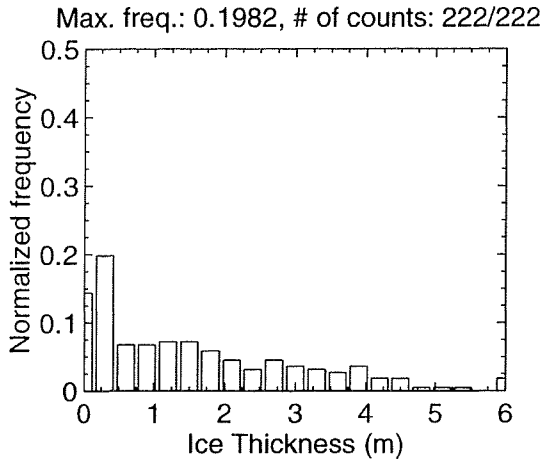

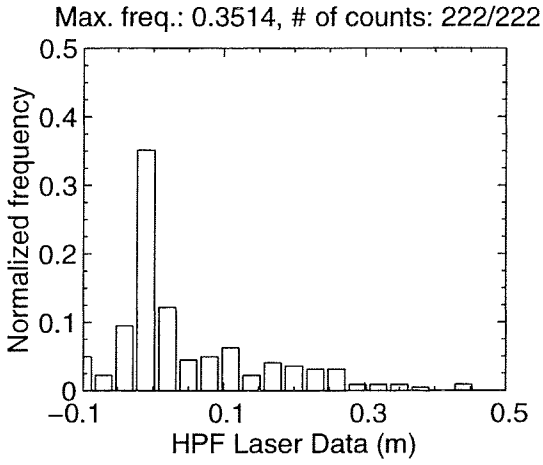

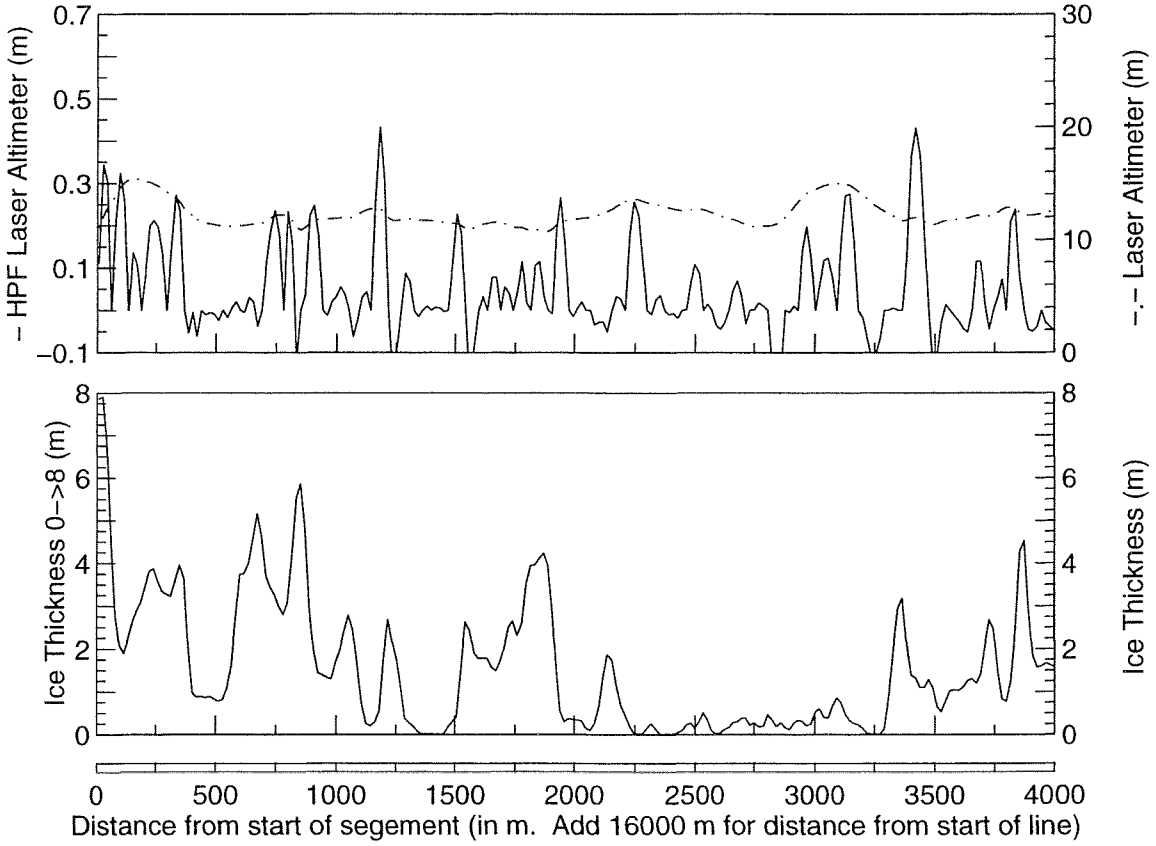

MAR 07 Flight #01 Line #10040 part 6 of 6

Line Starting Coordinates (53.4212,–55.5781) ending at (53.4107,–55.5592)

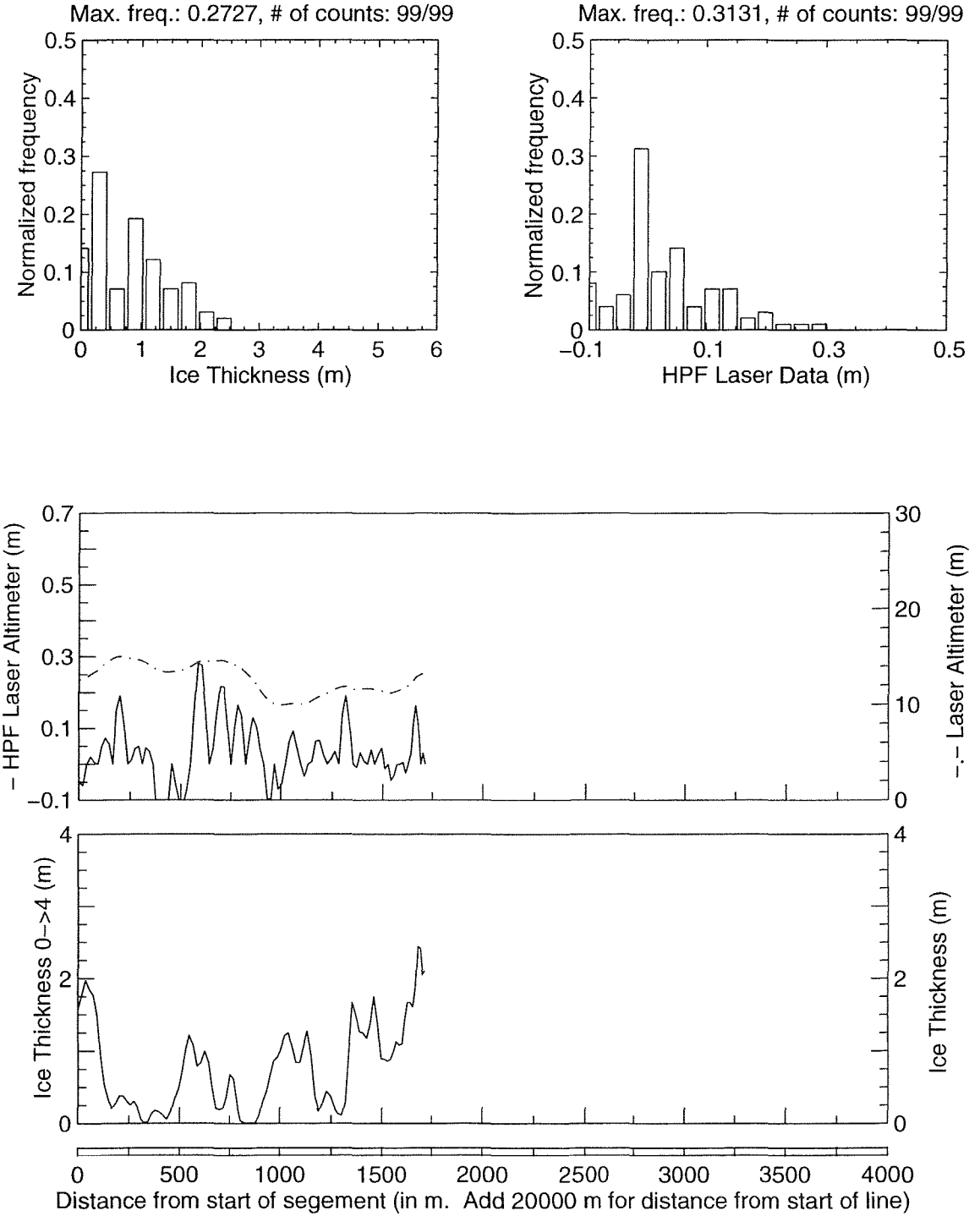

MAR 07 Flight #01 Line #10050 part 1 of 5

Line Starting Coordinates (53.3629,−55.5715) ending at (53.3292,−55.5924)

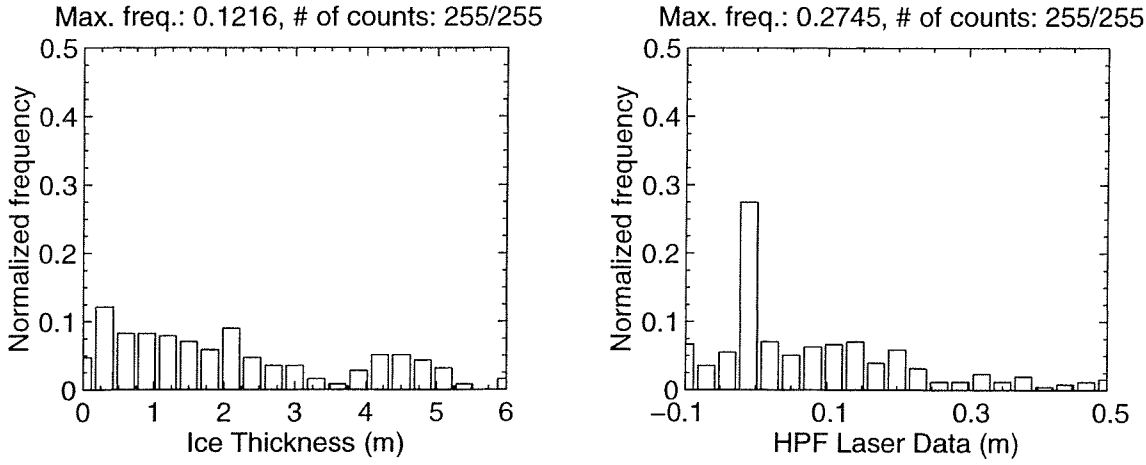

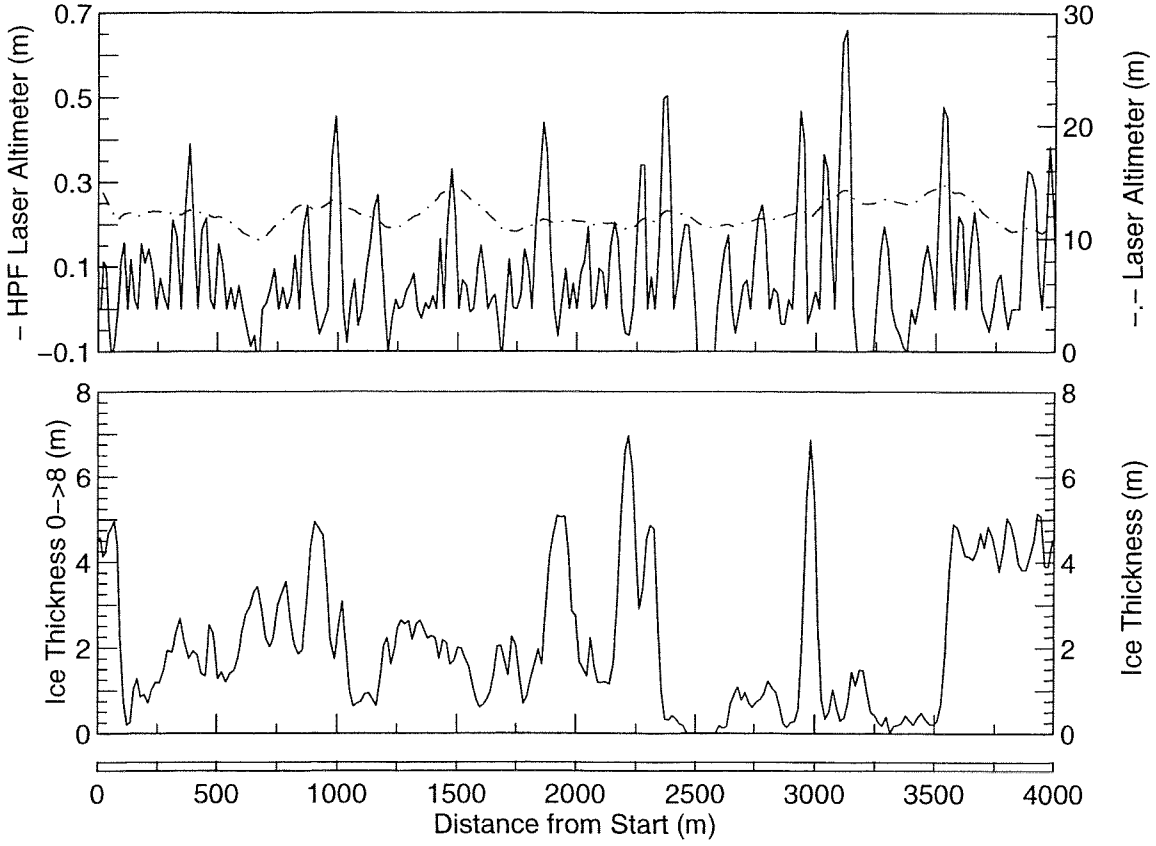

MAR 07 Flight #01 Line #10050 part 2 of 5

Line Starting Coordinates (53.3292,–55.5924) ending at (53.2954,–55.6127)

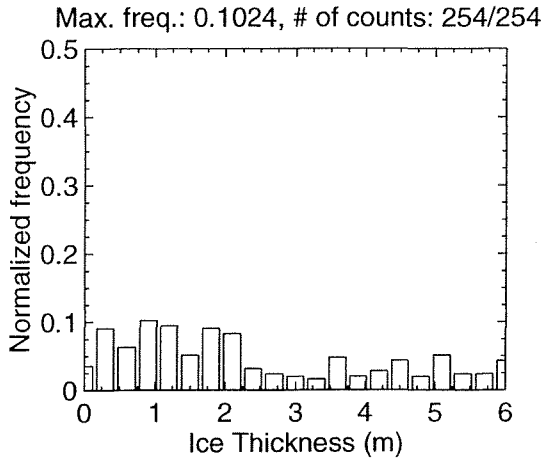

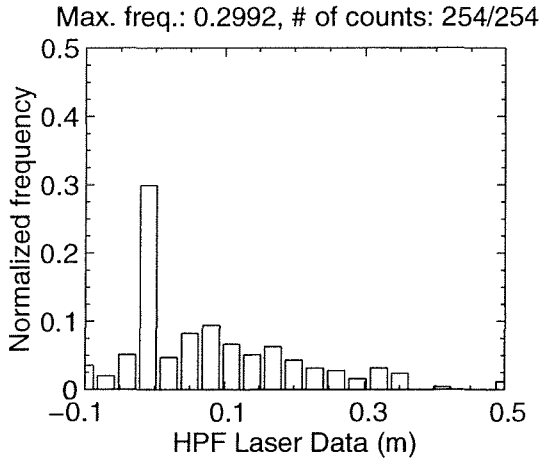

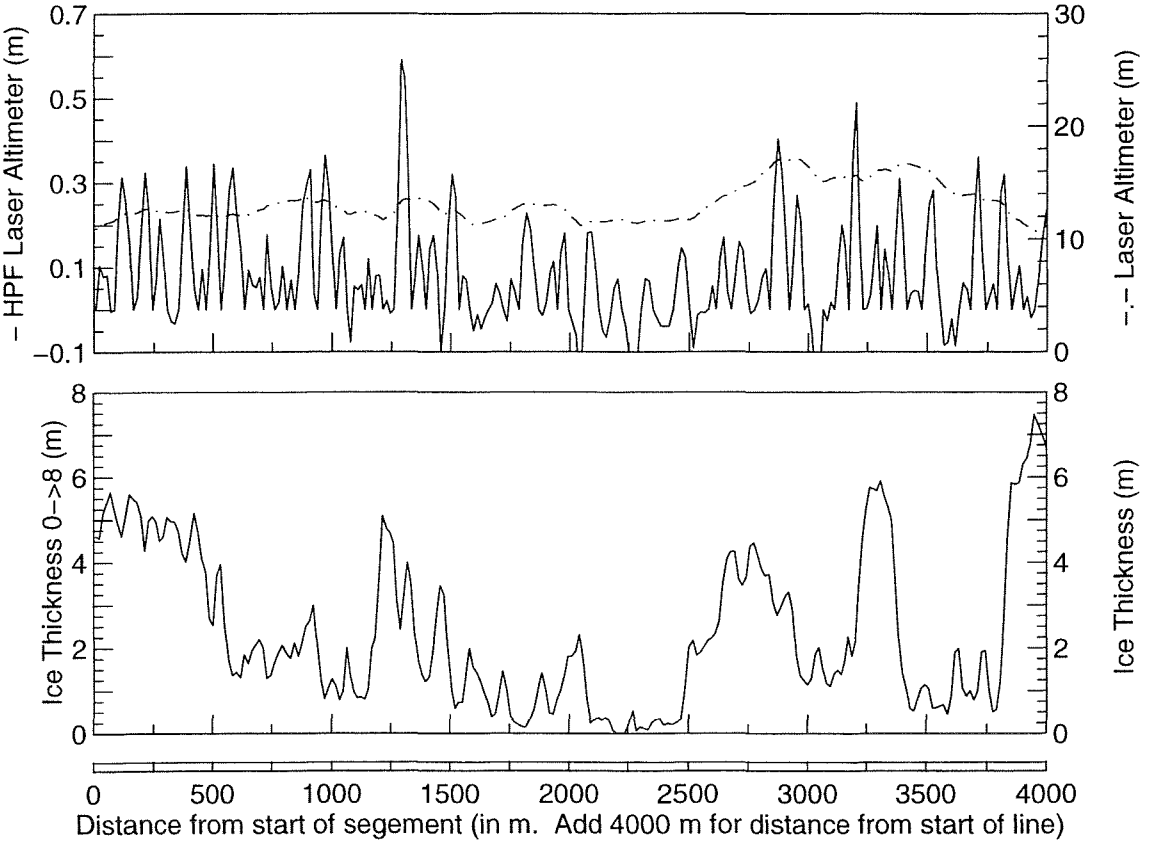

MAR 07 Flight #01 Line #10050 part 3 of 5

Line Starting Coordinates (53.2954,–55.6127) ending at (53.2612,–55.6307)

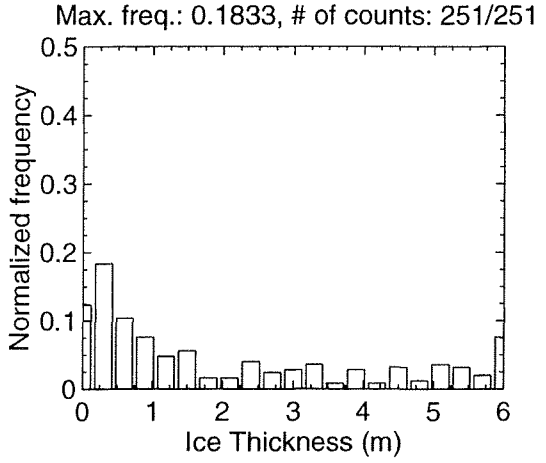

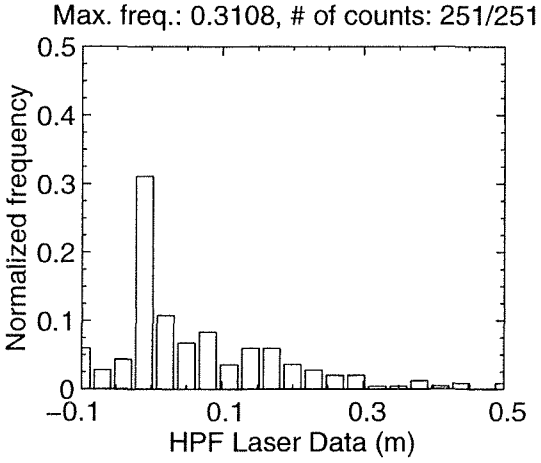

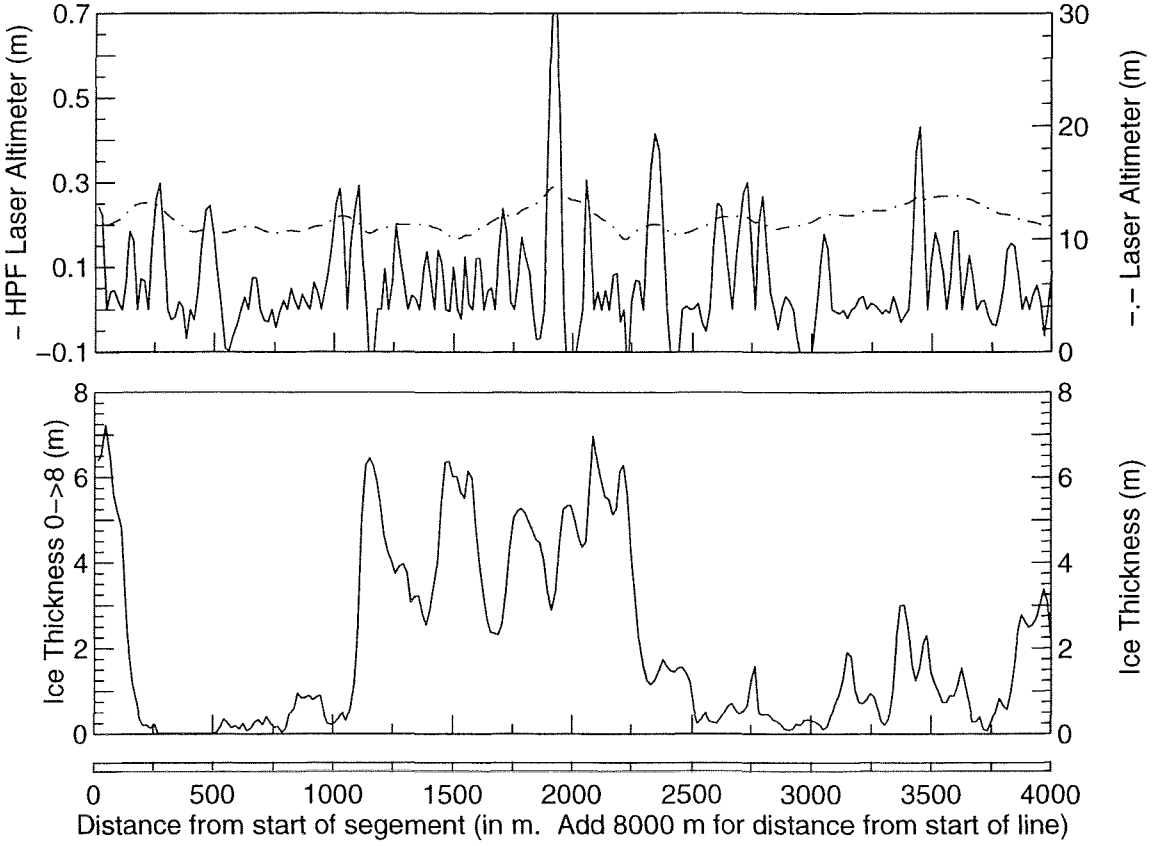

MAR 07 Flight #01 Line #10050 part 4 of 5

Line Starting Coordinates (53.2612,–55.6307) ending at (53.2269,–55.6489)

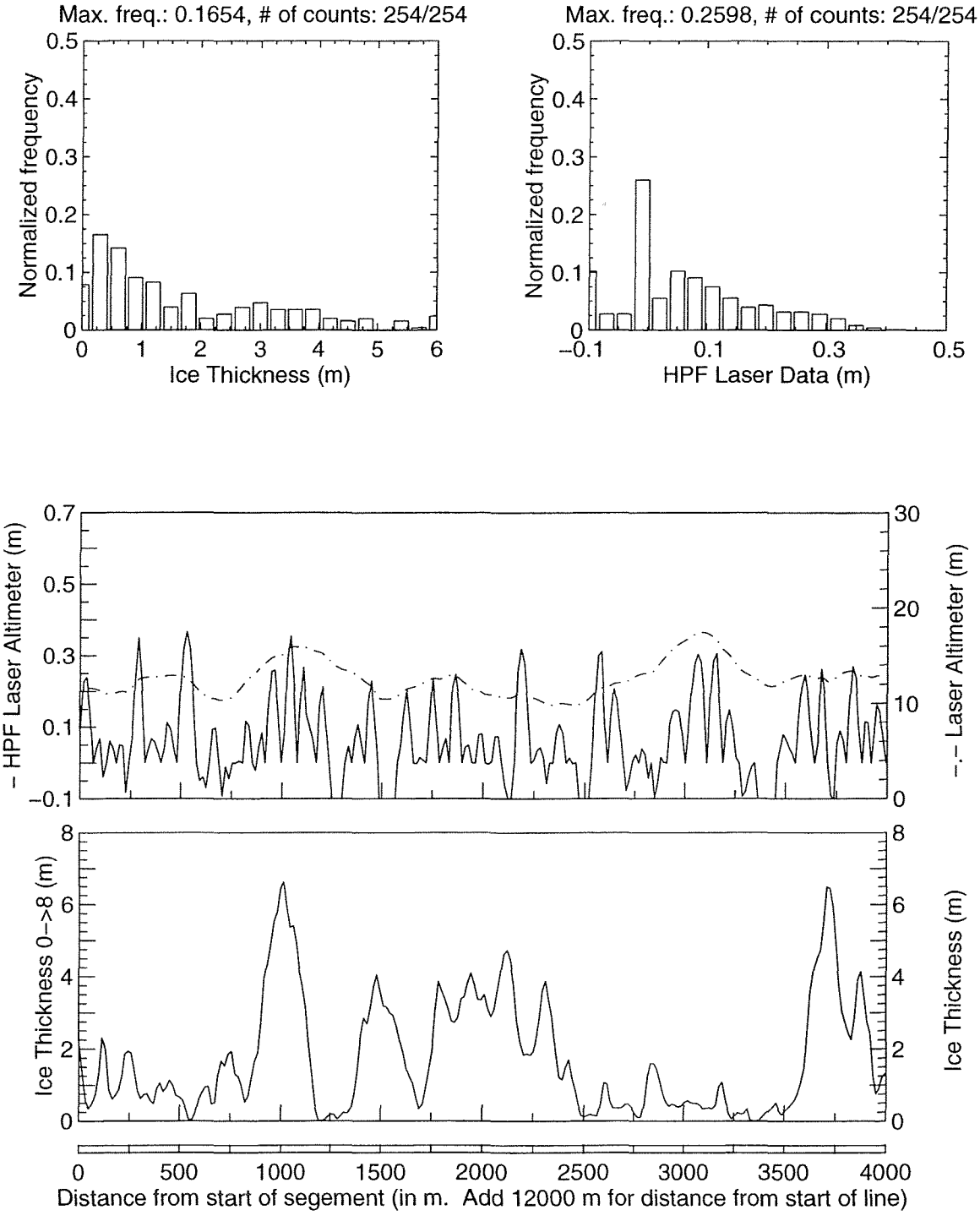

MAR 07 Flight #01 Line #10050 part 5 of 5

Line Starting Coordinates (53.2269,–55.6489) ending at (53.2131,–55.6553)

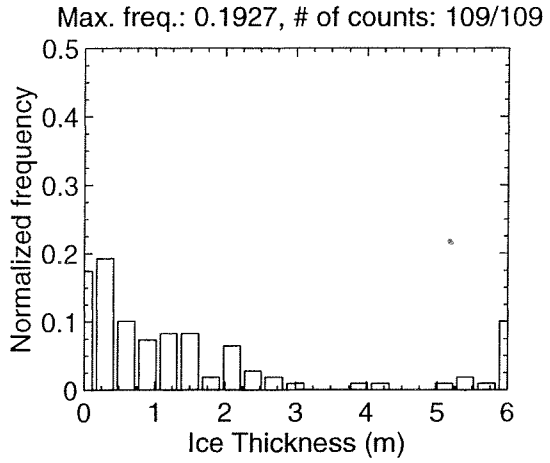

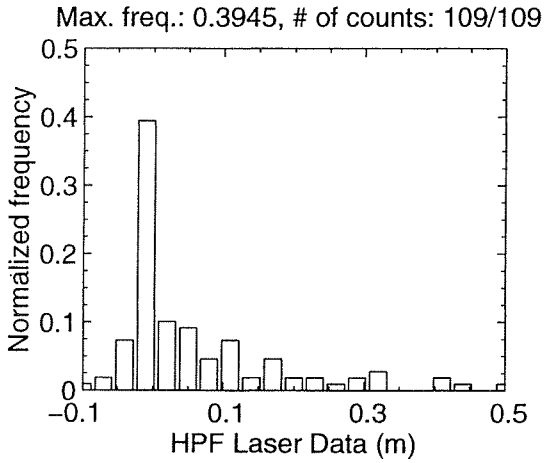

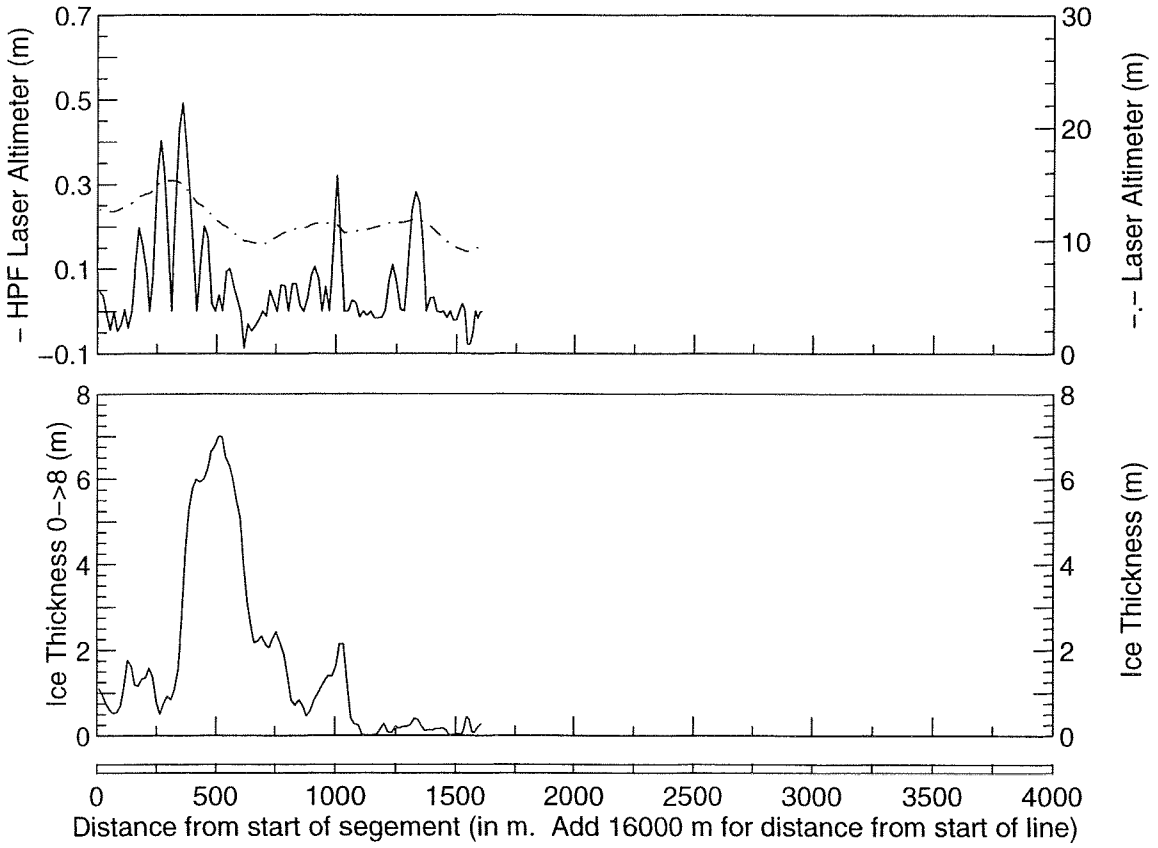

MAR 07 Flight #01 Line #10071 part 1 of 2

Line Starting Coordinates (53.0989,–55.6999) ending at (53.1119,–55.6441)

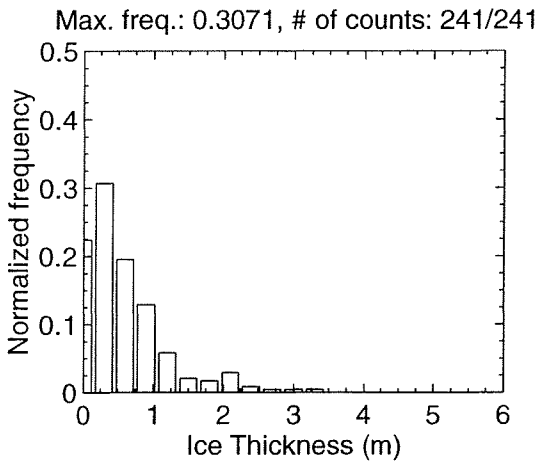

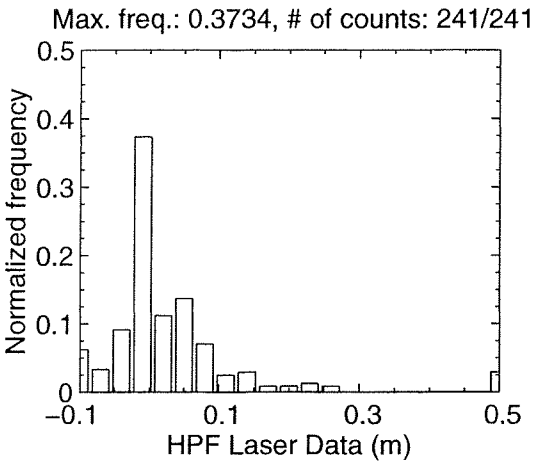

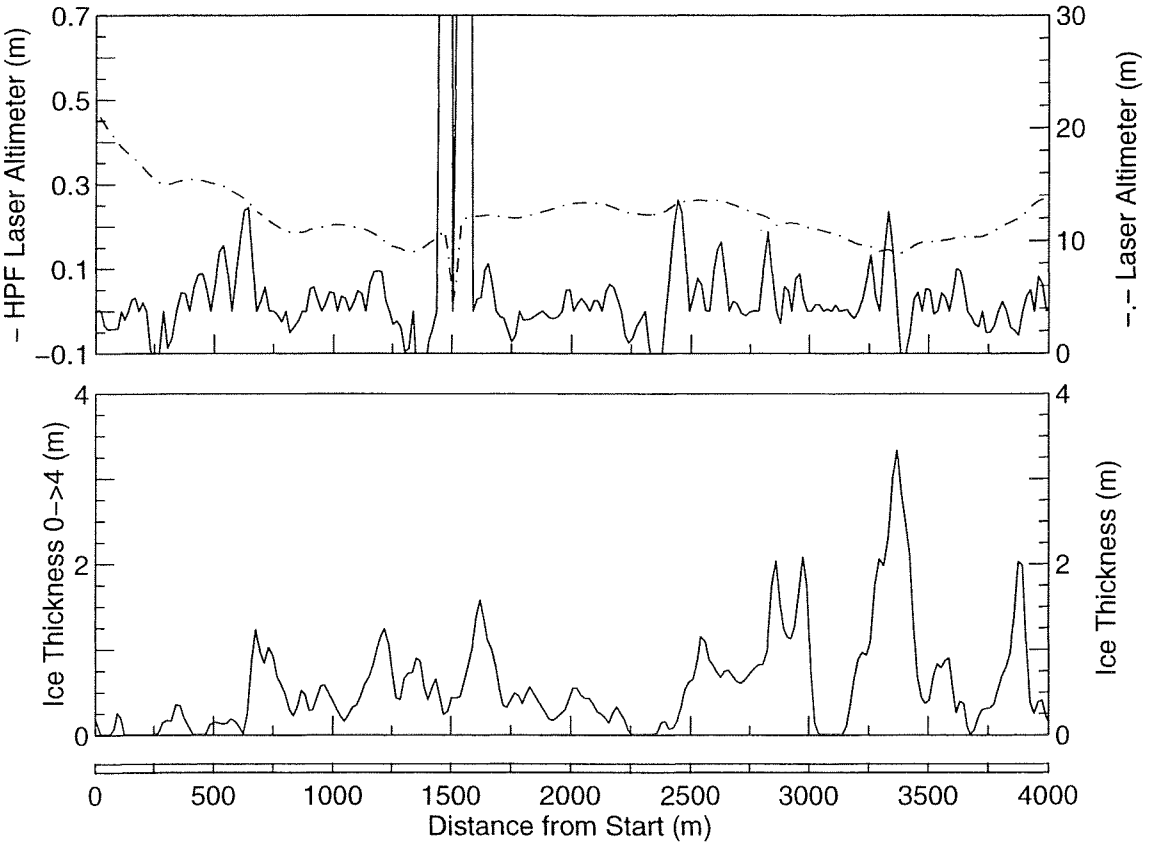

MAR 07 Flight #01 Line #10071 part 2 of 2

Line Starting Coordinates (53.1119,–55.6441) ending at (53.1257,–55.5974)

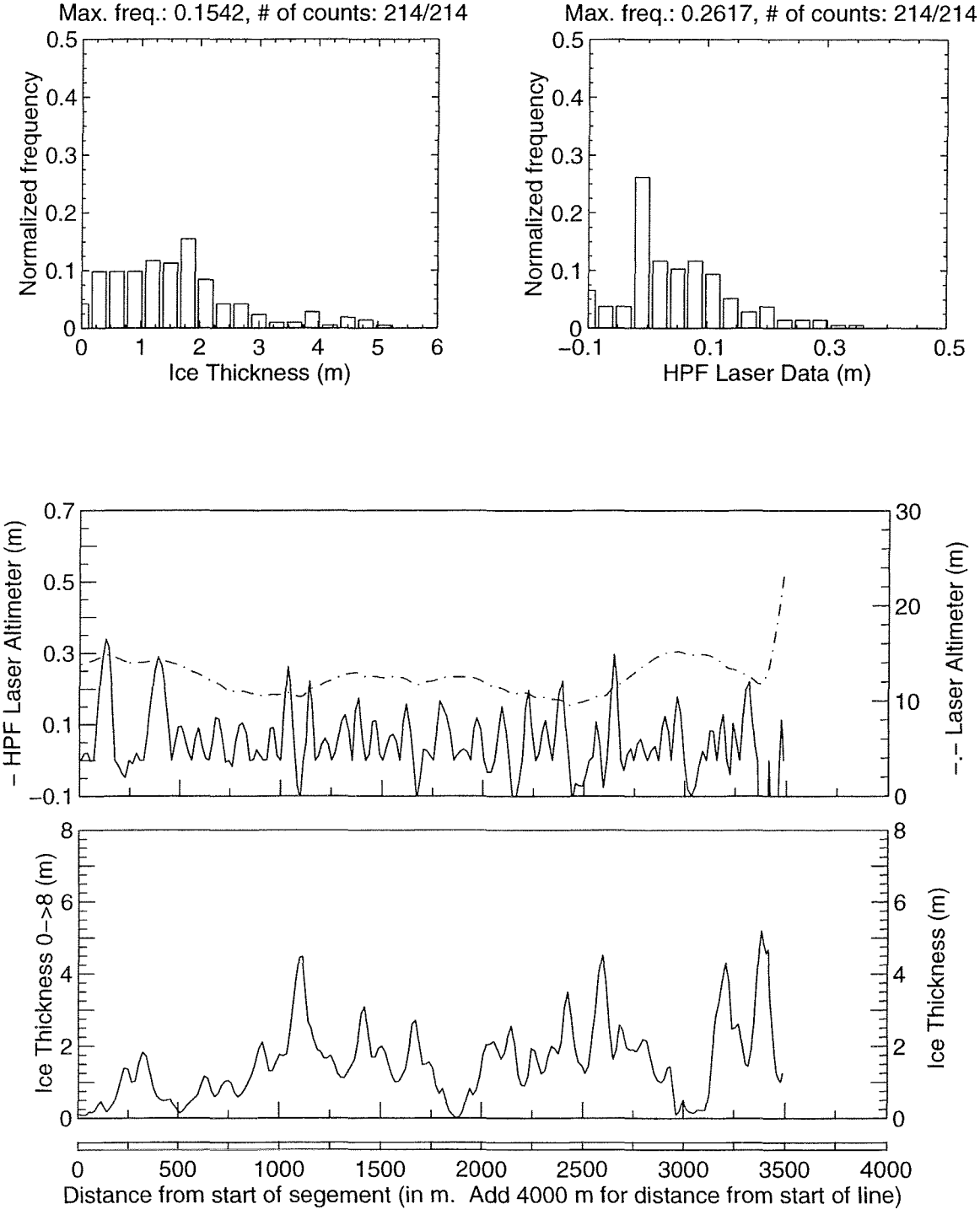

MAR 07 Flight #01 Line #10081 part 2 of 4

Line Starting Coordinates (53.3165,–55.6671) ending at (53.3510,–55.6835)

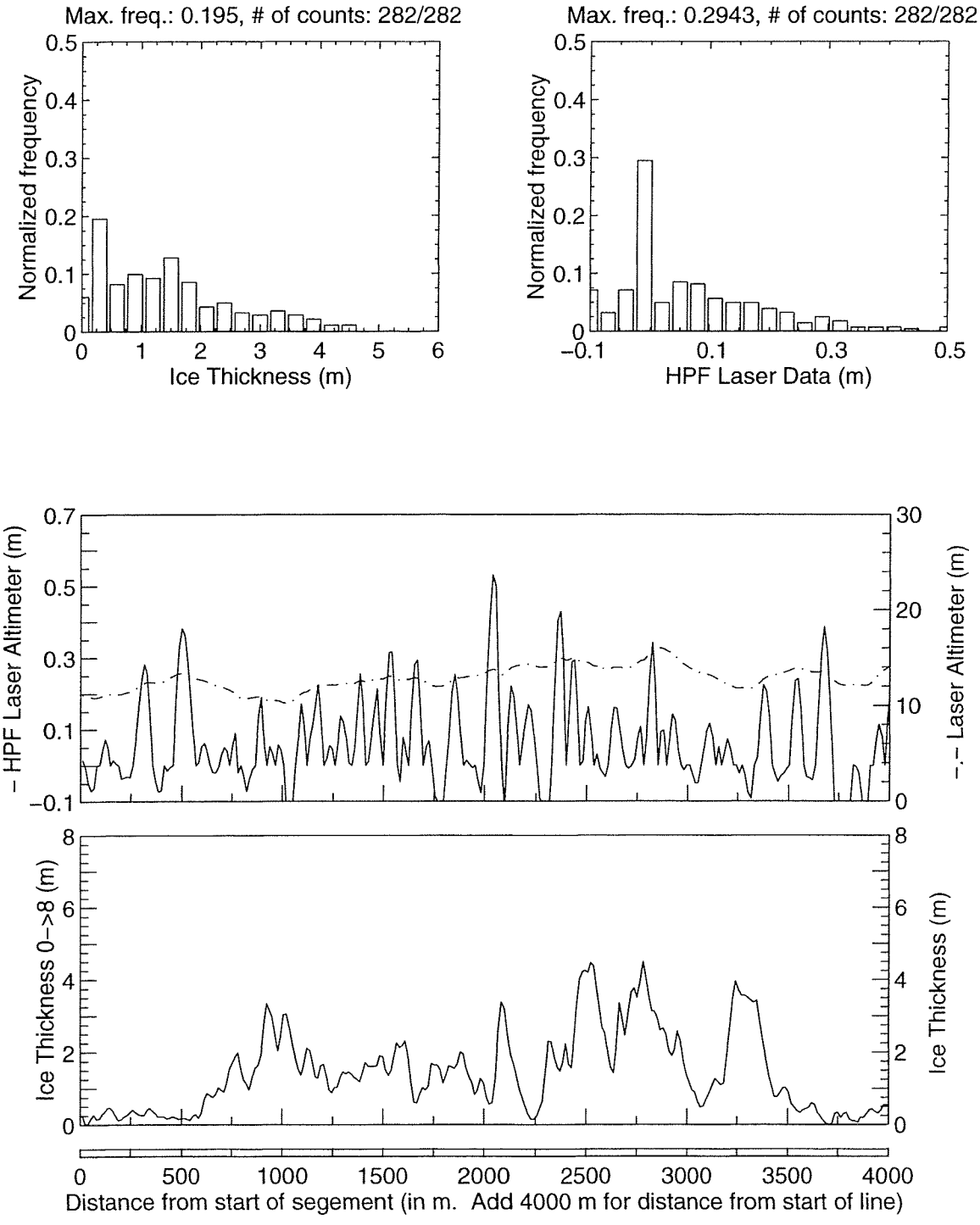

MAR 07 Flight #01 Line #10081 part 3 of 4

Line Starting Coordinates (53.3510,–55.6835) ending at (53.3859,–55.6975)

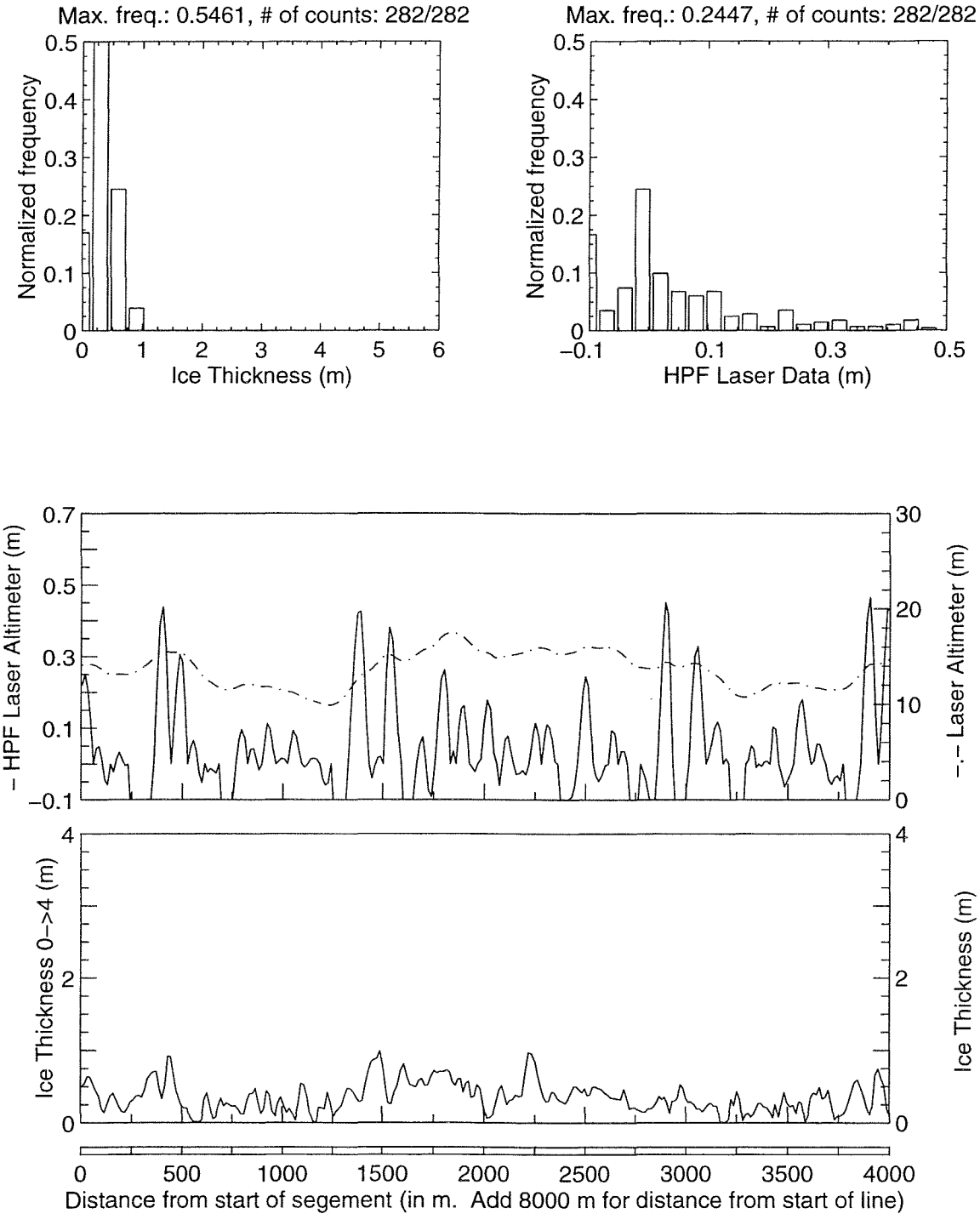

MAR 07 Flight #01 Line #10081 part 4 of 4

Line Starting Coordinates (53.3859,–55.6975) ending at (53.4209,–55.7076)

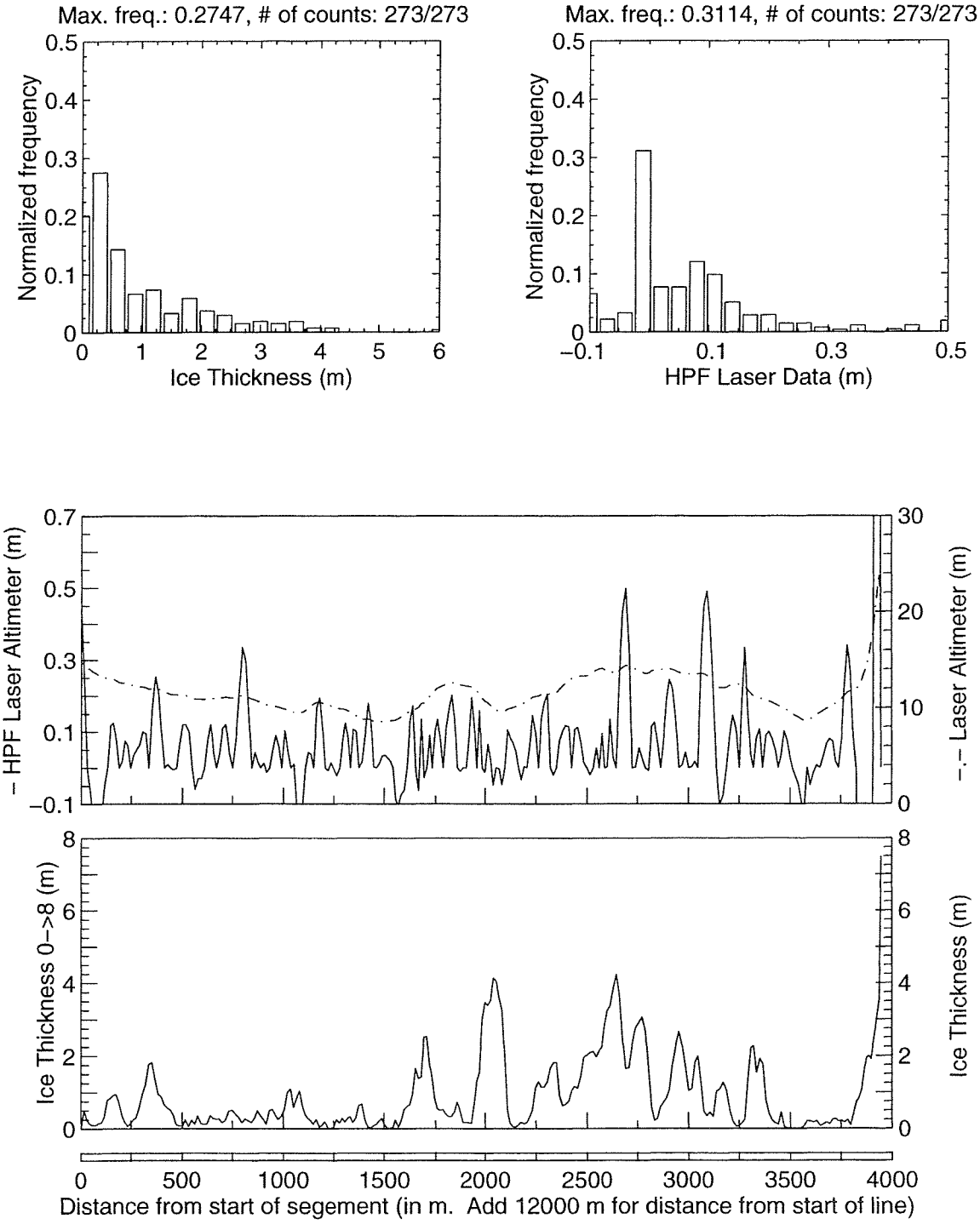

MAR 07 Flight #01 Line #10090 part 1 of 3

Line Starting Coordinates (53.4110,–55.8923) ending at (53.4231,–55.9492)

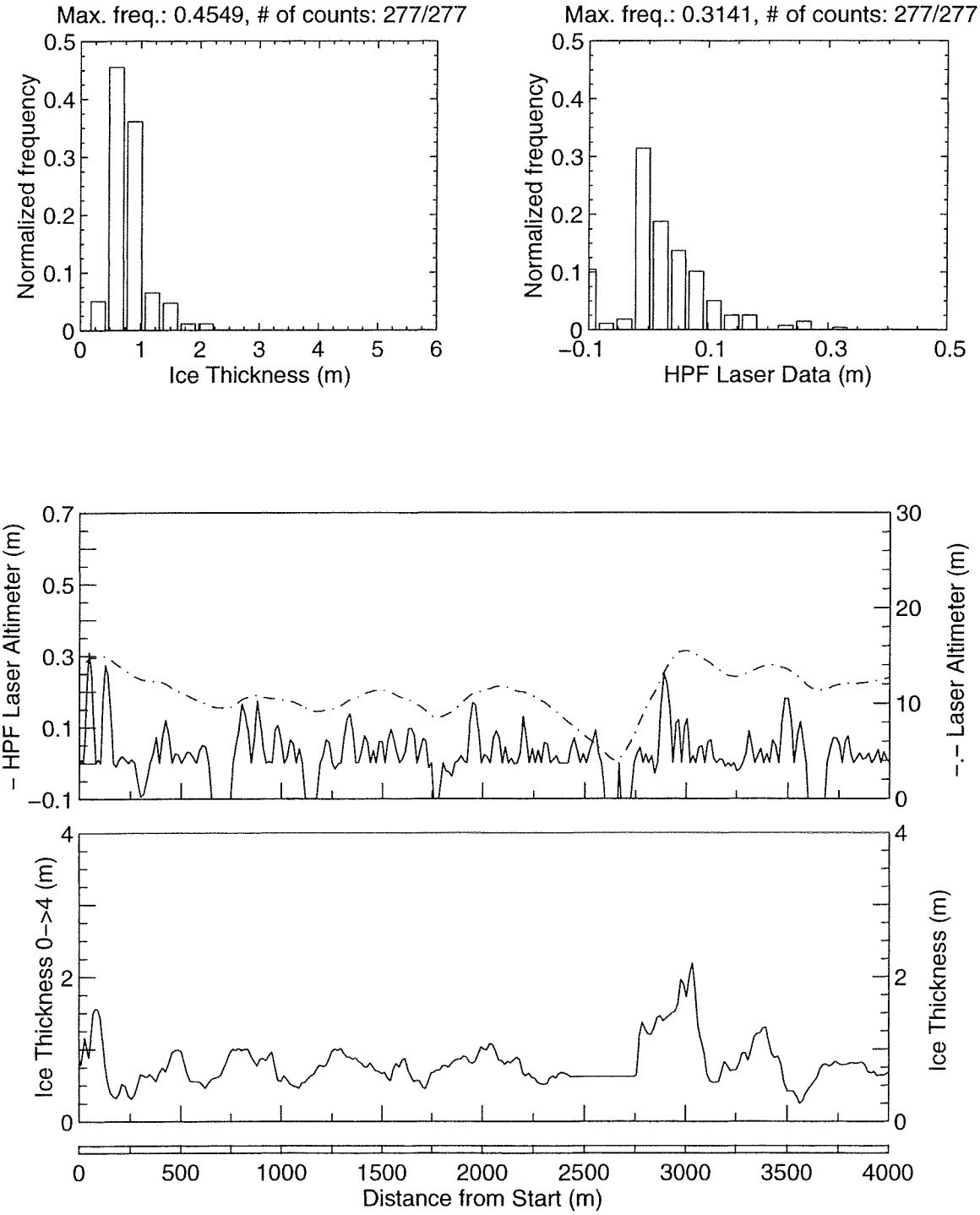

MAR 07 Flight #01 Line #10090 part 2 of 3

Line Starting Coordinates (53.4231,–55.9492) ending at (53.4451,–55.9957)

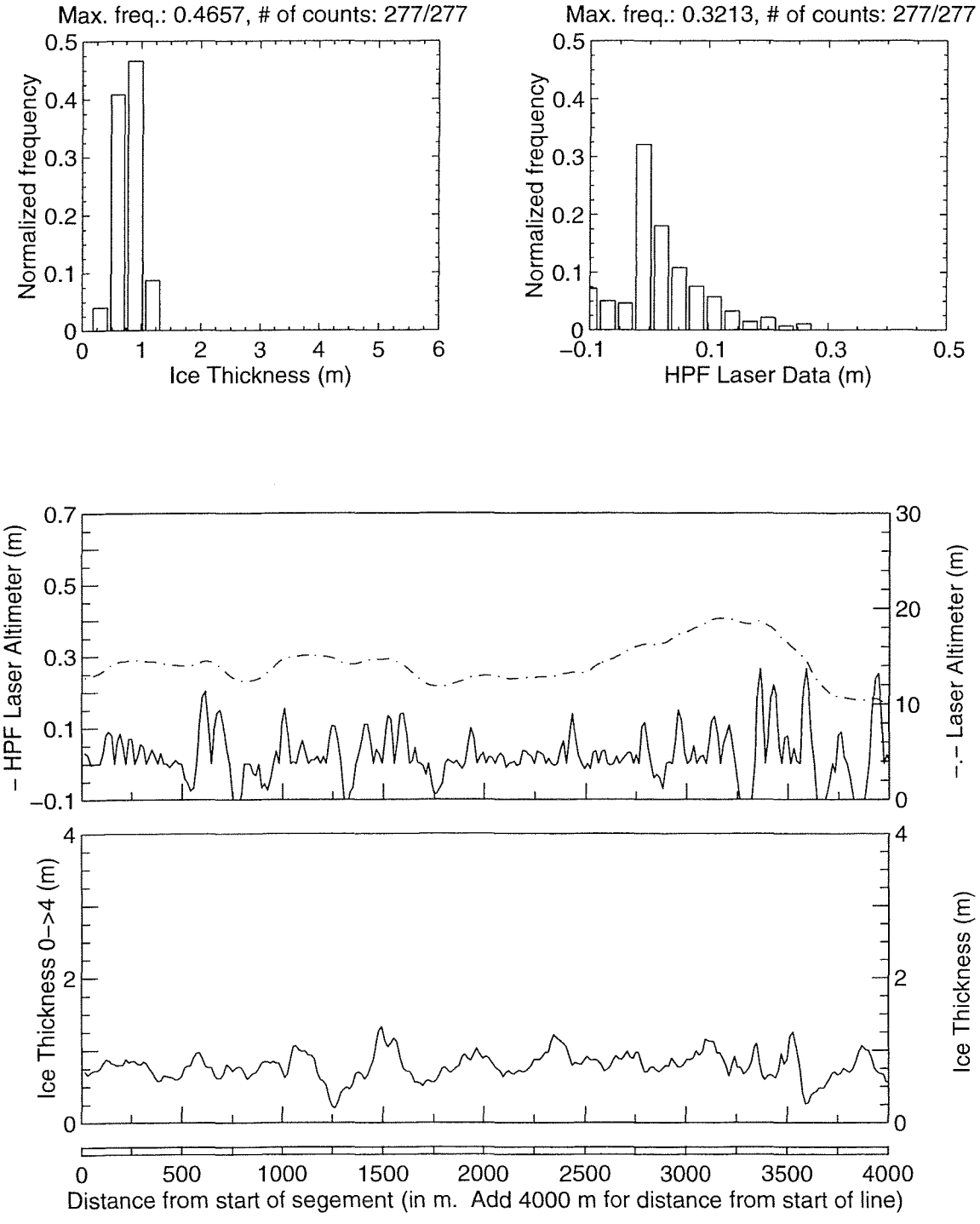

MAR 07 Flight #01 Line #10090 part 3 of 3

Line Starting Coordinates (53.4451,–55.9957) ending at (53.4521,–56.0065)

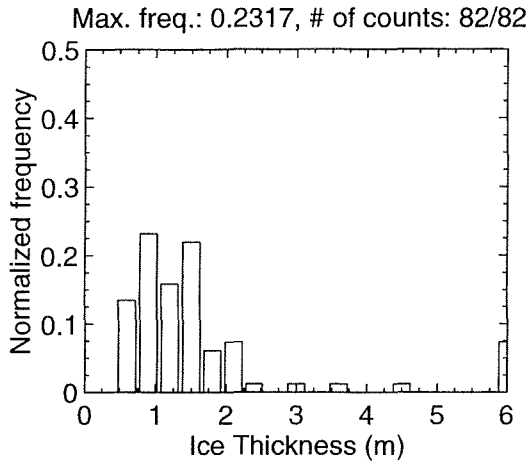

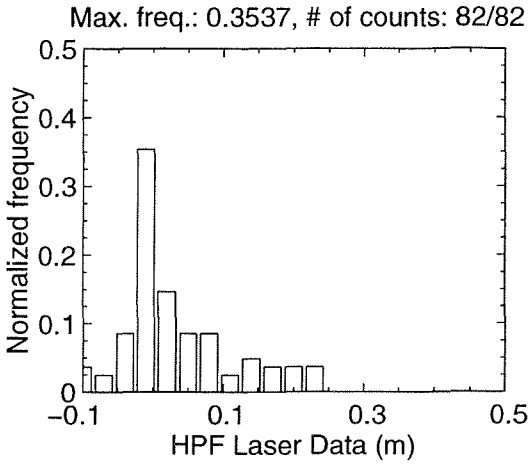

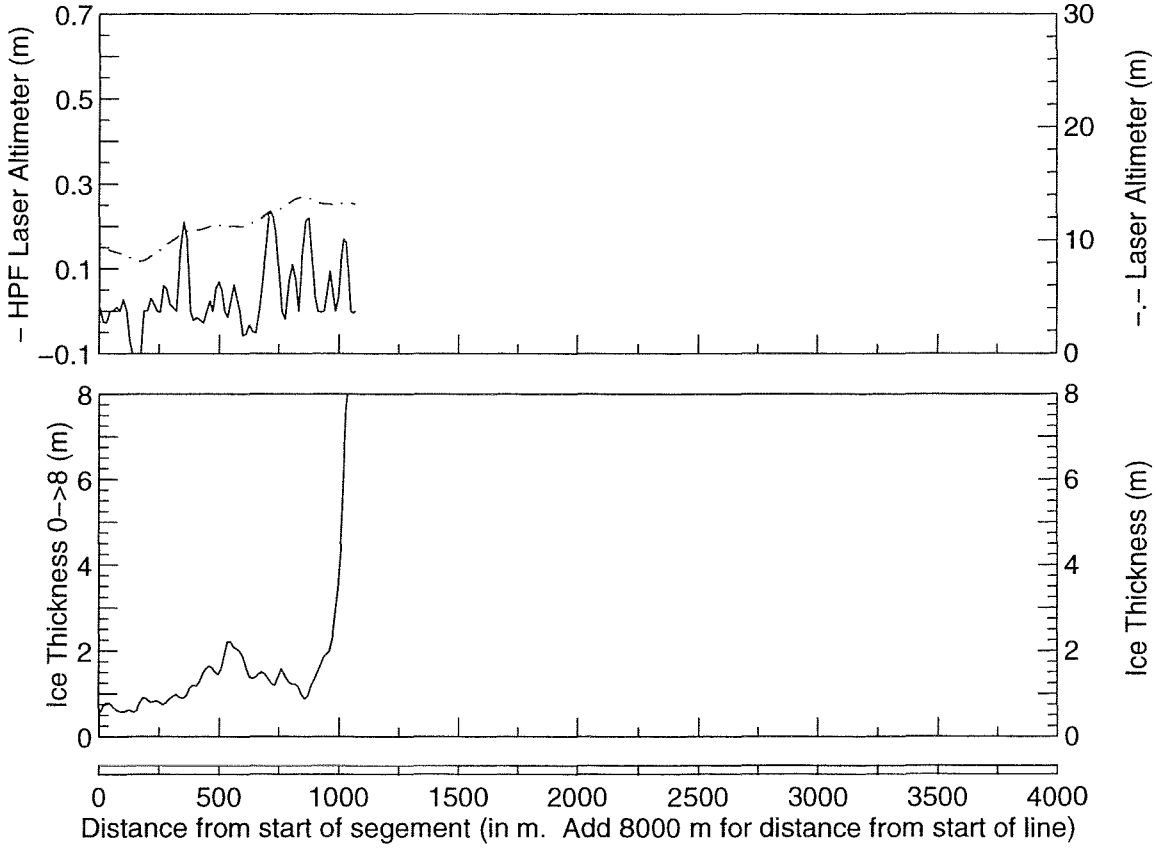

MAR 07 Flight #01 Line #10100 part 1 of 4

Line Starting Coordinates (53.4633,–56.0083) ending at (53.4938,–55.9760)

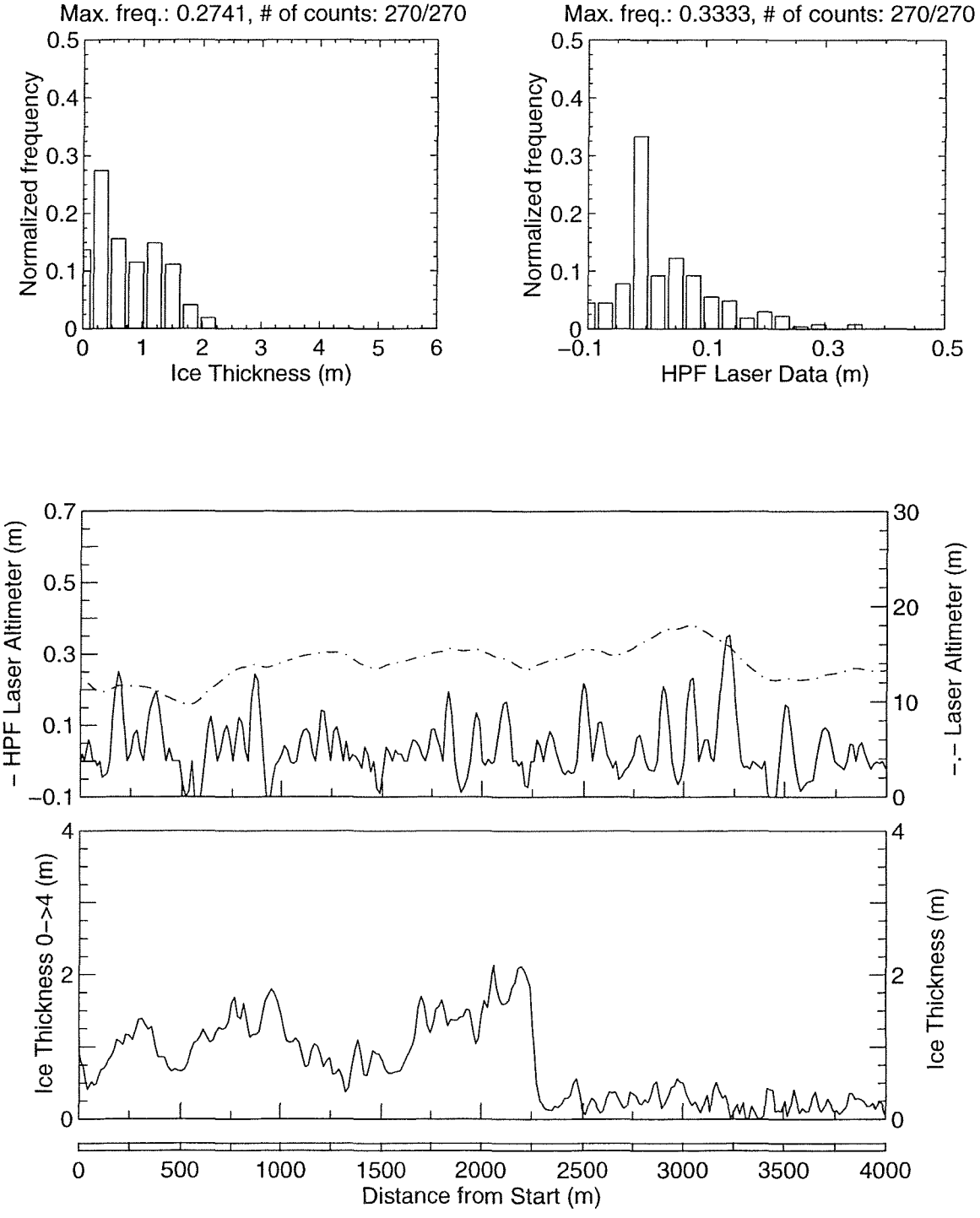

MAR 07 Flight #01 Line #10100 part 2 of 4

Line Starting Coordinates (53.4938,–55.9760) ending at (53.5234,–55.9421)

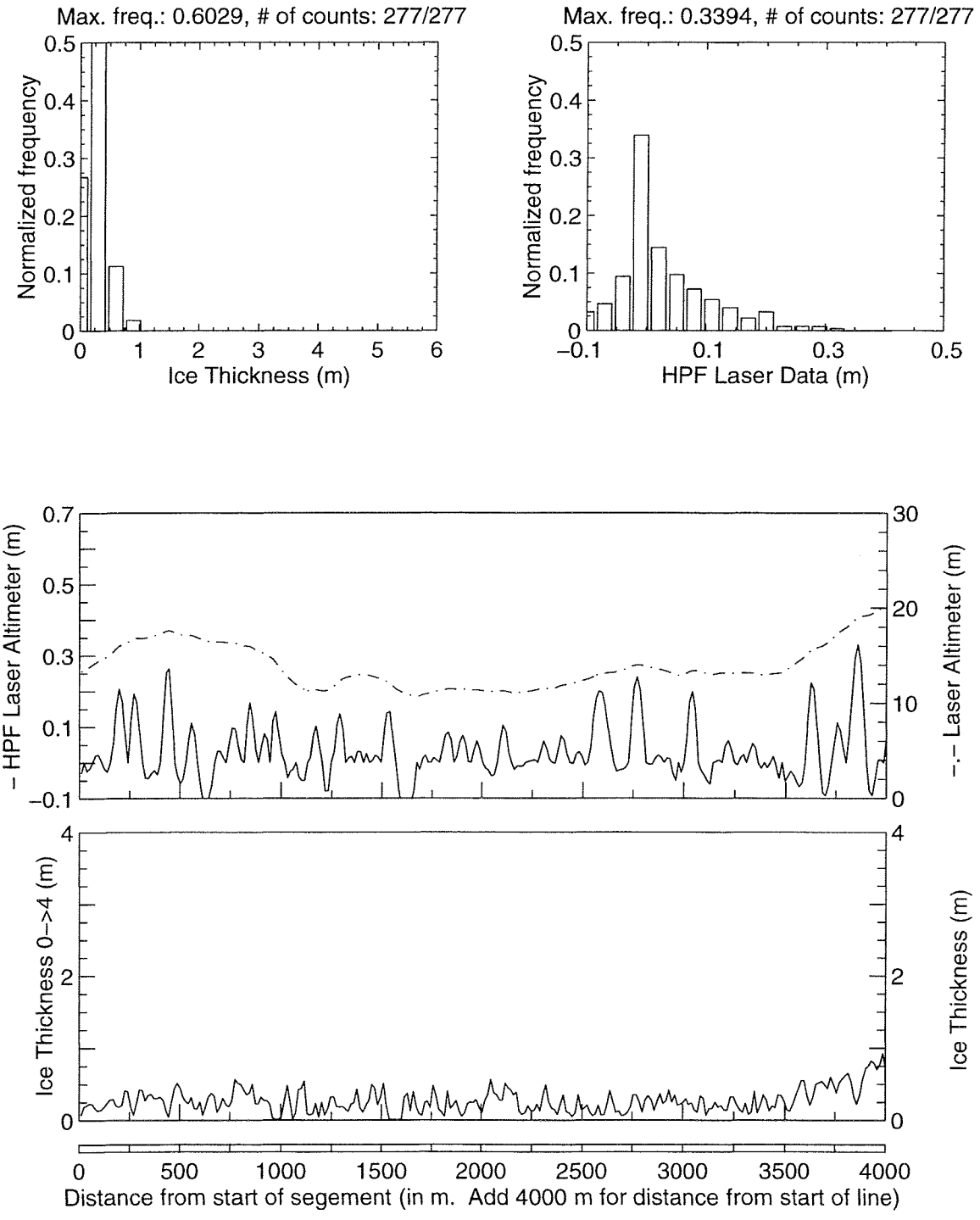

MAR 07 Flight #01 Line #10100 part 3 of 4

Line Starting Coordinates (53.5234,–55.9421) ending at (53.5534,–55.9087)

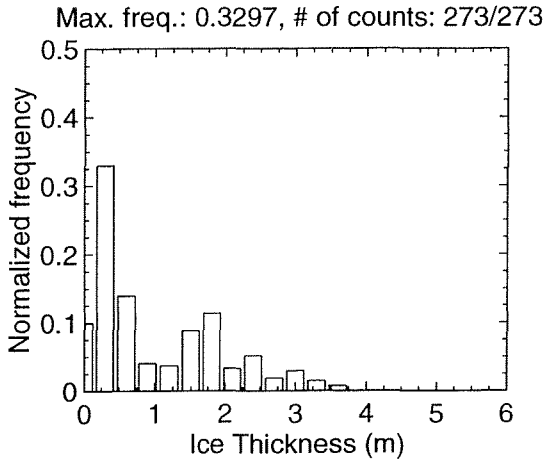

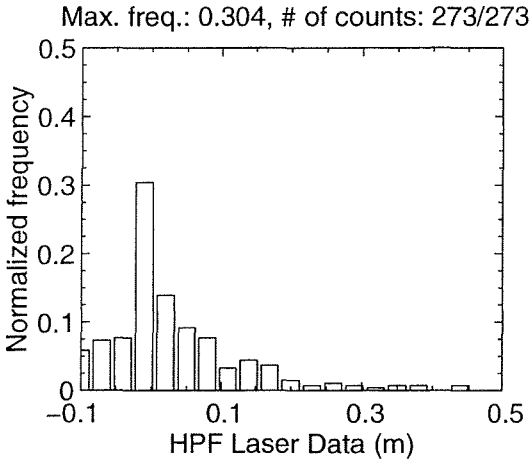

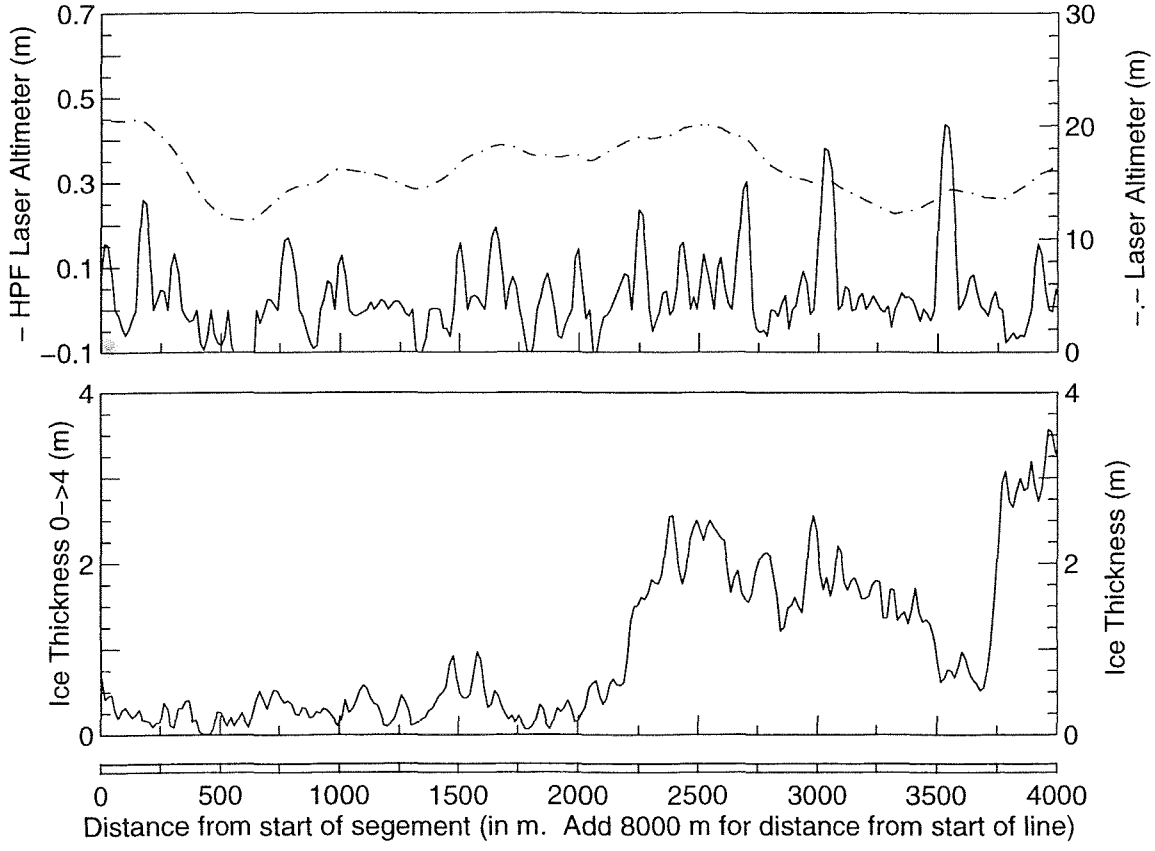

MAR 07 Flight #01 Line #10100 part 4 of 4

Line Starting Coordinates (53.5534,–55.9087) ending at (53.5609,–55.9000)

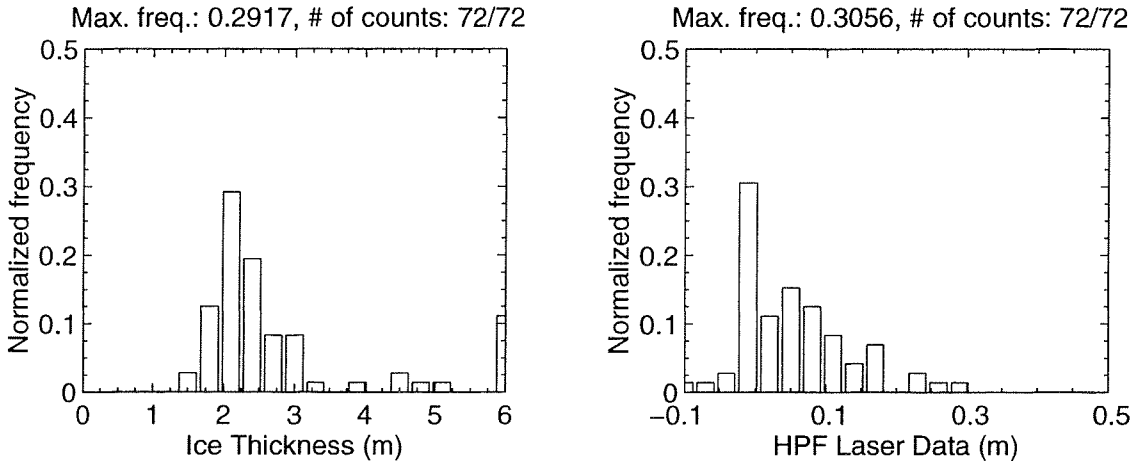

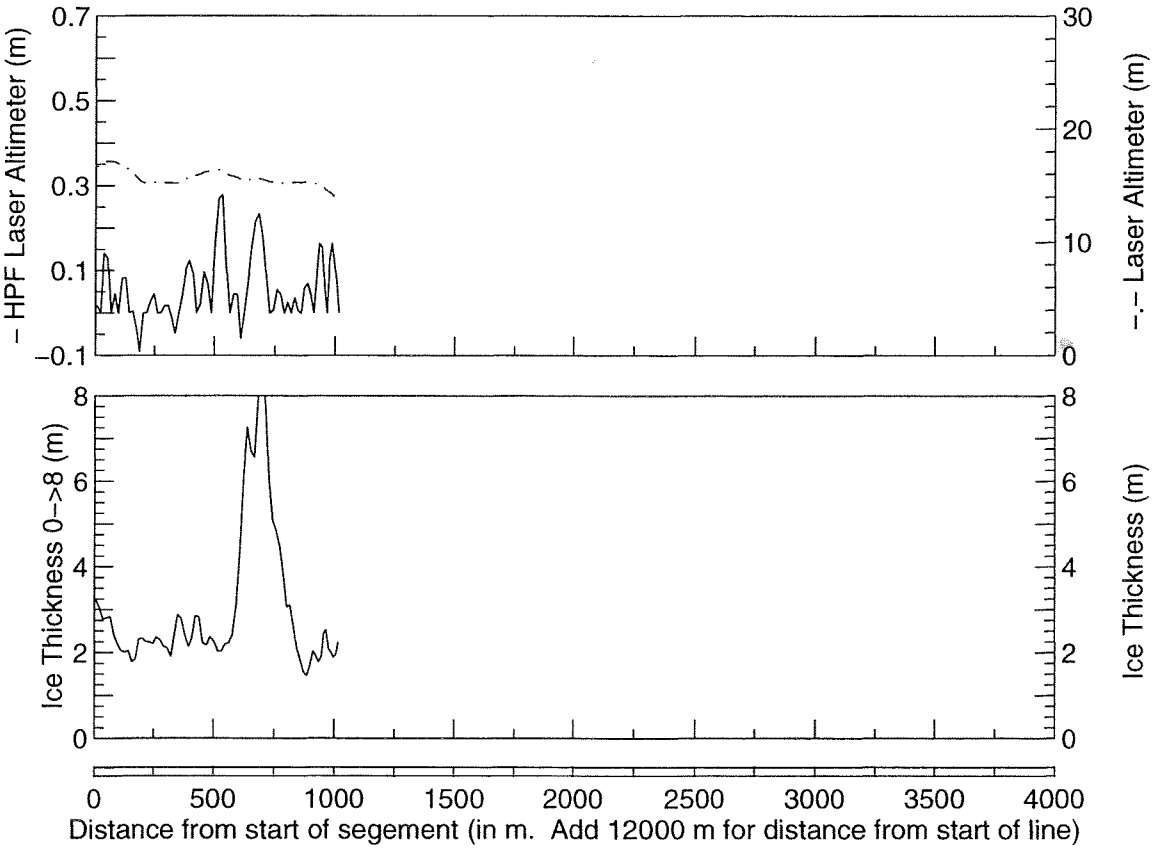

MAR 07 Flight #01 Line #10110 part 1 of 6

Line Starting Coordinates (53.5803,–55.9143) ending at (53.5915,–55.9719)

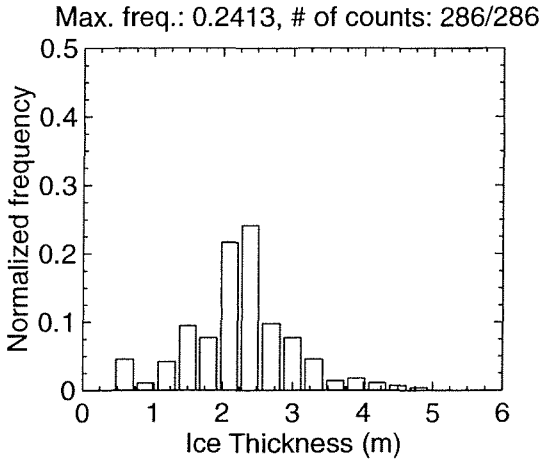

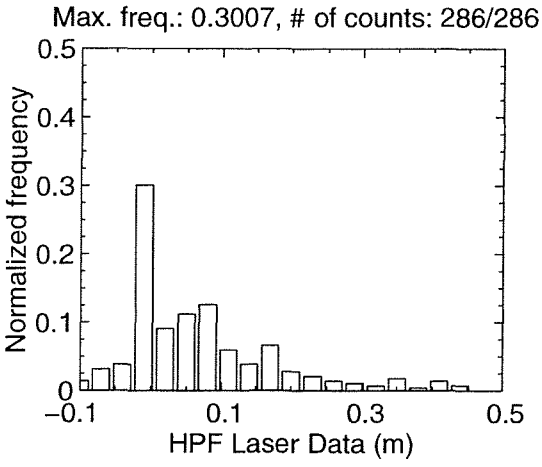

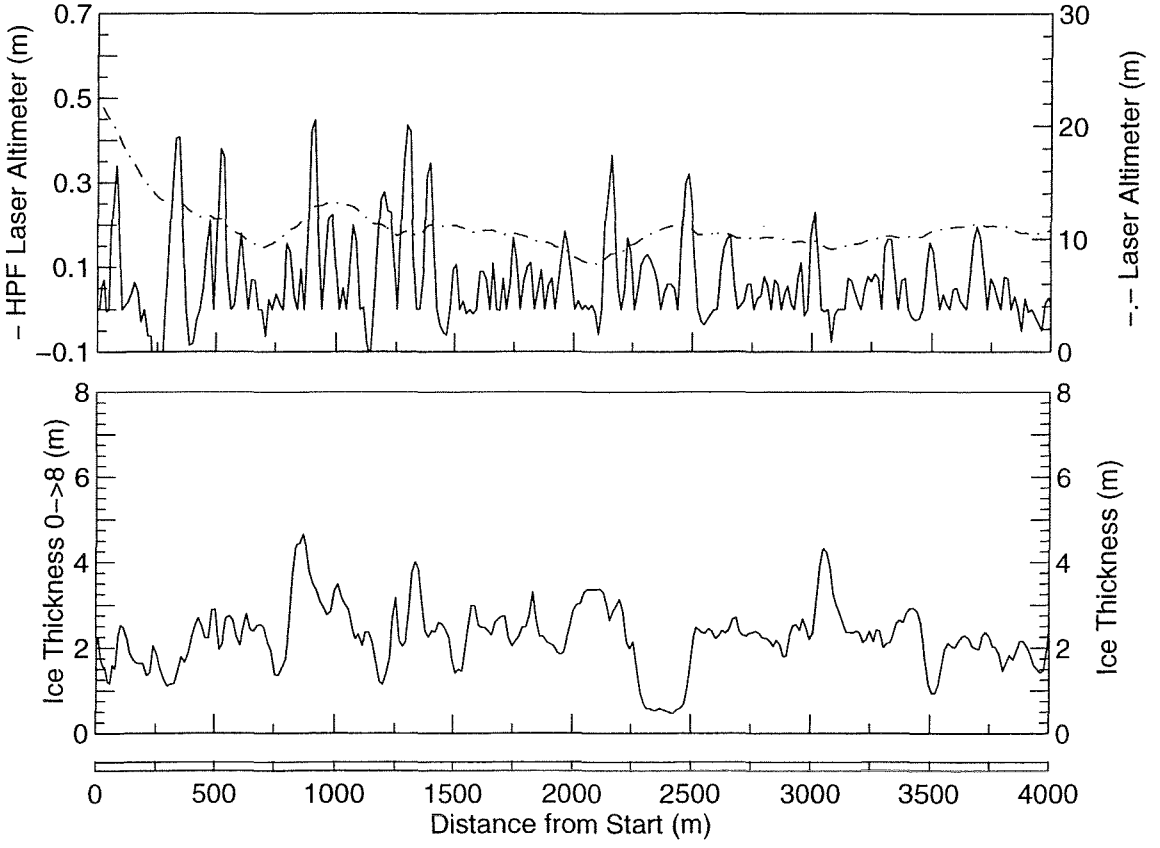

MAR 07 Flight #01 Line #10110 part 2 of 6

Line Starting Coordinates (53.5915,–55.9719) ending at (53.6026,–56.0295)

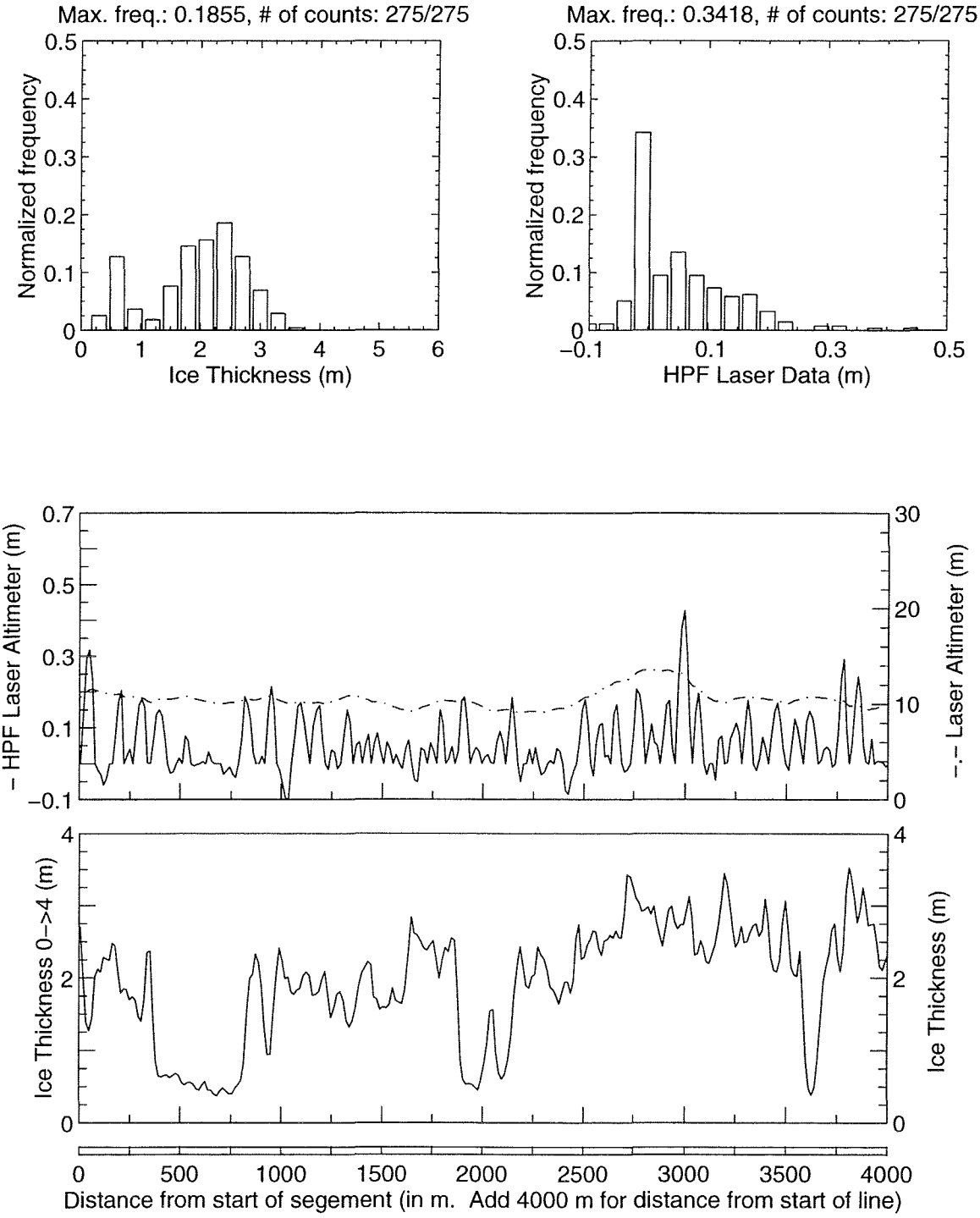

MAR 07 Flight #01 Line #10110 part 3 of 6

Line Starting Coordinates (53.6026,–56.0295) ending at (53.6136,–56.0873)

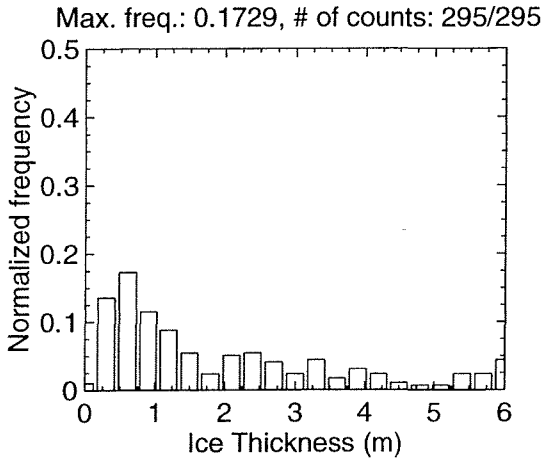

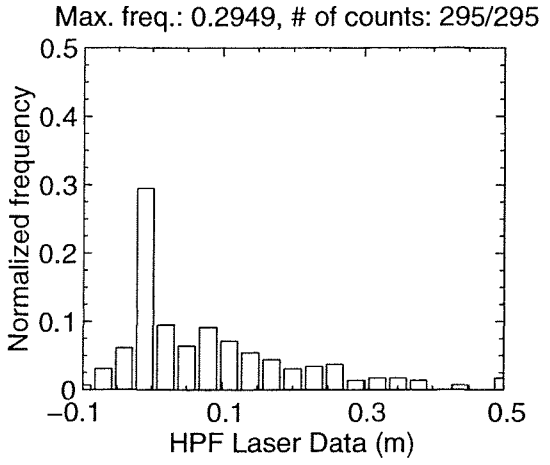

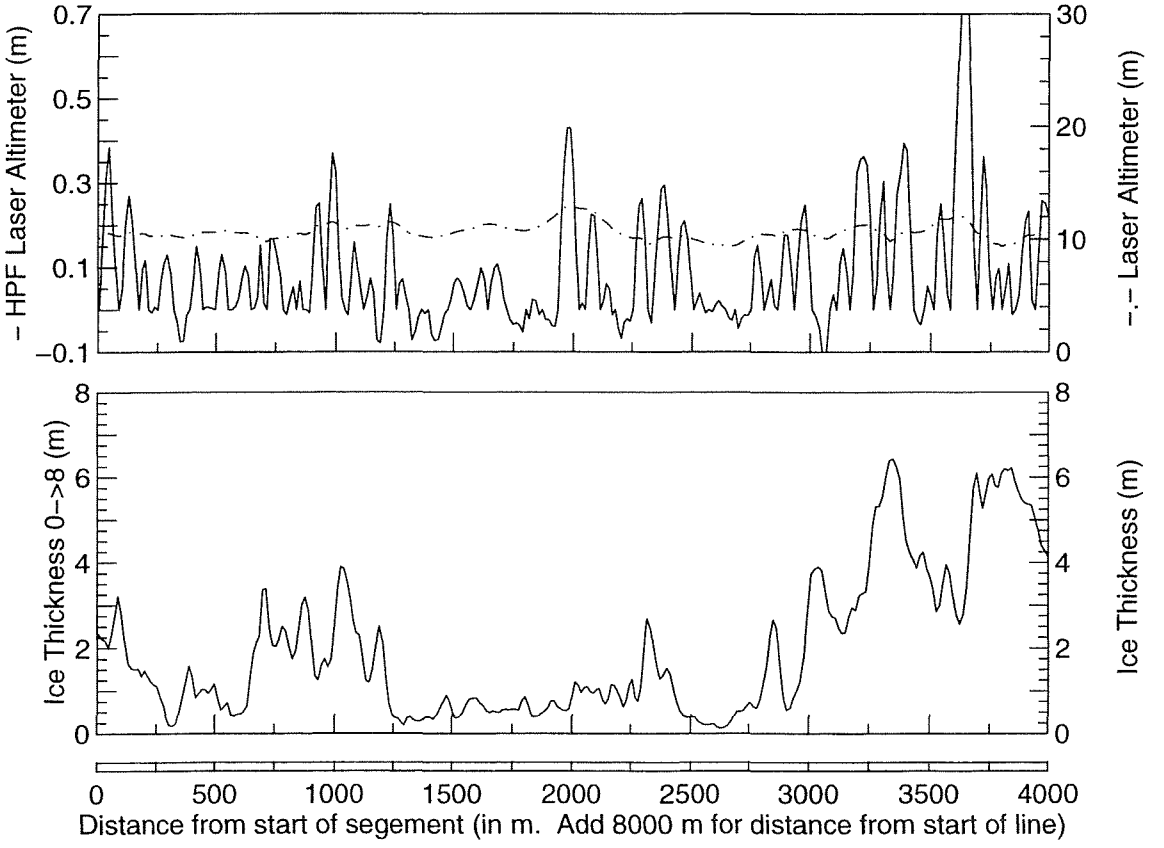

MAR 07 Flight #01 Line #10110 part 4 of 6

Line Starting Coordinates (53.6136,–56.0873) ending at (53.6243,–56.1451)

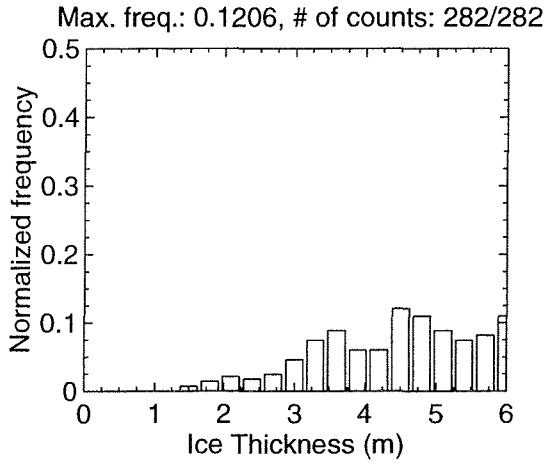

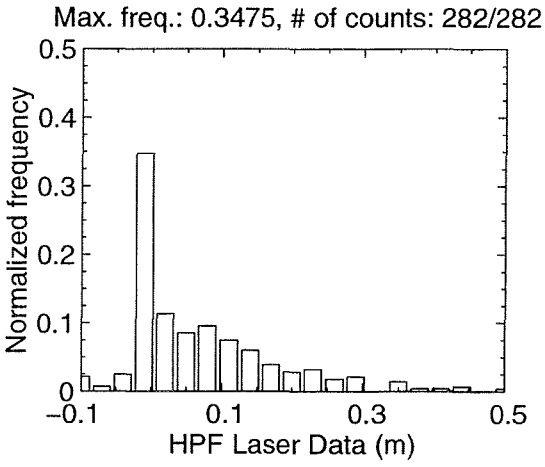

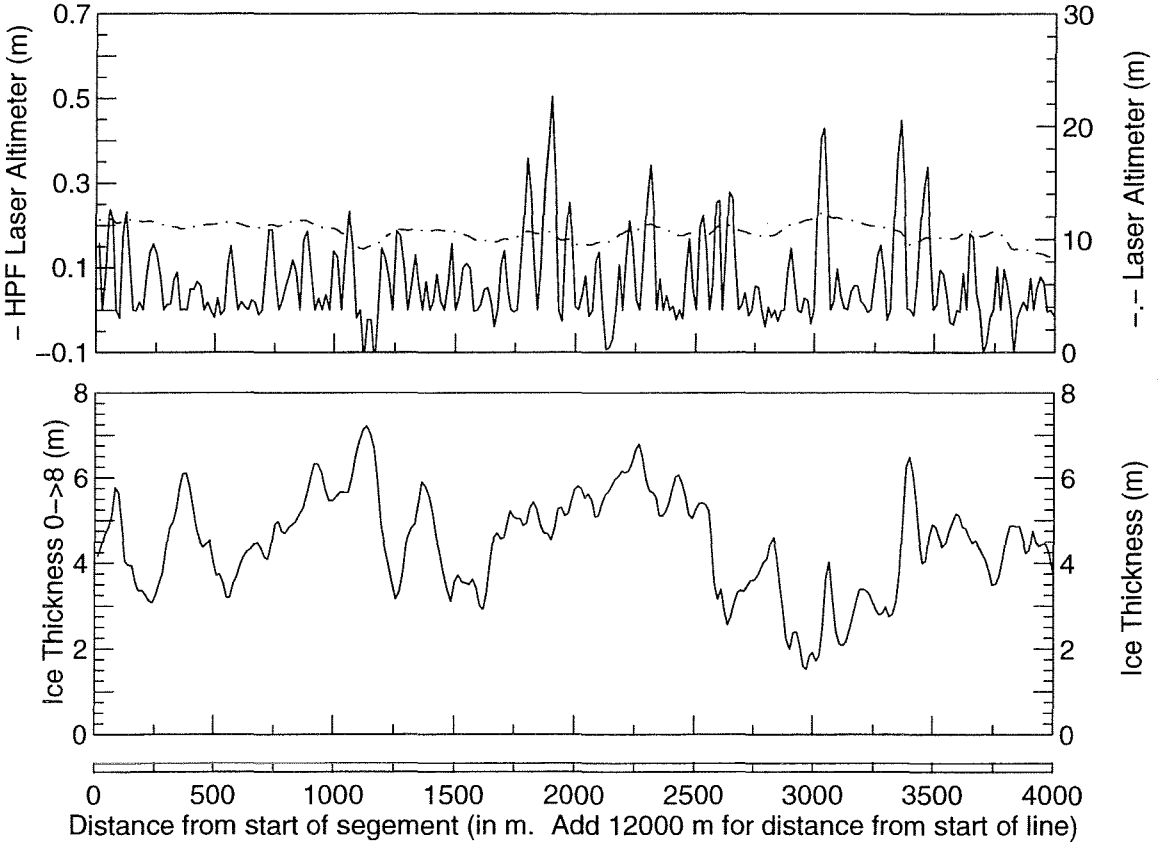

MAR 07 Flight #01 Line #10110 part 5 of 6

Line Starting Coordinates (53.6243,–56.1451) ending at (53.6361,–56.2023)

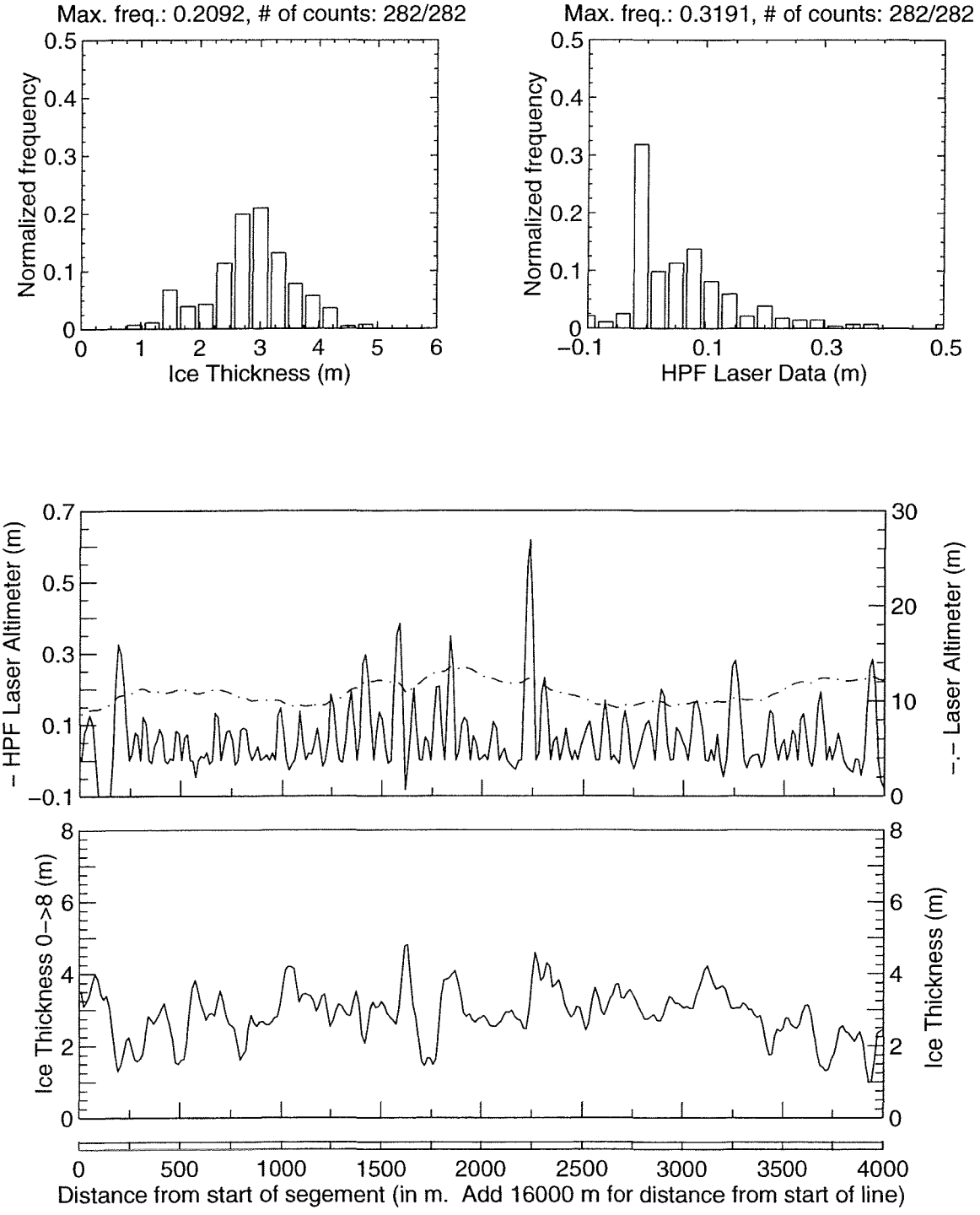

MAR 07 Flight #01 Line #10110 part 6 of 6

Line Starting Coordinates (53.6361,–56.2023) ending at (53.6478,–56.2580)

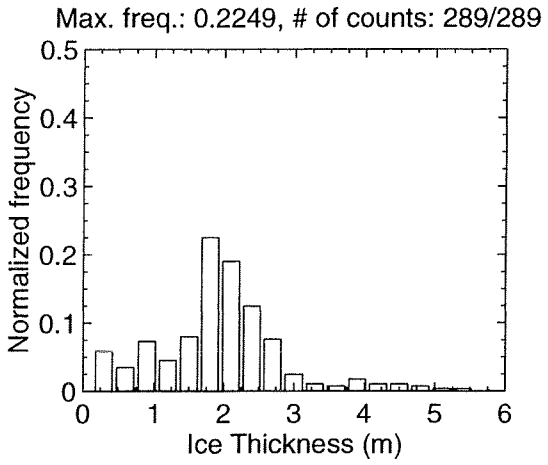

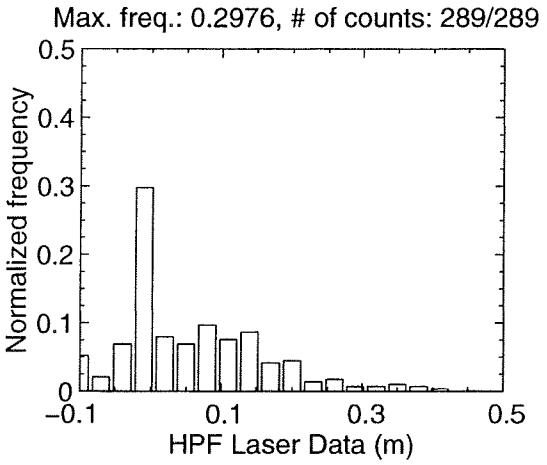

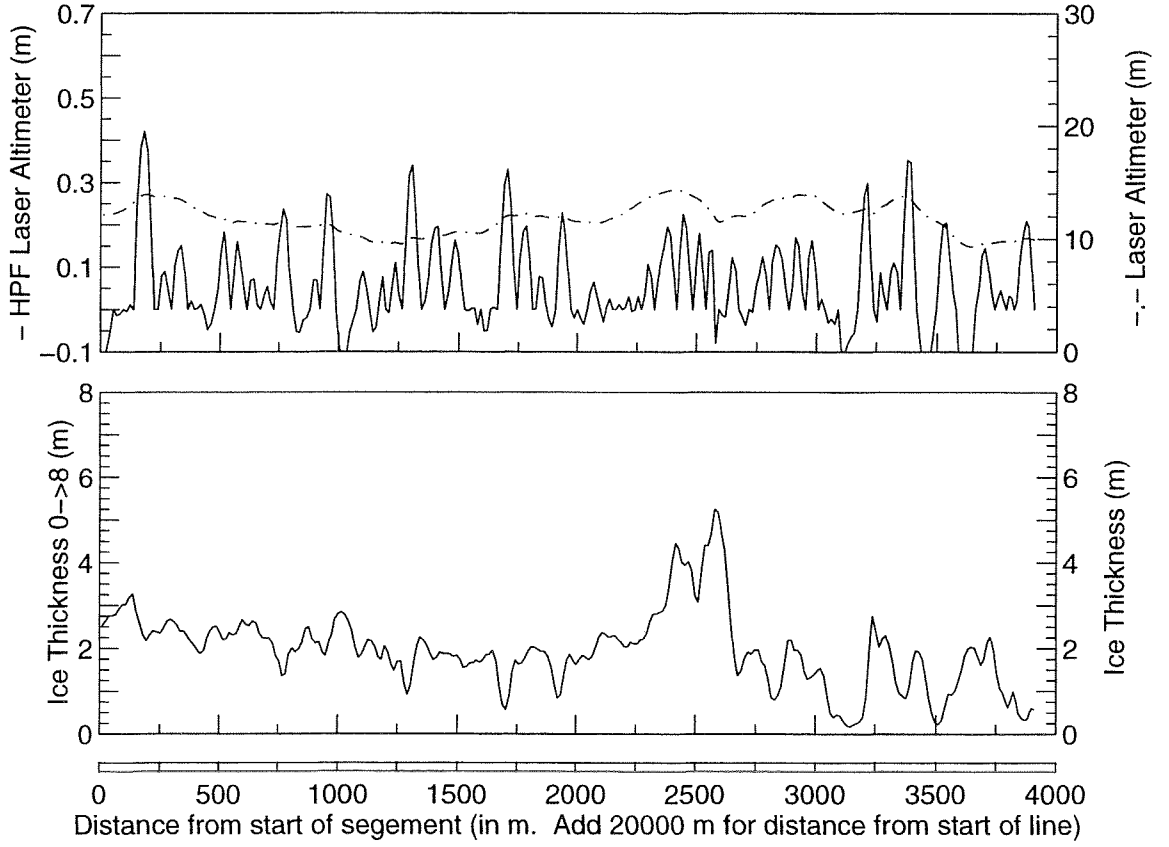

MAR 07 Flight #01 Line #10120 part 1 of 4

Line Starting Coordinates (53.6513,–56.2899) ending at (53.6616,–56.3478)

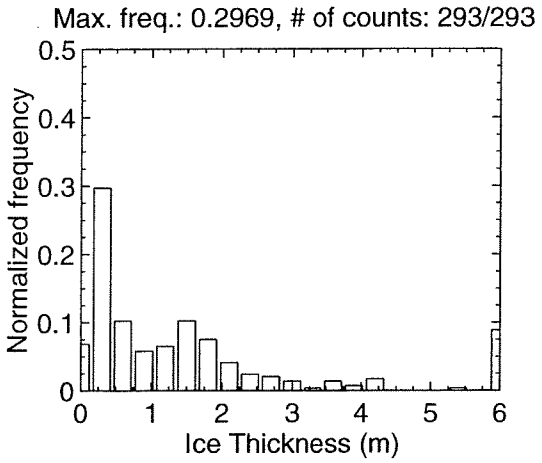

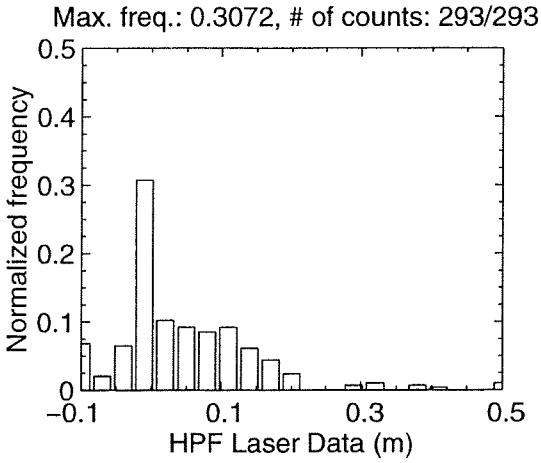

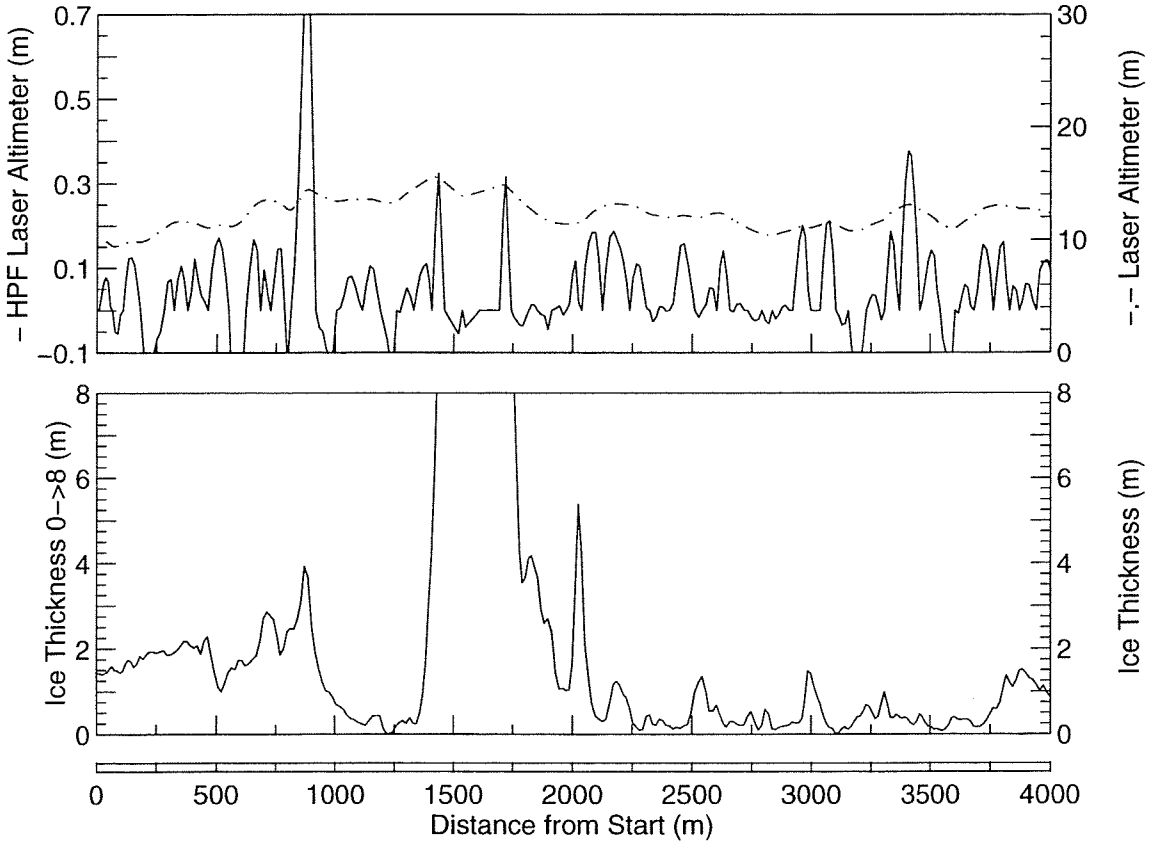

MAR 07 Flight #01 Line #10120 part 2 of 4

Line Starting Coordinates (53.6616,−56.3478) ending at (53.6781,−56.4018)

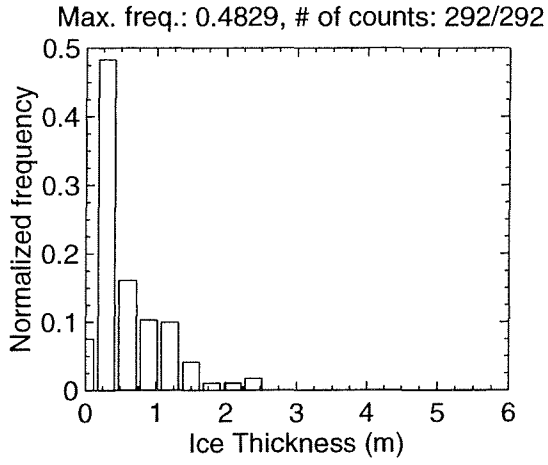

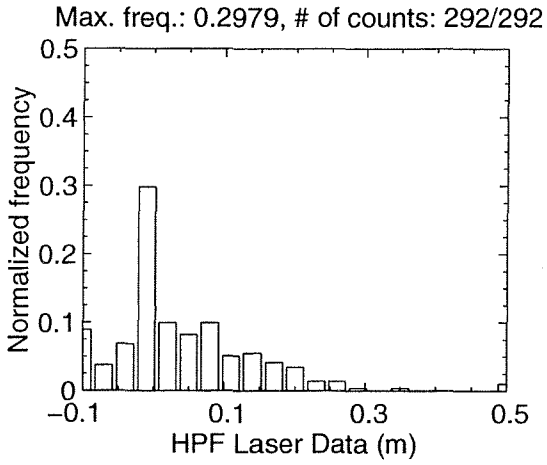

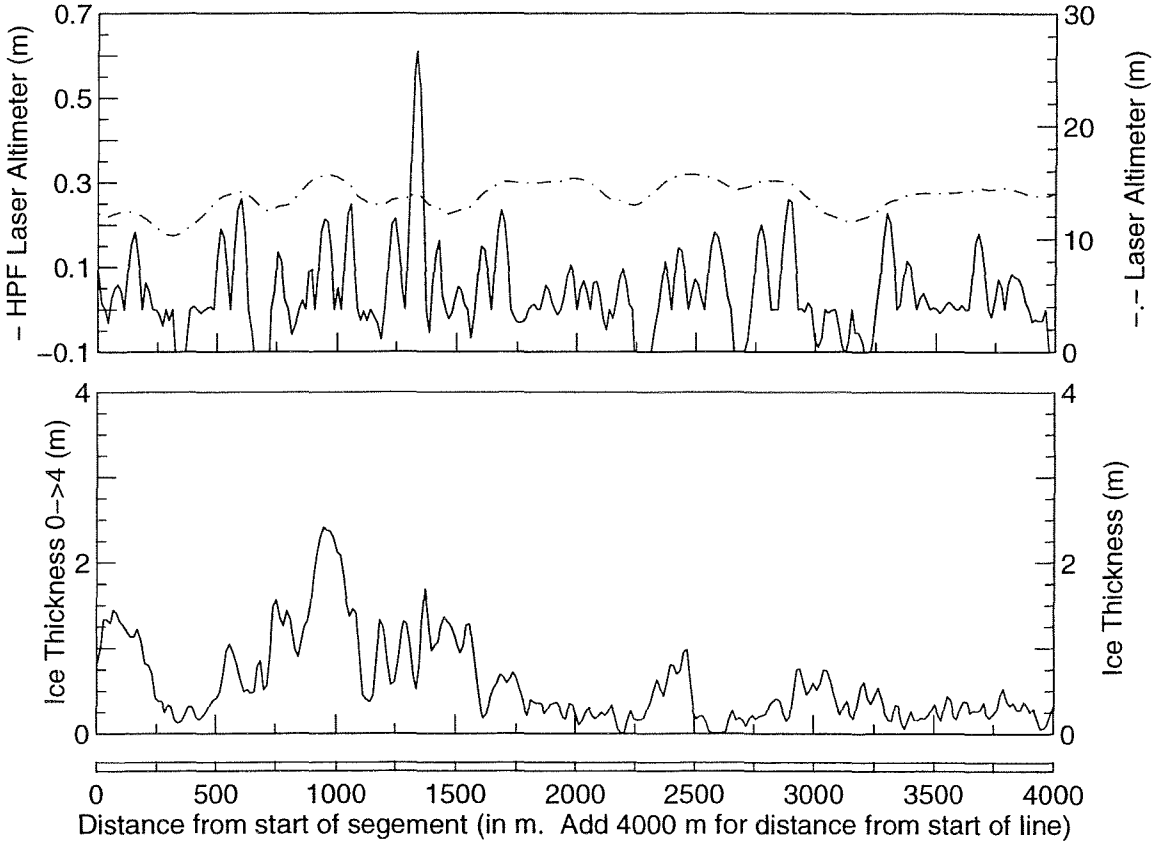

MAR 07 Flight #01 Line #10120 part 3 of 4

Line Starting Coordinates (53.6781,–56.4018) ending at (53.6994,–56.4505)

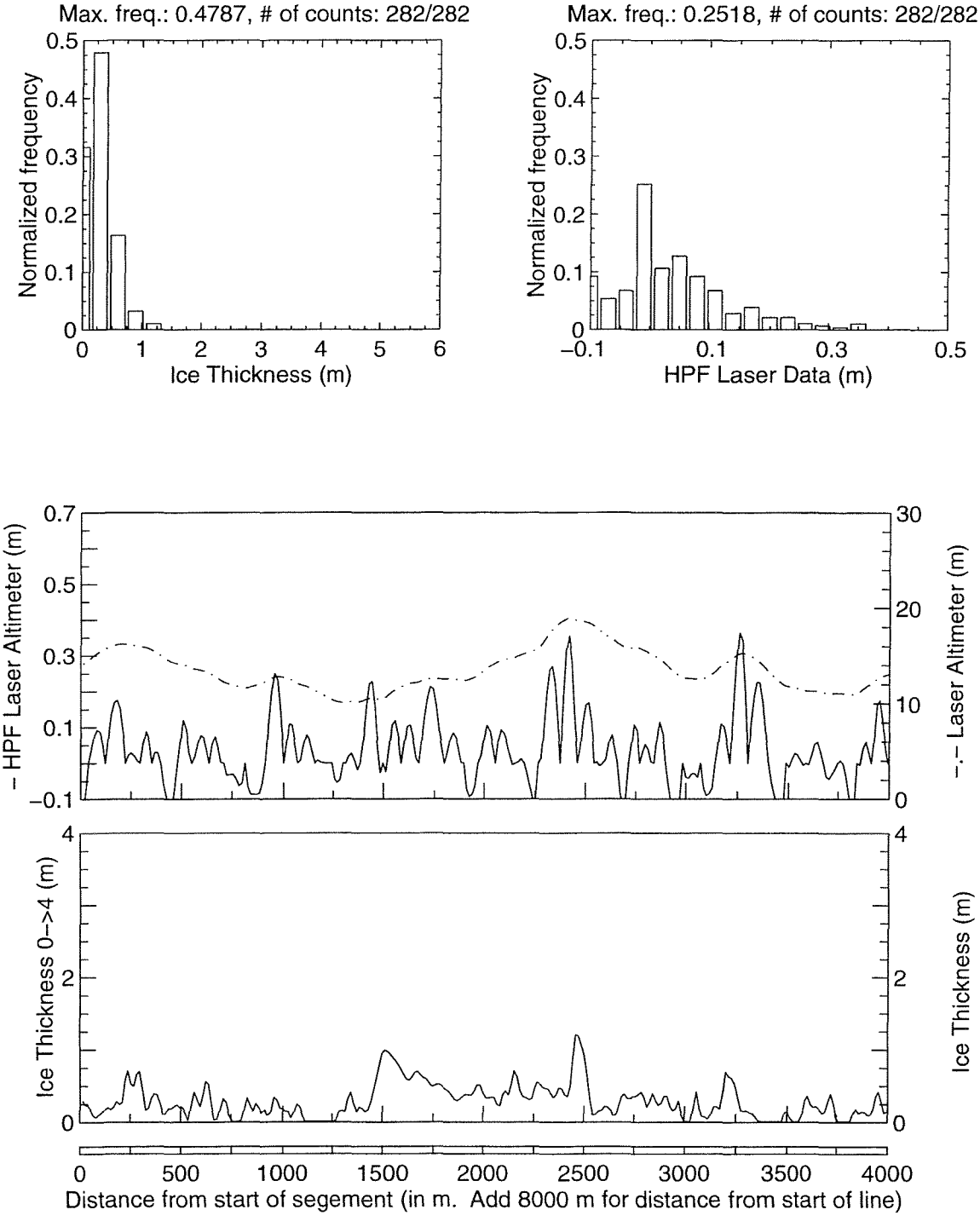

MAR 07 Flight #01 Line #10120 part 4 of 4

Line Starting Coordinates (53.6994,–56.4505) ending at (53.7125,–56.4846)

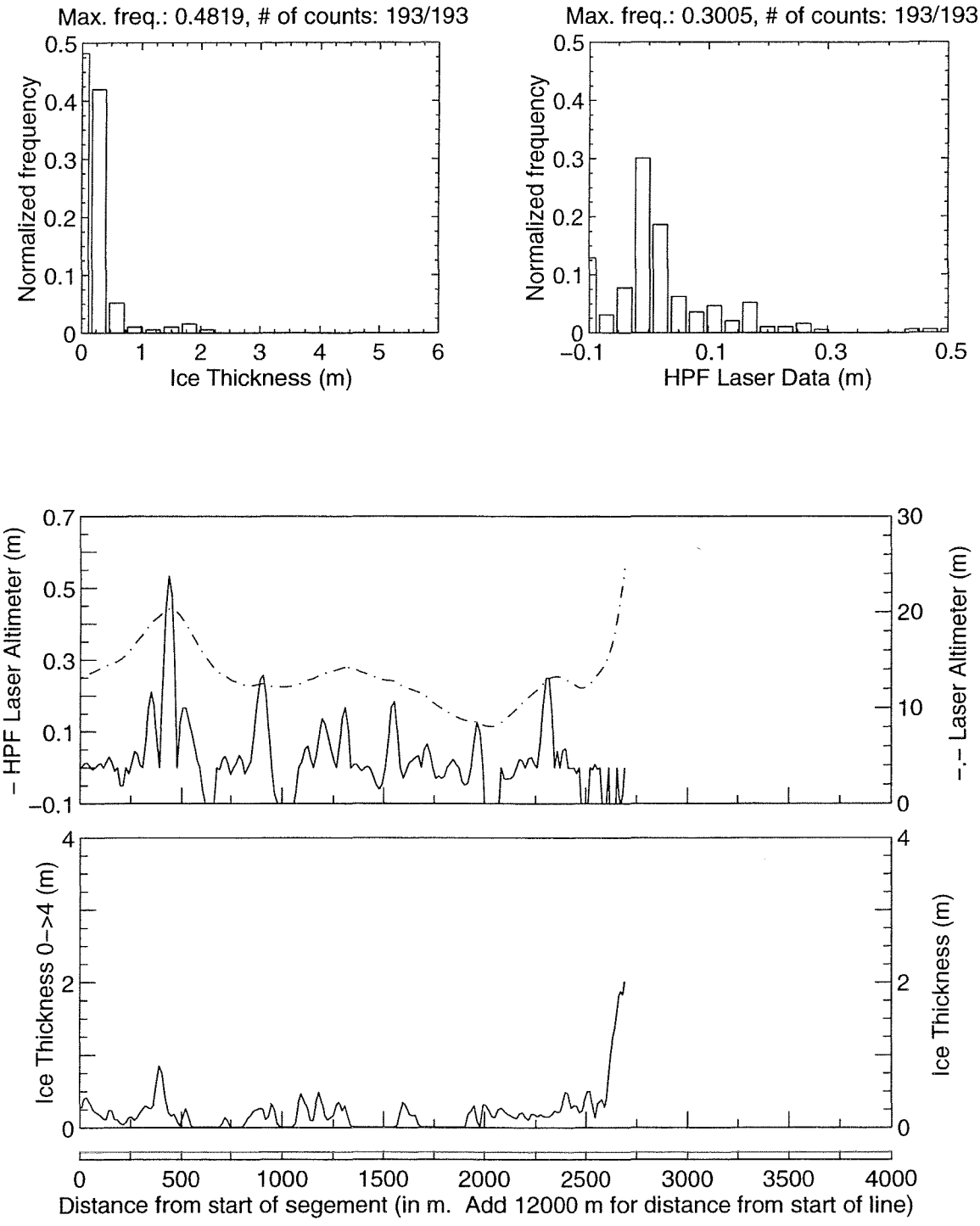

MAR 07 Flight #01 Line #10060 part 1 of 4

Line Starting Coordinates (53.2107,-55.6565) ending at (53.1768,-55.6762)

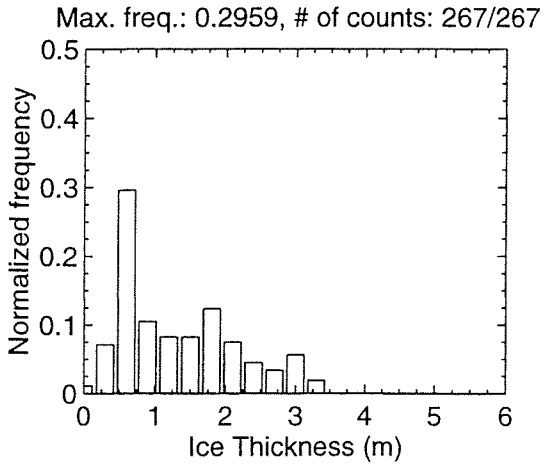

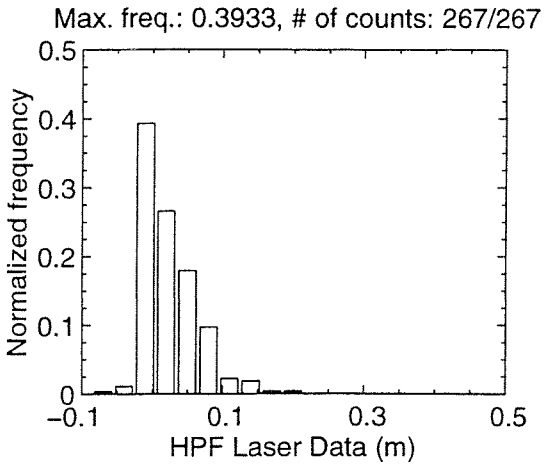

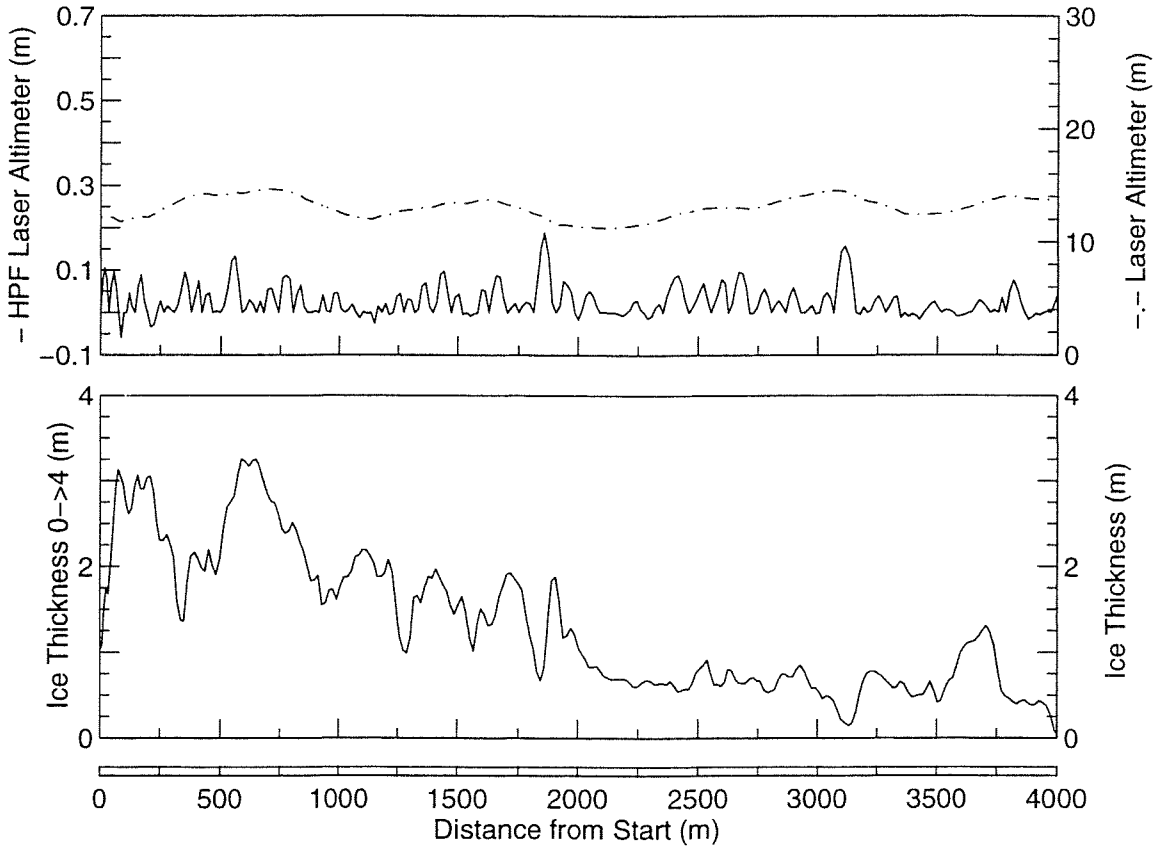

MAR 07 Flight #01 Line #10060 part 2 of 4

Line Starting Coordinates (53.1768,–55.6762) ending at (53.1440,–55.7007)

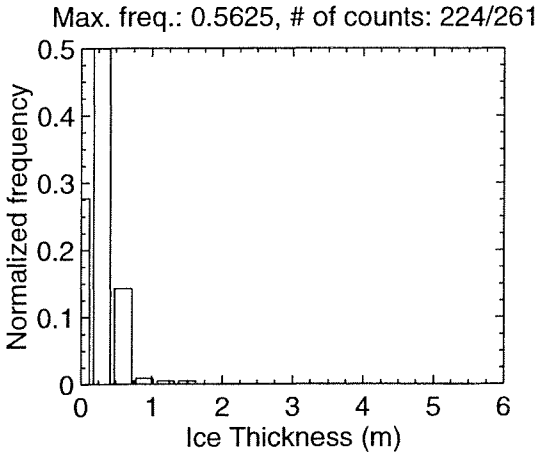

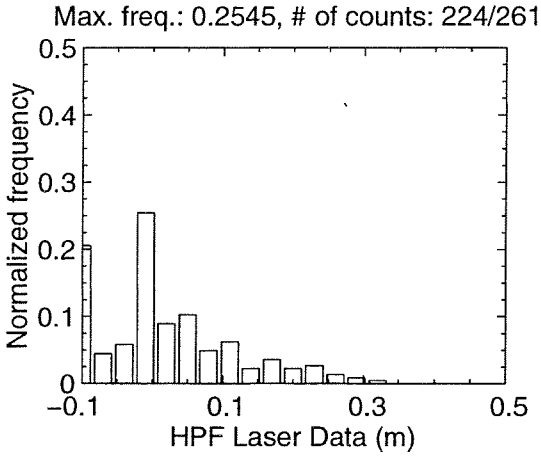

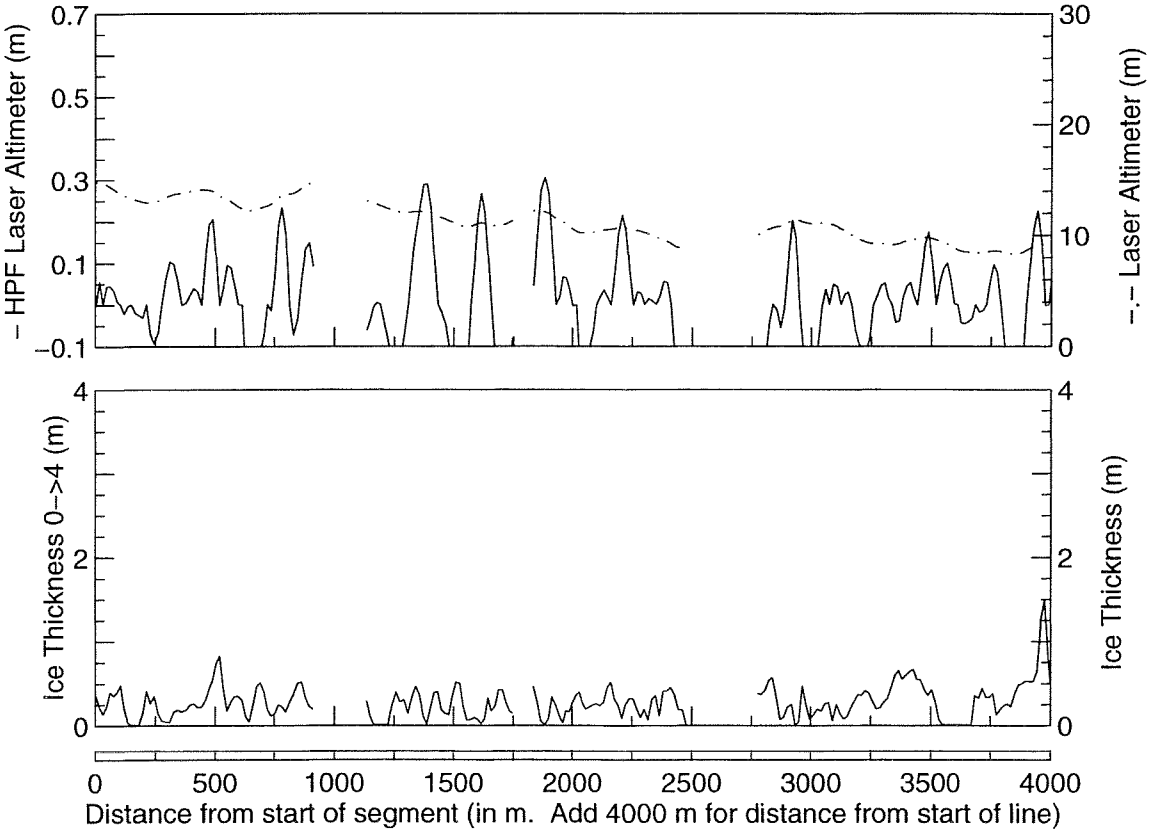

MAR 07 Flight #01 Line #10060 part 3 of 4

Line Starting Coordinates (53.1440,–55.7007) ending at (53.1130,–55.7312)

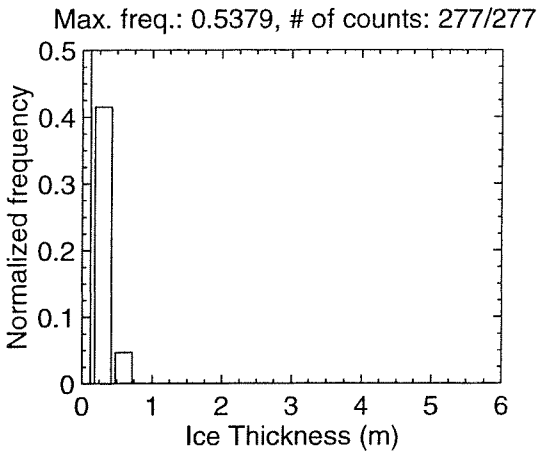

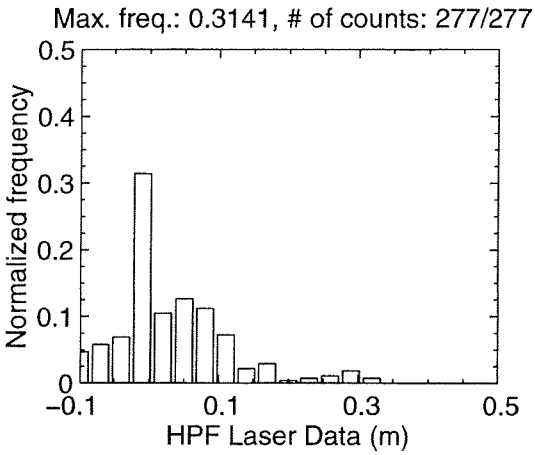

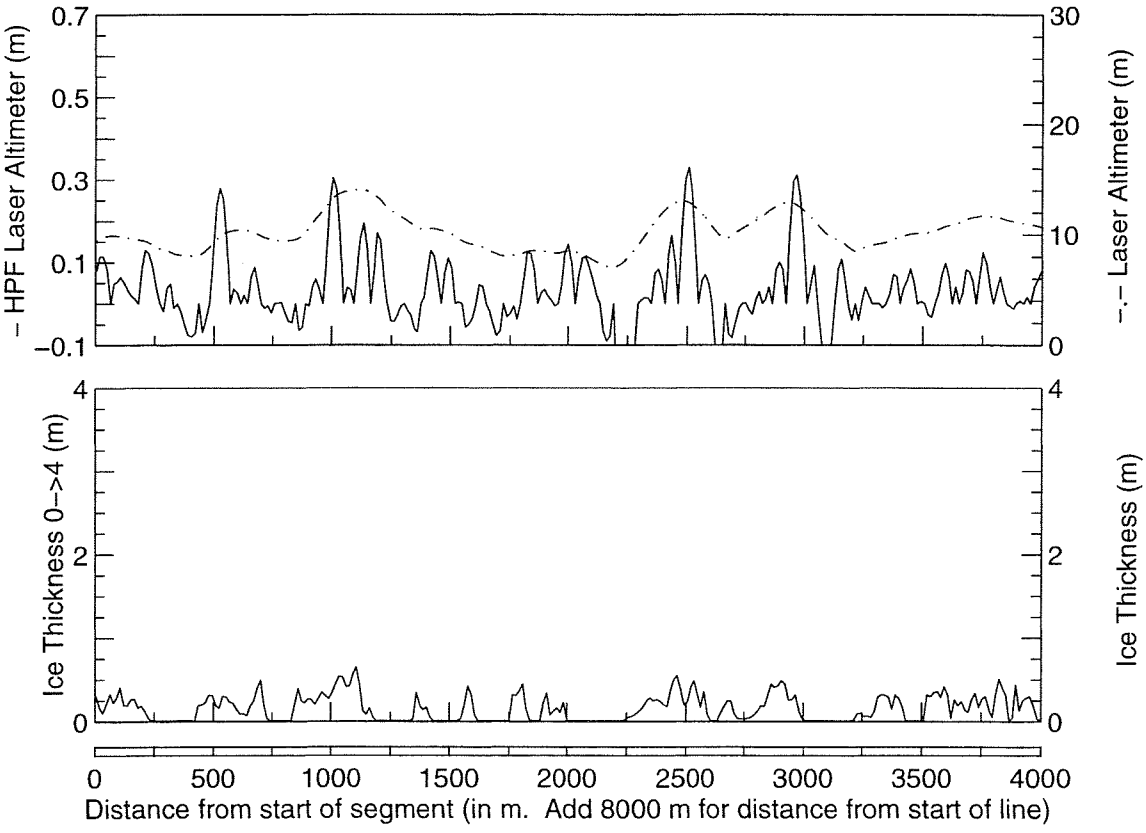

MAR 07 Flight #01 Line #10060 part 4 of 4

Line Starting Coordinates (53.1130,–55.7312) ending at (53.0825,–55.7608)

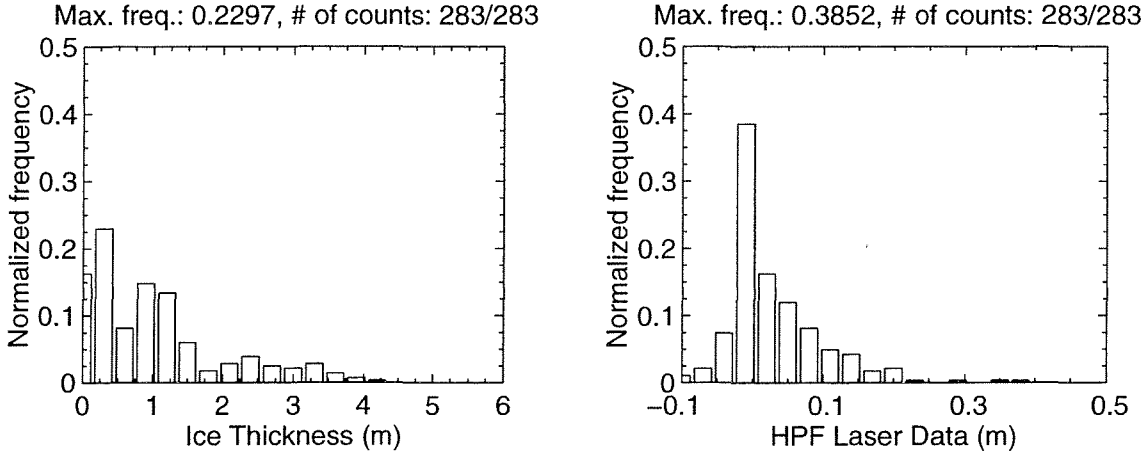

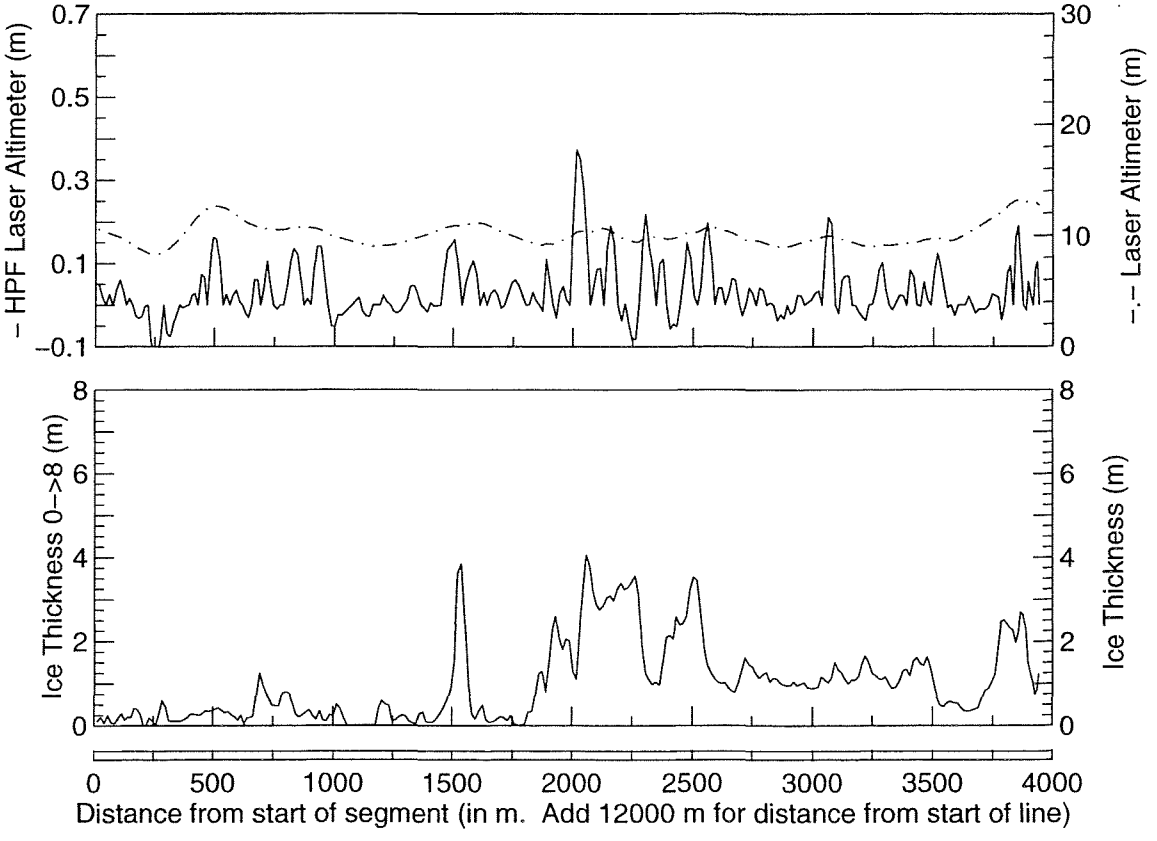

MAR 07 Flight #01 Line #10072 part 1 of 4

Line Starting Coordinates (53.1536,–55.5934) ending at (53.1881,–55.6106)

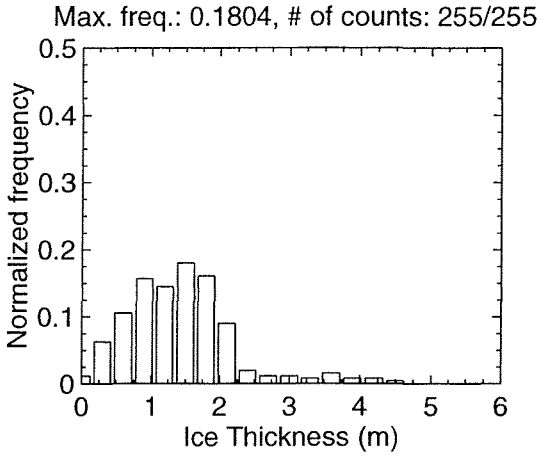

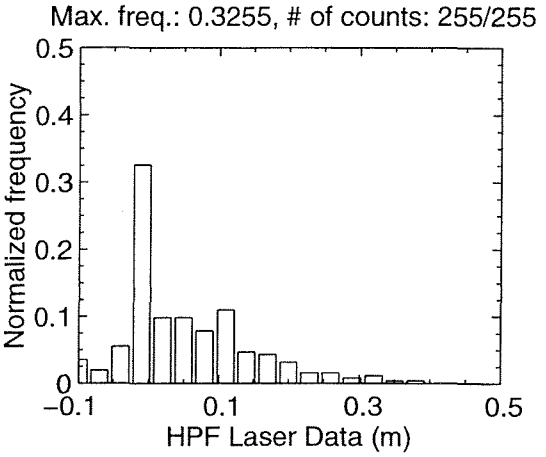

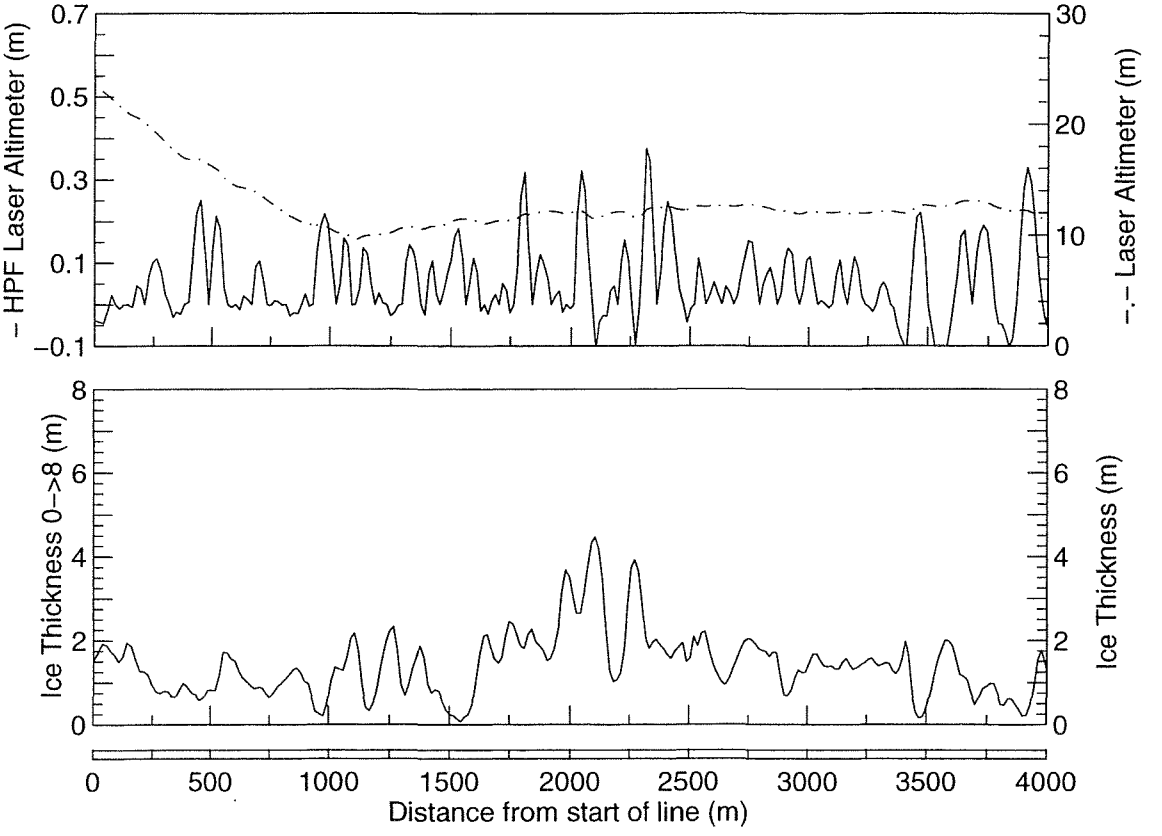

MAR 07 Flight #01 Line #10072 part 2 of 4

Line Starting Coordinates (53.1881,–55.6106) ending at (53.2230,–55.6246)

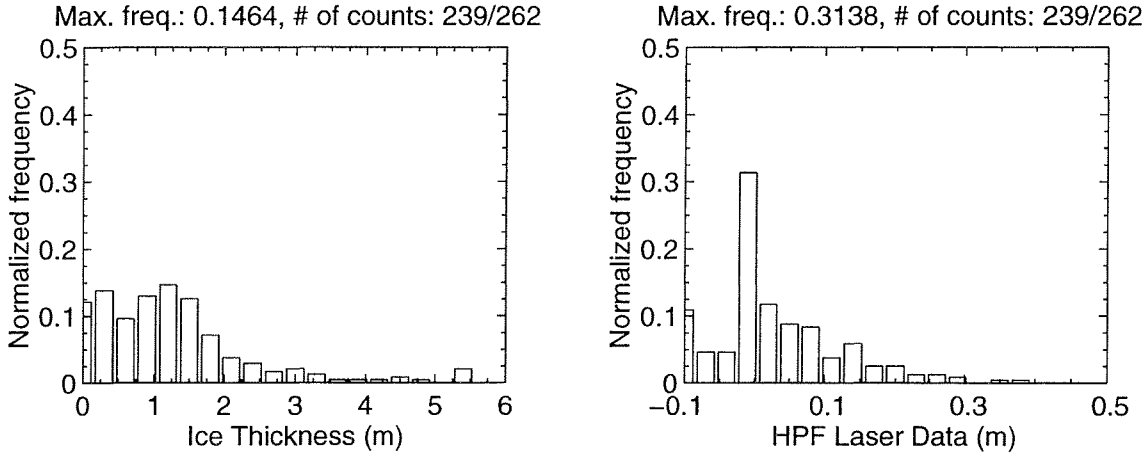

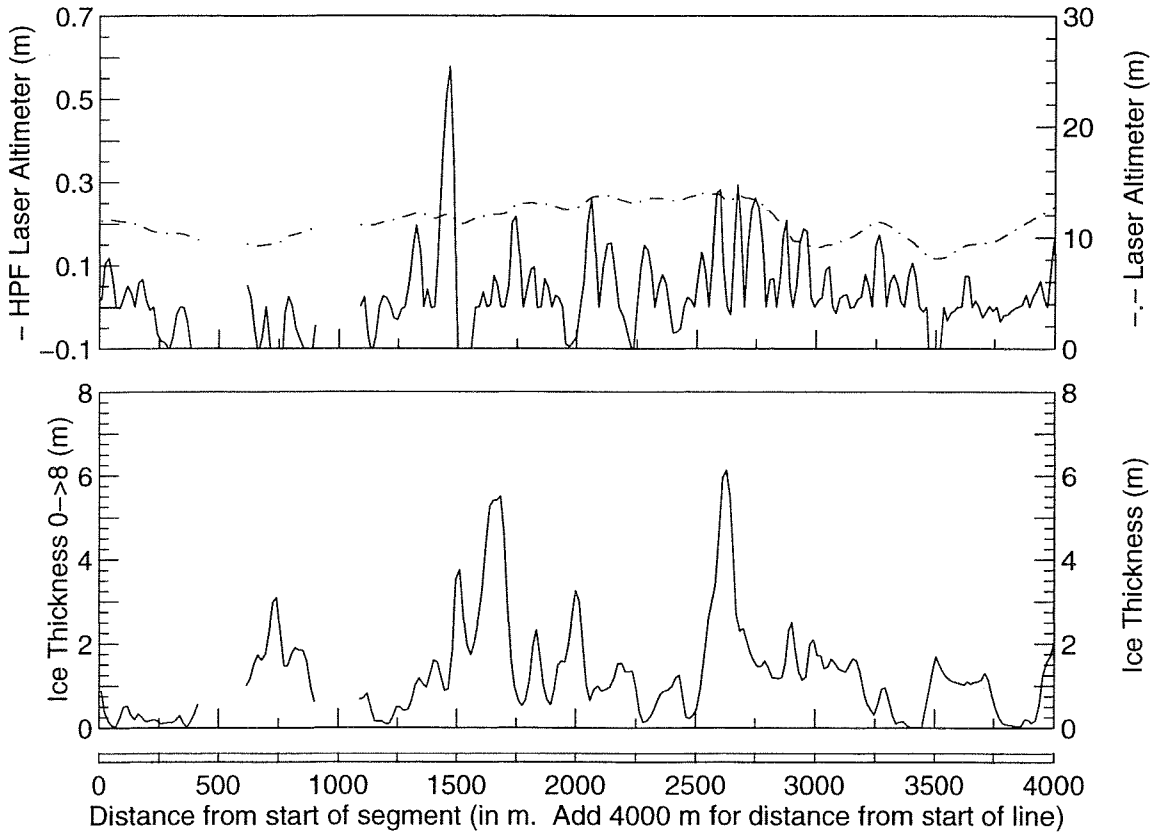

MAR 07 Flight #01 Line #10072 part 3 of 4

Line Starting Coordinates (53.2230,–55.6246) ending at (53.2580,–55.6388)

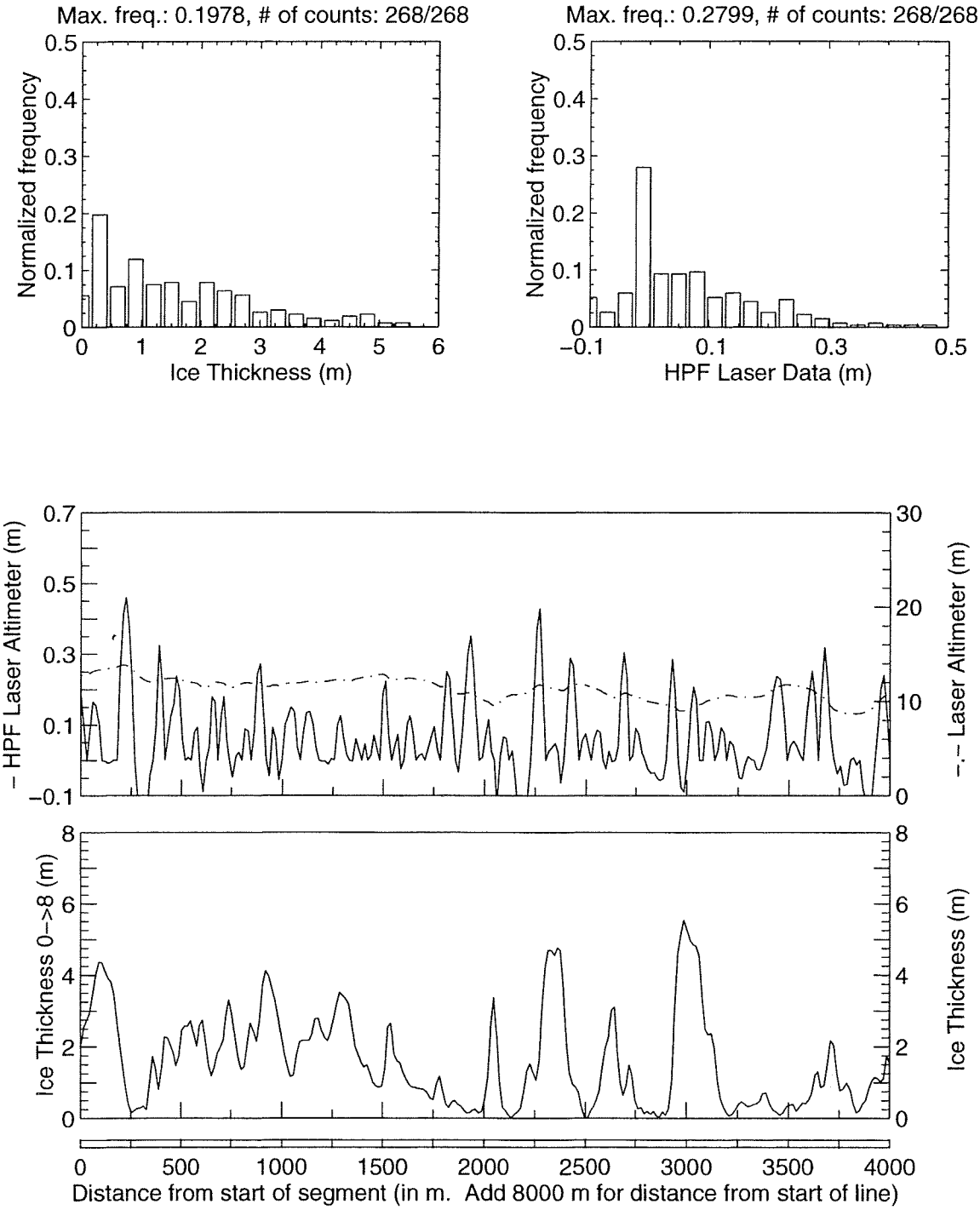

MAR 07 Flight #01 Line #10072 part 4 of 4

Line Starting Coordinates (53.2580,–55.6388) ending at (53.2807,–55.6500)

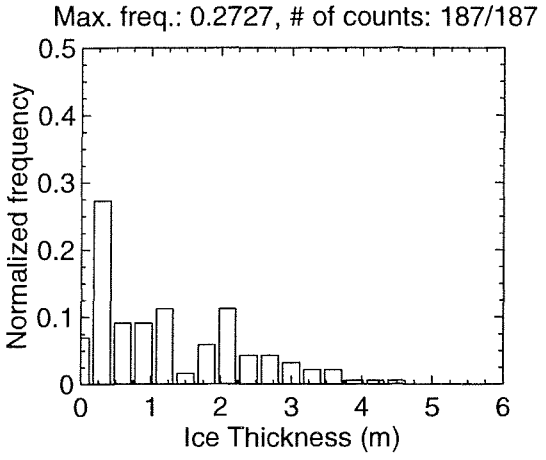

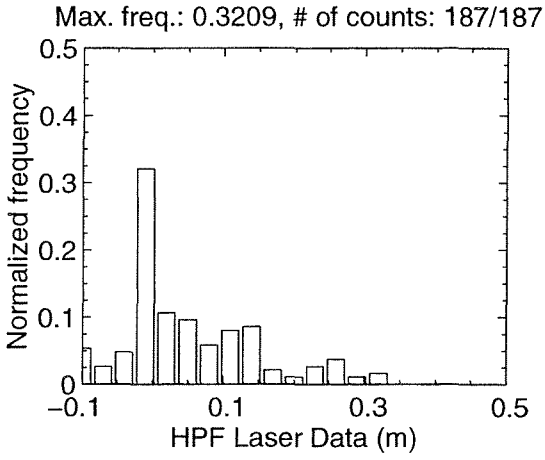

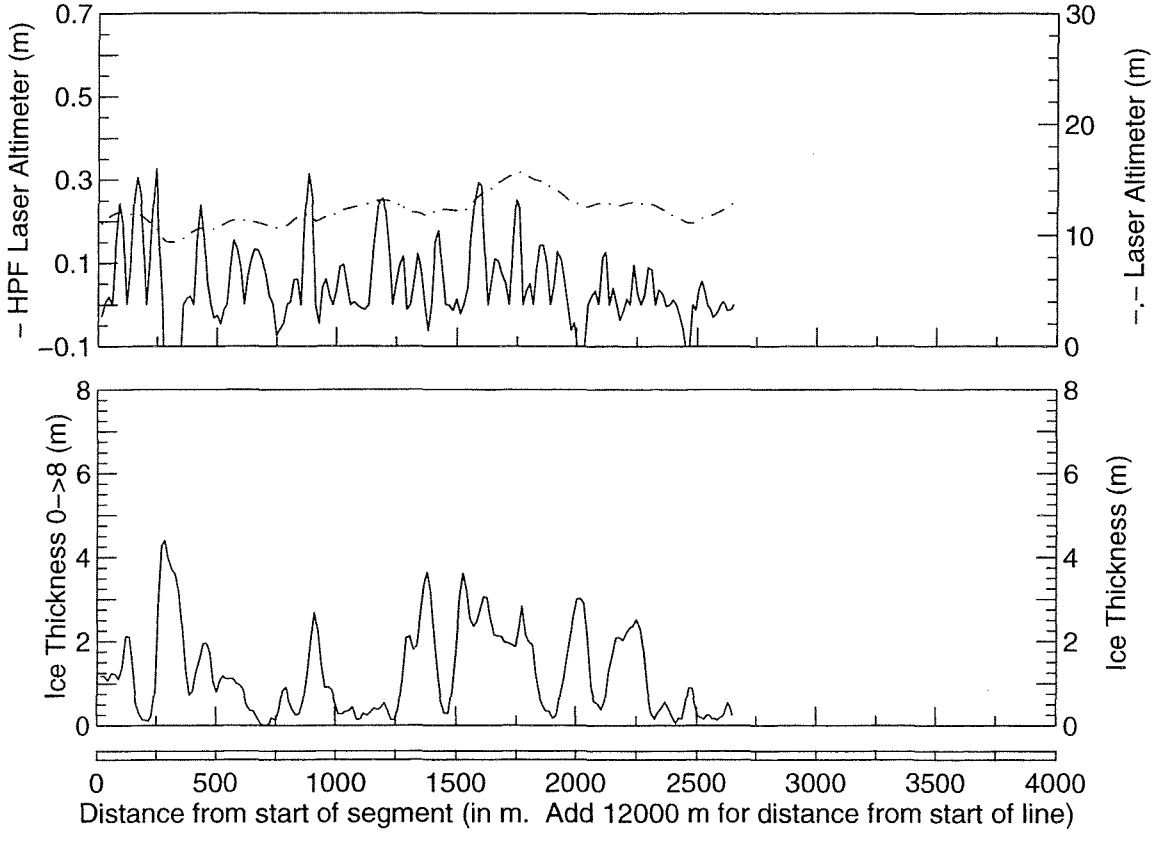

MAR 07 Flight #01 Line #10082 part 1 of 1

Line Starting Coordinates (53.4294,–55.7535) ending at (53.4310,–55.8051)

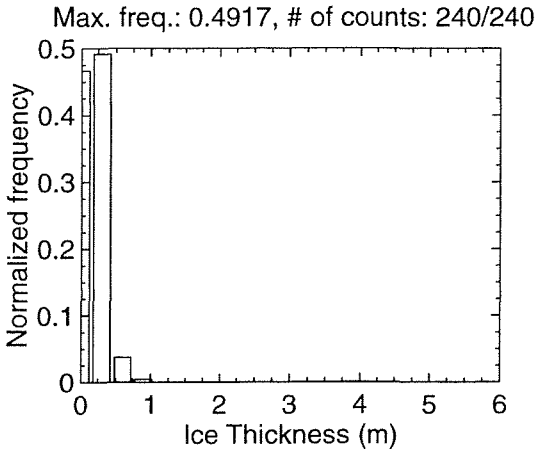

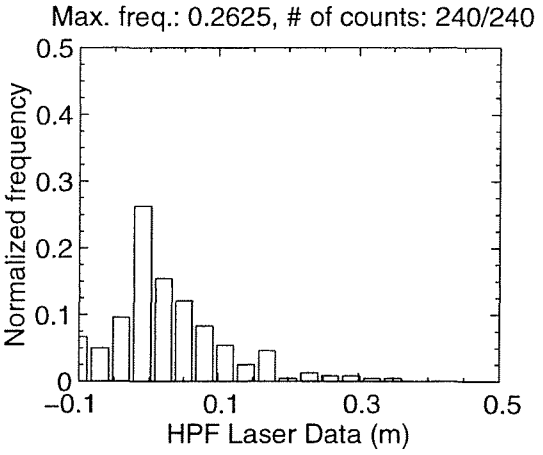

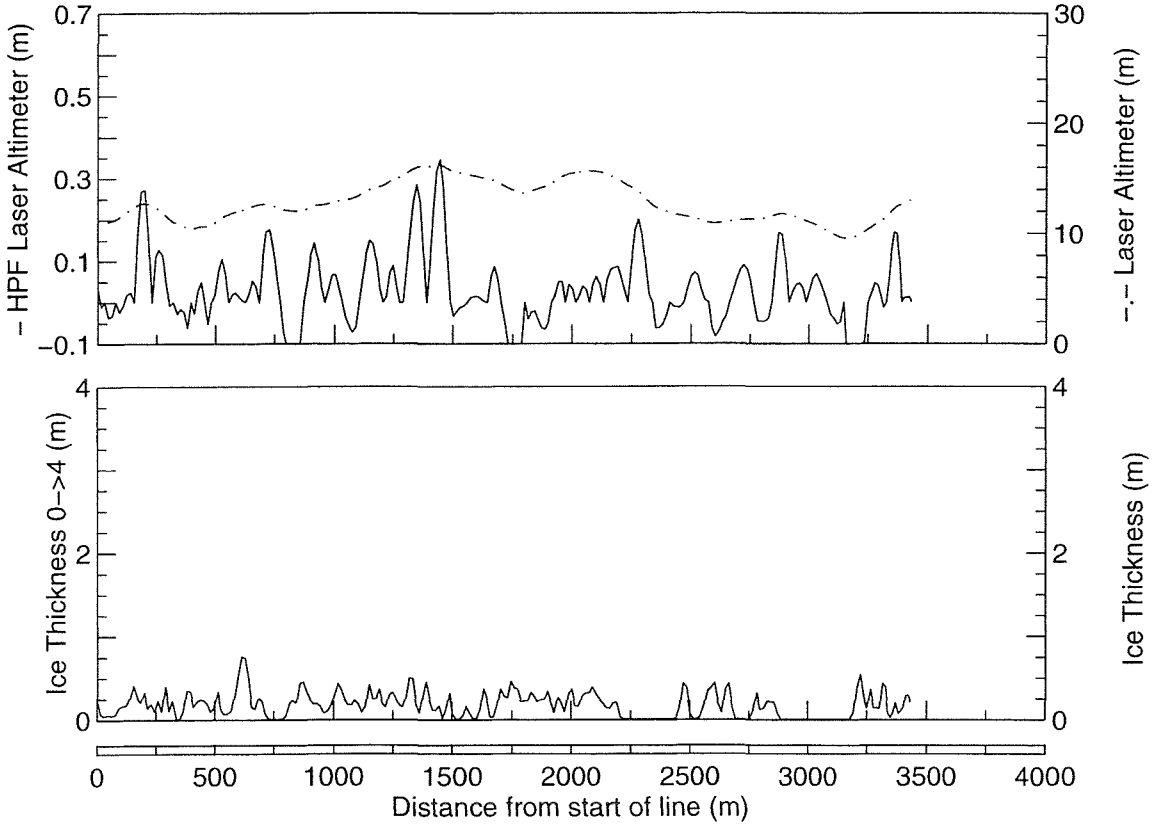

MAR 07 Flight #02 Line #10011 part 1 of 1

Line Starting Coordinates (53.6672,−56.6265) ending at (53.6565,−56.5791)

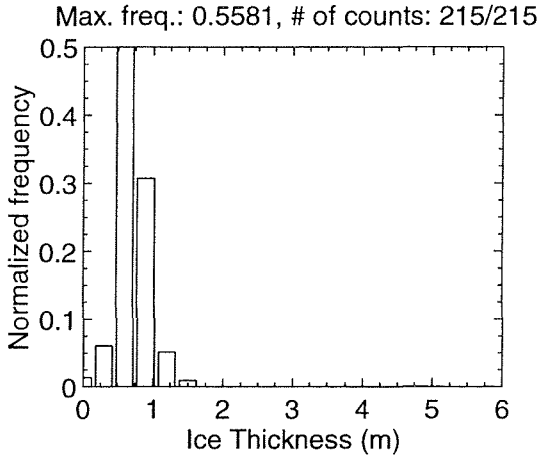

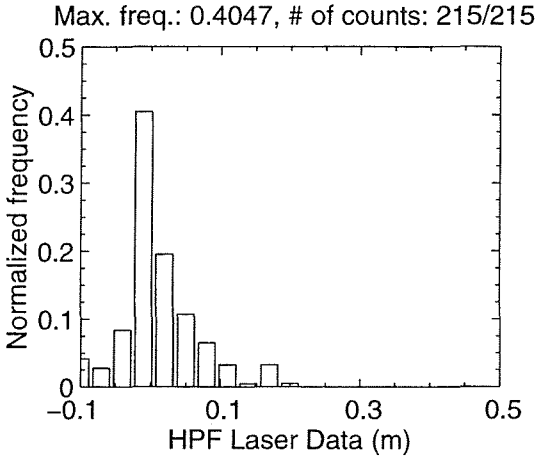

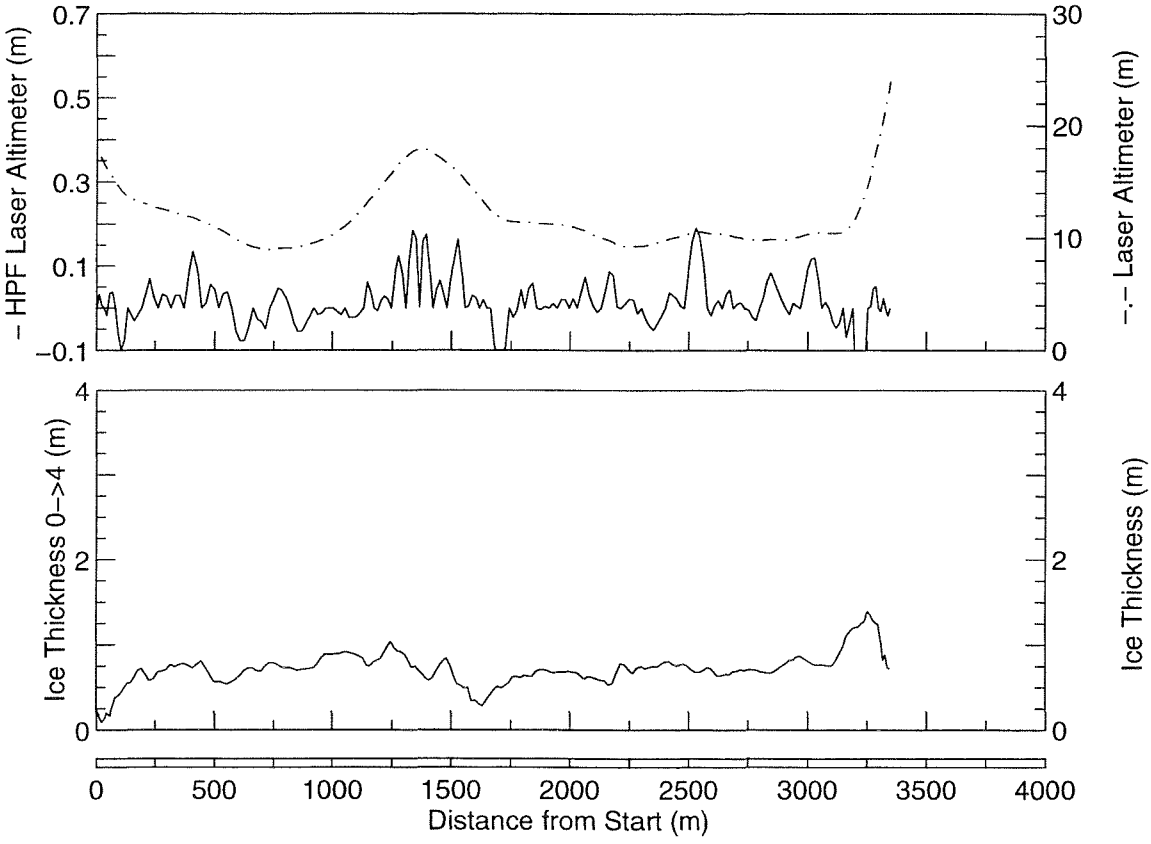

MAR 07 Flight #02 Line #10012 part 1 of 2

Line Starting Coordinates (53.6444,–56.4877) ending at (53.6415,–56.4271)

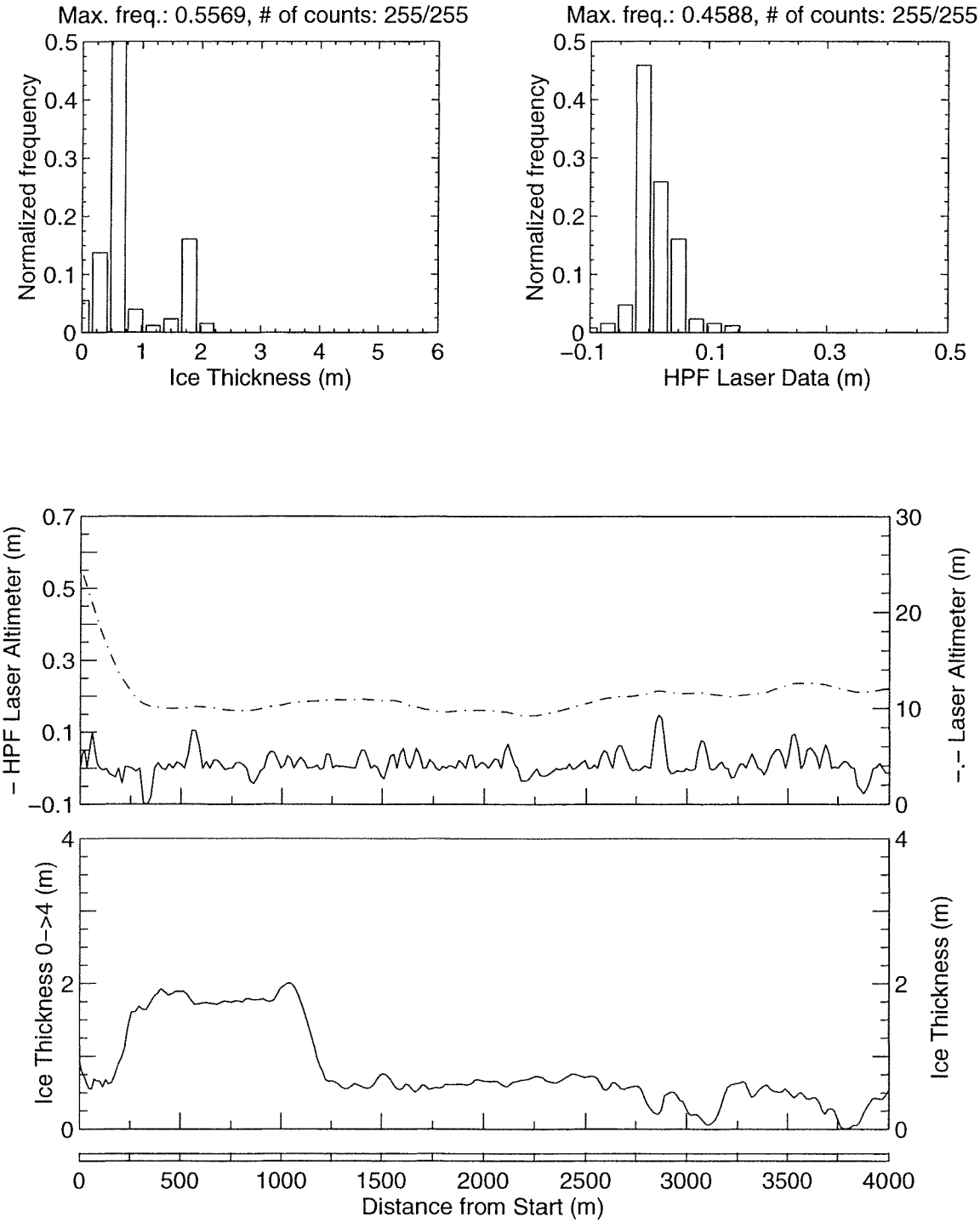

MAR 07 Flight #02 Line #10012 part 2 of 2

Line Starting Coordinates (53.6415,–56.4271) ending at (53.6384,–56.3694)

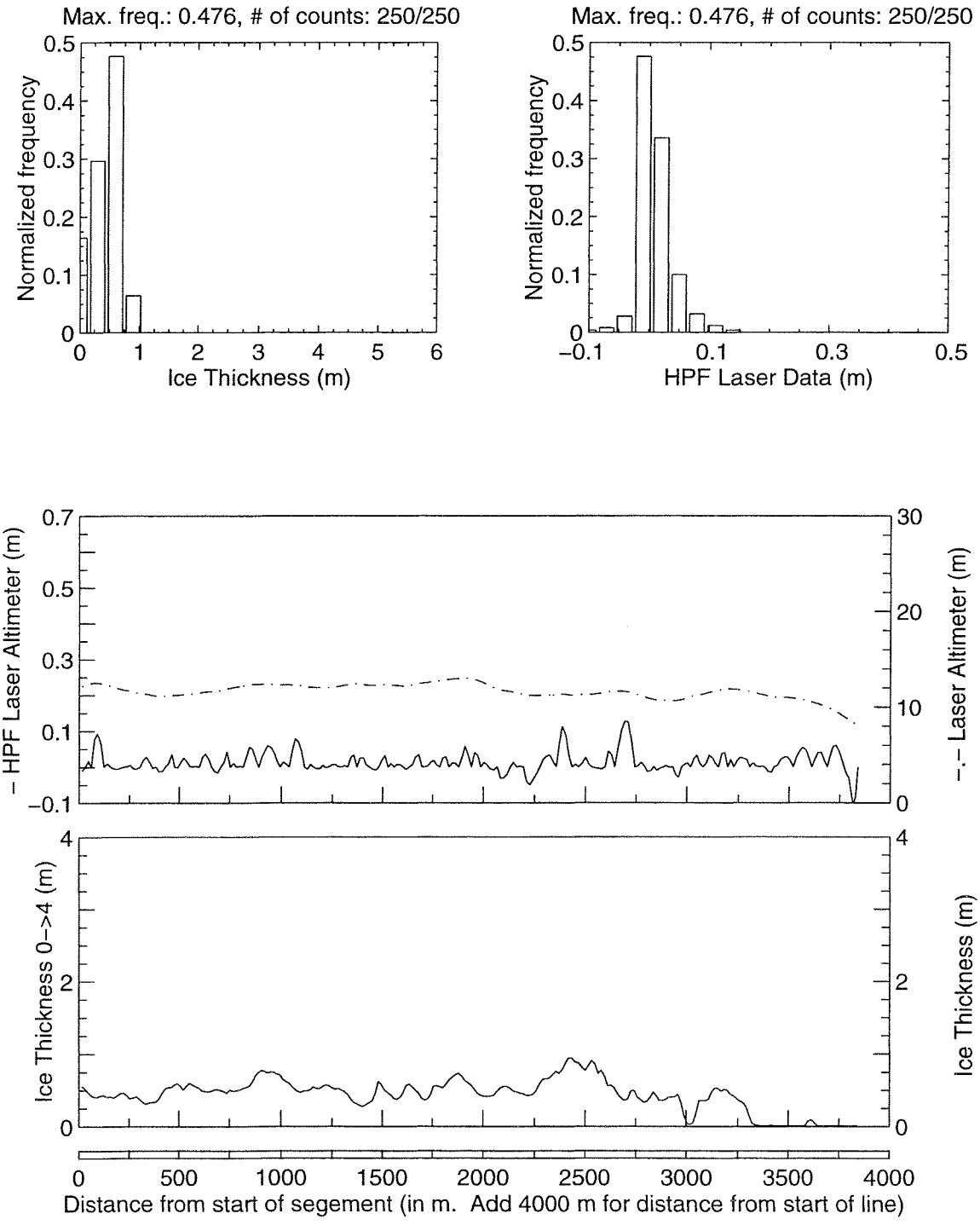

MAR 07 Flight #02 Line #10020 part 1 of 6

Line Starting Coordinates (53.6370,–56.3664) ending at (53.6318,–56.3065)

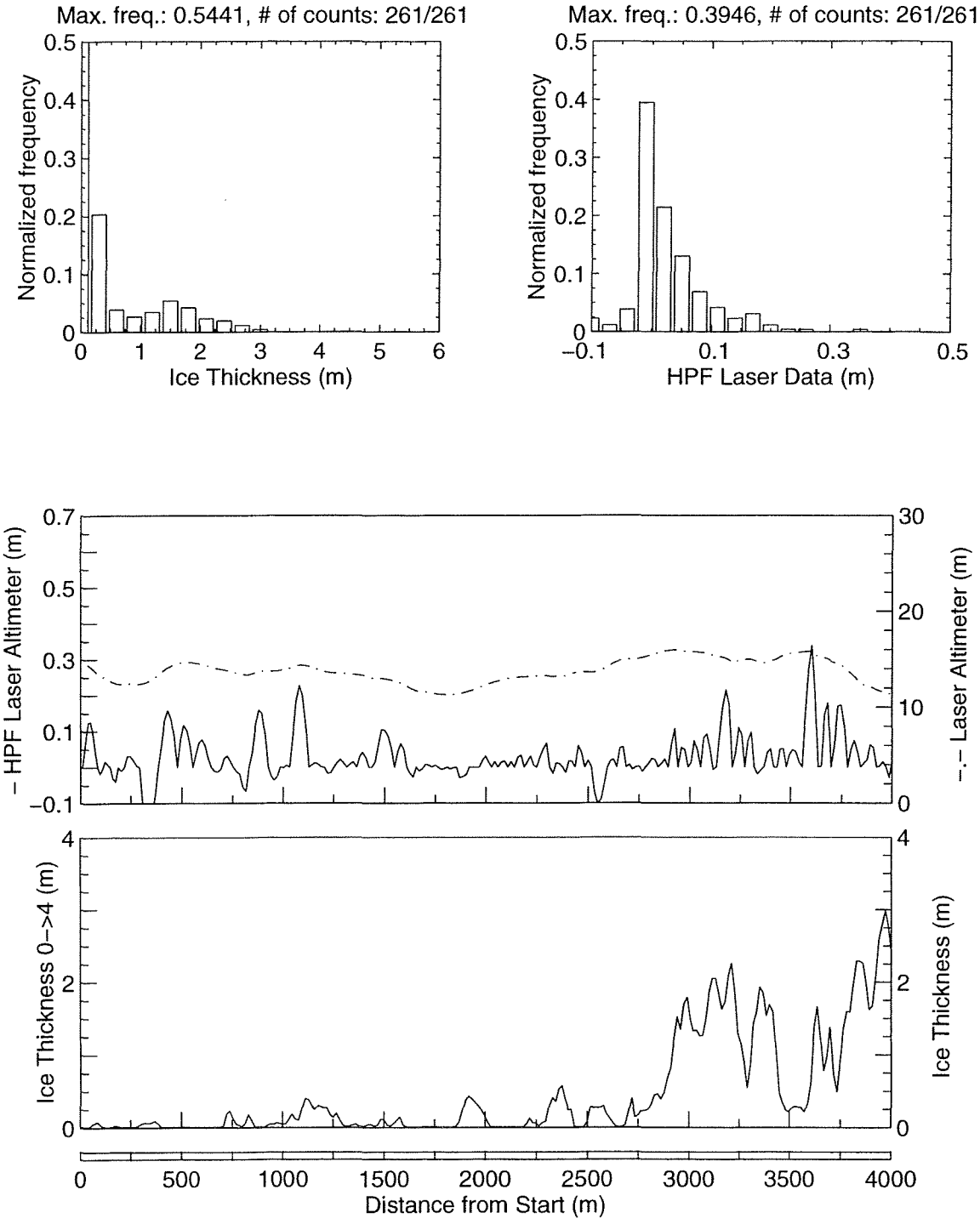

MAR 07 Flight #02 Line #10020 part 2 of 6

Line Starting Coordinates (53.6318,–56.3065) ending at (53.6236,–56.2475)

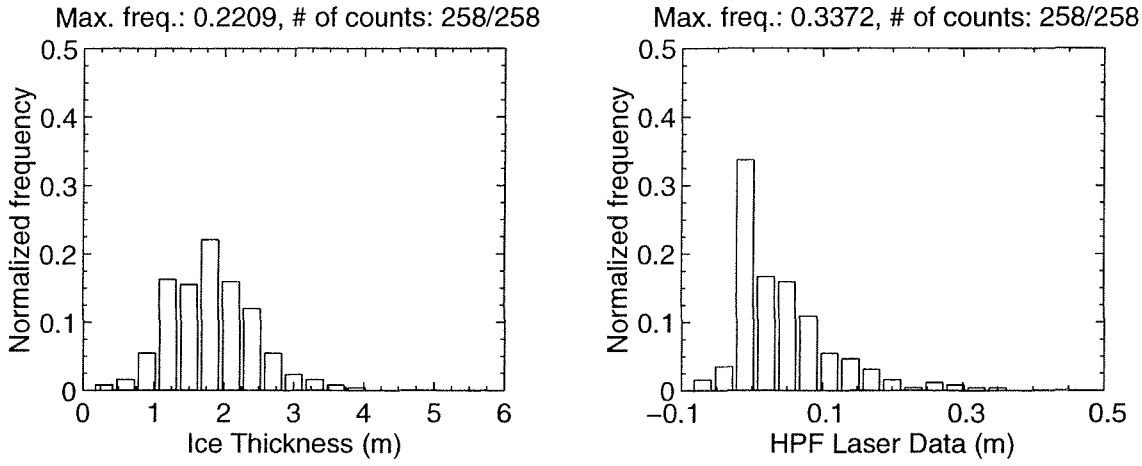

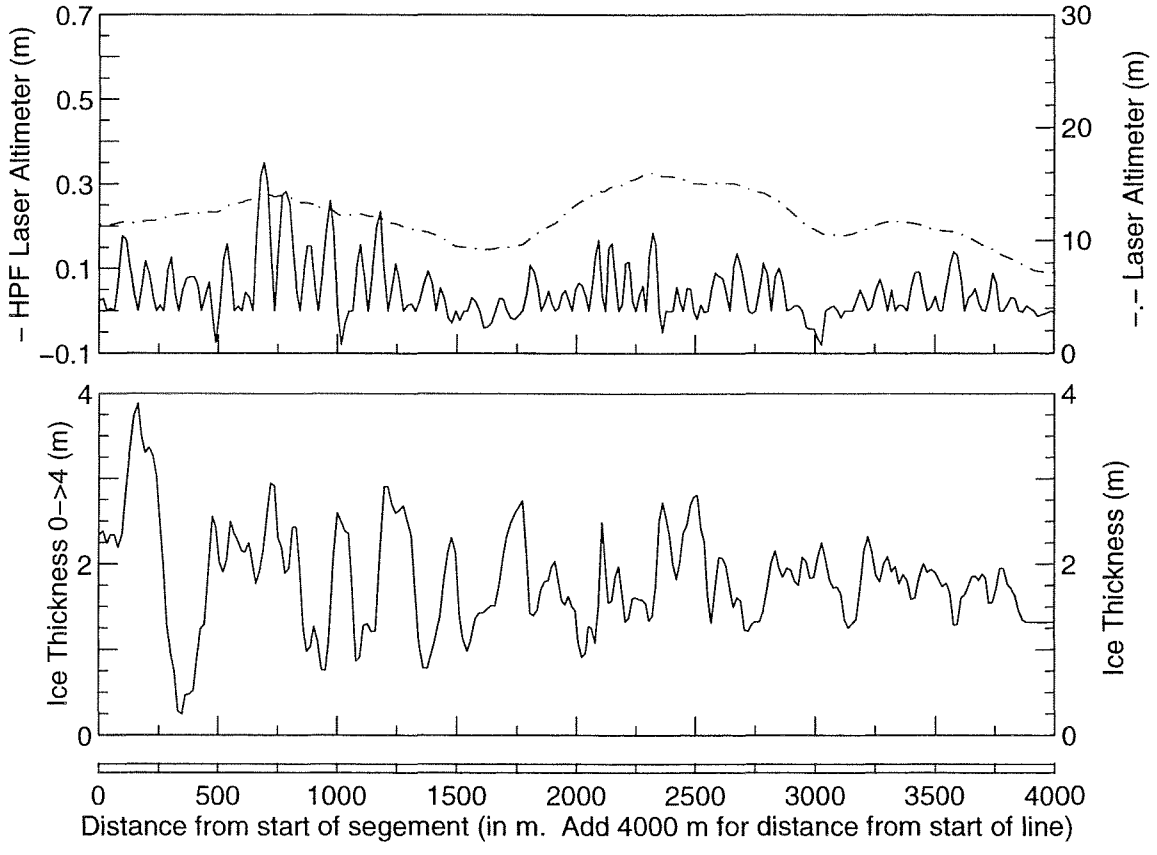

MAR 07 Flight #02 Line #10020 part 3 of 6

Line Starting Coordinates (53.6236,–56.2475) ending at (53.6152,–56.1885)

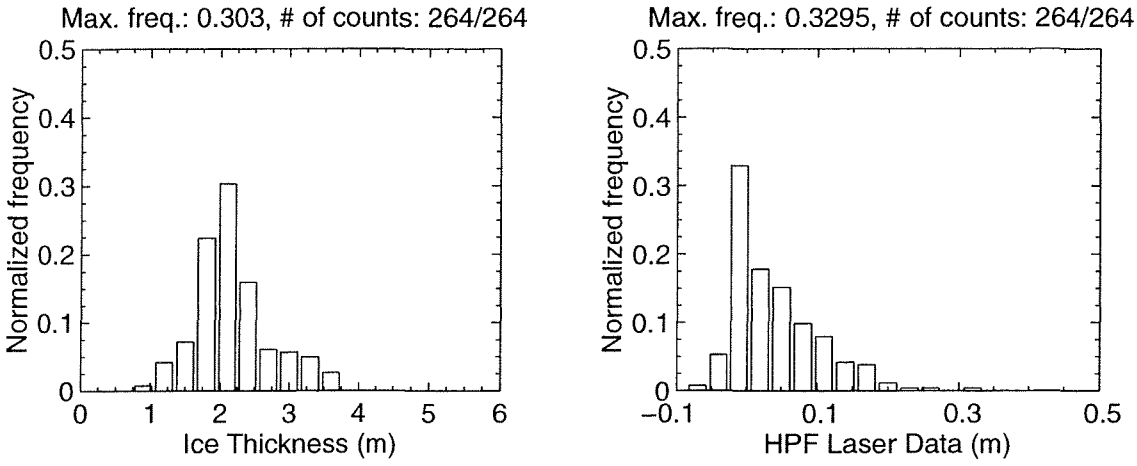

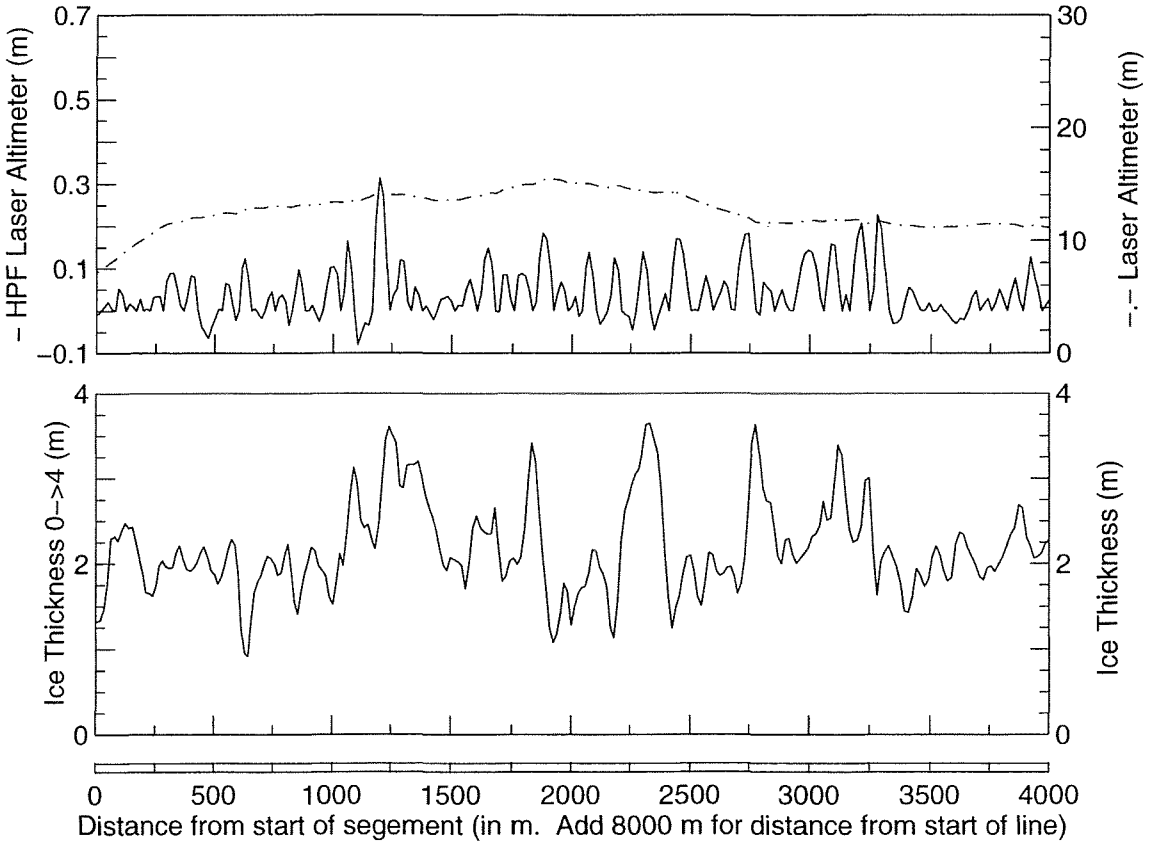

MAR 07 Flight #02 Line #10020 part 4 of 6

Line Starting Coordinates (53.6152,–56.1885) ending at (53.6044,–56.1308)

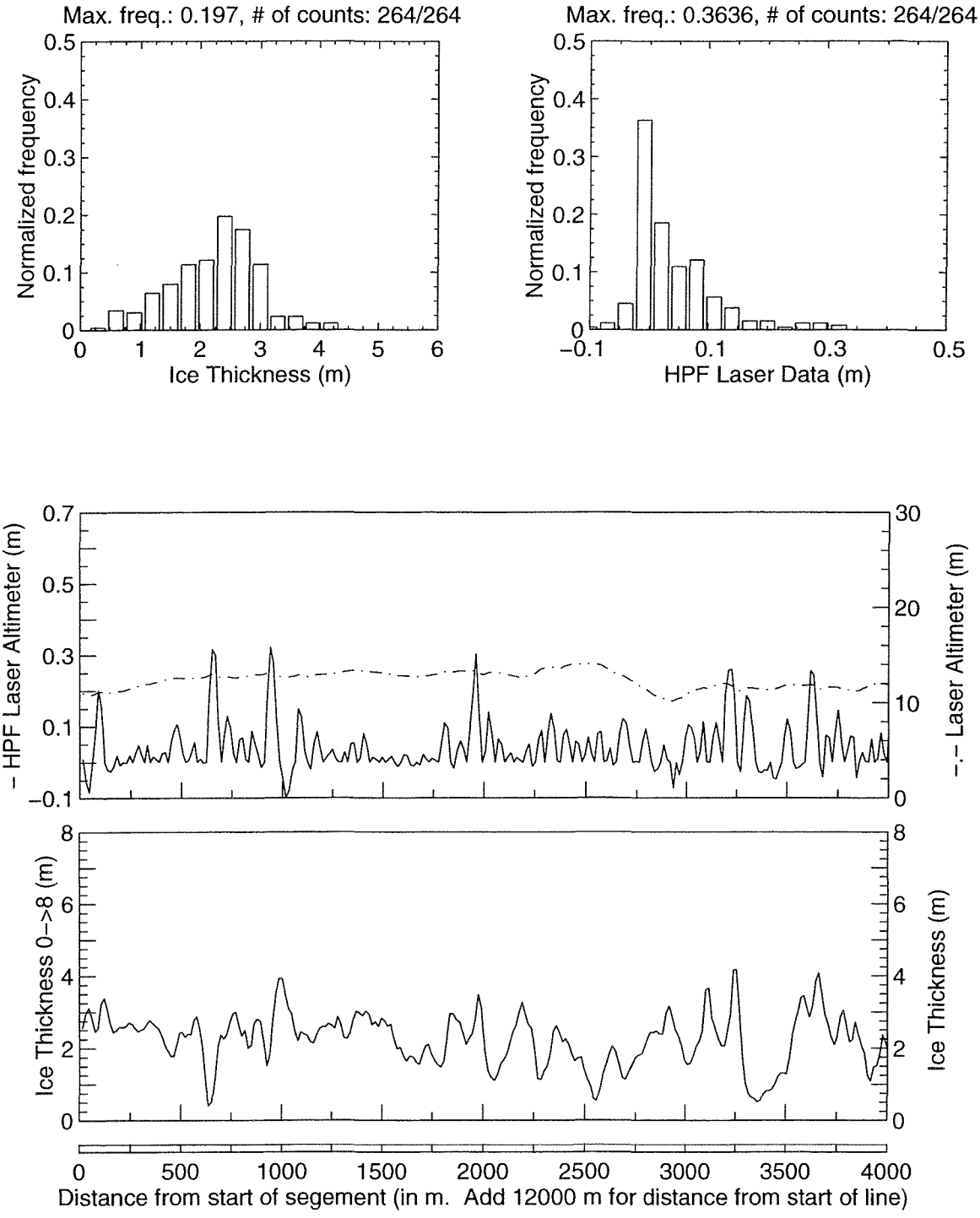

MAR 07 Flight #02 Line #10020 part 5 of 6

Line Starting Coordinates (53.6044,–56.1308) ending at (53.5948,–56.0725)

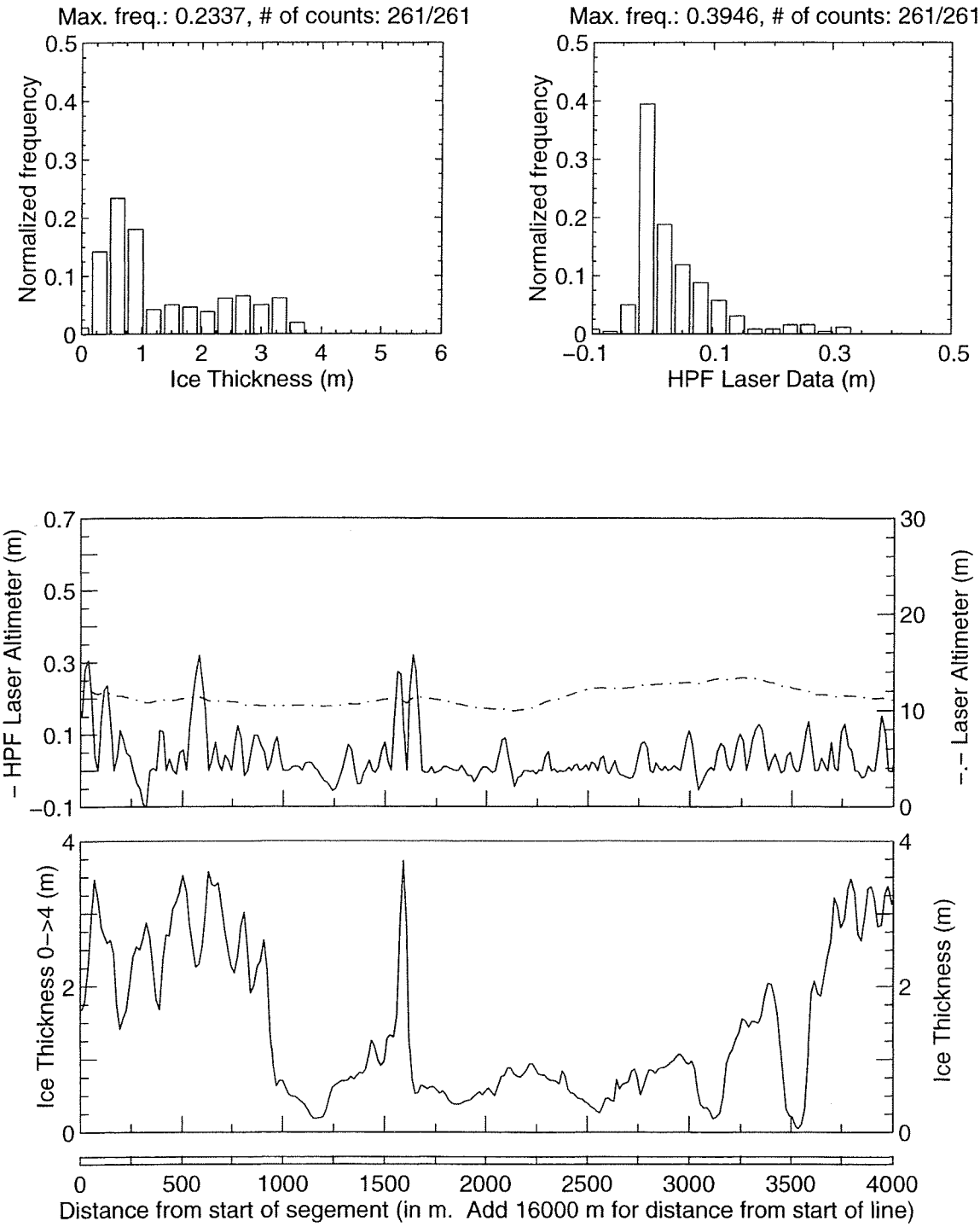

MAR 07 Flight #02 Line #10020 part 6 of 6

Line Starting Coordinates (53.5948,–56.0725) ending at (53.5924,–56.0522)

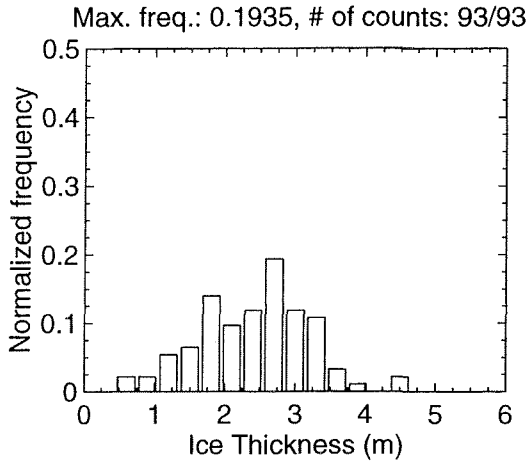

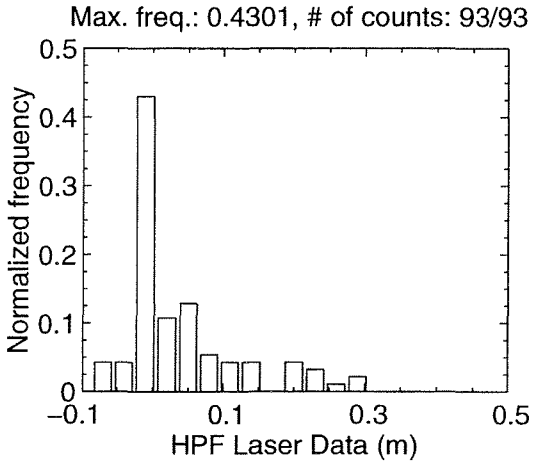

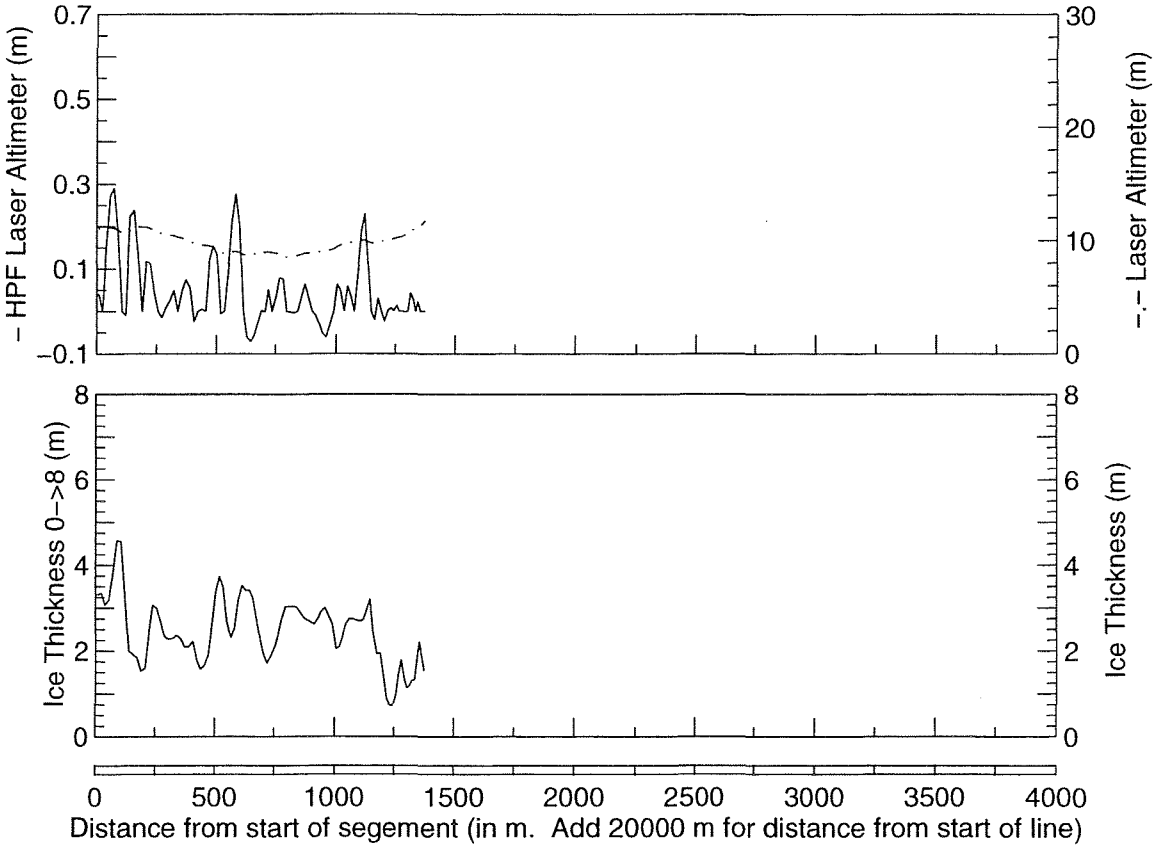

MAR 07 Flight #02 Line #10030 part 1 of 2

Line Starting Coordinates (53.5860,–56.0313) ending at (53.5594,–55.9906)

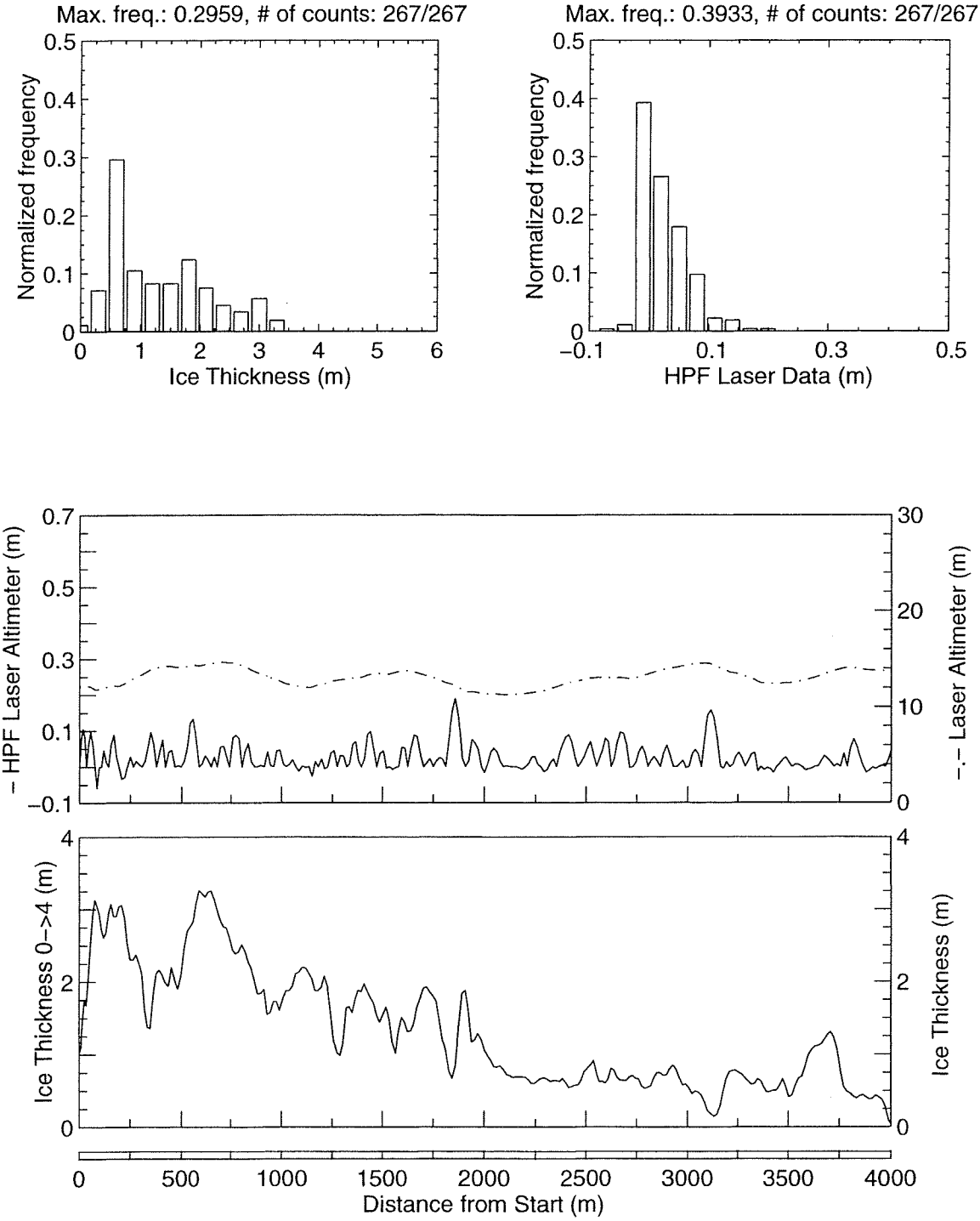

MAR 07 Flight #02 Line #10030 part 2 of 2

Line Starting Coordinates (53.5594,–55.9906) ending at (53.5560,–55.9846)

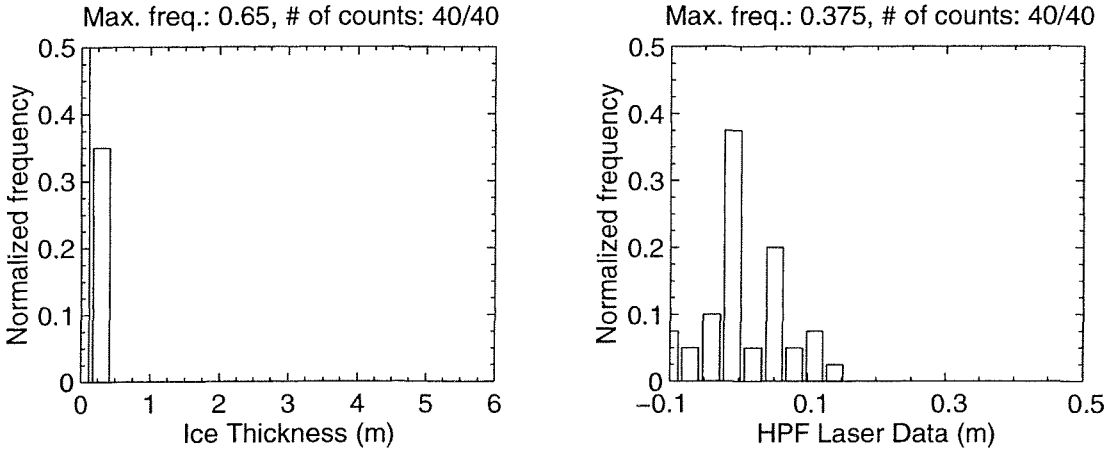

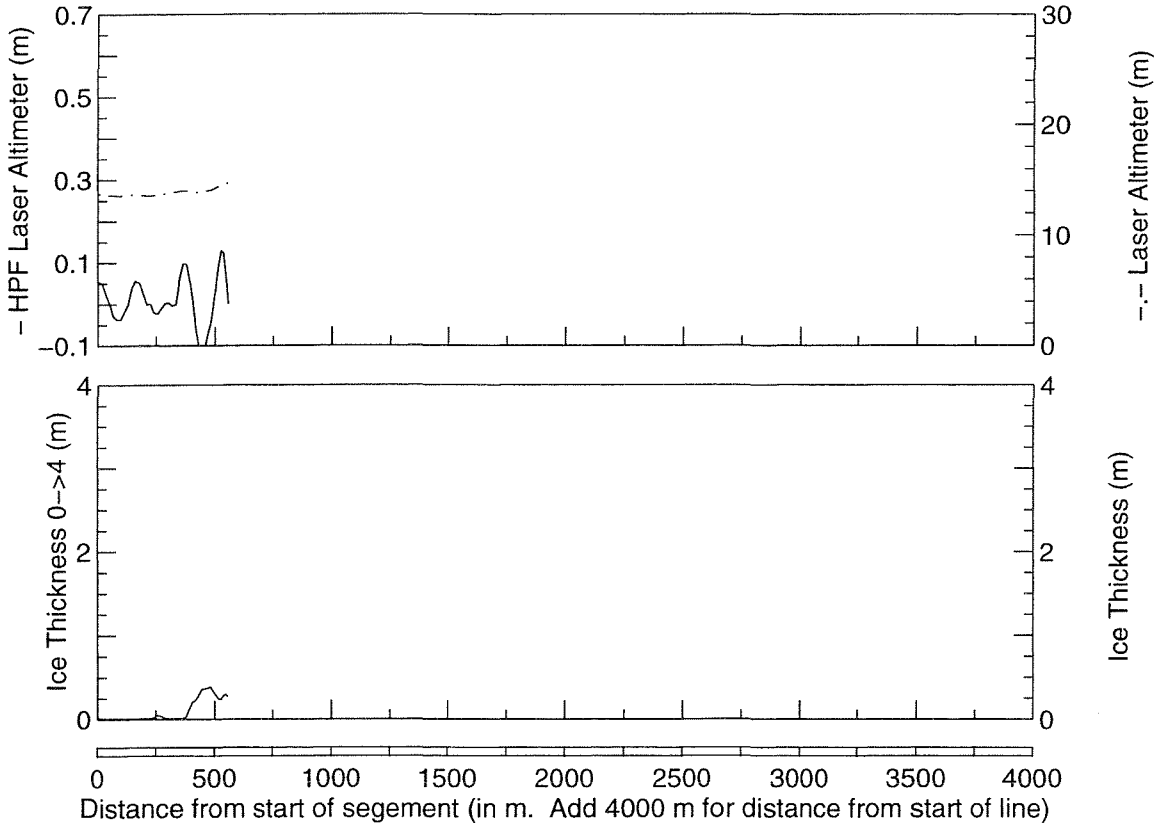

MAR 07 Flight #02 Line #10040 part 1 of 7

Line Starting Coordinates (53.5522,–55.9762) ending at (53.5336,–55.9242)

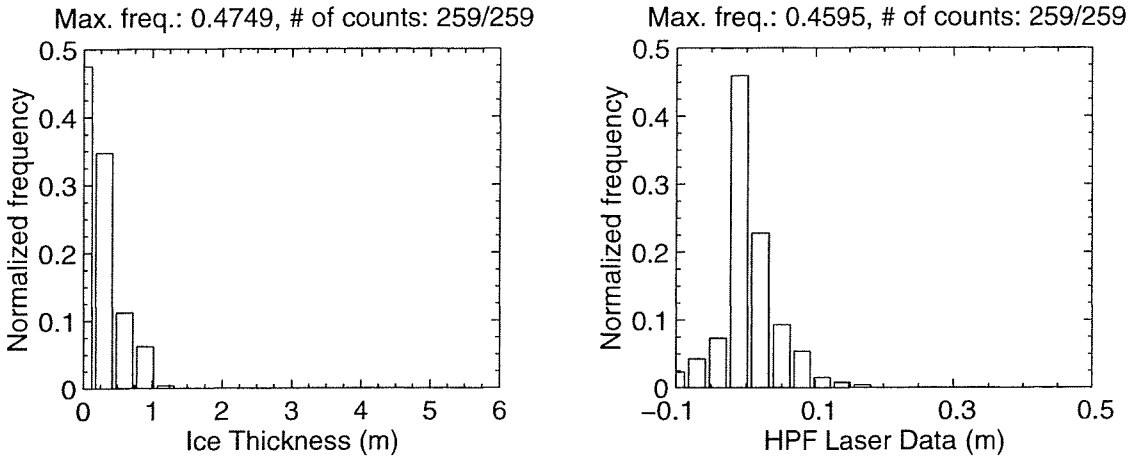

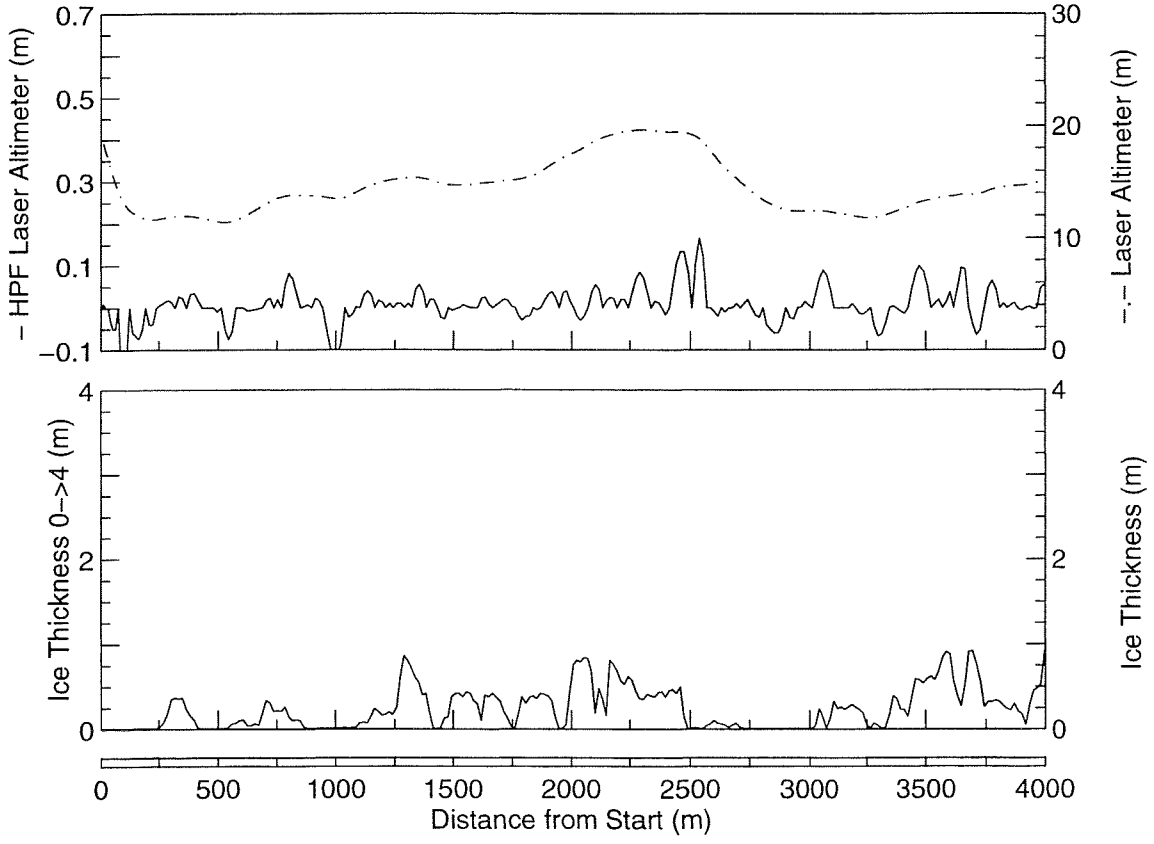

MAR 07 Flight #02 Line #10040 part 2 of 7

Line Starting Coordinates (53.5336,–55.9242) ending at (53.5138,–55.8737)

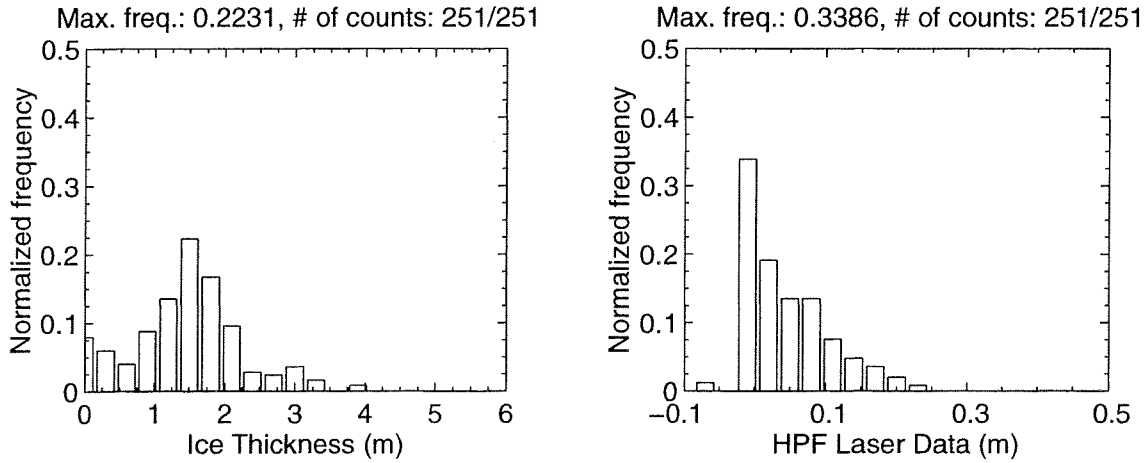

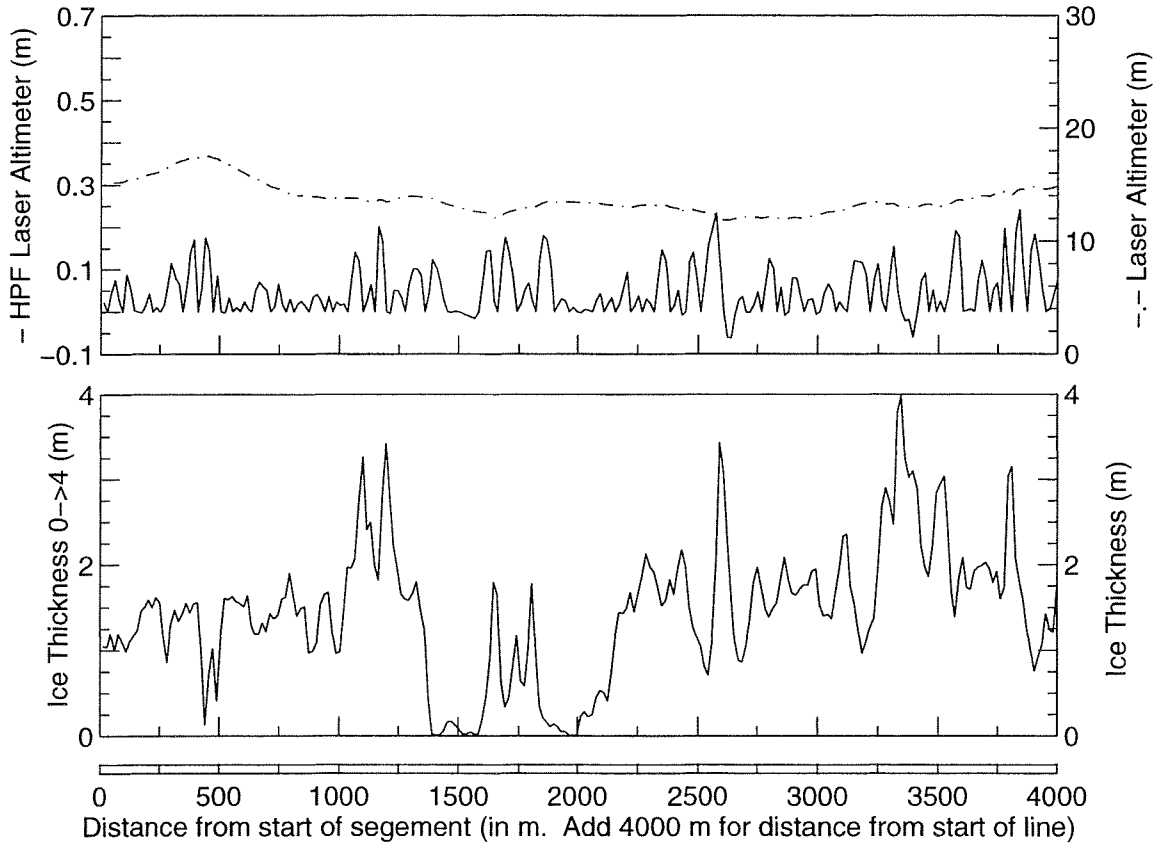

MAR 07 Flight #02 Line #10040 part 3 of 7

Line Starting Coordinates (53.5138,–55.8737) ending at (53.4964,–55.8211)

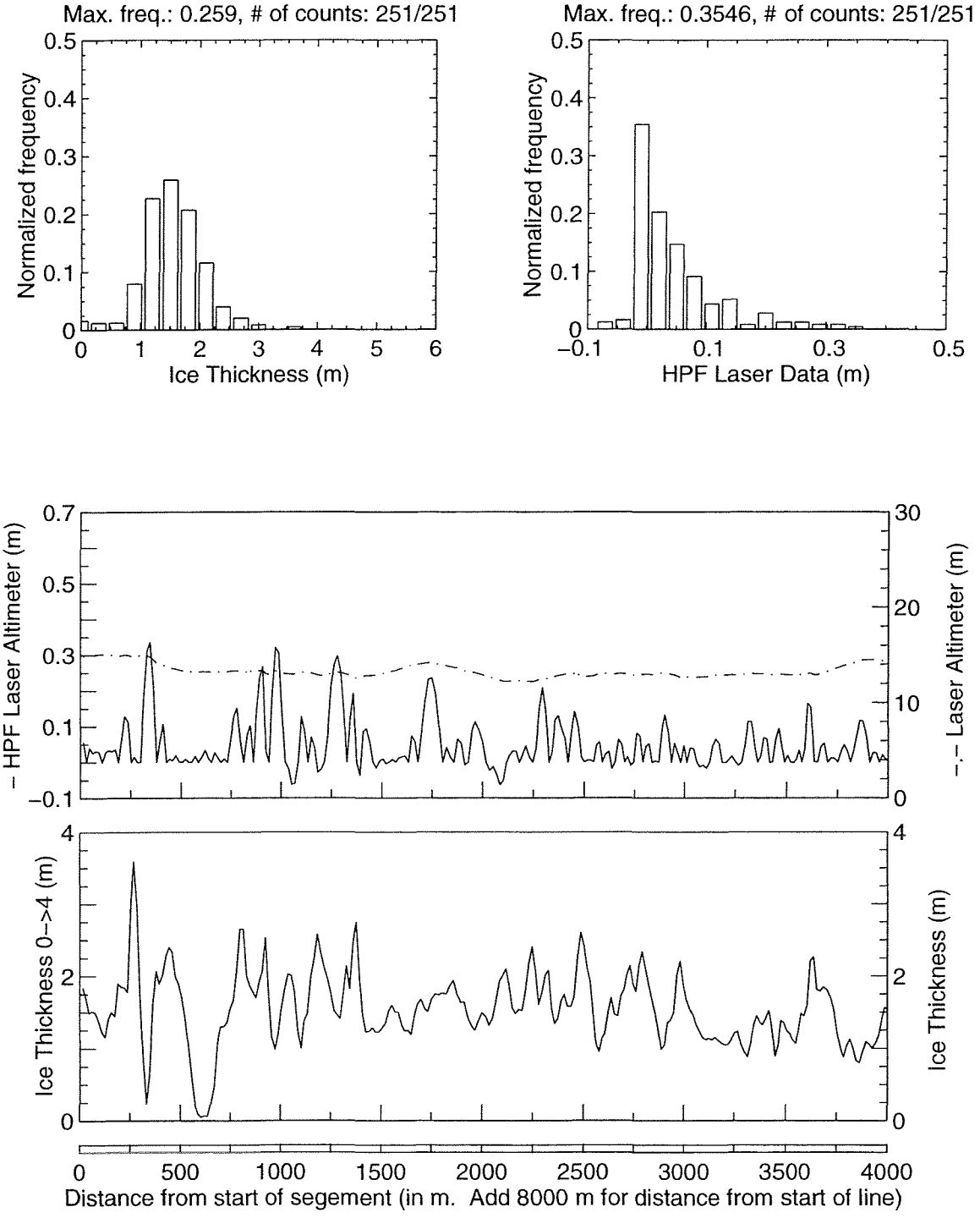

MAR 07 Flight #02 Line #10040 part 4 of 7

Line Starting Coordinates (53.4964,-55.8211) ending at (53.4800,-55.7673)

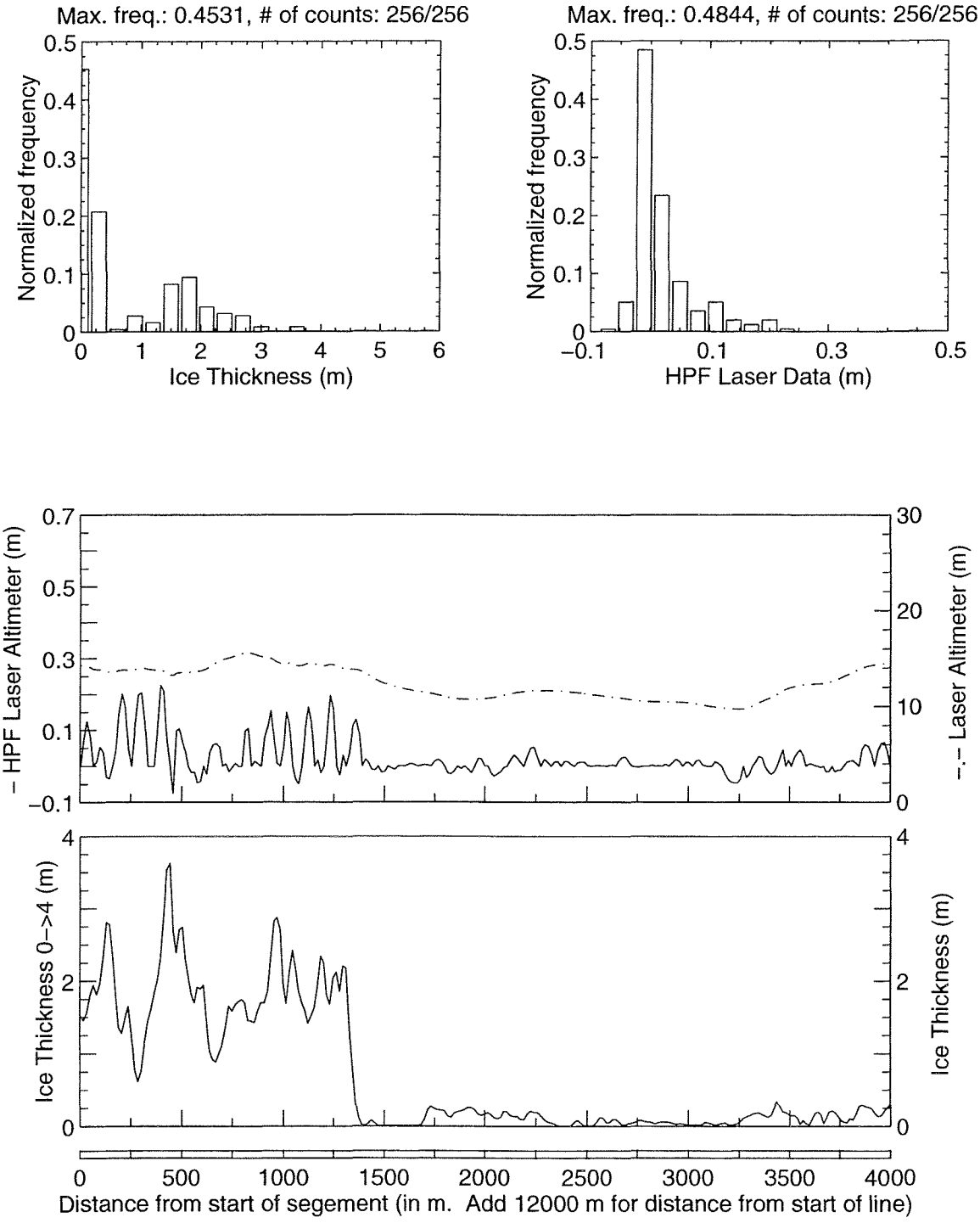

MAR 07 Flight #02 Line #10040 part 5 of 7

Line Starting Coordinates (53.4800,–55.7673) ending at (53.4650,–55.7126)

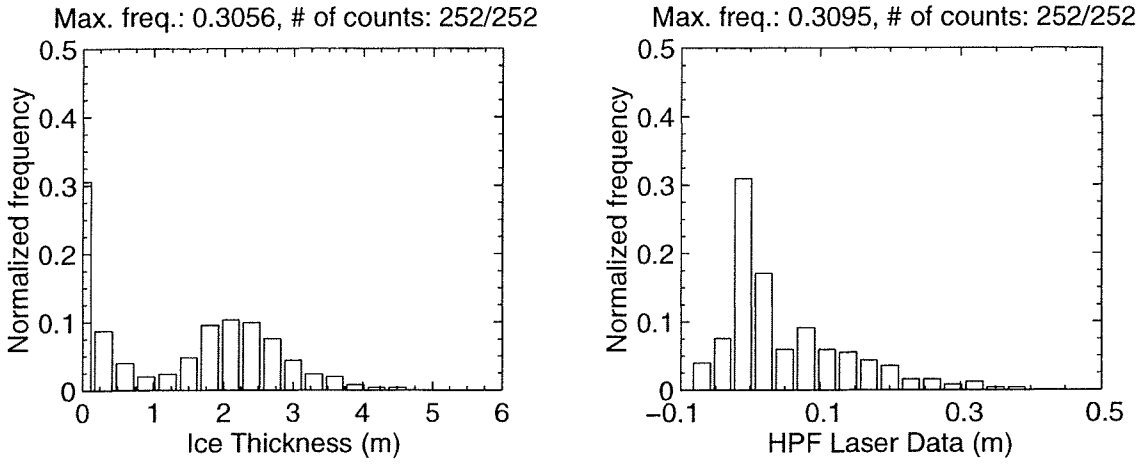

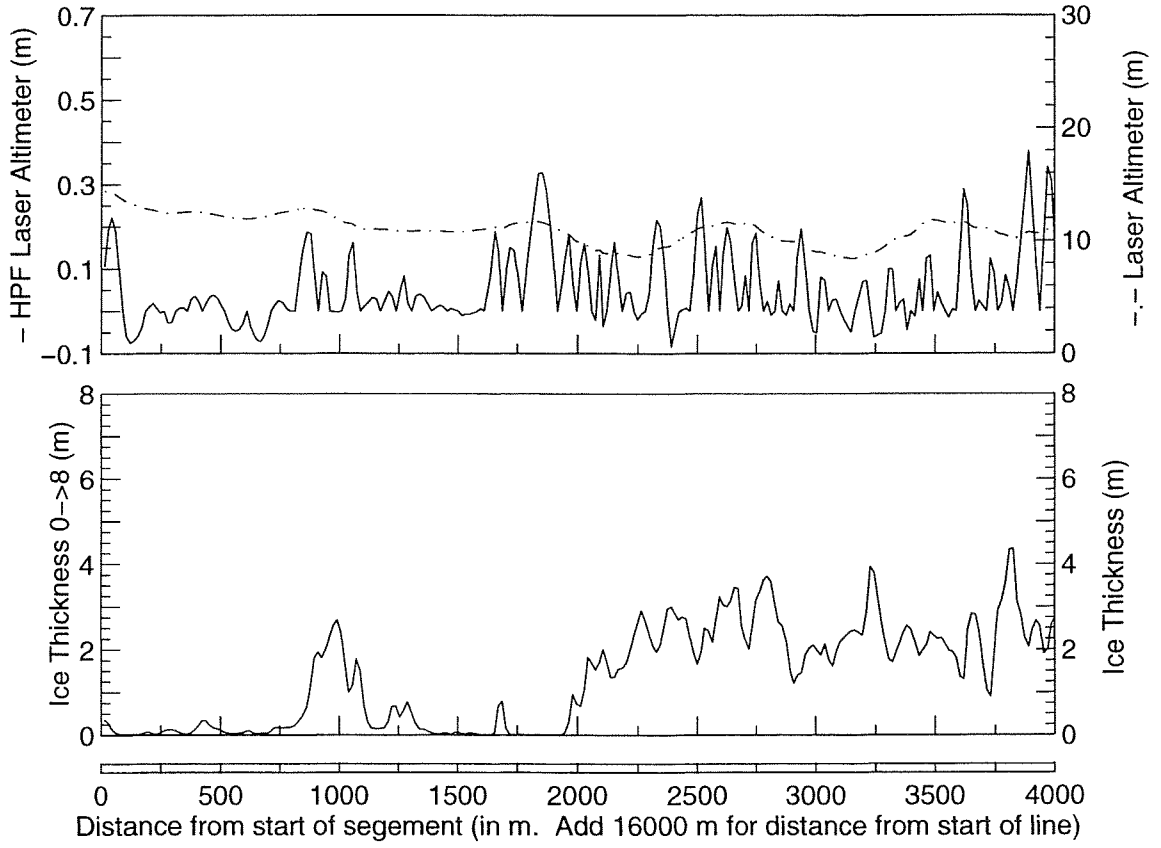

MAR 07 Flight #02 Line #10040 part 6 of 7

Line Starting Coordinates (53.4650,–55.7126) ending at (53.4483,–55.6593)

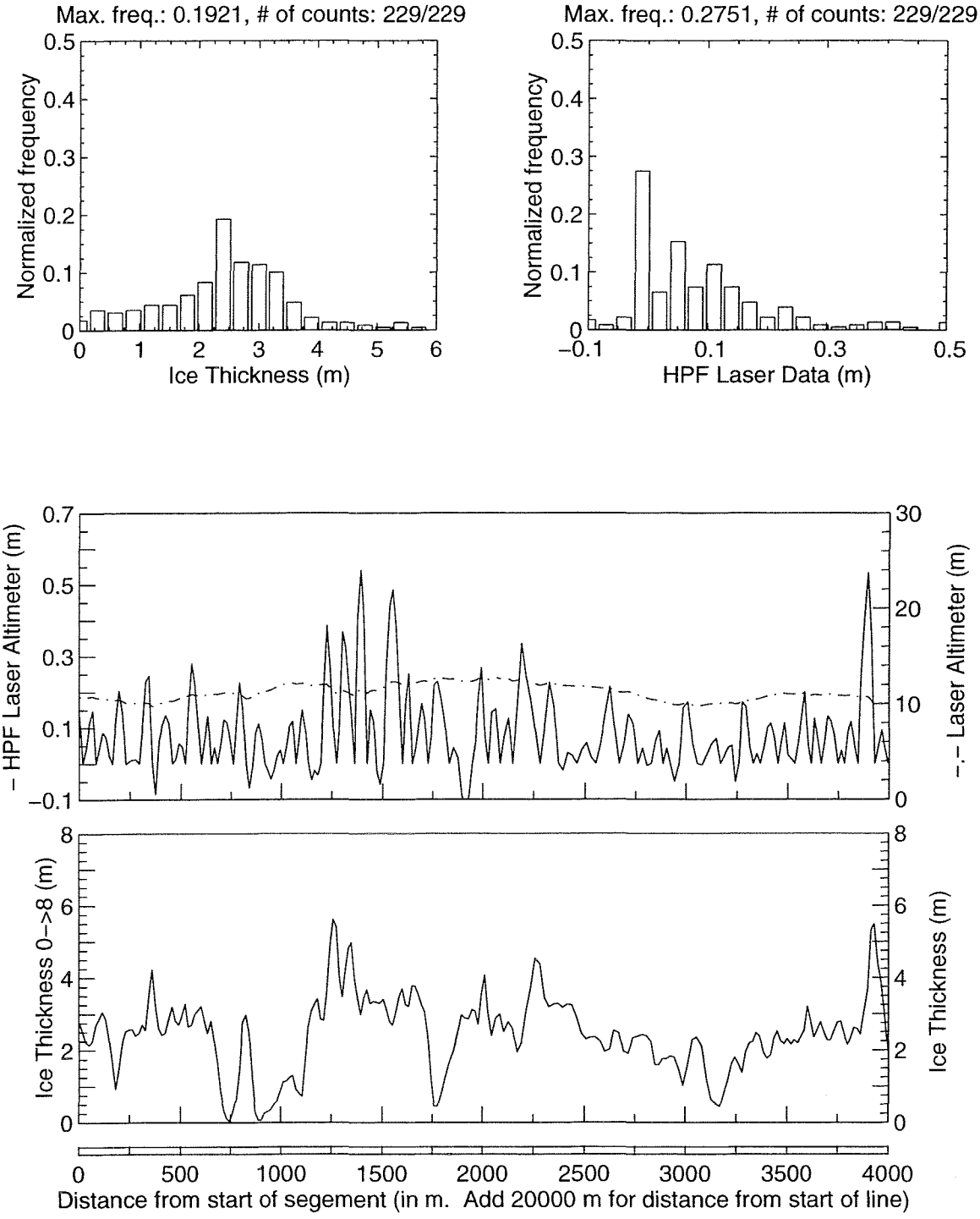

MAR 07 Flight #02 Line #10040 part 7 of 7

Line Starting Coordinates (53.4483,–55.6593) ending at (53.4404,–55.6241)

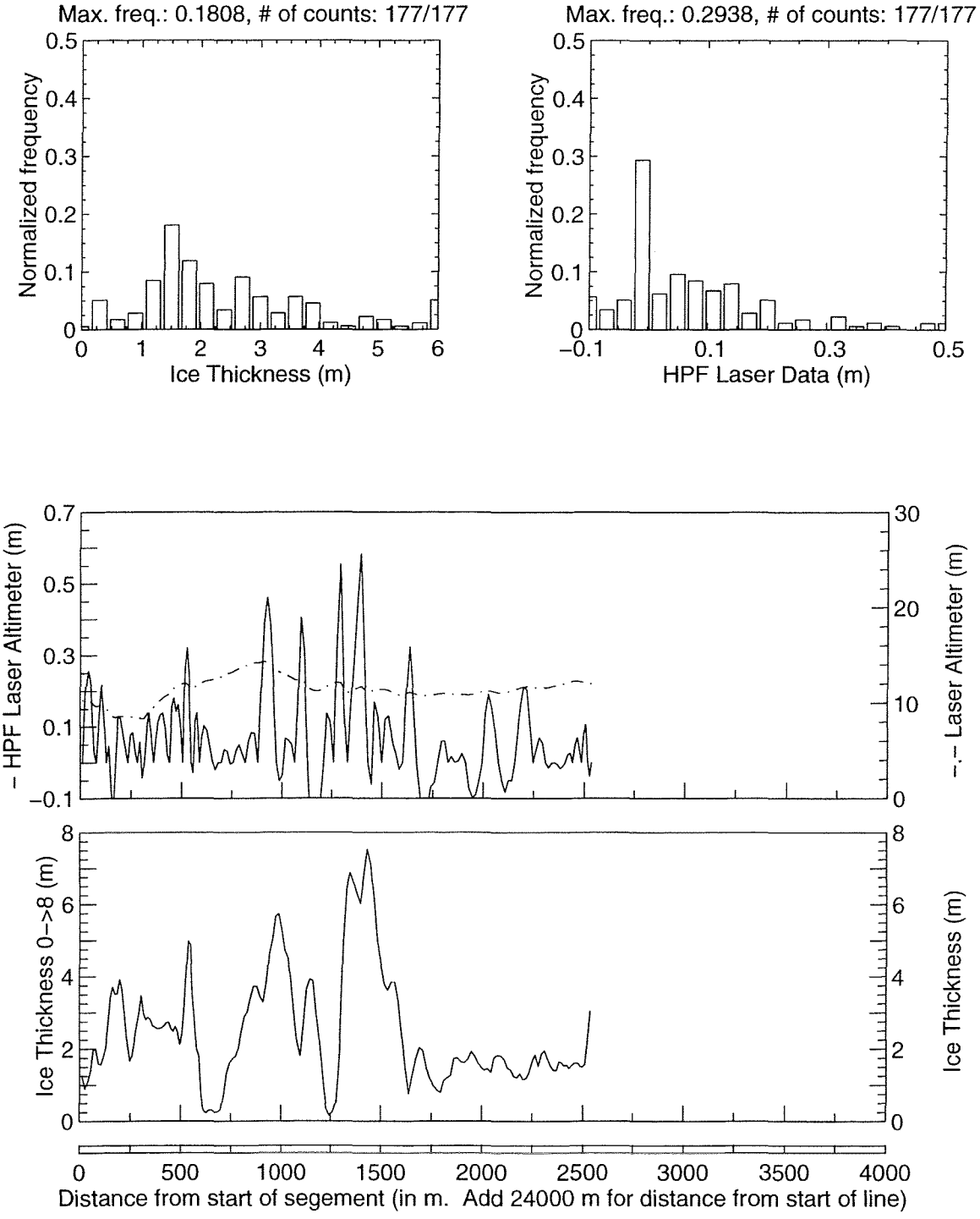

MAR 07 Flight #02 Line #10051 part 1 of 4

Line Starting Coordinates (53.4593,–55.6041) ending at (53.4951,–55.6108)

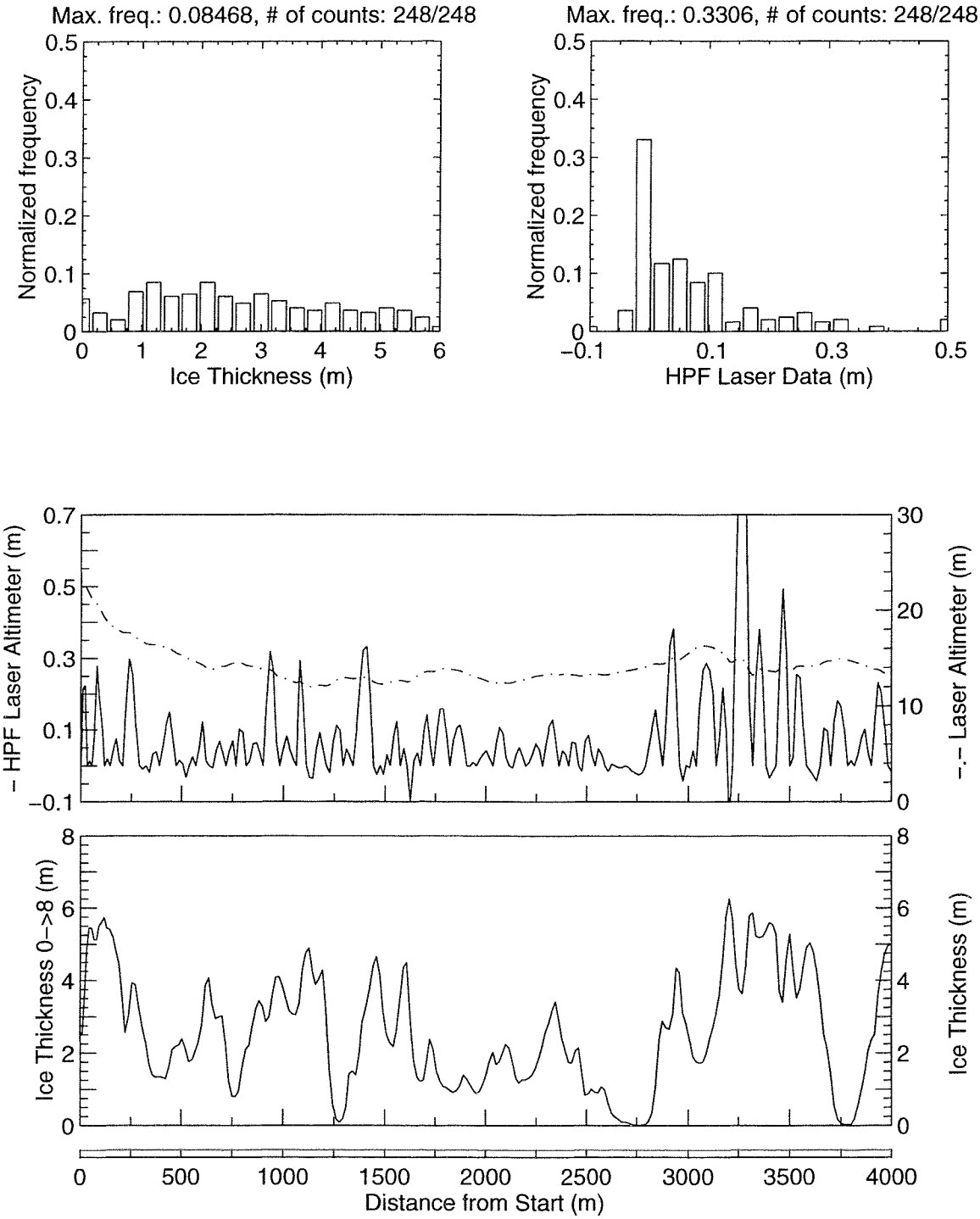

MAR 07 Flight #02 Line #10051 part 2 of 4

Line Starting Coordinates (53.4951,–55.6108) ending at (53.5309,–55.6158)

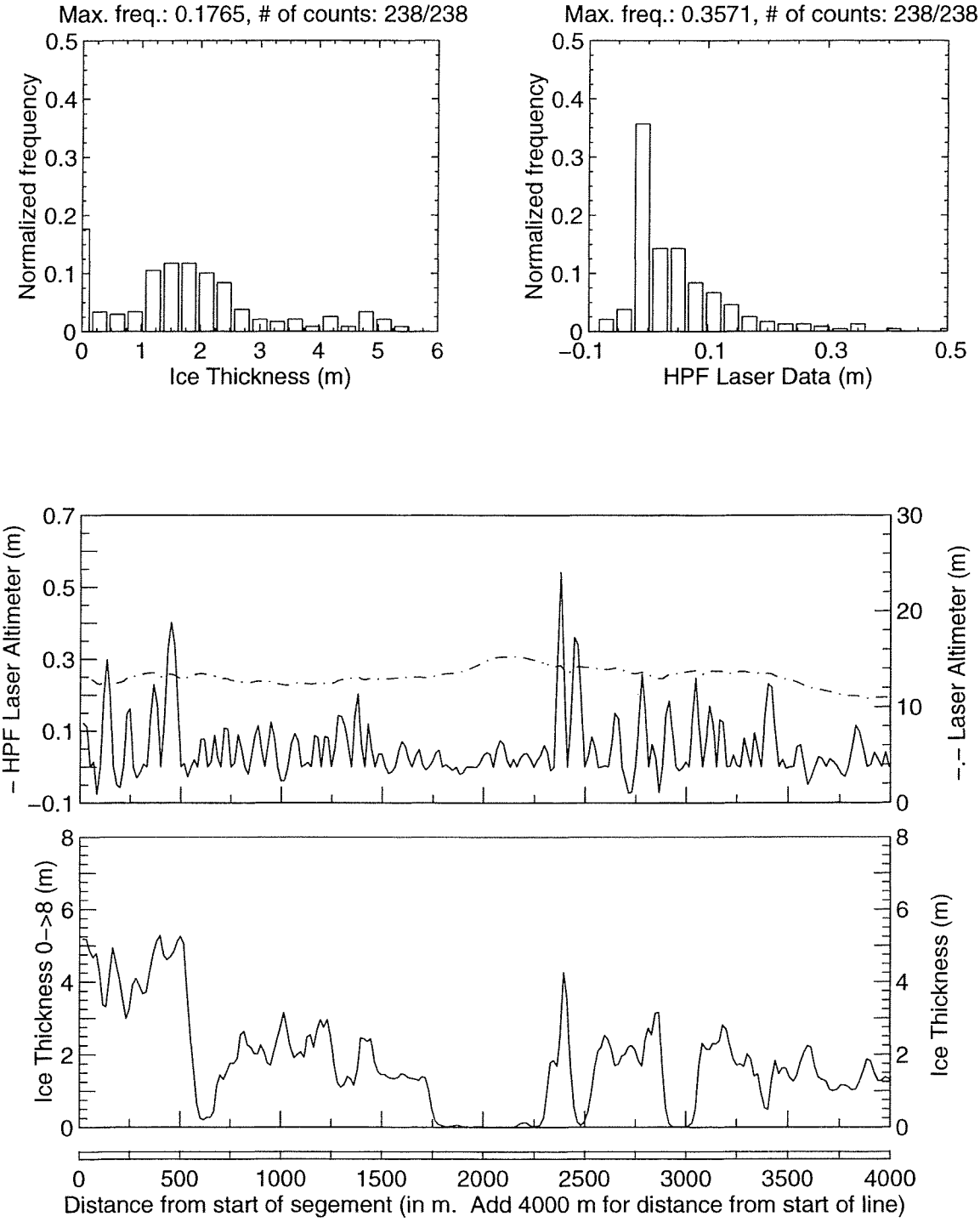

MAR 07 Flight #02 Line #10051 part 3 of 4

Line Starting Coordinates (53.5309,–55.6158) ending at (53.5668,–55.6175)

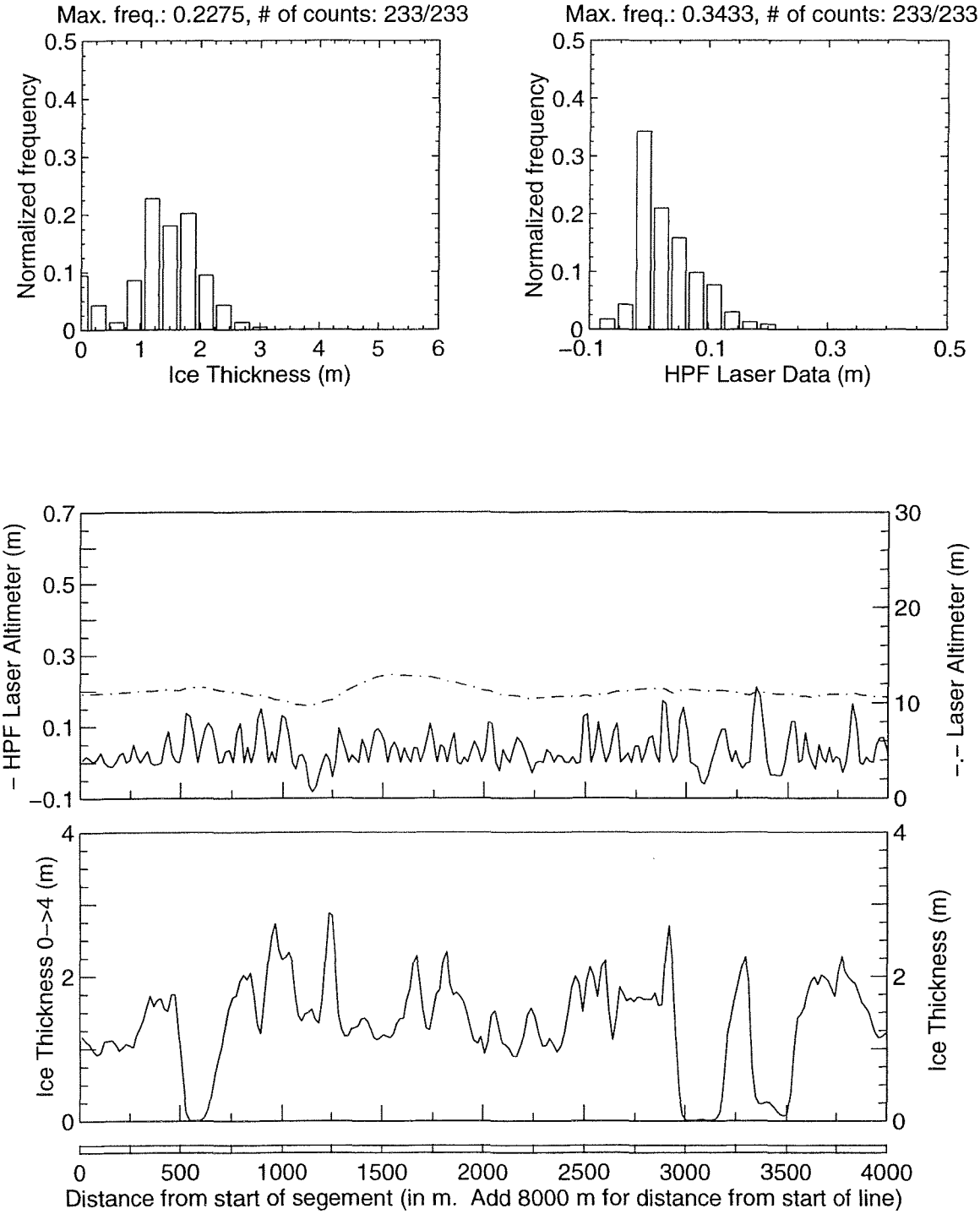

MAR 07 Flight #02 Line #10051 part 4 of 4

Line Starting Coordinates (53.5668,–55.6175) ending at (53.5695,–55.6175)

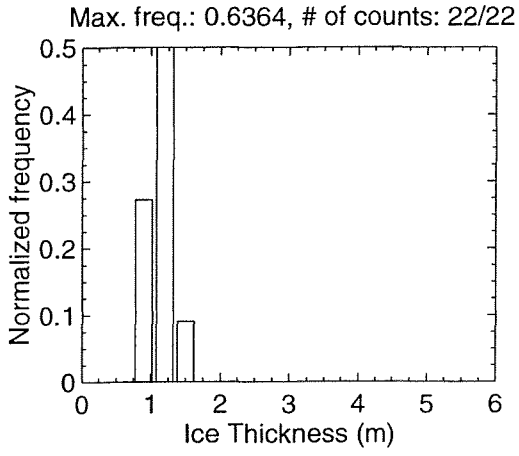

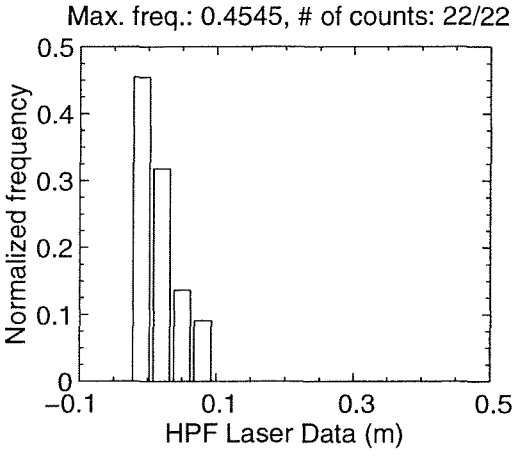

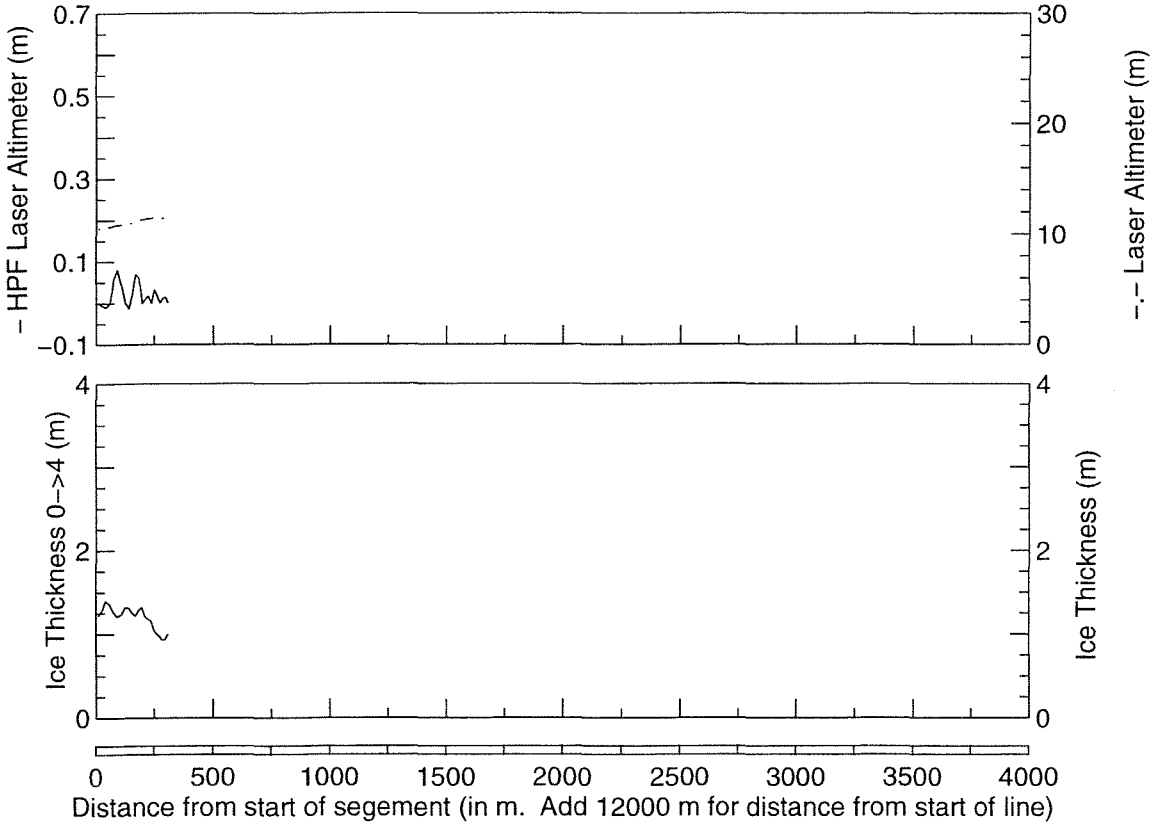

MAR 07 Flight #02 Line #10052 part 1 of 1

Line Starting Coordinates (53.5708,–55.6175) ending at (53.5994,–55.6154)

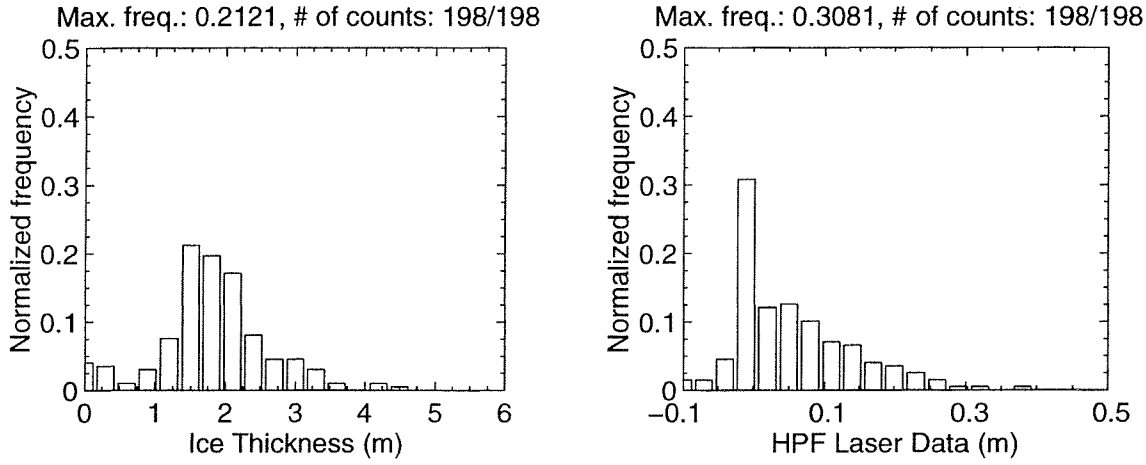

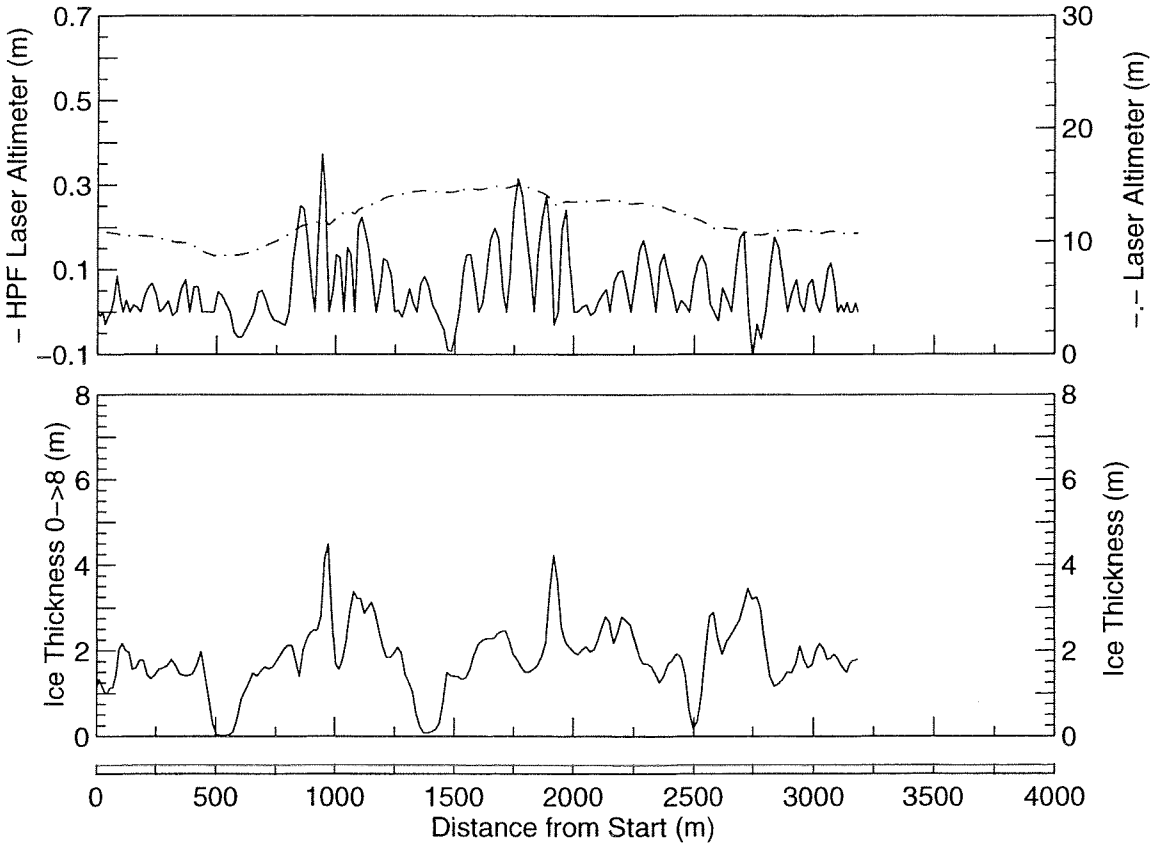

MAR 07 Flight #02 Line #10053 part 1 of 2

Line Starting Coordinates (53.6009,–55.6154) ending at (53.6369,–55.6192)

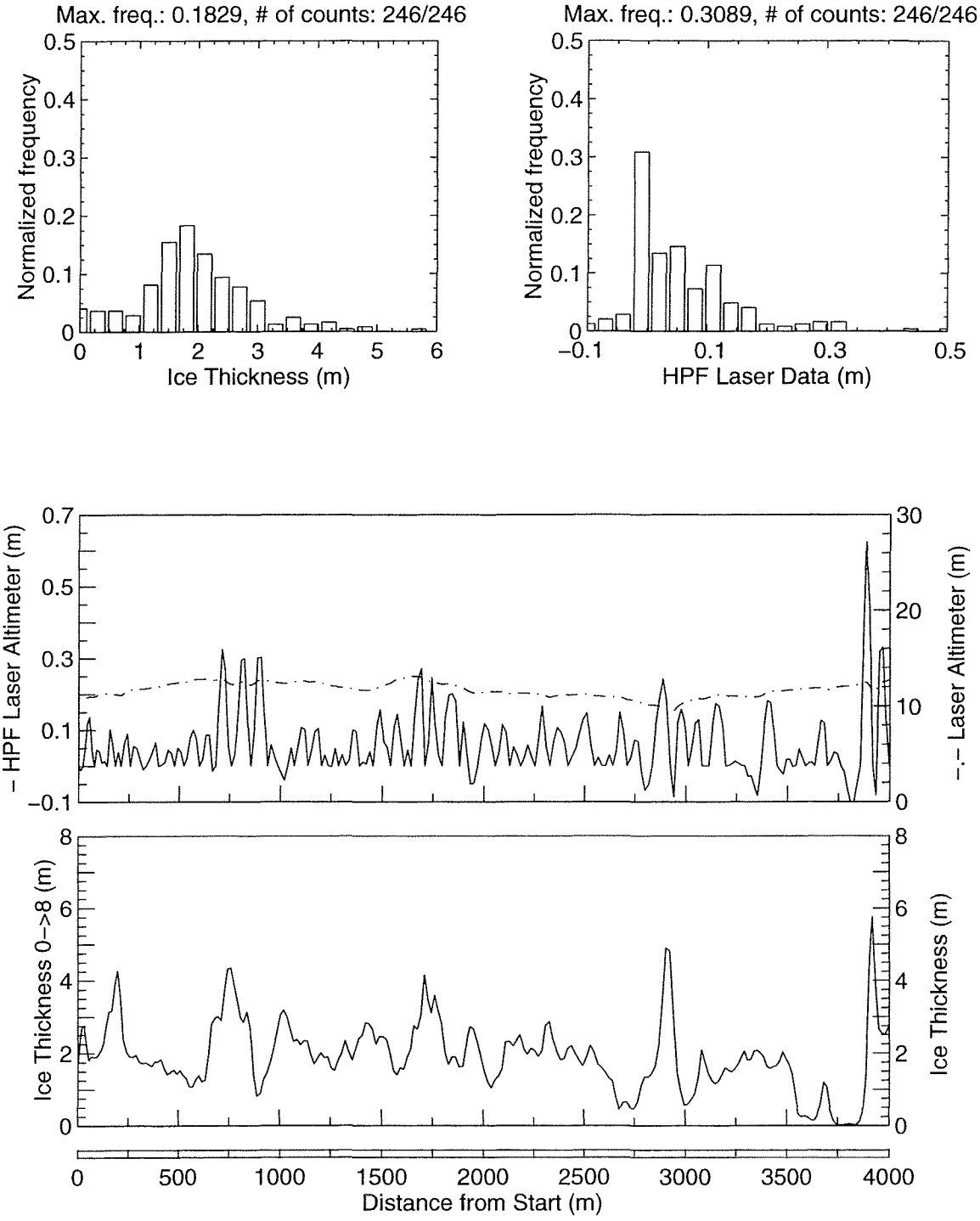

MAR 07 Flight #02 Line #10053 part 2 of 2

Line Starting Coordinates (53.6369,–55.6192) ending at (53.6467,–55.6207)

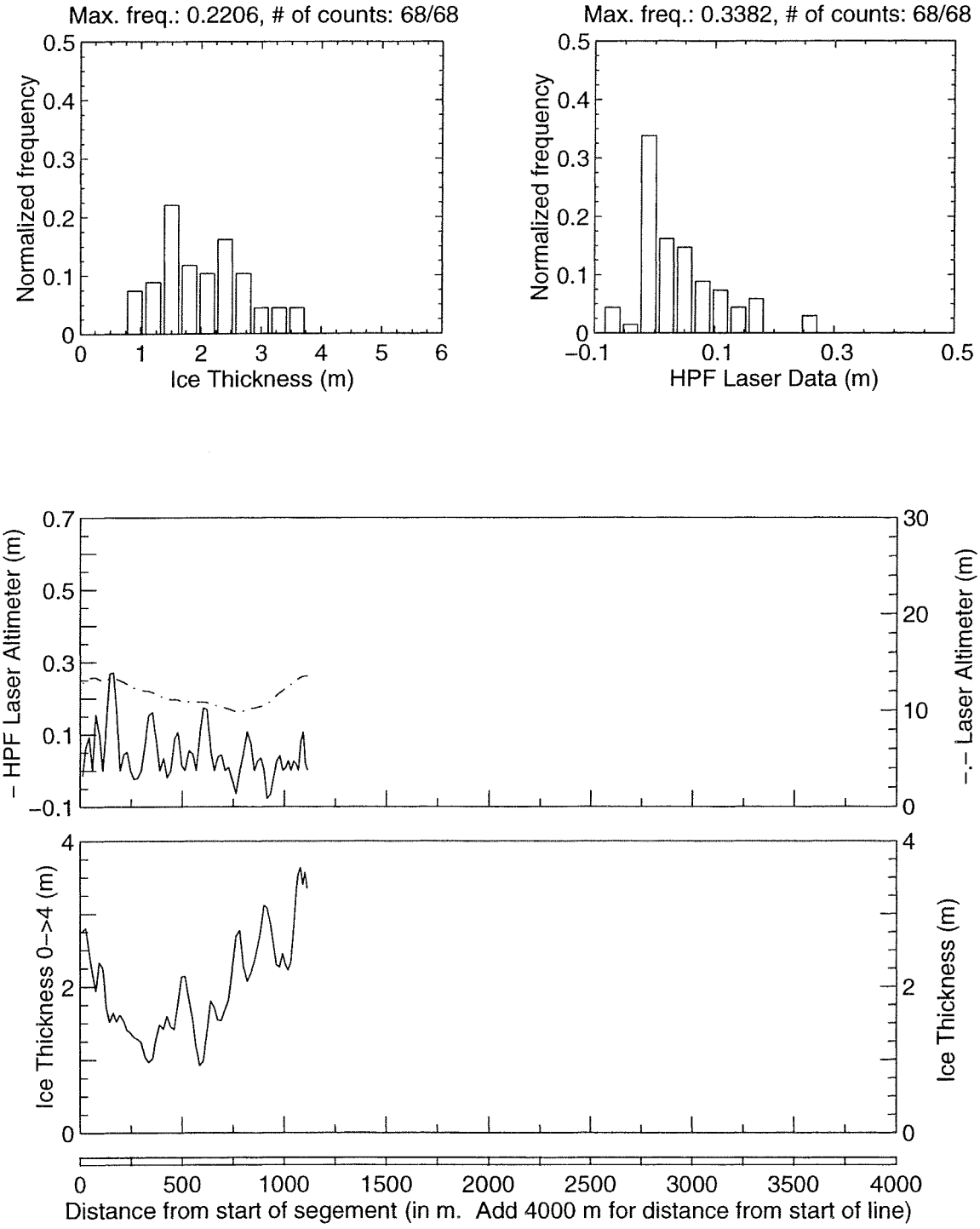

MAR 07 Flight #02 Line #10061 part 1 of 2

Line Starting Coordinates (53.6898,–55.6241) ending at (53.7259,–55.6263)

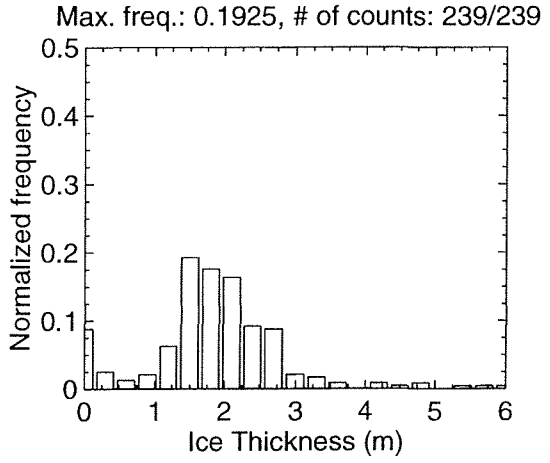

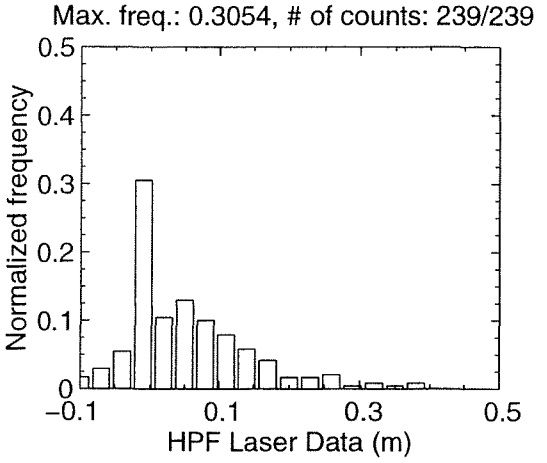

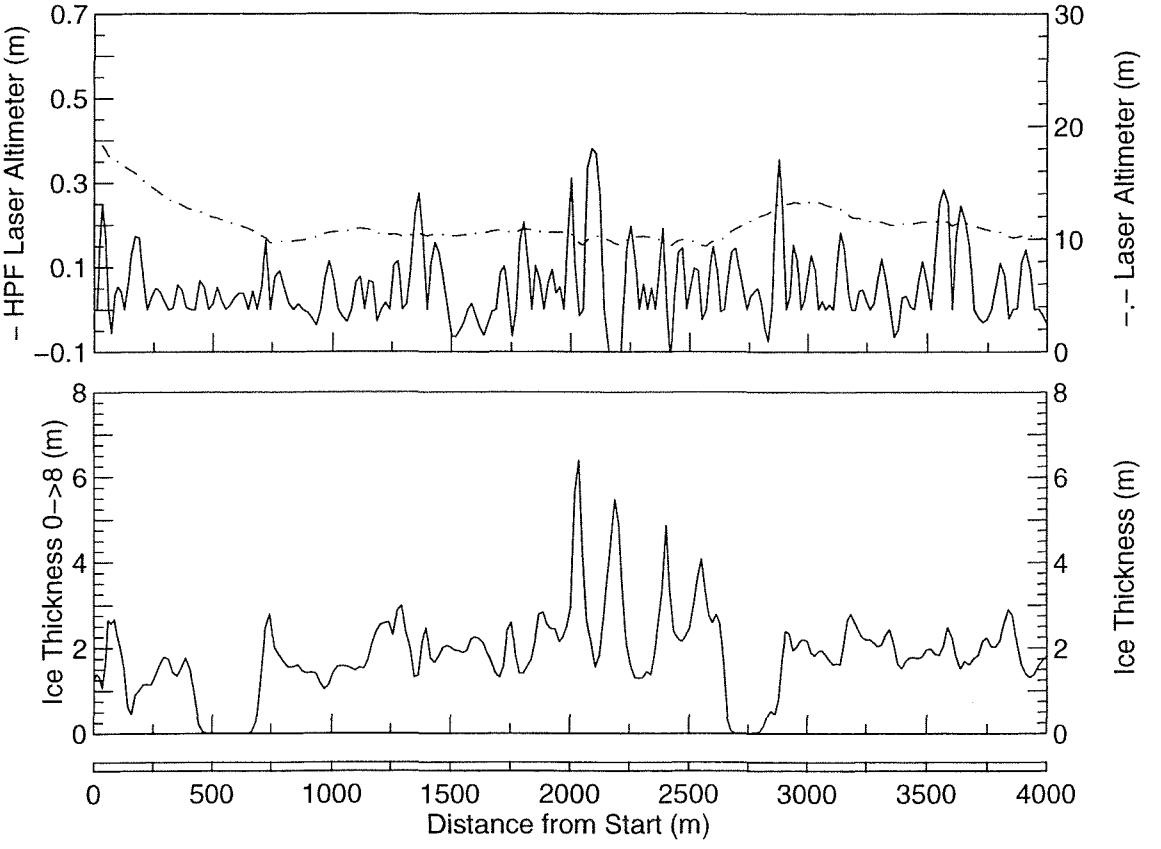

MAR 07 Flight #02 Line #10061 part 2 of 2

Line Starting Coordinates (53.7259,–55.6263) ending at (53.7392,–55.6268)

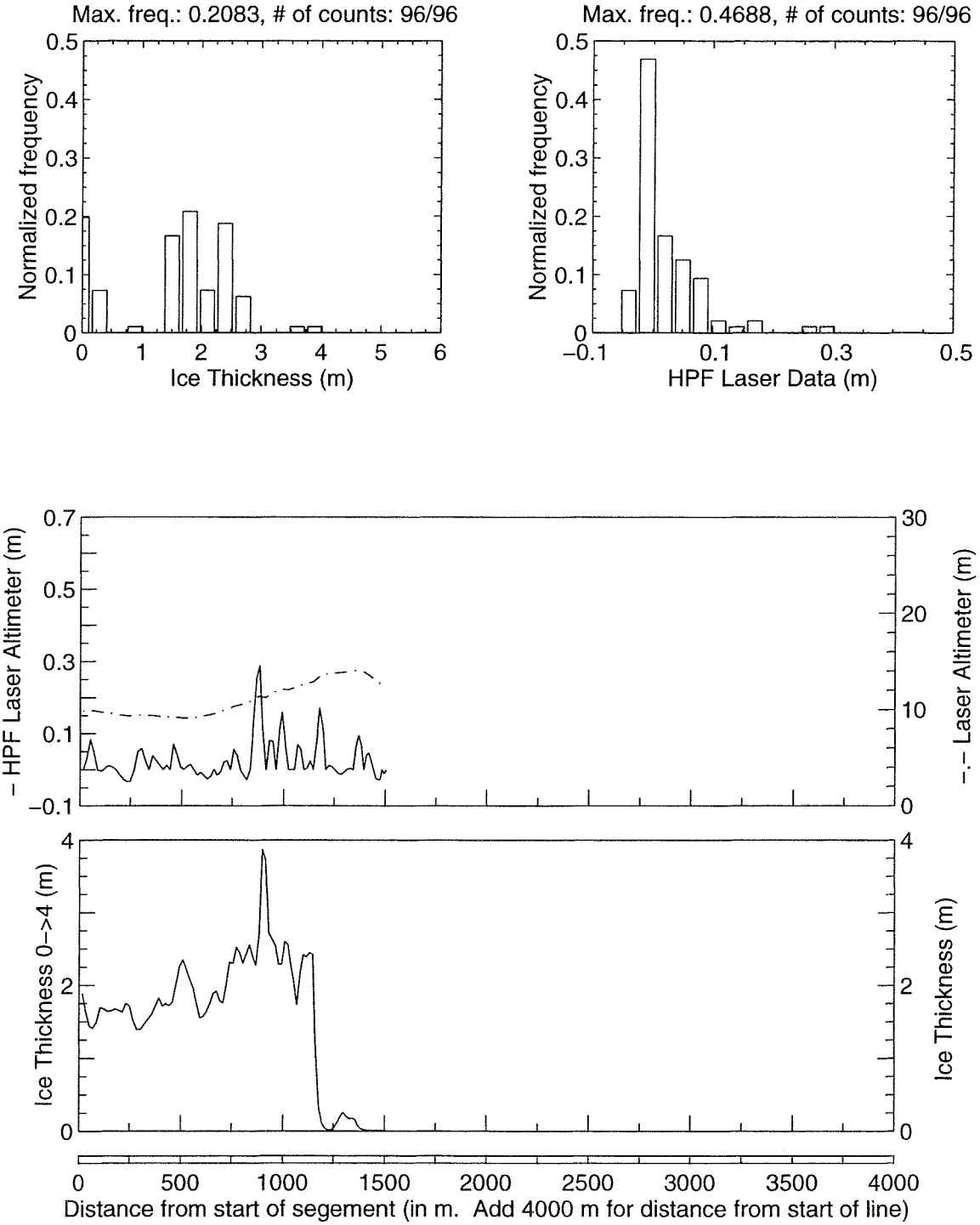

MAR 07 Flight #02 Line #10062 part 1 of 4

Line Starting Coordinates (53.7406,–55.6268) ending at (53.7767,–55.6245)

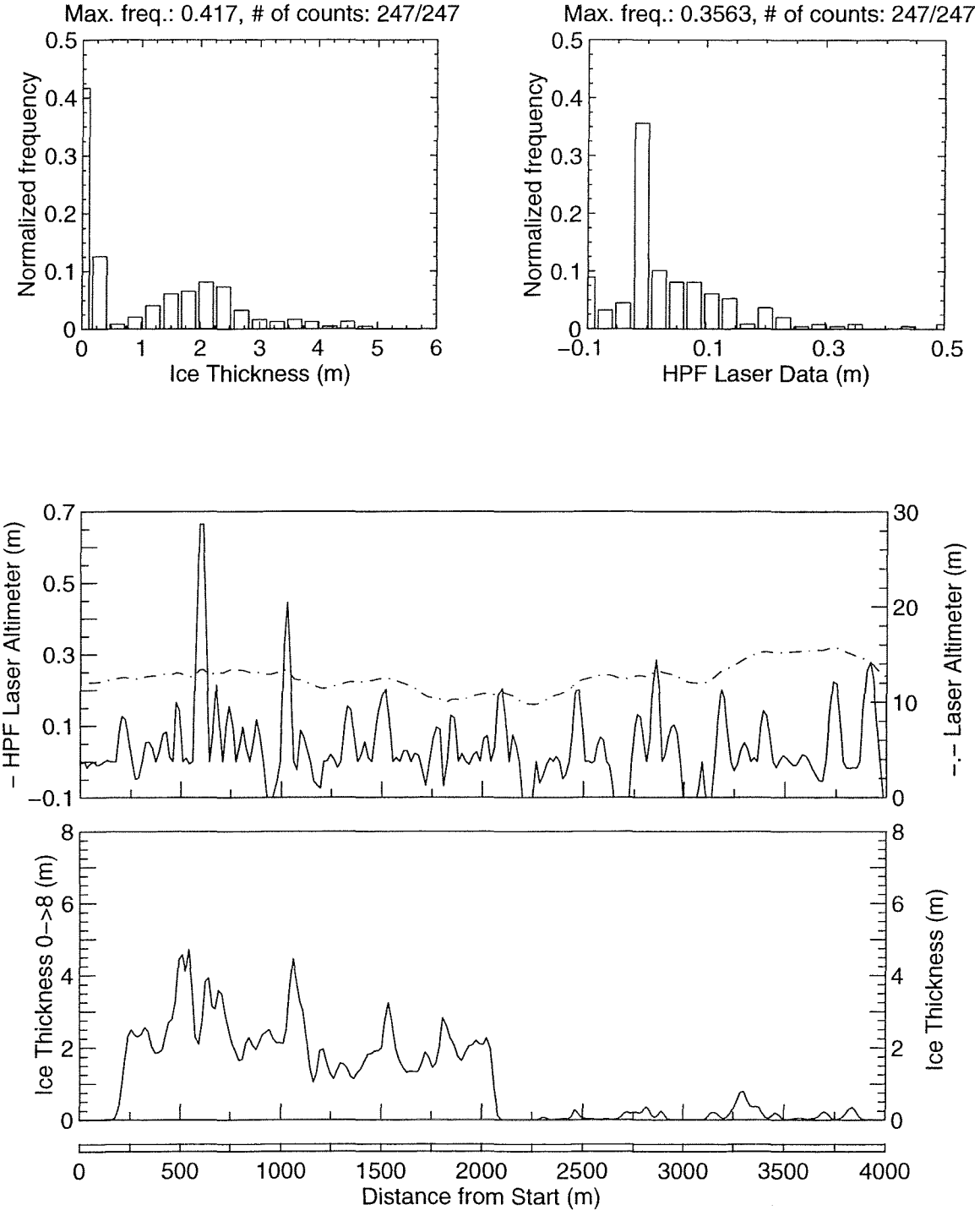

MAR 07 Flight #02 Line #10062 part 2 of 4

Line Starting Coordinates (53.7767,–55.6245) ending at (53.8125,–55.6210)

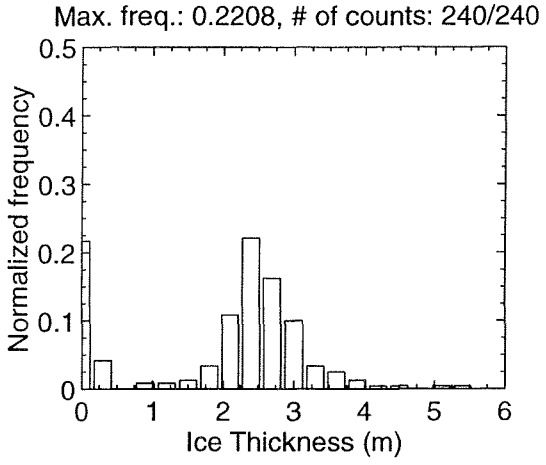

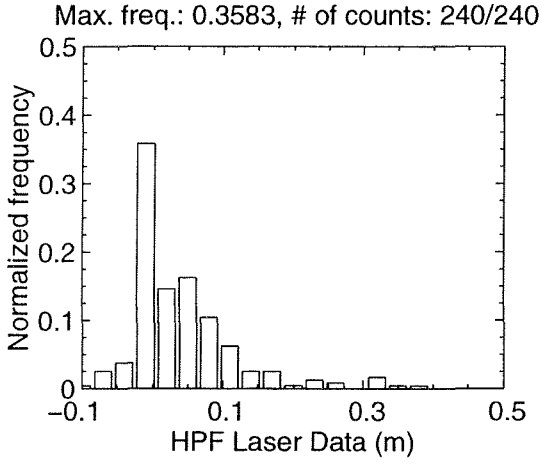

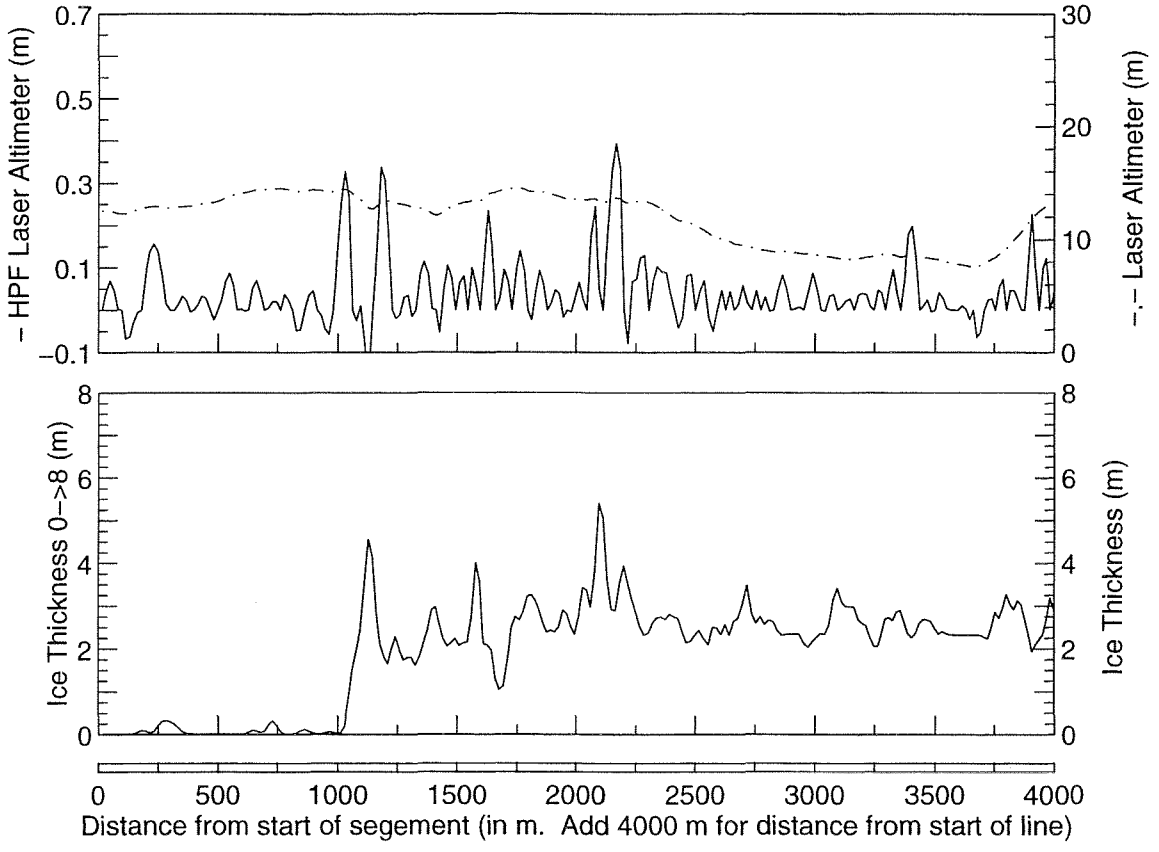

MAR 07 Flight #02 Line #10062 part 3 of 4

Line Starting Coordinates (53.8125,-55.6210) ending at (53.8483,-55.6190)

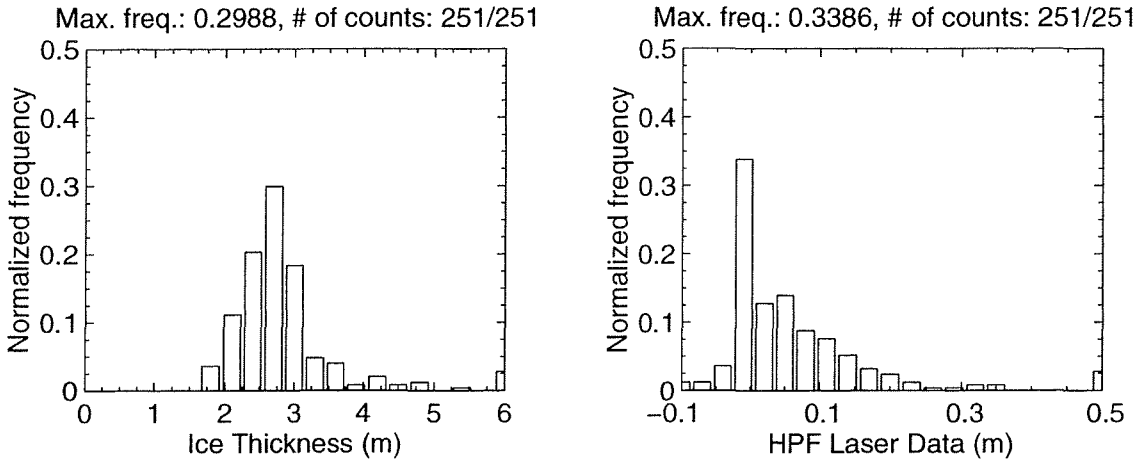

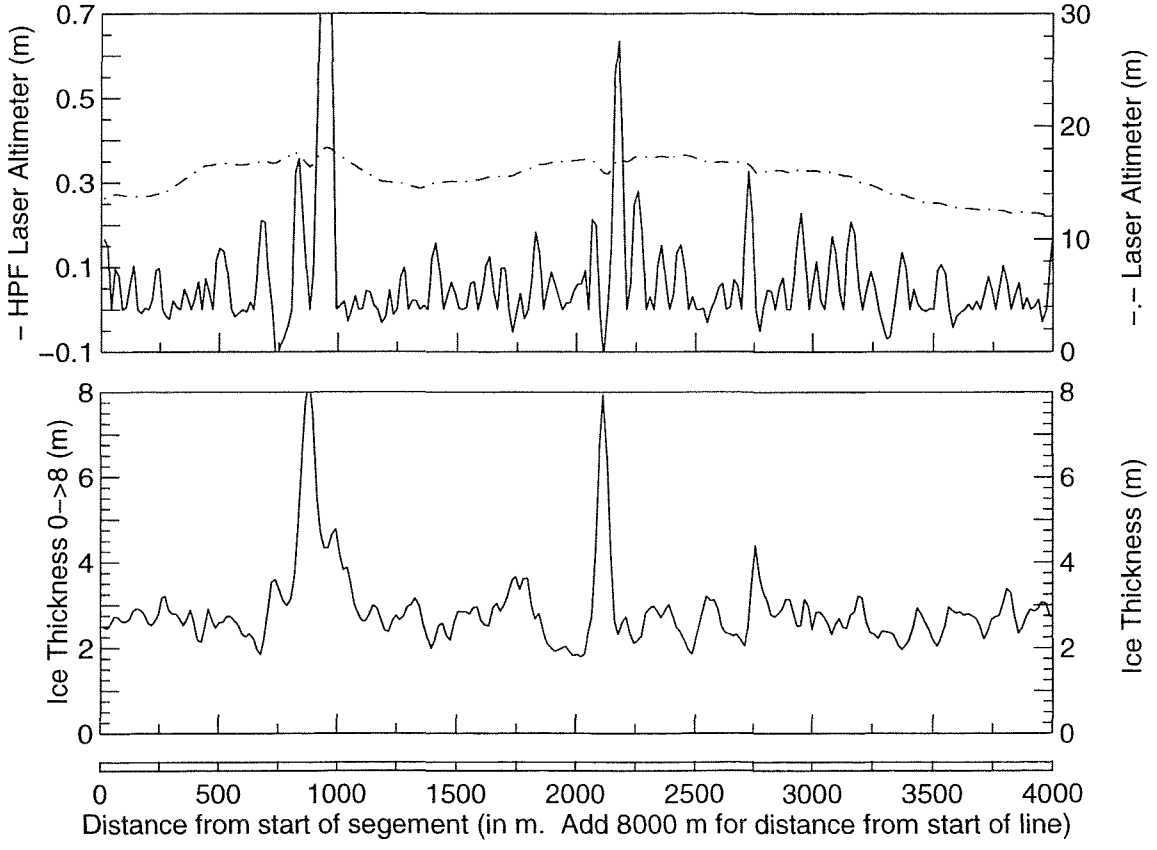

MAR 07 Flight #02 Line #10062 part 4 of 4

Line Starting Coordinates (53.8483,–55.6190) ending at (53.8577,–55.6184)

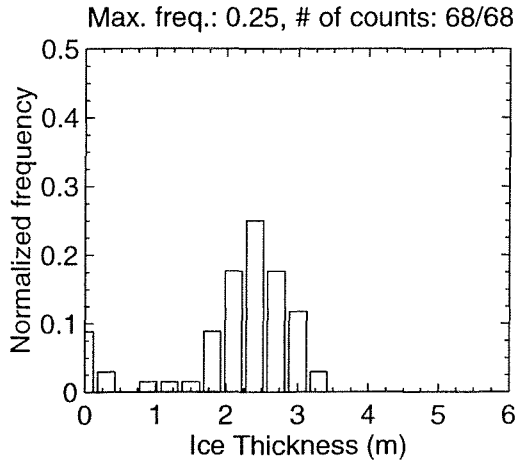

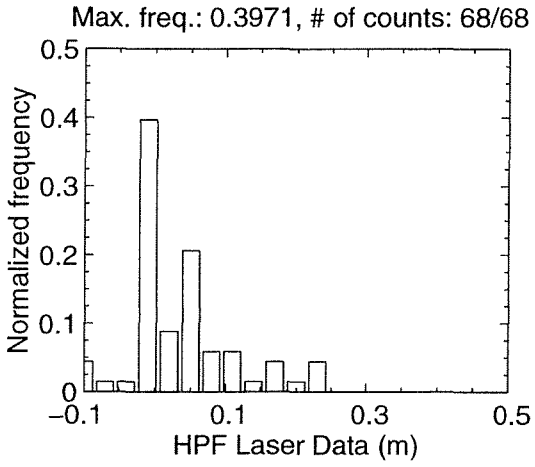

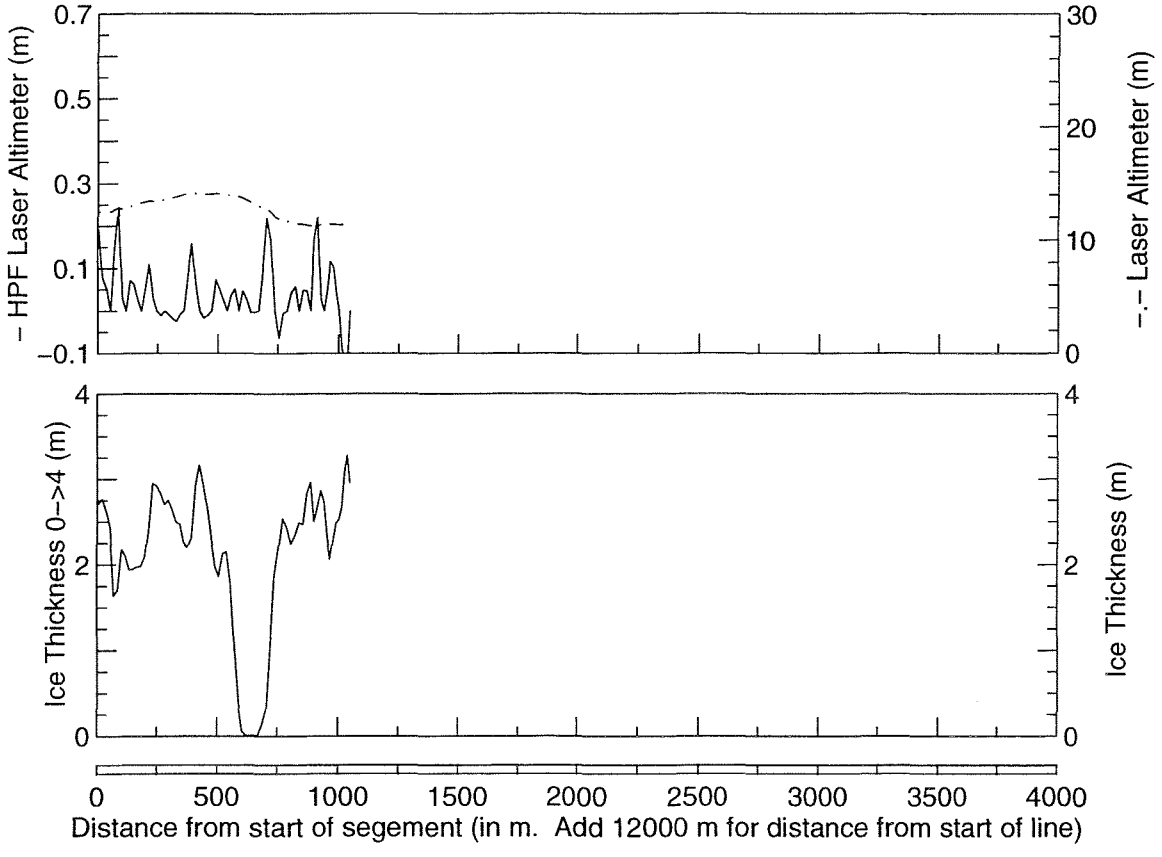

MAR 07 Flight #02 Line #10070 part 1 of 5

Line Starting Coordinates (53.8662,–55.6856) ending at (53.8666,–55.7467)

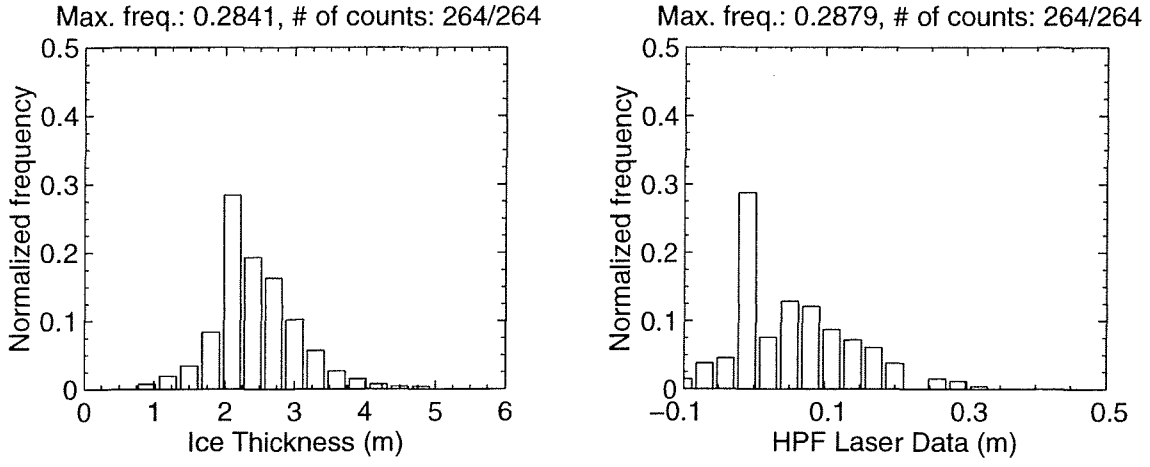

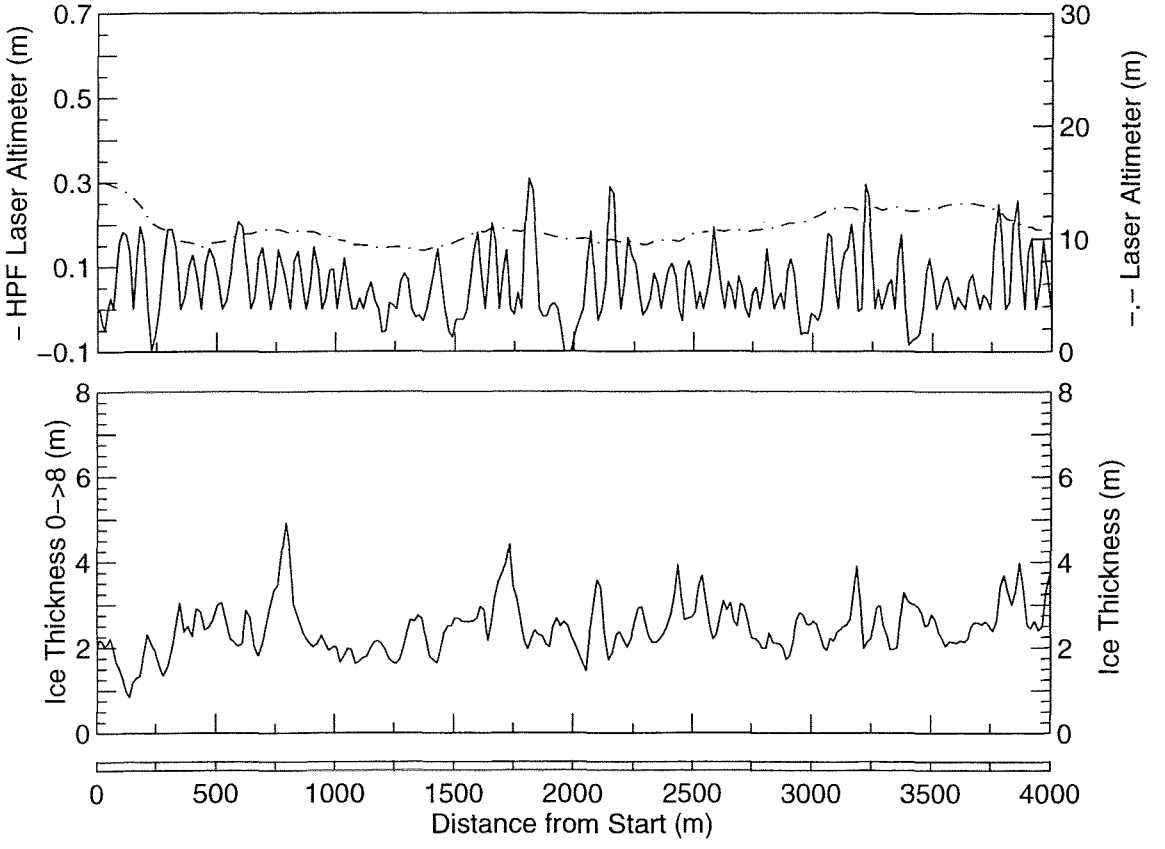

MAR 07 Flight #02 Line #10070 part 2 of 5

Line Starting Coordinates (53.8666,–55.7467) ending at (53.8677,–55.8075)

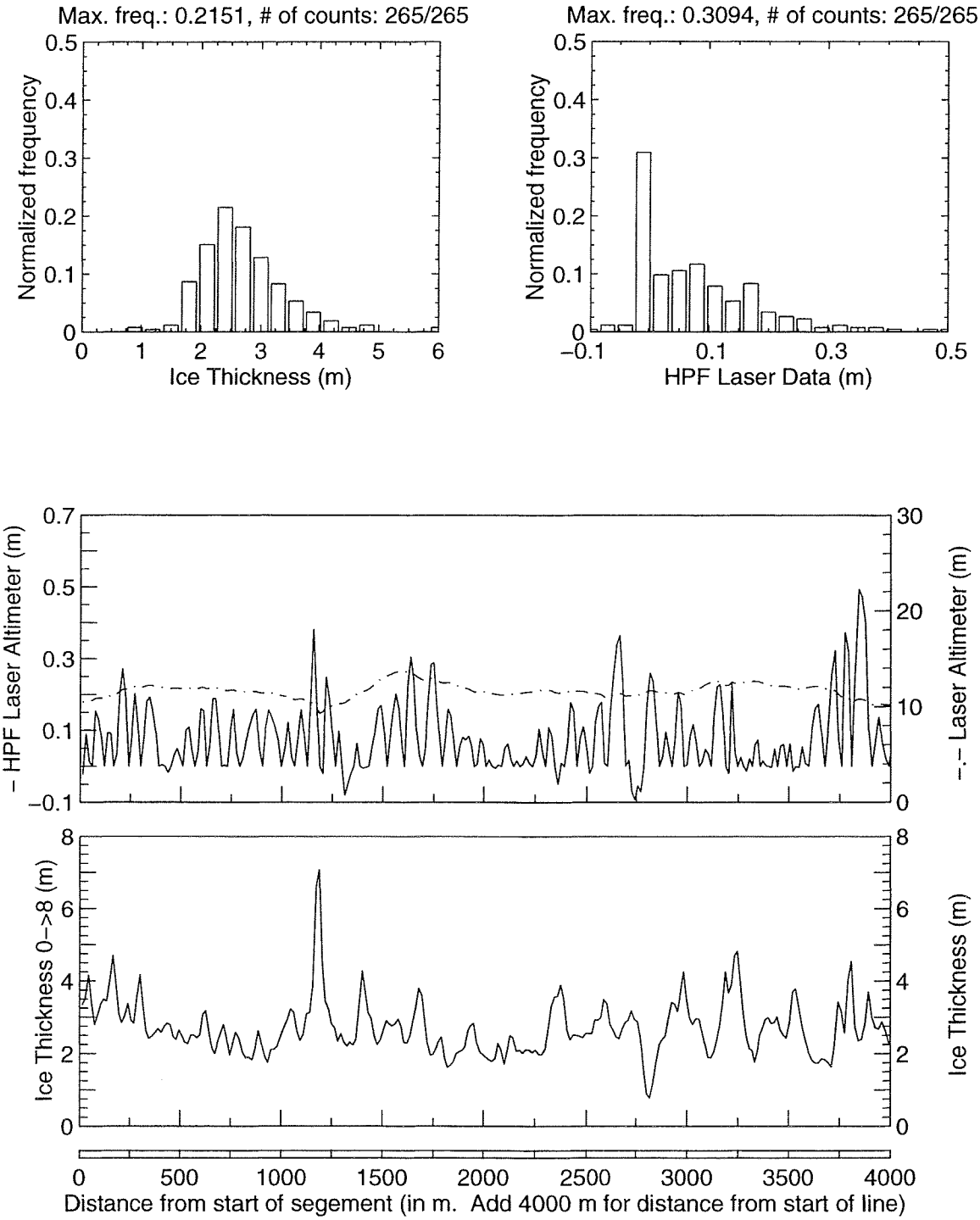

MAR 07 Flight #02 Line #10070 part 3 of 5

Line Starting Coordinates (53.8677,–55.8075) ending at (53.8689,–55.8684)

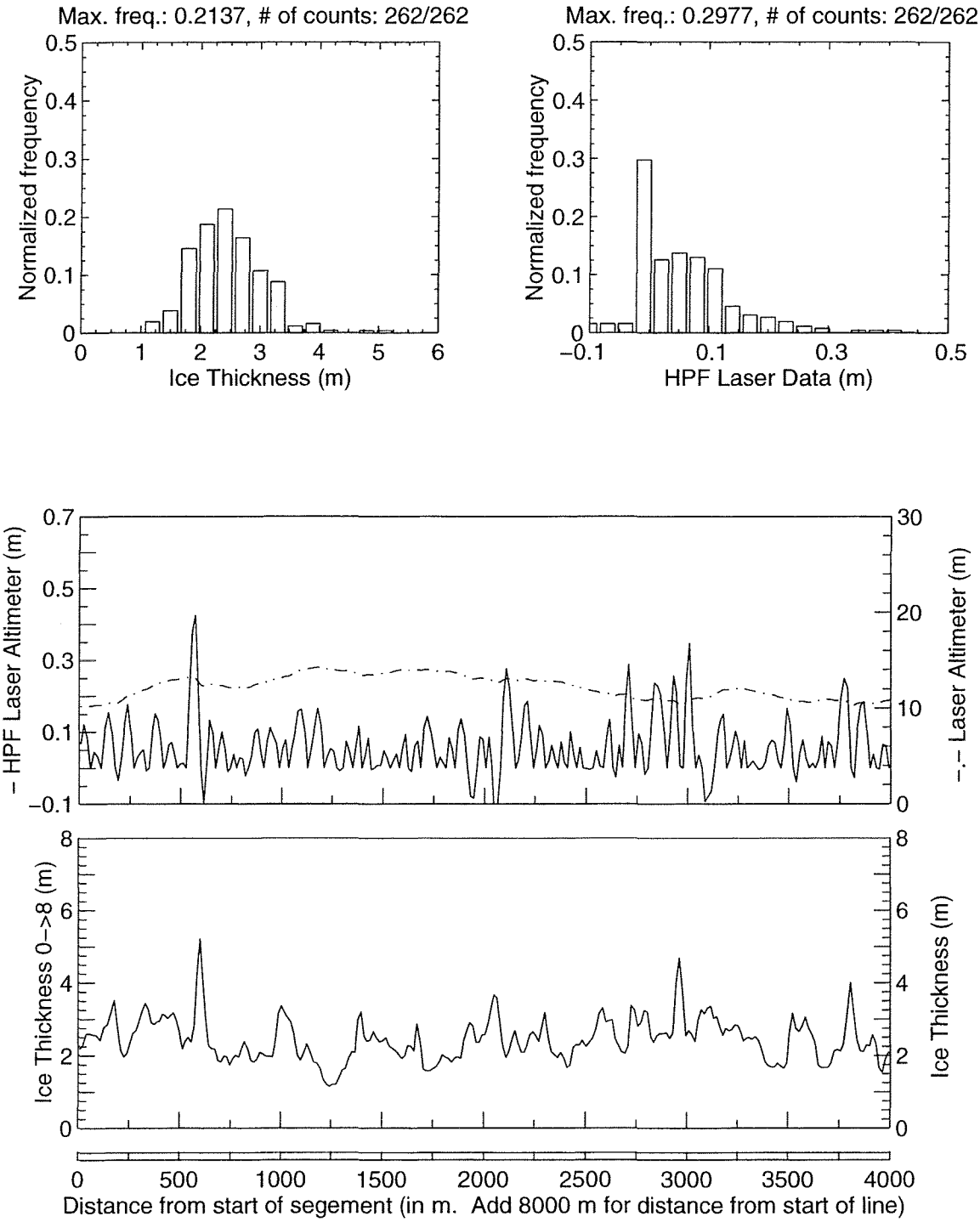

MAR 07 Flight #02 Line #10070 part 4 of 5

Line Starting Coordinates (53.8689,–55.8684) ending at (53.8705,–55.9293)

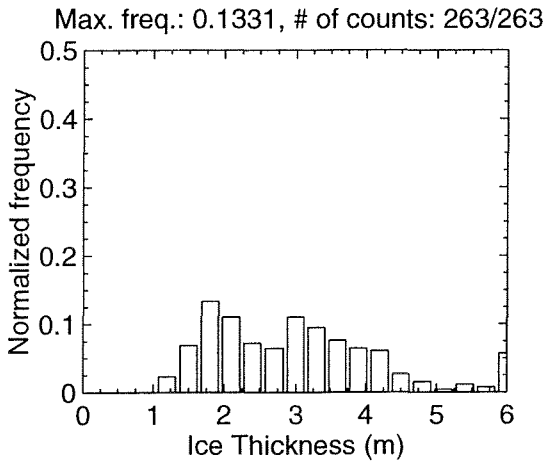

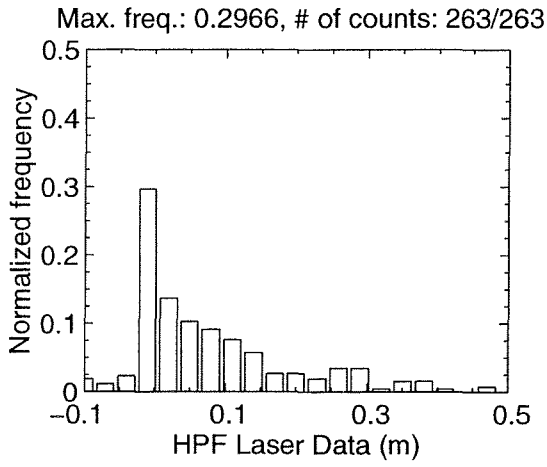

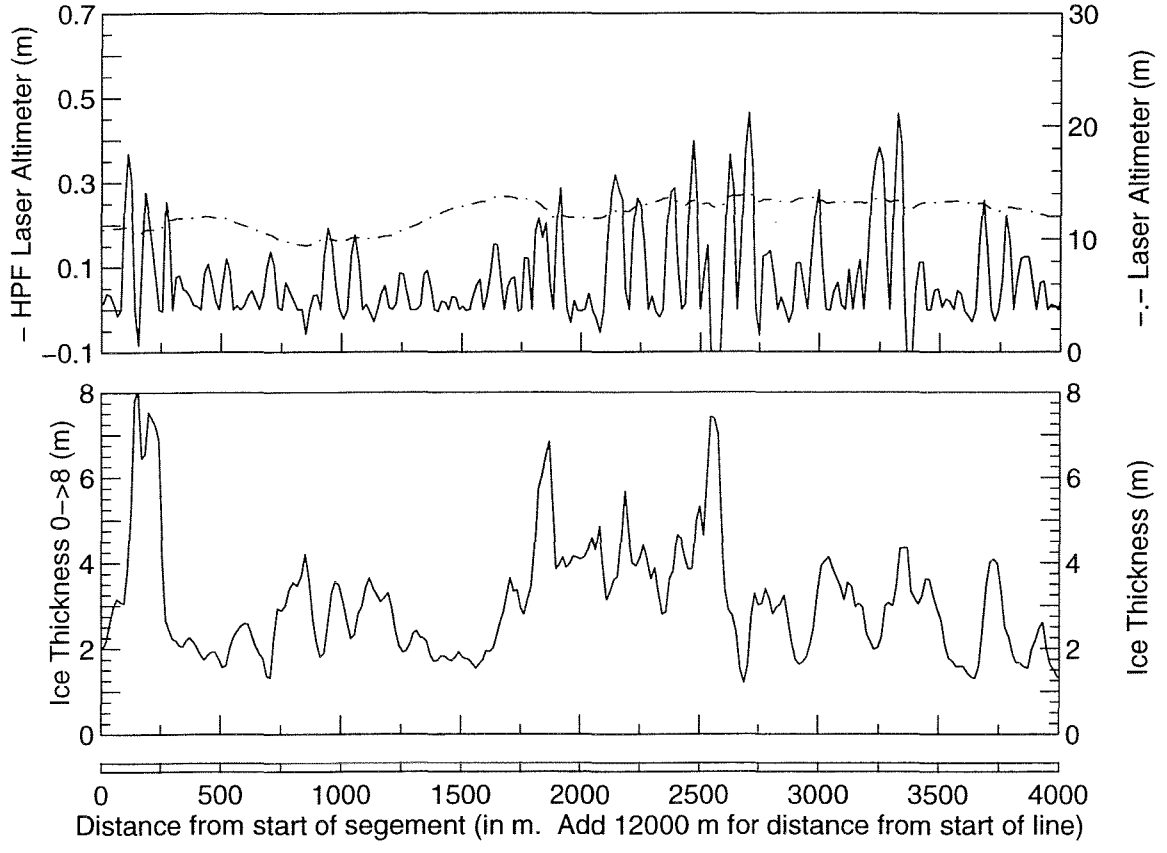

MAR 07 Flight #02 Line #10070 part 5 of 5

Line Starting Coordinates (53.8705,–55.9293) ending at (53.8710,–55.9550)

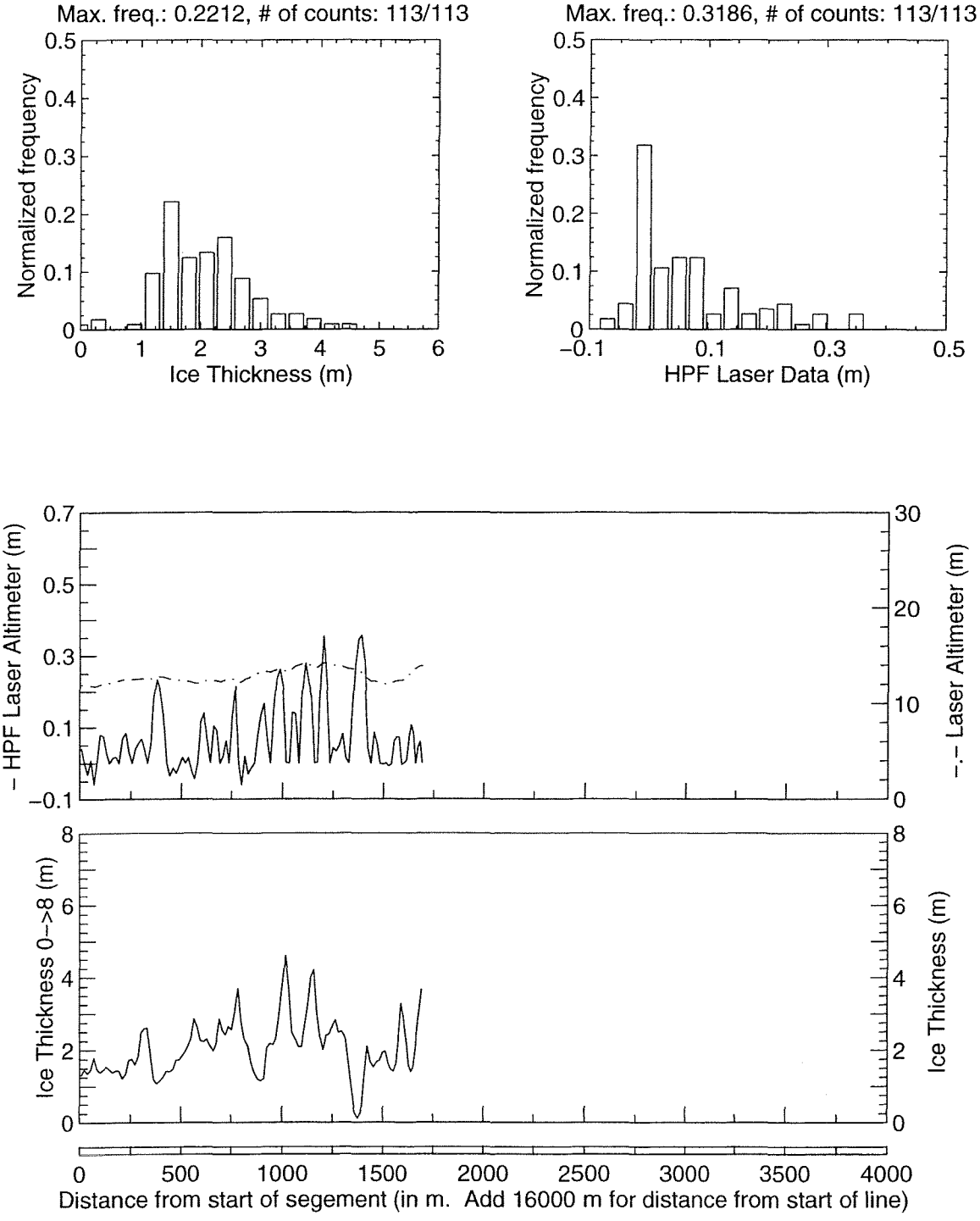

MAR 07 Flight #02 Line #10080 part 1 of 1

Line Starting Coordinates (53.8710,–55.9620) ending at (53.8717,–56.0109)

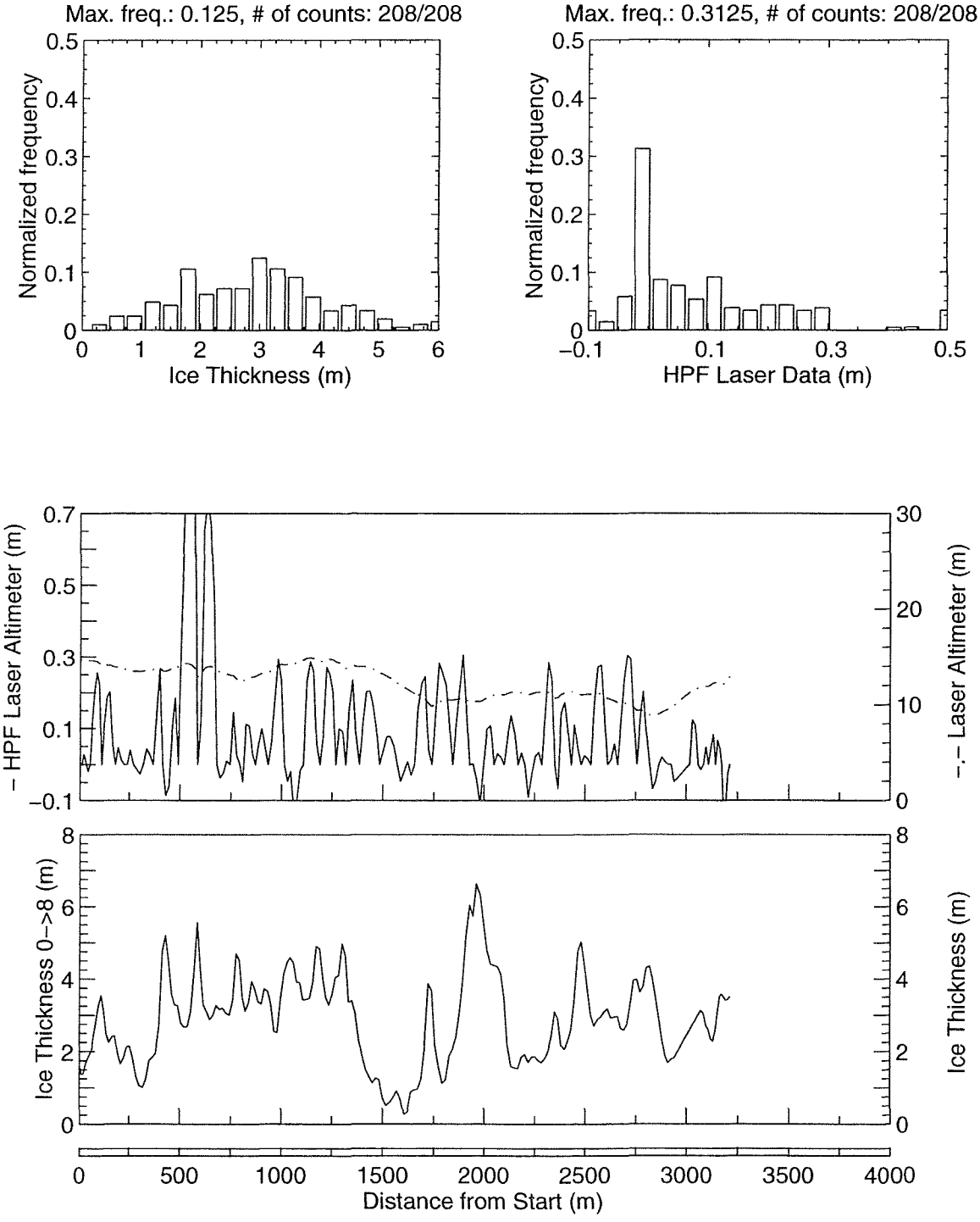

MAR 07 Flight #02 Line #10090 part 1 of 6

Line Starting Coordinates (53.8737,–56.0913) ending at (53.8771,–56.1522)

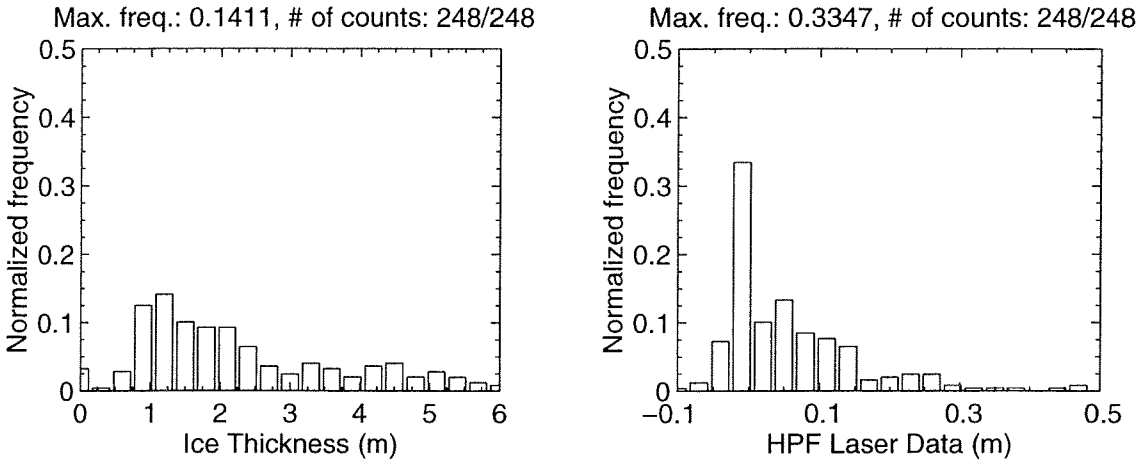

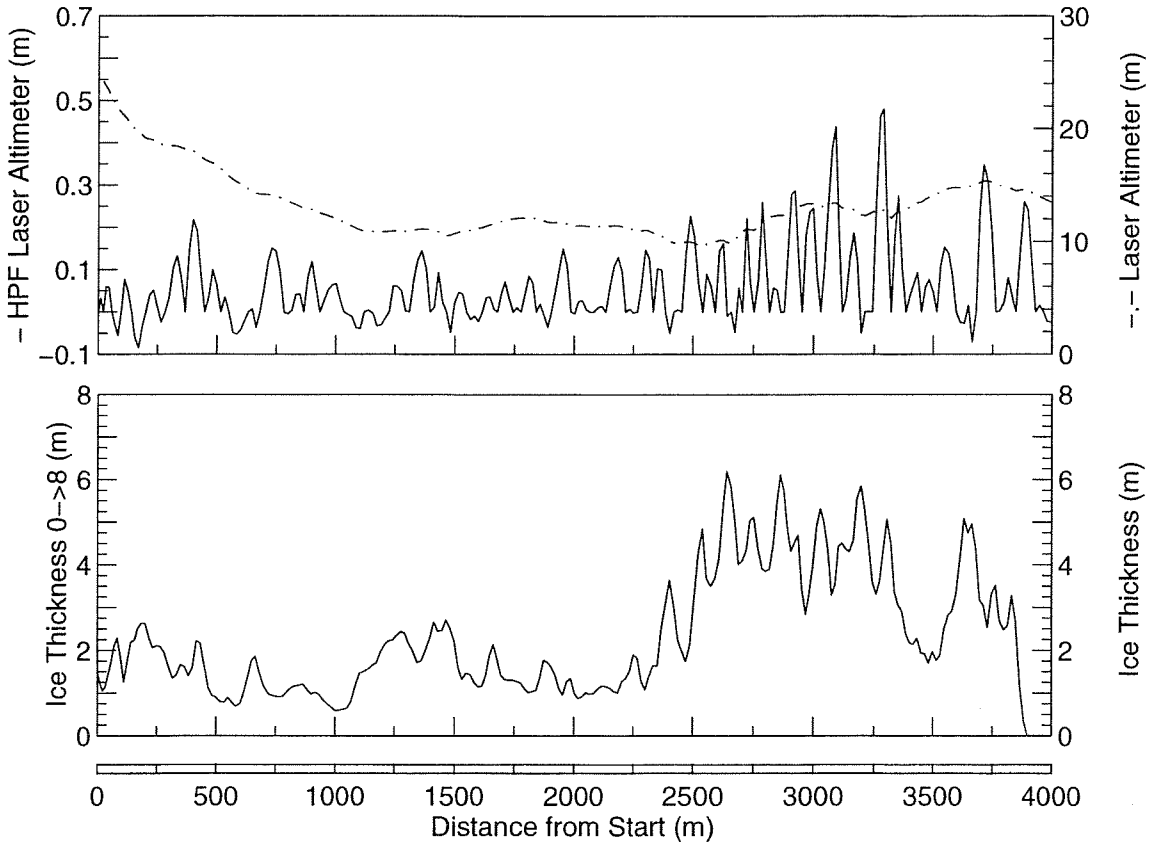

MAR 07 Flight #02 Line #10090 part 2 of 6

Line Starting Coordinates (53.8771,–56.1522) ending at (53.8796,–56.2129)

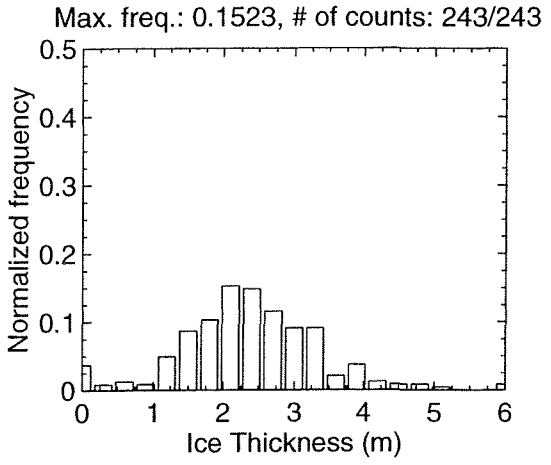

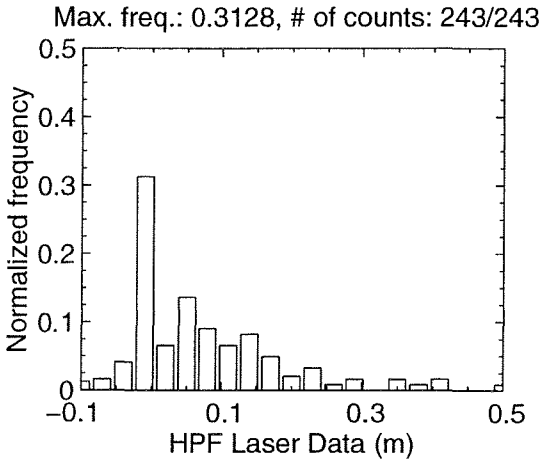

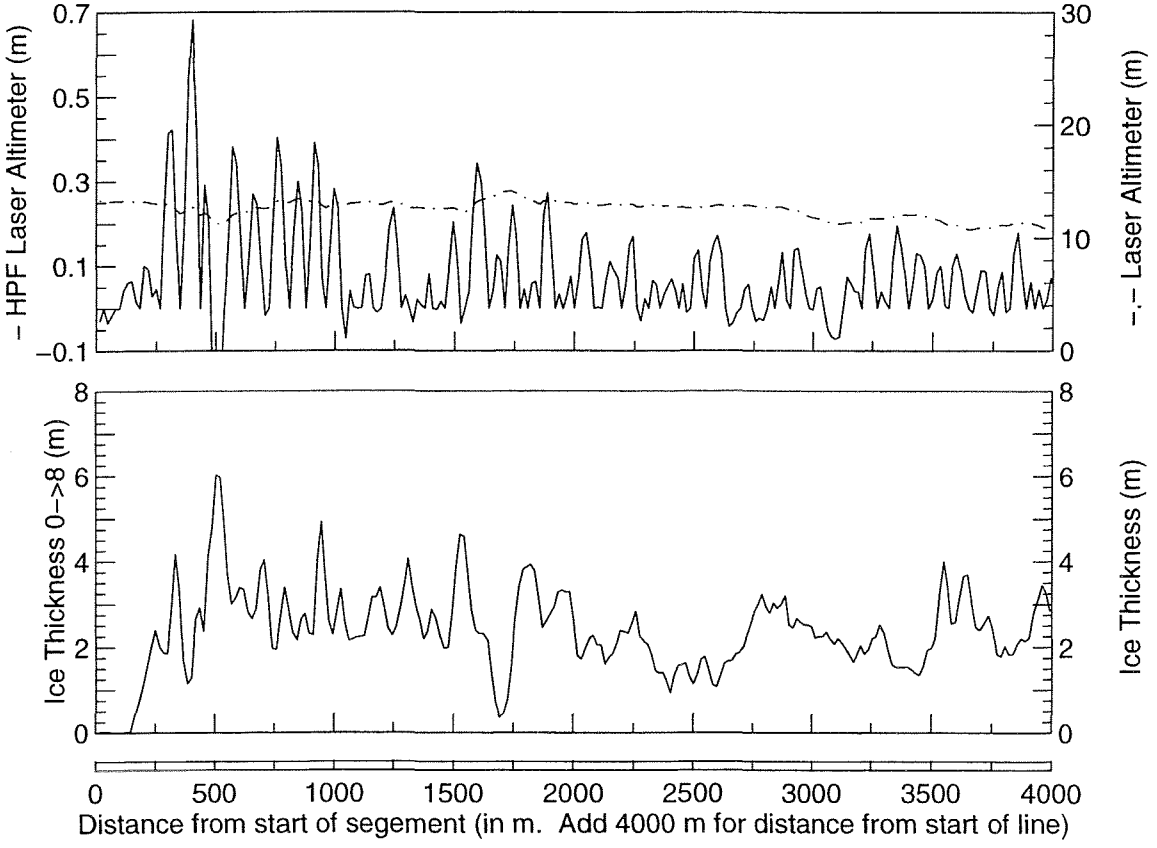

MAR 07 Flight #02 Line #10090 part 3 of 6

Line Starting Coordinates (53.8796,–56.2129) ending at (53.8825,–56.2737)

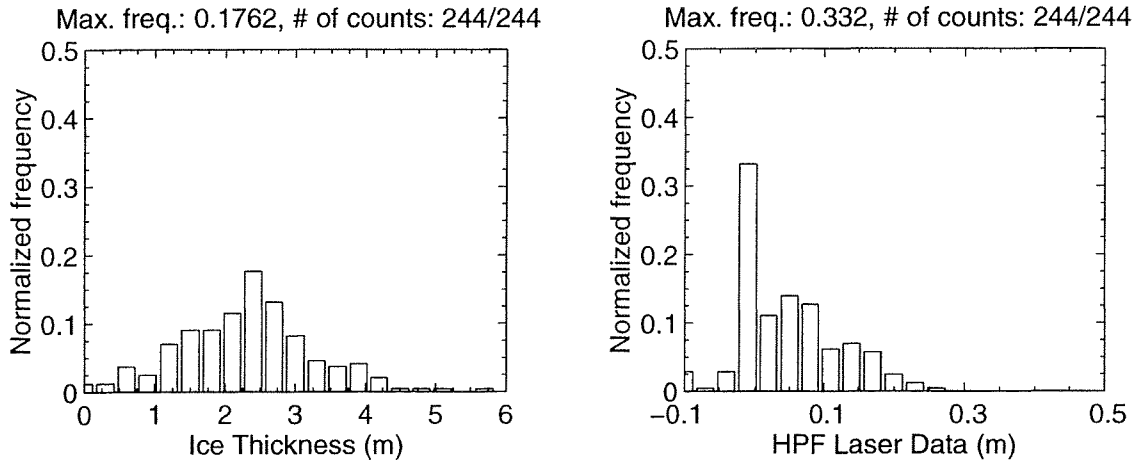

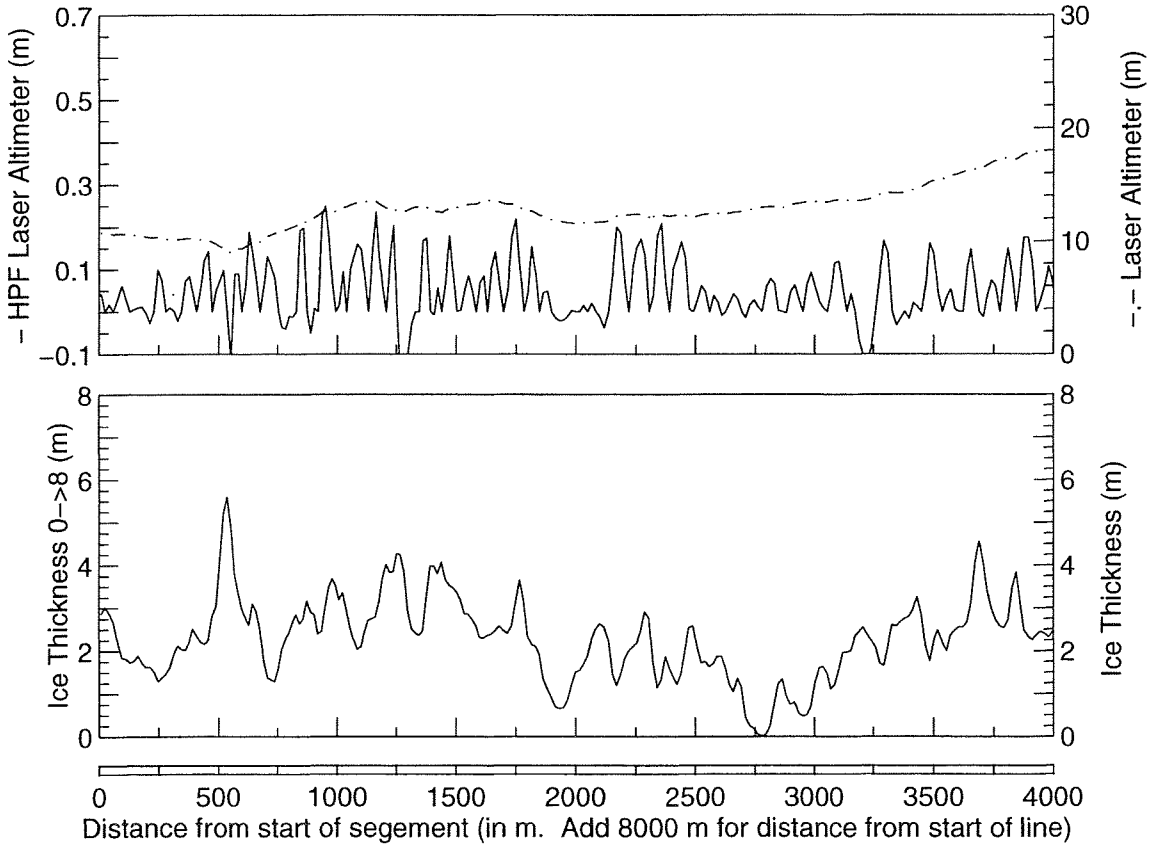

MAR 07 Flight #02 Line #10090 part 4 of 6

Line Starting Coordinates (53.8825,–56.2737) ending at (53.8883,–56.3339)

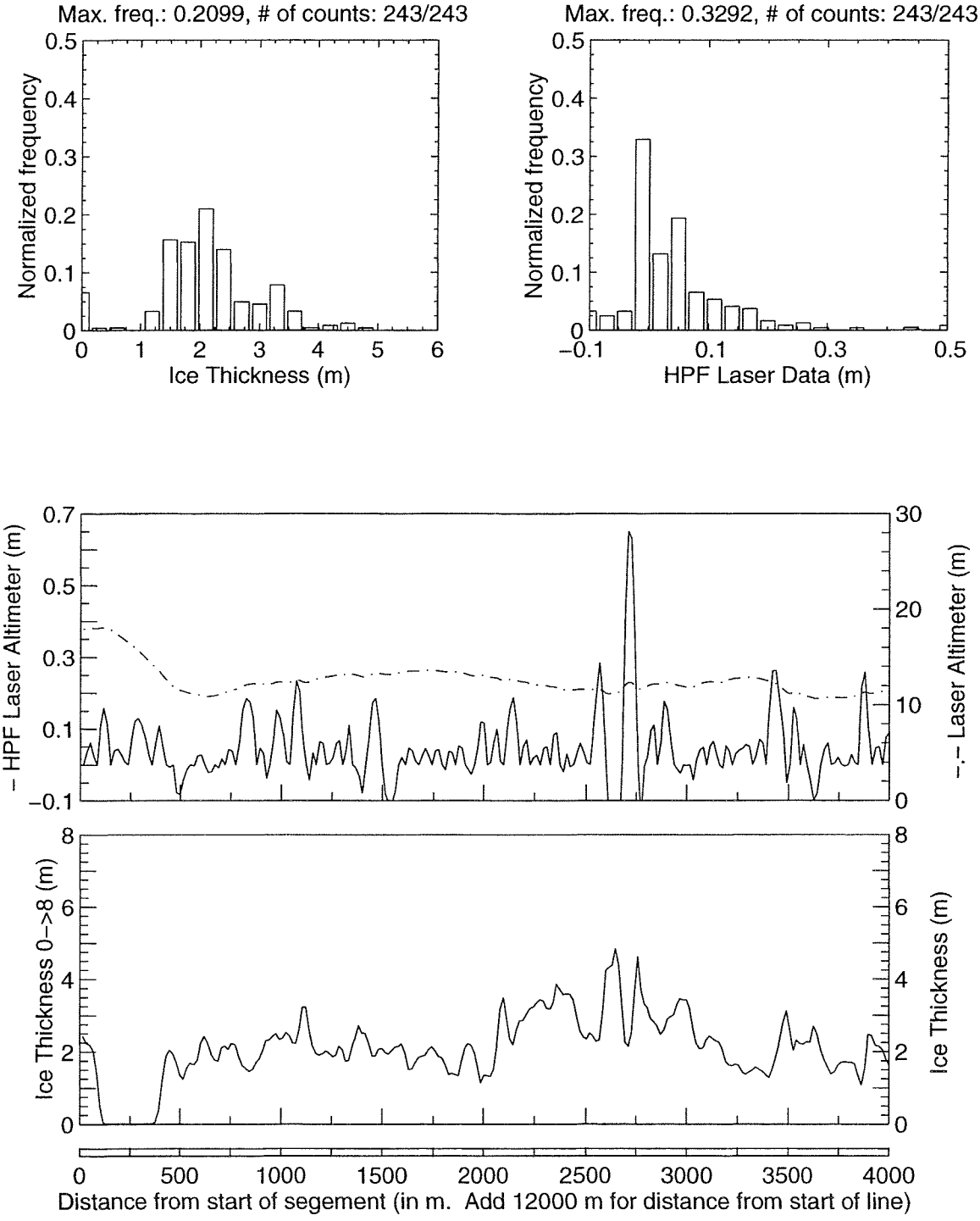

MAR 07 Flight #02 Line #10090 part 5 of 6

Line Starting Coordinates (53.8883,–56.3339) ending at (53.8930,–56.3942)

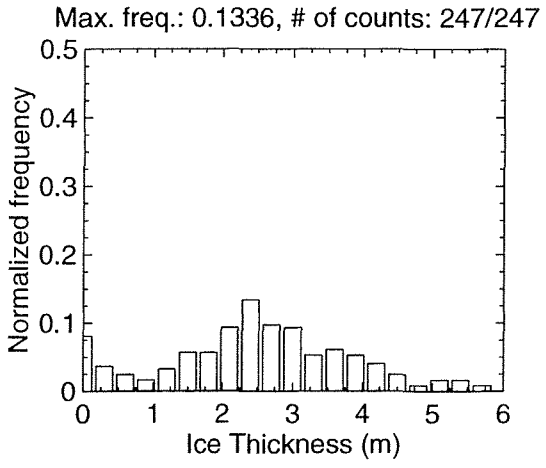

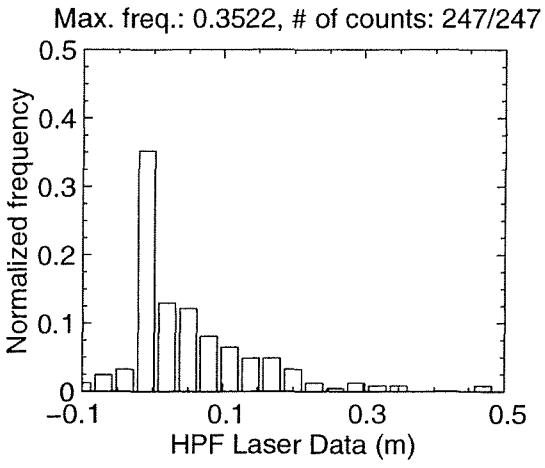

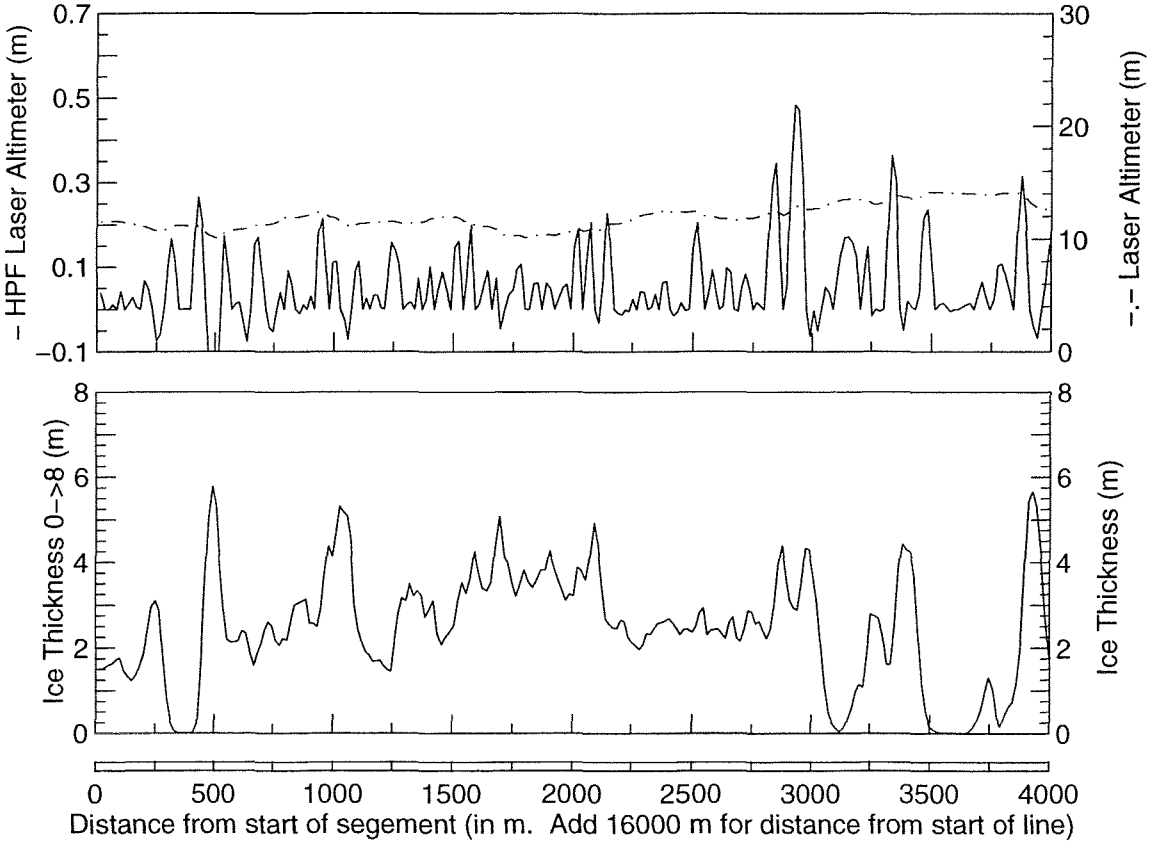

MAR 07 Flight #02 Line #10090 part 6 of 6

Line Starting Coordinates (53.8930,–56.3942) ending at (53.8979,–56.4527)

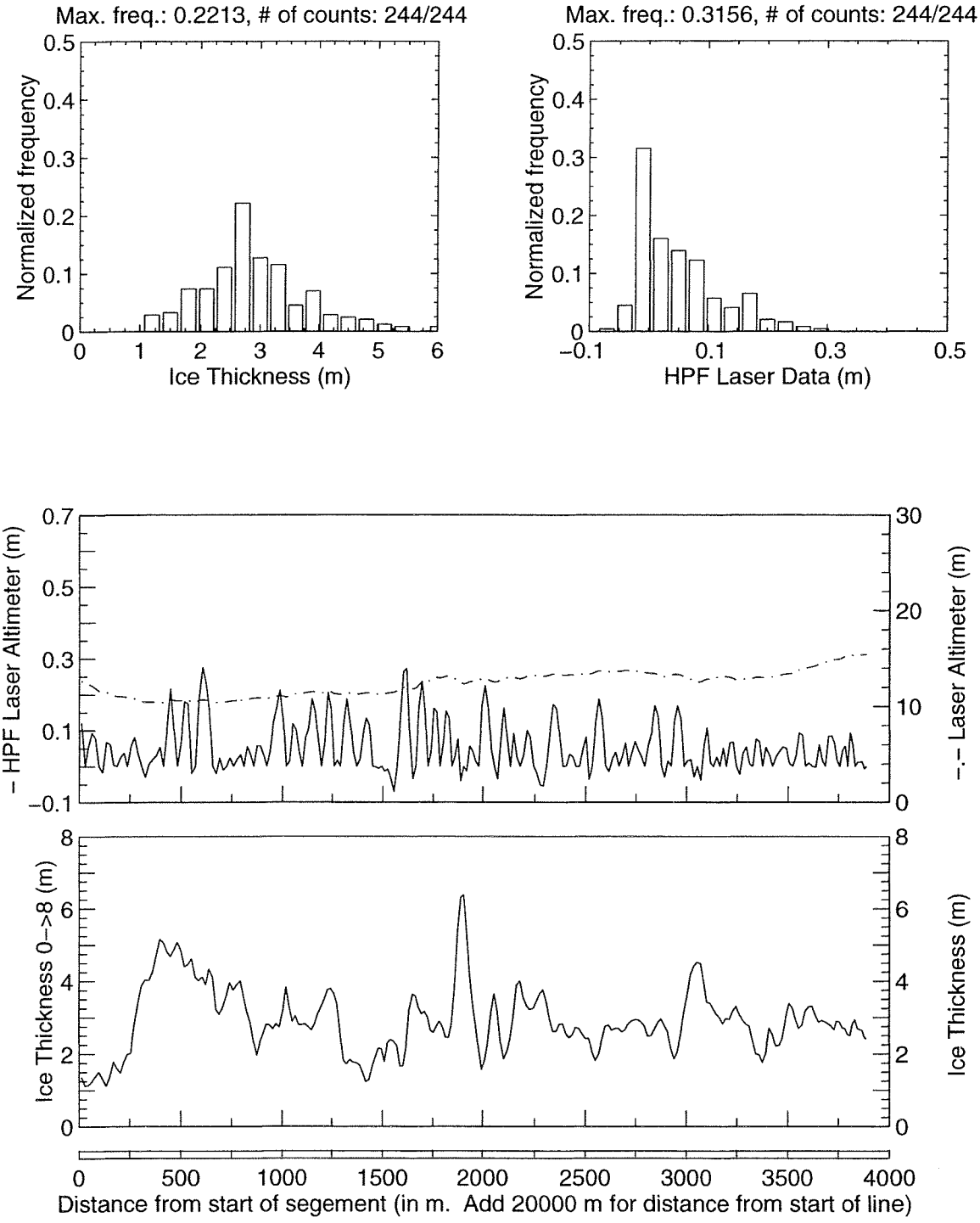

MAR 07 Flight #02 Line #10100 part 1 of 5

Line Starting Coordinates (53.8796,−56.5496) ending at (53.8656,−56.6058)

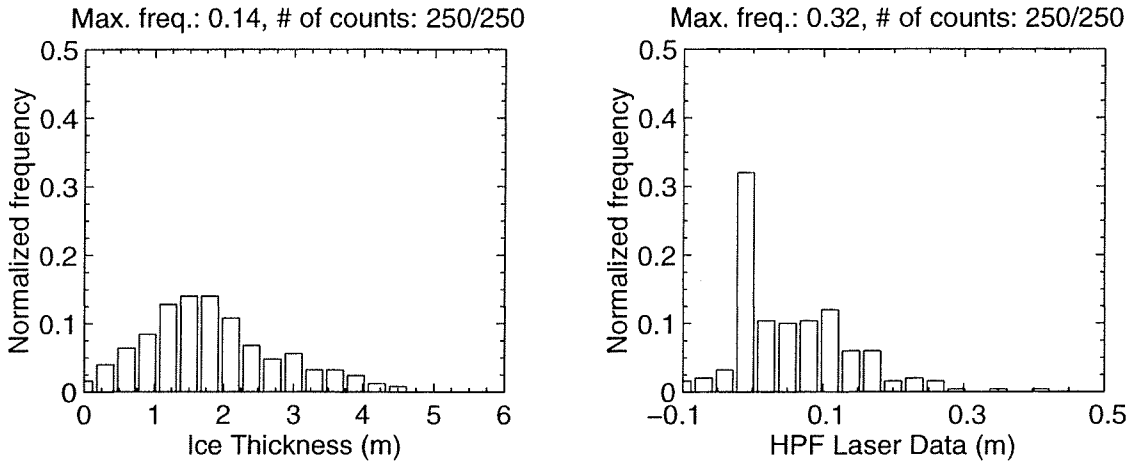

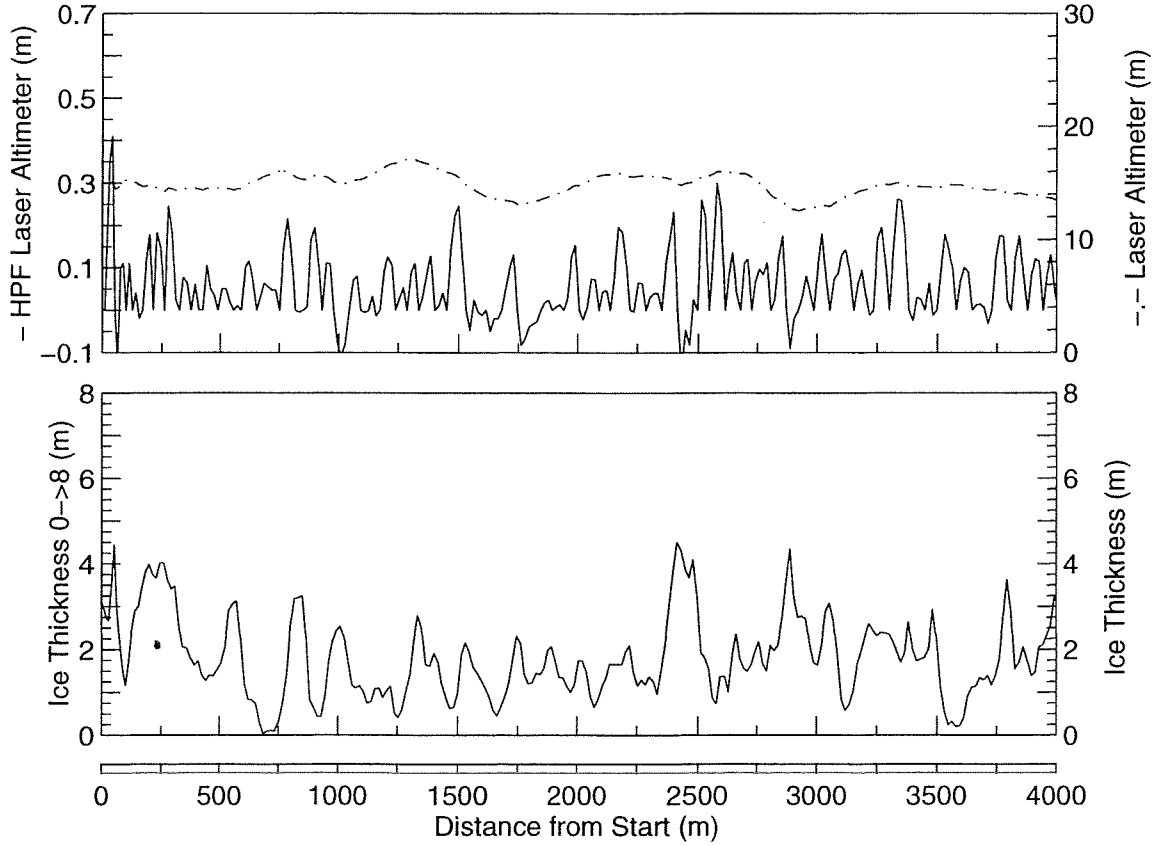

MAR 07 Flight #02 Line #10100 part 2 of 5

Line Starting Coordinates (53.8656,–56.6058) ending at (53.8520,–56.6621)

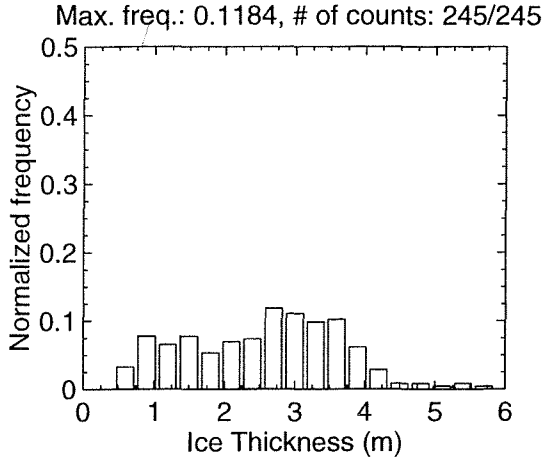

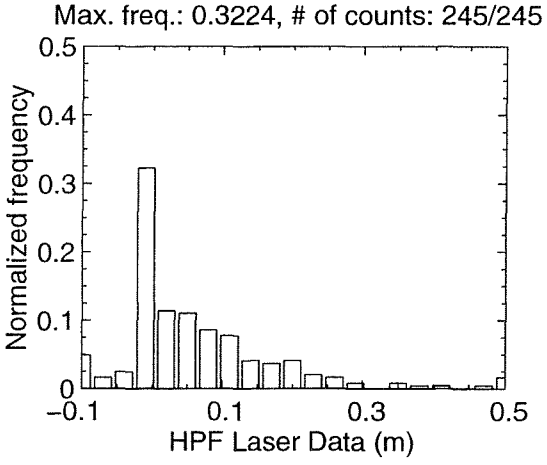

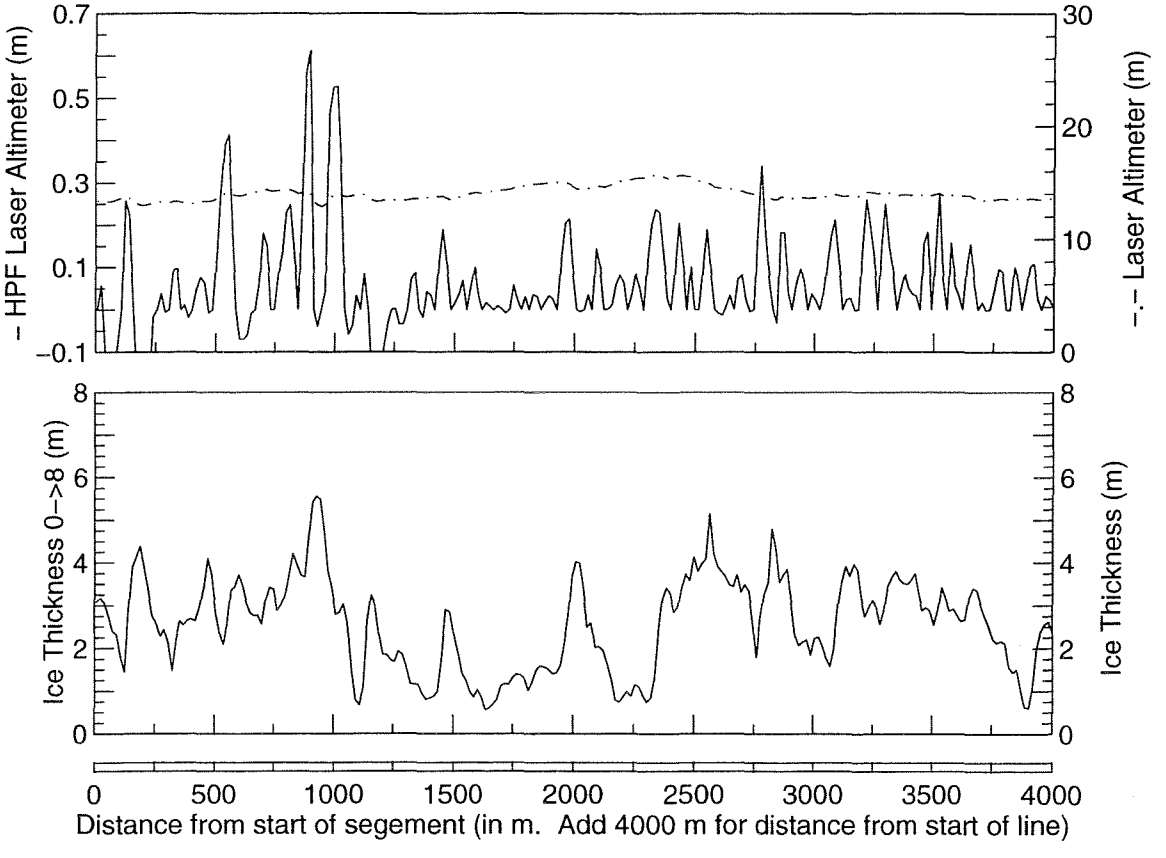

MAR 07 Flight #02 Line #10100 part 3 of 5

Line Starting Coordinates (53.8520,–56.6621) ending at (53.8377,–56.7179)

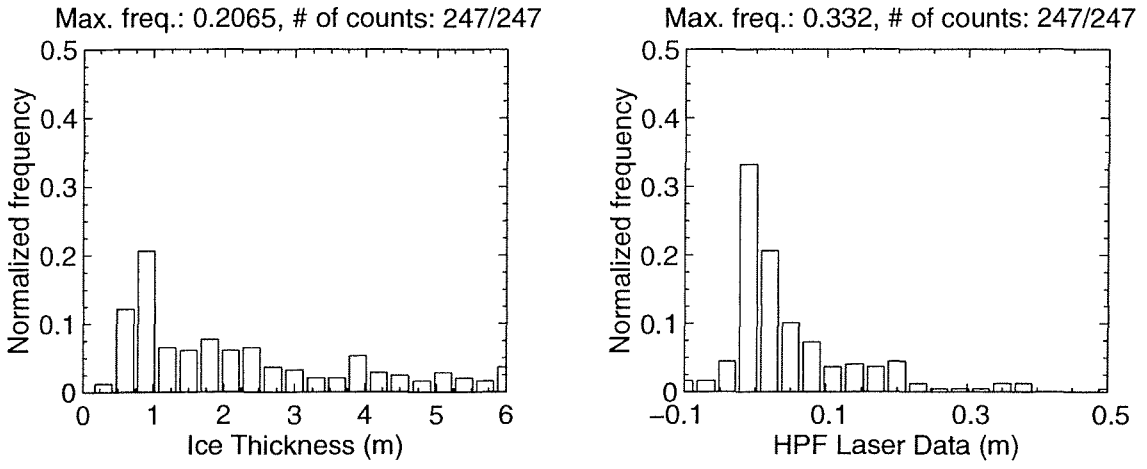

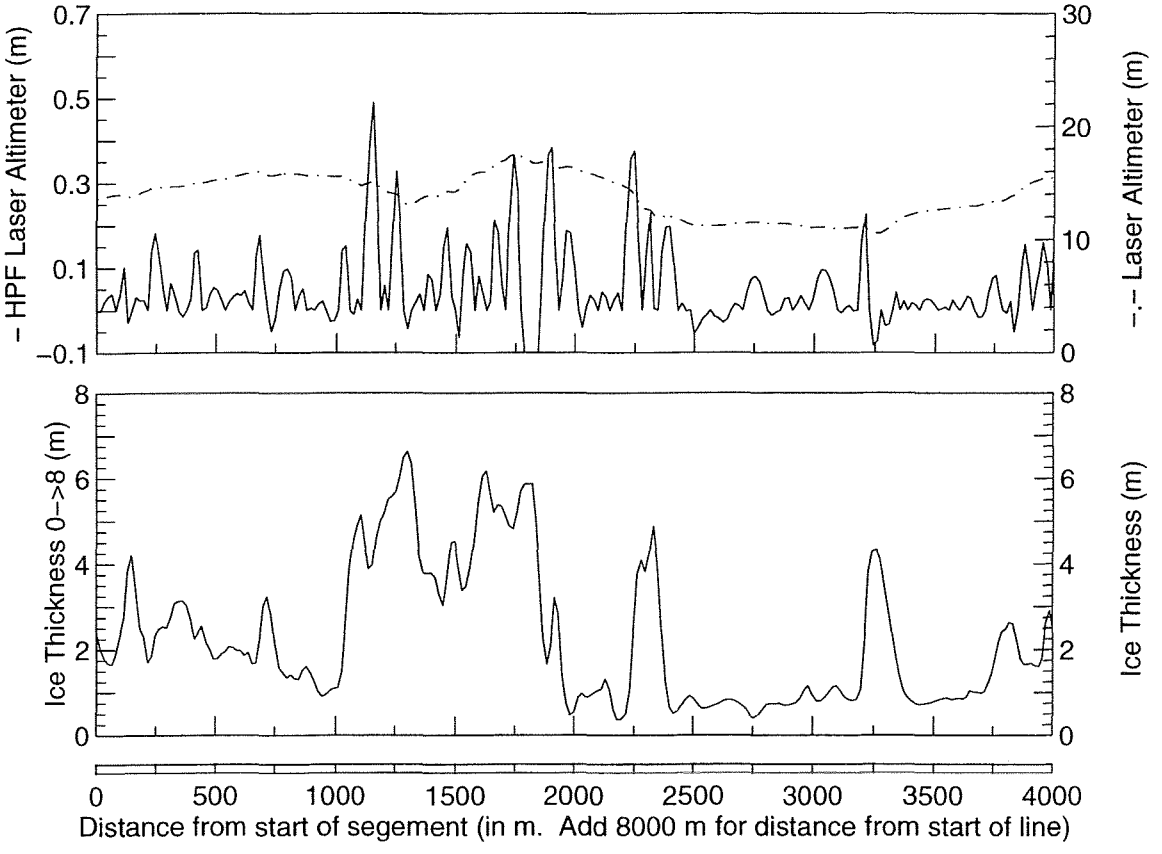

MAR 07 Flight #02 Line #10100 part 4 of 5

Line Starting Coordinates (53.8377,–56.7179) ending at (53.8196,–56.7706)

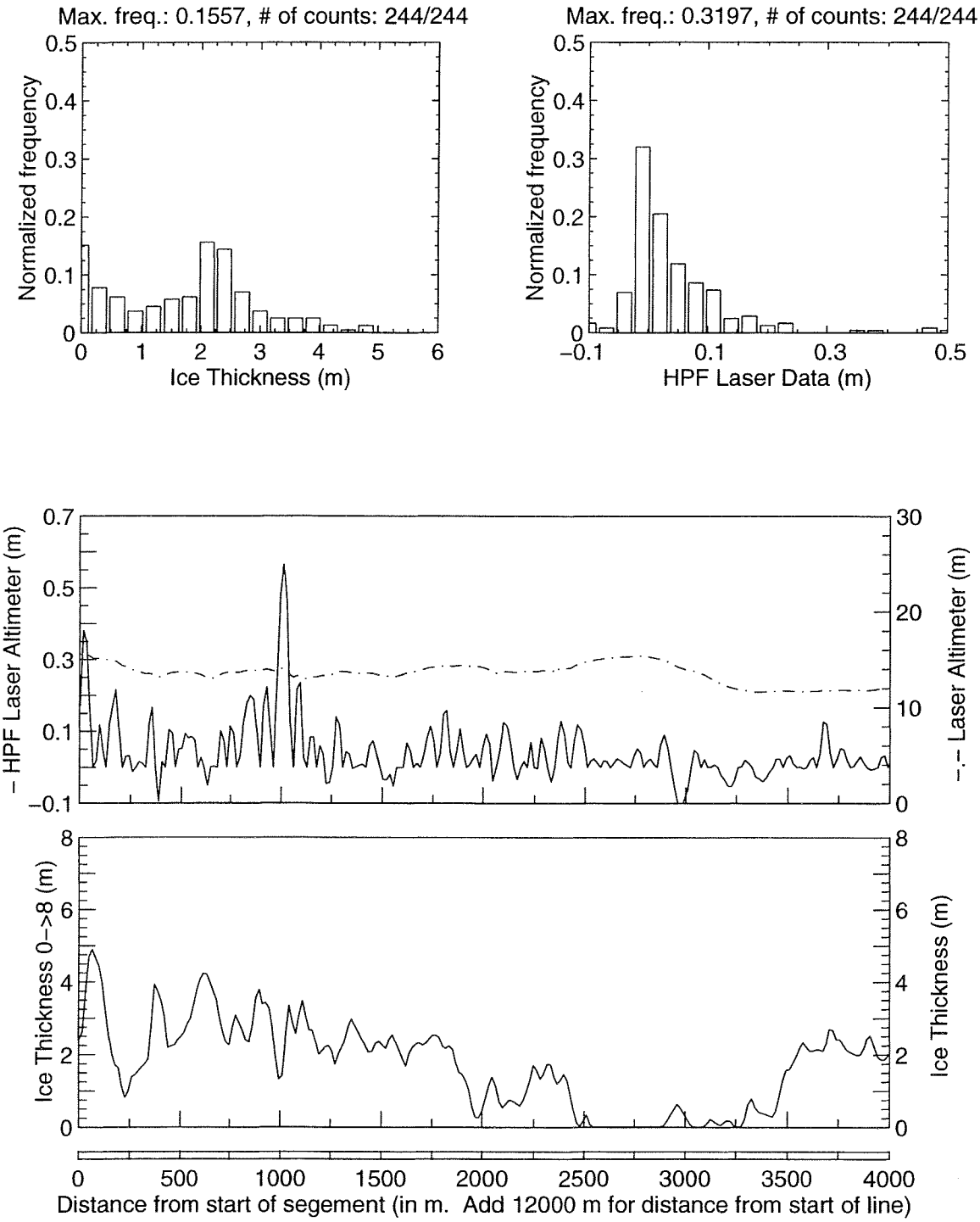

MAR 07 Flight #02 Line #10100 part 5 of 5

Line Starting Coordinates (53.8196,−56.7706) ending at (53.8041,−56.8149)

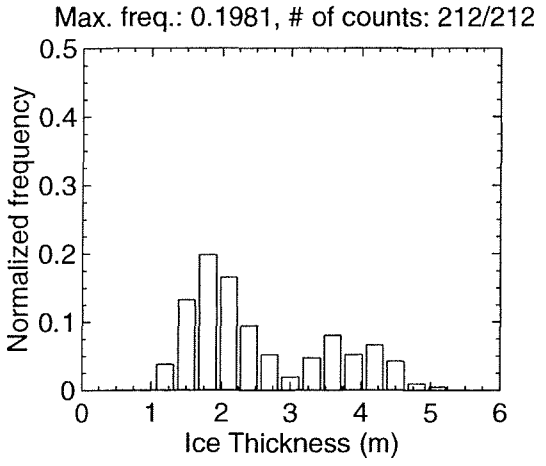

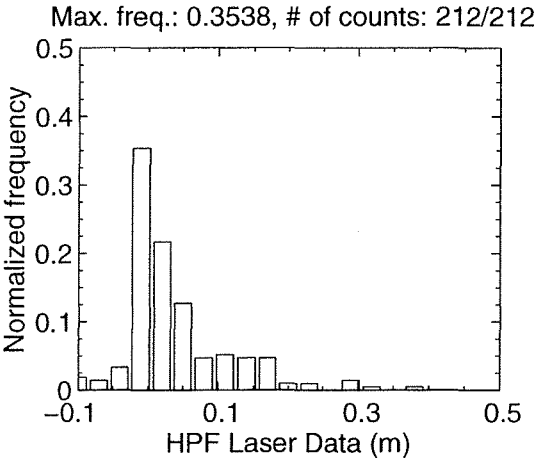

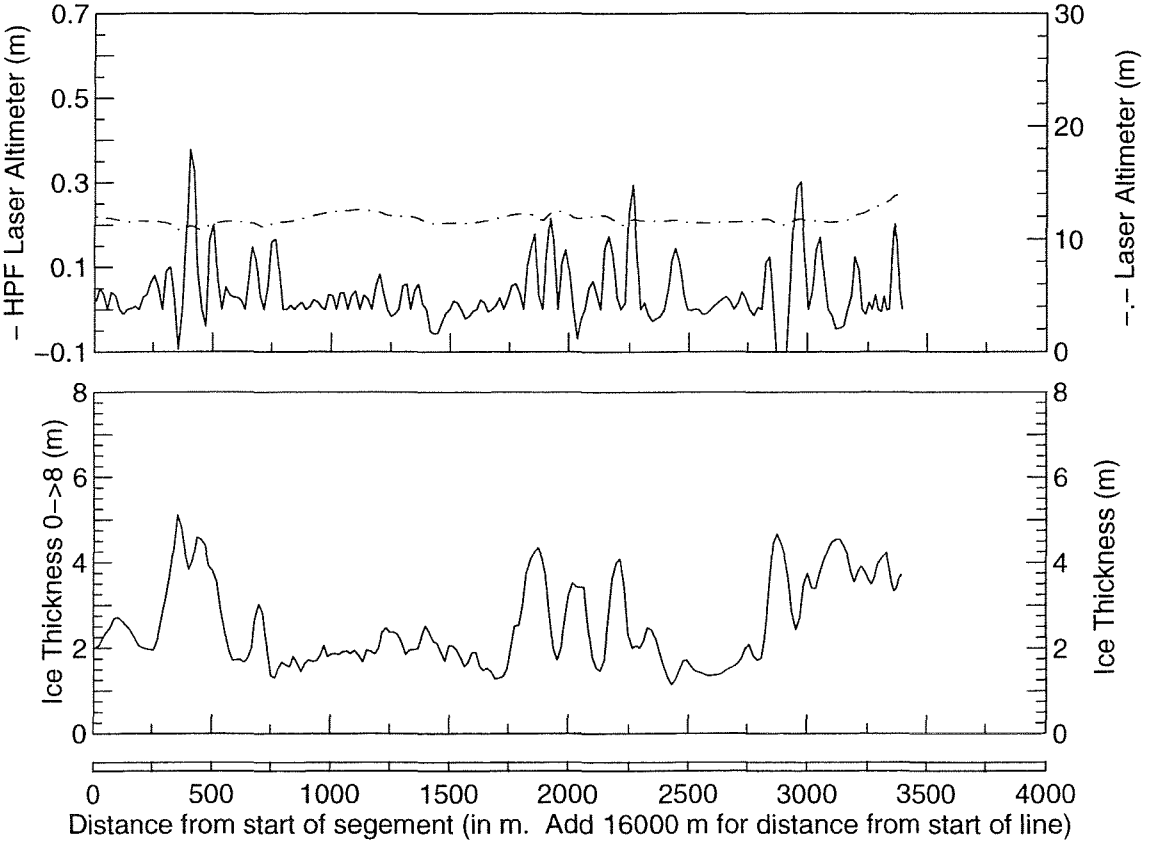

MAR 07 Flight #02 Line #10110 part 1 of 2

Line Starting Coordinates (53.7607,−56.9004) ending at (53.7409,−56.9510)

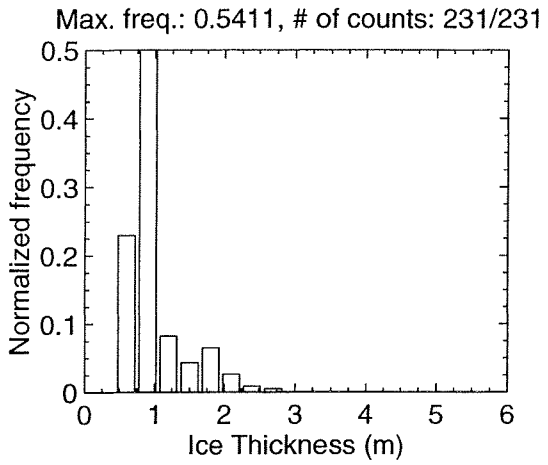

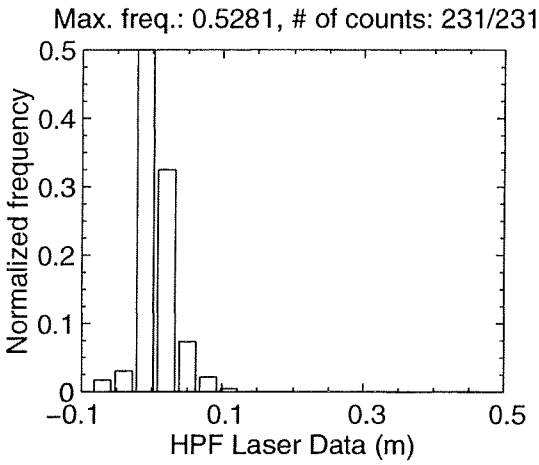

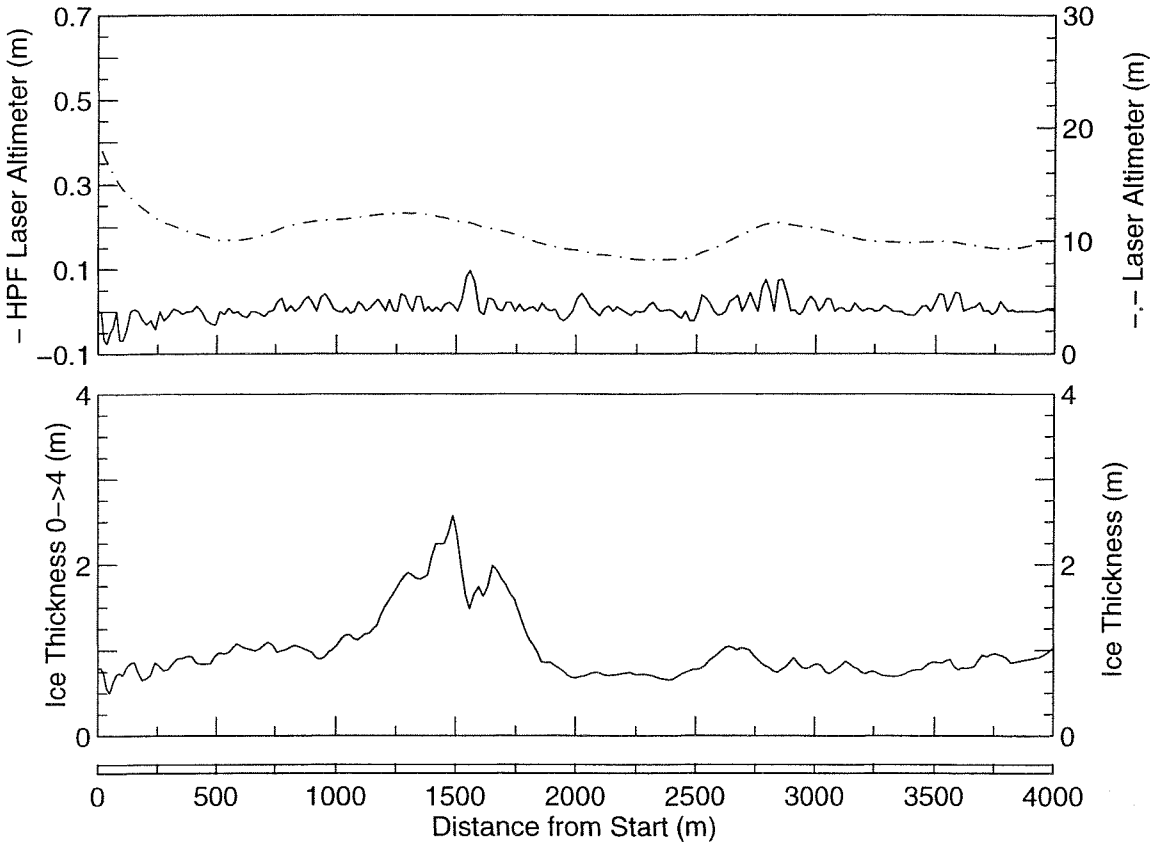

MAR 07 Flight #02 Line #10110 part 2 of 2

Line Starting Coordinates (53.7409,–56.9510) ending at (53.7277,–56.9852)

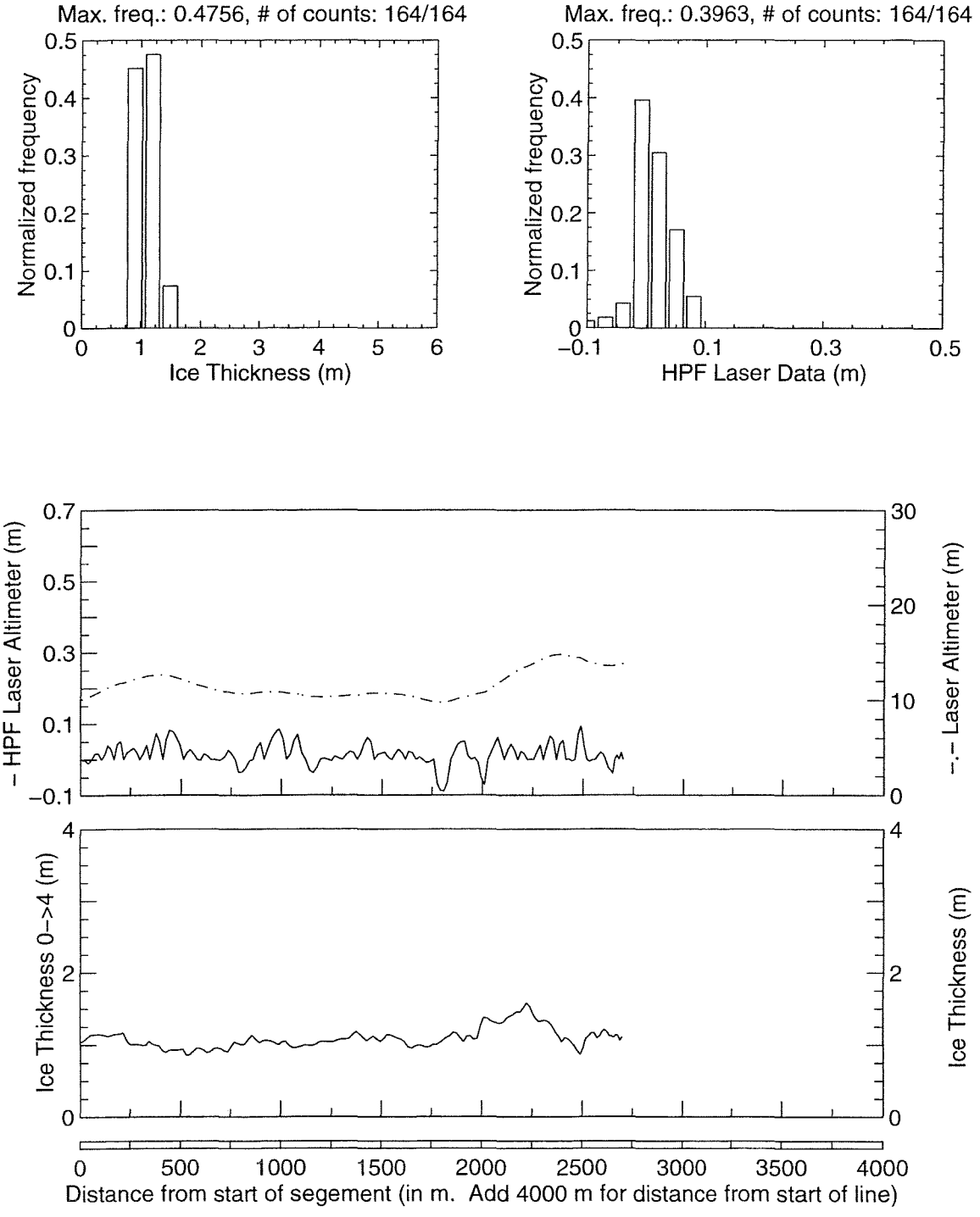

MAR 09 Flight #01 Line #10010 part 1 of 2

Line Starting Coordinates (53.7714,−56.7354) ending at (53.7831,−56.6778)

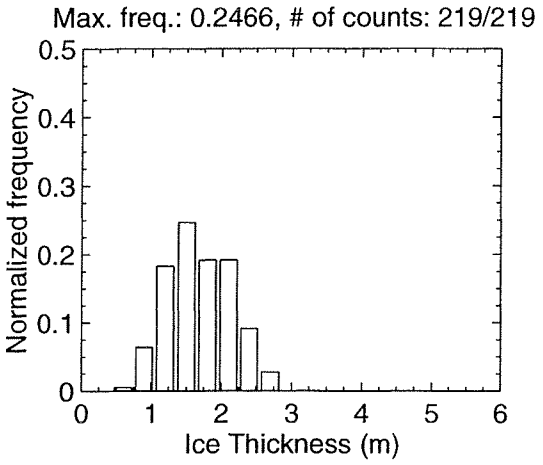

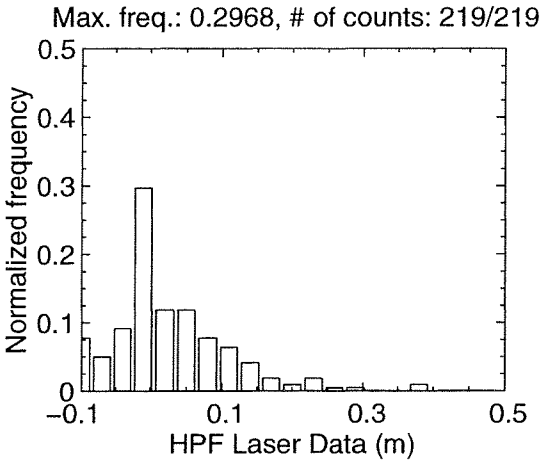

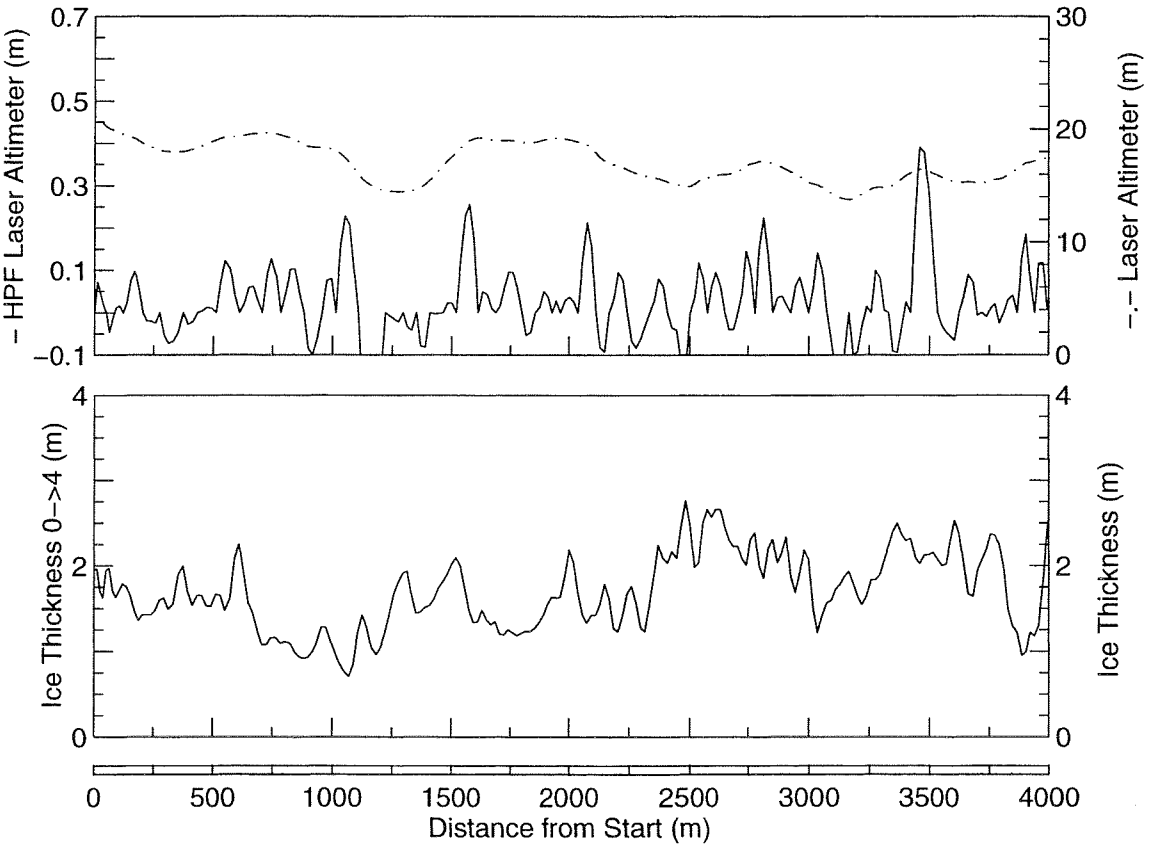

MAR 09 Flight #01 Line #10020 part 1 of 3

Line Starting Coordinates (53.8040,–56.5586) ending at (53.8145,–56.5004)

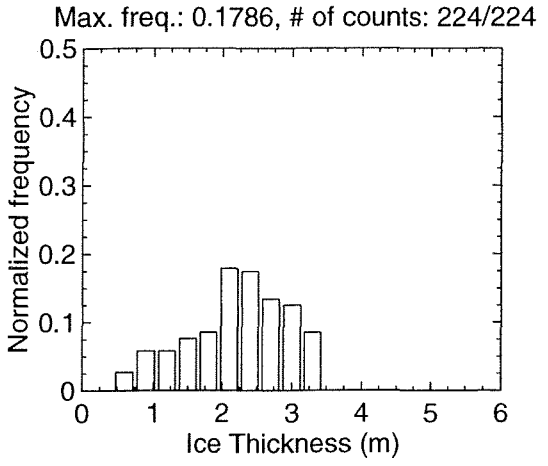

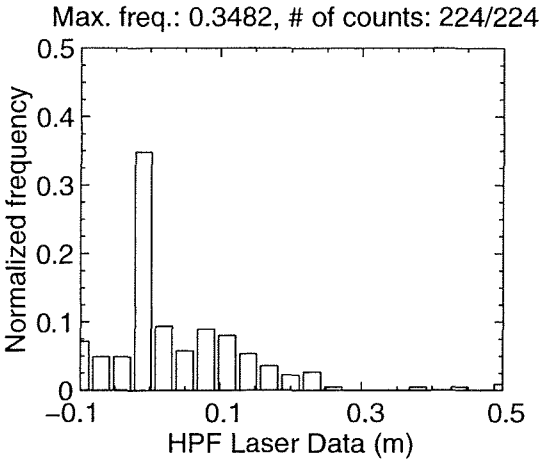

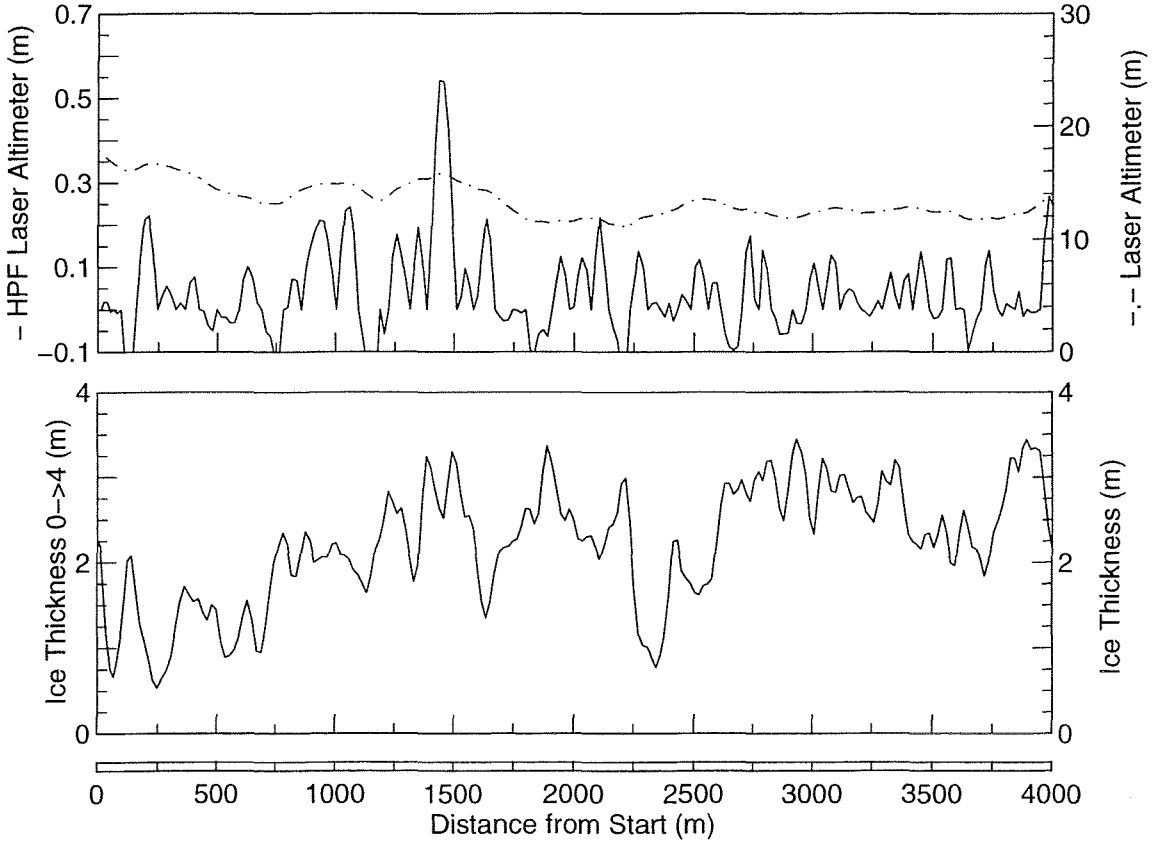

MAR 09 Flight #01 Line #10020 part 2 of 3

Line Starting Coordinates (53.8145,–56.5004) ending at (53.8241,–56.4417)

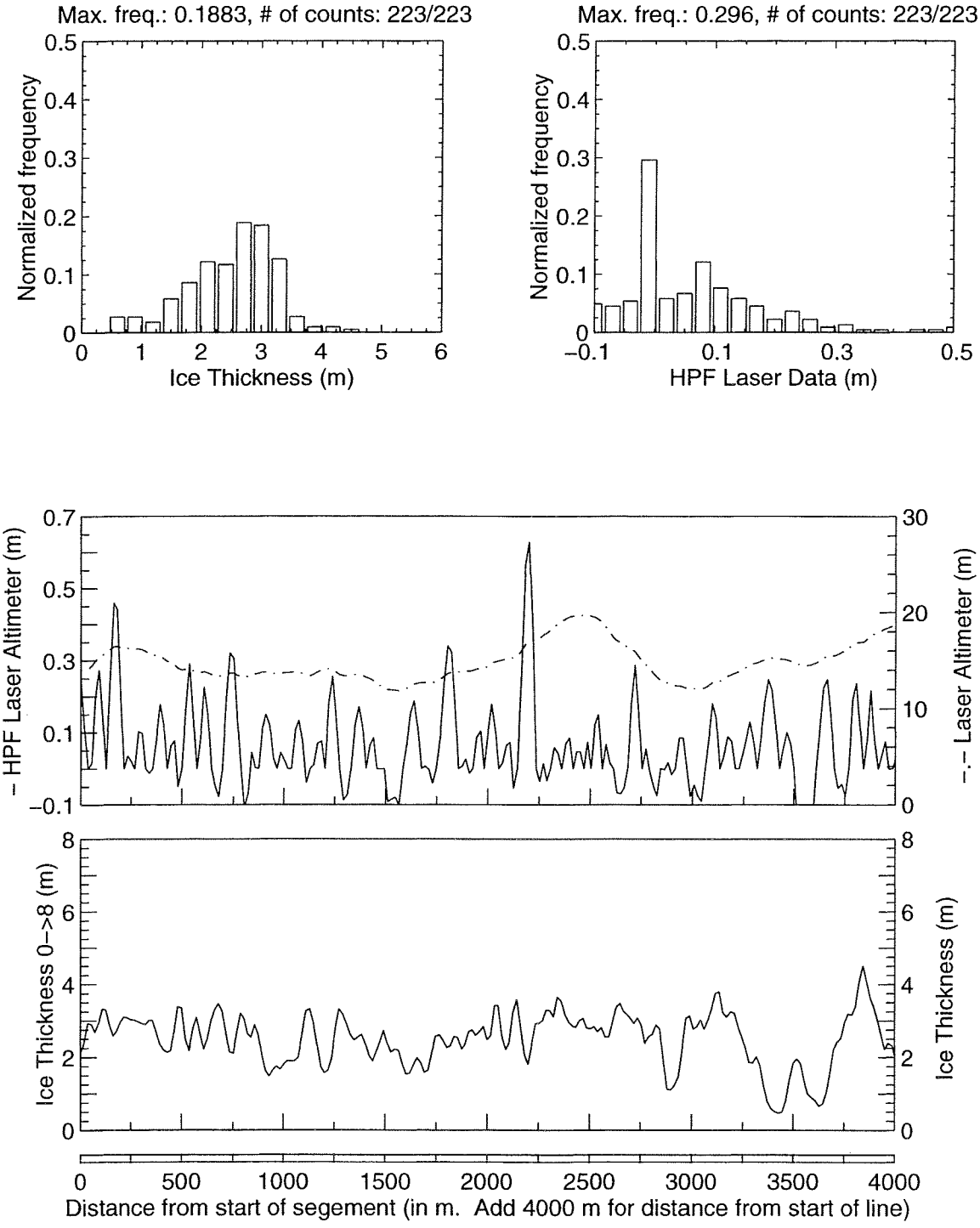

MAR 09 Flight #01 Line #10020 part 3 of 3

Line Starting Coordinates (53.8241,–56.4417) ending at (53.8279,–56.4161)

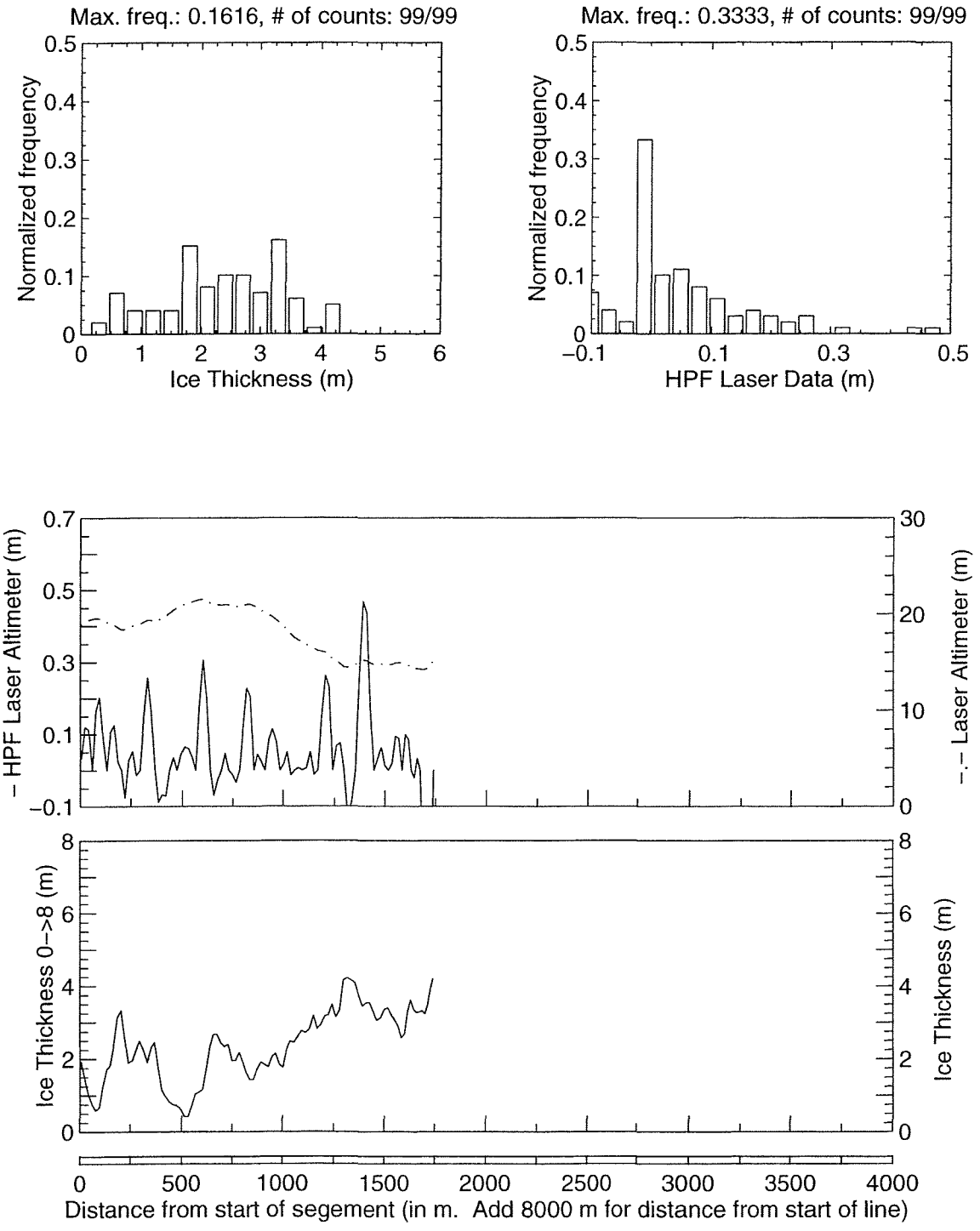

MAR 09 Flight #01 Line #10031 part 1 of 1

Line Starting Coordinates (53.8299,–56.4066) ending at (53.8347,–56.4049)

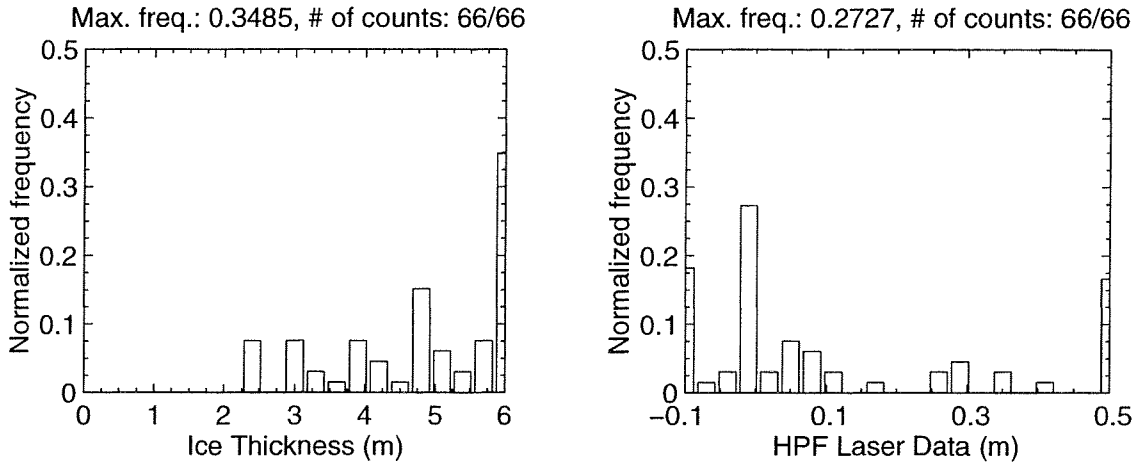

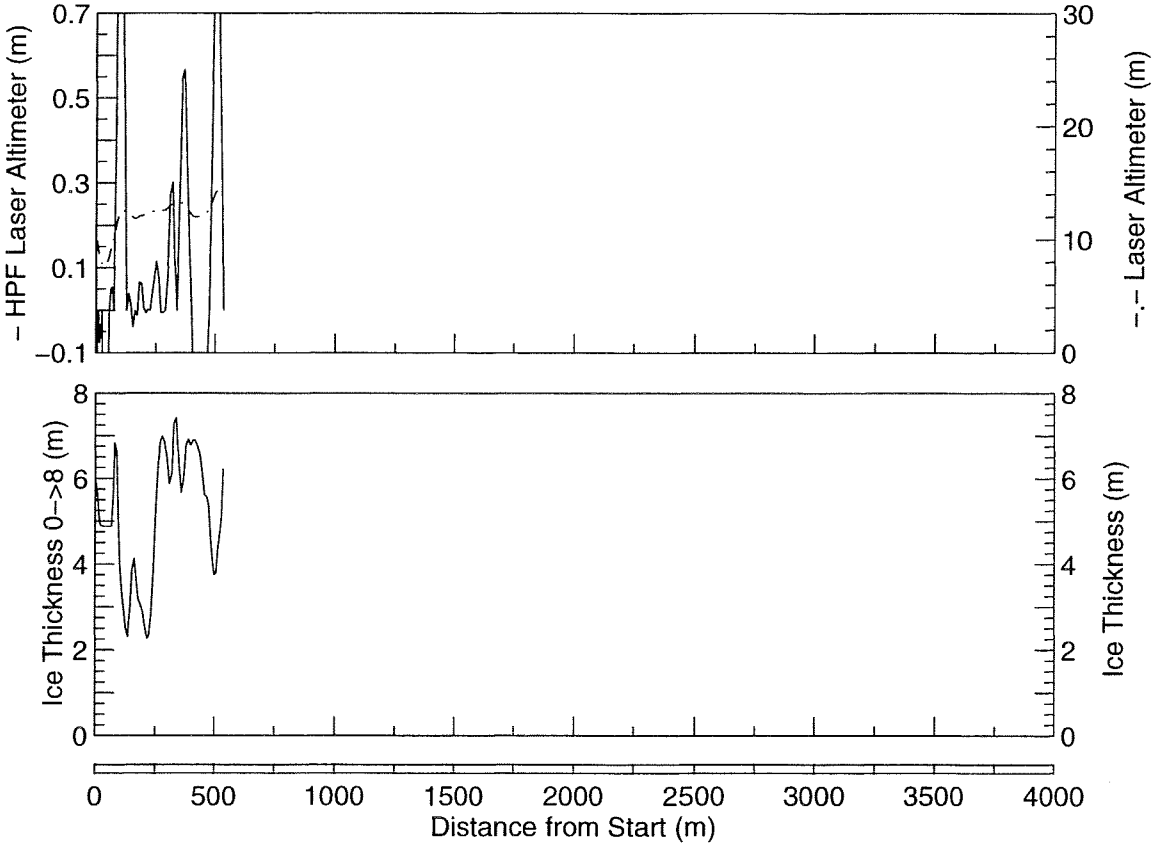

MAR 09 Flight #01 Line #10032 part 1 of 2

Line Starting Coordinates (53.8356,–56.4046) ending at (53.8642,–56.3933)

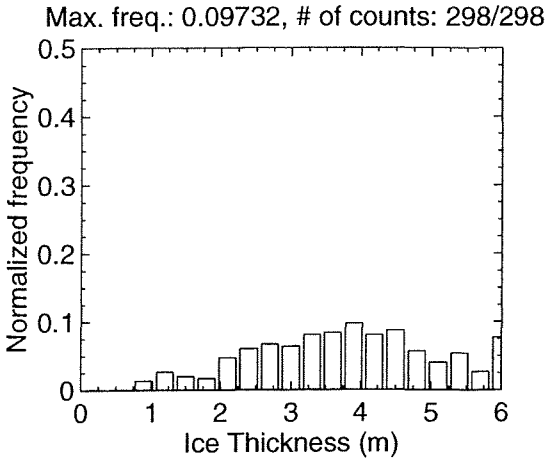

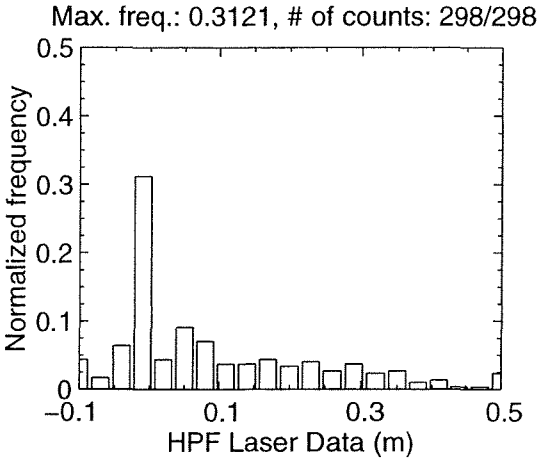

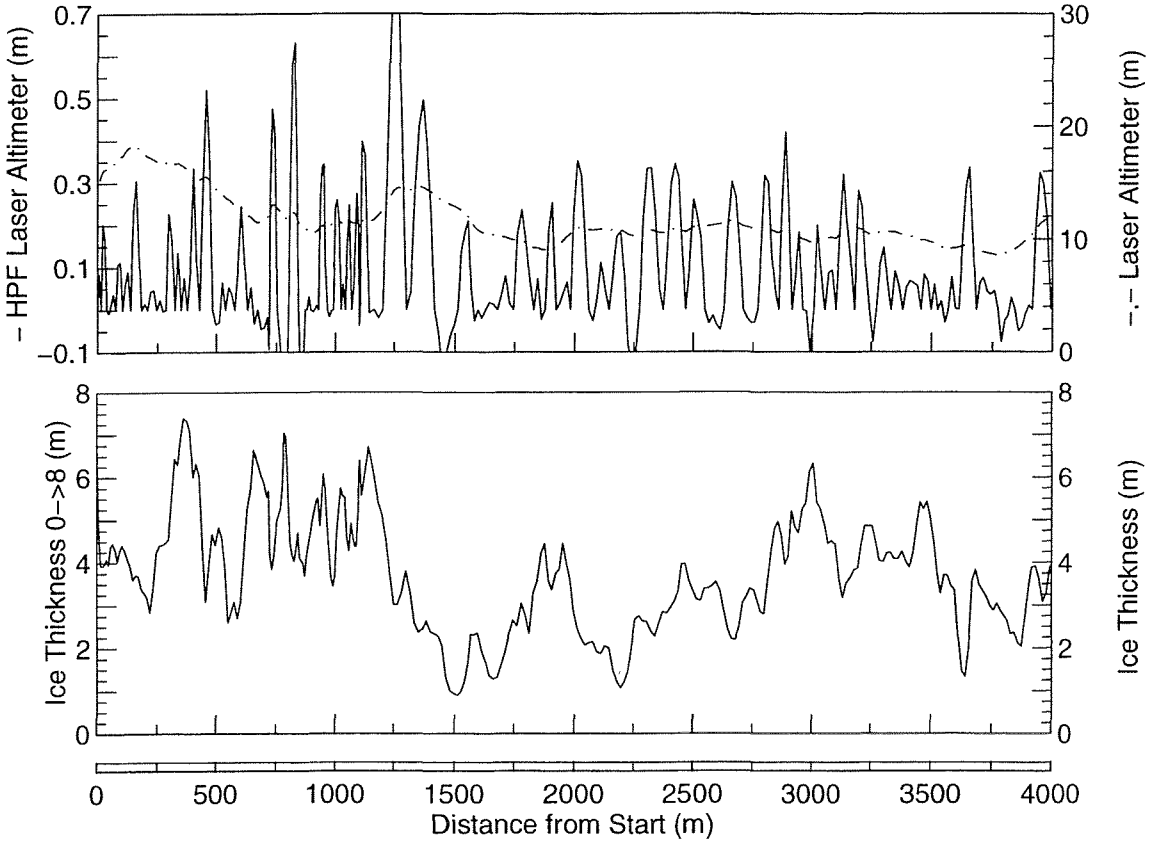

MAR 09 Flight #01 Line #10032 part 2 of 2

Line Starting Coordinates (53.8642,–56.3933) ending at (53.8836,–56.3844)

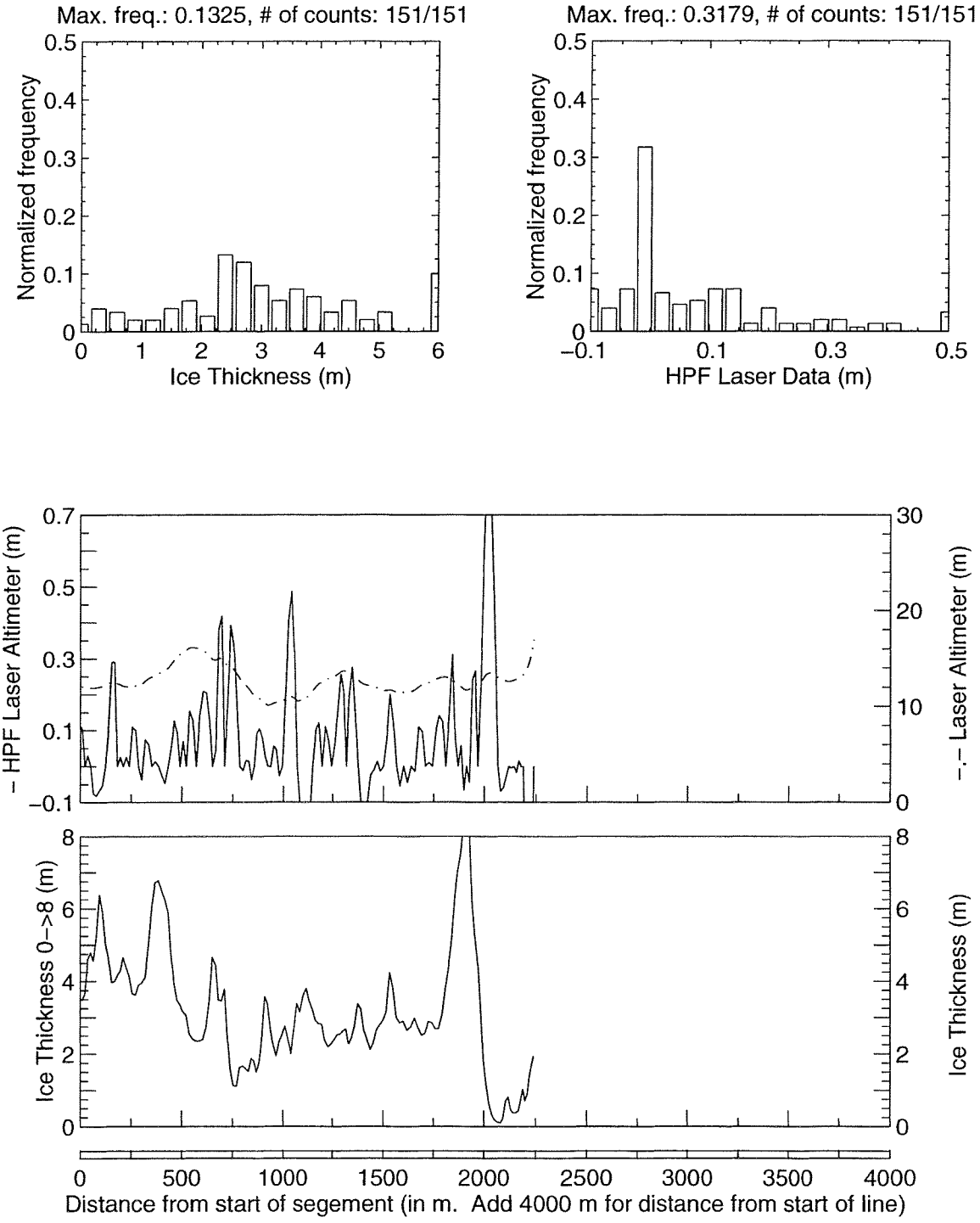

MAR 09 Flight #01 Line #10040 part 1 of 2

Line Starting Coordinates (53.9270,–56.3684) ending at (53.9626,–56.3602)

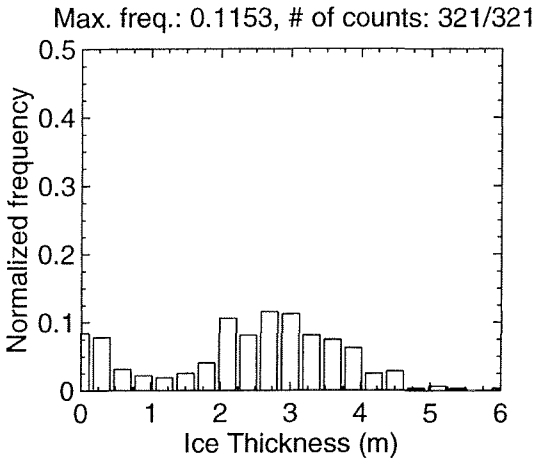

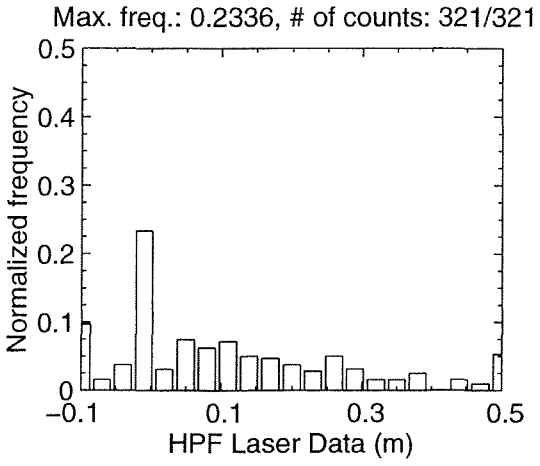

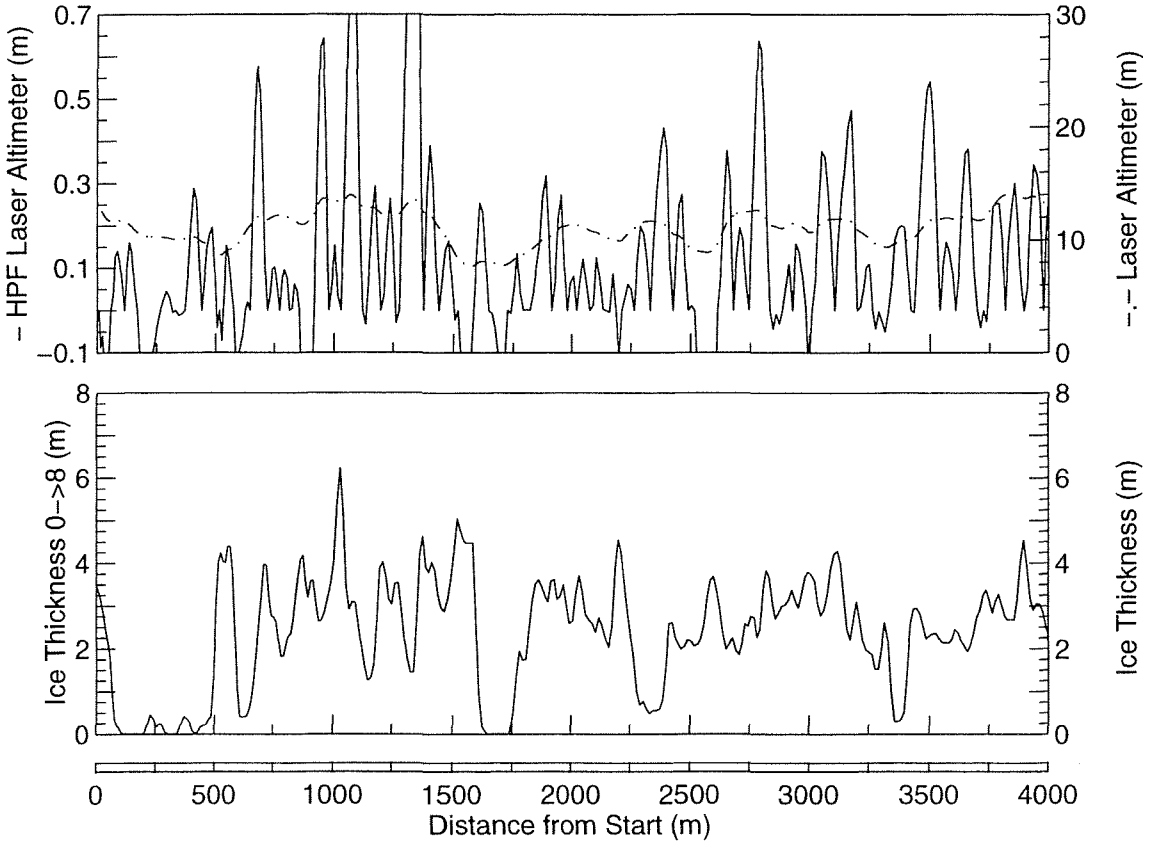

MAR 09 Flight #01 Line #10040 part 2 of 2

Line Starting Coordinates (53.9626,–56.3602) ending at (53.9951,–56.3532)

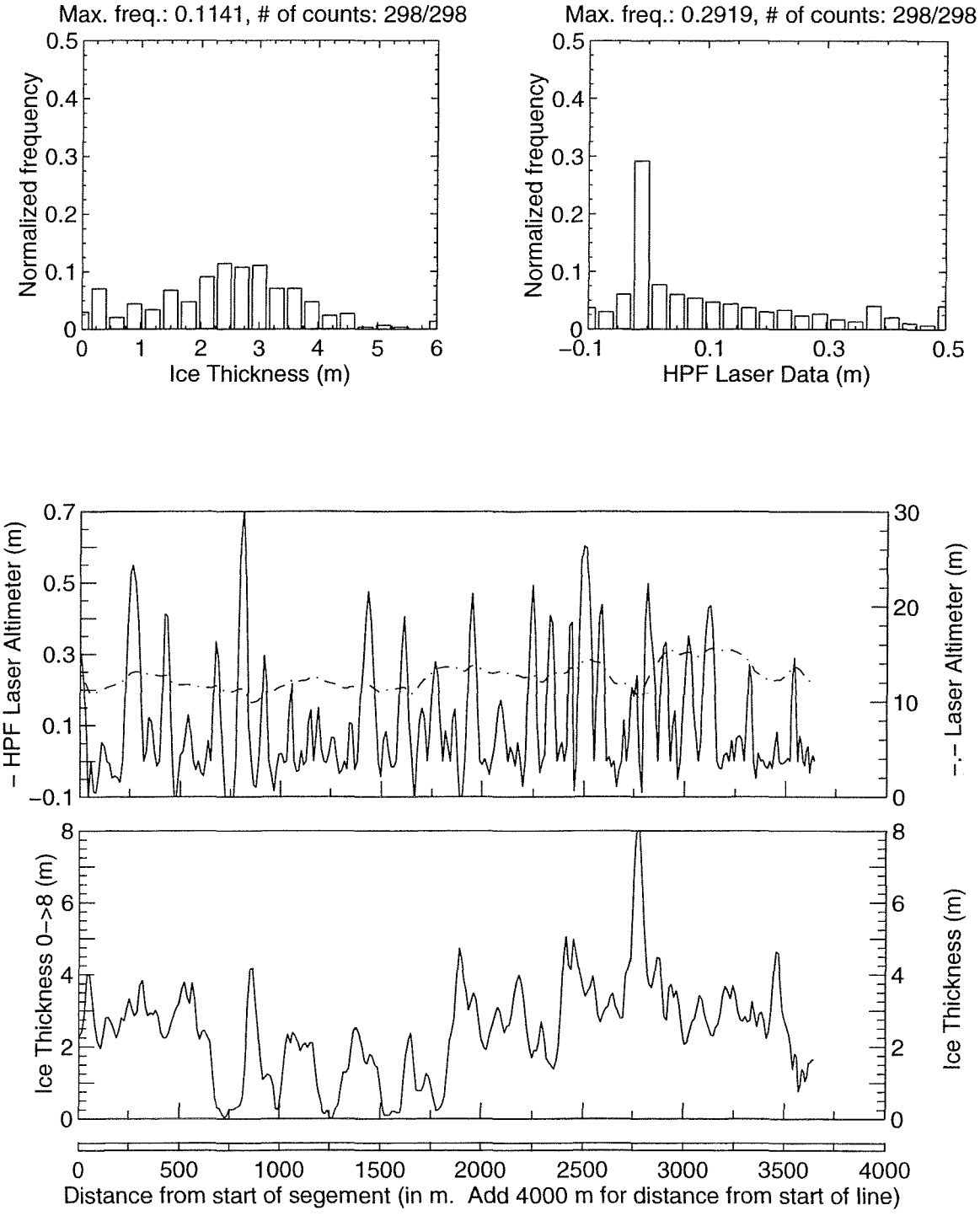

MAR 09 Flight #01 Line #10051 part 1 of 1

Line Starting Coordinates (54.0336,–56.3473) ending at (54.0606,–56.3524)

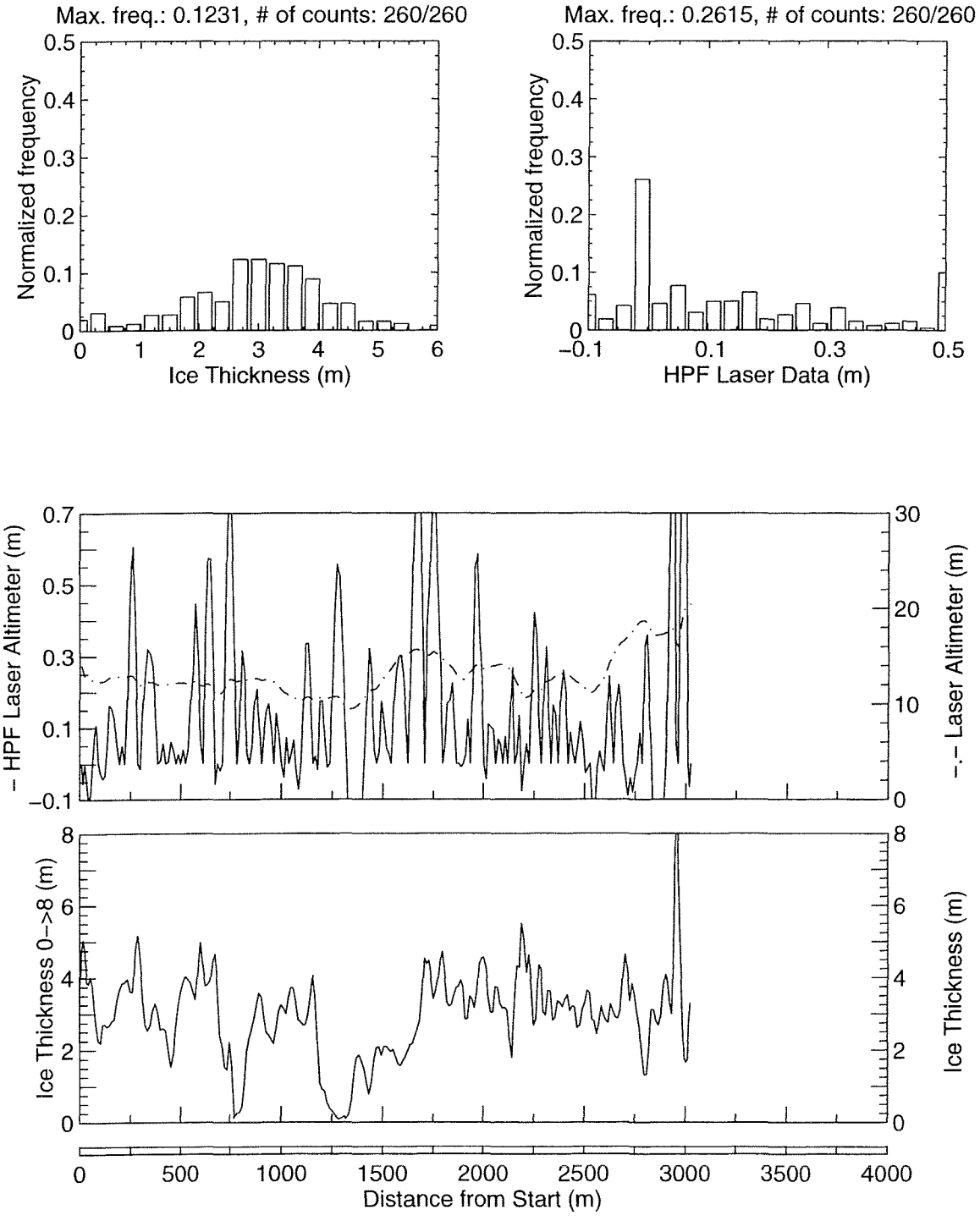

MAR 09 Flight #01 Line #10052 part 1 of 3

Line Starting Coordinates (54.0616,–56.3525) ending at (54.0969,–56.3409)

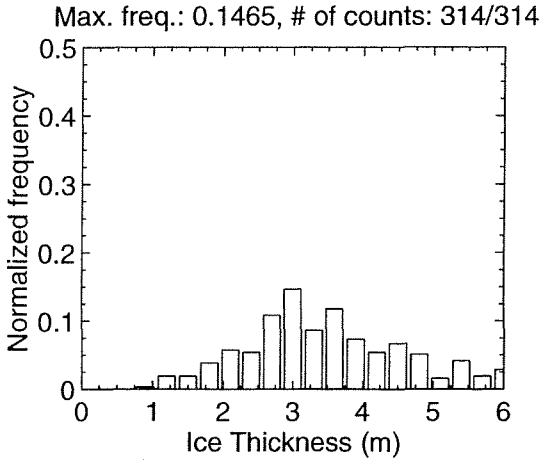

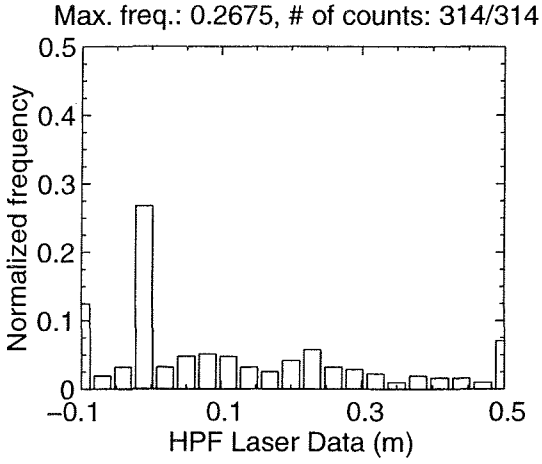

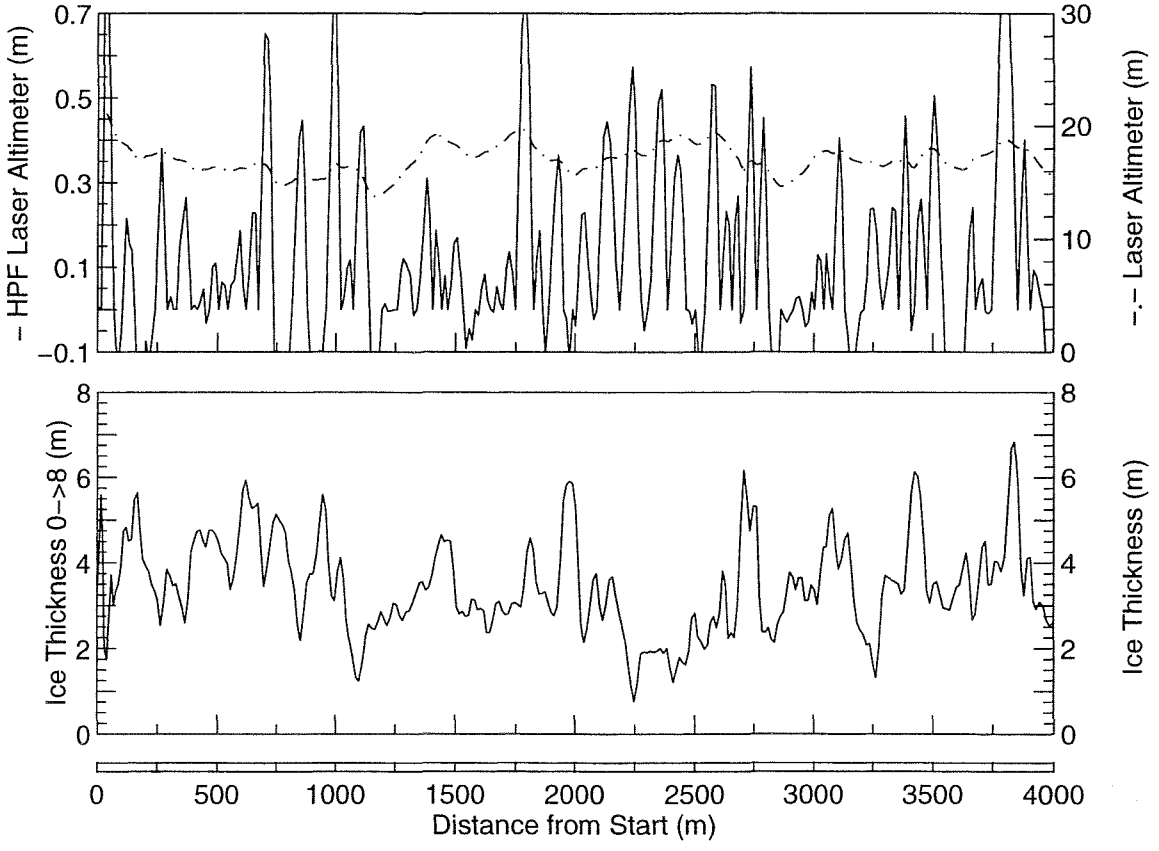

MAR 09 Flight #01 Line #10052 part 2 of 3

Line Starting Coordinates (54.0969,–56.3409) ending at (54.1322,–56.3302)

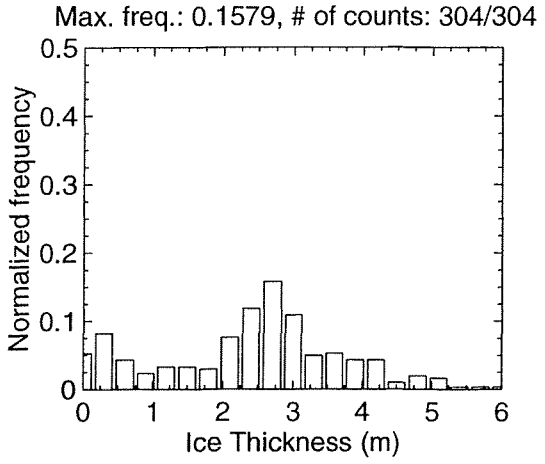

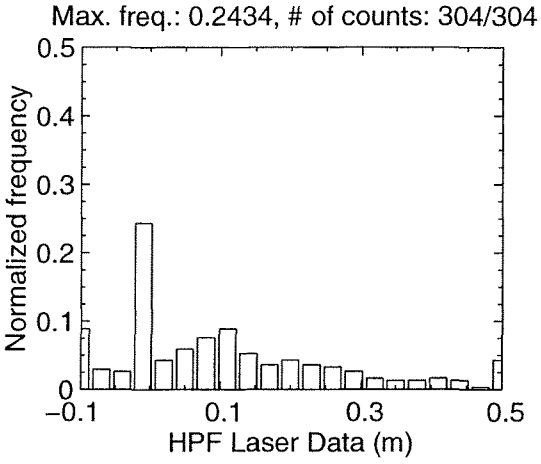

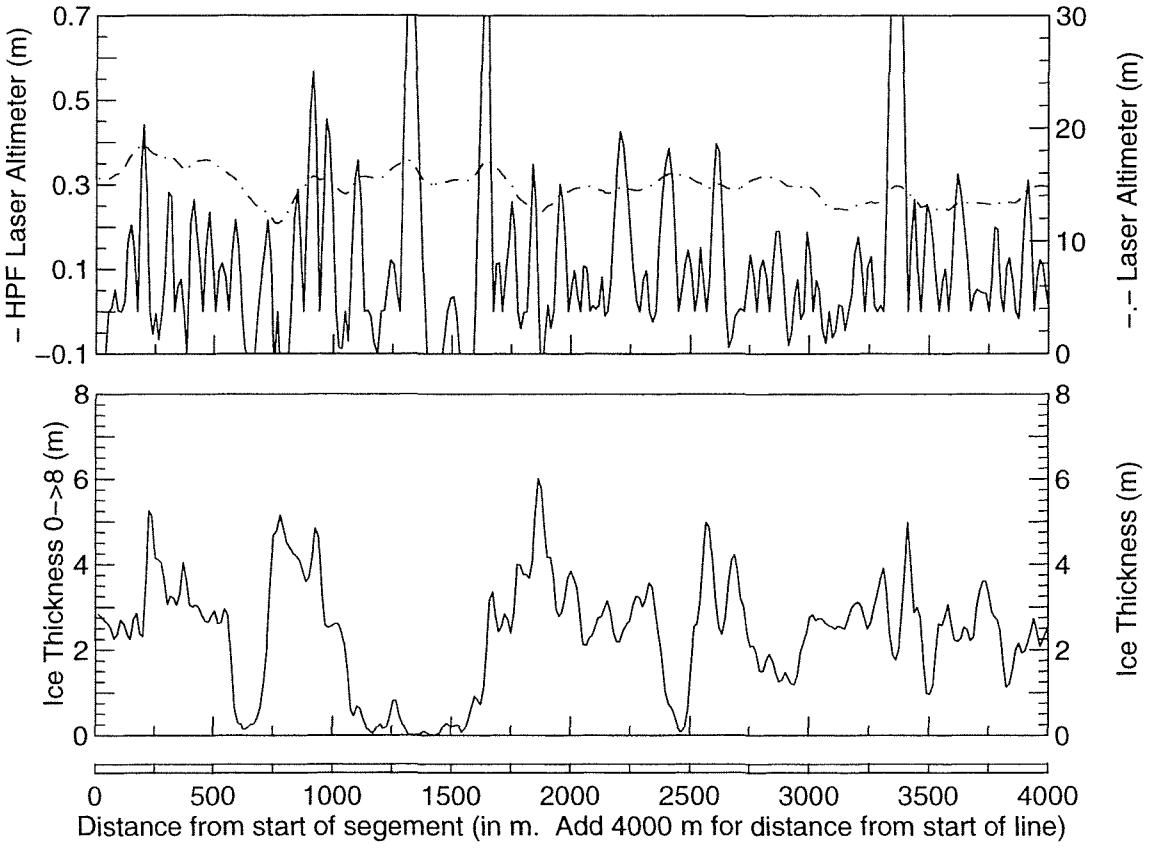

MAR 09 Flight #01 Line #10052 part 3 of 3

Line Starting Coordinates (54.1322,–56.3302) ending at (54.1567,–56.3235)

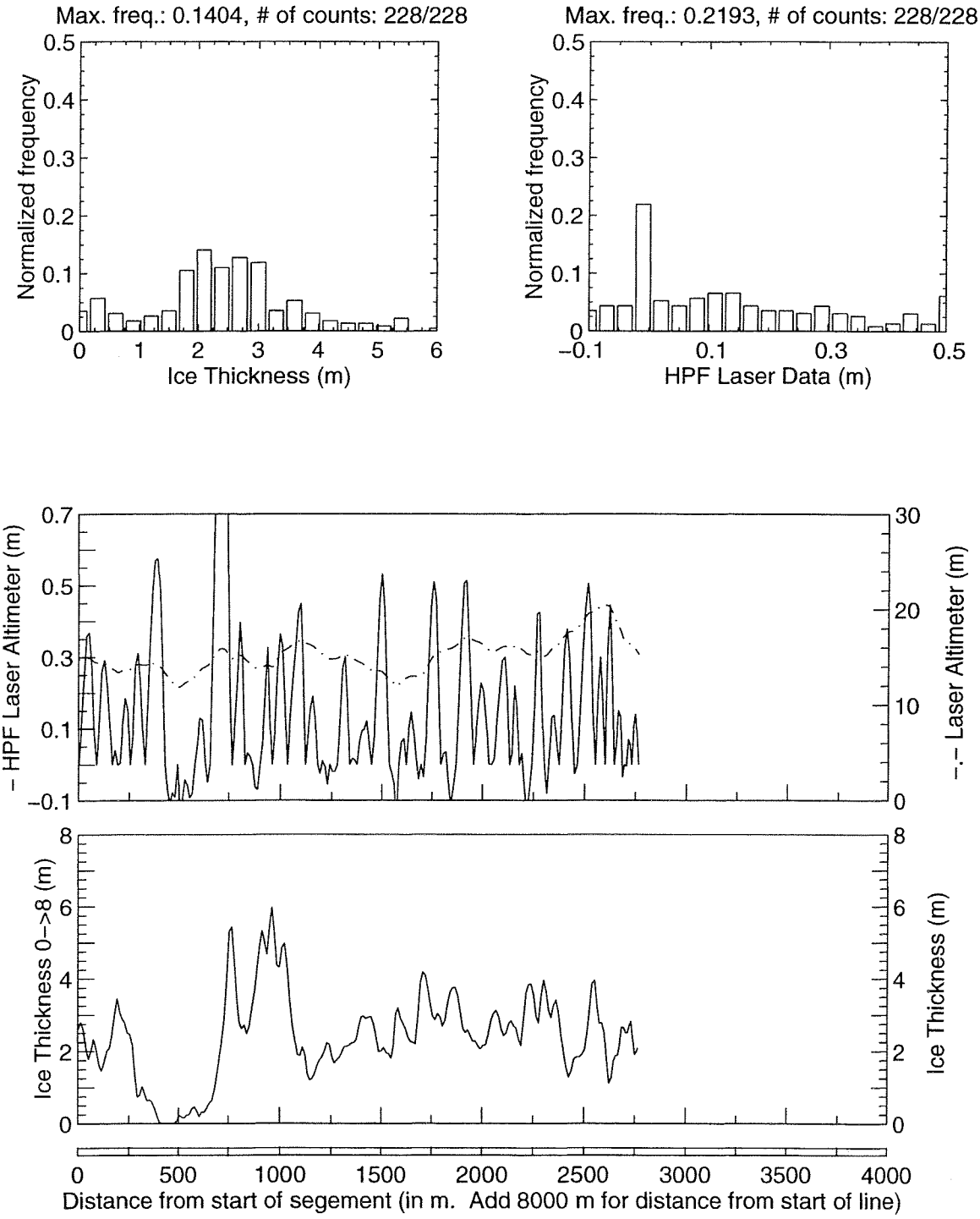

MAR 09 Flight #01 Line #10060 part 1 of 1

Line Starting Coordinates (54.1589,–56.3231) ending at (54.1611,–56.3228)

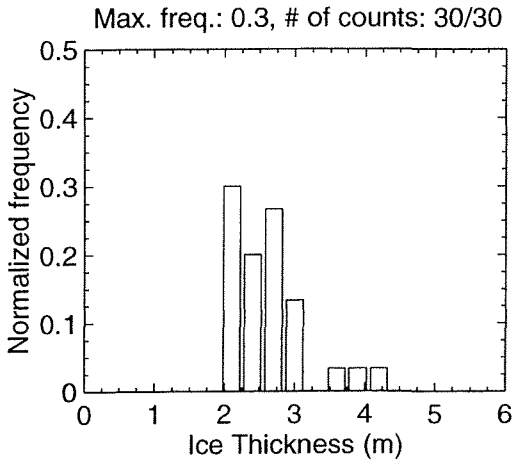

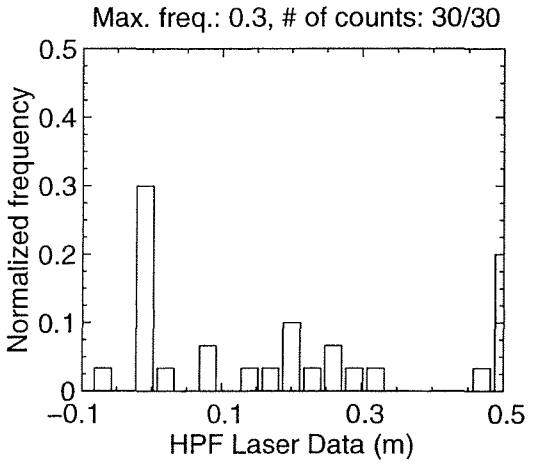

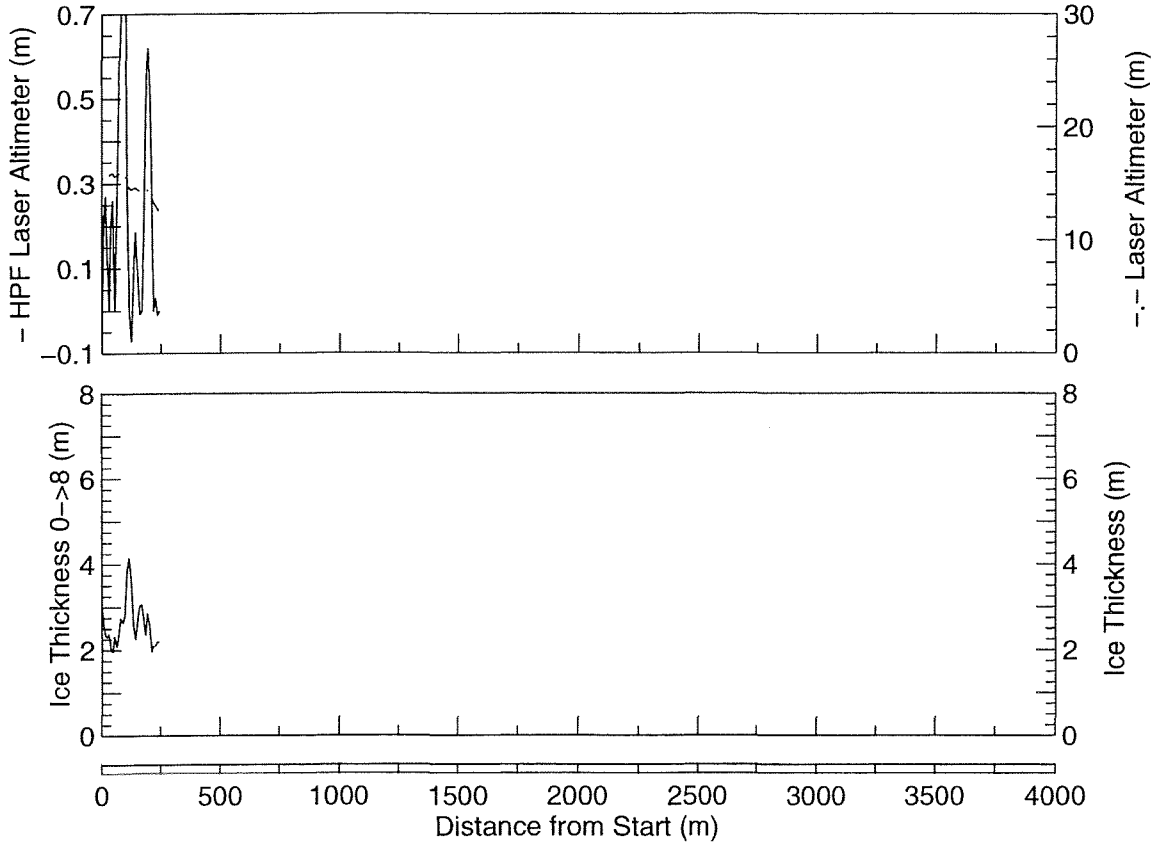

MAR 09 Flight #01 Line #10070 part 1 of 1

Line Starting Coordinates (54.1632,−56.3225) ending at (54.1701,−56.3216)

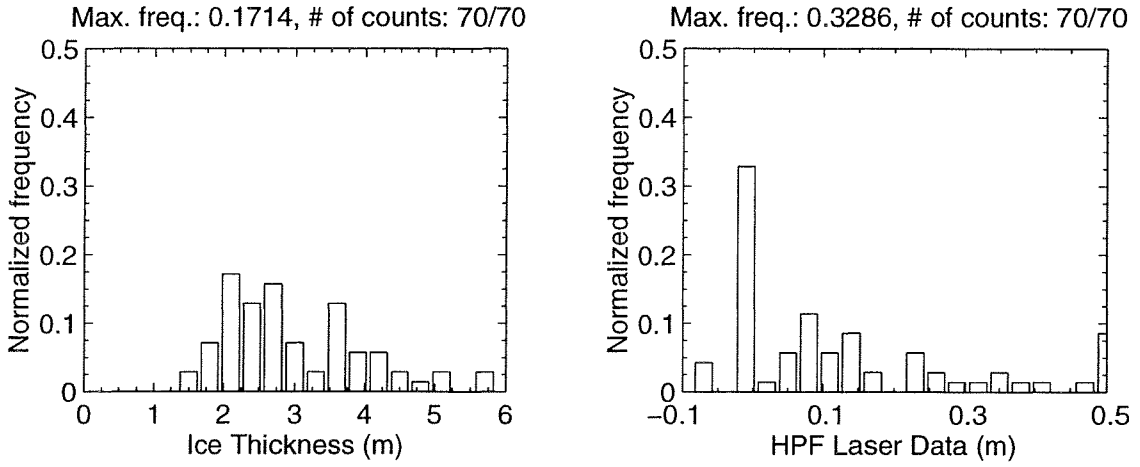

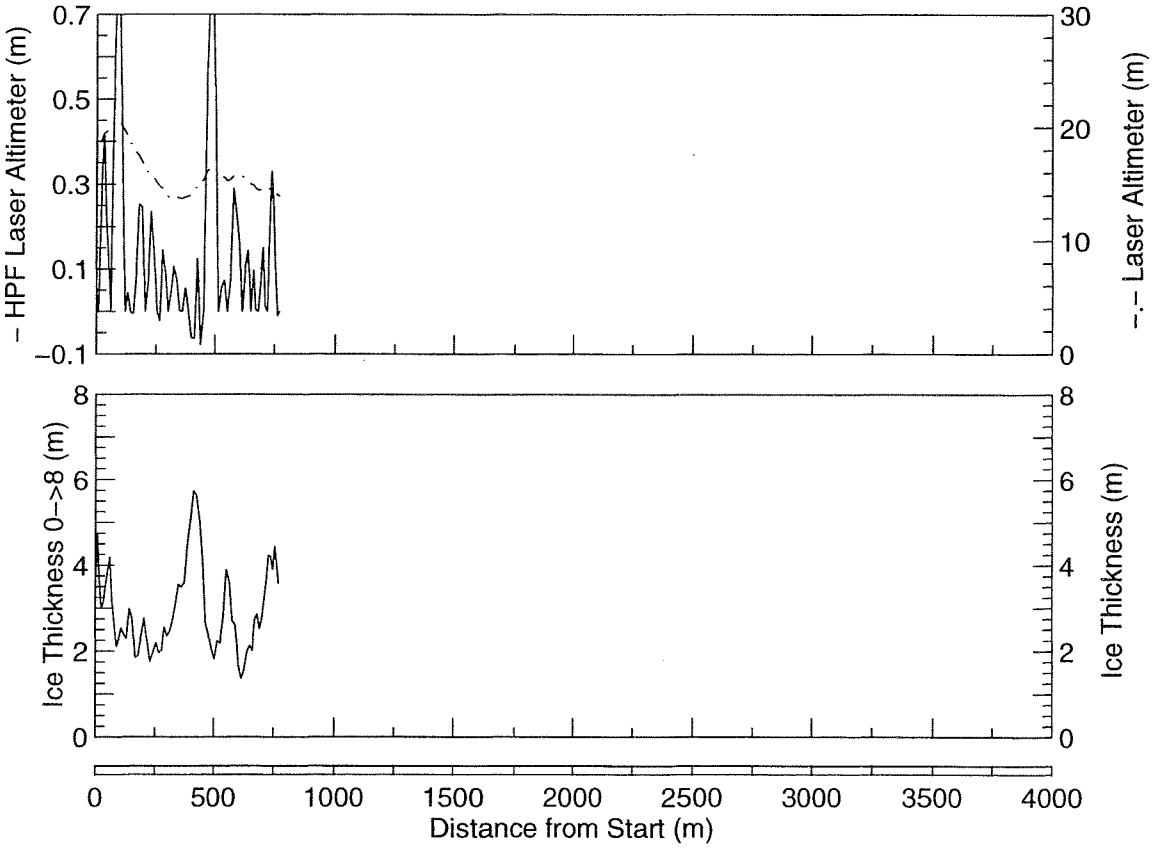

MAR 09 Flight #01 Line #10080 part 1 of 3

Line Starting Coordinates (54.1907,–56.3277) ending at (54.1701,–56.3781)

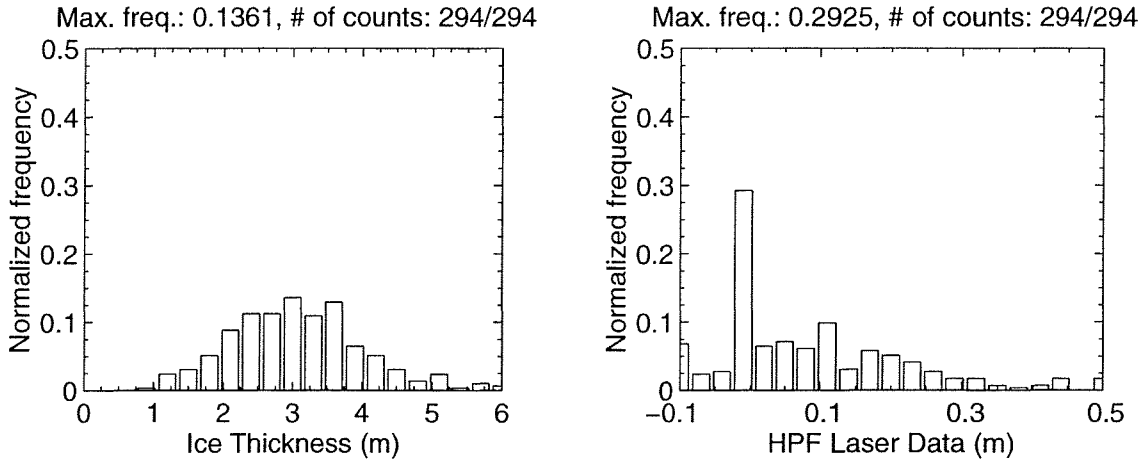

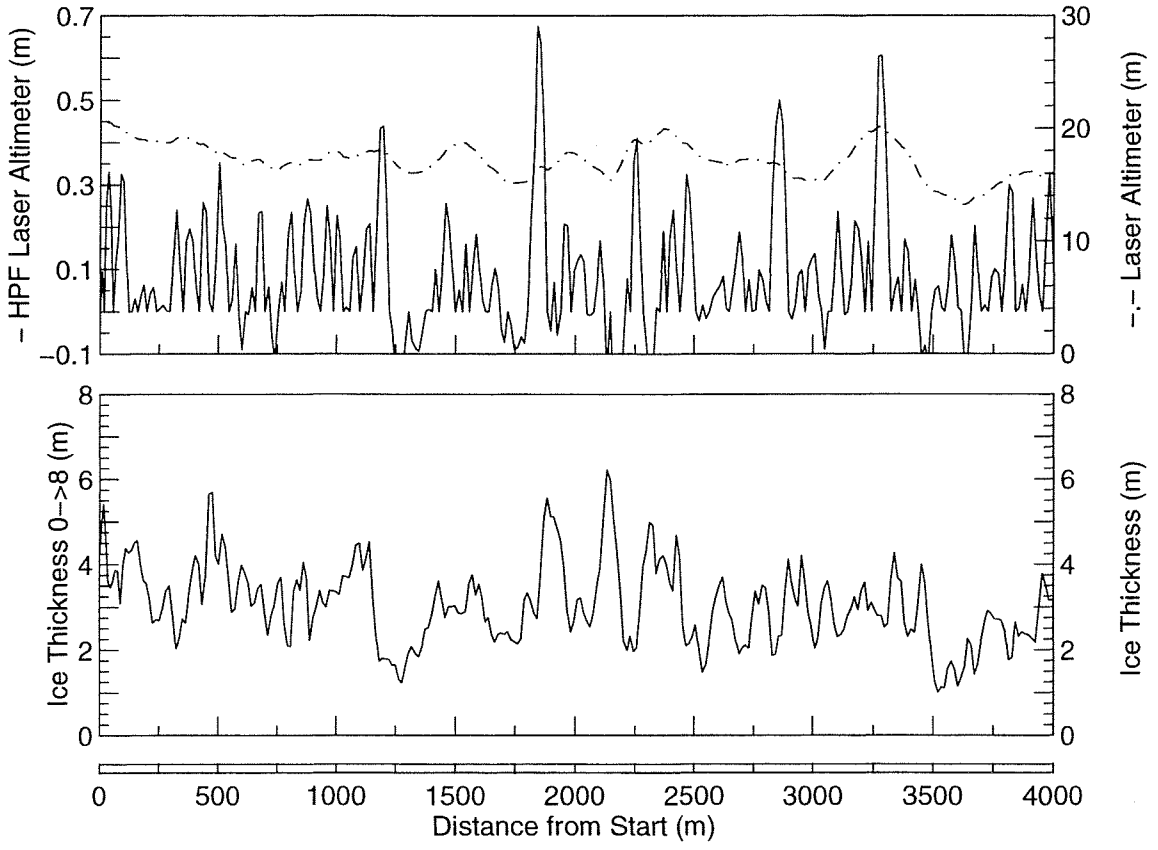

MAR 09 Flight #01 Line #10080 part 2 of 3

Line Starting Coordinates (54.1701,–56.3781) ending at (54.1502,–56.4292)

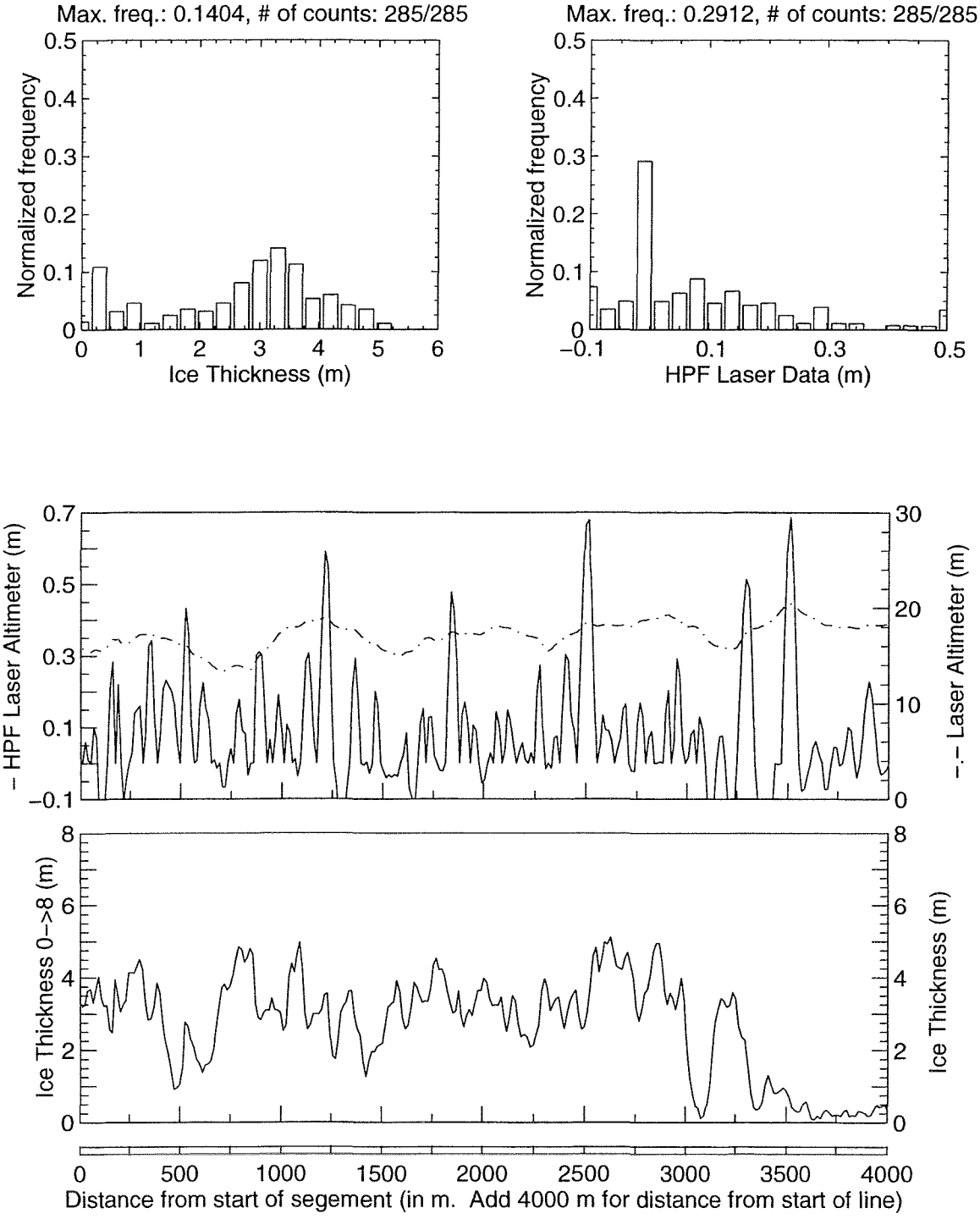

MAR 09 Flight #01 Line #10080 part 3 of 3

Line Starting Coordinates (54.1502,–56.4292) ending at (54.1318,–56.4813)

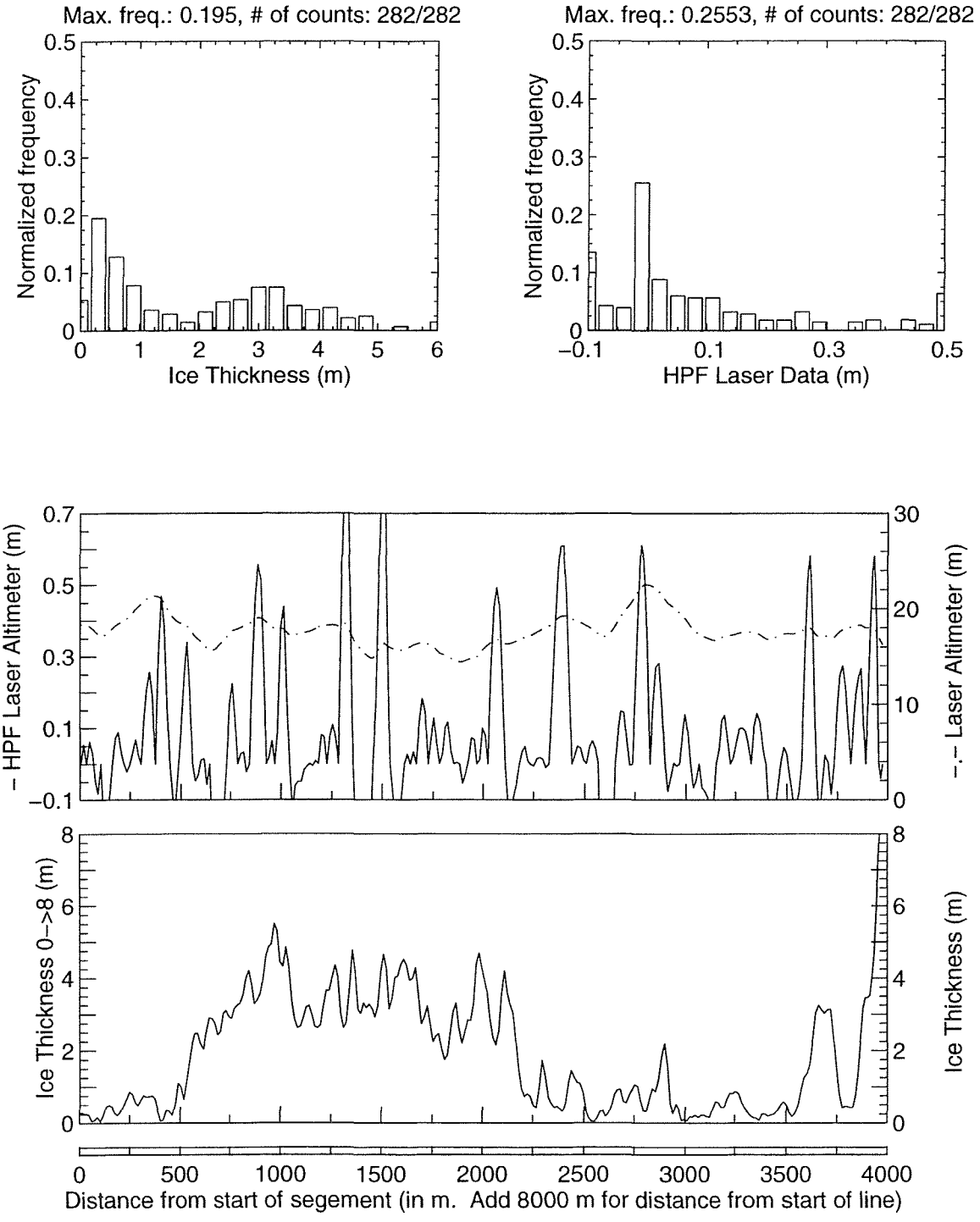

MAR 09 Flight #01 Line #10090 part 1 of 4

Line Starting Coordinates (54.1147,–56.5295) ending at (54.0955,–56.5813)

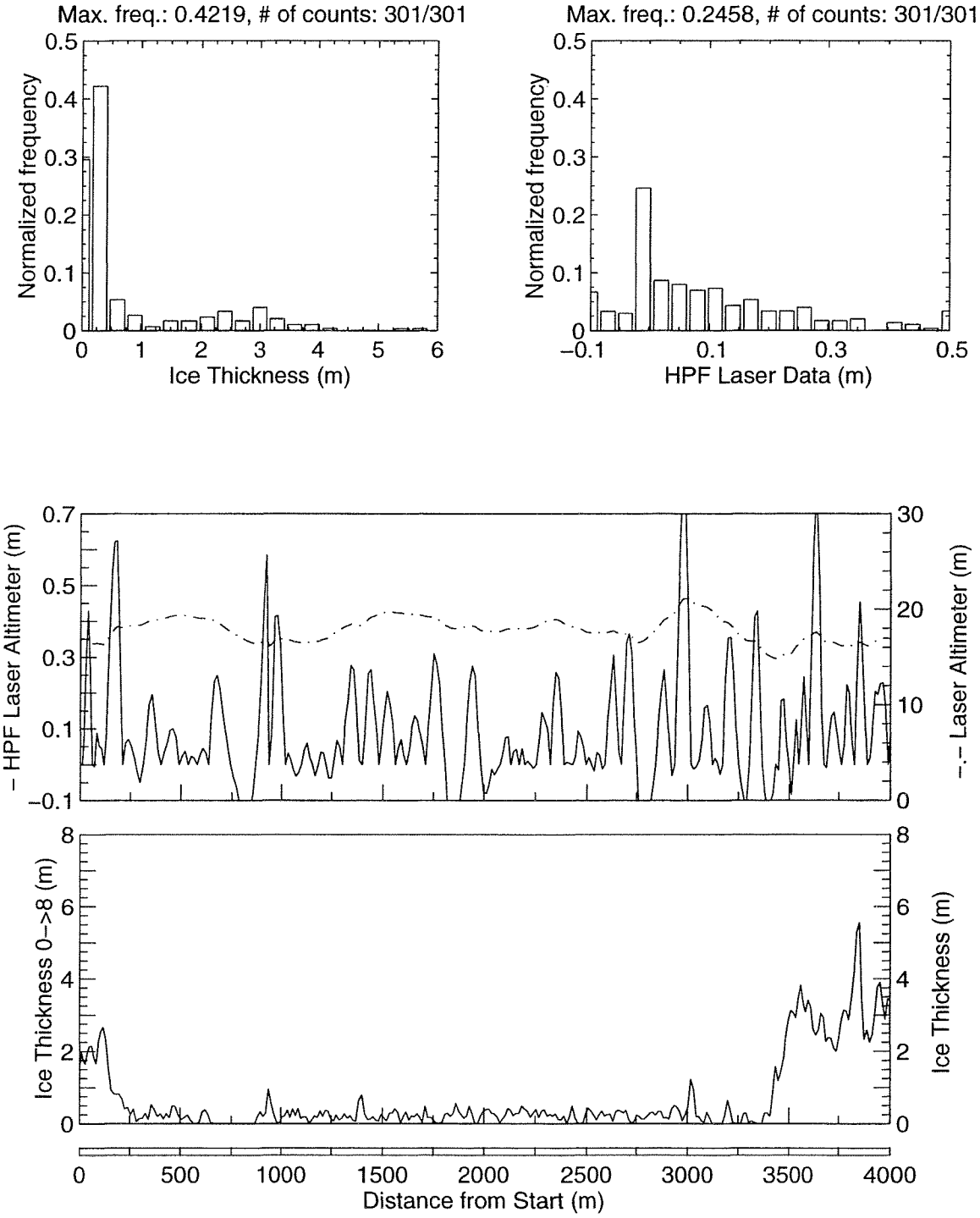

MAR 09 Flight #01 Line #10090 part 2 of 4

Line Starting Coordinates (54.0955,–56.5813) ending at (54.0774,–56.6343)

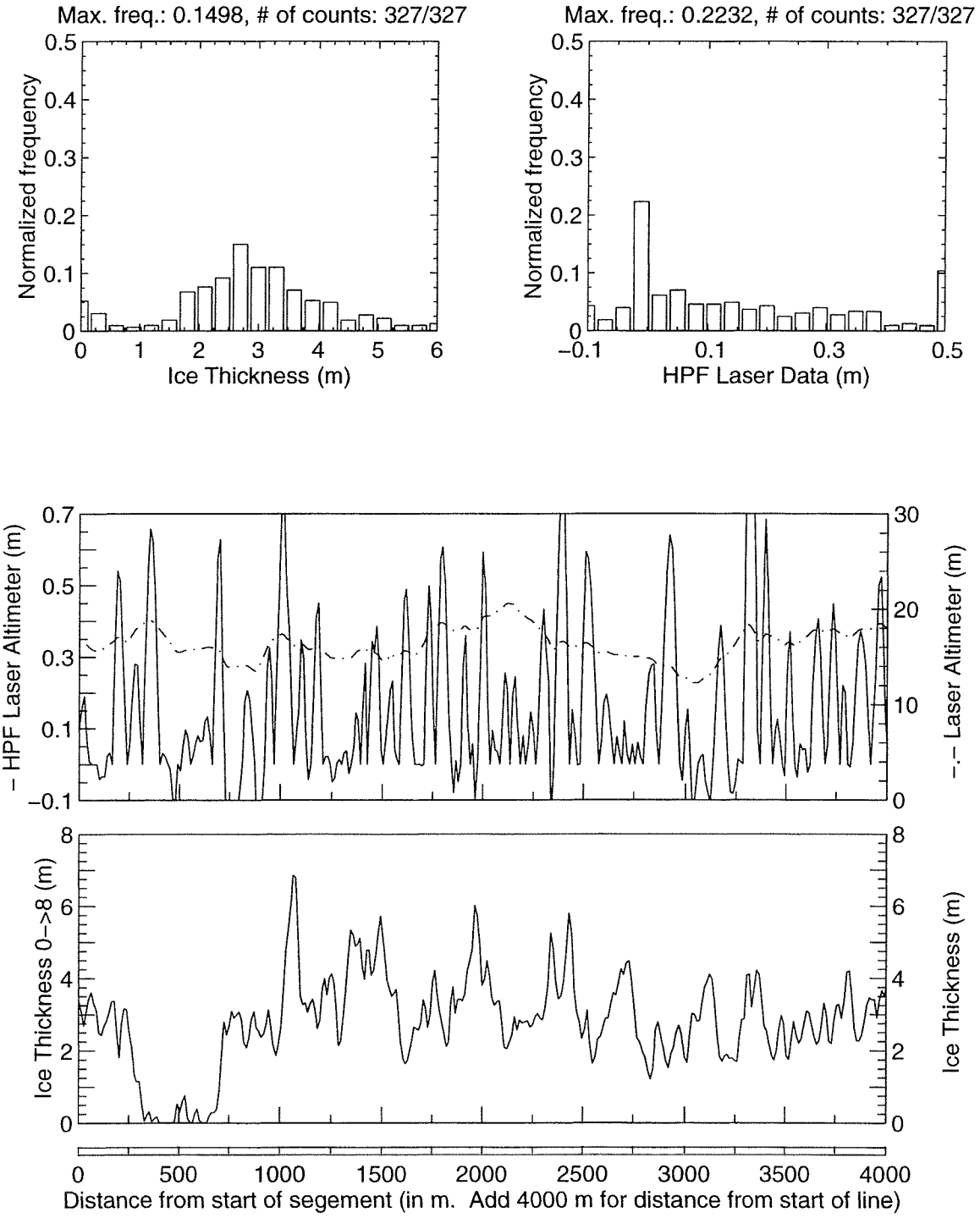

MAR 09 Flight #01 Line #10090 part 3 of 4

Line Starting Coordinates (54.0774,−56.6343) ending at (54.0622,−56.6896)

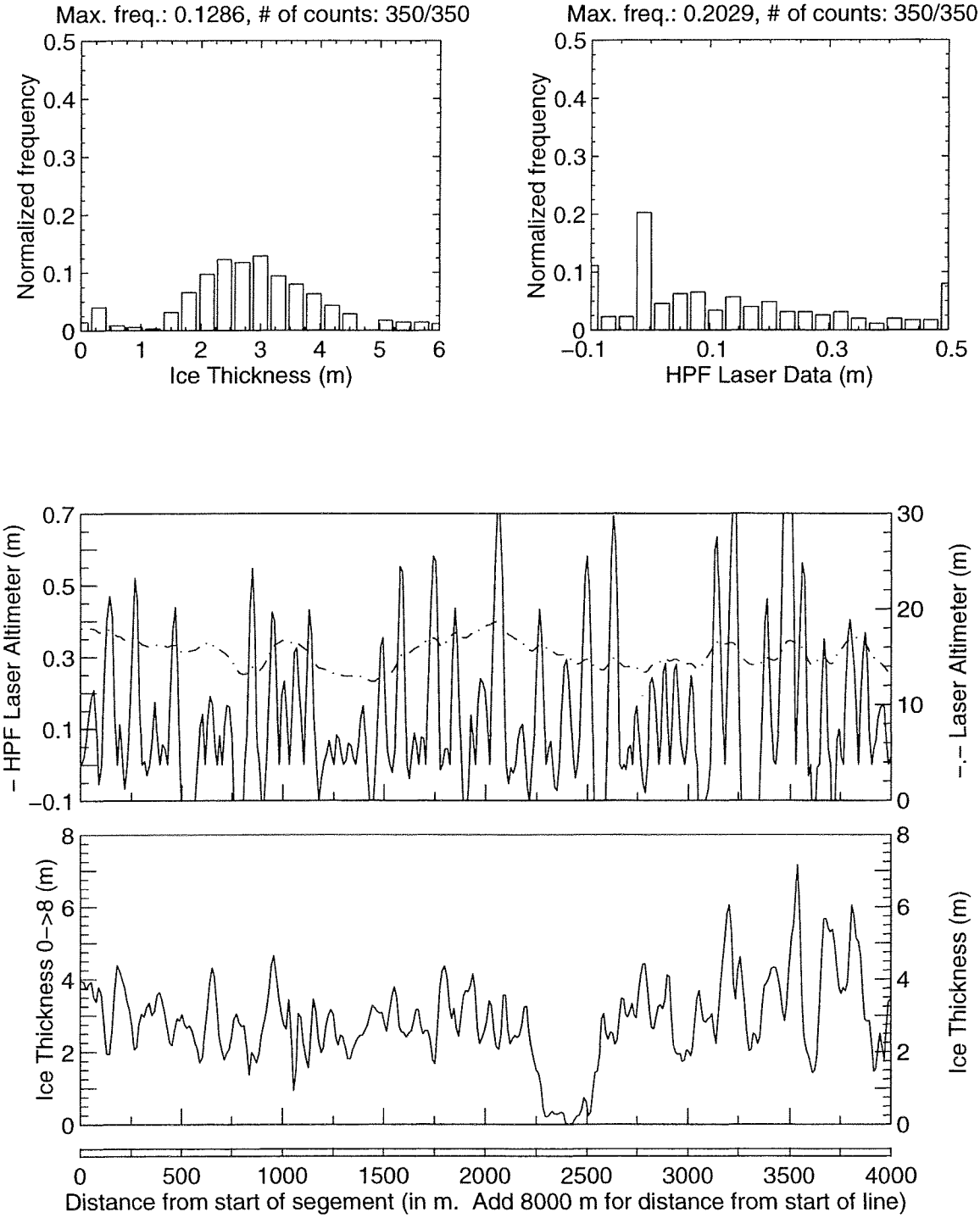

MAR 09 Flight #01 Line #10090 part 4 of 4

Line Starting Coordinates (54.0622,–56.6896) ending at (54.0505,–56.7462)

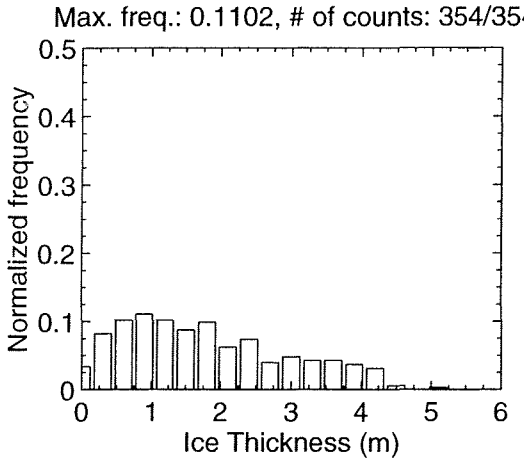

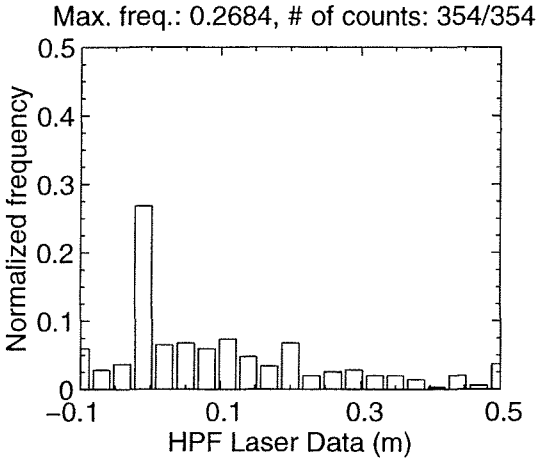

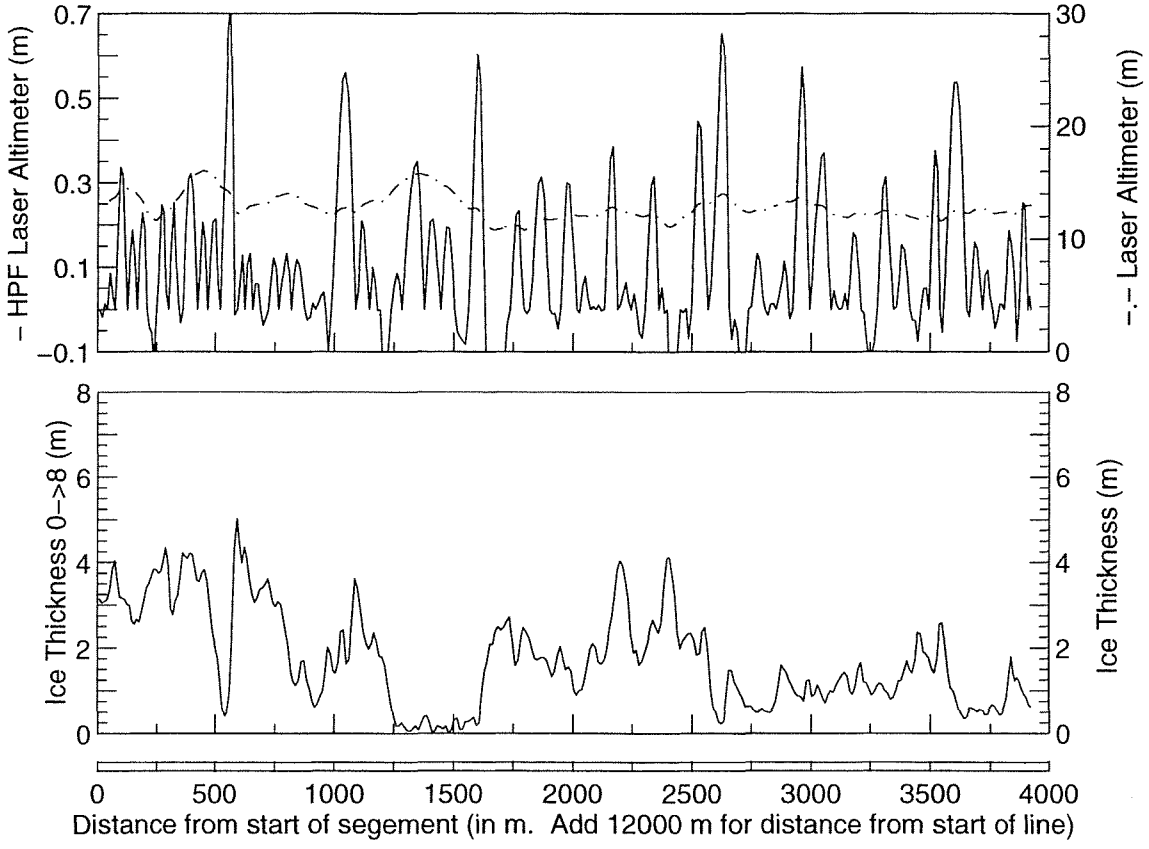

MAR 09 Flight #01 Line #10100 part 1 of 2

Line Starting Coordinates (54.0497,–56.7502) ending at (54.0367,–56.8074)

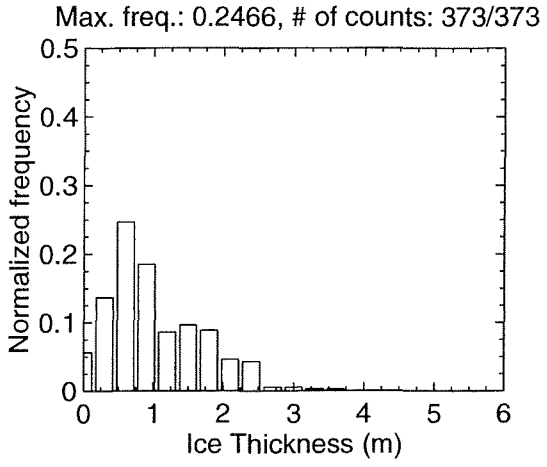

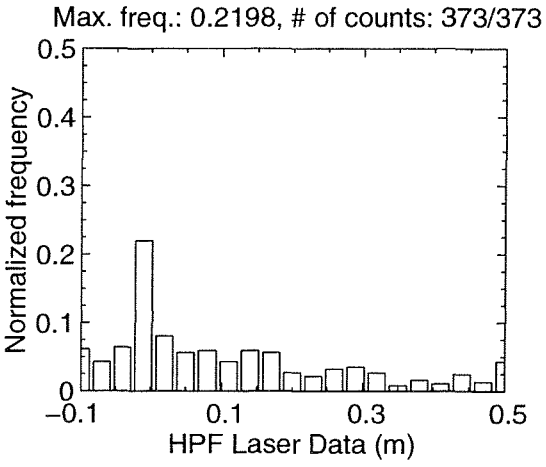

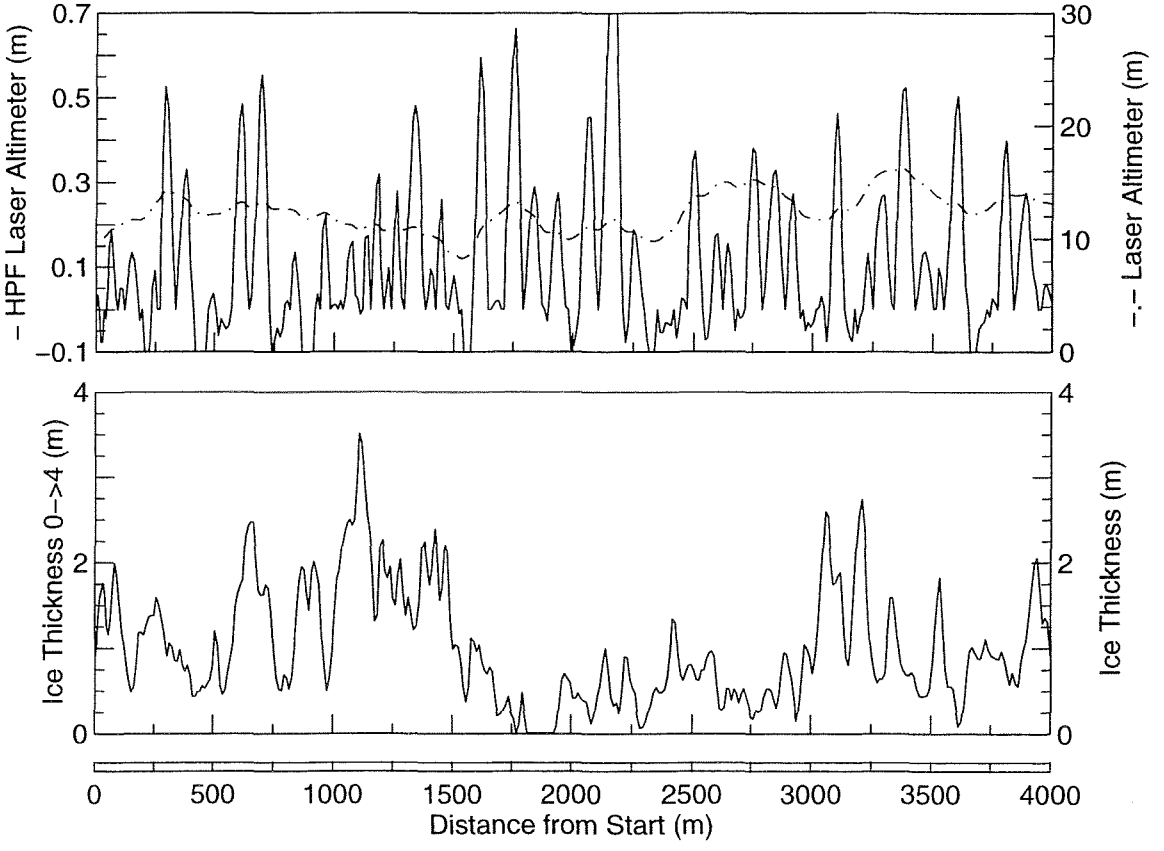

MAR 09 Flight #01 Line #10100 part 2 of 2

Line Starting Coordinates (54.0367,−56.8074) ending at (54.0280,−56.8437)

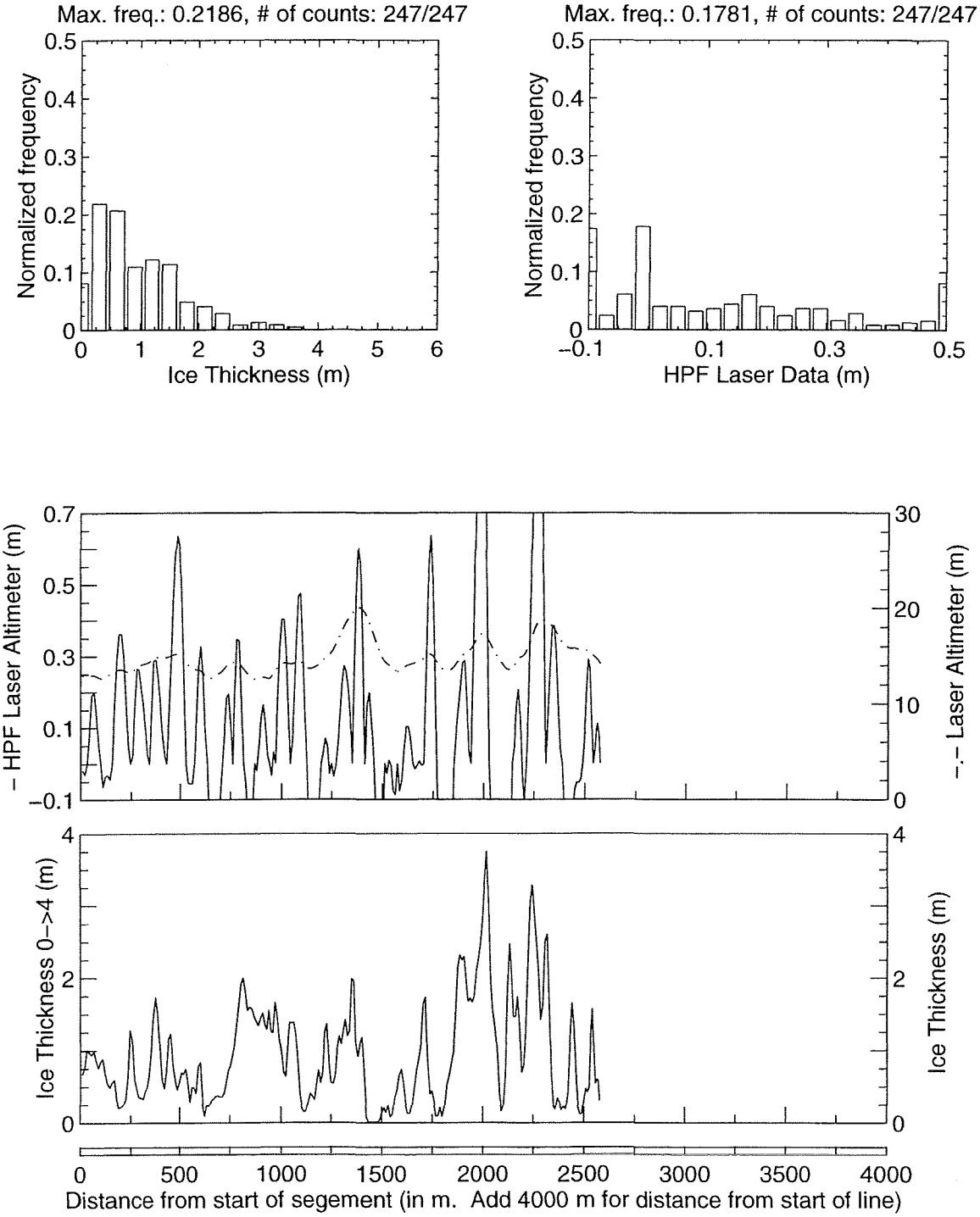

MAR 09 Flight #01 Line #10110 part 1 of 4

Line Starting Coordinates (54.0050,–56.8713) ending at (53.9731,–56.8998)

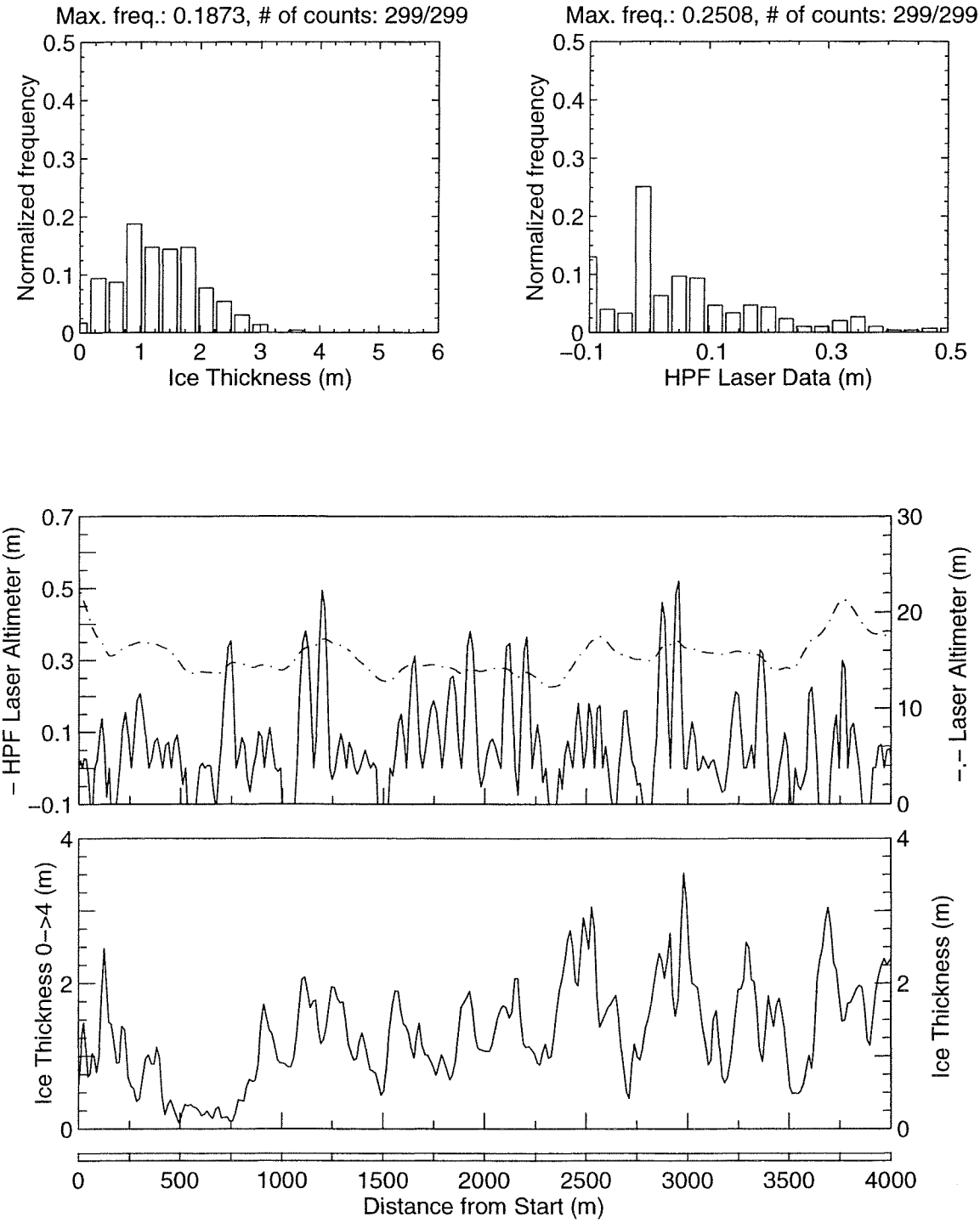

MAR 09 Flight #01 Line #10110 part 2 of 4

Line Starting Coordinates (53.9731,–56.8998) ending at (53.9411,–56.9273)

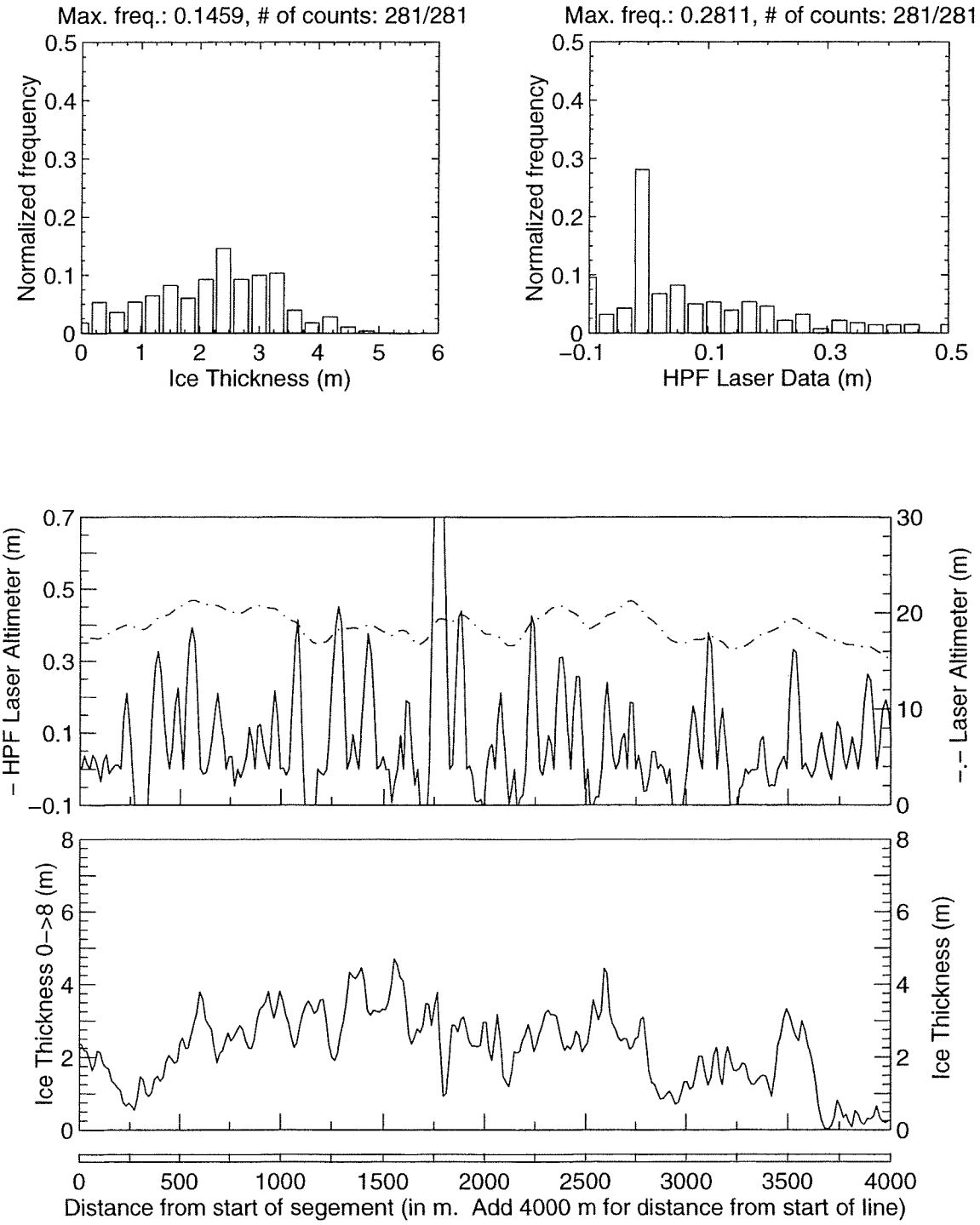

MAR 09 Flight #01 Line #10110 part 3 of 4

Line Starting Coordinates (53.9411,–56.9273) ending at (53.9088,–56.9542)

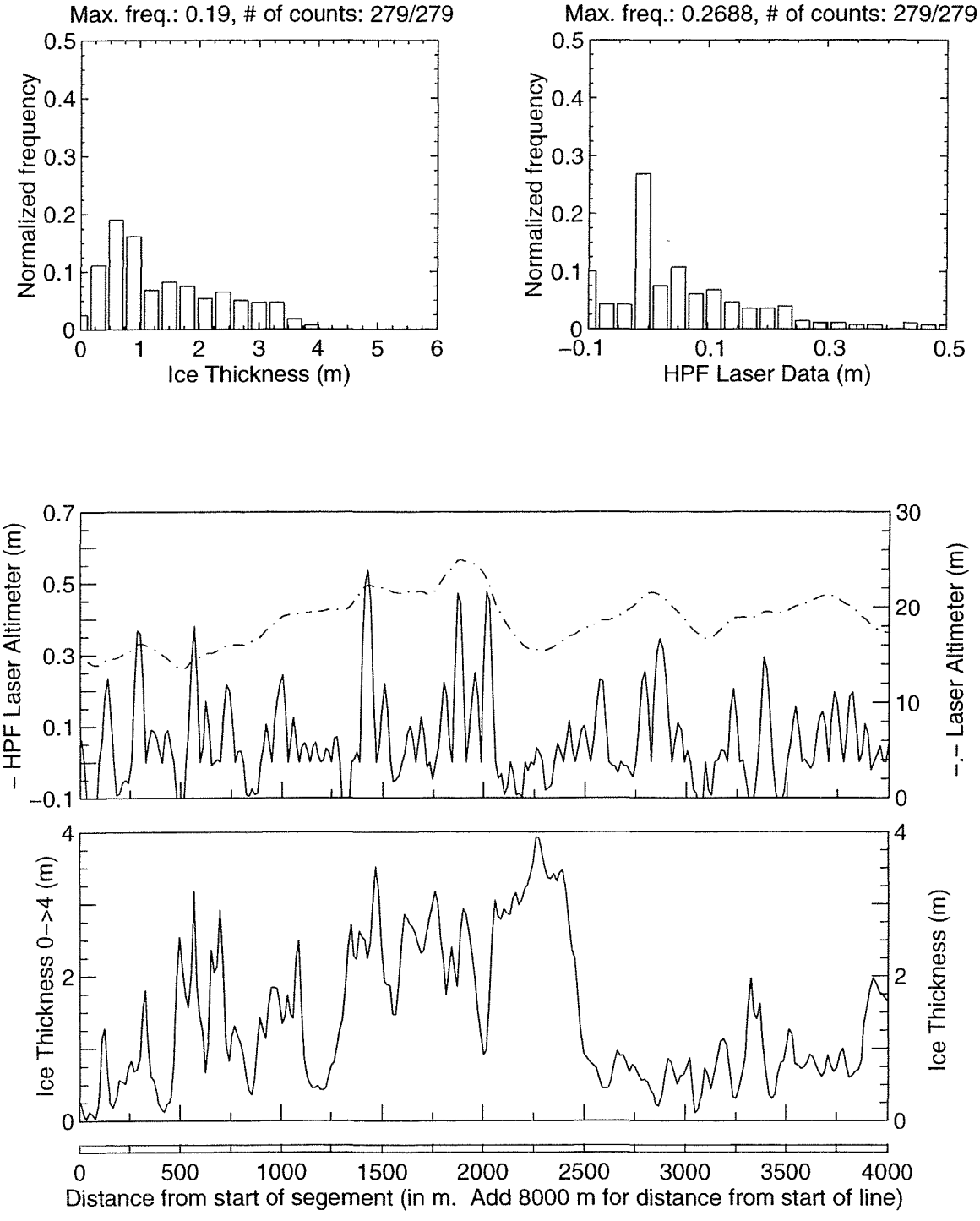

MAR 09 Flight #01 Line #10110 part 4 of 4

Line Starting Coordinates (53.9088,–56.9542) ending at (53.8944,–56.9660)

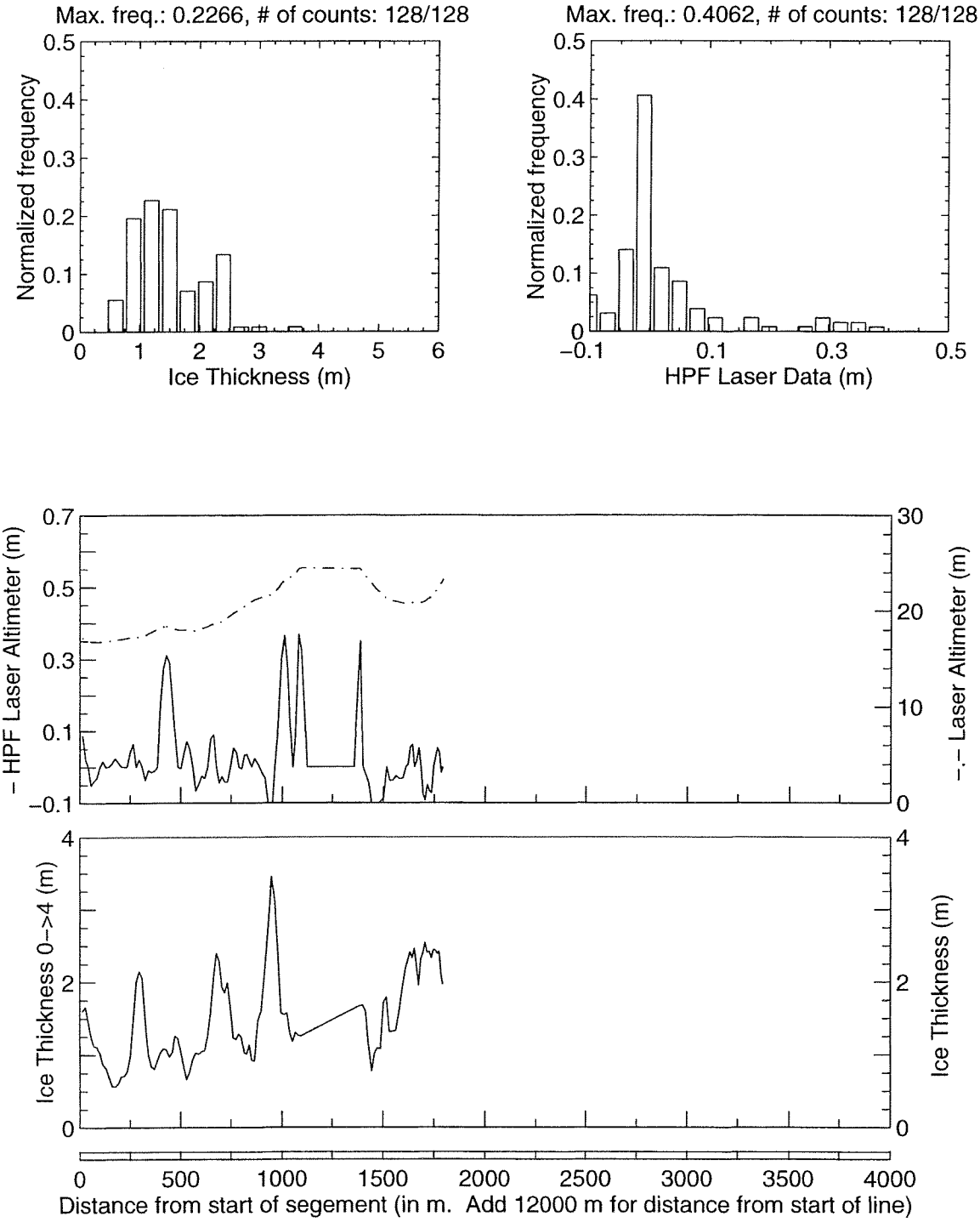

MAR 09 Flight #01 Line #10120 part 1 of 1

Line Starting Coordinates (53.8902,−56.9699) ending at (53.8799,−56.9796)